USING NEW METABOLIC APPROACHES TO TARGET AND ERADICATE CANCER STEM CELLS

EDITED BY: Michael P. Lisanti, Federica Sotgia and Stephen Byers
PUBLISHED IN: Frontiers in Oncology

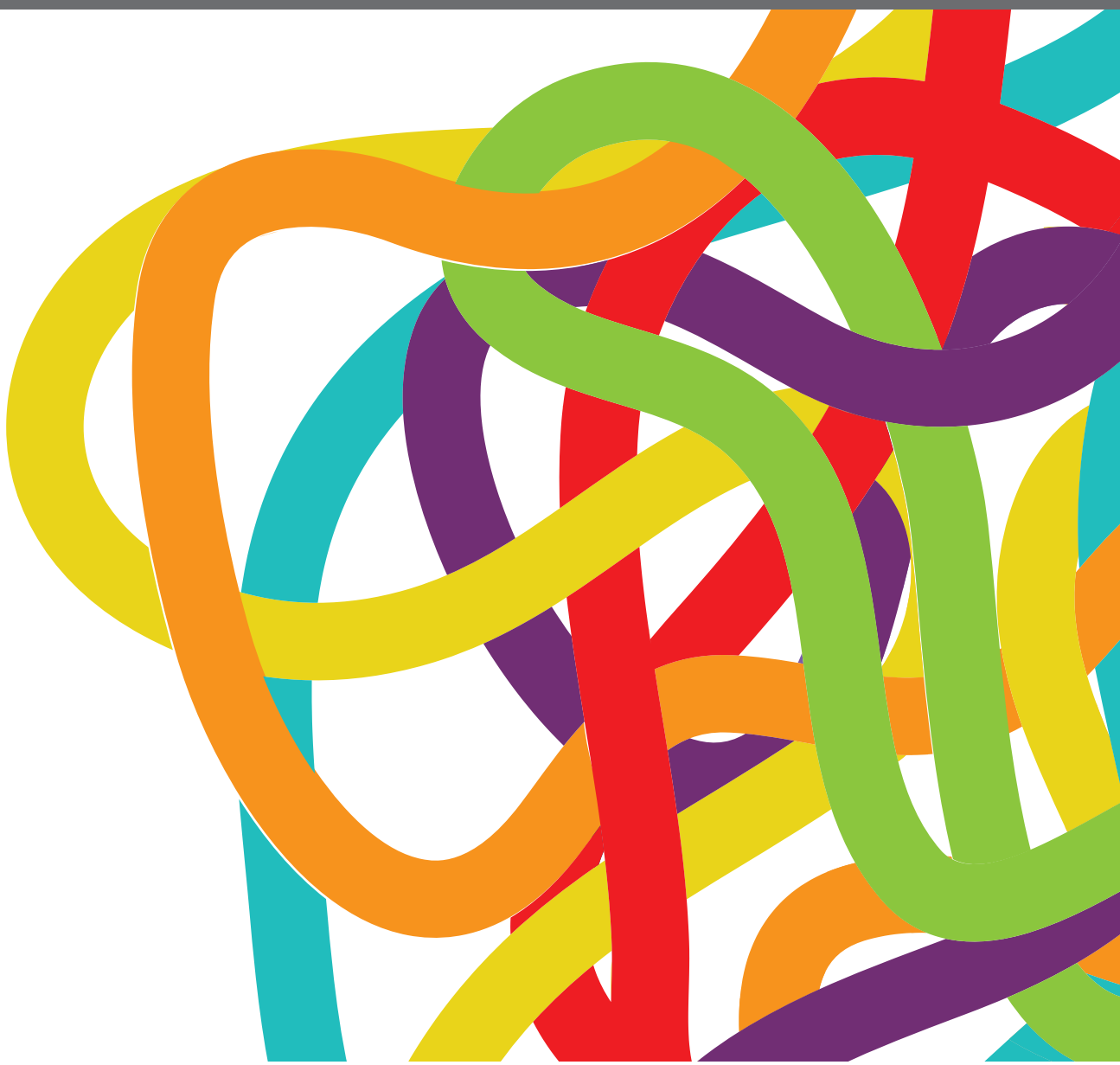

frontiers Research Topics

frontiers

ISSN 1664-8714
ISBN 978-2-88974-610-1
DOI 10.3389/978-2-88974-610-1

About Frontiers

Frontiers is more than just an open-access publisher of scholarly articles: it is a pioneering approach to the world of academia, radically improving the way scholarly research is managed. The grand vision of Frontiers is a world where all people have an equal opportunity to seek, share and generate knowledge. Frontiers provides immediate and permanent online open access to all its publications, but this alone is not enough to realize our grand goals.

Frontiers Journal Series

The Frontiers Journal Series is a multi-tier and interdisciplinary set of open-access, online journals, promising a paradigm shift from the current review, selection and dissemination processes in academic publishing. All Frontiers journals are driven by researchers for researchers; therefore, they constitute a service to the scholarly community. At the same time, the Frontiers Journal Series operates on a revolutionary invention, the tiered publishing system, initially addressing specific communities of scholars, and gradually climbing up to broader public understanding, thus serving the interests of the lay society, too.

Dedication to Quality

Each Frontiers article is a landmark of the highest quality, thanks to genuinely collaborative interactions between authors and review editors, who include some of the world's best academicians. Research must be certified by peers before entering a stream of knowledge that may eventually reach the public - and shape society; therefore, Frontiers only applies the most rigorous and unbiased reviews.
Frontiers revolutionizes research publishing by freely delivering the most outstanding research, evaluated with no bias from both the academic and social point of view. By applying the most advanced information technologies, Frontiers is catapulting scholarly publishing into a new generation.

What are Frontiers Research Topics?

Frontiers Research Topics are very popular trademarks of the Frontiers Journals Series: they are collections of at least ten articles, all centered on a particular subject. With their unique mix of varied contributions from Original Research to Review Articles, Frontiers Research Topics unify the most influential researchers, the latest key findings and historical advances in a hot research area! Find out more on how to host your own Frontiers Research Topic or contribute to one as an author by contacting the Frontiers Editorial Office: frontiersin.org/about/contact

USING NEW METABOLIC APPROACHES TO TARGET AND ERADICATE CANCER STEM CELLS

Topic Editors:
Michael P. Lisanti, University of Salford, United Kingdom
Federica Sotgia, University of Salford, United Kingdom
Stephen Byers, Georgetown University, United States

Topic Editors MPL and FS hold a minority interest in Lunella Biotech, Inc.

Citation: Lisanti, M. P., Sotgia, F., Byers, S., eds. (2022). Using New Metabolic Approaches to Target and Eradicate Cancer Stem Cells.
Lausanne: Frontiers Media SA. doi: 10.3389/978-2-88974-610-1

Table of Contents

frontiers in Oncology

ORIGINAL RESEARCH
published: 07 August 2019
doi: 10.3389/fonc.2019.00615

Dodecyl-TPP Targets Mitochondria and Potently Eradicates Cancer Stem Cells (CSCs): Synergy With FDA-Approved Drugs and Natural Compounds (Vitamin C and Berberine)

Ernestina Marianna De Francesco, Béla Ózsvári, Federica Sotgia and Michael P. Lisanti**

Translational Medicine, Biomedical Research Centre, School of Environment and Life Sciences, University of Salford, Greater Manchester, United Kingdom

OPEN ACCESS

Edited by:
Chris Albanese, Georgetown University, United States

Reviewed by:
Paul Dent, Virginia Commonwealth University, United States
Varda Shoshan-Barmatz, Ben-Gurion University of the Negev, Israel

***Correspondence:**
Federica Sotgia
fsotgia@gmail.com
Michael P. Lisanti
michaelp.lisanti@gmail.com

Specialty section:
This article was submitted to Cancer Metabolism, a section of the journal Frontiers in Oncology

Received: *13 May 2019*
Accepted: *21 June 2019*
Published: *07 August 2019*

Citation:
De Francesco EM, Ózsvári B, Sotgia F and Lisanti MP (2019) Dodecyl-TPP Targets Mitochondria and Potently Eradicates Cancer Stem Cells (CSCs): Synergy With FDA-Approved Drugs and Natural Compounds (Vitamin C and Berberine). Front. Oncol. 9:615. doi: 10.3389/fonc.2019.00615

Elevated mitochondrial biogenesis and/or metabolism are distinguishing features of cancer cells, as well as Cancer Stem Cells (CSCs), which are involved in tumor initiation, metastatic dissemination, and therapy resistance. In fact, mitochondria-impairing agents can be used to hamper CSCs maintenance and propagation, toward better control of neoplastic disease. Tri-Phenyl-Phosphonium (TPP)-based mitochondrially-targeted compounds are small non-toxic and biologically active molecules that are delivered to and accumulated within the mitochondria of living cells. Therefore, TPP-derivatives may represent potentially "powerful" candidates to block CSCs. Here, we evaluate the metabolic and biological effects induced by the TPP-derivative, termed Dodecyl-TPP (d-TPP) on breast cancer cells. By employing the 3D mammosphere assay in MCF-7 cells, we demonstrate that treatment with d-TPP dose-dependently inhibits the propagation of breast CSCs in suspension. Also, d-TPP targets adherent "bulk" cancer cells, by decreasing MCF-7 cell viability. The analysis of metabolic flux using Seahorse Xfe96 revealed that d-TPP potently inhibits the mitochondrial oxygen consumption rate (OCR), while simultaneously shifting cell metabolism toward glycolysis. Thereafter, we exploited this ATP depletion phenotype and strict metabolic dependency on glycolysis to eradicate the residual glycolytic CSC population, by using additional metabolic stressors. More specifically, we applied a combination strategy based on treatment with d-TPP, in the presence of a selected panel of natural and synthetic compounds, some of which are FDA-approved, that are known to behave as glycolysis (Vitamin C, 2-Deoxy-Glucose) and OXPHOS (Doxycyline, Niclosamide, Berberine) inhibitors. This two-hit scheme effectively decreased CSC propagation, at concentrations of d-TPP toxic only for cancer cells, but not for normal cells, as evidenced using normal human fibroblasts (hTERT-BJ1) as a reference point. Taken together, d-TPP halts CSCs propagation and targets "bulk" cancer cells, without eliciting the relevant undesirable off-target effects in normal cells.

These observations pave the way for further exploring the potential of TPP-based derivatives in cancer therapy. Moreover, TPP-based compounds should be investigated for their potential to discriminate between "normal" and "malignant" mitochondria, suggesting that distinct biochemical, and metabolic changes in these organelles could precede specific normal or pathological phenotypes. Lastly, our data validate the manipulation of the energetic machinery as useful tool to eradicate CSCs.

Keywords: Tri-Phenyl-Phosphonium (TPP), Cancer Stem Cells (CSCs), mitochondria, cancer therapy, vitamin C, Doxycycline, cancer metabolism, metabolic plasticity

INTRODUCTION

Intact and enhanced metabolic function are necessary to support the elevated bioenergetic and biosynthetic demands of cancer cells toward tumor growth and metastatic dissemination (1, 2). Not surprisingly, mitochondrially-dependent metabolic pathways provide an essential biochemical platform for cancer cells, by extracting energy from several distinct fuels sources (3).

Recently, energetic metabolism and mitochondrial function have been linked to certain dynamics involved in the maintenance and propagation of Cancer Stem Cells (CSCs), which are a distinct cell sub-population, within the tumor mass, involved in tumor initiation, metastatic spread and resistance to anti-cancer therapies (3–9). For instance, CSCs show a peculiar and unique increase in mitochondrial mass, as well as enhanced mitochondrial biogenesis and higher activation of mitochondrial protein translation, suggestive of a strict reliance on mitochondrial function (10–13).

Consistent with these observations, elevated mitochondrial metabolic function, and OXPHOS have been detected in CSCs, across multiple tumor types (10–13). Likewise, the fluorescent mitochondrial dye, MitoTracker, has been used to enrich and purify CSCs, due to its ability to accumulate in and distinguish between different cancer cell sub-populations, characterized by a higher degree of anchorage-independent growth and higher tumor-initiating capability (10). During asymmetric cell division, "newly-synthesized" mitochondria are clustered within daughter cells, that retain stem-like phenotype. In contrast, daughter cells committed to differentiation, progressively loose stem traits because they receive older, less-efficient mitochondria. This observation further supports the idea that the most functionally viable and undamaged mitochondria, are selected for supporting stemness traits in cancer cells (14).

Based on these observations, novel pharmacological approaches aimed at targeting mitochondria in CSCs have been proposed and successfully applied in pre-clinical and clinical studies (15–23). For instance, the antibiotic Doxycycline, which decreases mitochondrial protein translation as an off-target effect, has been suggested for repurposing in the clinical management of early breast cancer patients for its ability to selectively target CSCs (21). In addition, compounds carrying a Tri-Phenyl-Phosphonium (TPP) moiety, that serves as a Mitochondria Targeting Signal (MTS), have been shown to elicit selective inhibitory actions in cancer cells, and CSCs, but not in normal cells (24).

Nevertheless, certain limitations restrain the use of solely anti-mitochondrial agents in cancer therapy, as adaptive mechanisms can be adopted in the tumor mass, to overcome the lack of mitochondrial function (3, 25). These adaptive mechanisms include the ability of CSCs to shift from oxidative metabolism to alternate energetic pathways, in a multi-directional process of metabolic plasticity driven by both intrinsic and extrinsic factors within the tumor cells, as well as in the surrounding tumor stroma or niche (7, 26, 27). Notably, in CSCs the manipulation of such metabolic flexibility can be advantageous to enhance therapeutic efficacy (23, 26). For instance, synchronizing CSCs toward certain metabolic dependencies, thus blocking their ability to shift among several energetic pathways, may represent a useful strategy toward CSC eradication (23, 26).

Herein, we provide evidence that the TPP derivative dodecyl-TPP (d-TPP), acting as a potent inhibitor of mitochondrial function, selectively and preferentially targets cancer cells and CSCs. As a proof of concept, we show that pharmacological strategies based on the combined use of mitochondrial (i.e., d-TPP) and glycolysis inhibitors (i.e., Vitamin C), efficiently hinder CSCs propagation.

MATERIALS AND METHODS

Materials

Dodecyl-tri-phenyl-phosphonium (d-TPP) bromide, Doxycycline, Ascorbic Acid, 2-Deoxy-D-glucose (2-DG), Berberine Chloride, and Niclosamide were all purchased from Sigma Aldrich. All compounds were dissolved in DMSO (Dimethyl Sulfoxide), except Ascorbic Acid and 2-deoxy-D-glucose (2-DG), which were dissolved in cell culture medium.

Cell Cultures

MCF7 and MDA-MB-231 breast cancer cells were obtained from the ATCC. Human immortalized fibroblasts (hTERT-BJ1) were originally purchased from Clontech, Inc. Cells were cultured in Dulbecco's modified Eagle's medium (DMEM), supplemented with 10% FBS (fetal bovine serum), 2 mM GlutaMAX, and 1% Pen-Strep in a 37°C humidified atmosphere containing 5% CO_2.

Mammosphere Formation

A single cell suspension of MCF-7 or MDA-MB-231 cells was prepared using enzymatic (1x Trypsin-EDTA, Sigma Aldrich), and manual disaggregation (25 gauge needle) (28). Cells were

then plated at a density of 500 cells/cm^2 in mammosphere medium (DMEM-F12/ B27/EGF(20-ng/ml)/PenStrep) under non-adherent conditions, in culture dishes coated with (2-hydroxyethylmethacrylate) (poly-HEMA, Sigma Aldrich), in the presence of treatments, as required. Cells were grown for 5 days and maintained in a humidified incubator at 37°C at an atmospheric pressure in 5% (v/v) carbon dioxide/air mixture. After 5 days for culture, spheres >50 μm were counted using an eye-piece (graticule), and the percentage of cells plated which formed spheres was calculated and is referred to as percentage mammosphere formation. Mammosphere assays were performed in triplicate and repeated three times independently.

Seahorse XFe-96 Metabolic Flux Analysis

Extracellular acidification rates (ECAR) and real-time oxygen consumption rates (OCR) for MCF-7 cells were determined using the Seahorse Extracellular Flux (XFe-96) analyzer (Seahorse Bioscience) (11). Briefly, 15,000 MCF-7 cells per well were seeded into XFe-96 well cell culture plates, and incubated overnight to allow attachment. Cells were then treated with increasing concentrations of d-TPP (50–500 nM) for 24 h. Vehicle alone (DMSO) control cells were processed in parallel. Then, cells were washed in pre-warmed XF assay media (or for OCR measurement, XF assay media supplemented with 10 mM glucose, 1 mM Pyruvate, 2 mM L-glutamine, and adjusted at 7.4 pH). Cells were then maintained in 175 μL/well of XF assay media at 37C, in a non-CO_2 incubator for 1 h. During the incubation time, 5 μL of 80 mM glucose, 9 μM oligomycin, and 1 M 2-deoxyglucose (for ECAR measurement) or 10 μM oligomycin, 9 μM FCCP, 10 μM Rotenone, 10 μM antimycin A (for OCR measurement), were loaded in XF assay media into the injection ports in the XFe-96 sensor cartridge. Data sets was analyzed using XFe-96 software and afterwards the measurements were normalized by protein content (via the SRB assay). All experiments were performed three times independently.

Sulphorhodamine B Assay

Protein content in viable cells was assessed in MCF-7 and hTERT-BJ1 cells, by using the sulphorhodamine (SRB) assay, based on the measurement of cellular protein content. After treatment with d-TPP (50–1 μM) for 24, 48, or 72 h, cells were fixed with 10% trichloroacetic acid (TCA) for 1 h in the cold room, and dried overnight at room temperature. Then, cells were incubated with SRB for 15 min, washed twice with 1% acetic acid, and air dried for at least 1 h. Finally, the protein-bound dye was dissolved in a 10 mM Tris pH 8.8 solution and read using a plate reader at 540 nm.

xCELLigence RTCA System (ACEA Biosciences Inc.)

The xCELLigence RTCA system provides a useful approach for the real-time monitoring of the biological status of adherent cells, by measuring their electrical impedance, expressed as a cell index (CI) value. Five thousand MCF-7 cells were seeded in a 16-well plate (E-plate). Twenty-four hours after seeding, cells were treated with vehicle or increasing concentrations of d-TPP (from 50 to 250 nM) for additional 72 h. Real-time cell-analysis (RTCA) was performed by measuring the cell-induced electrical impedance values, which were automatically recorded every 15 min for 96 h. This approach allows the quantification of the onset and kinetics of the cellular response. Experiments were repeated three times independently, using quadruplicate samples for each condition.

Statistical Analysis

Data is represented as the mean ± standard error of the mean (SEM), taken over ≥3 independent experiments, with ≥3 technical replicates per experiment, unless otherwise stated. Statistical significance was measured, using the *t*-test. The $p \leq 0.05$ was considered to be statistically significant.

RESULTS

We have recently established that compounds carrying a (TPP) moiety inhibit mitochondrial function and, therefore, reduce CSC propagation (24). More specifically, using an ATP (Adenosine Triphosphate) depletion assay as a surrogate marker of mitochondrial dysfunction, we identified, among 9 TPP-derivatives subjected to screening, the compound 2-butene-1,4-bis-TPP (b-TPP), as the most effective in inhibiting CSC propagation (IC-50 ∼ 500 nM) (24). The TPP moiety, which acts as a mitochondrial targeting signal (MTS), is chemically attached to a cargo molecule via a covalent bond. The intrinsic nature of the cargo molecule and its binding to the TPP structure may deeply influence the accumulation of the TPP-derivative in the mitochondria of living cells, thereafter impacting its overall biological function.

Herein, we characterized the metabolic and biological properties of dodecyl-TPP (d-TPP), establishing a combination strategy that efficiently targets the energetic cell machinery of CSCs to achieve their eradication.

d-TPP Inhibits CSC Propagation

Figure 1A shows the structure of d-TPP, which contains a long hydrophobic saturated aliphatic chain with 12 carbons, covalently-linked to a TPP moiety. **Figure 1B** shows the structure of b-TPP, which contains two TPP moieties. In contrast, note that d-TPP has only one TPP moiety.

Firstly, we performed the mammosphere formation assay as a read-out for CSC propagation, in the Estrogen Receptor (ER)-positive MCF-7 breast cancer cells, treated with increasing concentration of d-TPP. As shown in **Figure 1C**, treatment with d-TPP resulted in an 80% reduction in CSC activity at the highest concentrations tested (500 nM and 1 μM); a slight (20%), but significant reduction, in mammosphere formation was already observed at very low concentrations (50 and 100 nM). In a parallel analysis of CSC activity, d-TPP was more than twice as potent as b-TPP (**Figure 1C**). A similar inhibitory trend for CSC propagation was observed in the triple-negative breast cancer cells line MDA-MB-231 (**Figure 1D**).

Our previous study has indicated that certain TPP-derivatives may interfere with mitochondrial function in cancer cells, impairing their metabolic activity and ultimately leading to a reduction in cancer cell viability. Of interest, the actions of certain

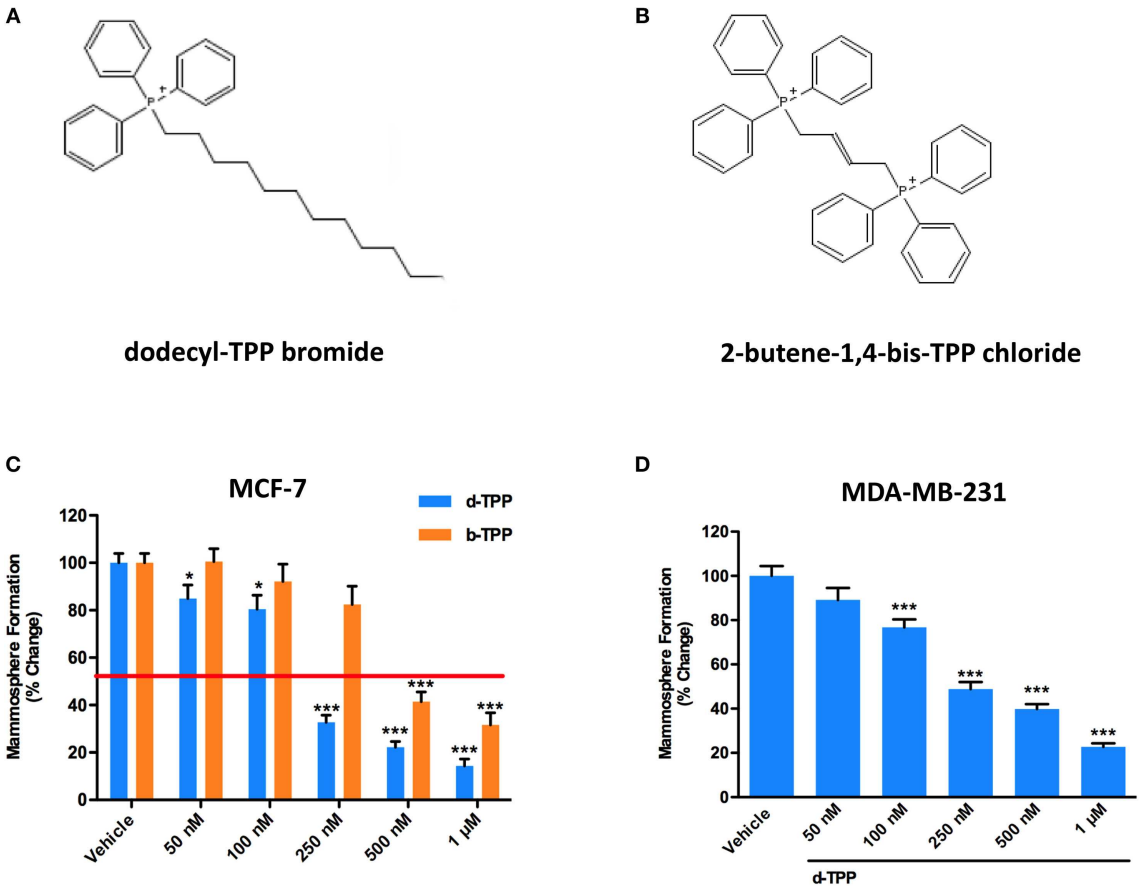

FIGURE 1 | d-TPP dose-dependently inhibits mammosphere formation in both ER(+) and triple-negative cell lines. **(A,B)** Structures of the TPP derivatives d-TPP (dodecyl-TPP) and b-TPP (2-butene-1,4-bis-TPP). **(C,D)** Differential inhibition of the mammosphere-forming activity of MCF-7 and MDA-MB-231 breast CSCs, after treatment with d-TPP (blue) and b-TPP (orange). Cells were treated for 5 days in mammosphere media with vehicle alone (DMSO) or increasing concentrations of the drugs (50 nM–1 μM). Note that d-TPP is approximately twice as potent as b-TPP in inhibiting mammosphere formation, with an IC-50 of approximately 250 nM. Data shown are the mean ± SEM of at least three independent experiments performed in triplicate. *$p < 0.05$; ***$p < 0.001$ indicates significance, all relative to the vehicle-alone treated cells.

TPP-compounds are selectively elicited on cancer cells, but not on normal cells (24). Thereafter, we tested the ability of d-TPP to decrease cell viability in MCF-7 breast cancer cells treated with increasing concentrations of d-TPP (from 50 nM to 1 μM), over different period of time (from 24 to 72 h). A similar experimental approach was used in normal human fibroblasts (hTERT-BJ1). As shown in **Figure 2**, d-TPP reduced MCF-7 cell viability in a time- and dose-dependent manner. The highest concentrations of the compound (250–500 nM and 1 μM), led to early reductions in cell viability (nearly 30%), which was evident already after 24 h of treatment. After 72 h of treatment, the reduction in cell viability was nearly 80% for the highest concentrations (250–500 nM and 1 μM) and a slight (nearly 30%) but significant inhibitory action was detected also at the lowest concentrations (50 and 100 nM).

On the other hand, in hTERT-BJ1 cells only the highest concentrations of the compound (250–500 nM and 1 μM) led to a reduction in cell viability, whereas the lowest concentrations (50 and 100 nM) showed little or no toxicity (**Figures 2B–F**). These results support the idea that d-TPP could be selectively used to target cancer cells, rather than normal cells, when used at low concentrations.

d-TPP Inhibits OXPHOS and Activates Glycolysis Toward the Acquisition of Metabolic Inflexibility

In cancer cells, the intrinsic ability to flexibly shift from one fuel source to another, according to the local availability, is a pre-requisite for abnormally high proliferation, cell survival, and metastatic dissemination to distant sites (26, 27, 29). Any pharmacological or metabolic approach aimed at compromising this flexibility in the energetic cancer cell machinery will negatively impact tumor progression [reviewed in (26)].

To understand the effects of d-TPP treatment on cancer cell metabolism, we performed metabolic flux analysis using the Seahorse XFe96. In MCF-7 cells, a dramatic reduction in (OCR) was observed after 24 h of treatment, with increasing concentrations of d-TPP (**Figure 3**). Basal mitochondrial

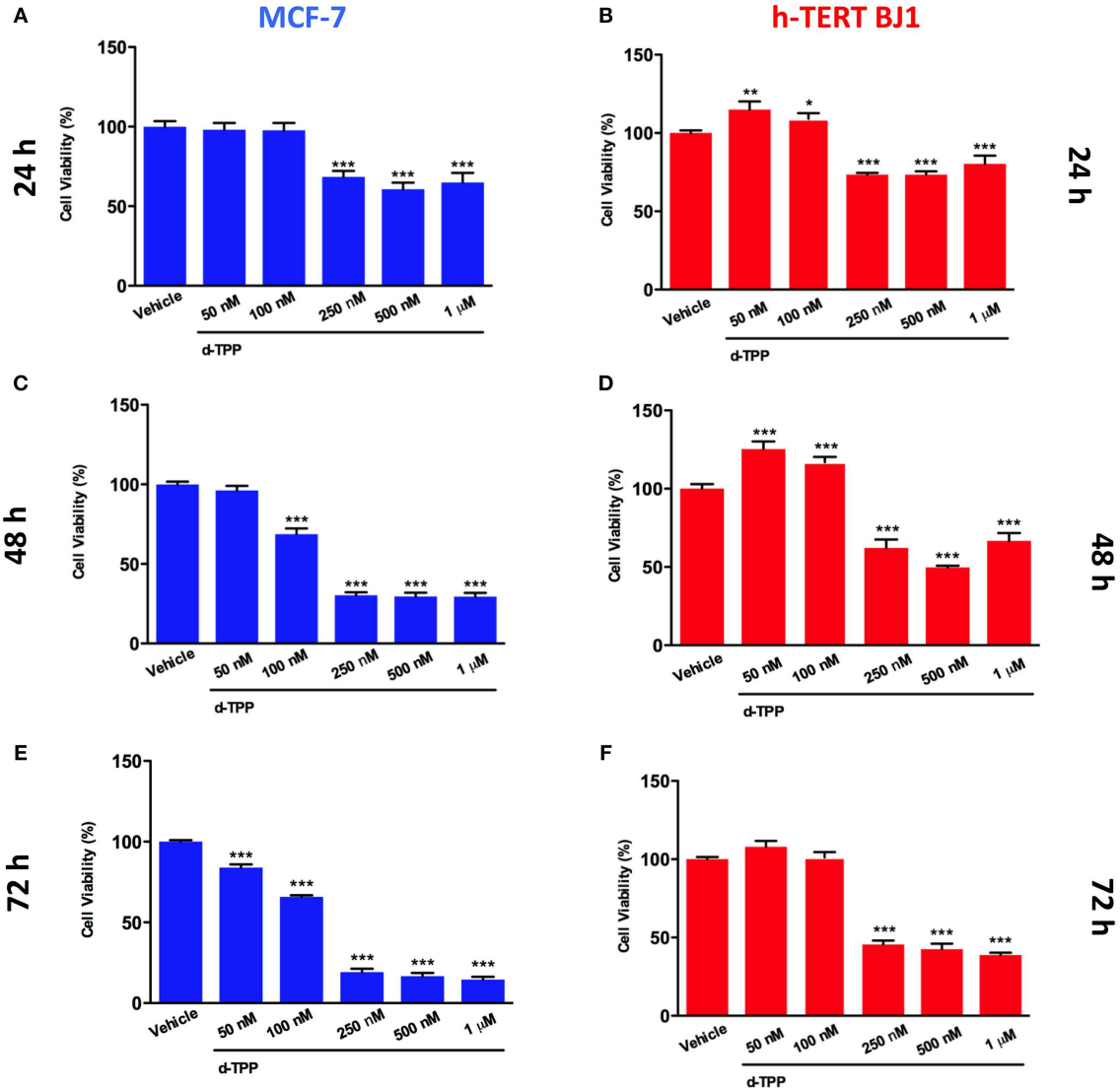

FIGURE 2 | Effects of d-TPP on cell viability. Evaluation of cell viability using the SBR assay in MCF-7 **(A,C,E)** and h-TERT BJ1 **(B,D,F)** cells treated with increasing concentrations of d-TPP (50 nM–1 μM) for 24, 48, and 72 h, as indicated. Data shown are the mean ± SEM of at least three independent experiments performed in triplicate. $^{*}p < 0.05$; $^{**}p < 0.01$; $^{***}p < 0.001$ indicates significance, all relative to the vehicle-alone treated cells.

respiration was reduced, with an IC-50 of ∼250 nM (the same concentration of the d-TPP necessary to halve CSC activity); likewise, ATP levels were also dose-dependently depleted.

Strikingly, the opposite trend was observed for glycolysis, which was substantially and dose-dependently increased, as indicated by the analysis of ECAR (extracellular acidification rate) in MCF-7 cells treated with d-TPP (**Figure 4**).

Taken together, these data indicate that d-TPP impairs mitochondrial function, thereafter compromising the ability to obtain ATP from oxidative phosphorylation. In order to cope with this stressful metabolic setting, cancer cells are forced toward a purely glycolytic phenotype, more strictly depending on glucose to fulfill their high energetic demands. In this scenario, the anti-mitochondrial effect elicited by d-TPP treatment serves as a functional metabolic synchronizer toward an obligated and inflexible glycolytic dependence.

Using d-TPP in a "Two-Hit" Metabolic Strategy to Potently Target CSCs Vulnerabilities

As we previously observed, this scenario of energetic inflexibility can be further exploited to metabolically weaken CSCs, by the addition of other metabolic stressors (23, 26). Therefore, we performed 3D mammosphere assays using d-TPP in combination with selected glycolysis and OXPHOS inhibitors, of both synthetic and natural origin, including two FDA approved drugs, as detailed below.

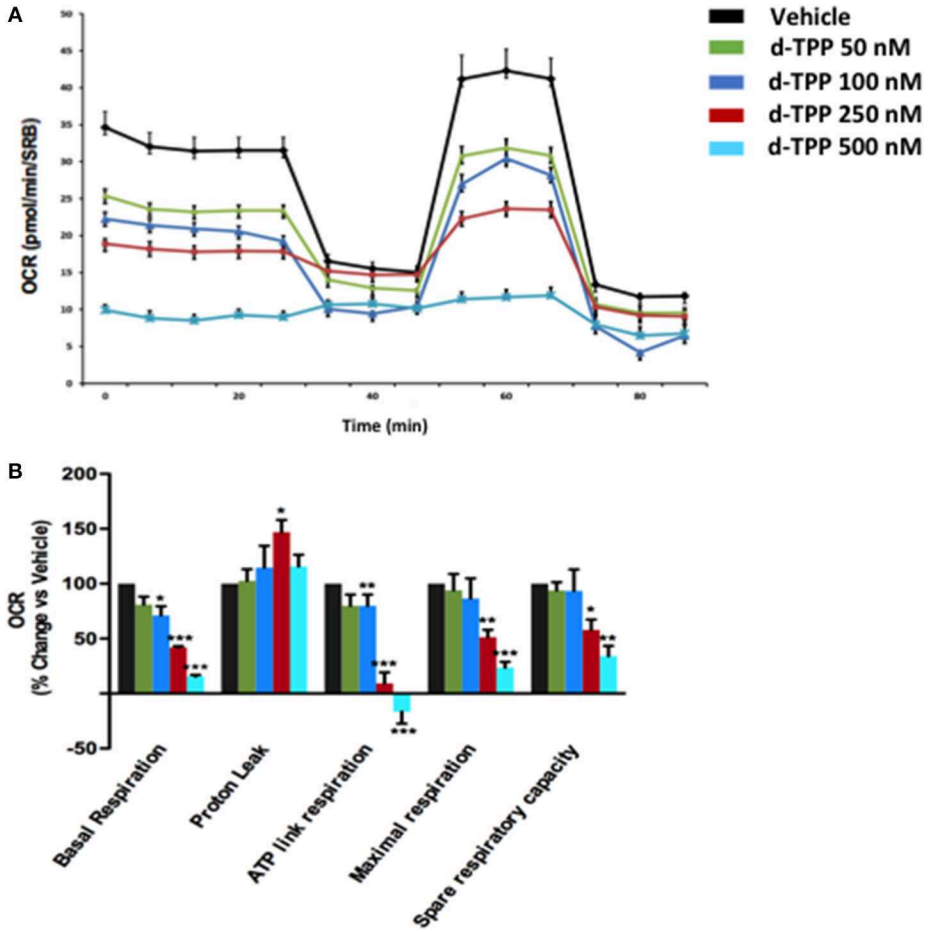

FIGURE 3 | Mitochondrial respiration is inhibited in MCF-7 cells treated with d-TPP. The metabolic profile of MCF-7 cells treated with increasing concentrations of d-TPP (50–500 nM) was assessed using the Seahorse XFe96 analyzer. **(A)** Representative tracings of metabolic flux. Dose-dependent significant reductions in basal respiration, maximal respiration, ATP levels, and spare respiratory capacity were observed **(B)**. Data shown are the mean ± SEM of 3 independent experiments performed in sextuplicate. $^{*}p < 0.05$; $^{**}p < 0.01$; $^{***}p < 0.001$ indicates significance, all relative to the vehicle-alone treated cells.

This drug combination strategy has been designed as a "two-hit" scheme, where the first metabolic hit is represented by d-TPP and the second metabolic hit is represented by either Vitamin C, 2-deoxy-glucose, Doxycycline, Niclosamide, or Berberine Chloride.

For this set of experiments, we selected a concentration of d-TPP equal to 100 nM, which is the dose of the chemical selectively toxic only to cancer cells, but not normal cells (**Figure 2**).

Of note, a natural (Vitamin C) as well as a synthetic (2-deoxy-glucose, 2-DG) glycolysis inhibitor were able to potentiate the inhibitory effect of d-TPP on CSC activity (**Figures 5A,B**). In particular, treatment with Vitamin C inhibited the propagation of CSCs by >50% at 250 μM and >70% at 500 μM, when used in combination with d-TPP (100 nM) (**Figure 5A**). Previously, we showed that the IC-50 for Vitamin C is 1 mM for MCF-7 CSC propagation (13). Therefore, treatment with d-TPP confers an approximate 4-fold increase in CSC sensitivity to Vitamin C.

The inhibitory effect of 2-DG was observed already at the concentration of 10 mM (which conferred a 2-fold increase in the inhibitory effect of d-TPP alone) and was more dramatic at 20 mM (almost completely suppressing CSC activity, with <10% residual mammosphere formation capability) (**Figure 5B**).

Next, we used two FDA-approved drugs, namely Doxycycline and Niclosamide, as well as the natural compound Berberine, all known to behave as OXPHOS inhibitors (11, 20, 30). This strategy is based on the assumption that in cancer cells weakened by d-TPP treatment, an additional metabolic mitochondrial stressor may help to eradicate the residual CSC population.

As shown in **Figure 5C**, low doses of the antibiotic Doxycycline (10 μM), which is known to impair mitochondrial biogenesis and function, were sufficient to double the efficacy of d-TPP on CSC activity; this effect was potentiated in the presence of 30 μM Doxycyline. Interestingly, the anti-tapeworm drug Niclosamide, which inhibits OXPHOS, increased the efficacy of d-TPP on CSC activity by nearly 2-fold at 250 nM and by nearly 3-fold at 500 nM (**Figure 5D**).

Finally, we used the natural compound and OXPHOS inhibitor Berberine, the main alkaloid extracted from Coptidis

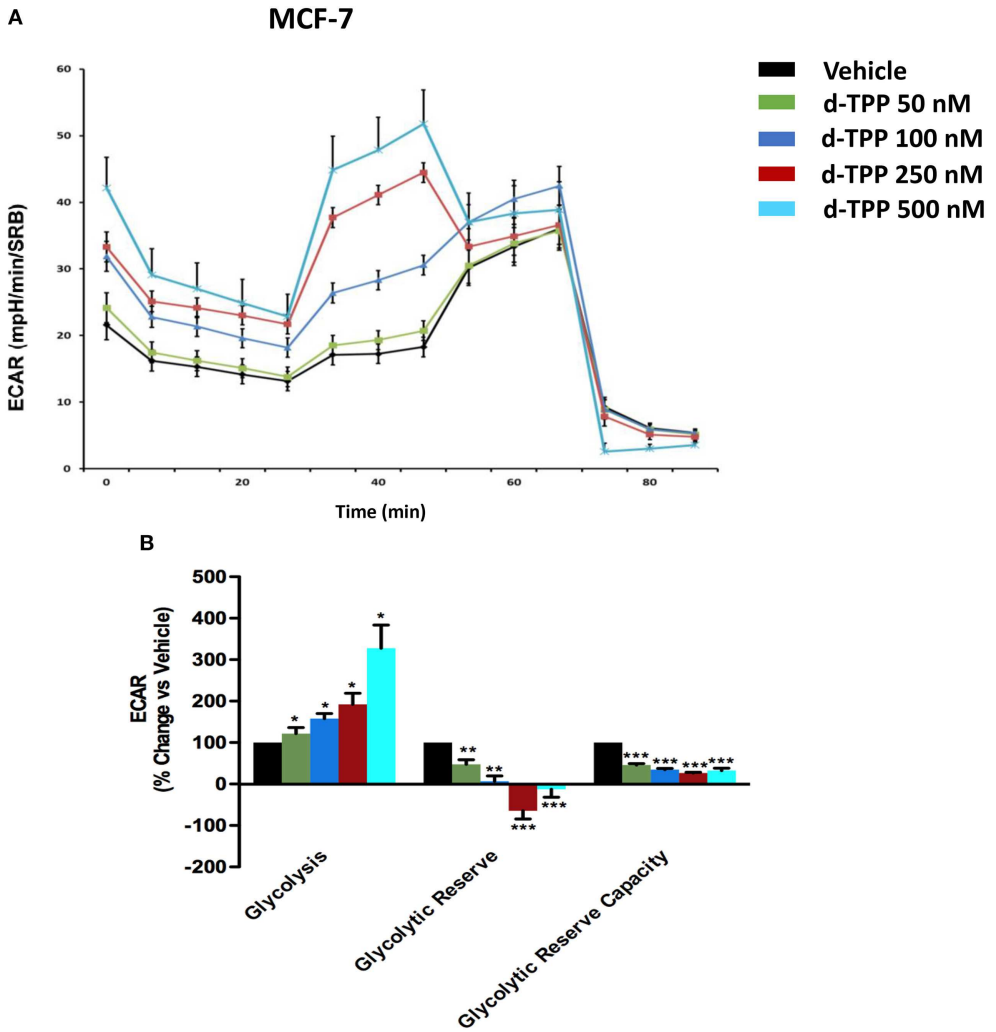

FIGURE 4 | Glycolysis is increased in MCF-7 cells treated with d-TPP. The metabolic profile of MCF-7 cells treated with increasing concentrations of d-TPP (50 nM to 500 nM) was assessed using the Seahorse XFe96 analyzer. **(A)** Representative tracings of metabolic flux. **(B)** Dose-dependent significant increases in glycolysis and decreases in glycolytic reserve, as well as glycolytic reserve capacity, were observed. Data shown are the mean ± SEM of three independent experiments performed in sextuplicate. $^{*}p < 0.05$; $^{**}p < 0.01$; $^{***}p < 0.001$ indicates significance, all relative to the vehicle-alone treated cells.

rhizoma (Coptis chinensis Franch) and Phellodendri cortex (Phellodendron amurense Ruprecht), with known anti-malarial, anti-inflammatory and antibiotic activity (31). At the highest concentration tested (10 μM), Berberine inhibited CSC formation by >80% thereafter increasing the efficacy of d-TPP by almost 5-fold, nevertheless Berberine's action was evident already at 1 μM (**Figure 5E**).

Taken together, these findings suggest that a mitochondrial-impairing agent like d-TPP compromises the normal functioning of the energetic cancer cell machinery, thus significantly narrowing the possibility to flexibly use alternate fuels and metabolic pathways. This has a negative impact on CSC biology and propagation, as well as cancer cell viability and proliferation. The kinetics of d-TPP action on the proliferation of adherent MCF-7 cells was independently evaluated using the xCELLigence system that allows the real-time, label-free, monitoring of cell health and behavior, by measuring electrical impedance, whose magnitude is strictly dependent on the number of cells.

As shown in **Figure 6**, the effects of d-TPP on MCF-7 cells are dose- and time-dependent, with a trend toward reduced cell number after 72 h of treatment, even with the lowest dose tested (50 nM d-TPP). At higher doses (100 nM), a major cytostatic effect was detected, whereas clear cytotoxicity was observed at the concentration of 250 nM.

DISCUSSION

In this report, we provide solid evidence to validate the use of an integrated metabolic strategy to eradicate CSCs. More specifically, we demonstrate that in breast cancer cells the

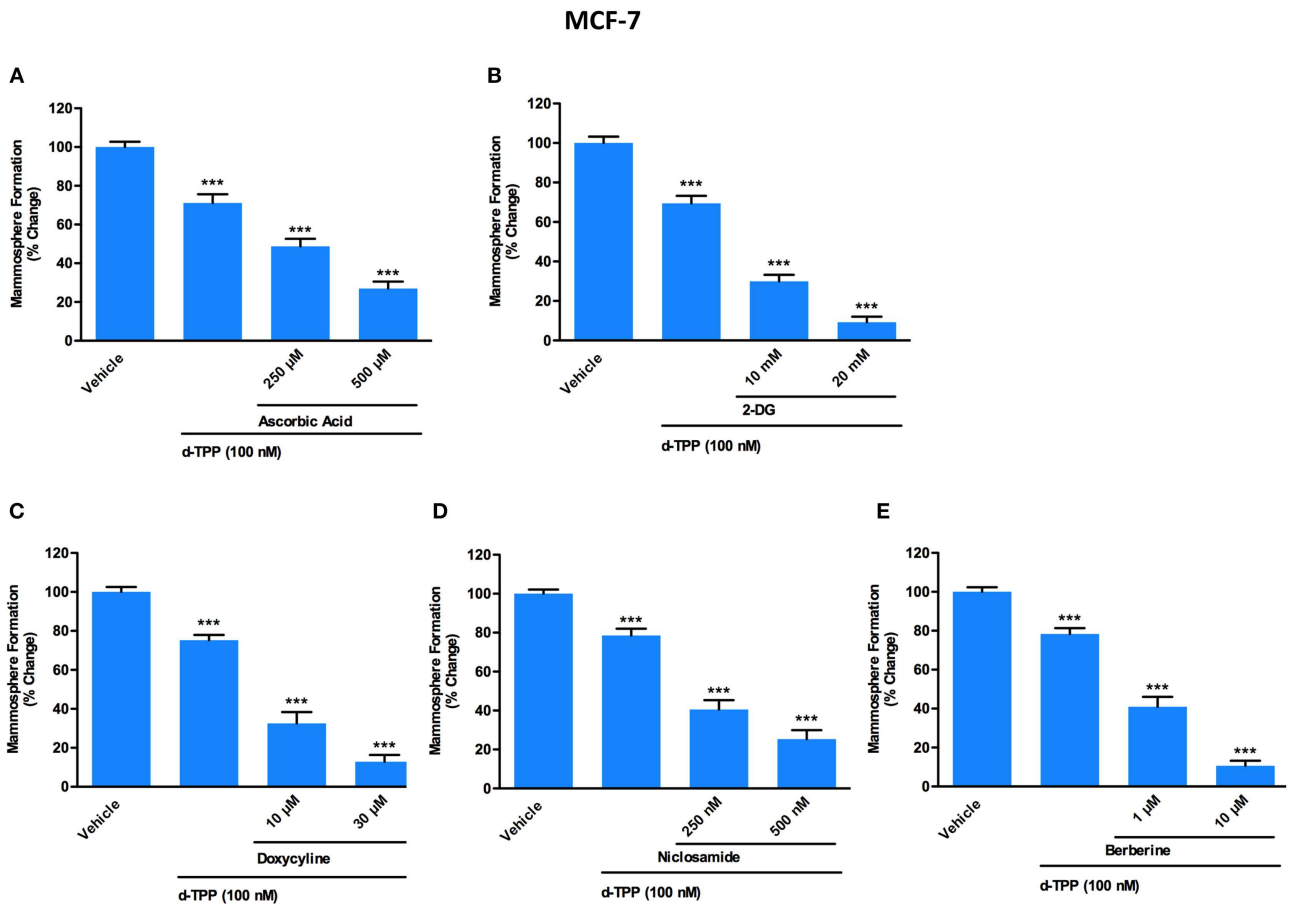

FIGURE 5 | A panel of clinically-approved drugs, natural compounds and synthetic chemicals, interfering with cell metabolism, potentiates d-TPP effects on mammosphere formation. Evaluation of mammosphere formation in MCF-7 cells cultured in low attachment plates and treated with Vehicle or d-TPP (100 nM), alone or in combination with the glycolysis inhibitors Ascorbic Acid (250 and 500 μM) **(A)**, 2-deoxy-glucose (2-DG) (10 and 20 mM) **(B)**; the OXPHOS inhibitors Doxycycline (10 and 30 μM) **(C)**, Niclosamide (250 and 500 nM) **(D)**, and Berberine (1 and 10 μM) **(E)**. Data shown are the mean ± SEM of at least three independent experiments performed in triplicate ***$p < 0.001$ indicates significance, all relative to the vehicle-alone treated cells.

compound d-TPP, which carries a mitochondria-targeting (TPP) motif, inhibits mitochondrial function, conferring a dose and time-dependent reduction in cell viability, as well as inhibiting the formation of 3D mammospheres, assayed as a read-out for CSC activity. Quantitatively similar results were obtained with both ER(+) [MCF7] and Triple Negative [MDA-MB-231] cell lines.

The analysis of metabolic flux revealed that d-TPP potently inhibits mitochondrial basal respiration, as well as ATP production, thereby providing a rational for the reduced functional capability observed in response to the treatment. As a consequence, d-TPP-treated breast cancer cells preferentially exhibit a glycolytic phenotype, which allows them to cope with the anti-mitochondrial effects elicited by d-TPP. Despite the acquisition of this compensatory glycolytic phenotype, d-TPP treatment weakens CSCs, rendering them more sensitive to the action of a second metabolic inhibitor, as evidenced using the glycolysis inhibitors Vitamin C and 2-DG, as well as the OXPHOS inhibitors Doxycycline, Niclosamide, and Berberine. Thus, functional validation of this approach is evidenced by the almost complete loss of CSCs activity in MCF-7 cells, simultaneously treated with d-TPP in the presence of other energetic inhibitors.

Inter- and intra-tumor heterogeneity is one of the main factors accounting for tumor progression and therapy failure (32). CSCs originate and drive such heterogeneity, due to their ability to give rise to a hierarchically differentiated progeny, which contributes toward the generation of a full repertoire of cell types within the tumor mass (33, 34). As a consequence, pharmacological strategies aimed at identifying, and selectively targeting CSCs are among the most promising, though challenging, therapeutic approaches (8, 26, 35, 36). Diverse theories have been proposed for the explanation of the origin of CSCs. According to the so-called "metabo-stemness" model, certain metabolic phenotypes may dictate the stemness properties of tumors, suggesting that specific metabolic dynamics may drive the *de novo* acquisition of stem cell traits in non-cancer or differentiated cancer cells (37, 38). Likewise, onco-metabolism has been included among the hallmarks of cancer (39). On the basis of these observations, it's not surprising that cancer metabolism has been regarded

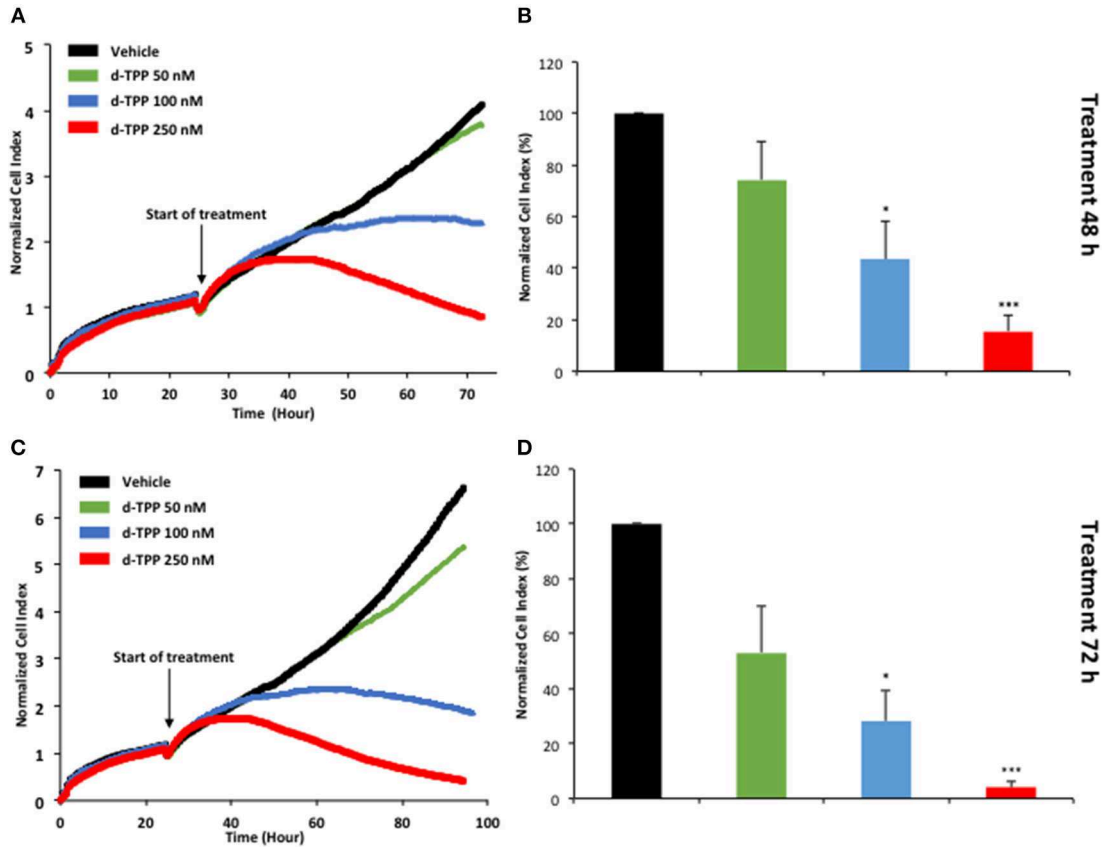

FIGURE 6 | Real-time profiling of cell viability using the xCELLigence system. The xCELLigence system allows for the real-time, label-free, monitoring of cell health, and behavior, via high frequency measurement of cell-induced electrical impedance. Five-thousand MCF-7 cells were seeded in a 16-well E-plate. Twenty-four hours after seeding, cells were treated with increasing concentrations of d-TPP (50–250 nM) for further 72 h. **(A,C)** Representative cell tracings of the impedance profile indicating the normalized cell index is shown at 48 h **(A)** and 72 h **(C)**. **(B,D)** The graphs show cell index values, normalized at the time of d-TPP stimulation, reached after 48 **(B)** or 72 h **(D)** of d-TPP treatment. Data shown are the mean ± SEM of at least three independent experiments performed in triplicate. $^{*}p < 0.05$; $^{***}p < 0.001$ indicates significance, all relative to the vehicle-alone treated cells.

as an opportunity to selectively target CSCs (26, 40). In this regard, our laboratory and others have demonstrated that CSCs across diverse tumor types show peculiar metabolic features, for instance an increased capacity for OXPHOS, elevated mitochondrial biogenesis, as well as higher mitochondrial mass, compared to the non-stem or "bulk" cancer cell population [reviewed in (26)]. Corroborating these findings, cancer cells with higher telomerase ($hTERT^{high}$) activity and therefore higher immortality features, exhibit an increased mitochondrial mass, compared to their $hTERT^{low}$ counterparts (41, 42). Furthermore, a metabolic rewiring due to mitochondrial dysfunction has been shown to inhibit cancer cell proliferation, encourage cell differentiation and halt tumor growth *in vivo* (43, 44).

Clearly these observations suggest that mitochondrial-impairing agents could be used to specifically inhibit the CSC population, paving the way for the identification of chemical strategies aimed at selectively targeting mitochondria in CSCs (4, 17, 18, 45, 46). In this regard, the covalent linkage of a compound to a (TPP) cation represents a well-established method to deliver probes and imaging agents to mitochondria (47). TPP^{+} lipophilic cations may serve as very efficient chemical "vehicles" to transport small molecules to the mitochondria. In addition, their chemical synthesis is easily achievable, and the degree of accumulation in the mitochondria is elevated, because of the chemical attraction between the positively charged TPP-cation and the negative membrane potential of the mitochondrial inner membrane (47). This peculiar chemical structure would also explain at least some of the biochemical effects induced by TPP-derivatives, like the dissipation of the mitochondrial membrane potential, together with the inhibition of the respiratory chain complexes (48). Recently, we have demonstrated that the compound 2-butene-1,4-bis-TPP impairs mitochondrial metabolic function leading to the inhibition of breast CSC activity (24). The TPP-based compound tested in the current study, namely dodecyl-TPP, is at least twice as potent as b-TPP in inhibiting CSC propagation (see **Figure 1C**). Also, d-TPP targets the bulk of cancer cells, resulting in a time-dependent reduction in their viability. According to our data, it is conceivable to hypothesize that after short time treatment with d-TPP (24h), cells would have enough metabolic reserves to cope with the metabolic stress induced by the treatment; whereas upon stimulation with d-TPP for longer time (48–72 h), no spare

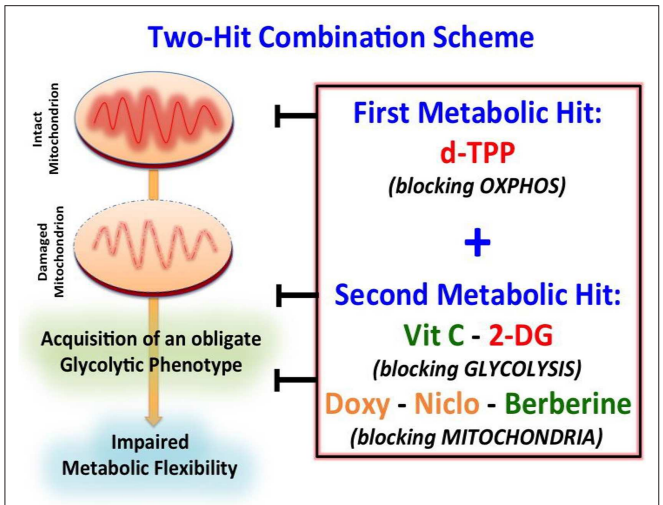

FIGURE 7 | Schematic diagram showing the proposed "two-hit" metabolic strategy for eradicating CSCs. Our results suggest that CSCs may be more efficiently eradicated by using a "two-hit" metabolic strategy based on the use of a first metabolic inhibitor (i.e., d-TPP), which would weaken CSCs and their energetic machinery. The starved residual CSC population would be more sensitive to the detrimental effects of a second metabolic inhibitor (i.e., Vitamin C, Berberine, Doxycycline, Niclosamide, 2-Deoxy-Glucose). **Green**: Natural Compounds; **Orange**: FDA-approved Drugs; **Red**: Synthetic drugs.

metabolic fuels would be progressively available for cancer cells to survive. On the other hand, the compound has limited toxicity effect on normal fibroblasts. One of the possible explanations of this effect is that in cancer cells and CSCs, the mitochondrial membrane potential is higher than in normal cells, and this could account for the differential effects observed.

As such, TPP-based strategies would therefore be able to distinguish between "normal" and "malignant" mitochondria, mainly on the basis of the intrinsic chemical-physical characteristics of these organelles in health and disease. Of note, d-TPP treatment caused a shift in energetic metabolism toward the activation of the glycolytic pathway, which very likely represents a compensatory response to the anti-mitochondrial effects elicited by d-TPP.

This metabolic shift has unveiled a strict dependency of cancer cells on glycolysis after d-TPP treatment, immediately suggesting the use of a second metabolic (glycolysis or OXPHOS) inhibitor to further "starve" the residual CSCs population. This two-hit metabolic strategy had already been implemented and validated in our previous study (23). This approach is based on the use of a first metabolic inhibitor (for instance a mitochondrial-impairing agent) that serves as a first-hit, followed by the use of a second metabolic inhibitor (for instance a glycolysis or an OXPHOS inhibitor) that acts as a second-hit (**Figure 7**). For example, we have previously demonstrated that: (i) the antibiotic Doxycycline, acting as a mitochondrial inhibitor, impairs CSCs activity; (ii) that prolonged treatment with Doxycycline turns on the glycolytic pathway, in response to the mitochondrial dysfunction; and (iii) the use of a glycolysis inhibitor, such as Vitamin C, in combination with Doxycycline completely eradicates CSCs. These findings indicate that a combination of Doxycycline plus Vitamin C might conceivably represent a safe approach for the clinical management of cancer patients. Indeed, at biologically active concentrations Doxycycline has a very manageable spectrum of side effects, whereas Vitamin C has potentially no side effects, being used as additive to a number of preparations. Adding to this, data coming from meta-analysis of 21 published studies, as well as pre-clinical investigations have demonstrated that oral doses of vitamin C reduce cancer risk, overall mortality and disease-specific mortality in lung and breast cancer (49–52); furthermore, a 1-week oral administration of ascorbate, performed before cell inoculation, significantly decreased tumor development in a lymphoma xenograft model (53).

Clinical validation of these findings, at least for Doxycycline, has been provided in our recent pilot study, where we enrolled early breast cancer patients for a short-term (14-day) pre-operative Doxycycline administration. Notably, the analysis of post-operative vs. pre-operative breast tumor specimens showed a selective reduction in the stem markers, namely CD44 and ALDH1, in the patients receiving Doxycycline compared with controls. This provides exciting clinical evidence that mitochondrial-targeting strategies may be used to efficiently halt CSC propagation in cancer patients; nevertheless, additional studies are still necessary to investigate the action of Doxycycline together with Vitamin C, in breast cancer patients.

The data herein presented further validate the use of a metabolic "Two-Hit" approach to manipulate cancer cell metabolism, turning the metabolic plasticity of CSCs into an obligate metabolic inflexibility, which would be used to more efficiently eradicate CSCs. The potential of d-TPP to act as a safe driver of such a metabolic shift paves the way for further investigating the role of this compound in cancer biology and bioenergetics. However, further studies are still warranted to support the use of TPP-based compounds in combination with other metabolic inhibitors, as an add-on to conventional chemotherapy.

DATA AVAILABILITY

All datasets generated for this study are included in the manuscript/supplementary files.

AUTHOR CONTRIBUTIONS

ML and FS conceived and initiated this project. All experiments described in this paper were performed by ED and BÓ. More specifically, BÓ performed experiments of cell kinetics evaluation using the xCELLigence system. ED analyzed the data, generated the final figures, and wrote the first draft of the paper, which was then further edited by ML, FS, and BÓ.

FUNDING

This work was supported by research grant funding, provided by Lunella Biotech, Inc., (to FS and ML).

ACKNOWLEDGMENTS

We are grateful to Rumana Rafiq, for her kind and dedicated assistance, in keeping the Translational Medicine Laboratory at Salford running very smoothly. We would like to thank the Foxpoint Foundation and the Healthy Life Foundation for their philanthropic donations toward new equipment and infrastructure, in the Translational Medicine Laboratory, at the University of Salford.

REFERENCES

1. Zhu J, Thompson CB. Metabolic regulation of cell growth and proliferation. *Nat Rev Mol Cell Biol*. (2019) 20:436–50. doi: 10.1038/s41580-019-0123-5
2. Pavlova NN, Thompson CB. The emerging hallmarks of cancer metabolism. *Cell Metabol*. (2016) 23:27–47. doi: 10.1016/j.cmet.2015.12.006
3. Vyas S, Zaganjor E, Haigis MC. Mitochondria and cancer. *Cell*. (2016) 166:555–66. doi: 10.1016/j.cell.2016.07.002
4. Shin M-K, Cheong J-H. Mitochondria-centric bioenergetic characteristics in cancer stem-like cells. *Arch Pharm Res*. (2019) 42:113–27. doi: 10.1007/s12272-019-01127-y
5. Altieri DC. Mitochondrial dynamics and metastasis. *Cell Mol Life Sci*. (2019) 76:827–35. doi: 10.1007/s00018-018-2961-2
6. Peiris-Pagès M, Bonuccelli G, Sotgia F, Lisanti MP. Mitochondrial fission as a driver of stemness in tumor cells: mDIVI1 inhibits mitochondrial function, cell migration and cancer stem cell (CSC) signalling. *Oncotarget*. (2018) 9:13254–75. doi: 10.18632/oncotarget.24285
7. Peiris-Pagès M, Martinez-Outschoorn UE, Pestell RG, Sotgia F, Lisanti MP. Cancer stem cell metabolism. *Breast Cancer Res*. (2016) 18:55. doi: 10.1186/s13058-016-0712-6
8. Clevers H. The cancer stem cell: premises, promises and challenges. *Nat Med*. (2011) 17:313–9. doi: 10.1038/nm.2304
9. Batlle E, Clevers H. Cancer stem cells revisited. *Nat Med*. (2017) 23:1124–34. doi: 10.1038/nm.4409
10. Farnie G, Sotgia F, Lisanti MP. High mitochondrial mass identifies a sub-population of stem-like cancer cells that are chemo-resistant. *Oncotarget*. (2015) 6:30472–86. doi: 10.18632/oncotarget.5401
11. De Luca A, Fiorillo M, Peiris-Pagès M, Ozsvari B, Smith DL, Sanchez-Alvarez R, et al. Mitochondrial biogenesis is required for the anchorage-independent survival and propagation of stem-like cancer cells. *Oncotarget*. (2015) 6:14777–95. doi: 10.18632/oncotarget.4401
12. Lamb R, Bonuccelli G, Ozsvári B, Peiris-Pagès M, Fiorillo M, Smith DL, et al. Mitochondrial mass, a new metabolic biomarker for stem-like cancer cells: understanding WNT/FGF-driven anabolic signaling. *Oncotarget*. (2015) 6:30453–71. doi: 10.18632/oncotarget.5852
13. Bonuccelli G, De Francesco EM, de Boer R, Tanowitz HB, Lisanti MP. NADH autofluorescence, a new metabolic biomarker for cancer stem cells: identification of Vitamin C and CAPE as natural products targeting "stemness." *Oncotarget*. (2017) 8:20667–78. doi: 10.18632/oncotarget.15400
14. Katajisto P, Dohla J, Chaffer CL, Pentinmikko N, Marjanovic N, Iqbal S, et al. Asymmetric apportioning of aged mitochondria between daughter cells is required for stemness. *Science*. (2015) 348:340–3. doi: 10.1126/science.1260384
15. Sotgia F, Ozsvari B, Fiorillo M, De Francesco EM, Bonuccelli G, Lisanti MP. A mitochondrial based oncology platform for targeting cancer stem cells (CSCs): MITO-ONC-RX. *Cell Cycle*. (2018) 17:2091–100. doi: 10.1080/15384101.2018.1515551
16. Skoda J, Borankova K, Jansson PJ, Huang ML-H, Veselska R, Richardson DR. Pharmacological targeting of mitochondria in cancer stem cells: an ancient organelle at the crossroad of novel anti-cancer therapies. *Pharmacol Res*. (2019) 139:298–313. doi: 10.1016/j.phrs.2018.11.020
17. Ozsvari B, Sotgia F, Simmons K, Trowbridge R, Foster R, Lisanti MP. Mitoketoscins: novel mitochondrial inhibitors for targeting ketone metabolism in cancer stem cells (CSCs). *Oncotarget*. (2017) 8:78340–50. doi: 10.18632/oncotarget.21259
18. Ozsvari B, Fiorillo M, Bonuccelli G, Cappello AR, Frattaruolo L, Sotgia F, et al. Mitoriboscins: mitochondrial-based therapeutics targeting cancer stem cells (CSCs), bacteria and pathogenic yeast. *Oncotarget*. (2017) 8:67457–72. doi: 10.18632/oncotarget.19084
19. Peiris-Pagès M, Sotgia F, Lisanti MP. Doxycycline and therapeutic targeting of the DNA damage response in cancer cells: old drug, new purpose. *Oncoscience*. (2015) 2:696–9. doi: 10.18632/oncoscience.215
20. Lamb R, Fiorillo M, Chadwick A, Ozsvari B, Reeves KJ, Smith DL, et al. Doxycycline down-regulates DNA-PK and radiosensitizes tumor initiating cells: implications for more effective radiation therapy. *Oncotarget*. (2015) 6:14005–25. doi: 10.18632/oncotarget.4159
21. Scatena C, Roncella M, Di Paolo A, Aretini P, Menicagli M, Fanelli G, et al. Doxycycline, an inhibitor of mitochondrial biogenesis, effectively reduces Cancer Stem Cells (CSCs) in early breast cancer patients: a clinical pilot study. *Front Oncol*. (2018) 8:452. doi: 10.3389/fonc.2018.00452
22. De Francesco EM, Maggiolini M, Tanowitz HB, Sotgia F, Lisanti MP. Targeting hypoxic cancer stem cells (CSCs) with doxycycline: implications for optimizing anti-angiogenic therapy. *Oncotarget*. (2017) 8:56126–42. doi: 10.18632/oncotarget.18445
23. De Francesco EM, Bonuccelli G, Maggiolini M, Sotgia F, Lisanti MP. Vitamin C and Doxycycline: a synthetic lethal combination therapy targeting metabolic flexibility in cancer stem cells (CSCs). *Oncotarget*. (2017) 8:67269–86. doi: 10.18632/oncotarget.18428
24. Ozsvari B, Sotgia F, Lisanti MP. Exploiting mitochondrial targeting signal(s), TPP and bis-TPP, for eradicating cancer stem cells (CSCs). *Aging*. (2018) 10:229–40. doi: 10.18632/aging.101384
25. Dickerson T, Jauregui CE, Teng Y. Friend or foe? Mitochondria as a pharmacological target in cancer treatment. *Future Med Chem*. (2017) 9:2197–210. doi: 10.4155/fmc-2017-0110
26. De Francesco EM, Sotgia F, Lisanti MP. Cancer stem cells (CSCs): metabolic strategies for their identification and eradication. *Biochem J*. (2018) 475:1611–34. doi: 10.1042/BCJ20170164
27. Krstic J, Trivanovic D, Jaukovic A, Santibanez JF, Bugarski D. Metabolic plasticity of stem cells and macrophages in cancer. *Front Immunol*. (2017) 8:939. doi: 10.3389/fimmu.2017.00939
28. Shaw FL, Harrison H, Spence K, Ablett MP, Simões BM, Farnie G, et al. A detailed mammosphere assay protocol for the quantification of breast stem cell activity. *J Mammary Gland Biol Neoplasia*. (2012) 17:111–7. doi: 10.1007/s10911-012-9255-3
29. Nakajima EC, Van Houten B. Metabolic symbiosis in cancer: refocusing the Warburg lens. *Mol Carcinog*. (2013) 52:329–37. doi: 10.1002/mc.21863
30. Turner N, Li J-Y, Gosby A, To SWC, Cheng Z, Miyoshi H, et al. Berberine and its more biologically available derivative, dihydroberberine, inhibit mitochondrial respiratory complex I: a mechanism for the action of berberine to activate AMP-activated protein kinase and improve insulin action. *Diabetes*. (2008) 57:1414–8. doi: 10.2337/db07-1552
31. Liu D, Meng X, Wu D, Qiu Z, Luo H. A natural isoquinoline alkaloid with antitumor activity: studies of the biological activities of berberine. *Front Pharmacol*. (2019) 10:9. doi: 10.3389/fphar.2019.00009
32. Meacham CE, Morrison SJ. Tumour heterogeneity and cancer cell plasticity. *Nature*. (2013) 501:328–37. doi: 10.1038/nature12624
33. Prasetyanti PR, Medema JP. Intra-tumor heterogeneity from a cancer stem cell perspective. *Mol Cancer*. (2017) 16:41. doi: 10.1186/s12943-017-0600-4
34. Visvader JE. Cells of origin in cancer. *Nature*. (2011) 469:314–22. doi: 10.1038/nature09781
35. Apostoli AJ, Ailles L. Clonal evolution and tumor-initiating cells: new dimensions in cancer patient treatment. *Crit Rev Clin Lab Sci*. (2016) 53:40–51. doi: 10.3109/10408363.2015.1083944
36. Dawood S, Austin L, Cristofanilli M. Cancer stem cells: implications for cancer therapy. *Oncology*. (2014) 28:1101–7, 1110.
37. Menendez JA, Alarcón T. Metabostemness: a new cancer hallmark. *Front Oncol*. (2014) 4:262. doi: 10.3389/fonc.2014.00262

38. Menendez JA. The metaboloepigenetic dimension of cancer stem cells: evaluating the market potential for new metabostemness-targeting oncology drugs. *Curr Pharm Des*. (2015) 21:3644–53. doi: 10.2174/1381612821666150710150327
39. Hanahan D, Weinberg RA. Hallmarks of cancer: the next generation. *Cell*. (2011) 144:646–74. doi: 10.1016/j.cell.2011.02.013
40. Jagust P, de Luxán-Delgado B, Parejo-Alonso B, Sancho P. Metabolism-based therapeutic strategies targeting cancer stem cells. *Front Pharmacol*. (2019) 10:203. doi: 10.3389/fphar.2019.00203
41. Lamb R, Ozsvari B, Bonuccelli G, Smith DL, Pestell RG, Martinez-Outschoorn UE, et al. Dissecting tumor metabolic heterogeneity: telomerase and large cell size metabolically define a sub-population of stem-like, mitochondrial-rich, cancer cells. *Oncotarget*. (2015) 6:21892–905. doi: 10.18632/oncotarget.5260
42. Bonuccelli G, Peiris-Pages M, Ozsvari B, Martinez-Outschoorn UE, Sotgia F, Lisanti MP. Targeting cancer stem cell propagation with palbociclib, a CDK4/6 inhibitor: telomerase drives tumor cell heterogeneity. *Oncotarget*. (2017) 8:9868–84. doi: 10.18632/oncotarget.14196
43. Arif T, Amsalem Z, Shoshan-Barmatz V. Metabolic reprograming via silencing of mitochondrial VDAC1 expression encourages differentiation of cancer cells. *Mol Ther Nucleic Acids*. (2019) 17:24–37. doi: 10.1016/j.omtn.2019.05.003
44. Arif T, Paul A, Krelin Y, Shteinfer-Kuzmine A, Shoshan-Barmatz V. Mitochondrial VDAC1 silencing leads to metabolic rewiring and the reprogramming of tumour cells into advanced differentiated states. *Cancers (Basel)*. (2018) 10. doi: 10.3390/cancers10120499
45. Zhu Y, Dean AE, Horikoshi N, Heer C, Spitz DR, Gius D. Emerging evidence for targeting mitochondrial metabolic dysfunction in cancer therapy. *J Clin Invest*. (2018) 128:3682–91. doi: 10.1172/JCI120844
46. Lamb R, Harrison H, Hulit J, Smith DL, Lisanti MP, Sotgia F. Mitochondria as new therapeutic targets for eradicating cancer stem cells: quantitative proteomics and functional validation via MCT1/2 inhibition. *Oncotarget*. (2014) 5:11029–37. doi: 10.18632/oncotarget.2789
47. Zielonka J, Joseph J, Sikora A, Hardy M, Ouari O, Vasquez-Vivar J, et al. Mitochondria-targeted triphenylphosphonium-basedcompounds: syntheses, mechanisms of action, and therapeutic and diagnostic applications. *Chem Rev*. (2017) 117:10043–120. doi: 10.1021/acs.chemrev.7b00042
48. Trnka J, Elkalaf M, Anděl M. Lipophilic triphenylphosphonium cations inhibit mitochondrial electron transport chain and induce mitochondrial proton leak. *PLoS One*. (2015) 10:e0121837. doi: 10.1371/journal.pone.0121837
49. Luo J, Shen L, Zheng D. Association between vitamin C intake and lung cancer: a dose-response meta-analysis. *Sci Rep*. (2014) 4:6161. doi: 10.1038/srep06161
50. Harris HR, Orsini N, Wolk A. Vitamin C and survival among women with breast cancer: a meta-analysis. *Eur J Cancer*. (2014) 50:1223–31. doi: 10.1016/j.ejca.2014.02.013
51. Harris HR, Bergkvist L, Wolk A. Vitamin C intake and breast cancer mortality in a cohort of Swedish women. *Br J Cancer*. (2013) 109:257–64. doi: 10.1038/bjc.2013.269
52. Ngo B, Van Riper JM, Cantley LC, Yun J. Targeting cancer vulnerabilities with high-dose vitamin C. *Nat Rev Cancer*. (2019) 9:271–82. doi: 10.1038/s41568-019-0135-7
53. Gao P, Zhang H, Dinavahi R, Li F, Xiang Y, Raman V, et al. HIF-dependent antitumorigenic effect of antioxidants *in vivo*. *Cancer Cell*. (2007) 12:230–8. doi: 10.1016/j.ccr.2007.08.004

Conflict of Interest Statement: ML and FS hold a minority interest in Lunella Biotech, Inc.

The remaining authors declare that the research was conducted in the absence of any commercial or financial relationships that could be construed as a potential conflict of interest.

frontiers in Oncology

CASE REPORT
published: 05 May 2020
doi: 10.3389/fonc.2020.00578

Managing Metastatic Thymoma With Metabolic and Medical Therapy: A Case Report

Matthew C. L. Phillips[1], Deborah K. J. Murtagh[2], Sanjay K. Sinha[3] and Ben G. Moon[4]*

[1] Department of Neurology, Waikato Hospital, Hamilton, New Zealand, [2] Healthy Kitchen Christchurch Ltd., Hamilton, New Zealand, [3] Department of Pathology, Waikato Hospital, Hamilton, New Zealand, [4] Department of Radiology, Waikato Hospital, Hamilton, New Zealand

Thymomas consist of neoplastic thymic cells intermixed with variable numbers of non-neoplastic lymphocytes. Metastatic thymomas are typically managed with non-curative chemotherapy to control tumor-related symptoms; no prolonged survival is expected. Metabolic-based approaches, such as fasting and ketogenic diets, target cancer cell metabolism by creating an increased reliance on ketones while decreasing glucose, glutamine, and growth factor availability, theoretically depriving cancer cells of their metabolic fuels while creating an unfavorable environment for cancer growth, which may be beneficial in metastatic thymoma. We report the case of a 37-year-old woman with myasthenia gravis, diagnosed with an inoperable type AB, stage IVA thymoma, who pursued a metabolic intervention consisting of periodic fasting (7-day, fluid-only fasts every 1–2 months), combined with a modified ketogenic diet on feeding days, for 2 years. Fasting-related adverse effects included cold intolerance, fatigue, and generalized muscle aches, all of which resolved during the second year. She experienced two myasthenia relapses, each associated with profoundly reduced oral intake, marked weight loss, and tumor regression-the first relapse was followed by a 32% decrease in tumor volume over 4 months, the second relapse by a dramatic 96% decrease in tumor volume over 4 months. The second relapse also required prednisone to control the myasthenia symptoms. We hypothesize that 2 years of fasting and ketogenic diet therapy metabolically weakened the neoplastic thymic cell component of the thymoma, "setting the stage" for immune activation and extreme energy restriction to destroy the majority of cancer cells during both relapses, while prednisone-induced apoptosis eradicated the remaining lymphocytic component of the thymoma during the second relapse. This case is unique in that a metabolic-based fasting and ketogenic diet intervention was used as the primary management strategy for a metastatic cancer in the absence of surgery, chemotherapy, or radiotherapy, culminating in a near-complete regression. Nearly 3 years after being diagnosed with inoperable metastatic cancer, our patient shows no signs of disease and leads a full and active life.

Keywords: metastatic thymoma, fasting, ketogenic diet, prednisone, cancer

OPEN ACCESS

Edited by:
Michael P. Lisanti,
University of Salford Manchester,
United Kingdom

Reviewed by:
Giuseppe Nicoló Fanelli,
University of Padova, Italy
Stephen John Ralph,
Griffith University, Australia

****Correspondence:***
Matthew C. L. Phillips
matthew.phillips@waikatodhb.health.nz

Specialty section:
This article was submitted to Cancer Metabolism, a section of the journal Frontiers in Oncology

Received: *28 January 2020*
Accepted: *30 March 2020*
Published: *05 May 2020*

Citation:
Phillips MCL, Murtagh DKJ, Sinha SK and Moon BG (2020) Managing Metastatic Thymoma With Metabolic and Medical Therapy: A Case Report. Front. Oncol. 10:578. doi: 10.3389/fonc.2020.00578

INTRODUCTION

Thymomas, the most common tumor of the anterior mediastinum, are composed of neoplastic thymic epithelial cells intermixed with variable numbers of non-neoplastic lymphocytes (1, 2). Thymomas are usually asymptomatic but may present with chest pain, dyspnea, and a variety of autoimmune disorders, most commonly myasthenia gravis which presents with ocular, bulbar, and limb weakness and fatiguability (3). Nearly 30% of thymomas are inoperable (4), resulting in 5-year survival rates of 36–53% (5, 6). Inoperable, metastatic thymomas are typically managed with chemotherapy to control tumor-related symptoms; no prolonged survival is expected (4). Novel therapeutic strategies are needed for metastatic thymomas.

Cancer is generally regarded as a primarily genetic disorder, yet it may also be perceived as a primarily metabolic disorder, with most of the genetic abnormalities arising as secondary phenomena (7). Cancer cells show a dramatically increased uptake of glucose, a feature common to over 90% of malignant cancers (8), and some cancer cells also show increased uptake of the amino acid glutamine (9, 10). Cancer cells rely upon these fermentable metabolites to compensate for mitochondria dysfunction and impaired cell respiration, which are characteristic of most cancers (7). Cancer cells also rely heavily on growth signaling pathways, particularly those involving insulin, insulin-like growth factor-1 (IGF-1), and mammalian target of rapamycin (mTOR) (11), to support a "reprogrammed" cell metabolism redirected toward unbridled growth and proliferation (12). Given these facts, cancer cells may be vulnerable to interventions that selectively target their abnormal metabolism.

Metabolic interventions, such as fasting and ketogenic diets, target cancer cell metabolism and may be effective alongside medical therapies in treating advanced cancers (7, 13). Fasting is a voluntary abstinence from food and drink for specified, recurring periods of time, with the fasting periods typically ranging from 12 h to 3 weeks in humans, whereas ketogenic diets are high-fat, adequate-protein, low-carbohydrate diets that stimulate the body to mimic a fasted metabolic state (14). Both interventions increase fat metabolism within the body, the former utilizing endogenous (body) fat and the latter exogenous (dietary) fat. After several days of fasting or a ketogenic diet, the human body enters a state of physiological ketosis characterized by low blood glucose levels, emptied liver glycogen stores, and hepatic production of ketones, which serve as a major energy source for brain and muscle. Ketones cannot be effectively utilized by cancer cells and may inhibit their growth (15, 16). Moreover, both interventions can decrease glucose, glutamine, and growth factor availability, depriving cancer cells of their major fuels and creating an unfavorable physiological environment for unchecked growth and proliferation. To our knowledge, neither fasting nor ketogenic diets have been utilized as the primary management strategy for metastatic cancer in the absence of surgery, chemotherapy, or radiotherapy.

CASE REPORT

We report the case of a 37-year-old, 37 weeks pregnant marketing consultant who presented with 2 months of eyelid weakness worsening on activity as well as 1 month of pleuritic chest pain and dyspnea. She was diagnosed with myasthenia gravis at age 26, during which time a coexisting mediastinal mass was laparoscopically resected and diagnosed as a World Health Organization (WHO) type B2 invasive thymoma. Although she had been intermittently managed with pyridostigmine, prednisone, and intravenous immunoglobulin (IVIg) in the interim, her only current medication was azathioprine 50 mg orally daily. She weighed 53 kg. A neurological examination revealed subtle bilateral asymmetric ptosis and mild eyelid fatiguability. Examination findings regarding upper and lower limb power, reflexes, plantar responses, and sensation were normal.

A computed tomography (CT) scan of the neck and chest revealed several large soft tissue masses in the left lung, the largest being 10 × 5 × 14 cm (total tumor volume 549.6 cm^3); several masses invaded the left pleura, and there was a small left pleural effusion. Our patient was treated with IVIg (1 g/kg, administered over 5 days) to ensure the uncomplicated delivery of a healthy baby girl 2 weeks later. She underwent a left pleural percutaneous needle biopsy the day after delivery and was diagnosed with a WHO type AB (indicating oval/spindle cells admixed with abundant small lymphocytes), Masaoka stage IVA (indicating pleural or pericardial dissemination) thymoma [**Figure 1**; (3)]. The thymoma was deemed unresectable at a multidisciplinary meeting, and she was offered non-curative chemotherapy, which she declined. Following this, a combined metabolic intervention was offered; after all foreseeable risks and benefits had been explained, she chose this course.

Our patient's health and myasthenia gravis were regularly monitored by a neurologist during the metabolic intervention, which consisted of a periodic fasting regimen (starting with a 12-day, water-only fast followed by a series of 7-day, fluid-only fasts every 1–2 months) combined with a modified ketogenic diet (60% fat, 30% protein, 5% fiber, and 5% net carbohydrate by weight, consisting largely of green vegetables, meats, eggs, nuts, seeds, creams, and natural oils) on feeding days (**Figure 2**). She monitored and recorded her blood glucose and beta-hydroxybutyrate (BHB) levels (Freestyle Neo; Abbott Diabetes Care, Whitney, UK) three times per week (17). All adverse effects were documented. An oncologist monitored the thymoma with a CT scan every 4–5 months, and a radiologist blinded to treatment simultaneously assessed all CT scans with volumetric analysis at the end of the intervention (**Figure 3**). Tumor volumes were calculated by Hounsfield unit threshold segmentation followed by manual correction of all tumor margins.

The first 3 months of the combined metabolic intervention was uneventful, but during months 4–7, our patient experienced reduced appetite and oral intake in the setting of several weeks of diarrhea (up to 10 motions per day), resulting in 6-kg weight loss; the diarrhea was extensively investigated

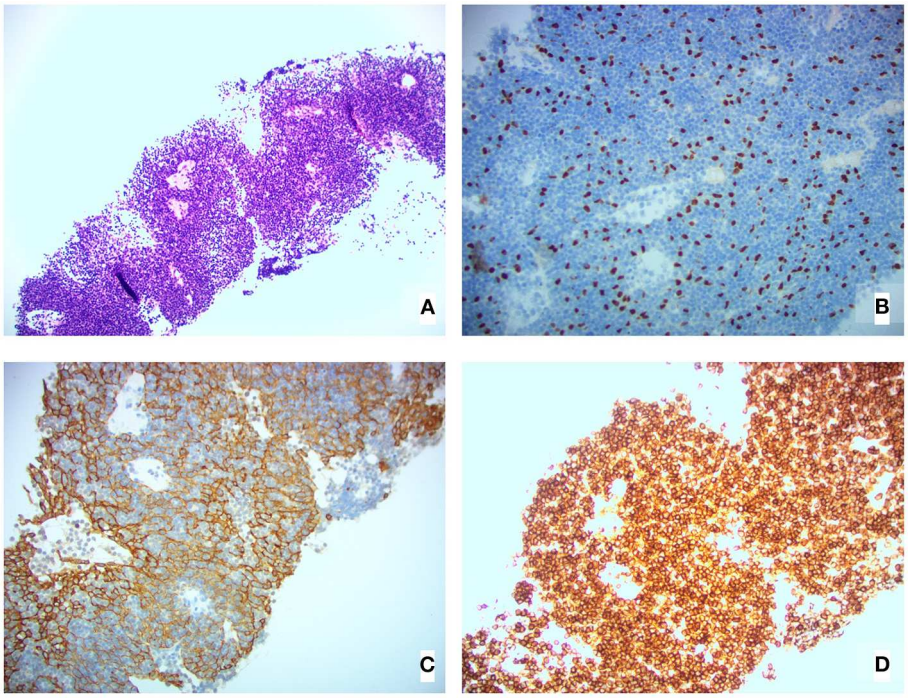

FIGURE 1 | Pleural biopsy histological images showing **(A)** H&E stain, **(B)** 20×P63 stain (highlighting epithelial cell nuclei), **(C)** 20×AE1/AE3 stain (highlighting epithelial cell cytoplasm), and **(D)** 20×CD45 stain (highlighting lymphoid cells).

and thought to be a thymoma-associated autoimmune enteropathy (18). Coincident with the diarrhea, she developed a myasthenia relapse resulting in worsening bilateral ptosis, dysphagia, and four-limb weakness with fatiguability. Our patient chose not to commence prednisone as she had experienced disrupted mood, insomnia, and weight gain several years previously while taking this medication. She was therefore commenced on 4-weekly IVIg for 4 months, after which her 8-month CT scan revealed a partial regression of the tumor (376.4 cm^3, representing a 32% decrease in diagnosis volume), moderate bilateral pleural effusions, and a small pericardial effusion. Given that the myasthenia symptoms persisted combined with the possibility that the IVIg may have contributed to the partial regression, the azathioprine was stopped and the IVIg frequency increased to 3-weekly.

During months 9–12, our patient's diarrhea ceased, she regained her weight, and the myasthenia symptoms resolved. However, the 12-month CT demonstrated that the thymoma had regrown to its original diagnosis volume. Given her ongoing myasthenia control and lack of IVIg inhibitory effect on the growth of the tumor, the IVIg frequency was decreased to 6-weekly.

During months 13–24, our patient remained largely free of diarrhea and maintained her diagnosis body weight, and the myasthenia symptoms remained controlled. Her IVIg frequency was decreased to 8-weekly and then 12-weekly. By the time of the 25-month CT, the thymoma showed minimal growth (632.7 cm^3, representing a 13% increase in diagnosis volume), and all effusions had disappeared.

After 2 years on the combined fasting and ketogenic diet intervention, our patient weighed 54 kg and her mean 2-year blood glucose and BHB levels (±standard deviation) were measured at 4.98 ± 0.55 and 3.50 ± 1.27 mmol/L, respectively. During each 7-day fasting period, she lost an average of 2.9 ± 0.72 kg of body weight, with mean blood glucose and BHB levels during the fasting periods measured at 3.92 ± 0.73 and 6.31 ± 1.55 mmol/L, respectively. There were several fasting-related adverse effects including cold intolerance, fatigue, and generalized muscle aches, all of which peaked during the first 3 days of each fasting period and progressively resolved over the first year such that they no longer occurred by the second year. No adverse effects occurred in relation to the ketogenic diet.

During months 25–29, our patient experienced several weeks of drastically reduced oral intake and diarrhea, resulting in 15-kg weight loss. She also developed a second, more severe myasthenia relapse resulting in bilateral ptosis, dysarthria, four-limb weakness with fatiguability, and respiratory failure requiring 2 weeks of intubation and mechanical ventilation in the intensive care unit. She was treated with plasma exchange followed by 3- to 4-weekly IVIg and 10 days of octreotide 1.5 mg subcutaneously daily (followed by a single dose of long-acting octreotide 20 mg intramuscularly 1 month later). Despite the previous adverse effects experienced by our patient in relation to prednisone, we decided to commence prednisone 40 mg orally daily. Her myasthenia symptoms resolved, and the 29-month CT

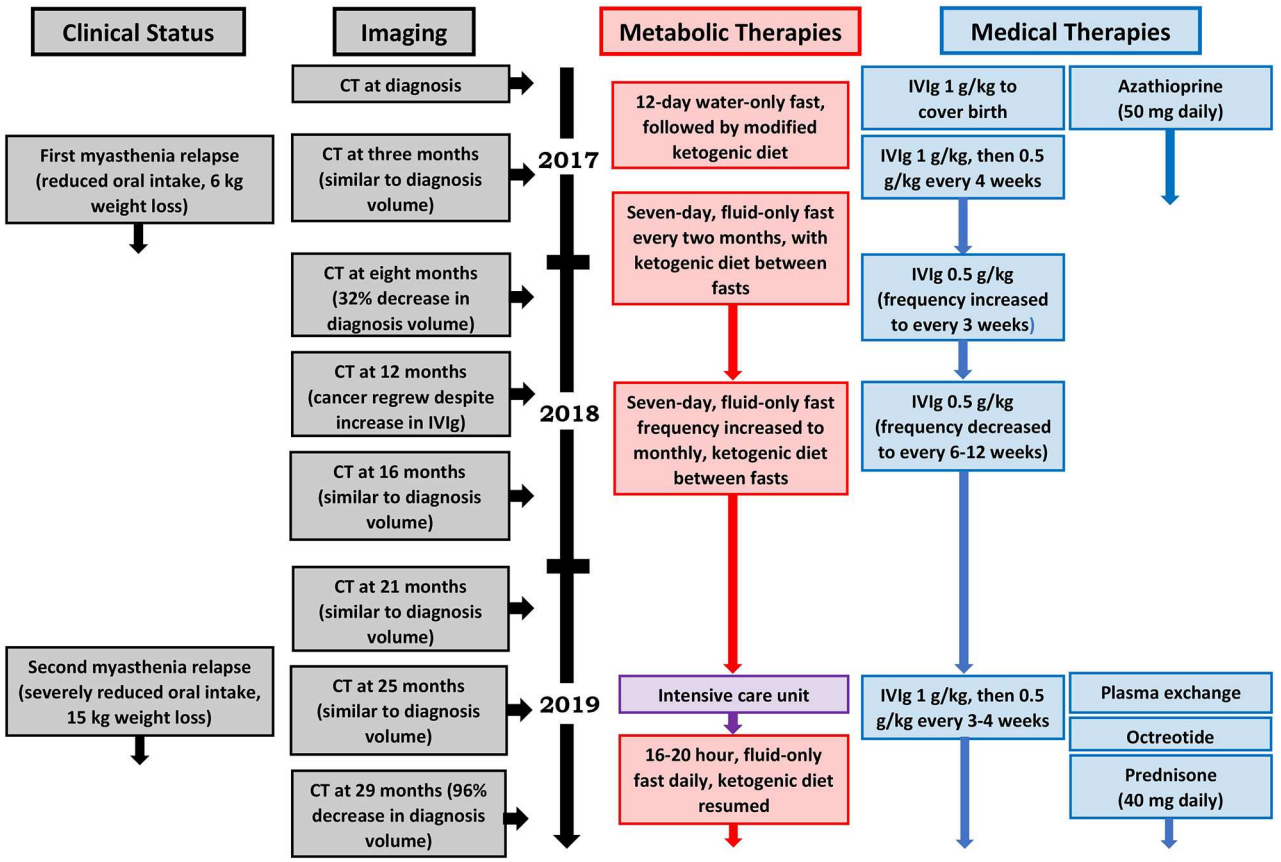

FIGURE 2 | Patient timeline.

revealed a near-complete regression of the thymoma (21.3 cm^3, representing a 96% decrease in diagnosis volume).

DISCUSSION

In this case, a metabolic-based fasting and ketogenic diet intervention, along with adjunctive medications aimed at controlling myasthenia symptoms, culminated in the near-complete regression of a metastatic thymoma. For 2 years, our patient relied almost completely upon a metabolic strategy to manage her metastatic cancer, during which time she remained active, maintained her diagnosis body weight, and the tumor volume increased by a modest 13%. There were several fasting-related adverse effects including cold intolerance, fatigue, and generalized muscle aches, all of which resolved by the second year. She then experienced a 4-month myasthenia relapse, accompanied by severe weight loss and requiring prednisone, during which time the thymoma decreased in volume by 96%. Nearly 3 years after being diagnosed with metastatic cancer, our patient shows no signs of disease and leads a full and active life. She continues her metabolic therapy and her only remaining medical therapy is prednisone 10 mg orally daily.

Various metabolic approaches are theoretically capable of targeting cancer cell energy metabolism by creating an increased cell reliance on ketone and fat metabolism, a decreased reliance on glucose as the primary metabolic fuel, and reduced levels of tumor growth-promoting factors such as insulin, IGF-1, and mTOR (11, 14). Normal cells are metabolically flexible and readily adapt to ketone and fat metabolism; in contrast, metabolically inflexible cancer cells undergo physiological stress (19). The metabolic intervention supported by the most evidence is calorie restriction, defined as a chronic 20–40% reduction in calorie intake with maintained meal frequency (20). Calorie restriction reduces tumor incidence by 75% in rodents and by 50% in rhesus monkeys (21, 22). However, long-term adherence to calorie restriction is challenging in cancer patients (11); from a practical standpoint, fasting and ketogenic diets are more suitable. Periodic fasting (fasting periods lasting 2 days or longer) holds a particular therapeutic edge by inducing more extreme changes in ketone, glucose, glutamine, and growth factor levels compared to calorie restriction or ketogenic diets, as shown by the lower glucose and higher BHB levels measured by our patient during the fasts. Although the benefits of fasting interventions in preventing cancer in animals are somewhat variable (21), they can exceed those of calorie restriction (23, 24); there is also mounting evidence that fasting may

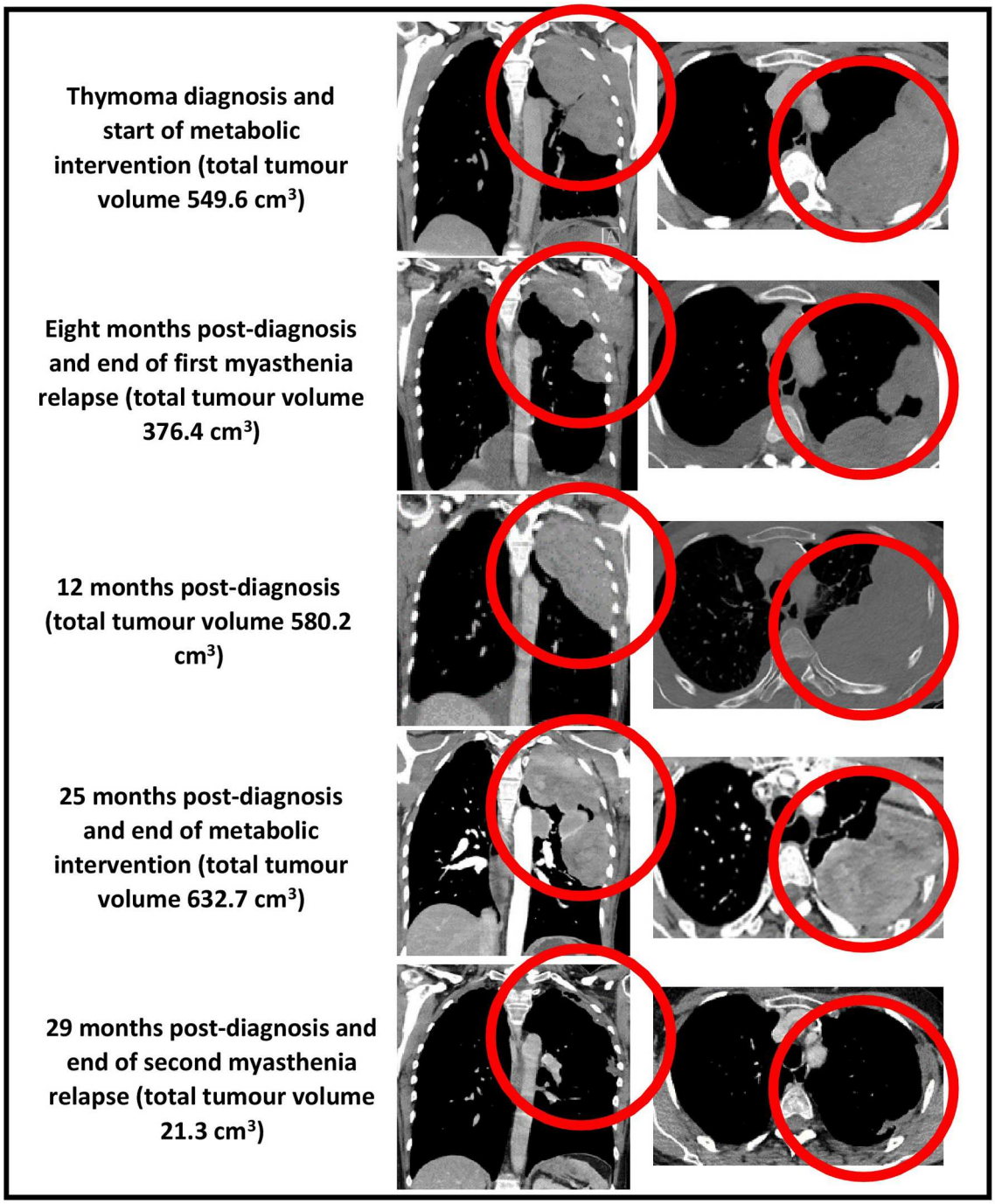

FIGURE 3 | CT chest (coronal and axial views, bulk of tumor circled in red) showing total tumor volumes at diagnosis, 8, 12, 25, and 29 months post-diagnosis.

benefit human cancer patients, particularly when combined with conventional treatments such as chemotherapy (25–27). Regarding ketogenic diets, many animal studies suggest an antitumor effect; however, evidence of improved outcomes in human cancer patients is currently limited to individual cases (28).

It is important to note that although 2 years of a combined fasting and ketogenic diet intervention may have limited the growth of our patient's metastatic thymoma, the tumor had not decreased in volume by the end of this approach; it was only in the setting of two myasthenia relapses that significant volume reduction occurred, with a 32% decrease in tumor diagnosis

volume during the first 4-month relapse and a 96% decrease in volume during the second 4-month relapse. Given that both relapses in our patient were characterized by abnormal immune function and marked weight loss, it is possible that immune activation and extreme energy restriction contributed to the regressions, and since both relapses were treated medically, one or more of the myasthenia medications may have contributed to the regressions. These possibilities warrant discussion.

First, it is possible that immune activation contributed to both regressions. So-called "spontaneous" regressions have been documented for thousands of years in a variety of cancers (29). The mechanism of spontaneous regression remains unknown but may involve the activation of antigen recognition mechanisms such that the immune system becomes capable of recognizing cancer cells, allowing for the establishment of active immunity against tumors (30). In the case of thymomas, which are generally asymptomatic, the few documented cases of spontaneous regression presented with fever, chest pain, and pleural effusions which are thought to result from a massive inflammatory reaction within the tumor (31). Given the similar findings in this case, an immunity-induced regression may have occurred in our patient, although it must be noted that the spontaneous regression of a metastatic thymoma in the absence of any other treating factors is exceedingly rare; to our knowledge, only one case of a stage IVA thymoma undergoing a spontaneous (and only partial) regression has been reported (31).

Second, extreme energy restriction may have contributed to both regressions. During each relapse, our patient experienced a profound reduction in appetite resulting in minimal calorie intake over several weeks. The ensuing weight loss was considerable—for example, during each 1-week, fluid-only fast, our patient typically lost 2.9 kg (5% of body weight), whereas during the first and second relapses, she lost 6 kg (11% of body weight), and 15 kg (28% of body weight), respectively. In both cases, such a degree of weight loss would have created drastic alterations in ketone, glucose, glutamine, and growth factor levels, fostering a hostile physiological environment for metabolically inflexible cancer cells. Thus, it is possible that an extreme metabolic-induced regression occurred in our patient.

Third, one or more of the medications used to treat our patient's myasthenia symptoms may have contributed to the regressions. The possibility that IVIg contributed to the first regression was considered and partially formed the rationale for increasing the IVIg frequency from 4- to 3-weekly in week 9. Despite this adjustment, the thymoma regrew to its original size by week 12, which suggests that IVIg did not contribute to either regression. In the second and more pronounced regression, octreotide and prednisone were additionally used to placate the myasthenia gravis and autoimmune enteropathy. Octreotide inhibits somatostatin receptors, dampening angiogenesis and growth factor availability, which can produce objective response rates of 10–37% in thymic tumors (32, 33). However, due to funding restrictions, octreotide was only administered for 10 days in our patient, followed by a single long-acting dose 1 month later; it seems unlikely that so small a dose could significantly contribute to the dramatic reduction in thymoma volume that occurred. Although extremely rare, corticosteroid-induced regressions of advanced thymomas in the absence of other treatments have been documented (34–36); however, all cases involved subtype B1 thymomas which contain more CD4+ and CD8+ double-positive immature lymphocytes compared to other subtypes (37). Double-positive lymphocytes show a high expression of glucocorticoid receptors, rendering the lymphocytic component of subtype B1 thymomas susceptible to glucocorticoid-induced apoptosis, whereas neoplastic thymic cells and hence other subtypes (including type AB, as in this case) are resistant to this mechanism (37). Nonetheless, it remains possible that prednisone-induced lymphocytic apoptosis contributed to the second regression seen in our patient, although it cannot explain the first regression.

Taken together, it is likely that several factors culminated in the near-complete regression of our patient's metastatic thymoma. It is difficult to ignore 2 years of periodic fasting combined with a ketogenic diet, which would have immersed the tumor in ketones while depriving it of glucose, glutamine, and growth-promoting factors. It is equally difficult to ignore the two myasthenia relapses in which immune activation and extreme energy restriction may have contributed to both regressions; in the case of the second relapse, it is possible that prednisone-induced apoptosis of the lymphocytic component of the tumor contributed to the dramatic second regression. Overall, we hypothesize that 2 years of a combined fasting and ketogenic diet intervention metabolically weakened the neoplastic thymic cell component of the thymoma, "setting the stage" for immune activation and extreme energy restriction to destroy the majority of cancer cells during the relapses, with prednisone-induced apoptosis destroying most of the lymphocytic component of the thymoma during the second relapse, culminating in the virtual eradication of the tumor.

Given that this study involved one patient, its major limitation is obvious, and it is difficult to draw definitive conclusions. Additional potential limitations include concerns that periodic fasting and ketogenic diets may produce unwanted weight loss and other adverse effects in patients with metastatic cancer. It is therefore important to note that our patient did not experience weight loss after 2 years undergoing both metabolic interventions. Furthermore, although she experienced several fasting-related adverse effects, these were all transient and improved as she adapted to each successive fasting period.

In conclusion, this case is unique in that a metabolic-based fasting and ketogenic diet intervention was used as the primary management strategy for a metastatic cancer in the absence of surgery, chemotherapy, or radiotherapy, culminating in the near-complete regression of an inoperable metastatic thymoma, with our patient experiencing only transient, fasting-related side effects. Nearly 3 years after being diagnosed with inoperable metastatic cancer, our patient shows no signs of disease and leads a full and active life. Although we cannot be certain of the mechanism underlying this remarkable outcome, the most plausible explanation is that 2 years of fasting and ketogenic diet therapy metabolically weakened the thymoma, setting the stage for a combined immunity-induced, metabolic-induced, and prednisone-induced near-complete regression. Despite our uncertainty, the extraordinary outcome in our patient highlights the importance of exploring metabolic-based

therapies in advanced cancer cases, in the hope that more options may be offered to patients in the years to come.

ETHICS STATEMENT

Written informed consent was obtained from the patient in this case report for the publication of any potentially identifiable images or data included in this article.

AUTHOR CONTRIBUTIONS

MP: conception, design, interpretation, and write-up of final article. DM: diet implementation and advice, and proof-reading of final article. SS: histology analysis and advice, and proof-reading of final article. BM: imaging analysis and advice, and proof-reading of final article.

REFERENCES

1. Levine G, Rosai J. Thymic hyperplasia and neoplasia: a review of current concepts. *Hum Pathol.* (1978) 9:495–515. doi: 10.1016/s0046-8177(78)80131-2
2. Verley J, Hollmann K, Thymoma. A comparative study of clinical stages, histologic features, and survival in 200 cases. *Cancer*. (1985) 55:1074–86. doi: 10.1002/1097-0142(19850301)55:5<1074::aid-cncr2820550524>3.0.co2-t
3. Falkson C, Bezjak A, Darling G, Gregg R, Malthaner R, Maziak D, et al. The management of thymoma: a systematic review and practice guideline. *J Thorac Oncol.* (2009) 4:911–19. doi: 10.1097/jto.0b013e3181a4b8e0
4. Girard N. Thymic epithelial tumours: from basic principles to individualised treatment strategies. *Eur Respir Rev.* (2013) 22:75–87. doi: 10.1183/09059180.00007312
5. Kondo K, Monden Y. Therapy for thymic epithelial tumors: a clinical study of 1,320 patients from Japan. *Ann Thorac Surg.* (2003) 76:878–84. doi: 10.1016/s0003-4975(03)00555-1
6. Gadalla S, Rajan A, Pfeiffer R, Kristinsson S, Björkholm M, Landgren O, et al. A population-based assessment of mortality and morbidity patterns among patients with thymoma. *Int J Cancer.* (2010) 128:2688–94. doi: 10.1002/ijc.25583
7. Seyfried T, Flores R, Poff A, D'Agostino D. Cancer as a metabolic disease: implications for novel therapeutics. *Carcinogenesis.* (2013) 35:515–27. doi: 10.1093/carcin/bgt480
8. Epstein T, Gatenby R, Brown J. The Warburg effect as an adaptation of cancer cells to rapid fluctuations in energy demand. *PLoS ONE.* (2017) 12:e0185085. doi: 10.1371/journal.pone.0185085
9. Eagle H. Nutrition needs of mammalian cells in tissue culture. *Science.* (1955) 122:501–4. doi: 10.1126/science.122.3168.501
10. Wise D, Thompson C. Glutamine addiction: a new therapeutic target in cancer. *Trends Biochem Sci.* (2010) 35:427–33. doi: 10.1016/j.tibs.2010.05.003
11. O'Flanagan C, Smith L, McDonell S, Hursting S. When less may be more: calorie restriction and response to cancer therapy. *BMC Med.* (2017) 15:106. doi: 10.1186/s12916-017-0873-x
12. Hanahan D, Weinberg R. Hallmarks of cancer: the next generation. *Cell.* (2011) 144:646–74. doi: 10.1016/j.cell.2011.02.013
13. Turbitt W, Demark-Wahnefried W, Peterson C, Norian L. Targeting glucose metabolism to enhance immunotherapy: emerging evidence on intermittent fasting and calorie restriction mimetics. *Front Immunol.* (2019) 10:1402. doi: 10.3389/fimmu.2019.01402
14. Phillips M. Fasting as a therapy in neurological disease. *Nutrients.* (2019) 11:2501. doi: 10.3390/nu11102501
15. Magee B, Potezny N, Rofe A, Conyers R. The inhibition of malignant cell growth by ketone bodies. *Aust J Exp Biol Med Sci.* (1979) 57:529–39. doi: 10.1038/icb.1979.54
16. Fine E, Miller A, Quadros E, Sequeira J, Feinman R. Acetoacetate reduces growth and ATP concentration in cancer cell lines which over-express uncoupling protein 2. *Cancer Cell Int.* (2009) 9:14. doi: 10.1186/1475-2867-9-14
17. Freestyle. *FreeStyle Optium Neo Blood Glucose and Ketone Monitoring System*. (2019). Available online at: https://www.myfreestyle.com.au/products/freestyle-optium-neo-blood-glucose-ketone-monitoring-system/# (accessed December 22, 2019).
18. Mais D, Mulhall B, Adolphson K, Yamamoto K. Thymoma-associated autoimmune enteropathy: a report of two cases. *Am J Clin Pathol.* (1999) 112:810–15. doi: 10.1093/ajcp/112.6.810
19. Lee C, Raffaghello L, Brandhorst S, Safdie F, Bianchi G, Martin-Montalvo A, et al. Fasting cycles retard growth of tumors and sensitize a range of cancer cell types to chemotherapy. *Sci Transl Med.* (2012) 4:124ra27. doi: 10.1126/scitranslmed.3003293
20. Longo V, Mattson M. Fasting: molecular mechanisms and clinical applications. *Cell Metab.* (2014) 19:181–92. doi: 10.1016/j.cmet.2013.12.008
21. Lv M, Zhu X, Wang H, Wang F, Guan W. Roles of caloric restriction, ketogenic diet and intermittent fasting during initiation, progression and metastasis of cancer in animal models: a systematic review and meta-analysis. *PLoS ONE.* (2014) 9:e115147. doi: 10.1371/journal.pone.0115147
22. Colman R, Anderson R, Johnson S, Kastman E, Kosmatka K, Beasley T, et al. Caloric restriction delays disease onset and mortality in rhesus monkeys. *Science.* (2009) 325:201–4. doi: 10.1126/science.1173635
23. Cleary M, Grossmann M. The manner in which calories are restricted impacts mammary tumor cancer prevention. *J Carcinog.* (2011) 10:21. doi: 10.4103/1477-3163.85181
24. Rogozina O, Bonorden M, Grande J, Cleary M. Serum insulin-like growth factor-i and mammary tumor development in *ad libitum*-Fed, chronic calorie-restricted, and intermittent calorie-restricted MMTV-TGF- mice. *Cancer Prev Res.* (2009) 2:712–19. doi: 10.1158/1940-6207.capr-09-0028
25. Safdie F, Dorff T, Quinn D, Fontana L, Wei M, Lee C, et al. Fasting and cancer treatment in humans: a case series report. *Aging.* (2009) 1:988–1007. doi: 10.18632/aging.100114
26. de Groot S, Vreeswijk M, Welters M, Gravesteijn G, Boei J, Jochems A, et al. The effects of short-term fasting on tolerance to (neo) adjuvant chemotherapy in HER2-negative breast cancer patients: a randomized pilot study. *BMC Cancer.* (2015) 15:652. doi: 10.1186/s12885-015-1663-5
27. Bauersfeld S, Kessler C, Wischnewsky M, Jaensch A, Steckhan N, Stange R, et al. The effects of short-term fasting on quality of life and tolerance to chemotherapy in patients with breast and ovarian cancer: a randomized cross-over pilot study. *BMC Cancer.* (2018) 18:476. doi: 10.1186/s12885-018-4353-2
28. Klement R. Beneficial effects of ketogenic diets for cancer patients: a realist review with focus on evidence and confirmation. *Med Oncol.* (2017) 34:132. doi: 10.1007/s12032-017-0991-5
29. Vernon L. William Bradley Coley, MD, and the phenomenon of spontaneous regression. *Immunotargets Ther.* (2018) 7:29–34. doi: 10.2147/itt.s163924
30. Jessy T. Immunity over inability: the spontaneous regression of cancer. *J Nat Sci Biol Med.* (2011) 2:43–9. doi: 10.4103/0976-9668.82318
31. Fukui T, Taniguchi T, Kawaguchi K, Yokoi K. Spontaneous regression of thymic epithelial tumours. *Interact Cardiovasc Thorac Surg.* (2013) 18:399–401. doi: 10.1093/icvts/ivt496
32. Palmieri G, Montella L, Martignetti A, Muto P, Di Vizio D, De Chiara A, et al. Somatostatin analogs and prednisone in advanced refractory thymic tumors. *Cancer.* (2002) 94:1414–20. doi: 10.1002/cncr.10374
33. Loehrer P, Wang W, Johnson D, Ettinger D. Octreotide alone or with prednisone in patients with advanced thymoma and thymic carcinoma: an eastern cooperative oncology group phase II trial. *J Clin Oncol.* (2004) 22:293–99. doi: 10.1200/jco.2004.02.047

34. Kirkove C, Berghmans J, Noel H, Van de Merckt J. Dramatic response of recurrent invasive thymoma to high doses of corticosteroids. *Clin Oncol.* (1992) 4:64–6. doi: 10.1016/s0936-6555(05)80783-6
35. Termeer A. Regression of invasive thymoma following corticosteroid therapy. *Neth J Med.* (2001) 58:181–4. doi: 10.1016/s0300-2977(01)00090-0
36. Barratt S, Puthucheary Z, Plummeridge M. Complete regression of a thymoma to glucocorticoids, commenced for palliation of symptoms. *Eur J Cardiothorac Surg.* (2007) 31:1142–43. doi: 10.1016/j.ejcts.2007.02.032
37. Kobayashi Y, Fujii Y, Yano M, Sasaki H, Yukiue H, Haneda H, et al. Preoperative steroid pulse therapy for invasive thymoma. *Cancer.* (2006) 106:1901–7. doi: 10.1002/cncr.21875

Conflict of Interest: DM was employed by the company Healthy Kitchen Christchurch Ltd.

The remaining authors declare that the research was conducted in the absence of any commercial or financial relationships that could be construed as a potential conflict of interest.

frontiers in Oncology

REVIEW
published: 15 May 2020
doi: 10.3389/fonc.2020.00776

Proline Metabolism in Tumor Growth and Metastatic Progression

Cristina D'Aniello[1]*, *Eduardo J. Patriarca*[1], *James M. Phang*[2]* and *Gabriella Minchiotti*[1]

[1] Stem Cell Fate Laboratory, Institute of Genetics and Biophysics "Adriano Buzzati-Traverso", CNR, Naples, Italy, [2] Mouse Cancer Genetics Program, Center for Cancer Research, National Cancer Institute at Frederick, NIH, Frederick, MD, United States

Cancer cells show a formidable capacity to survive under stringent conditions, to elude mechanisms of control, such as apoptosis, and to resist therapy. Cancer cells reprogram their metabolism to support uncontrolled proliferation and metastatic progression. Phenotypic and functional heterogeneity are hallmarks of cancer cells, which endow them with aggressiveness, metastatic capacity, and resistance to therapy. This heterogeneity is regulated by a variety of intrinsic and extrinsic stimuli including those from the tumor microenvironment. Increasing evidence points to a key role for the metabolism of non-essential amino acids in this complex scenario. Here we discuss the impact of proline metabolism in cancer development and progression, with particular emphasis on the enzymes involved in proline synthesis and catabolism, which are linked to pathways of energy, redox, and anaplerosis. In particular, we emphasize how proline availability influences collagen synthesis and maturation and the acquisition of cancer cell plasticity and heterogeneity. Specifically, we propose a model whereby proline availability generates a cycle based on collagen synthesis and degradation, which, in turn, influences the epigenetic landscape and tumor heterogeneity. Therapeutic strategies targeting this metabolic-epigenetic axis hold great promise for the treatment of metastatic cancers.

Keywords: proline, metabolic reprogramming, PRODH, ALDH18A1, PYCR1, collagen prolyl-hydroxylases, epigenetic remodeling, Budesonide

OPEN ACCESS

Edited by:
Stephen Byers, Georgetown University, United States

Reviewed by:
Domenica Scumaci, Magna Graecia University of Catanzaro, Italy
Mariafrancesca Scalise, University of Calabria, Italy

***Correspondence:**
Cristina D'Aniello
cristina.daniello@igb.cnr.it
James M. Phang
phangj@mail.nih.gov

Specialty section:
This article was submitted to Cancer Metabolism, a section of the journal Frontiers in Oncology

Received: *19 March 2020*
Accepted: *21 April 2020*
Published: *15 May 2020*

Citation:
D'Aniello C, Patriarca EJ, Phang JM and Minchiotti G (2020) Proline Metabolism in Tumor Growth and Metastatic Progression. Front. Oncol. 10:776. doi: 10.3389/fonc.2020.00776

INTRODUCTION

Metastatic seeding of tumor cells to distant body sites relies on the extraordinary phenotypic plasticity of cancer cells (1, 2). The acquisition of cancer cell plasticity is emerging as the adaptive response to a hostile tumor microenvironment. A paradigm of cell plasticity is the epithelial to mesenchymal transition (EMT) by which epithelial cells acquire mesenchymal traits while losing epithelial-specific gene expression. This phenotypic switch occurs through a continuum of intermediated cellular states in which cells acquire intermediate/metastable phenotypes, adopting phenotypic, and molecular features of both epithelial and mesenchymal cell types (3, 4). How this multistep process is controlled is a key question and a major unresolved issue.

A central role for metabolism is emerging in the control/modulation of cancer cell plasticity (5). Upon the activation of oncogenic pathways, cancer cells undergo metabolic reprogramming, adapting their metabolism to the energetic and anabolic requirements necessary for uncontrolled proliferation and motility (5). For instance, cancer cells become dependent on an exogenous source of non-essential amino acids (NEAAs), which are involved in synthesis of macromolecules redox balance, and post-translational and epigenetic modifications, i.e., the NEAAs take on regulatory

functions essential for malignant growth and metastasis. Thus, it has been hypothesized that during cancer progression, some NEAAs may become "conditionally essential," however, it is not only the product amino acid but also the metabolic pathway, itself, which is important (6–8).

In this context, a great interest is emerging on the role of the extracellular matrix (ECM) as a readily available source of limiting metabolites and an important component of the tumor cell plasticity. ECM proteins are a great reservoir of amino acids, mainly NEAAs, that can be released in the tumor microenvironment by the activity of matrix metalloproteinases/collagenases secreted by cancer cells (9) and thus influence cancer cells metabolism. Among NEAAs, ECM proteins are particularly rich of Glycine and Proline, and the regulatory functions and the impact of Proline metabolism on normal and cancer cell behavior has been deeply investigated and well-described (10–12).

The goal of this review is to describe the emerging knowledge on the role of Proline metabolism, mainly Proline synthesis, in the control of cancer cell plasticity, the genes/enzymes/pathways involved and their relevance as prognostic markers and potential therapeutic targets. Finally, we will discuss the emerging idea that cancer cells epigenetic and phenotypic plasticity rely on a Proline-dependent cycle, based on collagen-synthesis and degradation, which represents a potential target for the future development of novel anti-cancer therapies.

PROLINE CATABOLISM IN CANCER

The conversion of Proline into Δ^1- pyrroline-5-carboxylate (P5C) is the first step of Proline catabolism, and is catalyzed by Proline dehydrogenase/Proline oxidase (PRODH/POX) enzyme. During this enzymatic reaction, flavin adenine dinucleotide FAD is reduced to $FADH_2$, which may be used to generate ATP through the oxidative phosphorylation process. PRODH enzyme is bound to the inner mitochondrial membrane and its overexpression, concomitantly with high levels of free Proline, may concur to generate reactive oxygen species (ROS). In a second oxidative step, Proline-derived P5C can be converted into Glutamate in a reaction catalyzed by the pyrroline-5-carboxylate dehydrogenase (P5CDH) enzyme. Glutamate, after conversion into α-Ketoglutarate (α-KG), can be burned to CO_2 using the TCA cycle, gaining ATP. Thus, cells can use Proline to produce ATP, other metabolites (P5C, glutamate, αKG) and ROS. The role of PRODH-mediated Proline oxidation in the proliferation/survival of cancer cells has been exhaustively described elsewhere (11–14). Here we report a brief description of the contrasting effects (anti- vs. pro- tumor) of PRODH on cancer cell behavior.

Antitumor

PRODH is a p53-induced gene and its expression is down regulated in many tumors (15–18), most likely those carrying inactivated/mutated p53 variants. PRODH expression is also induced by the inflammatory factor peroxisome proliferator-activated receptor gamma (PPARγ) and AMP activated protein kinase (AMPK), whereas it is repressed by oncogenes, such as MYC, which acts through *miR-23b** (19). Overexpression of PRODH gene in colorectal cancer cells blocks cell cycle and reduces DNA synthesis (20). PRODH-induced ROS are strong inducers of apoptosis and autophagy. PRODH activity can also concur to suppress hypoxia-inducible factor 1 alpha (HIF1α)-mediated signaling by increasing the synthesis of α-KG, in hepatocellular carcinoma (21, 22).

Protumor

PRODH expression is induced under hypoxic conditions in different tumor cell lines and in a mouse xenograft model of human breast tumor, and contributes to cancer cell survival by inducing autophagy (23, 24). Moreover, PRODH is upregulated in a 3D spheroidal cell culture model of breast cancer (BC) compared to the 2D culture, as well as in metastases compared to primary tumors in BC patients (25) (**Table 1**). PRODH inhibition impairs spheroids growth and reduces lung metastases formation *in vivo* (25). PRODH/POX contributes to survival of triple negative breast cancer (TNBC) cells treated with HDAC inhibitors (**Table 1**). PRODH ablation reduces pro-survival autophagy and increases apoptosis induced by the HDAC inhibitors used (45). PRODH induces, *in vitro* and *in vivo*, non-small cell lung cancer (NSCLC) cells toward EMT, proliferation and migration, which are blocked by depletion of PRODH (46) (**Table 1**).

All together these findings support the idea that the pro- or anti-survival roles of PRODH in cancer cells may be context/environment- and cell type- dependent (75). Additionally, the product of PRODH activity P5C is the immediate precursor of Proline. The Proline-P5C cycle provides unique functions in amino acid metabolism (14).

PROLINE BIOSYNTHESIS GENES PREDICT POOR PROGNOSIS IN CANCER

De novo synthesis of Proline is supported by Glutamine-derived Glutamate. In a first step, the P5C synthetase enzyme, encoded by aldehyde dehydrogenase 18A1 (ALDH18A1) gene catalyzes the conversion of Glutamate to P5C. In a second reductive step, P5C is converted to Proline by P5C reductase (PYCR) enzymes (10). Three isoforms (PYCR1, PYCR2, and PYCRL) of P5C reductase, each with distinct properties, have been identified (76). PYCR1 and 2 share a high amino acid (aa) sequence similarity (84%), they are both located in the mitochondria and prefer NADH as electron donor. Conversely, PYCRL shares only 45% of the aa sequence similarity with PYCR1 and 2, is localized in the cytosol and preferentially uses NADPH as reducing agent. PYCR2 is more sensitive to feedback inhibition by Proline (Ki ∼0.15 mM) than PYCR1 (Ki ∼1.0 mM), whereas PYCRL appears insensitive to Proline inhibition (10, 14). Of note, the up regulation of Proline synthesis from Glutamine by cMYC (77), and NAD^+ $NADP^+$ produced during Proline synthesis are potent regulators of both glycolysis and the pentose phosphate pathway, strongly suggesting its importance in cancer (8).

The role played by PYCRs-mediated Proline synthesis in cancer progression is supported by unbiased transcriptomics,

TABLE 1 | Proline-related genes and associated cancer types.

Cancer Type/Organ	Proline-related genes										
	ALDH18A1	*PYCR1*	*PRODH*	*EIF5A*	*P4HA1*	*P4HA2*	*P4HB*	*LEPREL4*	*PLOD1/2*	*MMP9/1/13*	*ATF4*
Adrenal	■	■						■	■	■	
Bladder	■	■		■				■	■	■	■
Brain	■	■				■		■	■	■	■
Breast	■	■	■		■	■		■	■	■	■
Cervix	■	■		■		■		■	■	■	
Colon	■	■		■				■	■	■	■
Esophagus	■	■		■				■	■	■	■
Gastric	■	■		■			■	■	■	■	■
Germ Cell	■	■						■	■	■	
Head-Neck	■	■			■			■	■	■	■
Hepatic	■	■		■		■					
Kidney	■	■					■	■	■	■	
Leukemia	■	■		■				■	■	■	
Lung	■	■					■	■	■	■	■
Lymphoma	■	■				■		■	■	■	
Melanoma		■									
Myeloma	■	■						■		■	■
Ovary	■	■		■	■			■		■	
Pancreas	■	■		■	■			■		■	
Prostate		■			■						■
Thyroid	■	■				■		■	■	■	
Reference	(26–29)	(26, 27, 30) (28, 31) (32–44)	(15–18) (21–25, 45, 46)	(47)	(48) (49–56)	(57) (58–65) (66, 67)	(68–72)	(26)	(26)	(26)	(73, 74)

The gray boxes indicate that the specific gene has been associated to the specific cancer type.

metabolomics, and proteomics studies, indicating that PYCRs expression levels, especially PYCR1, influence the clinical course of cancer (**Table 1**).

A comprehensive study comparing the mRNA expression profiles of 1,454 metabolic enzymes across 1,981 tumors covering 19 different tumor types vs. 931 matched normal tissue controls, identify Proline biosynthesis genes (PYCR1 and ALDH18A1) among the most up regulated enzymes (26). The Cancer Genome Atlas (TCGA) database and gene expression profiles from a Singapore-based cohort reveal that PYCR1 and ALDH18A1 are among the most up-regulated genes in Hepatocellular Carcinoma (HCC). They both correlate with HCC grade, and predict a poor clinical outcome (27). PYCR1 knock-down (KD) cells show decreased cell proliferation, and a reduction of the NAD^+–induced glycolytic and $NADP^+$–dependent oxidative pentose phosphate pathways has been suggested (27). An independent study reveal that PYCR1 is induced in HCC tumor tissues compared to adjacent normal liver tissues and, remarkably, that PYCR1 ablation induces apoptosis, decreases cell proliferation, colony formation ability *in vitro*, and reduces *in vivo* tumor size (30). Moreover, a link between PYCR1 expression and activation of c-Jun N-terminal kinase (JNK) and insulin receptor substrate 1 (IRS1) signaling has been also suggested (30). Different studies reported that ablation of PYCR1 generates smaller tumors. However, besides reduced proliferation/cell number and/or increased apoptosis, lower tumor volume can be the consequence of reduced stroma/ECM. Indeed, lower levels of Proline affect collagen/ECM accumulation, which eventually results in smaller/more compact tumors that have less capacity to invade and generate metastasis (57).

In Breast Cancer (BC) tumors, PYCR1 and ALDH18A1 expression levels varies among specific BC subtype. An increase in PYCR1 copy number and PYCR1 mRNA level is associated with Luminal B type. Moreover, ALDH18A1 and Glutaminase protein levels are higher in high proliferative estrogen receptor positive (ER^+) /human epidermal growth factor receptor negative ($HER2^-$) (Luminal B) compared to low proliferative $ER^+/HER2^-$ (Luminal A) tumor cells, thus suggesting that the Glutamine-Proline axis is a poor prognosis marker in BC (28). By combining *in vitro* studies using BC cell lines and clinical data from human samples, Ding et al. found that PYCR1, but not PYCR2, is highly expressed in BCs independently of the specific subtype (ER^+ vs. ER^-), and positively correlates with tumor size, grade and invasiveness. Accordingly, PYCR1 KD reduces BC cells proliferation and invasiveness and increases the cytotoxicity of chemotherapeutic drugs, thus suggesting that PYCR1 may be a potential therapeutic target for BC (31). Complementary to these findings, Liu et al. developed a

tool to calculate electrons energy dissipation during metabolic transformations (29), and found that under hypoxic conditions in which the electron transfer chain (ETC) to oxygen is blocked, proliferating cells rewire their metabolism and use Proline biosynthesis and lipogenesis as alternative electron acceptors. Blocking simultaneously ALDH18A1 and lipogenesis inhibits breast tumor growth *in vivo* and *in vitro* (29). A recent study demonstrates that infection with oncogenic Kaposi's sarcoma-associated herpesvirus (KSHV), an etiological agent of Kaposi sarcoma, increases Proline synthesis in a 3D model of breast cancer. KSHV K1 oncoprotein interacts with and activates PYCR1, promoting tumor growth and development. Abrogation of PYCR1 abolishes the oncogenic activity of KSHV K1 protein (32).

PYCR1 is highly expressed also in prostate cancer tissues (33), in renal cell carcinoma (RCC) (34), in papillary renal cell carcinoma (PRCC) (35) and in human malignant melanoma (MM) (36). These studies showed that PYCR1 expression strongly influence cell behavior (proliferation, colony formation, apoptosis) in different cancer contexts, and correlate with poor outcome and decreased overall survival in patients. Of particular interest is the finding that PYCR1 ablation inhibits migration and invasion both in PRCC and MM cells, altering phosphorylation of AKT (36) and mTOR (35).

Independent studies bring to the findings that PYCR1 is overexpressed also in non-small cell lung cancer (NSCLC) and has been associated with poor prognosis in patients with NSCLC (37–40). Knocking down PYCR1 inhibits NSCLC cell proliferation and cell cycle (37). Interestingly, PYCR1 expression is negatively regulated by *miR-488*, which inhibits cell proliferation and clone formation ability, and promotes apoptosis. These effects are rescued by PYCR1, which in turn activates p38 MAPK pathway (38). PYCR1 was shown to regulate NSCLC cell migration and invasion, and the expression of the typical epithelial-mesenchymal transition markers E-cadherin, Vimentin, N-cadherin, and Snail1, suggesting that PYCR1 may be critical for NSCLC aggressiveness and a potential target for treating NSCLC (39). Accordingly, lung adenocarcinoma cell sensibility to cisplatin increased upon PYCR1 silencing, further supporting the idea that PYCR1 is a potential therapeutic target for lung adenocarcinoma (40). Finally, recent findings showed a correlation between cancer cells that have mutation in isocitrate dehydrogenase 1 (IDH1) and increased PYCR1 expression and Proline levels (41).

Altogether, these findings further support a critical role of Proline biosynthesis genes in cancer development and progression, independently of the tumor type.

Transcriptional and Post-translational Regulation of PYCR1 and ALDH18A1 in Cancer

Recent studies on the role of Proline biosynthetic enzymes in neuroblastoma (NB) progression unravel a novel mechanism of transcriptional regulation of the genes coding for these enzymes (42). Specifically, myeloid zinc finger 1 (MZF1) and MZF1 antisense RNA1 (MZF1-AS1) have been identified as transcriptional regulators of ALDH18A1 and PYCR1. MZF1 induces the expression of ALDH18A1 and PYCR1, promoting NB aggressiveness. Mechanistically, MZF1AS1 promotes the up-regulation of both MZF1 and of other oncogenic genes through the interaction with poly(ADP-ribose) polymerase 1 (PARP1), thus facilitating its interaction with E2F transcription factor 1 (E2F1). Interestingly, MZF1, MZF1AS1, PARP1, and E2F1 are all associated with poor prognosis of NB patients, and blocking MZF1AS1 and PARP1 interaction, using a small peptide, or targeting MZF1AS1 suppresses Proline synthesis and tuomorigenesis, thus representing potential targets for NB therapy (42).

Recently, a lncRNA *TRPM2-AS*/*miR-140-3p*/PYCR1 axis has been described in BC, which regulates cell proliferation and apoptosis. Specifically, while TRPM2-AS and PYCR1 are both overexpressed in BC, *miR-140-3p* is downregulated and directly targets both TRPM2-AS and PYCR1 (43).

To date the knowledge on PYCR1 post-translational regulation is still poor. Recently, it has been shown that SIRT3, a mitochondrial NAD^+-dependent deacetylase involved in the regulation of several metabolic pathways, interacts with PYCR1 both *in vitro* and *in vivo*. Acetylation of PYCR1 at K288 residue by cAMP response element- binding protein (CREB binding protein, CBP) acetylase reduces its activity and leads to inhibition of cell proliferation. These findings link Proline metabolism with SIRT3 and CBP and cell growth, and suggest that this axis may be a potential target for cancer therapy (44).

Finally, expression of P5CS, PYCR1/2/L is increased by c-MYC and PI3K signaling in luminal B breast cancer (28) as was previously shown in cultured cancer cells after ectopic expression of c-MYC (77).

PROLINE AVAILABILITY CONTROLS CANCER CELL BEHAVIOR

The emerging evidences that increased PYCR1 and ALDH18A1 expression is a poor prognosis factor in different tumor types are robust and convincing, and suggest an increased need of Proline biosynthesis in cancer cells. Proline can be used by cancer cells as energy source and/or as precursor of protein synthesis. An interesting finding regarding the requirement of Proline for proteinogenesis has been reported by Loayzcha-Puch and colleagues (78). The authors developed a protocol to measure differential ribosome codon reading (diricore), which is based on ribosome profiling measurements. The study reports a striking contrast between the diricore of cancer and normal surrounding kidney tissues and provides evidence for a cancer cells-specific limitation of Proline-tRNA availability for protein synthesis (78). These findings are complemented by the observation that PYCR1 gene is induced in cancer cells, likely as a compensatory feedback mechanism against a condition of Proline shortage. This can be provoked either by a reduced availability of exogenous Proline and Proline metabolic precursors (Glutamine and Glutamate), by a sudden increase of Proline consumption for proteogenic and energetic purposes and/or by both, i.e., an increased requirement with a reduced availability. The

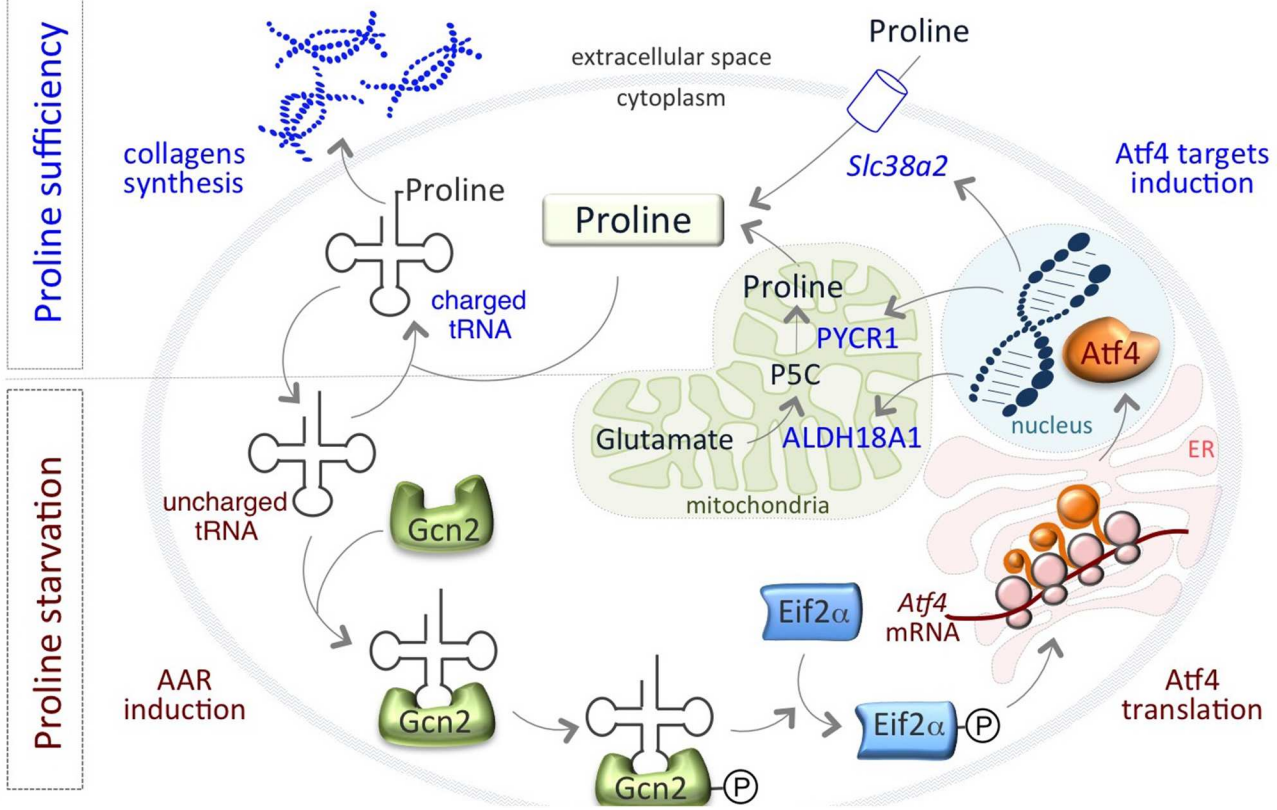

FIGURE 1 | An autoregulatory loop controls Proline biosynthesis. Proline biosynthetic enzymes, ALDH18A1 and PYCR1 are under the control of the amino acid starvation pathway (AAR-ATF4). Under Proline limiting conditions, uncharged tRNAs accumulate and activate/phosphorylate Gcn2-eIF2α inducing the expression of the transcription factor ATF4, which in turn activates the expression of PYCR1, ALDH18A1, and the amino acid transporter *Slc38a2/SNAT2* genes. When Proline levels increases, tRNAs are charged and AAR-ATF4 pathway is relieved.

requirement of PYCR1 activity for tumor growth, further support the idea that Proline availability controls cancer progression (78). Interestingly, Proline restriction is not an unique feature of kidney cancer cells, but also of breast cancer cells (78), thus raising the possibility that it may be a common feature of different tumors types. Accordingly, some cancer cell lines are starved of Proline and depend on exogenous Proline to restore their clonogenic potential, and resolve endoplasmic reticulum (ER) stress (79).

Remarkably, a finely regulated growth-limiting starvation of Proline is also a feature of mouse pluripotent embryonic stem cells (ESCs), which is required to preserve ESC identity. We have recently showed that the amino acid stress response (AAR)-ATF4 pathway, which is sensitive to nutrient starvation through the presence of uncharged tRNAs, is active in ESCs and controls the expression of the Proline biosynthesis genes *Aldh18a1* and *Pycr1* (80) (**Figure 1**). This generates an autoregulatory loop by which ATF4 induces Proline synthesis/accumulation, which in turn down regulates ATF4 through the relief of the AAR pathway (**Figure 1**). Interestingly, also the amino acid transporter *Slc38a2/Snat2,* which madiates Proline uptake in ESCs (81), is an ATF4 target gene (82, 83) (**Figure 1**). This autoregulatory loop causes a specific shortage of Proline that preserves ESC behavior/identity. When Proline levels suddenly increase, for instance as a consequence of Proline supplementation, the prolyl-tRNA is loaded and the synthesis of Proline-rich proteins, such as collagens, is induced (80). Consequent to the rapid increase of Proline availability, mESCs undergo a phenotypic transition named embryonic-stem-to-mesenchymal like transition (esMT). During esMT, the cells acquire mesenchymal-like, motile and invasive features, resembling the main characteristics of the migrating cancer cells (80, 84). Remarkably, pharmacological blocking of the prolyl-tRNA synthetase activity with the specific inhibitor halofuginone (85, 86) antagonizes Proline-induced esMT (80). These findings, together with the observations that the prolyl-tRNA synthetase-coding gene (26) and the transcription factor ATF4 (73) are overexpressed in different tumor types, and promote cancer metabolic homeostasis and survival (74) (**Table 1**), point to the key role of Proline availability in regulating protein synthesis, which sustains cancer cell proliferation and preserves stem cell identity. Tumor cells undergo metabolic reprograming that may restrict the availability of specific amino acids. Thus, sensing of amino acid availability by different pathways, including mTOR and

AAR-ATF4 pathways, is crucial for cancer development, mainly by controlling the efficiency of protein synthesis and in particular of Proline-rich protein such as collagens.

COLLAGEN-PROLYL HYDROXYLATION IN CANCER PROGRESSION

Tumor microenvironment and remodeling of the extracellular matrix (ECM) have gained increasing interest as mechanisms that contribute to the development of many solid tumors and in particular, to the reprogramming of cancer cells, conferring them with aggressive features, e.g., invasiveness, ability to undergo EMT and therapeutic resistance (87–89). Collagen is the most abundant protein in the human body and is the principal component of ECM. In this view, collagen biosynthesis, and maturation play a critical role. About 25% of the amino acids in collagen are incorporated as Proline and half of them are hydroxylated by a group of Fe^{2+} αKG/VitC- dependent dioxygenases, the prolyl-4-hydroxylase (P4H), within the endoplasmic reticulum (ER) (90). Hydroxylation of Proline residues is a critical modification required to stabilize the triple helix of collagens. It is thus reasonable to expect that incorporation of Proline into collagen may have metabolic consequences. P4H enzymes are tetramers made of 2α catalytic subunits and 2β subunits, and the genes encoding for these enzymes have been implicated in cancer progression (**Table 1**). High levels of P4HA2 correlate with poor prognosis in glioma, and P4HA2 knockdown blocks glioma cells proliferation, migration and acquisition of EMT-like phenotypes (58). Overexpression of P4HA2 has been implicated also in cervical cancer (59); papillary thyroid cancer (60); B-cell lymphoma (61); oral cavity squamous cell carcinoma development and recurrence (62, 63). P4HA2 is correlated to liver fibrosis and hepatocellular carcinoma (HCC) (64). Interestingly, TCGA database analysis reveal higher levels of P4HA2 in HCC patients with a shorter overall survival and a higher cancer grade (65). P4HA2 is thus emerging as a potential target for the development of novel therapeutic anti-cancer strategies. Elevated P4HA2 and 1 predict patient mortality in human breast cancers (48, 66). Moreover, prolyl hydroxylase gene expression is induced by hypoxia and promotes invasiveness and lung metastasis (48). Conversely, depletion of P4HA2 inhibited BC cell proliferation and invasiveness *in vitro* and *in vivo*, by reducing collagen deposition (66). P4HA2 has been recently reported to play a role in the progression of breast ductal carcinoma *in situ* (DCIS) (67). Furthermore, high levels of P4HA2 has been associated with decreased survival in a breast cancer dataset with almost 2000 patients, and is an independent predictor of disease outcome with respect to standard clinopathological parameters (57). Accordingly, silencing of P4HA2 converted Triple Negative Breast Cancer (TNBC) cells to a more epithelial phenotype, and reduces invasiveness in a 3D organotypic culture (57).

Deregulated P4HA1 expression has been also implicated in cancer development and progression. P4HA1 expression is induced in TNBC and correlates with short relapse-free survival in patients treated with chemotherapy (49). The authors show that P4HA1 promotes HIF1α-dependent cancer stemness and chemoresistance by reducing the availability of α-KG, and support the idea that P4H is a promising target to inhibit tumor progression and sensitize TNBC to chemotherapy (49). Elevated P4HA1 expression was recently described in pancreatic ductal adenocarcinoma (PDAC) and predicts poor prognosis. Of note, the authors found a P4HA1-HIF1α positive feedback loop, which regulates the glycolytic and oncogenic activities of PDAC, their stemness and chemoresistance (50). Additionally, high P4HA1 expression is a poor prognostic factor for head and neck squamous cell carcinoma (51), oral squamous cell carcinoma (52), and prostate cancer (53). In ovarian cancer P4HA1 promotes migration, invasion, EMT and metastasis formation (54). In glioma, P4HA1 promotes the transdifferentiation of glioma stem cells into endothelial cells leading to the formation of vascular basement membranes (55) and has been considered as a prognostic marker for high-grade glioma (56).

Prolyl-4 hydroxylases beta polypeptide (P4HB) is the beta subunit of P4H and belongs to the family of protein disulfide isomerase (PDI), which acts as chaperone in the ER to inhibit the aggregation of misfolded proteins. P4HB is overexpressed in different types of tumors, such as hepatocellular carcinoma (68), non-small-cell lung cancer (69), and in gastric cancer (GC) for which it has been considered to have a prognostic value (70). High levels are mainly associated with invasiveness and lymphatic metastases of cancers (71). Zhang et al. suggested a correlation between hypoxia/hypoxic microenvironment, which plays critical roles in the process of EMT, and P4HB in the context of GC. Specifically, HIF-1α up-regulates P4HB expression in gastric cancer and together they cooperate to promote GC invasion and metastases (72).

In line with the idea that collagen hydroxylation and maturation underlie tumor progression and metastasis formation, PLOD1/2 and LEPREL4 genes, which are both involved in collagen biosynthesis, are upregulated in 19 different tumor types, (26) (**Table 1**).

Interestingly, recent phosphoproteomic analysis reveal that P4HA2 and P4HB are targets of the tyrosine kinase PKDCC/VLK, which phosphorylates a broad range of secreted and ER-located proteins (91). Of note, PKDCC/VLK is one of the most up regulated genes in Proline-induced esMT (80, 84).

In most cases, P4H expression has been linked to the acquisition of mesenchymal/invasive features and metastasis formation. In particular, (i) the accumulation/deposition of collagen near tumors has been associated with metastasis formation, (ii) inhibition of P4H reduces tumor aggressiveness both *in vitro* and *in vivo*. Despite extensive studies, the mechanisms underlying P4H-dependent tumor aggressiveness are still poorly understood.

COLLAGEN-EPIGENETIC INTERPLAY IN CANCER CELL IDENTITY AND PLASTICITY

Increased collagen synthesis and maturation may in turn influence cancer cell growth and behavior by acting at different levels. The most studied role of collagen processing in tumors

development/progression is focused on its downstream signaling. Different signaling pathways control synthesis/accumulation of collagens, including TGFβ. In the context of TGFβ-dependent activation of fibroblast and consequent production and secretion of matrix protein and wound healing, TGFβ promotes Proline biosynthesis in a SMAD4-dependent manner, to support collagen production (92). Collagens interact with specific receptors, e.g., discoidin domain receptors (DDRs) and integrins, and in turn activate downstream pathways including ERK, PI3K/AKT - NFkB, Focal adhesion kinase (FAK) and enhance migration and promotion of EMT. This complex, context- specific role of collagen signaling in cancer development and progression has been extensively investigated and recently reviewed (93).

It is now evident that signals from the microenvironment influence cancer cell behavior, and that tumor microenvironment, including ECM composition, largely influences tumor progression. Indeed, the changing in the ECM mechanical properties, the increased collagen deposition and stiffness influence cell plasticity, endowing cancer cells with elevated invasiveness, migration and metastatic dissemination properties (87–89). In this context, it has been recently shown that epigenetic silencing of the tumor suppressor RASSF1A in lung cancer induces P4HA2 expression, which leads to increased collagen deposition, ECM stiffness and triggers metastatic dissemination (94). An interesting interplay between Proline metabolism/collagen synthesis and microenvironment has been reported in a recent study on lung cancer, where the authors show the interaction of PYCR1 in the mitochondria with Kindlin-2, a protein critical for integrin-mediated cell-ECM adhesion. When ECM stiffness rises, as in cancer, Kindlin-2 translocates in the mithocondria where it interacts with PYCR1, increasing PYCR1 and proline levels. Kindlin-2 KD reduces PYCR1 levels and ECM stiffening-dependent increase of Proline synthesis. *In vivo* Kindlin-2 ablation strongly reduces PYCR1 and Proline levels, fibrosis, tumor growth and mortality rate (95).

The aforementioned mechanisms allow cancer cells to survive and adjust to rapid, transient changes. Genetic mutations do not explain the heterogeneity/plasticity of cancer cells, which can be better explained by metabolic, epigenetic mechanisms. In this respect, we have recently proposed a novel mechanism underlying cancer cells plasticity by which collagen maturation may act as an epigenetic signal (57). Data provided in recently published papers underscore the existence of a functional link between Proline metabolism and epigenetic remodeling (84, 96, 97) and demonstrate that Proline availability influences mouse embryonic stem cell (mESC) identity and behavior through modulating AAR-ATF4 pathway (see above paragraph *Proline availability controls cancer cell behavior*). Of particular relevance is the finding that a sudden increase of Proline availability in mESCs induces a mesenchymal-like transition (esMT), which resembles the EMT that occurs at the invasive border of metastatic tumors (80, 84). This phenotypic transition is accompanied with metabolic and epigenetic changes similar to that observed in cancer cells. First, the acquisition of mesenchymal-like invasive features in Proline-treated ESCs (PiCs) is accompanied by a metabolic reprogramming shift from a bivalent to a glycolytic metabolism. Furthermore, esMT is accompanied by epigenetic remodeling, which results in a genome-wide increase of DNA and histone methylation (84, 98). While several metabolites act as cofactors or substrates of epigenetic enzymes and may thus influence the epigenetic landscape (99), a different mechanism has been recently proposed underlying Proline's epigenetic activity, which relies on collagen synthesis/maturation that requires Vitamin C (VitC) (**Figure 2**) (57). Following this model, consequently to a rapid increase of Proline-dependent collagen synthesis, the activity of Prolyl-hydroxylase (P4h) enzymes for collagen maturation, consumes VitC in the ER. This results in a reduced nuclear availability of VitC, which becomes limiting for the VitC/ αKG /Fe^{+2}-dependent epigenetic enzymes, i.e., the JumonjiC-domain containing (JmjC) histone dioxygenases and the Ten-eleven Translocation (Tet) DNA demethylases, and determines a genome-wide increase of histones and DNA methylation (57, 98) (**Figure 2**). This functional interplay between P4H and JmjC/Tet enzymes explains, at least in part, the mechanism through which Proline induces the epigenetic remodeling associated with reversible esMT/MesT (57, 98). This previously unexplored functional interplay between Proline metabolism/collagen hydroxylation and epigenetic remodeling is not unique of ESCs but similarly occurs in cancer cells and contribute to breast cancer cell plasticity and metastatic progression (57) (**Figure 2**).

These findings lead us to hypothesize the existence of a Proline metabolism-dependent cycle of collagen synthesis and degradation in the same cell (**Figure 2**). Concomitant to continuous synthesis and maturation of collagen inside the cells, which promotes cancer cell invasiveness, collagen is degraded in the tumor microenvironment through the activity of the metalloproteinases (MMPs) and collagenases. This serves as reservoir of free extracellular Proline that in turn is taken up by the cell and used for protein synthesis/collagen biosynthesis, potentiating the cycle itself, and causing the epigenetic remodeling (**Figure 2**). Interestingly, genes encoding for MMP9, 1 and 13 and PREP, involved in proteins/collagen degradation are overexpressed in many different tumor types (26) (**Table 1**). Additional crucial enzymes required for collagen degradation and uptake may also contribute to the regeneration of this cycle, including prolidases (100), which hydrolyzes di- or tri-peptides with C-terminal Proline or hydroxyproline residues, and other collagenases.

In this context, interesting findings have been recently reported in pancreatic ductal adenocarcinoma (PDAC), which is characterized by cells organized in gland-like structures embedded in a dense collagen meshwork, which limits the delivery of nutrients and oxygen (101). Under nutrients starvation, PDAC cells can survive by using collagen-derived Proline as a source of energy. In fact, PDAC cells express Proline metabolic enzymes and are able to uptake collagen both through macropinocytosis (102) and uPARAP/Endo180 collagen receptor (101). Tracer experiments showed that upon collagen uptake, free Proline primarily contributes to biomass through incorporation into proteins, while only at small ratio in non-protein metabolic compartments. Genetic and pharmacological inhibition of PRODH, whose expression is increased in PDAC, significantly

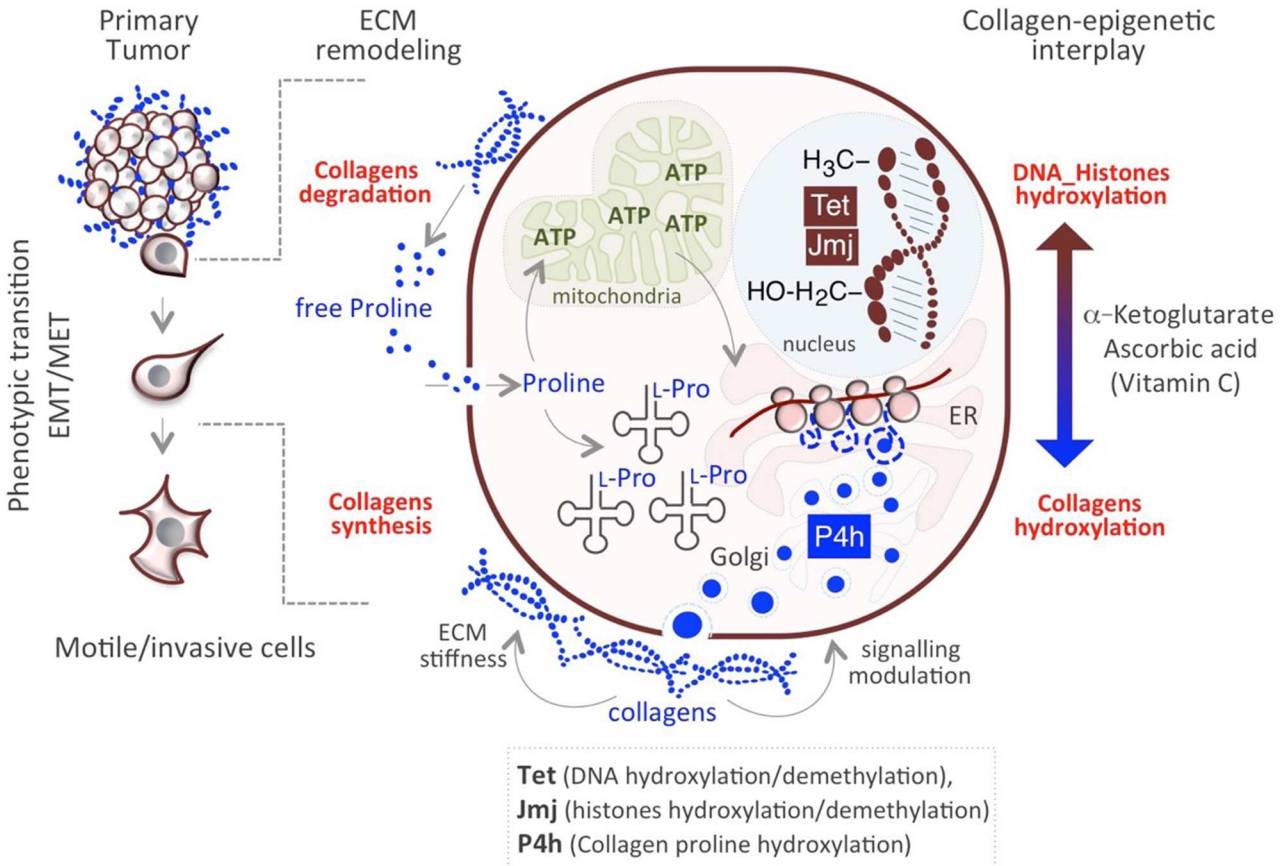

FIGURE 2 | Impact of Proline/Epigenetic axis on tumor progression. Extracellular Proline released from collagen degradation influences cell identity/behavior at different levels. Proline may serve as (i) energy source (ATP) through degradation in the mitochondria and (ii) building block for collagens synthesis. Nascent collagens are hydroxylated in the ER through the activity of Prolyl-4-hydroxylases (P4h) and secreted in the ECM. A sudden increase of collagen synthesis/hydroxylation provokes a compartmentalized (ER->nucleus) metabolic perturbation of the substrates/cofactors (VitC and/or α-KG) of DNA/Histone hydroxylases (Tet, JMJ).

reduces PDAC cells clonogenicity *in vitro*, which is rescued by exogenous Proline, and strongly reduces pancreatic tumor growth *in vivo* (101). The authors suggest that collagen-derived Proline may promote cancer cell survival and proliferation through TCA cycle metabolism and cellular respiration; however, it would be interesting to investigate the fate of collagen-derived free Proline to protein synthesis as an additional/alternative mechanism of PDAC cells survival and invasiveness.

POTENTIAL THERAPEUTIC STRATEGIES TARGETING PROLINE METABOLISM IN CANCER

The critical role of Proline on cancer cell identity and behavior prompted researchers to develop novel therapeutic anti-cancer strategies targeting different levels of Proline metabolism (**Figure 3**). Among them, halofuginone (HF) holds great promise. HF is a derivative of febrifugine, a fundamental herb of traditional Chinese medicine, used to treat malaria for almost 2,000 years. HF binds the glutamyl-prolyl-tRNA synthetase (EPRS) and inhibits prolyl-tRNA formation (tRNA loading) (85, 86). This inhibition leads to the activation of the aminoacid stress response (AAR) pathway, which senses amino acid restriction through the accumulation of uncharged tRNAs, phosphorylation of Gcn2-eIF2α, and ATF4 expression (80). Increased levels of ATF4 activates the transcription of a set of genes that are crucial for the adaptation of cells to a stress environment (103). HF-dependent inhibition is reversed by exogenous supplementation of Proline.

HF has gained increasing interest for its potential application in the treatment of fibrosis and cancer since many studies have demonstrated its efficacy in inhibiting growth and progression of many types of tumors, mainly reducing collagen, and stroma accumulation, metalloproteinases, angiogenesis, and immune responses. In glioma tumors HF reduces collagen accumulation (104), in leiomyoma HF reduces cell proliferation *in vitro* (105) and *in vivo* (106); in bladder carcinoma HF inhibits angiogenesis, tumor stroma and growth (107). HF disrupts the stromal barriers also in PDAC, and modulates the immune response, leading to reduced tumor volume (108), and reduced subcutaneous pancreatic tumor development in a xenograft model (109). HF

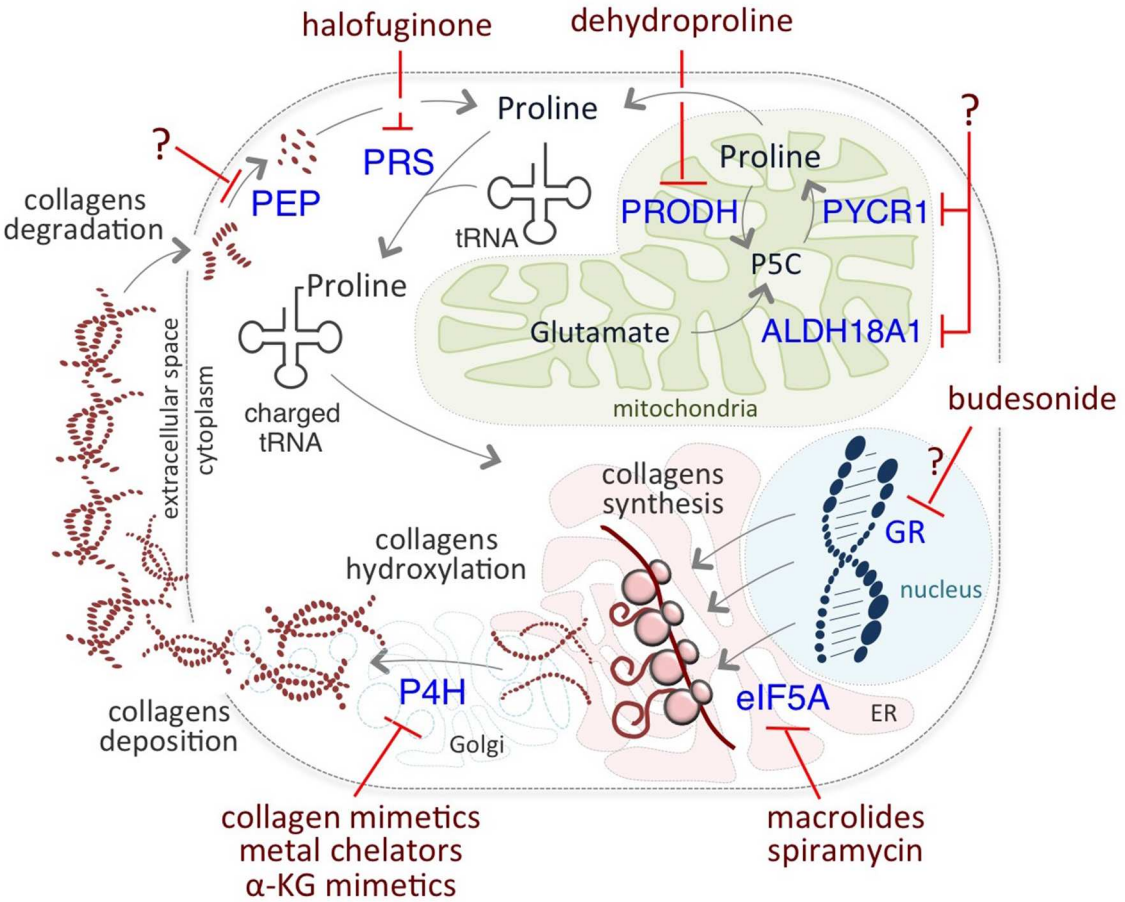

FIGURE 3 | Putative therapeutic targets of Proline metabolism. Halofuginone (HF) binds to the glutamyl-prolyl-tRNA synthetase (PRS) and inhibits the prolyl-tRNA loading, reducing Proline-rich protein synthesis, such as collagens. Inhibitors of P4H enzymes include collagen mimetics, metal chelators, and α-KG mimetic. Macrolides, such as Spiramycin, inhibit the translation of mRNAs coding for Proline- rich stretches/motifs by blocking the elongation (eIF5A) of Proline- rich polypeptides. Budesonide reduces collagen synthesis and maturation, most likely acting as a GR antagonist. Dehydroproline (DHP) and L-tetrahydro-2-furoic acid (L-THFA) is a PRODH/POX inhibitor.

efficacy has been reported on prostate cancer growth *in vivo* (110) and on pheochromocytoma with vasculature reduction (111). Independent studies indicate that HF inhibits breast cancer growth by different mechanisms, including the induction of ROS production, which in turn activate apoptosis, and the inhibition of cell migration by down regulation of the matrix metalloproteinase 9 (MMP9) (112), or through activation of autophagy (113). HF reduces breast and prostate bone metastasis, by inhibiting TGFβ- and BMP- signaling (114). Recently, HF has been found to block breast cancer cells growth by controlling the exosome production of miRNAs involved in cell cycle and growth control (115). HF blocks colorectal cancer growth *in vitro* and *in vivo* through inhibition of AKT/mTORC1 pathway (116) and induction of autophagy under nutrient-rich conditions, and inhibition of autophagy under nutrient- poor conditions (117). HF suppresses HCC growth and progression (118, 119), lung metastasis by decreasing MMP activity (120). HF suppresses acute promyelocytic leukemia cell proliferation and promotes apoptosis (121), resulting in hematological remission *in vivo* (122); and inhibits multiple myeloma cell proliferation (123). HF augmented the sensitivity of different cancer cell lines to radiotherapy (124) and enhances the chemo-sensitivity of cancer cells (125), HF potentiates the radiotherapy effects of Lewis lung cancer cell *in vitro* and *in vivo* (126), reverting radiotherapy-dependent induction of TGFβ and EMT (127). HF is effective for the treatment of metastatic brain tumors (128), reduces melanoma bone metastasis, (129). Hence some pre- clinic models (130), and phase I and II clinical trials have been developed (131), showing the great potential of this molecule for cancer treatment.

The elongation factor P (EF-P, also known as eIF5A) is implicated in the translation of mRNAs coding for Proline- rich stretches/motifs (132, 133). Of note, eIF5A was associated to development of human cancers, and considered as an oncogene (47), and a potential therapeutic target (**Table 1**).

Macrolide antibiotics have been proposed as potential therapeutic targets relevant for inhibition of Proline-rich protein synthesis. Accordingly, it has been recently reported that macrolides can induce ribosome stalling, blocking the elongation

of Proline- rich polypeptides (134). Interestingly, the macrolide Spiramycin is a potent inhibitor of Proline- induced esMT (57), suggesting that it may exert anti metastatic activities although it has not been yet tested in the cancer cell models.

Based on the well-known role of TGFβ in inducing collagens gene expression, other potential therapeutic targets that must be included in this section, as an extension of Proline metabolism targets for cancer treatment, are TGFβ inhibitors, which are the focus of many research projects and clinical trials (135).

The findings that collagen hydroxylation enzymes play a key role in cancer progression, and that their expression positively correlates with patient mortality, encouraged development of chemical inhibitors of P4H enzymes. These include metal ions and chelators, mimetics of the co-substrate α-KG, and collagen mimetic peptides. However, so far the majority of them have shown low clinical relevance, mainly because of high toxicity and/or low efficacy *in vivo* (136), suggesting that although promising, this field still needs further investigations.

In a very recent study, Budesonide, which is a drug commonly used to treat asthma and reduce collagen in pathological fibrotic conditions, has been identified as a candidate for the treatment of metastatic cancer (57). Indeed, Budesonide has been identified in a high-through-put phenotypic screening of 1200 FDA-approved drugs searching for esMT inhibitors. Budesonide not only antagonizes Proline-dependent esMT but also impairs the acquisition of mesenchymal and motile/invasive features in human lung and breast cancer cell lines, reducing collagen synthesis/accumulation *in vitro*. Furthermore, Budesonide impairs ECM and collagen accumulation in an orthotopic model of human breast cancer development *in vivo* and reduces metastasis formation (57). Although the mechanism of action of Budesonide is still far from fully elucidated, it may act as a glucocorticoid receptor (GR) antagonist. Interestingly, asthmatic patients under long-term treatment with Budesonide show reduced risk to develop pancreatic ductal adenocarcinoma (137). Moreover, Budesonide has been recently identified, using a combined connectivity mapping and pharmacoepidemiology approach, as a potential treatment for preventing breast cancer (138). Finally, by blocking collagen synthesis and hydroxylation in the ER, Budesonide increases VitC availability in the nucleus, resulting in epigenetic remodeling, i.e., a global reduction of DNA and histone methylation levels (57), thus showing its potential for targeting cancer cell plasticity and identity.

Finally, PYCR1 is considered a potential therapeutic target in HCC (27) and in BC (31) but so far, specific inhibitors of PYCR1 are not available.

CONCLUSIONS AND PERSPECTIVES

Proline is abundantly incorporated into collagen and provides the structural strength in higher animals. Besides this well-know function of Proline/collagen, increasing attention has been drawn to the impact of Proline and collagen metabolism, i.e., collagen synthesis/hydroxylation and degradation, on cell identity and behavior (14, 57). In this context, our recent findings that VitC-dependent collagen hydroxylation influences the epigenetic landscape and contributes to cellular plasticity (57) open new and important perspectives.

It has been proposed that oncogenic mutations may perturb the function of metabolic enzymes, which may in turn act as oncogenes. We suggest that such mutations, along with cancer cell metabolic reprogramming, may alter the availability of specific metabolites/cofactors required by epigenetic enzymes, e.g., Vitamin C, and alter the epigenetic signature of cancer cells causing, at least in part, tumor heterogeneity.

Following our proposed model, a functional interplay between Proline metabolism/collagen biosynthesis and epigenetic remodeling may generate a cycle based on the concomitant collagen synthesis and degradation, which sustains the cycle itself and controls cancer cell plasticity and behavior. Development of therapeutic strategies targeting this metabolic axis may provide novel options to target cancer cell heterogeneity.

A critical aspect is that proliferating cancer cells develop significant metabolic heterogeneity in order to survive to changing microenvironment (5). This heterogeneity is of particular relevance when envisioning therapeutic strategies and represents the main roadblock to attempts to control cell proliferation. The combination of cocktails of drugs that target metabolic pathways at different levels may represent a successful strategy to ultimately eradicate metastasizing cancer cells. In this context, several therapeutic strategies have been proposed that target Proline metabolism at different levels, including inhibitors at the level of prolyl-tRNA synthetase/collagen synthesis and collagen prolyl-hydroxylation. Although these options hold great promise, further investigations and clinical applications are needed to validate potential efficacy.

AUTHOR CONTRIBUTIONS

CD'A prepared the draft of the manuscript with input from all the authors. EP designed and prepared the figures. EP, JP, and GM revised the draft. All authors read, edited and approved the final manuscript.

FUNDING

This study was supported by AIRC (IG 20736), Project SATIN-POR Campania FESR 2014/2020 and MIUR project PRIN 2017XJ38A4 to GM. JP was supported as Scientist Emeritus by the Office of the Chief, MCGP, CCR, NCI at Frederick.

ACKNOWLEDGMENTS

We apologize to those whose work has not been cited.

REFERENCES

1. Gupta PB, Pastushenko I, Skibinski A, Blanpain C, Kuperwasser C. Phenotypic plasticity: driver of cancer initiation, progression, and therapy resistance. *Cell Stem Cell.* (2019) 24:65–78. doi: 10.1016/j.stem.2018.11.011
2. Saygin C, Matei D, Majeti R, Reizes O, and Lathia JD. Targeting cancer stemness in the clinic: from hype to hope. *Cell Stem Cell.* (2019) 24:25–40. doi: 10.1016/j.stem.2018.11.017
3. Valastyan S, Weinberg RA. Tumor metastasis: molecular insights and evolving paradigms. *Cell.* (2011) 147:275–92. doi: 10.1016/j.cell.2011.09.024
4. Pastushenko I, Brisebarre A, Sifrim A, Fioramonti M, Revenco T, Boumahdi S, et al. Identification of the tumour transition states occurring during EMT. *Nature.* (2018) 556:463–8. doi: 10.1038/s41586-018-0040-3
5. Pavlova NN, Thompson CB. The emerging hallmarks of cancer metabolism. *Cell Metab.* (2016) 23:27–47. doi: 10.1016/j.cmet.2015.12.006
6. Geck RC, Toker A. Nonessential amino acid metabolism in breast cancer. *Adv Biol Regul.* (2016) 62:11–17. doi: 10.1016/j.jbior.2016.01.001
7. Choi BH, Coloff JL. The diverse functions of non-essential amino acids in cancer. *Cancers.* (2019) 11:675. doi: 10.3390/cancers11050675
8. Liu W, Hancock CN, Fischer JW, Harman M, Phang JM. Proline biosynthesis augments tumor cell growth and aerobic glycolysis: involvement of pyridine nucleotides. *Sci Rep.* (2015) 5:17206. doi: 10.1038/srep17206
9. Page-McCaw, Ewald AJ, Werb Z. Matrix metalloproteinases and the regulation of tissue remodelling. *Nat Rev Mol Cell Biol.* (2007) 8:221–33. doi: 10.1038/nrm2125
10. Phang JM, Liu W, Hancock CN, Fischer JW. Proline metabolism and cancer: emerging links to glutamine and collagen. *Curr Opin Clin Nutr Metab Care.* (2015) 18:71–7. doi: 10.1097/MCO.0000000000000121
11. Phang JM, Liu W. Proline metabolism and cancer. *Front Biosci.* (2012) 17:1835–45. doi: 10.2741/4022
12. Phang JM. The regulatory functions of proline and pyrroline-5-carboxylic acid. *Curr Top Cell Regul.* (1985) 25:91–132. doi: 10.1016/B978-0-12-152825-6.50008-4
13. Huynh TYL, Zareba I, Baszanowska W, Lewoniewska S, Palka J. Understanding the role of key amino acids in regulation of proline dehydrogenase/proline oxidase. (prodh/pox)-dependent apoptosis/autophagy as an approach to targeted cancer therapy. *Mol Cell Biochem.* (2020) 466:35–44. doi: 10.1007/s11010-020-03685-y
14. Phang JM. Proline metabolism in cell regulation and cancer biology: recent advances and hypotheses. *Antioxid Redox Signal.* (2019) 30:635–49. doi: 10.1089/ars.2017.7350
15. Maxwell SA, Davis GE. Differential gene expression in p53-mediated apoptosis-resistant vs. apoptosis-sensitive tumor cell lines. *Proc Natl Acad Sci USA.* (2000) 97:13009–14. doi: 10.1073/pnas.230445997
16. Maxwell SA, Rivera A. Proline oxidase induces apoptosis in tumor cells, and its expression is frequently absent or reduced in renal carcinomas. *J Biol Chem.* (2003) 278:9784–9. doi: 10.1074/jbc.M210012200
17. Donald SP, Sun XY, Hu CA, Yu J, Mei JM, Valle D, Phang JM. Proline oxidase, encoded by p53-induced gene-6, catalyzes the generation of proline-dependent reactive oxygen species. *Cancer Res.* (2001) 61:1810–5.
18. Polyak K, Xia Y, Zweier JL, Kinzler KW, Vogelstein B. A model for p53-induced apoptosis. *Nature.* (1997) 389:300–5. doi: 10.1038/38525
19. Liu W, Zabirnyk O, Wang H, Shiao YH, Nickerson ML, Khalil S, et al. miR-23b targets proline oxidase, a novel tumor suppressor protein in renal cancer. *Oncogene.* (2010) 29:4914–24. doi: 10.1038/onc.2010.237
20. Phang JM, Liu W, Zabirnyk O. Proline metabolism and microenvironmental stress. *Annu Rev Nutr.* (2010) 30:441–63. doi: 10.1146/annurev.nutr.012809.104638
21. Tang L, Zeng J, Geng P, Fang C, Wang Y, Sun M, et al. Global metabolic profiling identifies a pivotal role of proline and hydroxyproline metabolism in supporting hypoxic response in hepatocellular carcinoma. *Clin Cancer Res.* (2018) 24:474–85. doi: 10.1158/1078-0432.CCR-17-1707
22. Liu Y, Borchert GL, Donald SP, Diwan BA, Anver M, Phang JM. Proline oxidase functions as a mitochondrial tumor suppressor in human cancers. *Cancer Res.* (2009) 69:6414–22. doi: 10.1158/0008-5472.CAN-09-1223
23. Liu W, Phang JM. Proline dehydrogenase. (oxidase), a mitochondrial tumor suppressor, and autophagy under the hypoxia microenvironment. *Autophagy.* (2012) 8:1407–9. doi: 10.4161/auto.21152
24. Liu W, Phang JM. Proline dehydrogenase. (oxidase) in cancer. *Biofactors.* (2012) 38:398–406. doi: 10.1002/biof.1036
25. Elia I, Broekaert D, Christen S, Boon R, Radaelli E, Orth MF, et al. Proline metabolism supports metastasis formation and could be inhibited to selectively target metastasizing cancer cells. *Nat Commun.* (2017) 8:15267. doi: 10.1038/ncomms15267
26. Nilsson R, Jain M, Madhusudhan N, Sheppard NG, Strittmatter L, Kampf C, et al. Metabolic enzyme expression highlights a key role for MTHFD2 and the mitochondrial folate pathway in cancer. *Nat Commun.* (2014) 5:3128. doi: 10.1038/ncomms4128
27. Ding Z, Ericksen RE, Escande-Beillard N, Lee QY, Loh A, Denil S, et al. Metabolic pathway analyses identify proline biosynthesis pathway as a promoter of liver tumorigenesis. *J Hepatol.* (2019) 72:725–35. doi: 10.1016/j.jhep.2019.10.026
28. Craze ML, Cheung H, Jewa N, Coimbra NDM, Soria D, El-Ansari R, et al. MYC regulation of glutamine-proline regulatory axis is key in luminal B breast cancer. *Br J Cancer.* (2018) 118:258–65. doi: 10.1038/bjc.2017.387
29. Liu M, Wang Y, Yang C, Ruan Y, Bai C, Chu Q, et al. Inhibiting both proline biosynthesis and lipogenesis synergistically suppresses tumor growth. *J Exp Med.* (2020) 217:e20191226. doi: 10.1084/jem.20191226
30. Zhuang J, Song Y, Ye Y, He S, Ma X, Zhang M, et al. PYCR1 interference inhibits cell growth and survival via c-Jun N-terminal kinase/insulin receptor substrate 1. (JNK/IRS1) pathway in hepatocellular cancer. *J Transl Med.* (2019) 17:343. doi: 10.1186/s12967-019-2091-0
31. Ding J, Kuo ML, Su L, Xue L, Luh F, Zhang H, et al. Human mitochondrial pyrroline-5-carboxylate reductase 1 promotes invasiveness and impacts survival in breast cancers. *Carcinogenesis.* (2017) 38:519–31. doi: 10.1093/carcin/bgx022
32. Choi UY, Lee JJ, Park A, Zhu W, Lee HR, Choi YJ, et al. Oncogenic human herpesvirus hijacks proline metabolism for tumorigenesis. *Proc Natl Acad Sci USA.* (2020) 117:8083–93. doi: 10.1073/pnas.1918607117
33. Zeng T, Zhu L, Liao M, Zhuo W, Yang S, Wu W, et al. Knockdown of PYCR1 inhibits cell proliferation and colony formation via cell cycle arrest and apoptosis in prostate cancer. *Med Oncol.* (2017) 34:27. doi: 10.1007/s12032-016-0870-5
34. Weijin F, Zhibin X, Shengfeng Z, Xiaoli Y, Qijian D, Jiayi L, et al. The clinical significance of PYCR1 expression in renal cell carcinoma. *Medicine.* (2019) 98:e16384. doi: 10.1097/MD.0000000000016384
35. Wang QL, Liu L. PYCR1 is associated with papillary renal cell carcinoma progression. *Open Med.* (2019) 14:586–92. doi: 10.1515/med-2019-0066
36. Ye Y, Wu Y, Wang J. Pyrroline-5-carboxylate reductase 1 promotes cell proliferation via inhibiting apoptosis in human malignant melanoma. *Cancer Manag Res.* (2018) 10:6399–407. doi: 10.2147/CMAR.S166711
37. Cai F, Miao Y, Liu C, Wu T, Shen S, Su X, et al. Pyrroline-5-carboxylate reductase 1 promotes proliferation and inhibits apoptosis in non-small cell lung cancer. *Oncol Lett.* (2018) 15:731–40. doi: 10.3892/ol.2017.7400
38. Wang D, Wang L, Zhang Y, Yan Z, Liu L, et al. PYCR1 promotes the progression of non-small-cell lung cancer under the negative regulation of miR-488. *Biomed Pharmacother.* (2019) 111:588–95. doi: 10.1016/j.biopha.2018.12.089
39. Sang S, Zhang C, Shan J. Pyrroline-5-carboxylate reductase 1 accelerates the migration and invasion of nonsmall cell lung cancer *in vitro*. *Cancer Biother Radiopharm.* (2019) 34:380–7. doi: 10.1089/cbr.2019.2782
40. She Y, Mao A, Li F, Wei X. P5CR1 protein expression and the effect of gene-silencing on lung adenocarcinoma. *PeerJ.* (2019) 7:e6934. doi: 10.7717/peerj.6934
41. K.Hollinshead ER, Munford H, Eales KL, Bardella C, Li C, Escribano-Gonzalez C, et al. Oncogenic IDH1 mutations promote enhanced proline synthesis through PYCR1 to support the maintenance of mitochondrial redox homeostasis. *Cell Rep.* (2018) 22:3107–14. doi: 10.1016/j.celrep.2018.02.084
42. Fang E, Wang X, Yang F, Hu A, Wang J, Li D, et al. Therapeutic Targeting of MZF1-AS1/PARP1/E2F1 axis inhibits proline synthesis and neuroblastoma progression. *Adv Sci.* (2019) 6:1900581. doi: 10.1002/advs.201900581

43. Sun T, Song Y, Yu H, Luo X. Identification of lncRNA TRPM2-AS/miR-140–3p/PYCR1 axis's proliferates and anti-apoptotic effect on breast cancer using co-expression network analysis. *Cancer Biol Ther.* (2019) 20:760–73. doi: 10.1080/15384047.2018.1564563
44. Chen S, Yang X, Yu M, Wang Z, Liu B, Liu M, et al. SIRT3 regulates cancer cell proliferation through deacetylation of PYCR1 in proline metabolism. *Neoplasia*. (2019) 21:665–75. doi: 10.1016/j.neo.2019.04.008
45. Fang H, Du G, Wu Q, Liu R, Chen C, Feng J. HDAC inhibitors induce proline dehydrogenase. (POX) transcription and anti-apoptotic autophagy in triple negative breast cancer. *Acta Biochim Biophys Sin. (Shanghai).* (2019) 51:1064–70. doi: 10.1093/abbs/gmz097
46. Liu Y, Mao C, Wang M, Liu N, Ouyang L, Liu S, et al. Cancer progression is mediated by proline catabolism in non-small cell lung cancer. *Oncogene*. (2020) 39:2358–76. doi: 10.1038/s41388-019-1151-5
47. Mathews MB, Hershey JW. The translation factor eIF5A and human cancer. *Biochim Biophys Acta.* (2015) 1849:836–44. doi: 10.1016/j.bbagrm.2015.05.002
48. Gilkes DM, Chaturvedi P, Bajpai S, Wong CC, Wei H, Pitcairn S, Hubbi ME, et al. Collagen prolyl hydroxylases are essential for breast cancer metastasis. *Cancer Res*. (2013) 73:3285–96. doi: 10.1158/0008-5472.CAN-12-3963
49. Xiong G, Stewart RL, Chen J, Gao T, Scott TL, Samayoa LM, et al. Collagen prolyl 4-hydroxylase 1 is essential for HIF-1alpha stabilization and TNBC chemoresistance. *Nat Commun*. (2018) 9:4456. doi: 10.1038/s41467-018-06893-9
50. Cao XP, Cao Y, Li WJ, Zhang HH, Zhu ZM. P4HA1/HIF1alpha feedback loop drives the glycolytic and malignant phenotypes of pancreatic cancer. *Biochem Biophys Res Commun.* (2019) 516:606–12. doi: 10.1016/j.bbrc.2019.06.096
51. Li Q, Shen Z, Wu Z, Shen Y, Deng H, Zhou C, et al. High P4HA1 expression is an independent prognostic factor for poor overall survival and recurrent-free survival in head and neck squamous cell carcinoma. *J Clin Lab Anal.* (2019) e23107. doi: 10.1002/jcla.23107
52. Kappler M, Kotrba J, Kaune T, Bache M, Rot S, Bethmann D, et al. P4HA1: a single-gene surrogate of hypoxia signatures in oral squamous cell carcinoma patients. *Clin Transl Radiat Oncol.* (2017) 5:6–11. doi: 10.1016/j.ctro.2017.05.002
53. Chakravarthi BV, Pathi SS, Goswami MT, Cieslik M, Zheng H, Nallasivam S, et al. The miR-124-prolyl hydroxylase P4HA1-MMP1 axis plays a critical role in prostate cancer progression. *Oncotarget*. (2014) 5:6654–69. doi: 10.18632/oncotarget.2208
54. Duan Y, Dong Y, Dang R, Hu Z, Yang Y, Hu Y, et al. MiR-122 inhibits epithelial mesenchymal transition by regulating P4HA1 in ovarian cancer cells. *Cell Biol Int.* (2018) 42:1564–74. doi: 10.1002/cbin.11052
55. Zhou Y, Jin G, Mi R, Zhang J, Zhang J, Xu H, et al. Knockdown of P4HA1 inhibits neovascularization via targeting glioma stem cell-endothelial cell transdifferentiation and disrupting vascular basement membrane. *Oncotarget.* (2017) 8:35877–89. doi: 10.18632/oncotarget.16270
56. Hu WM, Zhang J, Sun SX, Xi SY, Chen ZJ, Jiang XB, et al. Identification of P4HA1 as a prognostic biomarker for high-grade gliomas. *Pathol Res Pract.* (2017) 213:1365–9. doi: 10.1016/j.prp.2017.09.017
57. D'Aniello C, Cermola F, Palamidessi A, Wanderlingh LG, Gagliardi M, Migliaccio A, et al. Collagen prolyl hydroxylation-dependent metabolic perturbation governs epigenetic remodeling and mesenchymal transition in pluripotent and cancer cells. *Cancer Res.* (2019) 79:3235–50. doi: 10.1158/0008-5472.CAN-18-2070
58. Lin J, Wu J, Wei X, Gao C, Jin Z, Cui Y, et al. P4HA2, a prognostic factor, promotes glioma proliferation, invasion, migration and EMT through collagen regulation and PI3K/AKT pathway. *bioRxiv [preprint]* (2020). doi: 10.1101/2020.02.05.935221
59. Li Q, Wang Q, Zhang Q, Zhang J, Zhang J. Collagen prolyl 4-hydroxylase 2 predicts worse prognosis and promotes glycolysis in cervical cancer. *Am J Transl Res.* (2019) 11:6938–51.
60. Jarzab B, Wiench M, Fujarewicz K, Simek K, Jarzab M, Oczko-Wojciechowska M, et al. Gene expression profile of papillary thyroid cancer: sources of variability and diagnostic implications. *Cancer Res.* (2005) 65:1587–97. doi: 10.1158/0008-5472.CAN-04-3078
61. Jiang W, Zhou X, Li Z, Liu K, Wang W, Tan R, et al. Prolyl 4-hydroxylase 2 promotes B-cell lymphoma progression via hydroxylation of Carabin. *Blood.* (2018) 131:1325–36. doi: 10.1182/blood-2017-07-794875
62. Chang KP, Yu JS, Chien KY, Lee CW, Liang Y, Liao CT, et al. Identification of PRDX4 and P4HA2 as metastasis-associated proteins in oral cavity squamous cell carcinoma by comparative tissue proteomics of microdissected specimens using iTRAQ technology. *J Proteome Res.* (2011) 10:4935–47. doi: 10.1021/pr200311p
63. Reis PP, Waldron L, Perez-Ordonez B, Pintilie M, Galloni NN, Xuan Y, et al. A gene signature in histologically normal surgical margins is predictive of oral carcinoma recurrence. *BMC Cancer*. (2011) 11:437. doi: 10.1186/1471-2407-11-437
64. Feng GX, Li J, Yang Z, Zhang SQ, Liu YX, Zhang WY, et al. Hepatitis B virus X protein promotes the development of liver fibrosis and hepatoma through downregulation of miR-30e targeting P4HA2 mRNA. *Oncogene*. (2017) 36:6895–905. doi: 10.1038/onc.2017.291
65. Wang T, Fu X, Jin T, Zhang L, Liu B, Wu Y, et al. Aspirin targets P4HA2 through inhibiting NF-kappaB and LMCD1-AS1/let-7g to inhibit tumour growth and collagen deposition in hepatocellular carcinoma. *EBioMedicine*. (2019) 45:168–80. doi: 10.1016/j.ebiom.2019.06.048
66. Xiong G, Deng L, Zhu J, Rychahou PG, Xu R. Prolyl-4-hydroxylase alpha subunit 2 promotes breast cancer progression and metastasis by regulating collagen deposition. *BMC Cancer*. (2014) 14:1. doi: 10.1186/1471-2407-14-1
67. Toss MS, Miligy IM, Gorringe KL, AlKawaz A, Khout H, Ellis IO, et al. Prolyl-4-hydroxylase Alpha subunit 2. (P4HA2) expression is a predictor of poor outcome in breast ductal carcinoma in situ. (DCIS). *Br J Cancer.* (2018) 119:1518–26. doi: 10.1038/s41416-018-0337-x
68. Xia W, Zhuang J, Wang G, Ni J, Wang J, Ye Y. P4HB promotes HCC tumorigenesis through downregulation of GRP78 and subsequent upregulation of epithelial-to-mesenchymal transition. *Oncotarget*. (2017) 8:8512–21. doi: 10.18632/oncotarget.14337
69. Wang SM, Lin LZ, Zhou DH, Zhou JX, Xiong SQ. Expression of prolyl 4-hydroxylase beta-polypeptide in non-small cell lung cancer treated with Chinese medicines. *Chin J Integr Med*. (2015) 21:689–96. doi: 10.1007/s11655-013-1535-2
70. Zhang J, Wu Y, Lin YH, Guo S, Ning PF, Zheng ZC, et al. Prognostic value of hypoxia-inducible factor-1 alpha and prolyl 4-hydroxylase beta polypeptide overexpression in gastric cancer. *World J Gastroenterol.* (2018) 24:2381–91. doi: 10.3748/wjg.v24.i22.2381
71. Sun S, Wong TS, Zhang XQ, Pu JK, Lee NP, Day PJ, et al. Protein alterations associated with temozolomide resistance in subclones of human glioblastoma cell lines. *J Neurooncol*. (2012) 107:89–100. doi: 10.1007/s11060-011-0729-8
72. Zhang J, Guo S, Wu Y, Zheng ZC, Wang Y, Zhao Y. P4HB, a novel hypoxia target gene related to gastric cancer invasion and metastasis. *Biomed Res Int.* (2019) 2019:9749751. doi: 10.1155/2019/9749751
73. I.Wortel MN, van der Meer LT, Kilberg MS, van Leeuwen FN. Surviving stress: modulation of ATF4-mediated stress responses in normal and malignant cells. *Trends Endocrinol Metab*. (2017) 28:794–806. doi: 10.1016/j.tem.2017.07.003
74. Singleton DC, Harris AL. Targeting the ATF4 pathway in cancer therapy. *Expert Opin Ther Targets*. (2012) 16:1189–202. doi: 10.1517/14728222.2012.728207
75. Tanner JJ, Fendt SM, Becker DF. The proline cycle as a potential cancer therapy target. *Biochemistry*. (2018) 57:3433–44. doi: 10.1021/acs.biochem.8b00215
76. De Ingeniis J, Ratnikov B, Richardson AD, Scott DA, Aza-Blanc P, De SK, et al. Functional specialization in proline biosynthesis of melanoma. *PLoS ONE*. (2012) 7:e45190. doi: 10.1371/journal.pone.0045190
77. Liu W, Le A, Hancock C, Lane AN, Dang CV, Fan TW, et al. Reprogramming of proline and glutamine metabolism contributes to the proliferative and metabolic responses regulated by oncogenic transcription factor c-MYC. *Proc Natl Acad Sci USA*. (2012) 109:8983–8. doi: 10.1073/pnas.1203244109
78. Loayza-Puch F, Rooijers K, Buil LC, Zijlstra J, Oude Vrielink JF, Lopes R, et al. Tumour-specific proline vulnerability uncovered by differential ribosome codon reading. *Nature*. (2016) 530:490–4. doi: 10.1038/nature16982
79. Sahu N, Dela Cruz D, Gao M, Sandoval W, Haverty PM, Liu J, et al. Proline starvation induces unresolved ER stress and hinders mTORC1-dependent tumorigenesis. *Cell Metab.* (2016) 24:753–61. doi: 10.1016/j.cmet.2016.08.008

80. D'Aniello C, Fico A, Casalino L, Guardiola O, Di Napoli G, Cermola F, et al. A novel autoregulatory loop between the Gcn2-Atf4 pathway and. (L)-Proline [corrected] metabolism controls stem cell identity. *Cell Death Differ.* (2015) 22:1094–5. doi: 10.1038/cdd.2015.24
81. Tan BS, Lonic A, Morris MB, Rathjen PD, Rathjen J. The amino acid transporter SNAT2 mediates L-proline-induced differentiation of ES cells. American journal of physiology. *Cell Physiol.* (2011) 300:C1270–9. doi: 10.1152/ajpcell.00235.2010
82. Han J, Back SH, Hur J, Lin YH, Gildersleeve R, Shan J, et al. ER-stress-induced transcriptional regulation increases protein synthesis leading to cell death. *Nature Cell Biol.* (2013) 15:481–90. doi: 10.1038/ncb2738
83. Palii SS, Chen H, Kilberg MS. Transcriptional control of the human sodium-coupled neutral amino acid transporter system A gene by amino acid availability is mediated by an intronic element. *J Biol Chem.* (2004) 279:3463–71. doi: 10.1074/jbc.M310483200
84. Comes S, Gagliardi M, Laprano N, Fico A, Cimmino A, Palamidessi A, et al. L-Proline induces a mesenchymal-like invasive program in embryonic stem cells by remodeling H3K9 and H3K36 methylation. *Stem Cell Reports.* (2013) 1:307–21. doi: 10.1016/j.stemcr.2013.09.001
85. Keller TL, Zocco D, Sundrud MS, Hendrick M, Edenius M, Yum J, et al. Halofuginone and other febrifugine derivatives inhibit prolyl-tRNA synthetase. *Nat Chem Biol.* (2012) 8:311–7. doi: 10.1038/nchembio.790
86. Zhou H, Sun L, Yang XL, Schimmel P. ATP-directed capture of bioactive herbal-based medicine on human tRNA synthetase. *Nature*. (2013) 494:121–4. doi: 10.1038/nature11774
87. Morrison SJ, Spradling AC. Stem cells and niches: mechanisms that promote stem cell maintenance throughout life. *Cell*. (2008) 132:598–611. doi: 10.1016/j.cell.2008.01.038
88. Scadden DT. Nice neighborhood: emerging concepts of the stem cell niche. *Cell*. (2014) 157:41–50. doi: 10.1016/j.cell.2014.02.013
89. Lane SW, Williams DA, Watt FM. Modulating the stem cell niche for tissue regeneration. *Nat Biotechnol.* (2014) 32:795–803. doi: 10.1038/nbt.2978
90. Myllyharju J. Prolyl 4-hydroxylases, the key enzymes of collagen biosynthesis. *Matrix Biol*. (2003) 22:15–24. doi: 10.1016/S0945-053X(03)00006-4
91. Bordoli MR, Yum J, Breitkopf SB, Thon JN, Italiano JE Jr, Xiao J, et al. A secreted tyrosine kinase acts in the extracellular environment. *Cell*. (2014) 158:1033–44. doi: 10.1016/j.cell.2014.06.048
92. Schworer S, Berisa M, Violante S, Qin W, Zhu J, Hendrickson RC, et al. Proline biosynthesis is a vent for TGFbeta-induced mitochondrial redox stress. *EMBO J.* (2020) 5:e103334. doi: 10.15252/embj.2019103334
93. Xu S, Xu H, Wang W, Li S, Li H, Li T, et al. The role of collagen in cancer: from bench to bedside. *J Transl Med.* (2019) 17:309. doi: 10.1186/s12967-019-2058-1
94. Pankova D, Jiang Y, Chatzifrangkeskou M, Vendrell I, Buzzelli J, Ryan A, et al. RASSF1A controls tissue stiffness and cancer stem-like cells in lung adenocarcinoma. *EMBO J.* (2019) 38:e100532. doi: 10.15252/embj.2018100532
95. Guo L, Cui C, Zhang K, Wang J, Wang Y, Lu Y, et al. Kindlin-2 links mechano-environment to proline synthesis and tumor growth. *Nat Commun.* (2019) 10:845. doi: 10.1038/s41467-019-08772-3
96. Casalino L, Comes S, Lambazzi G, De Stefano B, Filosa S, De Falco S, et al. Control of embryonic stem cell metastability by L-proline catabolism. *J Mol Cell Biol.* (2011) 3:108–22. doi: 10.1093/jmcb/mjr001
97. D'Aniello C, Cermola F, Patriarca EJ, Minchiotti G. Vitamin C in stem cell biology: impact on extracellular matrix homeostasis and epigenetics. *Stem Cells Int.* (2017) 2017:8936156. doi: 10.1155/2017/8936156
98. D'Aniello C, Habibi E, Cermola F, Paris D, Russo F, Fiorenzano A, et al. Vitamin C and l-proline antagonistic effects capture alternative states in the pluripotency continuum. *Stem Cell Reports.* (2017) 8:11. doi: 10.1016/j.stemcr.2016.11.011
99. D'Aniello C, Cermola F, Patriarca EJ, Minchiotti G. Metabolic–epigenetic axis in pluripotent state transitions. *Epigenomes*. (2019) 3:13. doi: 10.3390/epigenomes3030013
100. Surazynski A, Miltyk W, Palka J, Phang JM. Prolidase-dependent regulation of collagen biosynthesis. *Amino Acids.* (2008) 35:731–8. doi: 10.1007/s00726-008-0051-8
101. Olivares O, Mayers JR, Gouirand V, Torrence ME, Gicquel T, Borge L, et al. Collagen-derived proline promotes pancreatic ductal adenocarcinoma cell survival under nutrient limited conditions. *Nat Commun.* (2017) 8:16031. doi: 10.1038/ncomms16031
102. Kerr MC, Teasdale RD. Defining macropinocytosis. *Traffic*. (2009) 10:364–71. doi: 10.1111/j.1600-0854.2009.00878.x
103. Kilberg MS, Pan YX, Chen H, Leung-Pineda V. Nutritional control of gene expression: how mammalian cells respond to amino acid limitation. *Annu Rev Nutr.* (2005) 25:59–85. doi: 10.1146/annurev.nutr.24.012003.132145
104. Abramovitch R, Dafni H, Neeman M, Nagler A, Pines M. Inhibition of neovascularization and tumor growth, and facilitation of wound repair, by halofuginone, an inhibitor of collagen type I synthesis. *Neoplasia*. (1999) 1:321–9. doi: 10.1038/sj.neo.7900043
105. Grudzien MM, Low PS, Manning PC, Arredondo M, Belton RJ Jr, Nowak RA. The antifibrotic drug halofuginone inhibits proliferation and collagen production by human leiomyoma and myometrial smooth muscle cells. *Fertil Steril.* (2010) 93:1290–8. doi: 10.1016/j.fertnstert.2008.11.018
106. Koohestani F, Qiang W, MacNeill AL, Druschitz SA, Serna VA, Adur M, et al. Halofuginone suppresses growth of human uterine leiomyoma cells in a mouse xenograft model. *Hum Reprod*. (2016) 31:1540–51. doi: 10.1093/humrep/dew094
107. Elkin M, Ariel I, Miao HQ, Nagler A, Pines M, de-Groot N, et al. Inhibition of bladder carcinoma angiogenesis, stromal support, and tumor growth by halofuginone. *Cancer Res.* (1999) 59:4111–8.
108. Elahi-Gedwillo KY, Carlson M, Zettervall J, Provenzano PP. Antifibrotic therapy disrupts stromal barriers and modulates the immune landscape in pancreatic ductal adenocarcinoma. *Cancer Res*. (2019) 79:372–86. doi: 10.1158/0008-5472.CAN-18-1334
109. Spector I, Honig H, Kawada N, Nagler A, Genin O, Pines M. Inhibition of pancreatic stellate cell activation by halofuginone prevents pancreatic xenograft tumor development. *Pancreas*. (2010) 39:1008–15. doi: 10.1097/MPA.0b013e3181da8aa3
110. Gavish Z, Pinthus JH, Barak V, Ramon J, Nagler A, Eshhar Z, et al. Growth inhibition of prostate cancer xenografts by halofuginone. *Prostate*. (2002) 51:73–83. doi: 10.1002/pros.10059
111. Gross DJ, Reibstein I, Weiss L, Slavin S, Dafni H, Neeman M, et al. Treatment with halofuginone results in marked growth inhibition of a von Hippel-Lindau pheochromocytoma *in vivo. Clin Cancer Res*. (2003) 9:3788–93.
112. Jin ML, Park SY, Kim YH, Park G, Lee SJ. Halofuginone induces the apoptosis of breast cancer cells and inhibits migration via downregulation of matrix metalloproteinase-9. *Int J Oncol.* (2014) 44:309–18. doi: 10.3892/ijo.2013.2157
113. Xia X, Wang L, Zhang X, Wang S, Lei L, Cheng L, et al. Halofuginone-induced autophagy suppresses the migration and invasion of MCF-7 cells via regulation of STMN1 and p53. *J Cell Biochem*. (2018) 119:4009–20. doi: 10.1002/jcb.26559
114. Juarez P, P.Fournier GJ, Mohammad KS, McKenna RC, Davis HW, Peng XH, et al. Halofuginone inhibits TGF-beta/BMP signaling and in combination with zoledronic acid enhances inhibition of breast cancer bone metastasis. *Oncotarget.* (2017) 8:86447–62. doi: 10.18632/oncotarget.21200
115. Xia X, Wang X, Zhang S, Zheng Y, Wang L, Xu Y, et al. miR-31 shuttled by halofuginone-induced exosomes suppresses MFC-7 cell proliferation by modulating the HDAC2/cell cycle signaling axis. *J Cell Physiol.* (2019) 234:18970–84. doi: 10.1002/jcp.28537
116. Chen GQ, Tang CF, Shi XK, Lin CY, Fatima S, Pan XH, et al. Halofuginone inhibits colorectal cancer growth through suppression of Akt/mTORC1 signaling and glucose metabolism. *Oncotarget*. (2015) 6:24148–62. doi: 10.18632/oncotarget.4376
117. Chen GQ, Gong RH, Yang DJ, Zhang G, Lu AP, Yan SC, et al. Halofuginone dually regulates autophagic flux through nutrient-sensing pathways in colorectal cancer. *Cell Death Dis.* (2017) 8:e2789. doi: 10.1038/cddis.2017.203
118. Nagler A, Ohana M, Shibolet O, Shapira MY, Alper R, Vlodavsky I, et al. Suppression of hepatocellular carcinoma growth in mice by the alkaloid coccidiostat halofuginone. *Eur J Cancer*. (2004) 40:1397–403. doi: 10.1016/j.ejca.2003.11.036
119. Huo S, Yu H, Li C, Zhang J, Liu T. Effect of halofuginone on the inhibition of proliferation and invasion of hepatocellular carcinoma HepG2 cell line. *Int J Clin Exp Pathol.* (2015) 8:15863–70.

120. Taras D, Blanc JF, Rullier A, Dugot-Senant N, Laurendeau I, Bieche I, et al. Halofuginone suppresses the lung metastasis of chemically induced hepatocellular carcinoma in rats through MMP inhibition. *Neoplasia*. (2006) 8:312–8. doi: 10.1593/neo.05796
121. de Figueiredo-Pontes LL, Assis PA, Santana-Lemos BA, Jacomo RH, Lima AS, Garcia AB, et al. Halofuginone has anti-proliferative effects in acute promyelocytic leukemia by modulating the transforming growth factor beta signaling pathway. *PLoS ONE*. (2011) 6:e26713. doi: 10.1371/journal.pone.0026713
122. Assis PA, De Figueiredo-Pontes LL, Lima AS, Leao V, Candido LA, Pintao CT, et al. Halofuginone inhibits phosphorylation of SMAD-2 reducing angiogenesis and leukemia burden in an acute promyelocytic leukemia mouse model. *J Exp Clin Cancer Res*. (2015) 34:65. doi: 10.1186/s13046-015-0181-2
123. Leiba M, Jakubikova J, Klippel S, Mitsiades CS, Hideshima T, Tai YT, et al. Halofuginone inhibits multiple myeloma growth in vitro and in vivo and enhances cytotoxicity of conventional and novel agents. *Br J Haematol*. (2012) 157:718–31. doi: 10.1111/j.1365-2141.2012.09120.x
124. Cook JA, Choudhuri R, Degraff W, Gamson J, Mitchell JB. Halofuginone enhances the radiation sensitivity of human tumor cell lines. *Cancer Lett*. (2010) 289:119–26. doi: 10.1016/j.canlet.2009.08.009
125. Tsuchida K, Tsujita T, Hayashi M, Ojima A, Keleku-Lukwete N, Katsuoka F, Otsuki A, et al. Halofuginone enhances the chemo-sensitivity of cancer cells by suppressing NRF2 accumulation. *Free Radic Biol Med*. (2017) 103:236–47. doi: 10.1016/j.freeradbiomed.2016.12.041
126. Lin R, Yi S, Gong L, Liu W, Wang P, Liu N, et al. Inhibition of TGF-beta signaling with halofuginone can enhance the antitumor effect of irradiation in Lewis lung cancer. *Onco Targets Ther*. (2015) 8:3549–59. doi: 10.2147/OTT.S92518
127. Chen Y, Liu W, Wang P, Hou H, Liu N, Gong L, et al. Halofuginone inhibits radiotherapy-induced epithelial-mesenchymal transition in lung cancer. *Oncotarget*. (2016) 7:71341–52. doi: 10.18632/oncotarget.11217
128. Abramovitch R, Itzik A, Harel H, Nagler A, Vlodavsky I, Siegal T. Halofuginone inhibits angiogenesis and growth in implanted metastatic rat brain tumor model–an MRI study. *Neoplasia*. (2004) 6:480–9. doi: 10.1593/neo.03520
129. Juarez P, Mohammad KS, Yin JJ, Fournier PG, McKenna RC, Davis HW, et al. Halofuginone inhibits the establishment and progression of melanoma bone metastases. *Cancer Res*. (2012) 72:6247–56. doi: 10.1158/0008-5472.CAN-12-1444
130. Lamora A, Mullard M, Amiaud J, Brion R, Heymann D, Redini F, et al. Anticancer activity of halofuginone in a preclinical model of osteosarcoma: inhibition of tumor growth and lung metastases. *Oncotarget*. (2015) 6:14413–27. doi: 10.18632/oncotarget.3891
131. de Jonge MJ, Dumez H, Verweij J, Yarkoni S, Snyder D, Lacombe D, et al. Phase I and pharmacokinetic study of halofuginone, an oral quinazolinone derivative in patients with advanced solid tumours. *Eur J Cancer*. (2006) 42:1768–74. doi: 10.1016/j.ejca.2005.12.027
132. Gutierrez E, Shin BS, Woolstenhulme CJ, Kim JR, Saini P, Buskirk AR, et al. eIF5A promotes translation of polyproline motifs. *Mol Cell*. (2013) 51:35–45. doi: 10.1016/j.molcel.2013.04.021
133. Doerfel LK, Wohlgemuth I, Kothe C, Peske F, Urlaub H, Rodnina MV. EF-P is essential for rapid synthesis of proteins containing consecutive proline residues. *Science*. (2013) 339:85–8. doi: 10.1126/science.1229017
134. Davis AR, Gohara DW, Yap MN. Sequence selectivity of macrolide-induced translational attenuation. *Proc Natl Acad Sci USA*. (2014) 111:15379–84. doi: 10.1073/pnas.1410356111
135. Lahn M, Kloeker S, Berry BS. TGF-beta inhibitors for the treatment of cancer. *Exp Opin Investig Drugs*. (2005) 14:629–43. doi: 10.1517/13543784.14.6.629
136. Vasta JD, Raines RT. Collagen Prolyl 4-hydroxylase as a therapeutic target. *J Med Chem*. (2018) 61:10403–411. doi: 10.1021/acs.jmedchem.8b00822
137. Gomez-Rubio P, Zock JP, Rava M, Marquez M, Sharp L, Hidalgo M, et al. Reduced risk of pancreatic cancer associated with asthma and nasal allergies. *Gut*. (2017) 66:314–22. doi: 10.1136/gutjnl-2015-310442
138. Busby J, Murray L, Mills K, Zhang SD, Liberante F, Cardwell CR. A combined connectivity mapping and pharmacoepidemiology approach to identify existing medications with breast cancer causing or preventing properties. *Pharmacoepidemiol Drug Saf*. (2018) 27:78–86. doi: 10.1002/pds.4345

Conflict of Interest: The authors declare that the research was conducted in the absence of any commercial or financial relationships that could be construed as a potential conflict of interest.

frontiers in Oncology

ORIGINAL RESEARCH
published: 15 September 2020
doi: 10.3389/fonc.2020.01528

A Myristoyl Amide Derivative of Doxycycline Potently Targets Cancer Stem Cells (CSCs) and Prevents Spontaneous Metastasis, Without Retaining Antibiotic Activity

Béla Ózsvári[1], Luma G. Magalhães[1], Joe Latimer[2], Jussi Kangasmetsa[3], Federica Sotgia[1,4] and Michael P. Lisanti[1,4]**

[1] Translational Medicine, School of Science, Engineering and Environment (SEE), University of Salford, Manchester, United Kingdom, [2] Salford Antibiotic Research Network, School of Science, Engineering and Environment (SEE), University of Salford, Manchester, United Kingdom, [3] Eurofins Integrated Discovery UK Ltd., Essex, United Kingdom, [4] Lunella Biotech, Inc., Ottawa, ON, Canada

OPEN ACCESS

Edited by:
Anna Sebestyén, Semmelweis University, Hungary

Reviewed by:
Anna Maria Tokes, Semmelweis University, Hungary
Chris Albanese, Georgetown University, United States

***Correspondence:**
Federica Sotgia
fsotgia@gmail.com
Michael P. Lisanti
michaelp.lisanti@gmail.com

Specialty section:
This article was submitted to Cancer Metabolism, a section of the journal Frontiers in Oncology

Received: *23 May 2020*
Accepted: *16 July 2020*
Published: *15 September 2020*

Citation:
Ózsvári B, Magalhães LG, Latimer J, Kangasmetsa J, Sotgia F and Lisanti MP (2020) A Myristoyl Amide Derivative of Doxycycline Potently Targets Cancer Stem Cells (CSCs) and Prevents Spontaneous Metastasis, Without Retaining Antibiotic Activity. Front. Oncol. 10:1528. doi: 10.3389/fonc.2020.01528

Here, we describe the chemical synthesis and biological activity of a new Doxycycline derivative, designed specifically to more effectively target cancer stem cells (CSCs). In this analog, a myristic acid (14 carbon) moiety is covalently attached to the free amino group of 9-amino-Doxycycline. First, we determined the IC_{50} of Doxy-Myr using the 3D-mammosphere assay, to assess its ability to inhibit the anchorage-independent growth of breast CSCs, using MCF7 cells as a model system. Our results indicate that Doxy-Myr is >5-fold more potent than Doxycycline, as it appears to be better retained in cells, within a peri-nuclear membranous compartment. Moreover, Doxy-Myr did not affect the viability of the total MCF7 cancer cell population or normal fibroblasts grown as 2D-monolayers, showing remarkable selectivity for CSCs. Using both gram-negative and gram-positive bacterial strains, we also demonstrated that Doxy-Myr did not show antibiotic activity, against *Escherichia coli* and *Staphylococcus aureus*. Interestingly, other complementary Doxycycline amide derivatives, with longer (16 carbon; palmitic acid) or shorter (12 carbon; lauric acid) fatty acid chain lengths, were both less potent than Doxy-Myr for the targeting of CSCs. Finally, using MDA-MB-231 cells, we also demonstrate that Doxy-Myr has no appreciable effect on tumor growth, but potently inhibits tumor cell metastasis *in vivo*, with little or no toxicity. In summary, by using 9-amino-Doxycycline as a scaffold, here we have designed new chemical entities for their further development as anti-cancer agents. These compounds selectively target CSCs, e.g., Doxy-Myr, while effectively minimizing the risk of driving antibiotic resistance. Taken together, our current studies provide proof-of-principle, that existing FDA-approved drugs can be further modified and optimized, to successfully target the anchorage-independent growth of CSCs and to prevent the process of spontaneous tumor cell metastasis.

Keywords: cancer stem-like cells (CSCs), Doxycycline, myristic acid, fatty acylation, cancer cell metastasis, prophylaxis of metastasis, 9-amino-Doxycycline, antimitoscins

INTRODUCTION

Cancer stem cells (CSCs) are thought to be the root cause of recurrence, metastasis, and drug-resistance, in a host of cancer types (1–5). As a consequence, there is an unmet need to develop new therapeutics to target and selectively kill CSCs, while avoiding side effects, especially severe chemo-toxicity. Metastasis is believed to be driven by this unique sub-population of cancer-initiating cells (1–3). CSCs have the ability to generate *de novo* tumors in immuno-deficient host organisms. Moreover, they have the capacity to engage in anchorage-independent growth, which facilitates their invasive spread throughout the various tissues and organ systems, resulting in local, and distant disseminated lesions (4, 5). Remarkably, these metastatic lesions are resistant to both chemo-therapy and radiation treatments. Unfortunately, the Achilles' heel of these pro-metastatic CSCs remains largely unknown. As a consequence, currently there are no anti-cancer drugs that are FDA-approved for the prevention of metastasis.

Over the last 5 years, we identified that mitochondria in CSCs may be a novel tractable therapeutic target, for inhibiting their anchorage-independent growth (5). More specifically, increased mitochondrial biogenesis may facilitate efficient high energy production, resulting in the rapid propagation of CSCs (6–10). In addition, within metastatic lymph nodes isolated from breast cancer patients, disseminated cancer cells show elevated levels of mitochondrial activity, especially Complex IV activation, as revealed by functional activity assays (11).

Interestingly, mitochondrial biogenesis is critically linked to the activity of mitochondrial ribosomal proteins, that functionally translate key mitochondrial proteins, which are genetically encoded by mitochondrial DNA (mt-DNA); this includes 13 proteins that are necessary to functionally maintain OXPHOS and mitochondrial ATP synthesis (6–13).

The reason that mitochondria have their own DNA and specific machinery for protein translation is that they originally evolved from engulfed aerobic bacteria, over the last 1.4 billion years, after invading eukaryotic cells. This evolutionary symbiotic relationship has certain functional consequences that could be safely exploited to achieve anti-mitochondrial therapy, specifically targeting CSCs. For example, because of the similarities between bacteria and mitochondria, a subset of bacteriostatic antibiotics block mitochondrial protein translation, as a manageable side effect (6, 10, 13). In this context, Doxycycline inhibits the activity of the small mito-ribosome, while Azithromycin blocks the large mito-ribosome, both as off-target side effects (6, 10, 13). Similarly, Doxycycline and Azithromycin both inhibit the propagation of CSCs, in an anchorage-independent fashion, in numerous breast cancer cell lines, as well as in cell lines derived from many other solid tumor types (6, 10, 13). As such, we have suggested that these side-effects could be re-purposed to clinically target and therapeutically eradicate CSCs.

In direct support of this notion, a Phase II clinical trial has documented that brief treatment with Doxycycline, in early breast cancer patients, is indeed sufficient to significantly decrease the content of CSCs in the tumor mass, by employing CD44-staining as an established marker of CSCs in ER(+) patients (14). Overall, the response rate approached 90%, resulting in reductions of up to nearly 67% in CSC tumor burden (14). Quantitatively similar results were obtained in HER2(+) patients, using ALDH1 as a CSC marker. As such, blocking mitochondrial protein synthesis may be a viable approach for targeting and removing CSCs *in vivo,* prior to surgical excision, possibly preventing the development of metastases.

Consistent with the above observations, other groups have shown that Doxycycline treatment effectively reduces the expression of a panel of CSC markers, in breast cancer cell lines, such as CD44, ALDH, Oct4, Sox2, and Nanog (9, 12). Moreover, Doxycycline treatment functionally inhibits multiple CSC signaling pathways, including Wnt, Notch, Hedgehog, and STAT1/3-signaling (10).

Here, we describe a medicinal chemistry approach to design novel therapeutics to more selectively target CSCs. More specifically, we show that several new potent Doxycycline analogs can be generated by attaching a fatty acid onto 9-amino-Doxycycline, which is a relatively straightforward chemical modification. Importantly, these analogs, such as Doxy-Myr, lack antibiotic activity, but more potently target CSCs and effectively prevent metastasis, in an *in vivo* pre-clinical model. Therefore, Doxy-Myr could be used to eradicate CSCs, without exerting the selective pressures required for the development of antimicrobial resistance and without significant toxicity.

To better describe this general class of novel compounds which are lipid-modified FDA-approved antibiotics, we propose the term Antimitoscins, to specifically reflect their intrinsic anti-mitochondrial activity.

MATERIALS AND METHODS

Materials

MCF7 and MDA-MB-231 cells were obtained from the American Type Culture Collection (ATCC). hTERT-BJ1 fibroblasts were as we previously described (13). Cells were cultured in DMEM, supplemented with 10% fetal calf serum (FCS), Glutamine and Pen/Strep.

Chemical Synthesis

Custom-chemical syntheses were performed by Eurofins Integrated Discovery UK Ltd., (Essex, UK). Conventional peptide synthesis methods were used to covalently attach each free fatty acid to 9-amino-Doxycycline. The desired reaction products were identified, chromatographically purified and the chemical structures were validated, by using a combination of NMR and mass spectrometry. The IUPAC names for the chemical compounds are as follows.

Doxycycline

(4S,5S,6R,12aS)-4-(dimethylamino)-3,5,10,12,12a-pentahydroxy-6-methyl-1,11-dioxo-4a,5,5a,6-tetrahydro-4H-tetracene-2-carboxamide.

Doxycycline-Myr

(4S,5S,6R,12aS)-4-(dimethylamino)-3,5,10,12,12a-pentahydroxy-6-methyl-1,11-dioxo-9-(tetradecanoylamino)-4a,5,5a,6-tetrahydro-4H-tetracene-2-carboxamide.

Doxycycline-Laur

(4S,5S,6R,12aS)-4-(dimethylamino)-9-(dodecanoylamino)-3,5,10,12,12a-pentahydroxy-6-methyl-1,11-dioxo-4a,5,5a,6-tetrahydro-4H-tetracene-2-carboxamide.

Doxycycline-Pal

(4S,5S,6R,12aS)-4-(dimethylamino)-9-(hexadecanoylamino)-3,5,10,12,12a-pentahydroxy-6-methyl-1,11-dioxo-4a,5,5a,6-tetrahydro-4H-tetracene-2-carboxamide.

Doxycycline-TPP

[6-[[(5R,6S,7S,10aS)-9-carbamoyl-7-(dimethylamino)-1,6,8,10a,11-pentahydroxy-5-methyl-10,12-dioxo-5a,6,6a,7-tetrahydro-5H-tetracen-2-yl]amino]-6-oxo-hexyl]-triphenyl-phosphonium oxalate.

9-Amino-Doxycycline

(4S,5S,6R,12aS)-9-amino-4-(dimethylamino)-3,5,10,12,12a-pentahydroxy-6-methyl-1,11-dioxo-4a,5,5a,6-tetrahydro-4H-tetracene-2-carboxamide.

9-Amino-Doxycycline was synthesized, essentially as previously described (15).

See **Supplemental Materials and Methods**, and **Supplemental Figure 1**, for further details on the chemical synthesis of these Doxycycline derivatives.

3D-Mammosphere Assay

The mammosphere assay is considered as the gold-standard for functionally measuring "stemness" and CSC propagation in breast cancer cells. Single cells are first plated at low density on low-attachment plates and >90% of "bulk" cancer cells die under these conditions, in a process of programmed cell death, termed anoikis. Only stem-like cells survive and propagate in suspension. Each 3D mammosphere is formed from a single CSC. Test compounds are added at the moment of single cell plating and then the number of 3D mammospheres are counted 5 days after plating. More specifically, a single cell suspension of MCF7 cells was prepared using enzymatic (1x Trypsin-EDTA, Sigma Aldrich) and manual disaggregation (25-gauge needle) (16–19). Cells were then plated at a density of 500 cells/cm^2 in mammosphere medium (DMEM-F12/B27/ EGF (20-ng/ml)/PenStrep) in non-adherent conditions, in culture dishes coated with (2-hydroxyethylmethacrylate) (poly-HEMA, Sigma). Cells were then grown for 5 days and maintained in a humidified incubator at 37°C at an atmospheric pressure in 5% (v/v) carbon dioxide/air. After 5 days in culture, spheres >50 μm were counted using an eye-piece graticule, and the percentage of cells plated which formed spheres was calculated and is referred to as percent mammosphere formation, normalized to vehicle-alone treated controls. Mammosphere assays were performed in triplicate and repeated three times independently.

Fluorescence Imaging

Fluorescent images were taken after 72 h of incubation of MCF7 cells treated with either Doxycycline or Doxy-Myr (both at 10 μM), or vehicle control. Cell cultures were imaged with the EVOS Cell Imaging System (Thermo Fisher Scientific, Inc.), using the GFP channel. No fluorescent dye was used before imaging, therefore, any changes in signal were exclusively due to the auto-fluorescent nature of the Doxycycline compounds.

Cell Viability Assay

The Sulphorhodamine (SRB) assay is based on the measurement of cellular protein content (16–19). After treatment for 72 h in 96-well plates (8,000 cells/well), cells were fixed with 10% trichloroacetic acid (TCA) for 1 h in the cold room, and were dried overnight at room temperature. Then, cells were incubated with SRB for 15 min, washed twice with 1% acetic acid, and air dried for at least 1 h. Finally, the protein-bound dye was dissolved in a 10 mM Tris, pH 8.8, solution and read using the plate reader at 540-nm.

Cell Proliferation

Briefly, MCF7 cells were seeded in each well (10,000 cells/well) and employed to assess the efficacy of Doxycycline and Doxy-Myr, using RTCA (real-time cell analysis), via the measurement of cell-induced electrical impedance plate (Acea Biosciences Inc.) (18). This approach allows the quantification of the onset and kinetics of the cellular response. Experiments were repeated several times independently, using quadruplicate samples for each condition.

Cell Cycle Analysis

We performed cell-cycle analysis on MCF7 cells treated with Doxycycline, Doxy-Myr, or vehicle-alone. Briefly, after trypsinization, the re-suspended cells were incubated with 10 ng/ml of Hoechst solution (Thermo Fisher Scientific) for 40 min at 37°C under dark conditions. Following a 40 min period, the cells were washed and re-suspended in PBS Ca/Mg for acquisition on the Attune NxT flow cytometer (Thermo Scientific). We analyzed 10,000 events per condition. Gated cells were manually-categorized into cell-cycle stages (19).

Bacterial Growth Assays

Briefly, antibiotic activity was assessed using standard assay systems (20–22). The antibiotic activity of Doxycycline analogs was determined experimentally, using Resazurin (R7017; Sigma-Aldrich, Inc.) as an indicator of bacterial metabolism/vitality, in a 96-well plate format, using *Escherichia coli* and *Staphylococcus aureus*. The minimum inhibitory concentration (MIC) for the studied compounds was determined using the broth microdilution method, the reference susceptibility test for rapidly growing aerobic or facultative microorganism(s). The assays were performed according to the Clinical and Laboratory Standards Institute (CLSI) guidelines. The test compounds and positive control (doxycycline, Sigma Aldrich #D1822) stock solutions were prepared at 25 mM in DMSO and serially diluted (2-fold dilution from 200 to 1.56 μM) in cation adjusted Mueller Hinton Broth (MHB, Sigma Aldrich #90922) in 96-well transparent plates (VWR #734-2781) into a final volume of 50 μL/well. *Staphylococcus aureus* (ATCC 29213) and *E. coli* (ATCC 25922) cultures were maintained on Mueller Hinton Agar (MHA, Sigma Aldrich #70191). A single colony of each strain was then grown overnight at 37

°C in MHB until OD_{600} ∼ 0.6–0.8 and diluted into MHB to a concentration of 106 colony forming units (CFU)/mL, which was equivalent to an OD_{600} ∼ 0.01. Diluted inocula (50 μL) were transferred to the wells of the previously prepared 96-well plates containing the test compounds, negative control (1% DMSO in MHB) and positive control (Doxycycline). Final wells volume was 100 μL, final concentrations for the testing compounds were between 100 and 0.78 μM and final microorganism concentration was 5×10^5 CFU/mL. Subsequently, 10 μL of one negative control well was plated in a petri dish containing MHA to check CFU and the purity of the cultures. The plates were incubated at 37°C for 24 h after which 20 μL of resazurin solution (0.2 mg/mL) was added to the wells followed by 1 h 30 min incubation at 37°C. The OD_{570} and OD_{600} were measured in a microplate reader (BMG FLUOstar Omega). The ratio between OD_{570} and OD_{600} was determined and the MIC represents the lowest concentration of compound that inhibited bacterial growth (OD_{570}/OD_{600} ratio inferior to the average ratio determined for negative control wells). MIC values were determined by three independent experiments.

Assays for Tumor Growth, Metastasis, and Embryo Toxicity

These xenograft assays were carried out, essentially as previously described, without any major modifications (23–27).

Preparation of Chicken Embryos

Fertilized White Leghorn eggs were incubated at 37.5°C with 50% relative humidity for 9 days. At that moment (E9), the chorioallantoic membrane (CAM) was dropped down by drilling a small hole through the eggshell into the air sac, and a 1 cm^2 window was cut in the eggshell above the CAM.

Amplification and Grafting of Tumor Cells

The MDA-MB-231 tumor cell line was cultivated in DMEM medium supplemented with 10% FBS and 1% penicillin/streptomycin. On day E9, cells were detached with trypsin, washed with complete medium and suspended in graft medium. An inoculum of 1×10^6 cells was added onto the CAM of each egg (E9) and then eggs were randomized into groups.

Tumor Growth Assays

At day 18 (E18), the upper portion of the CAM was removed from each egg, washed in PBS and then directly transferred to paraformaldehyde (fixation for 48 h) and weighed. For tumor growth assays, at least 10 tumor samples were collected and analyzed per group ($n \geq 10$).

Metastasis Assays

On day E18, a 1 cm^2 portion of the lower CAM was collected to evaluate the number of metastatic cells in 8 samples per group ($n = 8$). Genomic DNA was extracted from the CAM (commercial kit) and analyzed by qPCR with specific primers for Human Alu sequences. Calculation of Cq for each sample, mean Cq, and relative amounts of metastases for each group are directly managed by the Bio-Rad® CFX Maestro software. A one-way ANOVA analysis with post-tests was performed on all the data.

Embryo Tolerability Assay

Before each administration, the treatment tolerability was evaluated by scoring the number of dead embryos.

Statistical Analysis

Statistical significance was determined using the Student's *t*-test, values of <0.05 were considered significant. Data are shown as the mean ± SEM, unless stated otherwise. Also, ANOVA was conducted, where appropriate.

RESULTS

Generating New Analogs of Doxycycline for Targeting CSCs: Doxy-Myr and Doxy-TPP

Doxycycline is known to function as an inhibitor of the propagation of CSCs, through its ability to inhibit the small mitochondrial ribosome, which is an off-target side-effect (6, 10, 13). Normally, Doxycycline is used as a broad-spectrum bacteriostatic antibiotic to treat a wide range of infections caused by gram-negative and gram-positive bacteria. Therefore, we sought to optimize the ability of Doxycycline for the targeting of CSCs, while minimizing its antibiotic activity, to derive a new chemical entity to selectively target CSCs.

As a first step, we synthesized 9-amino-Doxycycline, to which we covalently attached either a 14 carbon fatty acid moiety (myristic acid) or a six carbon spacer arm containing tri-phenyl-phosphonium (TPP). The chemical structures of these two Doxycycline analogs, as well as the parent compound, are all shown in **Figure 1**. We speculated that the TPP-moiety would better target Doxy-TPP to mitochondria in CSCs. In contrast, the addition of myristic acid could act as a membrane targeting signal, possibly leading to the increased retention of Doxy-Myr within membranous compartments, such as the plasma membrane, the endoplasmic reticulum (ER), the Golgi apparatus, and/or mitochondria.

To determine the functional activity of these Doxycycline analogs, we used the 3D-mammosphere assay, to assess their ability to inhibit the 3D anchorage-independent propagation of MCF7 CSCs. Interestingly, Doxy-TPP was not more potent that Doxycycline itself, so further assays with Doxy-TPP were not carried out (data not shown).

Figure 2 shows a direct comparison of Doxycycline with Doxy-Myr. Remarkably, Doxy-Myr was >5-fold more potent than Doxycycline, with an IC_{50} of 3.46 μM. In contrast, Doxycycline had an IC_{50} of 18.1 μM. Therefore, Doxy-Myr is more potent for targeting the 3D anchorage-independent propagation of CSCs.

To experimentally test the hypothesis that Doxy-Myr was better retained within cells, we took advantage of the observation that Doxycycline is fluorescent (Ex. 390–425 nm/Em. 520–560 nm). Doxy-Myr was more easily detected and retained in monolayer MCF7 cells, when compared to Doxycycline or cells

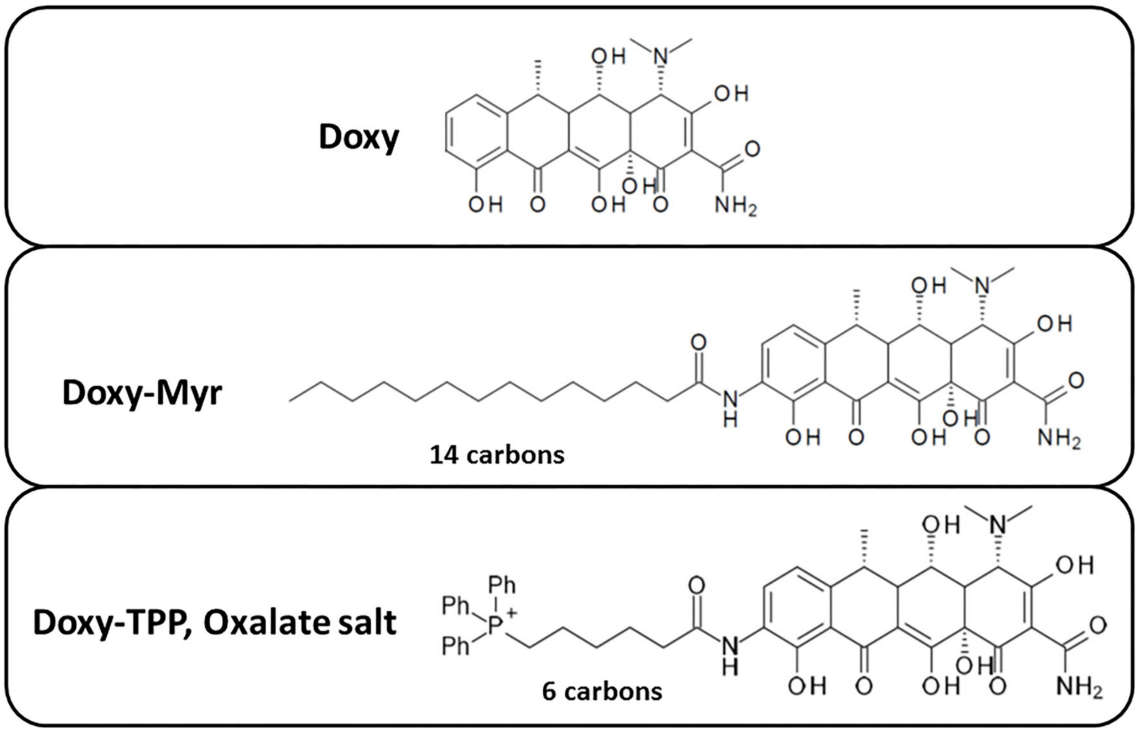

FIGURE 1 | Chemical structures of two new Doxycycline derivatives: Doxy-Myr and Doxy-TPP. Note that Doxy-Myr contains a 14-carbon fatty acid (myristate) covalently attached to 9-amino-Doxycycline and Doxy-TPP contains a TPP-moiety attached via a 6-carbon spacer to 9-amino-Doxycycline.

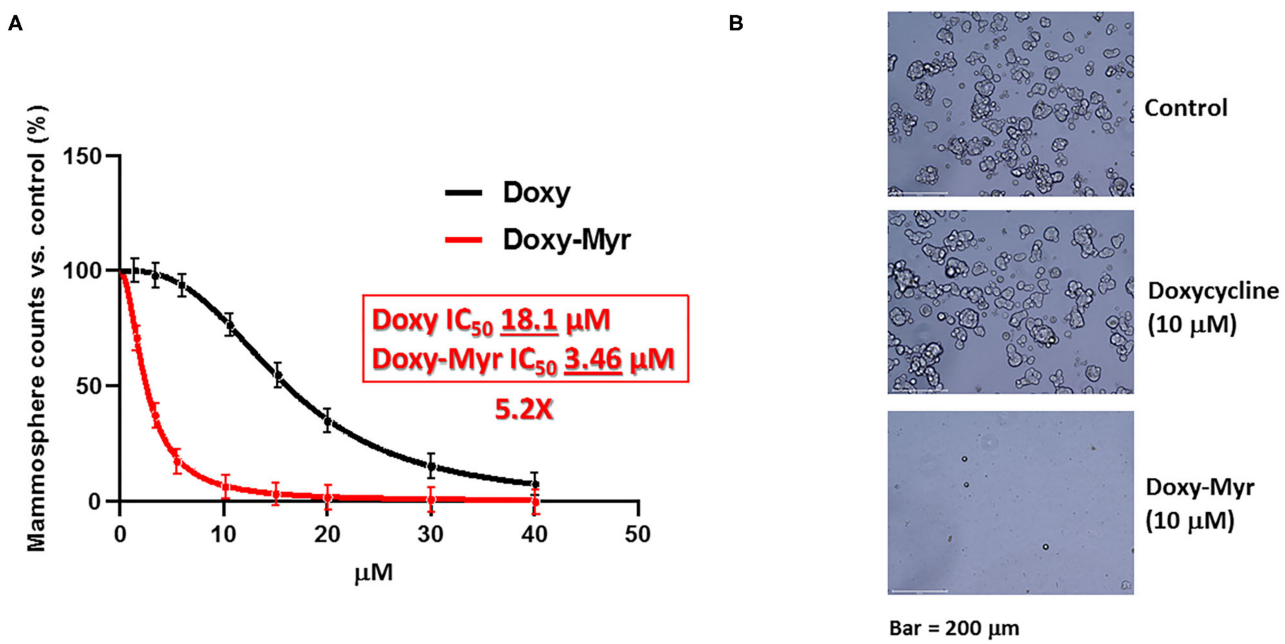

FIGURE 2 | Doxy-Myr more potently inhibits the anchorage-independent propagation of CSCs. **(A)** MCF7 cells were plated under anchorage-independent growth conditions and the number of 3D-mammospheres were counted after 5 days. Note that Doxycycline and Doxy-Myr both inhibited 3D-mammosphere formation, all relative to vehicle-alone controls. However, Doxy-Myr was >5-fold more potent than Doxycycline (IC-50 of 3.46 vs. 18.1 μM). **(B)** Representative phase images of 3D-mammospheres are shown. Bar = 200 μm.

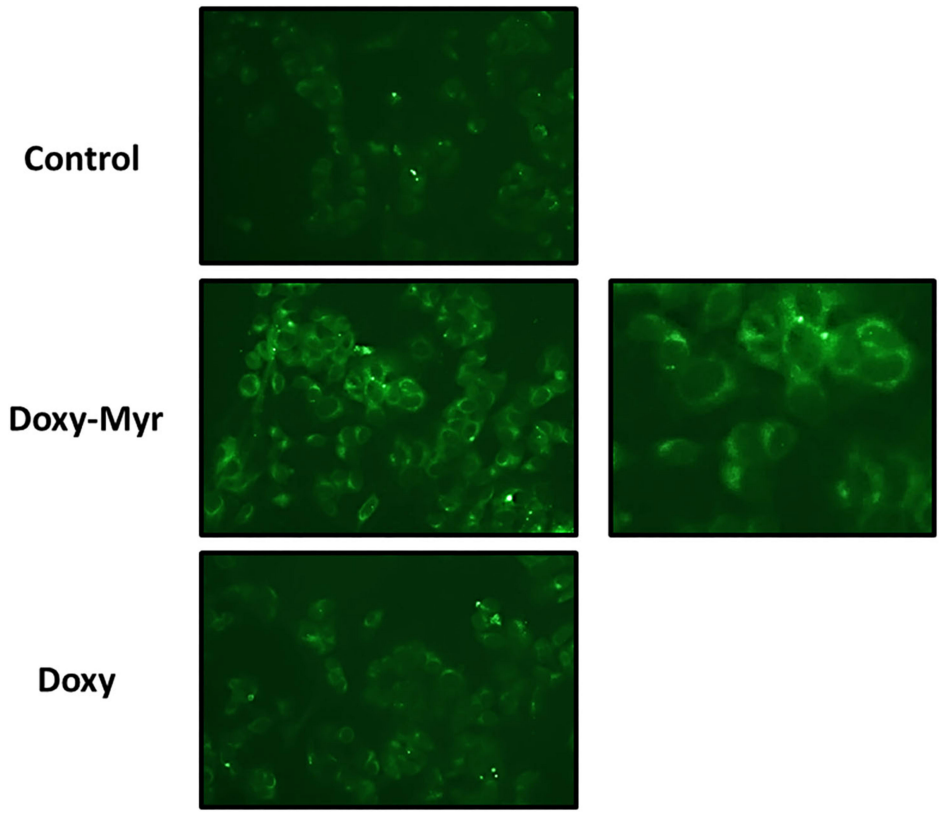

FIGURE 3 | Doxy-Myr is better retained within cells and reveals a peri-nuclear staining pattern. MCF7 cells were cultured for 72 h as 2D-monolayers, in the presence of Doxycycline or Doxy-Myr, at a concentration of 10 μM. Vehicle-alone controls were processed in parallel. Then, MCF7 cells were washed twice with PBS and subjected to live cell imaging to capture the auto-fluorescent signal retained within cells. Note that Doxy-Myr showed the strongest intracellular retention, and was concentrated within peri-nuclear intracellular compartments. No nuclear staining was observed. Quantitation of mean pixel intensity, using Image J software, revealed that relative to Doxycycline, Doxy-Myr showed a near 3-fold increase in intracellular fluorescence.

treated with vehicle alone (**Figure 3**). Doxy-Myr fluorescence showed a peri-nuclear staining pattern, consistent with its partitioning and retention within intracellular membranous compartments. This observation could mechanistically explain its increased potency. No nuclear staining for Doxy-Myr was observed, indicating that it was predominantly excluded from the nucleus.

Doxy-Myr Is Non-toxic in 2D-Monolayers of MCF7 Cells and Normal Human Fibroblasts

To further assess the effects of Doxy-Myr on 2D-cell growth, we next used MCF7 cells and normal human fibroblasts (hTERT-BJ1) treated over a period of 3 days. **Figure 4** shows that both Doxycycline and Doxy-Myr had no appreciable effects on cell viability, as determined over the concentration range of 5–20 μM.

Potential 2D-effects on cell proliferation and the cell cycle were also determined using MCF7 cell monolayers. Clearly, Doxycycline and Doxy-Myr did not inhibit the proliferation of MCF7 cells, as assessed using the xCELLigence (**Figure 5**). Similarly, relative to the parent compound Doxycycline, Doxy-Myr did not have any significant effects on reducing cell cycle progression in 2D-monolayers of MCF7 cells (**Figure 6**).

Therefore, overall Doxy-Myr did not significantly reduce the viability, proliferation or cell cycle progression of 2D-monolayers of MCF7 cells, indicating that its effects were specific for cell propagation under 3D anchorage-independent growth conditions.

Doxy-Laur and Doxy-Pal Are Less Potent Than Doxy-Myr in Targeting CSCs

We also synthesized two other new Doxycycline analogs to study the influence of the fatty acid chain length on their functional activity. These two analogs included Doxy-Laur (harboring a 12 carbon fatty acid) and Doxy-Pal (harboring a 16 carbon fatty acid) (**Figure 7**). Therefore, we directly compared the functional inhibitory activity of Doxy-Myr, Doxy-Laur, and Doxy-Pal in the 3D-mammosphere assay, using MCF7 cells. Interestingly, **Figure 8** demonstrates that the rank order potency is: Doxy-Myr > Doxy-Laur > Doxy-Pal > Doxycycline, with no direct correlation observed between chain length and activity. As such, the addition of myristic acid

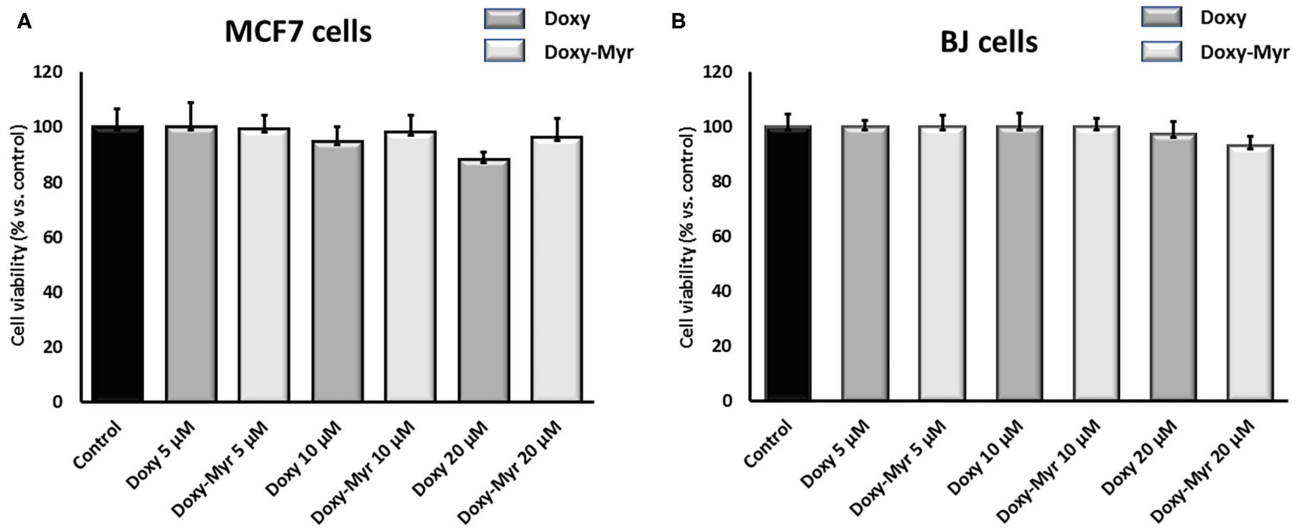

FIGURE 4 | Doxy-Myr does not affect the viability of MCF7 cells or normal fibroblasts, when grown as 2D-monolayers. To determine the effects of Doxy-Myr on cell viability, we next treated MCF7 cells and normal human fibroblasts (hTERT-BJ1) over a period of 3 days. Note that Doxycycline and Doxy-Myr had no appreciable effects on cell viability, in the concentration range of 5–20 μM. **(A)** MCF7 cells, **(B)** hTERT-BJ1 cells.

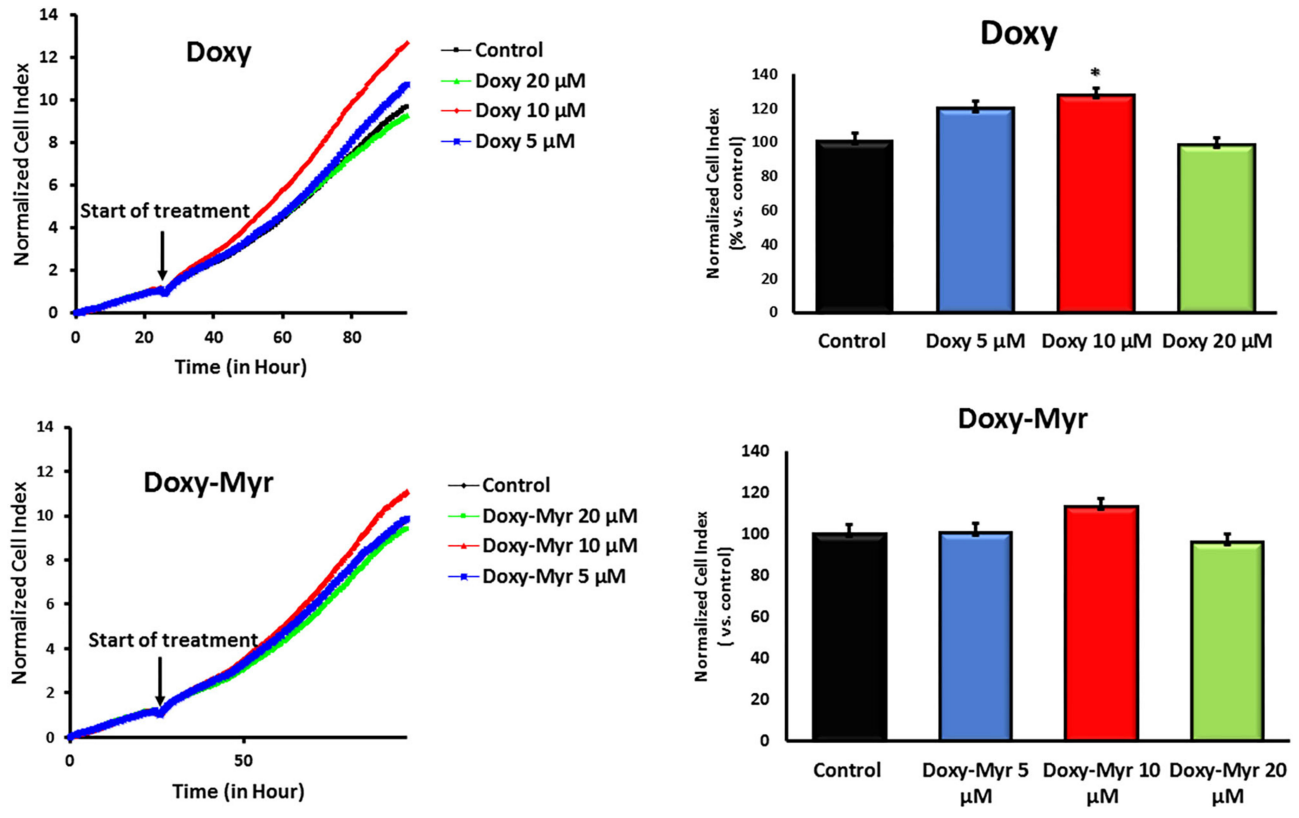

FIGURE 5 | Doxy-Myr does not inhibit the proliferation of MCF7 cell 2D-monolayers. Potential effects of Doxycycline and Doxy-Myr on cell proliferation were determined using MCF7 cell monolayers. Note that Doxycycline and Doxy-Myr did not inhibit the proliferation of MCF7 cells, as assessed using the xCELLigence, in the concentration range of 5–20 μM. *$p < 0.05$.

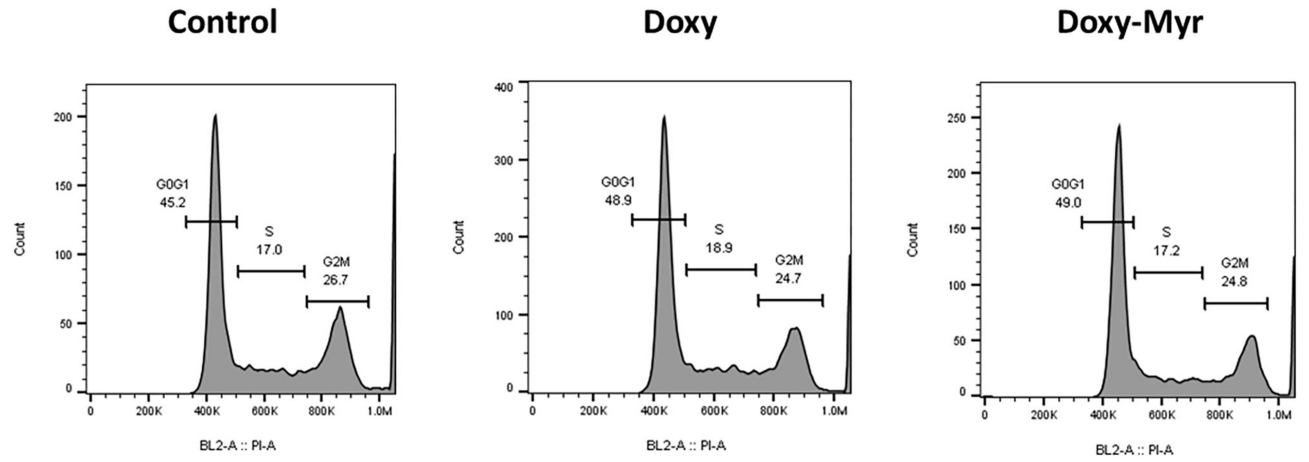

FIGURE 6 | Doxy-Myr does not induce cell cycle arrest, in MCF7 2D-monolayers. MCF7 cells were cultured for 72 h as 2D-monolayers, in the presence of Doxycycline or Doxy-Myr, at a concentration of 10 μM. Vehicle-alone controls were processed in parallel. Note that relative to the parent compound Doxycycline, Doxy-Myr did not have any significant effects on reducing cell cycle progression in 2D-monolayers of MCF7 cells. Representative FACS cell cycle profiles are shown.

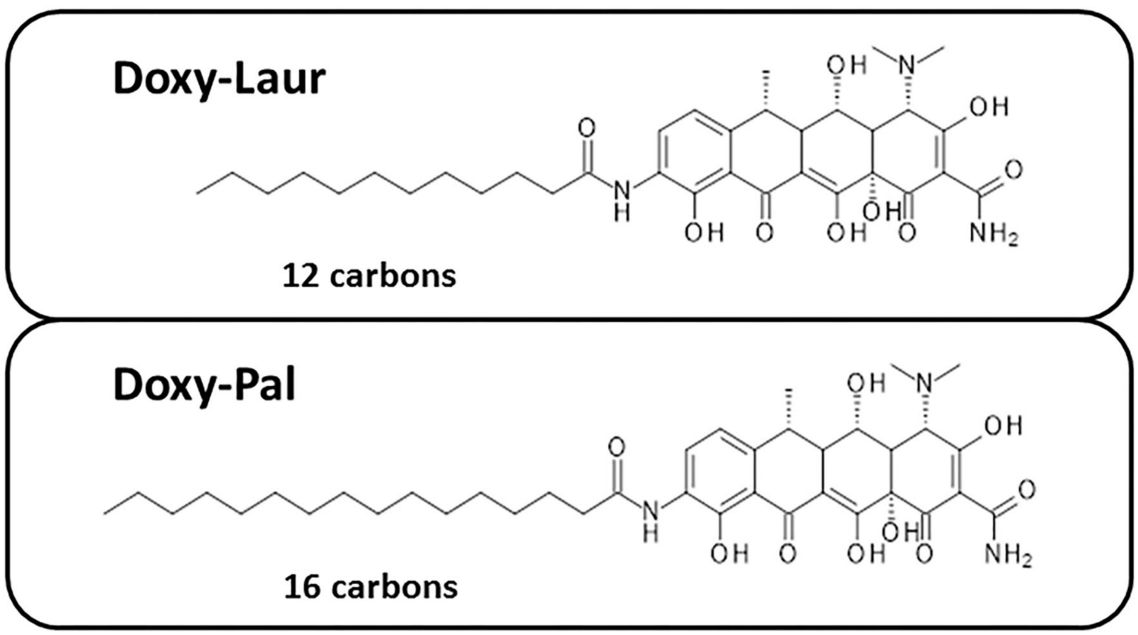

FIGURE 7 | Chemical structures of two other Doxycycline derivatives: Doxy-Laur and Doxy-Pal. We created two other new Doxycycline analogs by varying the chain length of the fatty acid attached to 9-amino-Doxycycline. These two analogs included Doxy-Laur (harboring a 12 carbon fatty acid) and Doxy-Pal (harboring a 16 carbon fatty acid). Their chemical structures are as shown.

(a 14 carbon fatty acid) appears to be the optimal chain length modification.

Doxy-Myr, Doxy-Laur, and Doxy-Pal Lack Antibiotic Activity Against Common Gram-Negative and Gram-Positive Bacteria

Doxycycline is a well-established broad-spectrum antibiotic, that is routinely used for therapeutically targeting both gram-negative and gram-positive bacterial infections. As a consequence, we also assessed the antibiotic activity of the Doxycycline analogs, as compared to the parent compound Doxycycline.

Figure 9 reveals that, as expected, Doxycycline potently and effectively inhibits the growth of both gram-negative (*E. coli*) and gram-positive (*S. aureus*) micro-organisms. Minimum inhibitory concentrations were 3.125 μM (1.3 mg/L) and 12.5 μM (5.5 mg/L), respectively. However, in striking contrast, Doxy-Myr,

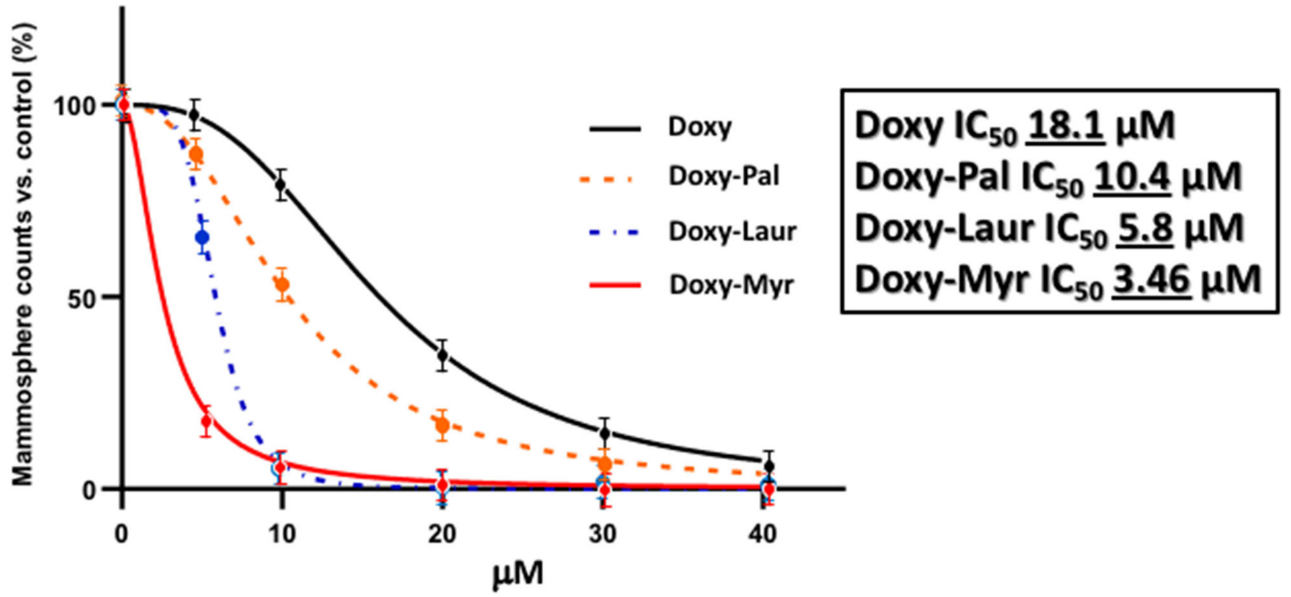

FIGURE 8 | Rank order potency of the new Doxycycline derivatives. Note that Doxy-Myr is the most potent Doxycycline derivative for targeting CSC propagation, as assayed using the 3D mammosphere assay to quantitatively measure anchorage-independent growth. The rank order potency is Doxy-Myr > Doxy-Laur > Doxy-Pal > Doxycycline.

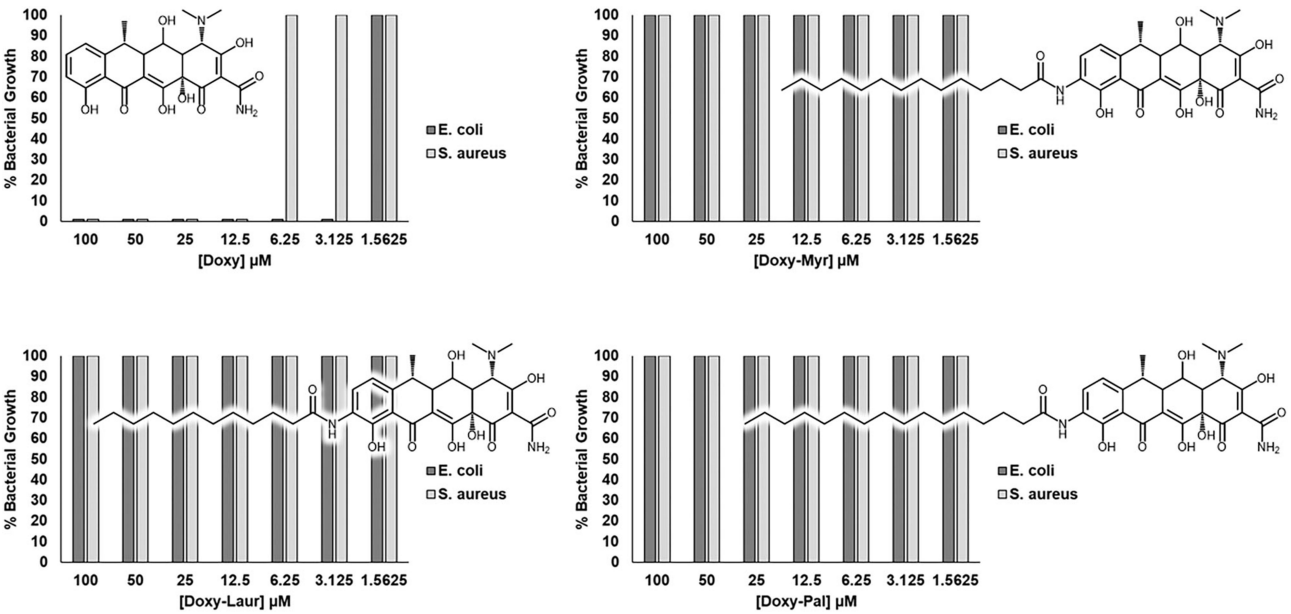

FIGURE 9 | Doxy-Myr, Doxy-Laur and Doxy-Pal do not show any residual antibiotic activity. The novel Doxycycline analogs (Doxy-Myr, Doxy-Laur, and Doxy-Pal) were screened against a gram-positive (*S. aureus*; ATCC 29213) and a gram-negative (*E. coli*; ATCC 25922) strain of bacteria to verify the maintenance of the antibiotic activity, when compared to the parent compound. While Doxycycline presented MIC values of 3.125 μM against *E. coli* and 12.5 μM against *S. aureus*, none of the Doxycycline analogs inhibited bacterial growth up to the concentration of 100 μM.

Doxy-Laur, and Doxy-Pal did not show any obvious antibiotic activity, in the same concentration range. Minimum inhibitory concentrations of the Doxycycline analogs were >100 μM (>65 mg/L). The clinical breakpoints for tetracyclines against *E. coli* and *S. aureus* are between 0.5–2.0 mg/L and 2.0–6.0 mg/L, respectively (28).

Therefore, these simple chemical modifications of Doxycycline have successfully removed its ability to act as a functional antibiotic, while simultaneously increasing its specificity for targeting CSCs.

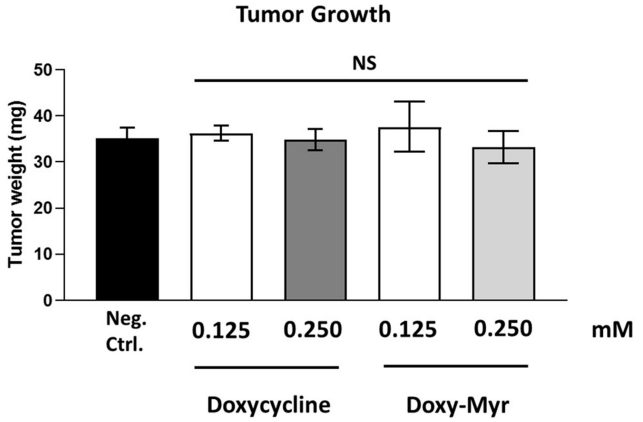

FIGURE 10 | Doxycycline and Doxy-Myr have no effect on tumor growth. MDA-MB-231 cells and the well-established chorio-allantoic membrane (CAM) assay in chicken eggs were used to quantitatively measure tumor growth. An inoculum of 1×10^6 MDA-MB-231 cells was added onto the Upper CAM of each egg (on Day E9) and then eggs were then randomized into groups. On day E10, tumors were detectable and they were then treated daily for 8 days with vehicle alone (1% DMSO in PBS), Doxycycline or Doxy-Myr. After 8 days of drug administration, on day E18 all tumors were weighed. Note that Doxycycline and Doxy-Myr did not have any significant effects on tumor growth. Averages are shown ± SEM. NS, not significant.

Doxy-Myr Potently Inhibits Cancer Cell Metastasis *in vivo*, Without Significant Toxicity

To experimentally evaluate the functional effects of Doxycycline and Doxy-Myr *in vivo*, we next used MDA-MB-231 cells and the well-established chorio-allantoic membrane (CAM) assay in chicken eggs, to quantitatively measure tumor growth and metastasis (16–19). MDA-MB-231 breast cancer cells were used for our *in vivo* studies, as they are estrogen-independent, intrinsically more aggressive, form larger tumors and are significantly more migratory, invasive and metastatic. As such, they are a better *in vivo* model, for simultaneously evaluating both tumor growth and spontaneous metastasis. Moreover, we have previously demonstrated that Doxycycline also effectively inhibits the 3D anchorage-independent growth of MDA-MB-231 cells (13).

Briefly, an inoculum of 1×10^6 MDA-MB-231 cells was added onto the Upper CAM of each egg (day E9) and then eggs were randomized into groups. On day E10, tumors were detectable and they were then treated daily for 8 days with vehicle alone (1% DMSO in PBS), Doxycycline or Doxy-Myr. After 8 days of drug administration, on day E18 all tumors were weighed, and the Lower CAM was collected to evaluate the number of metastatic cells, as analyzed by qPCR with specific primers for Human Alu sequences.

Morphologically, the CAM is constructed of two opposing sheets of epithelial cells, which are separated by a middle stromal layer, containing blood vessels and lymphatics. One epithelial layer is of ectodermal origin, while the other epithelial layer is of mesodermal/endodermal origin. Importantly, movement

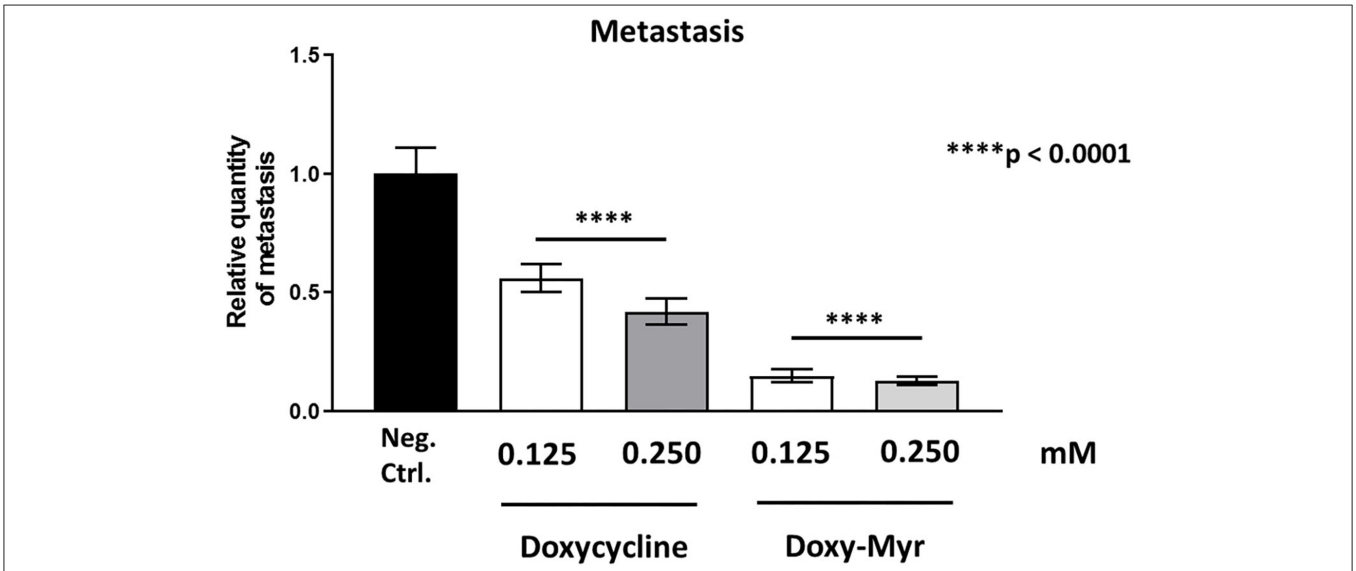

FIGURE 11 | Doxycycline and Doxy-Myr selectively target and prevent cancer metastasis. MDA-MB-231 cells and the well-established chorio-allantoic membrane (CAM) assay in chicken eggs were used to quantitatively measure spontaneous tumor metastasis. An inoculum of 1×10^6 MDA-MB-231 cells was added onto the Upper CAM of each egg (on day E9) and then eggs were then randomized into groups. On day E10, tumors were detectable and they were then treated daily for 8 days with vehicle alone (1% DMSO in PBS), Doxycycline or Doxy-Myr. After 8 days of drug administration, the Lower CAM was collected to evaluate the number of metastatic cells, as analyzed by qPCR with specific primers for Human Alu sequences. Note that Doxycycline and Doxy-Myr both showed significant effects on MDA-MB-231 metastasis. However, Doxy-Myr was clearly more effective than Doxycycline in inhibiting metastasis. Averages are shown ± SEM. $^{****}p < 0.0001$.

TABLE 1 | Chick embryo toxicity of Doxycycline and Doxy-Myr.

Group. #	Group description	Total	Alive	Dead	% Alive	% Dead
1	Neg. Ctrl.	18	15	3	83.33	16.67
2	Doxy, 0.125 mM	13	11	2	84.62	15.38
3	Doxy, 0.250 mM	13	10	3	76.92	23.08
4	Doxy-Myr, 0.125 mM	14	11	3	78.57	21.43
5	Doxy-Myr, 0.250 mM	13	12	1	92.31	7.69

of metastatic MDA-MB-231 cells from the Upper CAM to the Lower CAM involves their migration away from the primary tumor, cellular invasion, intravasation, extravasation, and the formation of a new distant lesion, all of the normal steps that are key features of spontaneous tumor cell metastasis (see **Supplemental Figure 2**).

Figure 10 shows the effects of Doxycycline and Doxy-Myr on MDA-MB-231 tumor growth. Note that that they both did not show any significant effects on tumor growth, as a result of the 8-day period of drug administration.

However, both Doxycycline and Doxy-Myr showed significant effects on MDA-MB-231 cancer cell metastasis. **Figure 11** illustrates that Doxycycline inhibited metastasis (by 44–57.5%). In contrast, Doxy-Myr inhibited metastasis (by 85–87%), at the same concentrations tested. Interestingly, the effects of Doxy-Myr on metastasis were significantly more pronounced.

Surprisingly, little or no embryo toxicity was observed for Doxycycline and Doxy-Myr (**Table 1**). Therefore, we conclude that Doxy-Myr can be further developed as an anti-metastatic agent, selectively inhibiting tumor metastasis, without showing significant toxicity or antibiotic activity.

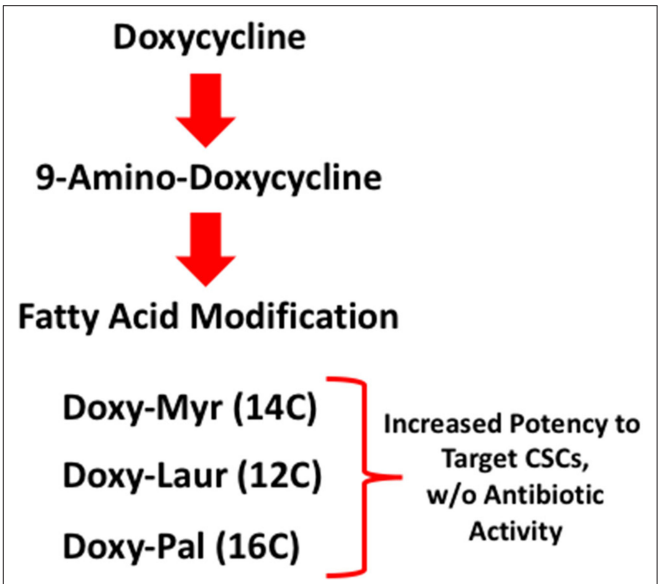

FIGURE 12 | Schematic diagram highlighting our systematic approach to generating Doxycycline derivatives, to target CSCs and prevent metastasis. Lipid moieties were covalently conjugated to 9-amino-Doxycycline. Importantly, these three Doxycycline derivatives lack anti-microbial activity.

DISCUSSION

Here, we report the chemical synthesis and biological activity of several new Doxycycline analogs, modified to increase their effectiveness in the targeting of CSCs. The most promising compound was Doxy-Myr, a Doxycycline analog in which a myristic acid (14 carbon) moiety is covalently attached to the free amino group of 9-amino-Doxycycline. We analyzed the potency of Doxy-Myr, using the 3D-mammosphere assay, to assess its potential inhibitory effects on the anchorage-independent propagation of breast CSCs. Overall, we observed that Doxy-Myr is >5-fold more potent than Doxycycline, the parent compound. Moreover, Doxy-Myr showed better intracellular retention, and was specifically localized within a peri-nuclear membranous compartment. In striking contrast, when MCF7 breast cancer cells or normal fibroblasts were grown as 2D-monolayers, Doxy-Myr did not reveal any effects on cell viability or proliferation, highlighting its unique selectivity for targeting the 3D-propagation of CSCs. In addition, we evaluated other Doxycycline analogs, with longer (16 carbon; palmitic acid) or shorter (12 carbon; lauric acid) chain lengths (**Figure 12**). However, these two analogs were less effective than Doxy-Myr for targeting of CSCs. Finally, using MDA-MB-231 cells, we demonstrated that Doxy-Myr has no appreciable effects on tumor growth, but potently inhibits tumor cell metastasis *in vivo*, with little or no chick embryo toxicity.

Our results also showed that the lipophilic amide substituents in Doxycycline on the C9 of the Tetracycline (TC) skeleton led to the loss of its antibacterial activity. Previously published structure-activity relationship (SAR) studies have shown that chemical modification of the TC skeleton on C9 can be tolerated, leading to diverse antibacterial activity, as is exemplified by the antibiotic Tigecycline. The lipophilicity of the TCs seems to play a key role in the biological potency of this family of drugs. There is a trend of decreased antibiotic activity with the increase of lipophilicity, specifically against gram-negative species, with eventual loss of activity when high lipophilicity is achieved, which could partially explain the loss of activity, we observed after the addition of fatty acids to the Doxycycline scaffold.

Importantly, our improvement in the biological properties of these Doxycycline analogs for targeting CSCs and the associated loss of the anti-microbial activity, make these new analogs extremely promising, because tetracycline resistance among gram-negative and gram-positive pathogens requires exposure to inhibitory concentrations as a selective pressure (28–30). MICs exceeding 65 mg/L also suggest that these analogs might be non-inhibitory to members of the human microbiome, the complex community of microorganisms which exerts wide-ranging effects on human immunity and disease (29, 30).

Interestingly, a previous study successfully used the parent compound, Doxycycline, to prevent bone metastasis in a mouse model, by employing MDA-MD-231 cells (31). However, these

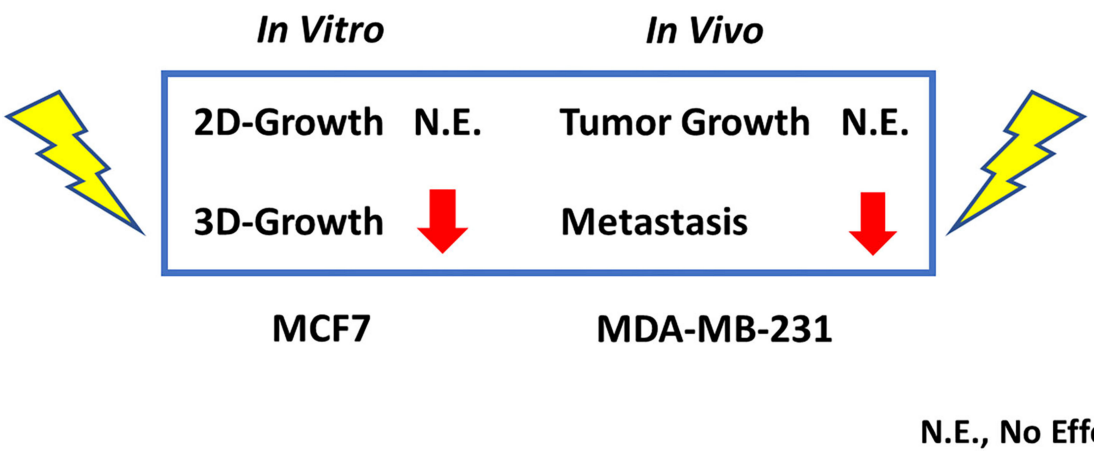

FIGURE 13 | *In vitro* inhibition of 3D-growth predicts *in vivo* inhibition of metastasis. Here, we used two complementary breast cancer cell lines for our *in vitro* screening (MCF7) and *in vivo* (MDA-MB-231) validation assays. More specifically, Doxy-Myr had no effect on 2D-growth *in vitro* and no effect on tumor growth *in vivo*. Conversely, we showed that Doxy-Myr potently inhibited 3D-growth *in vitro*, which directly correlated with inhibition of metastasis *in vivo*. In support of this observation, 3D anchorage-independent growth is thought to be a required step for metastasis *in vivo*. N.E., no effect.

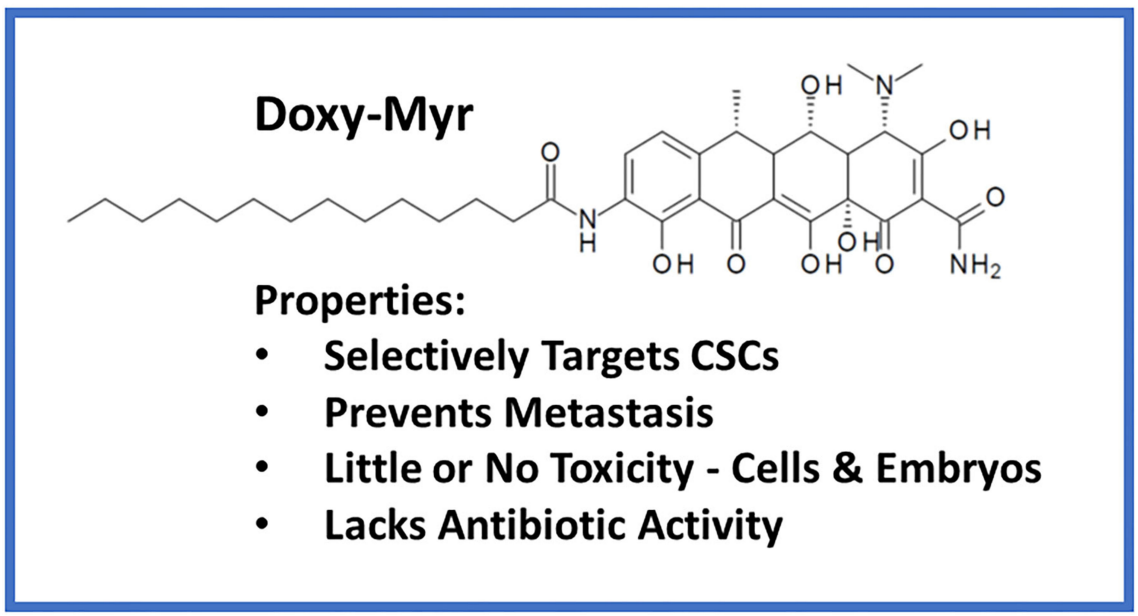

FIGURE 14 | Summary: Properties of Doxy-Myr. Briefly, Doxy-Myr is a lipid modified Doxycycline derivative. Our results show that Doxy-Myr potently targets CSCs and selectively prevents metastasis, without affecting tumor growth. Moreover, Doxy-Myr was non-toxic in the chick embryo assay and did not affect the viability of normal cells, or MCF7 cells, grown as a 2D-monolayer. Importantly, Doxy-Myr lacked antibiotic activity, and did not affect the growth of gram-positive (*E. coli*) or gram-negative (*S. aureus*) organisms.

authors did not examine the effects of Doxycycline on tumor growth, but only focused on bone metastasis. They attributed the efficacy of Doxycycline to its tropism for bone and to its ability to act as a protease inhibitor for lysosomal cysteine proteinases, the cathepsins, and MMPs, because Doxycycline behaves as a zinc chelator.

In contrast, herein, we have demonstrated that Doxycycline and Doxy-Myr both act as inhibitors of metastasis, by targeting the 3D anchorage-independent growth of CSCs, which is a completely different molecular mechanism (**Figures 13**, **14**). However, as predicted, Doxy-Myr was significantly more effective than Doxycycline, at the same concentrations examined. As such, based on these functional observations, we propose that this overall lipid modification strategy may be generally applicable, to facilitate the development and discovery of other drugs, for effectively preventing tumor progression, recurrence, and distant metastasis.

Moreover, our current results are consistent with recent studies showing that prophylaxis with other classes of mitochondrial inhibitors is indeed sufficient to prevent metastasis, using the same pre-clinical xenograft model, with little or no effect on tumor growth and minimal toxicity (32).

DATA AVAILABILITY STATEMENT

All datasets generated for this study are included in the article/**Supplementary Material**.

AUTHOR CONTRIBUTIONS

ML and FS conceived and initiated this project, they selected the clinically-approved drug Doxycycline for chemical modification and optimization by medicinal chemistry. JK performed the custom-chemical syntheses. The phenotypic drug screening and the majority of other wet-lab experiments described in this paper were performed by BÓ. LM determined the antibiotic activity of Doxycycline and its derivatives. BÓ, JK, and LM generated the final figures for the paper. ML and FS wrote the first draft of the manuscript, which was then further edited and approved by BÓ, LM, JL, JK, FS, and ML. ML generated the schematic summary diagrams. All authors contributed to the article and approved the submitted version.

FUNDING

This work was supported by research grant funding, provided by Lunella Biotech, Inc. The funder, Lunella Biotech, Inc., provided the necessary monetary resources to carry out the current study.

ACKNOWLEDGMENTS

We are grateful to Rumana Rafiq, for her kind and dedicated assistance, in keeping the Translational Medicine Laboratory at Salford running smoothly. We would like to thank the Foxpoint Foundation (Canada) and the Healthy Life Foundation (UK) for their philanthropic donations toward new equipment and infrastructure, in the Translational Medicine Laboratory at the University of Salford. We are thankful to Inovotion, Inc. (Grenoble, France), for independently performing the tumor growth and metastasis studies, using the CAM assay, as well as evaluating chicken embryo toxicity, through a research contract with Lunella Biotech, Inc. (Ottawa, Canada).

SUPPLEMENTARY MATERIAL

The Supplementary Material for this article can be found online at: https://www.frontiersin.org/articles/10.3389/fonc.2020.01528/full#supplementary-material

Supplemental Figure 1 | Chemical synthesis of Doxycycline derivatives.

Supplemental Figure 2 | CAM model for measuring tumor growth, metastasis, and embryo toxicity. On day E9, an inoculum of 1 million MDA-MB-231 breast tumor cells was layered on top of the Upper CAM and was allowed to form a primary tumor. Potential therapeutics were applied for a period of 8-days. Then, on day E18, the primary tumor was harvested from the upper CAM and the magnitude of distant metastases was quantitated in the Lower CAM, by performing qPCR with specific primers for recognizing Human Alu sequences. In order for the cells to metastasize, from the Upper CAM to the Lower CAM, it has been established that they need to undergo migration, invasion, intravasation, extravasation, and secondary lesion formation. Toxicity was measured by scoring embryo viability on day E18. See *Materials and Methods* for further details. Reproduced and modified, under a creative commons license, from the following source (33).

REFERENCES

1. De Francesco EM, Sotgia F, Lisanti MP. Cancer stem cells (CSCs): metabolic strategies for their identification and eradication. *Biochem J.* (2018) 475:1611–34. doi: 10.1042/BCJ20170164
2. Martinez-Outschoorn UE, Peiris-Pagés M, Pestell RG, Sotgia F, Lisanti MP. Cancer metabolism: a therapeutic perspective. *Nat Rev Clin Oncol.* (2017) 14:11–31. doi: 10.1038/nrclinonc.2016.60
3. Peiris-Pagès M, Martinez-Outschoorn UE, Pestell RG, Sotgia F, Lisanti MP. Cancer stem cell metabolism. *Breast Cancer Res.* (2016) 18:55. doi: 10.1186/s13058-016-0712-6
4. Yu Z, Pestell TG, Lisanti MP, Pestell RG. Cancer stem cells. *Int J Biochem Cell Biol.* (2012) 44:2144–51. doi: 10.1016/j.biocel.2012.08.022
5. Sotgia F, Ozsvari B, Fiorillo M, De Francesco EM, Bonuccelli G, Lisanti MP. A mitochondrial based oncology platform for targeting cancer stem cells (CSCs): MITO-ONC-RX. *Cell Cycle.* (2018) 17:2091–100. doi: 10.1080/15384101.2018.1515551
6. De Luca A, Fiorillo M, Peiris-Pagès M, Ozsvari B, Smith DL, Sanchez-Alvarez R, et al. Mitochondrial biogenesis is required for the anchorage-independent survival and propagation of stem-like cancer cells. *Oncotarget.* (2015) 6:14777–95. doi: 10.18632/oncotarget.4401
7. Farnie G, Sotgia F, Lisanti MP. High mitochondrial mass identifies a sub-population of stem-like cancer cells that are chemo-resistant. *Oncotarget.* (2015) 6:30472–86. doi: 10.18632/oncotarget.5401
8. Lamb R, Harrison H, Hulit J, Smith DL, Lisanti MP, Sotgia F. Mitochondria as new therapeutic targets for eradicating cancer stem cells: quantitative proteomics and functional validation via MCT1/2 inhibition. *Oncotarget.* (2014) 5:11029–37. doi: 10.18632/oncotarget.2789
9. Zhang L, Xu L, Zhang F, Vlashi E. Doxycycline inhibits the cancer stem cell phenotype and epithelial-to-mesenchymal transition in breast cancer. *Cell Cycle.* (2017) 16:737–45. doi: 10.1080/15384101.2016.1241929

10. Lamb R, Fiorillo M, Chadwick A, Ozsvari B, Reeves KJ, Smith L, et al. Doxycycline down-regulates DNA-PK and radiosensitizes tumor initiating cells: implications for more effective radiation therapy. *Oncotarget.* (2015) 6:14005–25. doi: 10.18632/oncotarget.4159
11. Sotgia F, Whitaker-Menezes D, Martinez-Outschoorn UE, Flomenberg N, Birbe RC, Witkiewicz K, et al. Mitochondrial metabolism in cancer metastasis: visualizing tumor cell mitochondria and the "reverse Warburg effect" in positive lymph node tissue. *Cell Cycle.* (2012) 11:1445–54. doi: 10.4161/cc.19841
12. Lin CC, Lo MC, Moody RR, Stevers NO, Tinsley SL, Sun D. Doxycycline targets aldehyde dehydrogenase-positive breast cancer stem cells. *Oncol Rep*. (2018) 39:3041–7. doi: 10.3892/or.2018.6337
13. Lamb R, Ozsvari B, Lisanti CL, Tanowitz HB, Howell A, Martinez-Outschoorn E, et al. Antibiotics that target mitochondria effectively eradicate cancer stem cells, across multiple tumor types: treating cancer like an infectious disease. *Oncotarget.* (2015) 6:4569–84. doi: 10.18632/oncotarget.3174
14. Scatena C, Roncella M, Di Paolo A, Aretini P, Menicagli M, Fanelli G, et al. Doxycycline, an inhibitor of mitochondrial biogenesis, effectively reduces Cancer Stem Cells (CSCs) in early breast cancer patients: a clinical pilot study. *Front Oncol.* (2018) 8:452. doi: 10.3389/fonc.2018.00452
15. Barden CT, Buckwalter LB, Testa TR, Petersen JP, Lee VJ. "Glycylcyclines". 3. 9-aminodoxycyclinecarboxamides. *J Med Chem.* (1994) 37:3205–11. doi: 10.1021/jm00046a003
16. Ozsvari B, Fiorillo M, Bonuccelli G, Cappello AR, Frattaruolo L, Sotgia F, et al. Mitoriboscins: mitochondrial-based therapeutics targeting cancer stem cells (CSCs), bacteria and pathogenic yeast. *Oncotarget.* (2017) 8:67457–72. doi: 10.18632/oncotarget.19084
17. Ozsvari B, Sotgia F, Lisanti MP. Exploiting mitochondrial targeting signal(s), TPP and bis-TPP, for eradicating cancer stem cells (CSCs). *Aging.* (2018) 10:229–40. doi: 10.18632/aging.101384
18. Ozsvari B, Nuttall JR, Sotgia F, Lisanti MP. Azithromycin and roxithromycin define a new family of "senolytic" drugs that target senescent human fibroblasts. *Aging.* (2018) 10:3294–307. doi: 10.18632/aging.101633
19. Fiorillo M, Sotgia F, Lisanti MP. "Energetic" cancer stem cells (e-CSCs): a new hyper-metabolic and proliferative tumor cell phenotype, driven by mitochondrial energy. *Front Oncol.* (2019) 8:677. doi: 10.3389/fonc.2018.00677
20. The European Committee on Antimicrobial Susceptibility Testing. *Routine Extended Internal Quality Control for MIC Determination Disk Diffusion as Recommended by EUCAST*, *Version 9*.0 (2019). Available online at: http://www.eucast.org (accessed August 12, 2020).
21. M02-A12. *Performance Standards for Antimicrobial Disk Susceptibility Tests; Approved Standard—Twelfth Edition*. Wayne, PA: Clinical and Laboratory Standards Institute. (2015).
22. Blackwood RK, English AR. Structure-activity relationships in the tetracycline series. In: Perlman D, editor. *Advances in Applied Microbiology*. London: Academic Press, Inc. (1970). p. 237–65. doi: 10.1128/AAC.01536-15
23. Alsamri H, El Hasasna H, Al Dhaheri Y, Eid AH, Attoub S, Iratni R. Carnosol, a natural polyphenol, inhibits migration, metastasis, and tumor growth of breast cancer via a ROS-dependent proteasome degradation of STAT3. *Front Oncol.* (2019) 9:743. doi: 10.3389/fonc.2019.00743
24. Nascimento BFO, Laranjo M, Pereira NAM, Dias-Ferreira J, Piñeiro M, Botelho MF, et al. Ring-fused diphenylchlorins as potent photosensitizers for photodynamic therapy applications: *in vitro* tumor cell biology and *in vivo* chick embryo chorioallantoic membrane studies. *ACS Omega.* (2019) 4:17244–50. doi: 10.1021/acsomega.9b01865
25. Gilson P, Couvet M, Vanwonterghem L, Henry M, Vollaire J, Baulin V, et al. The pyrrolopyrimidine colchicine-binding site agent PP-13 reduces the metastatic dissemination of invasive cancer cells *in vitro* and *in vivo*. *Biochem Pharmacol.* (2019) 160:1–13. doi: 10.1016/j.bcp.2018.12.004
26. El Hasasna H, Saleh A, Al Samri H, Athamneh K, Attoub S, Arafat K, et al. Rhus coriaria suppresses angiogenesis, metastasis and tumor growth of breast cancer through inhibition of STAT3, NFκB and nitric oxide pathways. *Sci Rep.* (2016) 6:21144. doi: 10.1038/srep21144
27. Al Dhaheri Y, Attoub S, Arafat K, Abuqamar S, Viallet J, Saleh A, et al. Anti-metastatic and anti-tumor growth effects of *Origanum majorana* on highly metastatic human breast cancer cells: inhibition of NFκB signaling and reduction of nitric oxide production. *PLoS ONE.* (2013) 8:e68808. doi: 10.1371/journal.pone.0068808
28. The European Committee on Antimicrobial Susceptibility Testing. *Breakpoint Tables for Interpretation of MICs and Zone Diameters, Version 10.0*. (2020). Available online at: https://eucast.org/ (accessed August 12, 2020).
29. Belkaid Y, Segre JA. Dialogue between skin microbiota and immunity. *Science*. (2014) 346:954–9. doi: 10.1126/science.1260144
30. Lazar V, Ditu LM, Pircalabioru GG, Gheorghe I, Curutiu C, Holban AM, et al. Aspects of gut microbiota and immune system interactions in infectious diseases, immunopathology, and cancer. *Front Immunol*. (2018) 9:1830. doi: 10.3389/fimmu.2018.01830
31. Duivenvoorden WC, Popović SV, Lhoták S, Seidlitz E, Hirte HW, Tozer RG, et al. Doxycycline decreases tumor burden in a bone metastasis model of human breast cancer. *Cancer Res.* (2002) 62, 1588–91.
32. Ózsvári B, Sotgia F, Lisanti MP. First-in-class candidate therapeutics that target mitochondria and effectively prevent cancer cell metastasis: mitoriboscins and TPP compounds. *Aging*. (2020) 12:10162–79. doi: 10.18632/aging.103336
33. Dünker N, Jendrossek V. Implementation of the Chick Chorioallantoic Membrane (CAM) model in radiation biology and experimental radiation oncology research. *Cancers*. (2019) 11:E1499. doi: 10.3390/cancers11101499

Conflict of Interest: JK is employed by the company Eurofins Integrated Discovery UK Ltd. FS holds a part-time affiliation with Lunella Biotech, Inc. ML holds a part-time affiliation with Lunella Biotech, Inc.

The remaining authors declare that the research was conducted in the absence of any commercial or financial relationships that could be construed as a potential conflict of interest.

frontiers in Oncology

ORIGINAL RESEARCH
published: 22 October 2020
doi: 10.3389/fonc.2020.01776

Mitochondrial Fission Factor (MFF) Inhibits Mitochondrial Metabolism and Reduces Breast Cancer Stem Cell (CSC) Activity

Rosa Sánchez-Alvarez[1†], Ernestina Marianna De Francesco[2,3†], Marco Fiorillo[2], Federica Sotgia[2] and Michael P. Lisanti[2*]*

[1] Division of Cancer Sciences, Faculty of Biology, Medicine and Health, School of Medical Sciences, University of Manchester, Manchester, United Kingdom, [2] Translational Medicine, School of Science, Engineering and Environment (SEE), Biomedical Research Centre (BRC), University of Salford, Greater Manchester, United Kingdom, [3] Department of Clinical and Experimental Medicine, University of Catania, and ARNAS Garibaldi, Catania, Italy

OPEN ACCESS

Edited by:
Philipp E. Scherer,
University of Texas Southwestern Medical Center, United States

Reviewed by:
Hsueh-Wei Chang,
Kaohsiung Medical University, Taiwan
Daeseok Kim,
University of Texas Southwestern Medical Center, United States

***Correspondence:**
Federica Sotgia
fsotgia@gmail.com
Michael P. Lisanti
michaelp.lisanti@gmail.com

[†] These authors have contributed equally to this work

Specialty section:
This article was submitted to Cancer Metabolism, a section of the journal Frontiers in Oncology

Received: 23 May 2020
Accepted: 10 August 2020
Published: 22 October 2020

Citation:
Sánchez-Alvarez R, De Francesco EM, Fiorillo M, Sotgia F and Lisanti MP (2020) Mitochondrial Fission Factor (MFF) Inhibits Mitochondrial Metabolism and Reduces Breast Cancer Stem Cell (CSC) Activity. Front. Oncol. 10:1776. doi: 10.3389/fonc.2020.01776

Elevated mitochondrial biogenesis and metabolism represent key features of breast cancer stem cells (CSCs), whose propagation is conducive to disease onset and progression. Therefore, interfering with mitochondria biology and function may be regarded as a useful approach to eradicate CSCs. Here, we used the breast cancer cell line MCF7 as a model system to interrogate how mitochondrial fission contributes to the development of mitochondrial dysfunction toward the inhibition of metabolic flux and stemness. We generated an isogenic MCF7 cell line transduced with Mitochondrial Fission Factor (MCF7-MFF), which is primarily involved in mitochondrial fission. We evaluated the biochemical, molecular and functional properties of MCF7-MFF cells, as compared to control MCF7 cells transduced with the empty vector (MCF7-Control). We observed that MFF over-expression reduces both mitochondrial mass and activity, as evaluated using the mitochondrial probes MitroTracker Red and MitoTracker Orange, respectively. The analysis of metabolic flux using the Seahorse XFe96 revealed the inhibition of OXPHOS and glycolysis in MCF7-MFF cells, suggesting that increased mitochondrial fission may impair the biochemical properties of these organelles. Notably, CSCs activity, assessed by 3D-tumorsphere assays, was reduced in MCF7-MFF cells. A similar trend was observed for the activity of ALDH, a well-established marker of stemness. We conclude that enhanced mitochondrial fission may compromise CSCs propagation, through the impairment of mitochondrial function, possibly leading to a quiescent cell phenotype. Unbiased proteomic analysis revealed that proteins involved in mitochondrial dysfunction, oxidative stress-response, fatty acid metabolism and hypoxia signaling are among the most highly up-regulated in MCF7-MFF cells. Of note, integrated analysis of top regulatory networks obtained from unbiased proteomics in MCF7-MFF cells predicts that this cell phenotype activates signaling systems and effectors involved in the inhibition of cell survival and adhesion, together with the activation of specific breast cancer cell death programs. Overall, our study shows that unbalanced and abnormal

activation of mitochondrial fission may drive the impairment of mitochondrial metabolic function, leading to inhibition of CSC propagation, and the activation of quiescence programs. Exploiting the potential of mitochondria to control pivotal events in tumor biology may, therefore, represent a useful tool to prevent disease progression.

Keywords: mitochondrial fission factor, CSCs, mitochondrial metabolism, breast cancer, mitochondrial dynamics, oxidative metabolism, metabo-stemness, mitochondrial mass

INTRODUCTION

Mitochondrial function is essential for supplying energy to fuel cancer cell growth and metastatic dissemination (1). Furthermore, enhanced mitochondrial metabolism has emerged as one of the novel features of cancer stem cells (CSCs), which exhibit tumorigenic and self-renewal properties, carry metastatic potential and provide resistance to anti-cancer therapies (2–4). In this regard, cancer cells biologically recapitulate certain stemness features, including anchorage-independent growth and higher tumor-initiating capacity, as well as increased mitochondrial mass, biogenesis and protein translation, across multiple tumor types (5). These observations, which clearly suggest a key role for mitochondria in CSC maintenance and propagation, are corroborated by the evidence that mitochondrial metabolic function and OXPHOS are augmented in cancer cells with stemness features, as compared to the non-stem cancer cell sub-population (6, 7). As a consequence of these findings, the ability of several classes of mitochondria-interfering agents to inhibit CSC dissemination has been explored, as reviewed in De Francesco et al. (8). In this regard, several antibiotics that impair mitochondrial protein translation, as a side effect, have been shown to be effective in depleting the CSC population *in vitro*, as well as in clinical studies (9–13). As such, a deeper understanding of mitochondrial biology in cancer would pave the way toward the identification of targeted therapeutics, aimed at selectively halting and eradicating CSCs.

Adequate mitochondrial function also depends on the intrinsic mechanical changes in the dynamic structure and architecture of these organelles (14, 15). For instance, changes in mitochondrial size and shape, as well as localization, are critical for the homeostasis of the energetic machinery. The main macro-mechanical events regulating mitochondrial architecture are represented by cycles of mitochondrial fusion and fission (fragmentation), that together constitute a mitochondrial network (16, 17). Given their important role in maintaining mitochondria homeostasis, fusion and fission are tightly regulated processes, whose de-regulation is associated with metabolic dysfunction, that may precede the establishment of pathological phenotypes (14, 17). In cancer, the elevated nutrient demands of proliferating cells are mainly fulfilled by drastic changes in energetic metabolism, largely supported by mitochondria, whose changes in function and shape are pivotal to tumor growth (1). Indeed, several oncogenic signals have been shown to influence the number of mitochondria, which is dependent on fusion-fission dynamics (15, 16, 18). Likewise, aberrant mitochondrial fission results in massive mitochondrial fragmentation, resulting in inhibition of oxidative metabolism and depletion of ATP (19). Mitochondrial Fission Factor (MFF) is an integral membrane protein of the outer mitochondrial membrane that serves as the main molecular mediator regulating mitochondria fragmentation (20). During fission, the cytosolic protein Drp1 is recruited to the mitochondrial surface via MFF and the proteins Fis1 (mitochondrial fission protein 1), MiD49 and MiD51 (mitochondrial dynamics proteins of 49 and 51 kDa, respectively) (21–23). Oligomeric Drp1 complexes are, thereafter, assembled into specific structures named *puncta*, which wrap around mitochondrial tubules, forcing them toward the fission reaction (24). Several studies have demonstrated that increased MFF expression is required for successive mitochondrial fission and is associated with disease states (25). Nevertheless, the role of MFF in regulating mitochondrial dynamics in breast cancer has not been thoroughly elucidated.

Herein, we provide evidence that aberrant MFF expression in breast cancer cells drastically inhibits mitochondrial mass and function, associated with a reduction of mitochondrial oxidative metabolism and ATP depletion. Proteomic profiling of MFF-overexpressing breast cancer cells reveals a phenotype associated with the inhibition of mitochondrial metabolism and a quiescent cell state. Biologically, MFF-overexpressing breast cancer cells exhibit impaired 3D mammosphere formation capacity, suggesting that the manipulation of mitochondrial structure and dynamics may represent a useful tool to control stemness traits in breast cancer.

MATERIALS AND METHODS

Cell Culture

MCF7 human breast cancer cells were purchased from ATCC. Cells were cultured in Dulbecco's modified Eagle's medium (DMEM), supplemented with 10% heat-inactivated fetal bovine serum, 100 units/mL of penicillin, 100 μg/mL of streptomycin and 2 mM Glutamax (ThermoScientific), in a 37°C humidified atmosphere containing 5% CO_2, unless otherwise noted.

Lentiviral Gene Transduction

Lentiviral plasmids, packaging cells and reagents were from Genecopoeia. Forty-eight hours after seeding, 293Ta packaging cells were transfected with lentiviral vectors encoding the mitochondrial fission factor (MFF, EX-Z4766-Lv-105), or empty vector (EV, EX-NEG-Lv105), using the Lenti-PacTM HIV Expression Packaging Kit, according to the manufacturer's instructions. Two days post-transfection, lentivirus-containing culture medium was passed through a 0.45 μm filter and added to the target cells (MCF7 cells) in the presence of 5 μg/ml polybrene. Transduced MCF7 cells were selected with 2.5 μg/ml puromycin.

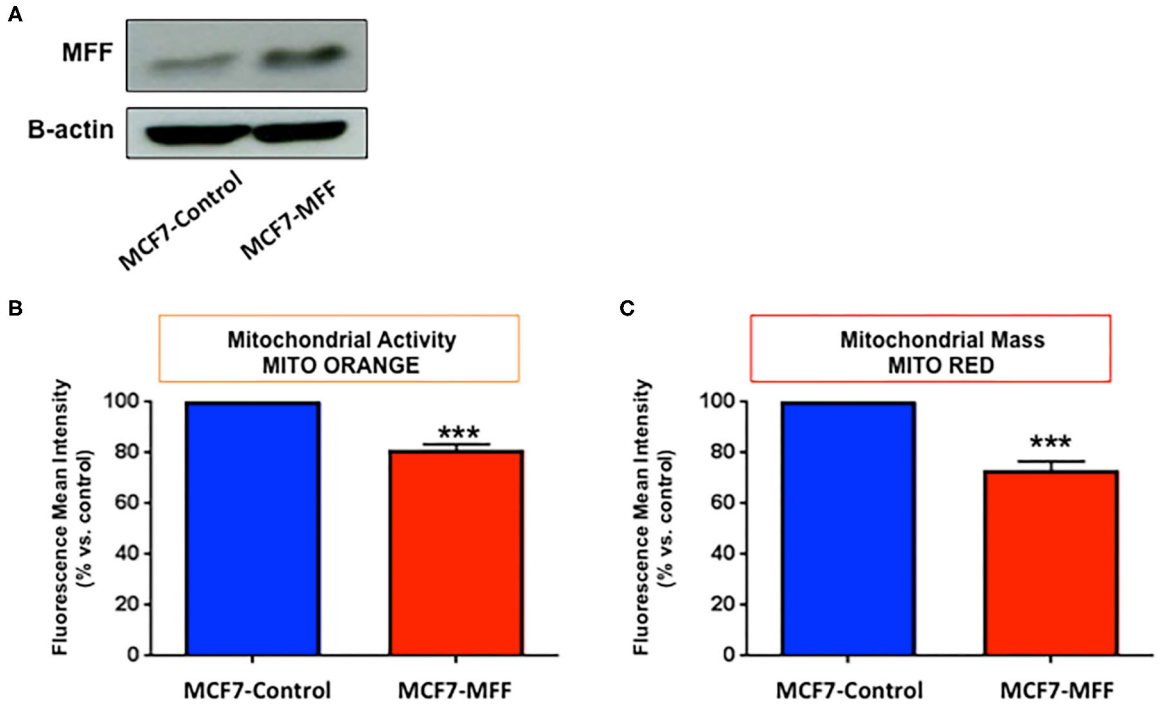

FIGURE 1 | Mitochondrial fission factor (MFF) decreases mitochondrial activity and mass. **(A)** Evaluation of MFF overexpression. MCF7 cells, stably transduced with a lentiviral vector encoding for mitochondrial fission factor (MCF-MFF) or the empty-vector (MCF-7 Control), were subjected to protein extraction and immunoblotted for MFF. β-actin is shown as equal loading control. **(B,C)** MFF overexpression decreases mitochondrial activity and mass. Stably transduced MCF7 cells harboring MFF (MCF-MFF) and the respective empty-vector (MCF-7 Control) were seeded for 24 h and then mitochondrial activity and mitochondrial mass were quantitated by FACS analysis using the probes MitoTracker Orange **(B)** and MitoTracker Deep-Red **(C)**. At least four replicates were performed in each experiment. Results are the average of the mean of three independent experiments and are expressed as percentages normalized to the control ± SEM. ***$p < 0.001$.

Western Blotting

Western blotting of stably transduced MCF7 cells was used to evaluate the efficiency of transduction. Briefly, 70–80% confluent stably-transduced MCF7 cells (harboring MFF and the respective Ex-Negative control) were harvested in lysis buffer (10 mM Tris pH 7.5, 150 mM NaCl, 1% Triton X-100, and 60 mM n-octyl-glucoside), containing protease (Roche) and phosphatase inhibitors (Sigma) and kept at 4°C for 40 min with rotation. Lysates were cleared by centrifugation for 10 min at 10, 000 × g and supernatants were collected. Equal amounts of protein lysate, as determined by using the BCA protein assay kit (Pierce), were diluted in SDS sample buffer and dry-boiled for 5 min, prior to separation by SDS-PAGE using 4–20% acrylamide gels (Biorad). Samples were then blotted onto nitrocellulose membranes (Biorad), blocked in 5% milk in TBS-Tween 20 (P9416, Sigma) for 1 h and probed with antibodies directed against MFF (Abcam), or β-actin (Sigma), which was used as loading control. Bound antibodies were detected using a horseradish peroxidase-conjugated secondary antibody (ab6789 and ab6721, Abcam) and the signal was visualized using Supersignal West Pico chemiluminescent substrate (ThermoScientific).

Mitochondrial Staining

Mitochondrial activity was assessed using the fluorescent probe MitoTracker Orange (CM-H2TMRos-reduced form) (ThermoFisher), whose accumulation in mitochondria is dependent upon membrane potential. Mitochondrial mass was determined using the fluorescent probe MitoTracker Deep-Red (ThermoFisher), which localizes to mitochondria regardless of mitochondrial membrane potential. Stably transduced MCF7 cells (harboring MFF or the Ex-Negative Control) were seeded for 48 h. After 48 h, the cells were incubated with pre-warmed MitoTracker staining solution (diluted in DMEM without serum to a final concentration of 10 nM) for 30 min at 37°C. All subsequent steps were performed in the dark. Cells were washed in PBS, harvested, and re-suspended in 300 μL of PBS/$Ca^{2+}Mg^{2+}$. Cells were then analyzed by flow cytometry using Fortessa (BD Bioscience). Data analysis was performed using FlowJo software. Results are the average of the mean of three independent experiments, were normalized to the control (Ex-Neg) and are expressed as percentages of mean fluorescence intensity. At least 4 biological replicates were performed in each experiment.

Seahorse XFe96 Metabolic Flux Analysis

Real time oxygen consumption rates (OCRs) and Extracellular acidification rates (ECARs) were determined for stably transduced MCF7 cells using the Seahorse Extracellular Flux (XFe96) analyzer (Seahorse Bioscience, MA, USA). Briefly, 10,000 cells per well were seeded into XFe96 well cell culture

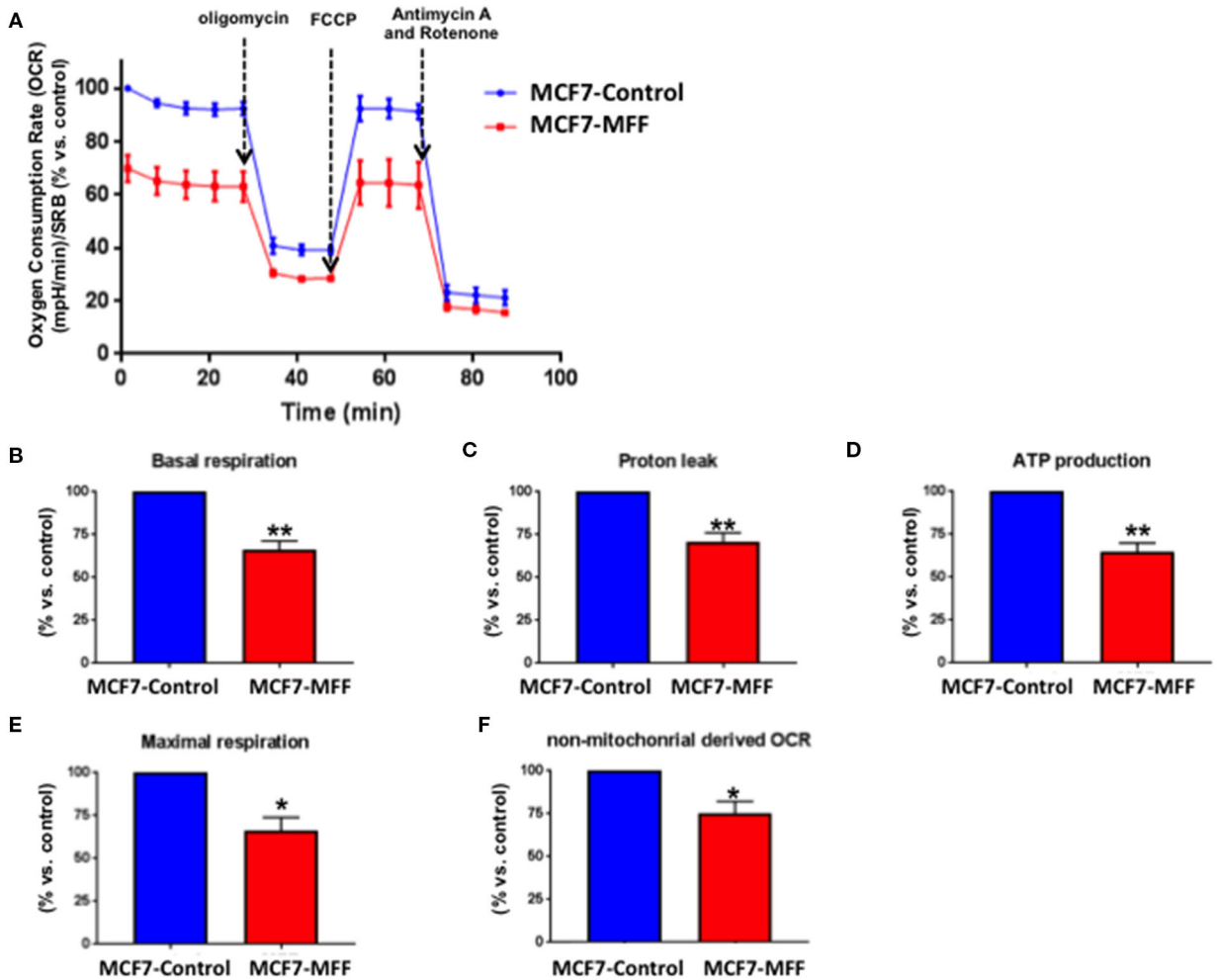

FIGURE 2 | Mitochondrial fission factor (MFF) reduces mitochondrial respiration. The metabolic profile of stably transduced MCF7 cells harboring MFF (MCF-MFF) and the respective empty-vector (MCF-7 Control) was examined using the Seahorse XFe96 analyzer. **(A)** Oxygen consumption rate (OCR) is significantly reduced in cells transduced with MFF as compared to control cells. **(B–F)** Significant reductions in respiration (basal and maximal), proton leak, ATP levels and non-mitochondrial derived OCR were observed in MCF7 cells transduced with MFF as compared to the control cells. At least six replicates were performed in each experiment. Results are the average of the mean of three independent experiments and are expressed as percentages normalized to the control ± SEM. $^{*}p < 0.05$, $^{**}p < 0.01$.

plates and incubated overnight with complete medium to allow attachment. After 24 h of incubation, cells were washed in either pre-warmed XF assay media containing 2 mM glutamine, pH 7.4 for ECAR measurements or in XF assay media supplemented with 10 mM glucose, 1 mM Pyruvate, 2 mM L-glutamine and adjusted at 7.4 pH for OCR measurements. Cells were then maintained in 175 μL/well of XF assay media at 37°C, in a non-CO_2 incubator for 1 h. During the incubation time, 25 μL of 80 mM glucose, 9 μM oligomycin, and 1M 2-deoxyglucose were loaded for ECAR measurement or 10 μM oligomycin, 9 μM FCCP, 10 μM rotenone, 10 μM antimycin A were loaded for OCR measurements, in XF assay media into the injection ports in the XFe96 sensor cartridge. Measurements were normalized by protein content, determined by SRB. Data sets were analyzed by employing XFe96 software and GraphPad Prism software, using Student's *t*-test calculations. Results are the average of the mean of three independent experiments normalized to the control and are expressed as percentages of mpH/min/SRB for ECAR or pmol/min/SRB for OCR measurements. At least six biological replicates were performed in each experiment.

3D Mammosphere Culture

A single cell suspension of stably transduced MCF7 cells was prepared using enzymatic (1x Trypsin-EDTA, Sigma Aldrich), and manual disaggregation (25 gauge needle) as previously described (26). Cells were plated at a density of 500 cells/cm^2 in DMEM-F12 phenol free supplemented with B27, 20,ng/ml EGF and 1% Pen/Strep in non-adherent conditions, in culture dishes coated with 2-hydroxyethylmethacrylate (poly-HEMA, Sigma-Aldrich). Cells were grown for 5 days and maintained in a humidified incubator at 37°C. After 5 days in culture, spheres > 50 μm were counted using an eyepiece graticule. Results

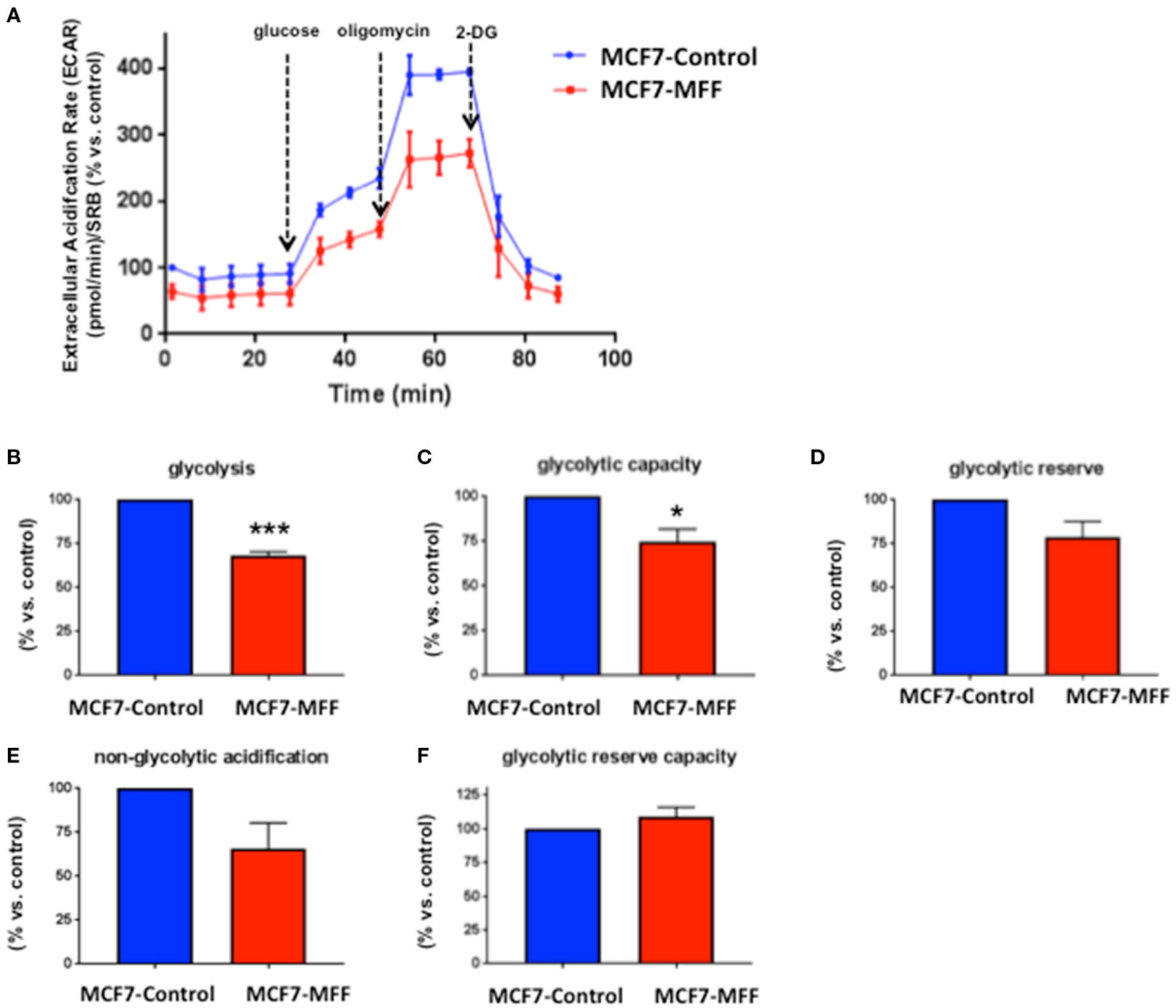

FIGURE 3 | Mitochondrial fission factor (MFF) reduces glycolysis. The metabolic profile of stably transduced MCF7 cells harboring MFF (MCF-MFF) and the respective empty-vector (MCF-7 Control) was examined using the Seahorse XFe96 analyzer. **(A)** Extracellular acidification rate (ECAR) is significantly reduced in cells transduced with MFF as compared to control cells. **(B,C)** Significant reduction in glycolysis and glycolytic capacity were observed in MCF7 cells transduced with MFF as compared to control cells, without significant changes in glycolytic reserve **(D)**, non-glycolytic acidification **(E)**, and glycolytic reserve capacity **(F)**. At least six replicates were performed in each experiment. Results are the average of the mean of three independent experiments and are expressed as percentages normalized to the control ± SEM. $^{*}p < 0.05$, $^{***}p < 0.001$.

are the average of the mean of three independent experiments normalized to the control (Ex-Neg) and are expressed as percentage of cells plated which formed spheres. Three biological replicates were performed in each experiment.

Aldefluor Assay

ALDH activity was assessed in stably transduced MCF7 cells, which were seeded in monolayer for 48 h. The ALDEFLUOR kit (StemCell Technologies) was used to isolate the population with high ALDH enzymatic activity by flow cytometry (Fortessa, BD Bioscience). Briefly, cells were harvested and incubated in 1 ml of ALDEFLUOR assay buffer containing ALDH substrate (5 μl/ml) for 40 min at 37°C. In each experiment, a sample of cells was stained under identical conditions with 30 mM of diethylaminobenzaldehyde (DEAB), a specific ALDH inhibitor, as a negative control. The ALDH-positive population was established, according to the manufacturer's instructions and was evaluated using 30,000 cells.

Proteomics and Ingenuity Pathway Analysis (IPA)

Samples were submitted to the CRUK Proteomics Core Facility, for label-free proteomic analysis. Proteomics and statistical analyses were carried out on a fee-for-service basis by Smith and his colleagues, at the Proteomics Core Facility at the Cancer Research UK Manchester Institute, University of Manchester. Briefly, stably transduced MCF7 cells were cultured in complete

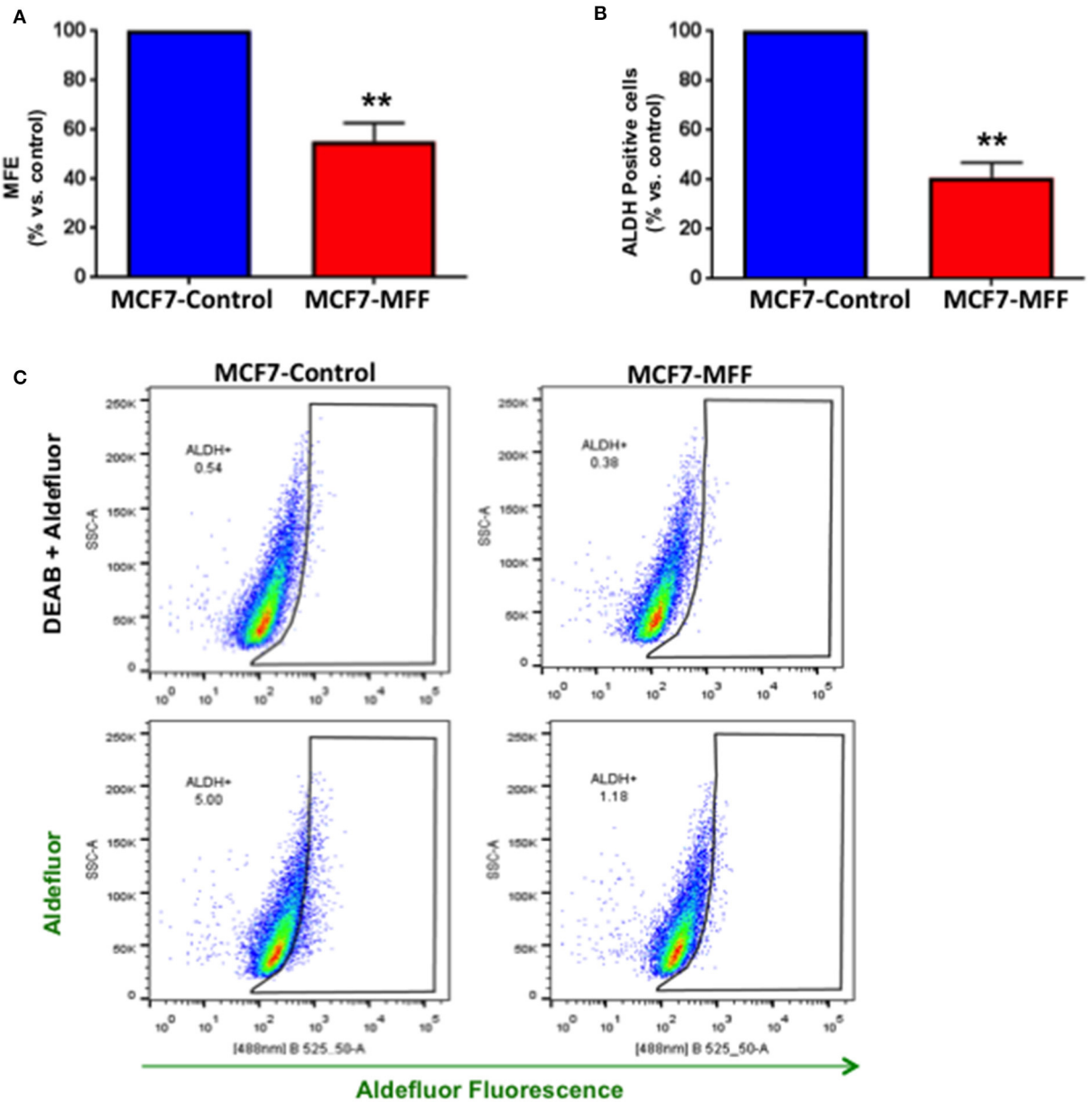

FIGURE 4 | Mitochondrial fission factor (MFF) inhibits 3D-spheroid formation and ALDH activity. **(A)** Evaluation of mammosphere formation efficiency (MFE) in stably transduced MCF7 cells harboring the mitochondrial fission factor (MCF7-MFF) and the respective empty-vector (MCF-7 Control), which were seeded on low-attachment plates for 5 days. Under these conditions, MCF7-MFF cells show a reduction by 45% in the mammosphere forming capacity as compared to MCF7-Control cells. **(B)** Evaluation of ALDEFLUOR activity, an independent marker of CSCs in MCF7 cells harboring MFF (MCF7-MFF) and the respective empty vector control (MCF-Control). Each sample was normalized using diethylaminobenzaldehyde (DEAB), a specific ALDH inhibitor, as negative control. **(C)** The tracing of representative samples is shown. Results are the average of the mean of three independent experiments performed in triplicate and are expressed as percentages normalized to the control ± SEM. $^{**}p < 0.01$.

media at a density of 1.8×10^6 in 10 cm dish. The day after plating, the media was changed to DMEM with 10% NuSerum, Pen-Strep and Glutamax. After 24 h, 70–75% of confluence was reached. Then, cells were washed twice with PBS and RIPA lysis buffer was added without protease inhibitors to detach the cells. The lysates were collected into pre-cooled tubes and kept on ice for 10 min. After centrifugation, the supernatants were collected and the samples were flash-frozen using liquid nitrogen. Previously, a small aliquot was removed for protein quantification. Samples were kept at −80°C until further analysis. Samples were subjected to proteomics following a protocol previously described (27). Briefly, cell lysates were prepared for trypsin digestion by sequential reduction of disulfide bonds with TCEP and alkylation with MMTS. Then, the

TABLE 1 | Significant changes in protein levels associated with mitochondrial biogenesis in MCF7 cells over-expressing mitochondrial fission factor (MFF).

Symbol	Gene name	Fold change
Mitochondrial biogenesis		
MFN2	Mitofusin 2	−31.184
MTERF1	Mitochondrial transcription termination factor 1	−5.38
MTFR1	Mitochondrial fission regulator 1	−9.616
TFAM	Transcription factor A, mitochondrial	1.519
TIMM50	Translocase of inner mitochondrial membrane 50	−83.102
TIMM10B	Translocase of inner mitochondrial membrane 10 homolog B (yeast)	−157.576
TIMM23B	Translocase of inner mitochondrial membrane 23 homolog B	1.56
TIMM8B	Translocase of inner mitochondrial membrane 8 homolog B	−5.662
TIMM13	Translocase of inner mitochondrial membrane 13	−2.266
TOMM34	Translocase of outer mitochondrial membrane 34	−5.272
TSFM	Ts translation elongation factor, mitochondrial	1.635
YY1	YY1 transcription factor	Infinity
SIRT6	Sirtuin 6	−8.746

Fold change of proteins detected in MCF7-MFF vs. MCF7-Control cells. Red: Up-regulated proteins; Green: down-regulated proteins. Proteomics was performed as described in Materials and Methods. Statistical analyses were performed using ANOVA and 1.5-fold-changes in proteins with a $p < 0.05$ were considered. Dataset containing proteins with significant altered expression profile were imported into the Ingenuity Pathway Analyses (IPA) software, which groups the differentially expressed proteins into known functions and pathways.

peptides were extracted and prepared for LC-MS/MS. All LC-MS/MS analyses were performed on an LTQ Orbitrap XL mass spectrometer (ThermoScientific) coupled to an Ultimate 3000 RSLCnano system (ThermoScientific). Xcalibur raw data files acquired on the LTQ-Orbitrap XL were directly imported into Progenesis LCMS software (Waters Corp.) for peak detection and alignment. Data were analyzed using the Mascot search engine. Five replicates were analyzed for each sample type ($N = 5$). Statistical analyses were performed using ANOVA and a 1.5-fold-change in protein levels, with a $p < 0.05$ were considered significant. The molecular function and biological pathways of the differentially expressed proteins were performed by the unbiased interrogation and analysis of proteomic data sets using IPA (Ingenuity systems, http://www.ingenuity.com). IPA assists with data interpretation, via the grouping of differentially expressed genes or proteins into known functions and pathways. Pathways with a z score of $> +2$ were considered as significantly activated, while pathways with a z score of <-2 were considered as significantly inhibited.

Statistical Analysis

Data is represented as the mean ± standard error of the mean (SEM), taken over ≥3 independent experiments, with ≥3 technical replicates per experiment, unless stated otherwise. Statistical significance was measured, using the Student *t*-test. A $p < 0.05$ was considered statistically significant.

TABLE 2 | Significant changes in protein levels associated with oxidative phosphorylation in MCF7 cells over-expressing the mitochondrial fission factor (MFF).

Symbol	Gene name	Fold change
Oxidative phosphorylation		
ATP5A1	ATP synthase, H+ transporting, mitochondrial F1 complex, alpha subunit 1, cardiac muscle	9.846
ATP5B	ATP synthase, H+ transporting, mitochondrial F1 complex, beta polypeptide	1781.432
ATP5C1	ATP synthase, H+ transporting, mitochondrial F1 complex, gamma polypeptide 1	−2.919
ATP5F1	ATP synthase, H+ transporting, mitochondrial Fo complex subunit B1	2.216
ATP5H	ATP synthase, H+ transporting, mitochondrial Fo complex subunit D	1.623
ATP5I	ATP synthase, H+ transporting, mitochondrial Fo complex subunit E	1.736
ATP5J	ATP synthase, H+ transporting, mitochondrial Fo complex subunit F6	1.673
ATP5J2	ATP synthase, H+ transporting, mitochondrial Fo complex subunit F2	−2.37
ATP5L	ATP synthase, H+ transporting, mitochondrial Fo complex subunit G	−15.581
ATP5O	ATP synthase, H+ transporting, mitochondrial F1 complex, O subunit	−601.813
COX4I1	Cytochrome c oxidase subunit 4I1	1.669
COX4I2	Cytochrome c oxidase subunit 4I2	−137.623
COX5A	Cytochrome c oxidase subunit 5A	1.913
COX5B	Cytochrome c oxidase subunit 5B	2.364
COX6B1	Cytochrome c oxidase subunit 6B1	1.87
COX6C	Cytochrome c oxidase subunit 6C	2.38
COX7A2	Cytochrome c oxidase subunit 7A2	−12.37
COX7A2L	Cytochrome c oxidase subunit 7A2 like	1.617
CYB5A	Cytochrome b5 type A	1.802
CYC1	Cytochrome c1	16.811
CYCS	Cytochrome c, somatic	1.821
MT-ATP6	ATP synthase F0 subunit 6	−280.464
MT-CO2	Cytochrome c oxidase subunit II	4.759
MT-ND1	NADH dehydrogenase, subunit 1 (complex I)	11.786
MT-ND2	Mitochondrially encoded NADH dehydrogenase 2	−7.366
MT-ND5	NADH dehydrogenase, subunit 5 (complex I)	−8.753
NDUFA2	NADH:ubiquinone oxidoreductase subunit A2	1.51
NDUFA4	NDUFA4, mitochondrial complex associated	2.201
NDUFA5	NADH:ubiquinone oxidoreductase subunit A5	1.527
NDUFA6	NADH:ubiquinone oxidoreductase subunit A6	−112.999
NDUFA8	NADH:ubiquinone oxidoreductase subunit A8	45.057
NDUFA9	NADH:ubiquinone oxidoreductase subunit A9	3.523
NDUFA10	NADH:ubiquinone oxidoreductase subunit A10	10.495
NDUFA12	NADH:ubiquinone oxidoreductase subunit A12	−60.713
NDUFA13	NADH:ubiquinone oxidoreductase subunit A13	1.767
NDUFAB1	NADH:ubiquinone oxidoreductase subunit AB1	−3.356
NDUFB3	NADH:ubiquinone oxidoreductase subunit B3	1.558
NDUFB4	NADH:ubiquinone oxidoreductase subunit B4	2.211
NDUFB5	NADH:ubiquinone oxidoreductase subunit B5	−338.956
NDUFB6	NADH:ubiquinone oxidoreductase subunit B6	2.247

(Continued)

TABLE 2 | Continued

Symbol	Gene name	Fold change
Oxidative phosphorylation		
NDUFB7	NADH:ubiquinone oxidoreductase subunit B7	−20.943
NDUFB9	NADH:ubiquinone oxidoreductase subunit B9	2.454
NDUFB10	NADH:ubiquinone oxidoreductase subunit B10	1.609
NDUFS1	NADH:ubiquinone oxidoreductase core subunit S1	−77.83
NDUFS2	NADH:ubiquinone oxidoreductase core subunit S2	−22.623
NDUFS3	NADH:ubiquinone oxidoreductase core subunit S3	−21.085
NDUFS5	NADH:ubiquinone oxidoreductase subunit S5	1.686
NDUFS6	NADH:ubiquinone oxidoreductase subunit S6	1.977
NDUFS7	NADH:ubiquinone oxidoreductase core subunit S7	−69.072
NDUFS8	NADH:ubiquinone oxidoreductase core subunit S8	−45.818
NDUFV1	NADH:ubiquinone oxidoreductase core subunit V1	1.552
NDUFV2	NADH:ubiquinone oxidoreductase core subunit V2	−5.91
SDHA	Succinate dehydrogenase complex flavoprotein subunit A	1.617
SDHB	Succinate dehydrogenase complex iron sulfur subunit B	2.018
UQCR10	Ubiquinol-cytochrome c reductase, complex III subunit X	2.354
UQCR11	Ubiquinol-cytochrome c reductase, complex III subunit XI	1.501
UQCRB	Ubiquinol-cytochrome c reductase binding protein	1.534
UQCRC1	Ubiquinol-cytochrome c reductase core protein I	−4.993
UQCRC2	Ubiquinol-cytochrome c reductase core protein II	373.541
UQCRH	Ubiquinol-cytochrome c reductase hinge protein	−40.845
UQCRQ	Ubiquinol-cytochrome c reductase complex III subunit VII	9.76

Fold change of proteins detected in MCF7-MFF vs. MCF7-Control cells. Red: Up-regulated proteins; Green: Down-regulated proteins. Proteomics was performed as described in Materials and Methods. Statistical analyses were performed using ANOVA and 1.5-fold-changes in proteins with a $p < 0.05$ were considered. Dataset containing proteins with significant altered expression profile were imported into the Ingenuity Pathway Analyses (IPA) software, which groups the differentially expressed proteins into known functions and pathways.

TABLE 3 | Significant changes in protein levels associated with the tricarboxylic acid cycle in MCF7 cells over-expressing mitochondrial fission factor (MFF).

Symbol	Gene name	Fold change
TCA cycle		
ACO1	Aconitase 1	−33.921
ACO2	Aconitase 2	−14.648
CS	Citrate synthase	−34.112
DHTKD1	Dehydrogenase E1 and transketolase domain containing 1	−3.207
DLD	Dihydrolipoamide dehydrogenase	3.814
DLST	Dihydrolipoamide S-succinyltransferase	−3.202
FH	Fumarate hydratase	14.079
IDH1	Isocitrate dehydrogenase [NADP(+)] 1, cytosolic	4.014
IDH2	Isocitrate dehydrogenase [NADP(+)] 2, mitochondrial	−176.206
IDH3A	Isocitrate dehydrogenase 3 [NAD(+)] alpha	−17.146
IDH3B	Isocitrate dehydrogenase 3 [NAD(+)] beta	1.752
IDH3G	Isocitrate dehydrogenase 3 [NAD(+)] gamma	3.159
MDH1	Malate dehydrogenase 1	24.472
MDH2	Malate dehydrogenase 2	−211.122
OGDH	Oxoglutarate dehydrogenase	−47.17
OGDHL	Oxoglutarate dehydrogenase-like	4.76
SDHA	Succinate dehydrogenase complex flavoprotein subunit A	1.617
SDHB	Succinate dehydrogenase complex iron sulfur subunit B	2.018
SUCLA2	Succinate-CoA ligase ADP-forming beta subunit	3.127
SUCLG1	Succinate-CoA ligase alpha subunit	6.425

Fold change of proteins detected in MCF7-MFF vs. MCF7-Control cells. Red: Up-regulated proteins; Green: Down-regulated proteins. Proteomics was performed as described in Materials and Methods. Statistical analyses were performed using ANOVA and 1.5-fold-changes in proteins with a $p < 0.05$ were considered. Dataset containing proteins with significant altered expression profile were imported into the Ingenuity Pathway Analyses (IPA) software, which groups the differentially expressed proteins into known functions and pathways.

RESULTS

Cancer stem cells (CSCs) are characterized by elevated mitochondrial biogenesis and metabolism (2). However, mitochondrial function is also largely dependent on a well-regulated balance between mitochondrial fusion and fission dynamics (19, 23). In fact, aberrantly activated fission results in mitochondrial fragmentation, which is associated to mitochondrial dysfunction.

Here, we interrogated how unopposed mitochondrial fission may promote alterations in mitochondrial biology and function, leading to inhibition of CSCs propagation in breast cancer.

MFF Inhibits Mitochondrial Biogenesis

In order to investigate the role of MFF in the regulation of mitochondrial activity in breast cancer cells, we generated an isogenic MCF7 cell line harboring MFF (MCF7-MFF), together with a matched isogenic cell line harboring the empty vector, which served as a control (MCF7-Control). After verifying MFF-overexpression by Western blotting (**Figure 1A**), the newly generated cell lines were subjected to functional phenotypic characterization. As a first step, cells were analyzed by FACS analysis using MitoTracker Deep-Red-FM, as a probe to estimate mitochondrial mass. As shown in **Figure 1C**, mitochondrial content was reduced by 30% in MCF7-MFF cells. A similar trend was observed for the evaluation of mitochondrial activity by FACS analysis, using the probe Mito-Orange (**Figure 1B**), suggesting an overall impairment in mitochondrial content and function in the presence of MFF-overexpression.

MFF Inhibits Breast Cancer Cell Metabolism

Data shown above immediately suggest that MFF may interfere with mitochondrial oxidative metabolism. To test this hypothesis, we directly evaluated metabolic flux using the Seahorse XFe96 and we found that Oxygen Consumption Rates (OCR) were significantly reduced in MCF7-MFF cells (**Figure 2**). More specifically, basal respiration and maximal respiration

TABLE 4 | Significant changes in protein levels associated with glycolysis in MCF7 cells over-expressing mitochondrial fission factor (MFF).

Symbol	Gene name	Fold change
Glycolysis		
GLUT1	Facilitated glucose transporter member 1	−27.22
HXK1	Hexokinase 1	−17.96
HXK2	Hexokinase 2	–Infinity
HXK3	Hexokinase 3	1.755
ALDOA	Aldolase, fructose-bisphosphate A	−63.01
ALDOC	Aldolase, fructose-bisphosphate C	3.304
ENO1	Enolase 1	−353.572
ENO2	Enolase 2	−14.088
ENO3	Enolase 3	4.658
FBP1	Fructose-bisphosphatase 1	−5.137
GAPDH	Glyceraldehyde-3-phosphate dehydrogenase	37.238
GPI	Glucose-6-phosphate isomerase	3.486
PFKM	Phosphofructokinase, muscle	−5.855
PFKP	Phosphofructokinase, platelet	–Infinity
PGAM1	Phosphoglycerate mutase 1	3.86
PGAM4	Phosphoglycerate mutase family member 4	1.668
PGK1	Phosphoglycerate kinase 1	250.959
PGK2	Phosphoglycerate kinase 2	−28.097
PKLR	Pyruvate kinase, liver and RBC	−11.843
PKM	Pyruvate kinase, muscle	−92.492
TPI1	Triosephosphate isomerase 1	−44.171
LDHA	Lactate dehydrogenase A	2.82
LDHA6LB	Lactate dehydrogenase A like 6B	−58.176

Fold change of proteins detected in MCF7-MFF vs. MCF7-Control cells. Red: Up-regulated proteins; Green: Down-regulated proteins. Proteomics was performed as described in Materials and Methods. Statistical analyses were performed using ANOVA and 1.5-fold-changes in proteins with a $p < 0.05$ were considered. Dataset containing proteins with significant altered expression profile were imported into the Ingenuity Pathway Analyses (IPA) software, which groups the differentially expressed proteins into known functions and pathways.

TABLE 5 | Significant changes in protein levels associated with the pentose phosphate pathway in MCF7 cells overexpressing mitochondrial fission factor (MFF).

Symbol	Gene name	Fold change
Pentose phosphate pathway		
G6PD	Glucose-6-phosphate dehydrogenase	−136.908
PGD	Phosphogluconate dehydrogenase	4.903
PGLS	6-phosphogluconolactonase	1.776
RPE	Ribulose-5-phosphate-3-epimerase	2.25
RPIA	Ribose 5-phosphate isomerase A	−11.28
TALDO1	Transaldolase 1	−6.741
TKT	Transketolase	−82.993

Fold change of proteins detected in MCF7-MFF vs. MCF7-Control cells. Red: Up-regulated proteins; Green: Down-regulated proteins. Proteomics was performed as described in Materials and Methods. Statistical analyses were performed using ANOVA and 1.5-fold-changes in proteins with a $p < 0.05$ were considered. Dataset containing proteins with significant altered expression profile were imported into the Ingenuity Pathway Analyses (IPA) software, which groups the differentially expressed proteins into known functions and pathways.

were reduced by nearly 40% (**Figures 2B,E**); accordingly, ATP levels were also depleted (**Figure 2D**). Notably, the analysis of Extracellular Acidification Rates (ECR) demonstrated that also the glycolytic pathway is inhibited in MCF7-MFF cells (**Figure 3**). In particular, a nearly 40 % decrease in glycolysis and glycolytic capacity (**Figures 3B,C**) were observed; an inhibitory, though not significant, trend was also observed for glycolytic reserve and non-glycolytic acidification (**Figures 3D,E**). Taken together, these data indicate that MFF over-expression negatively affects the metabolic cell machinery, by interfering with both oxidative phosphorylation and glycolysis in breast cancer cells.

MFF Inhibits Breast CSC Activity

We previously established that within the heterogeneous tumor mass, cancer cells exhibiting stemness features are also characterized by an elevated level of mitochondrial function (5, 6, 28). On the other hand, strategies aimed at targeting mitochondria have proven to be beneficial in halting CSCs, both in pre-clinical and clinical studies (9, 12, 29, 30). Based on these observations, we investigated whether aberrant mitochondrial fission may affect CSC propagation, together with the impairment of mitochondrial function. For this purpose, we used the 3D tumor-sphere formation assay as readout for CSCs activity. **Figure 4A** shows that mammosphere formation is inhibited by nearly 50% in MCF7-MFF cells. Likewise, ALDH activity, a surrogate marker of stemness, was reduced by >60% in MCF7-MFF cells (**Figures 4B,C**). These results clearly indicate that MFF over-expression hampers breast CSCs propagation.

Proteomic Profiling Reveals the MFF-Dependent Metabolic, Signaling, and Biological Landscape

Dysfunctional mitochondria activate a retrograde signaling network that shapes the nuclear transcriptomic program toward the regulation of cell morphology and function, for cells to response to disruption of energy metabolism (31). Adding to this, several lines of evidence indicate that mitochondrial dynamics might be involved in the regulation of stress signaling (14). Hence, we sought to depict the metabolic and signaling network landscape of MFF over-expressing breast cancer cells by using an "omics" approach. More specifically, unbiased proteomic analysis was performed in MCF7-MFF as well as in the matched MCF7-Control counterpart. Thereafter, the software Ingenuity Pathway was used to: (i) classify and group the proteins differentially regulated in response to MFF overexpression; (ii) predict how the upstream regulators may cause downstream phenotypic or functional changes in response to MFF overexpression.

Metabolomic Signature

Results, shown in **Tables 1**–**5**, indicate that increased expression of MFF fosters a transition toward a metabolically quiescent cell phenotype. In particular, proteins involved in mitochondrial biogenesis (**Table 1**), Oxidative Phosphorylation (**Table 2**) and TCA cycle (**Table 3**) are the most strongly down-regulated in MCF7-MFF, as compared to MCF-Control cells. Furthermore,

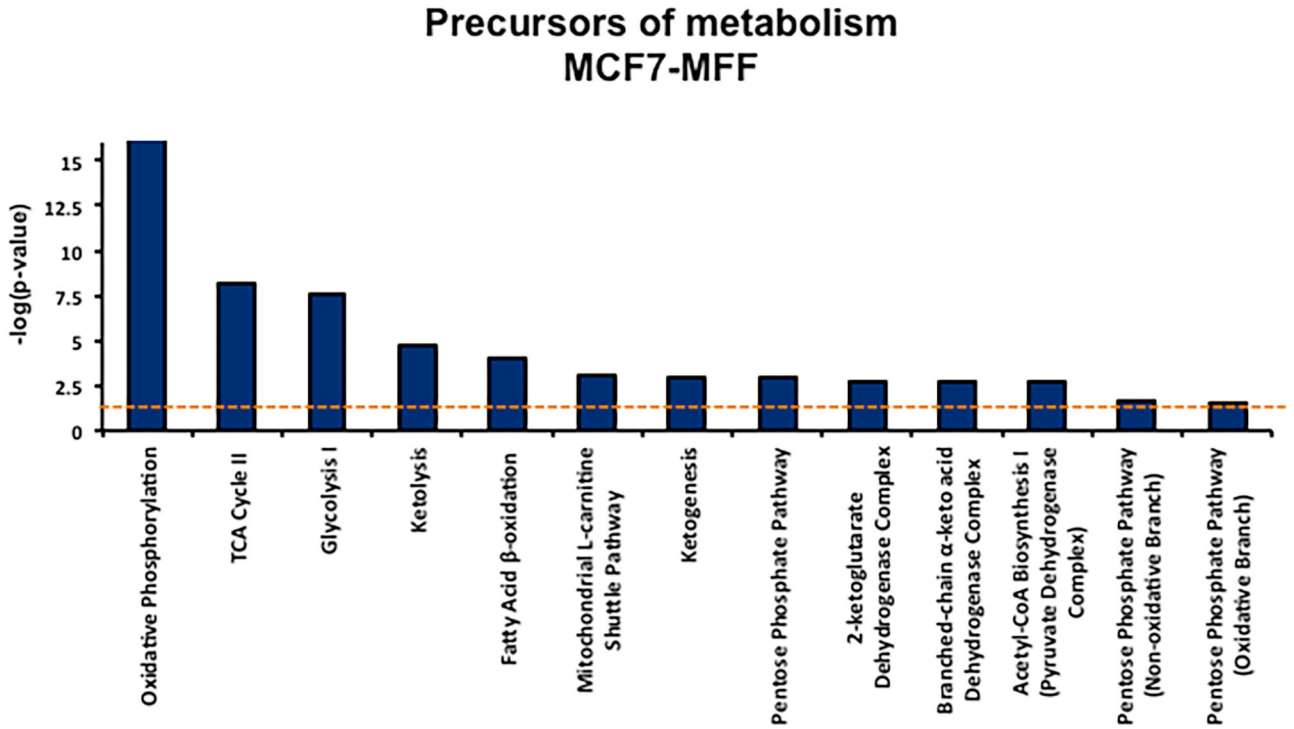

FIGURE 5 | Precursors of metabolism list. Precursor of metabolism list enriched by the proteins significantly regulated in MCF7 harboring mitochondrial fission factor (MFF) compared to MCF7 Control cells. The list has been generated by Ingenuity Pathway Analysis (IPA). The *p*-value for each pathway is represented by the height of the bars and is expressed as −1 times the log of the *p*-value. The orange dotted line represents the threshold of $p = 0.05$ as calculated by Fischer's test and denotes the cut-off for significance.

inhibition of proteins involved in the glycolytic and the pentose phosphate pathways is observed in MCF7-MFF cells (**Tables 4**, **5**). Likewise, a higher accumulation of proteins involved in the metabolism of metabolic precursors mainly for Oxidative phosphorylation, TCA cycle and Glycolysis is detected in MCF7-MFF cells, suggesting that the metabolic machinery is inhibited in the presence of enhanced mitochondrial fragmentation (**Figure 5**). Also, it appears that MFF over-expression triggers the up-regulation of a "toxicity network" of proteins, mainly related to cell metabolism (**Figure 6**). The most strongly up-regulated "toxicity" proteins are classified as regulators of mitochondrial dysfunction, together with oxidative stress response and fatty acid metabolism (**Figure 6**). Also, a "toxicity network" of proteins involved in the regulation of mitochondrial membrane potential and hypoxia signaling are engaged as relevant effectors in MCF7-MFF cells (**Figure 6**).

Signaling Pathways and Predicted Biological Responses

To interrogate how MFF over-expression would trigger the activation of specific intracellular signaling cascades, which are predicted to control distinct biological responses, a dataset containing proteins with significant altered expression profile was imported into the IPA tool. As shown in **Figure 7**, the most strongly differentially activated pathways in MCF7-MFF cells are predicted to regulate EI2F signaling, as well as epithelial adherens junctions and the cytoskeleton. Accordingly, down-regulation of proteins involved in Epithelial Mesenchymal Transition (EMT), Extracellular Matrix (ECM) and cytoskeleton remodeling is detected in MCF-MFF cells (**Table 6**). In addition, proteins involved in metastasis formation (MTA1 and MTA2), oxidative stress signaling (CAT, SOD2, TXNRD1, GLRX3, GSR, TXNL1, TXNRD2, TXNRD3), TGFß pathway (TGFB1, TGFBR3, TGFIF2lX, STAT1, STAT3) and TNF-alpha (TNFRSF12A, TRAF2) were all dramatically down-regulated in MCF7-MFF cells (**Table 7**). In order to further characterize the signaling landscape of MCF7-MFF cells, we performed a Regulator-Effects analysis, which integrates and merges together Upstream Regulator Networks with Downstream Effect Networks, thereby deriving how predicted regulators might impact biological processes. As shown in **Figure 8**, inhibition of cell adhesion and survival (A), and activation of cell death response (B) are the main biological events associated with MFF over-expression. The identification of the signaling mediators potentially linking upstream mediators with down-stream effects is also shown. Taken together, these data suggest that aberrant mitochondrial fragmentation may halt breast cancer cell survival and activate cell death programs by regulating a number of effectors also involved in ECM remodeling, the oxidative stress response, and mitochondrial metabolic function.

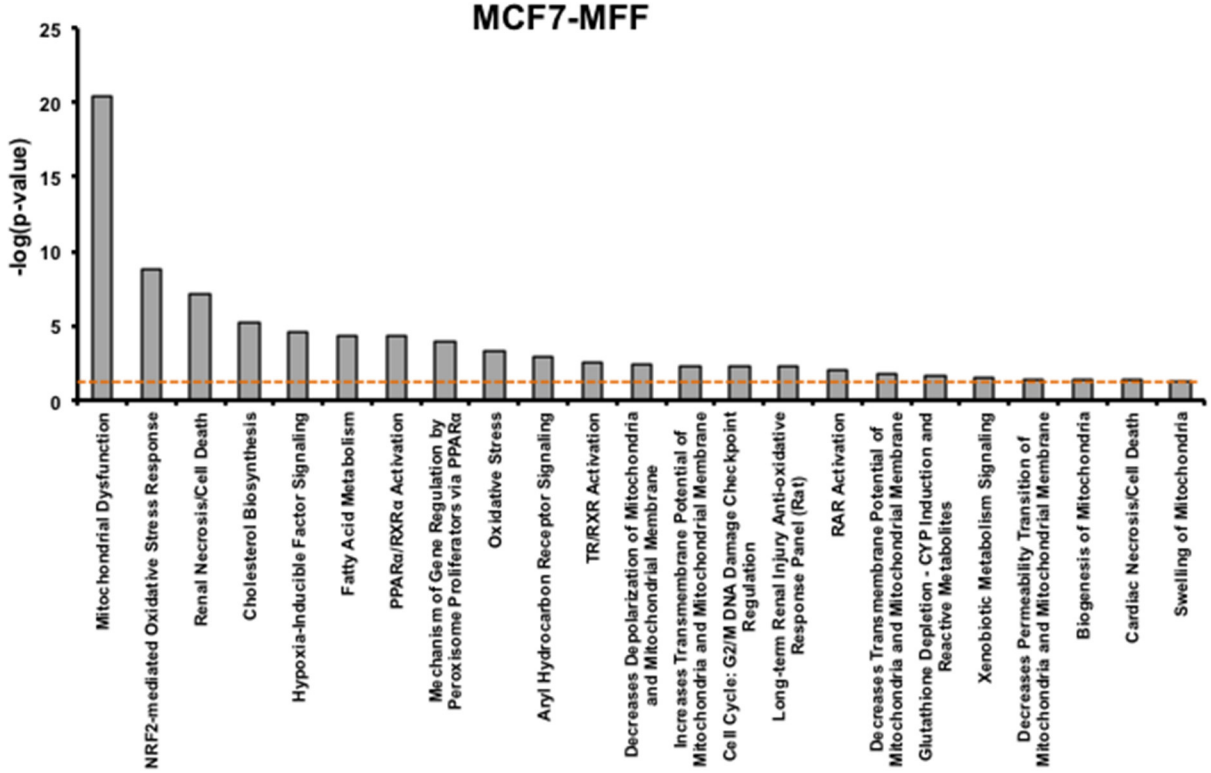

FIGURE 6 | Toxicological Pathways and Functions significantly regulated in MCF7 cells overexpressing the mitochondrial fission factor (MFF). Toxicity list enriched by the proteins significantly regulated in MCF7 harboring mitochondrial fission factor (MFF) has been generated by Ingenuity Pathway Analysis (IPA). The *p*-value for each pathway is represented by the height of the bars and is expressed as −1 times the log of the *p*-value. The orange dotted line represents the threshold of $p = 0.05$ as calculated by Fischer's test and denotes the cut-off for significance.

DISCUSSION

Here, we have generated a mitochondrial fission factor (MFF)-overexpressing breast cancer cell line in order to dissect the role of aberrant mitochondrial fission in the maintenance and dissemination of breast CSCs. We have found that MFF overexpression inhibits mitochondrial biogenesis and oxidative metabolism, depleting intracellular ATP levels. Furthermore, MFF-overexpressing breast cancer cells exhibit a reduction in stemness properties, as evidenced by the inhibition of 3D mammosphere formation capacity and decreases in the stem cell marker ALDH. Consistent with these observations, proteomic analysis performed in MFF-overexpressing breast cancer cells predicted a proteomic signature associated with the inhibition of mitochondrial function, and a metabolically quiescent cell phenotype, as well as the inhibition of cancer cell survival and the increase of cell death.

Mitochondria, which have classically been considered as the cell's "power-house," extract energy from oxidative phosphorylation to efficiently support tumor growth (1). Despite their unquestionable role in generating ATP from multiple fuels, mitochondria are now considered as central hubs which drive important tumor traits. For instance, mitochondria have been implicated in metastasis formation and spreading to distant sites, as well as drug resistance (18). In addition, mitochondria have been shown to support the survival of dormant tumor cells after oncogene ablation, thus promoting disease relapse (32). Many of these actions attributed to mitochondria have been correlated with the impact that these organelles exert on the biology of CSCs (33). Several lines of evidence have suggested that mitochondria support stem cell traits, thus facilitating self-renewal and resistance to differentiation (2). For instance, a strict reliance on young, viable and competent mitochondria is required during asymmetric cell division; in fact, older and aged mitochondria are clustered within daughter cells committed to differentiation, whereas "newly synthesized" and younger mitochondria are apportioned within daughter cells that retain a stem-like phenotype (34).

As the relationship between the mitochondrial-dependent bioenergetic responses and the CSC metabolic profile has been explored, it's not surprising that a mitochondria-centric regulation of cancer energy pathways can drive complex decision-making events, ultimately impacting CSC fate toward tumor progression. As a consequence

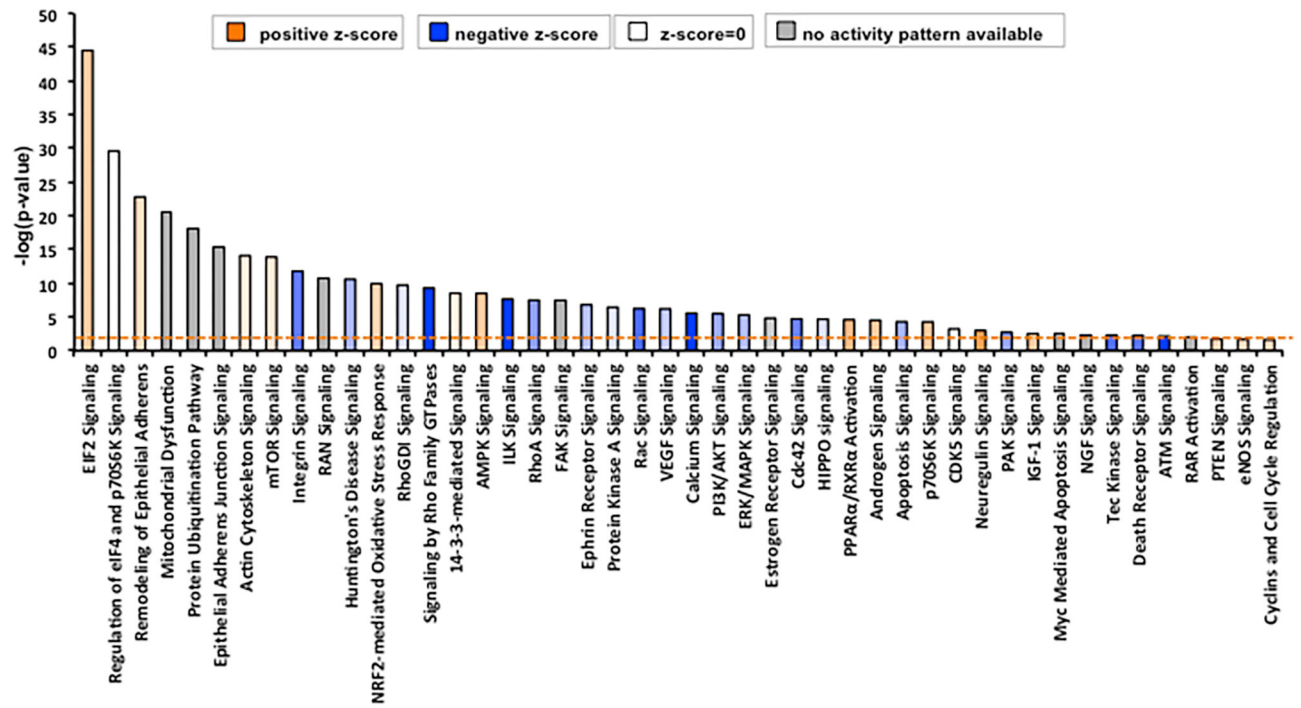

FIGURE 7 | Canonical pathways enriched in proteins differentially regulated in MCF7 cells overexpressing the mitochondrial fission factor (MFF). Significant canonical pathways associated to cell signaling were generated by Ingenuity Pathway Analysis (IPA). X axis represents pathways and Y axis represents –log (*p*-value) calculated with Fisher's exact test. A *p*-value threshold of 0.05 is applied and is represented by the orange dotted line.

of these findings, synthetic as well as natural compounds that impair mitochondrial function have been shown to selectively hamper CSC propagation in diverse tumor types (30, 35–38). Interestingly, as mitochondria evolutionary derive from the engulfment of an α-proteobacterium in eukaryotic host cells, several classes of FDA-approved antibiotics have been suggested in a repurposing effort for the selective targeting of mitochondria (12, 39). The most remarkable of these repurposing strategies is represented by the antibiotic Doxycycline, a relatively manageable and safe tetracycline analog, which inhibits CSC dissemination *in vitro*, by targeting mitochondria biogenesis, as well as mitochondrial-dependent bioenergetic metabolism (11). Of note, a Phase II clinical trial performed in early breast cancer patients, using the oral administration of Doxycycline, was sufficient to selective reduce the stemness markers ALDH1 and CD44 (9). These studies pave the way for further exploring the role of mitochondria in cancer, and the investigation of novel mitochondrial-based druggable targets to be exploited as anti-cancer strategies.

Mitochondrial fission and fusion dynamics play an integral role in the complex regulation of mitochondrial function (25). Fragmentation and fusion are tightly balanced processes which probably derive from the same endowment mechanisms through which bacteria were co-opted into host cells. As such, it's not surprising that alterations in fusion/fission balance may play a key role in the pathogenesis of several diseases, including cancer (16, 25).

Our data show that in breast cancer enhanced mitochondrial fragmentation reduces mitochondrial mass and membrane potential, suggesting that aberrant fission may compromise the efficiency of the energetic cell machinery. Mechanistically, this model could be explained by the bi-directional link existing between mitochondrial morphology and redox homeostasis. In fact, pro-fission programs leading to mitochondrial fragmentation have been shown to stimulate ROS production (40); furthermore, the activation of mitochondrial fission was required to generate ROS during hyperglycemic conditions (41), thereby suggesting that

TABLE 6 | Significant changes in protein levels associated with the epithelial-mesenchymal transition (EMT), extracellular matrix and cytoskeleton in MCF7 cells over-expressing mitochondrial fission factor (MFF).

Symbol	Gene name	Fold change
Epithelial-mesenchymal transition, ECM and cytoskeleton proteins		
VIM	Vimentin	−122.836
ACTA2	Actin, alpha 2, smooth muscle, aorta	−1.639
TNC	Tenascin C	−18.294
CNN2	Calponin 2	109.554
CALU	Calumenin	9.943
CAND1	Cullin associated and neddylation dissociated 1	−50.592
CANX	Calnexin	289.77
CFL1	Cofilin 1	−4.993
CTNNA1	Catenin alpha 1	15.851
CTNNA2	Catenin alpha 2	−46.852
CTNND1	Catenin delta 1	−50.914
GSN	Gelsolin	−9.378
KTN1	Kinectin 1	−27.16
VCL	Vinculin	2.965
THBS1	Thrombospondin 1	−26.041
TAGLN2	Transgelin 2	3.578
TAGLN3	Transgelin 3	−18.464
CUL1	Cullin 1	−24.7
CUL2	Cullin 2	−3.6
CUL3	Cullin 3	−43.342
CUL7	Cullin 7	−24.685
CUL4A	Cullin 4A	−4.282
CUL4B	Cullin 4B	−30.196
DES	Desmin	−2.734
COL11A1	Collagen type XI alpha 1 chain	−156.421
COL28A1	Collagen type XXVIII alpha 1 chain	−65.077
COL2A1	Collagen type II alpha 1 chain	−110.781
COL8A1	Collagen type VIII alpha 1	−7.542
ACTB	Actin beta	−378.155
ACTBL2	Actin, beta like 2	−100.94
ACTC1	Actin, alpha, cardiac muscle 1	−101.765
ACTG1	Actin gamma 1	4.483
ACTN1	Actinin alpha 1	−4.133
ACTN2	Actinin alpha 2	−2.295
ACT	Actin-like protein (ACT) gene	−20.682
ACTG1P4	Actin gamma 1 pseudogene 4	−2.329
ACTN4	Actinin alpha 4	30.372
MYH9	Myosin, heavy chain 9, non-muscle	820.527
MYH10	Myosin, heavy chain 10, non-muscle	7.969
MYH11	Myosin heavy chain 11	−46.952
MYH7B	Myosin heavy chain 7B	−13.017
MYL1	Myosin light chain 1	−10.816
MYL6	Myosin light chain 6	1.94
MYL12A	Myosin light chain 12A	2.173
MYL6B	Myosin light chain 6B	−Infinity
MYO1B	Myosin IB	1.551
MYO1C	Myosin IC	−51.931
TUBA8	Tubulin alpha 8	−15.245
TUBA1A	Tubulin alpha 1a	1.545
TUBA3E	Tubulin alpha 3e	1.5
TUBA4A	Tubulin alpha 4a	−22.152
TUBAL3	Tubulin alpha like 3	−3.393
TUBB3	Tubulin beta 3 class III	−3.965
TUBB6	Tubulin beta 6 class V	−18.369
TUBB8	Tubulin beta 8 class VIII	1.78
TUBB2A	Tubulin beta 2A class IIa	−2.783
TUBB2B	Tubulin beta 2B class IIb	2.353
TUBB4A	Tubulin beta 4A class IVa	2.216
TUBGCP2	Tubulin gamma complex associated protein 2	−Infinity
TUBGCP6	Tubulin gamma complex associated protein 6	−Infinity
TUBA1B	Tubulin alpha 1b	−5.529
TUBA1C	Tubulin alpha 1c	−11.125
TUBB	Tubulin beta class I	−90.993
TUBB4B	Tubulin beta 4B class IVb	−25.109
DNM1	Dynamin 1	−20.927
DNM2	Dynamin 2	−18.654
DNM3	Dynamin 3	−9.012
DNMBP	Dynamin binding protein	−4.552
LAMA3	Laminin subunit alpha 3	−58.838
LAMB2	Laminin subunit beta 2	−12.831
LAMB3	Laminin subunit beta 3	−77.639
LAMB4	Laminin subunit beta 4	−8.215

Fold change of proteins detected in MCF7-MFF vs. MCF7-Control cells. Red: Up-regulated proteins; Green: Down-regulated proteins. Proteomics was performed as described in Materials and Methods. Statistical analyses were performed using ANOVA and 1.5-fold-changes in proteins with a $p < 0.05$ were considered. Dataset containing proteins with significant altered expression profile were imported into the Ingenuity Pathway Analyses (IPA) software, which groups the differentially expressed proteins into known functions and pathways.

unopposed mitochondrial fragmentation is associated with enhanced ROS production and compromission of the energetic machinery.

Indeed, analysis of metabolic flux showed that in MFF-overexpressing breast cancer cells the capability to extract ATP from energetic sources is compromised. These data are in accordance with previous studies showing that natural or synthetic compounds that block mitochondrial biogenesis and thereby reduce mitochondrial mass, also interfere with mitochondrial energetic function [reviewed in (8)]. Likewise, the metabolic effects of abnormal mitochondrial fission may parallel the biochemical responses observed in breast cancer cells treated with mitochondrial-targeting agents. Our data from proteomic analyses provide supporting evidence that MFF over-expression mainly drives the acquisition of a metabolically suppressed cell phenotype, as demonstrated by the drastic reduction of proteins involved in several energetic pathways in MCF7-MFF vs.

TABLE 7 | Significant changes in other protein levels in MCF7 cells over-expressing mitochondrial fission factor (MFF).

Symbol	Gene name	Fold change
Other proteins		
MTA1	Metastasis associated 1	−41.671
MTA2	Metastasis associated 1 family member 2	−17.064
MTSS1L	Metastasis suppressor 1 like	2.028
UCP3	Uncoupling protein 3	−62.533
TIGAR	TP53 induced glycolysis regulatory phosphatase	−39.761
TGFBI	Transforming growth factor beta induced	–Infinity
TGFBR3	Transforming growth factor beta receptor 3	−8.57
TGIF2LX	TGFB induced factor homeobox 2 like, X-linked	−12.818
STAT1	Signal transducer and activator of transcription 1	−9.228
STAT3	Signal transducer and activator of transcription 3	−7.953
OXSR1	Oxidative stress responsive 1	6.331
PCNA	Proliferating cell nuclear antigen	3.128
HSF1	Heat shock transcription factor 1	−28.884
TRAP1	TNF receptor associated protein 1	−10.989
CAT	Catalase	−10.918
SOD2	Superoxide dismutase 2, mitochondrial	−33.389
TXNRD1	Thioredoxin reductase 1	−21.824
GLRX3	Glutaredoxin 3	−1.845
GSR	Glutathione-disulfide reductase	−1E+08
GSS	Glutathione synthetase	2.547
GSTM3	Glutathione S-transferase mu 3	18.065
ROMO1	Reactive oxygen species modulator 1	1.966
SMAD9	SMAD family member 9	−1.975
TXNL1	Thioredoxin like 1	−9.869
TXNRD2	Thioredoxin reductase 2	−3.538
TXNRD3	Thioredoxin reductase 3	–Infinity
TMX1	Thioredoxin related transmembrane protein 1	3.142
TMX4	Thioredoxin related transmembrane protein 4	1.518
TNFRSF12A	TNF receptor superfamily member 12A	–Infinity
TNFSF13B	Tumor necrosis factor superfamily member 13b	2.397
TRAF2	TNF receptor associated factor 2	−7.759

Fold change of proteins detected in MCF7-MFF vs. MCF7-Control cells. Red: Up-regulated proteins; Green: Down-regulated proteins. Note down-regulation of relevant proteins involved in the metastatic process and oxidative stress response. Proteomics was performed as described in Materials and Methods. Statistical analyses were performed using ANOVA and 1.5-fold-changes in proteins with a $p < 0.05$ were considered. Dataset containing proteins with significant altered expression profile were imported into the Ingenuity Pathway Analyses (IPA) software, which groups the differentially expressed proteins into known functions and pathways.

MCF7-Control cells. Therefore, unopposed mitochondrial fragmentation induces mitochondrial dysfunction, leading to the inability to extract ATP from fuels and an overall block in cell metabolism.

As cancer cells are strictly dependent on active energetic cellular machinery for their survival, any alteration in mitochondrial integrity may compromise cancer cell viability (42, 43). The proteomic analyses performed in MFF-overexpressing breast cancer cells showed that enhanced mitochondrial fission is associated not only with loss of mitochondrial proteins, impaired ability to cope with oxidative stress, and reduced metabolic function, but also with a quiescent cell phenotype. More specifically, the proteomic landscape of MFF over-expressing breast cancer cells highlights a clear inhibition of proteins involved in cell adhesion and cell junction, together with the inhibition of the EMT program, and metastasis-related mediators. Furthermore, our proteomic analysis predicts a substantial inhibition of cell survival pathways and the activation of cell death programs, consistent with a metabolically suppressed cell phenotype.

These data are in accordance with previous studies showing that MFF-dependent mitochondrial fission activates signaling pathways involved in the inhibition of cell viability and the activation of the apoptotic response (44). In particular, MFF and other mediators involved in mitochondrial fragmentation such as DRP1 play an integral role in cancer cell death in response to diverse stimuli, including several anticancer drugs (45, 46). At least some of these effects could be attributed to the generation of mitochondrial ROS, which would thereafter trigger apoptotic cell death (47).

Mitochondrial proteins are overexpressed in CSCs, which also exhibit increased mitochondrial metabolic function (2, 5, 7). Indeed, tracking mitochondrial mass represents an important metabolic tool to identify an enrichment of CSCs (7). Due to these unusual features, CSCs are selectively targeted by a number of mitochondria impairing agents, which have been shown to compromise mitochondrial function and thereafter halt CSC propagation (8). Likewise, in the present study we have shown that mitochondrial-driven impairment in metabolic function is associated with the loss of stemness features in MFF over-expressing breast cancer cells. These observations indicate that uncontrolled mitochondrial fission may drive the acquisition of an inactive metabolic phenotype associated with the starvation of the CSCs population. Therefore, the pharmacological manipulation of mitochondrial fission may serve as an actionable tool to eradicate cancer cells, with tumor initiating capabilities. Accordingly, it has been recently shown that an MFF peptidomimetic strategy elicits anti-cancer activity in patient-derived xenografts, primary breast and lung adenocarcinoma 3D organoids, as well as glioblastoma neurospheres (45).

Recently, drugs targeting mitochondrial dynamics are beginning to emerge as novel strategies in cancer treatment. It should be mentioned that their potential is still challenged by several controversies and awaits further confirmation. For instance, the inhibitor of mitochondrial fission named mdiv-1, which acts as a Drp1 GTPase activity inhibitor, can cause a loss of the functional properties of CSCs (48). However, this drug appears to also work as a reversible inhibitor of mitochondrial complex I, leading to alterations of mitochondrial ROS production (49). Additional layers of complexity have to be considered when exploring the contribution of mitochondrial shaping genes in tumor

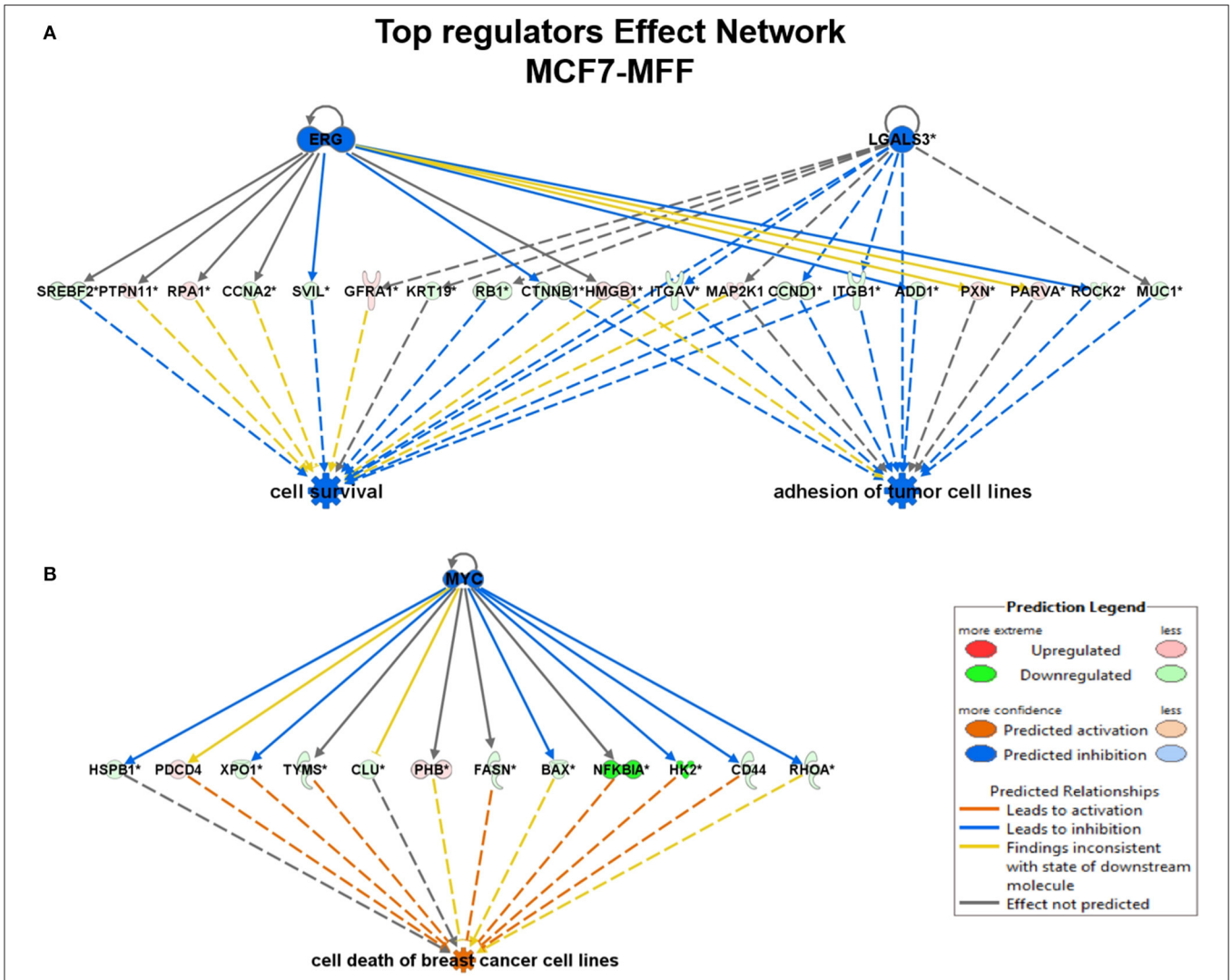

FIGURE 8 | Regulator effect networks generated by Ingenuity Pathway Analysis (IPA) in MCF7 over-expressed mitochondrial fission factor (MFF). IPA analysis generated several regulator effect networks in MCF7 cells over-expressing mitochondrial fission factor (MFF). Both upstream regulators and downstream cellular responses were identified in relation to certain proteins significantly altered in our dataset. Upstream regulators are shown at the top while functions and phenotypes are displayed at the bottom. Significantly regulated proteins connecting the upper and lower panel are displayed in the middle. Red and green colors represent significant up/down-regulation, respectively, with the intensity of the color reflecting the degree of change. Orange color predicts an overall activation of the pathway while blue indicates a prediction of an overall decrease based on z-score value. Inconsistent relationships are represented as yellow line. Note that in MCF7 harboring MFF some of the proteins in our dataset have been predicted to be inhibited by the upstream regulators ERG, LGALS3, and MYC leading to an overall inhibition (blue) of cell survival and/or activation (orange) of cell death. **(A)** Cell survival and adhesion; **(B)** Cell death.

biology. Indeed, tumor microevironmental conditions; the presence of hormonal/growth factors; and intrinsic features of the specific tumor cell types involved may affect mitodynamics pathways.

In conclusion, the data presented herein validate the use of a mitodynamic approach to target mitochondria architecture and function toward the eradication of CSCs. Further studies will be necessary to validate the use of this therapeutic strategy, especially in combination with additional metabolic inhibitors as novel tools to control stem traits in cancer.

DATA AVAILABILITY STATEMENT

The datasets generated for this study can be found in online repositories. The names of the repository/repositories and accession number(s) can be found here: ProteomeXchange via PRIDE dataset (identifier: PXD020802).

AUTHOR CONTRIBUTIONS

ML and FS conceived and initiated this project. All experiments described in this paper were performed by RS-A. MF performed

the 3D mammosphere assays. ED wrote the manuscript with input from RS-A. ML and FS edited the manuscript. All authors contributed to the article and approved the submitted version.

FUNDING

This work was supported by research grant funding, provided by Lunella Biotech, Inc. (to FS and ML).

ACKNOWLEDGMENTS

We are grateful to Rumana Rafiq, for her kind and dedicated assistance, in keeping the Translational Medicine Laboratory at Salford running very smoothly. We would like to thank the Foxpoint Foundation and the Healthy Life Foundation for their philanthropic donations toward new equipment and infrastructure, in the Translational Medicine Laboratory, at the University of Salford.

REFERENCES

1. Vyas S, Zaganjor E, Haigis MC. Mitochondria and cancer. *Cell.* (2016) 166:555–66. doi: 10.1016/j.cell.2016.07.002
2. Shin M-K, Cheong J-H. Mitochondria-centric bioenergetic characteristics in cancer stem-like cells. *Arch Pharm Res.* (2019) 42:113–27. doi: 10.1007/s12272-019-01127-y
3. Peiris-Pagès M, Martinez-Outschoorn UE, Pestell RG, Sotgia F, Lisanti MP. Cancer stem cell metabolism. *Breast Cancer Res.* (2016) 18:55. doi: 10.1186/s13058-016-0712-6
4. Visvader JE. Cells of origin in cancer. *Nature.* (2011) 469:314–22. doi: 10.1038/nature09781
5. Farnie G, Sotgia F, Lisanti MP. High mitochondrial mass identifies a sub-population of stem-like cancer cells that are chemo-resistant. *Oncotarget.* (2015) 6:30472–86. doi: 10.18632/oncotarget.5401
6. Lamb R, Ozsvari B, Bonuccelli G, Smith DL, Pestell RG, Martinez-Outschoorn UE, et al. Dissecting tumor metabolic heterogeneity: telomerase and large cell size metabolically define a sub-population of stem-like, mitochondrial-rich, cancer cells. *Oncotarget.* (2015) 6:21892–905. doi: 10.18632/oncotarget.5260
7. Lamb R, Bonuccelli G, Ozsvári B, Peiris-Pagès M, Fiorillo M, Smith DL, et al. Mitochondrial mass, a new metabolic biomarker for stem-like cancer cells: understanding WNT/FGF-driven anabolic signaling. *Oncotarget.* (2015) 6:30453–71. doi: 10.18632/oncotarget.5852
8. De Francesco EM, Sotgia F, Lisanti MP. Cancer stem cells (CSCs): metabolic strategies for their identification and eradication. *Biochem J.* (2018) 475:1611–34. doi: 10.1042/BCJ20170164
9. Scatena C, Roncella M, Di Paolo A, Aretini P, Menicagli M, Fanelli G, et al. Doxycycline, an inhibitor of mitochondrial biogenesis, effectively reduces Cancer Stem Cells (CSCs) in early breast cancer patients: a clinical pilot study. *Front Oncol.* (2018) 8:452. doi: 10.3389/fonc.2018.00452
10. Peiris-Pagès M, Sotgia F, Lisanti MP. Doxycycline and therapeutic targeting of the DNA damage response in cancer cells: old drug, new purpose. *Oncoscience.* (2015) 2:696–9. doi: 10.18632/oncoscience.215
11. Lamb R, Fiorillo M, Chadwick A, Ozsvari B, Reeves KJ, Smith DL, et al. Doxycycline down-regulates DNA-PK and radiosensitizes tumor initiating cells: implications for more effective radiation therapy. *Oncotarget.* (2015) 6:14005–25. doi: 10.18632/oncotarget.4159
12. Lamb R, Ozsvari B, Lisanti CL, Tanowitz HB, Howell A, Martinez-Outschoorn UE, et al. Antibiotics that target mitochondria effectively eradicate cancer stem cells, across multiple tumor types: treating cancer like an infectious disease. *Oncotarget.* (2015) 6:4569–84. doi: 10.18632/oncotarget.3174
13. De Francesco EM, Bonuccelli G, Maggiolini M, Sotgia F, Lisanti MP. Vitamin C and doxycycline: a synthetic lethal combination therapy targeting metabolic flexibility in cancer stem cells (CSCs). *Oncotarget.* (2017) 8:67269–86. doi: 10.18632/oncotarget.18428
14. Eisner V, Picard M, Hajnóczky G. Mitochondrial dynamics in adaptive and maladaptive cellular stress responses. *Nat Cell Biol.* (2018) 20:755–65. doi: 10.1038/s41556-018-0133-0
15. Maycotte P, Marín-Hernández A, Goyri-Aguirre M, Anaya-Ruiz M, Reyes-Leyva J, Cortés-Hernández P. Mitochondrial dynamics and cancer. *Tumour Biol.* (2017) 39:1010428317698391. doi: 10.1177/1010428317698391
16. Trotta AP, Chipuk JE. Mitochondrial dynamics as regulators of cancer biology. *Cell Mol Life Sci.* (2017) 74:1999–2017. doi: 10.1007/s00018-016-2451-3
17. Youle RJ, van der Bliek AM. Mitochondrial fission, fusion, and stress. *Science.* (2012) 337:1062–5. doi: 10.1126/science.1219855
18. Altieri DC. Mitochondrial dynamics and metastasis. *Cell Mol Life Sci.* (2019) 76:827–35. doi: 10.1007/s00018-018-2961-2
19. Westermann B. Bioenergetic role of mitochondrial fusion and fission. *Biochim Biophys Acta.* (2012) 1817:1833–8. doi: 10.1016/j.bbabio.2012.02.033
20. Gandre-Babbe S, van der Bliek AM. The novel tail-anchored membrane protein MFF controls mitochondrial and peroxisomal fission in mammalian cells. *Mol Biol Cell.* (2008) 19:2402–12. doi: 10.1091/mbc.e07-12-1287
21. Otera H, Wang C, Cleland MM, Setoguchi K, Yokota S, Youle RJ, et al. MFF is an essential factor for mitochondrial recruitment of Drp1 during mitochondrial fission in mammalian cells. *J Cell Biol.* (2010) 191:1141–58. doi: 10.1083/jcb.201007152
22. Palmer CS, Osellame LD, Laine D, Koutsopoulos OS, Frazier AE, Ryan MT. MiD49 and MiD51, new components of the mitochondrial fission machinery. *EMBO Rep.* (2011) 12:565–73. doi: 10.1038/embor.2011.54
23. Lee JE, Westrate LM, Wu H, Page C, Voeltz GK. Multiple dynamin family members collaborate to drive mitochondrial division. *Nature.* (2016) 540:139–43. doi: 10.1038/nature20555
24. Liu R, Chan DC. The mitochondrial fission receptor Mff selectively recruits oligomerized Drp1. *Mol Biol Cell.* (2015) 26:4466–77. doi: 10.1091/mbc.E15-08-0591
25. Westermann B. Mitochondrial fusion and fission in cell life and death. *Nat Rev Mol Cell Biol.* (2010) 11:872–84. doi: 10.1038/nrm3013
26. Shaw FL, Harrison H, Spence K, Ablett MP, Simões BM, Farnie G, et al. A detailed mammosphere assay protocol for the quantification of breast stem cell activity. *J Mammary Gland Biol Neoplasia.* (2012) 17:111–7. doi: 10.1007/s10911-012-9255-3
27. Lamb R, Harrison H, Hulit J, Smith DL, Lisanti MP, Sotgia F. Mitochondria as new therapeutic targets for eradicating cancer stem cells: quantitative proteomics and functional validation via MCT1/2 inhibition. *Oncotarget.* (2014) 5:11029–37. doi: 10.18632/oncotarget.2789
28. De Francesco EM, Maggiolini M, Tanowitz HB, Sotgia F, Lisanti MP. Targeting hypoxic cancer stem cells (CSCs) with doxycycline: implications for optimizing anti-angiogenic therapy. *Oncotarget.* (2017) 8:56126–42. doi: 10.18632/oncotarget.18445
29. Sotgia F, Ozsvari B, Fiorillo M, De Francesco EM, Bonuccelli G, Lisanti MP. A mitochondrial based oncology platform for targeting cancer stem cells (CSCs): MITO-ONC-RX. *Cell Cycle.* (2018) 17:2091–100. doi: 10.1080/15384101.2018.1515551
30. De Francesco EM, Ózsvári B, Sotgia F, Lisanti MP. Dodecyl-TPP targets mitochondria and potently eradicates Cancer Stem Cells (CSCs): synergy with FDA-approved drugs and natural compounds (vitamin C and berberine). *Front Oncol.* (2019) 9:615. doi: 10.3389/fonc.2019.00615
31. Guha M, Avadhani NG. Mitochondrial retrograde signaling at the crossroads of tumor bioenergetics, genetics and epigenetics. *Mitochondrion.* (2013) 13:577–91. doi: 10.1016/j.mito.2013.08.007
32. Viale A, Pettazzoni P, Lyssiotis CA, Ying H, Sánchez N, Marchesini M, et al. Oncogene ablation-resistant pancreatic cancer cells depend on mitochondrial function. *Nature.* (2014) 514:628–32. doi: 10.1038/nature13611
33. Cuyàs E, Verdura S, Folguera-Blasco N, Bastidas-Velez C, Martin ÁG, Alarcón T, et al. Mitostemness. *Cell Cycle.* (2018) 17:918–26. doi: 10.1080/15384101.2018.1467679

34. Katajisto P, Dohla J, Chaffer CL, Pentinmikko N, Marjanovic N, Iqbal S, et al. Asymmetric apportioning of aged mitochondria between daughter cells is required for stemness. *Science.* (2015) 348:340–3. doi: 10.1126/science.1260384
35. Fiorillo M, Peiris-Pagès M, Sanchez-Alvarez R, Bartella L, Di Donna L, Dolce V, et al. Bergamot natural products eradicate cancer stem cells (CSCs) by targeting mevalonate, Rho-GDI-signalling and mitochondrial metabolism. *Biochim Biophys Acta Bioenerg.* (2018) 1859:984–96. doi: 10.1016/j.bbabio.2018.03.018
36. Bonuccelli G, Sotgia F, Lisanti MP. Matcha green tea (MGT) inhibits the propagation of cancer stem cells (CSCs), by targeting mitochondrial metabolism, glycolysis and multiple cell signalling pathways. *Aging.* (2018) 10:1867–83. doi: 10.18632/aging.101483
37. Ozsvari B, Fiorillo M, Bonuccelli G, Cappello AR, Frattaruolo L, Sotgia F, et al. Mitoriboscins: mitochondrial-based therapeutics targeting cancer stem cells (CSCs), bacteria and pathogenic yeast. *Oncotarget.* (2017) 8:67457–72. doi: 10.18632/oncotarget.19084
38. Ozsvari B, Sotgia F, Simmons K, Trowbridge R, Foster R, Lisanti MP. Mitoketoscins: novel mitochondrial inhibitors for targeting ketone metabolism in cancer stem cells (CSCs). *Oncotarget.* (2017) 8:78340–50. doi: 10.18632/oncotarget.21259
39. Fiorillo M, Lamb R, Tanowitz HB, Cappello AR, Martinez-Outschoorn UE, Sotgia F, et al. Bedaquiline, an FDA-approved antibiotic, inhibits mitochondrial function and potently blocks the proliferative expansion of stem-like cancer cells (CSCs). *Aging.* (2016) 8:1593–607. doi: 10.18632/aging.100983
40. Picard M, Shirihai OS, Gentil BJ, Burelle Y. Mitochondrial morphology transitions and functions: implications for retrograde signaling? *Am J Physiol Regul Integr Comp Physiol.* (2013) 304:R393–406. doi: 10.1152/ajpregu.00584.2012
41. Yu T, Robotham JL, Yoon Y. Increased production of reactive oxygen species in hyperglycemic conditions requires dynamic change of mitochondrial morphology. *Proc Natl Acad Sci USA.* (2006) 103:2653–8. doi: 10.1073/pnas.0511154103
42. Hanahan D, Weinberg RA. Hallmarks of cancer: the next generation. *Cell.* (2011) 144:646–74. doi: 10.1016/j.cell.2011.02.013
43. Pavlova NN, Thompson CB. The emerging hallmarks of cancer metabolism. *Cell Metab.* (2016) 23:27–47. doi: 10.1016/j.cmet.2015.12.006
44. Xie Y, Lv Y, Zhang Y, Liang Z, Han L, Xie Y. LATS2 promotes apoptosis in non-small cell lung cancer A549 cells via triggering Mff-dependent mitochondrial fission and activating the JNK signaling pathway. *Biomed Pharmacother.* (2019) 109:679–89. doi: 10.1016/j.biopha.2018.10.097
45. Seo JH, Chae YC, Kossenkov AV, Lee YG, Tang H-Y, Agarwal E, et al. MFF regulation of mitochondrial cell death is a therapeutic target in cancer. *Cancer Res.* (2019) 79:6215–26. doi: 10.1158/0008-5472.CAN-19-1982
46. Tang Q, Liu W, Zhang Q, Huang J, Hu C, Liu Y, et al. Dynamin-related protein 1-mediated mitochondrial fission contributes to IR−783-induced apoptosis in human breast cancer cells. *J Cell Mol Med.* (2018) 22:4474–85. doi: 10.1111/jcmm.13749
47. Wan J, Cui J, Wang L, Wu K, Hong X, Zou Y, et al. Excessive mitochondrial fragmentation triggered by erlotinib promotes pancreatic cancer PANC-1 cell apoptosis via activating the mROS-HtrA2/Omi pathways. *Cancer Cell Int.* (2018) 18:165. doi: 10.1186/s12935-018-0665-1
48. Peiris-Pagès M, Bonuccelli G, Sotgia F, Lisanti MP. Mitochondrial fission as a driver of stemness in tumor cells: mDIVI1 inhibits mitochondrial function, cell migration and cancer stem cell (CSC) signalling. *Oncotarget.* (2018) 9:13254–75. doi: 10.18632/oncotarget.24285
49. Bordt EA, Clerc P, Roelofs BA, Saladino AJ, Tretter L, Adam-Vizi V, et al. The putative Drp1 inhibitor mdivi-1 is a reversible mitochondrial complex I inhibitor that modulates reactive oxygen species. *Dev Cell.* (2017) 40:583–94.e6. doi: 10.1016/j.devcel.2017.02.020

Conflict of Interest: ML and FS hold a minority interest in Lunella Biotech, Inc.

The remaining authors declare that the research was conducted in the absence of any commercial or financial relationships that could be construed as a potential conflict of interest.

frontiers in Oncology

MINI REVIEW
published: 22 December 2020
doi: 10.3389/fonc.2020.537930

Metabolic Targeting of Cancer Stem Cells

Anna Mukha[1,2*†] *and Anna Dubrovska*[1,2,3,4*]

[1] OncoRay-National Center for Radiation Research in Oncology, Faculty of Medicine and University Hospital Carl Gustav Carus, Technische Universität Dresden and Helmholtz-Zentrum Dresden-Rossendorf, Dresden, Germany, [2] Helmholtz-Zentrum Dresden - Rossendorf, Institute of Radiooncology – OncoRay, Dresden, Germany, [3] German Cancer Consortium (DKTK), Partner Site Dresden, Dresden, Germany, [4] German Cancer Research Center (DKFZ), Heidelberg, Germany

OPEN ACCESS

Edited by:
Federica Sotgia,
University of Salford, United Kingdom

Reviewed by:
Toshihiko Torigoe,
Sapporo Medical University, Japan
Michael P. Lisanti,
University of Salford Manchester, United Kingdom

***Correspondence:**
Anna Mukha
amukha@umcutrecht.nl
Anna Dubrovska
a.dubrovska@hzdr.de

†Present address:
Anna Mukha,
Center for Molecular Medicine, UMC Utrecht, Utrecht University, Utrecht, Netherlands

Specialty section:
This article was submitted to Cancer Metabolism, a section of the journal Frontiers in Oncology

Received: 25 February 2020
Accepted: 05 November 2020
Published: 22 December 2020

Citation:
Mukha A and Dubrovska A (2020) Metabolic Targeting of Cancer Stem Cells. Front. Oncol. 10:537930. doi: 10.3389/fonc.2020.537930

Most human tumors possess a high heterogeneity resulting from both clonal evolution and cell differentiation program. The process of cell differentiation is initiated from a population of cancer stem cells (CSCs), which are enriched in tumor-regenerating and tumor-propagating activities and responsible for tumor maintenance and regrowth after treatment. Intrinsic resistance to conventional therapies, as well as a high degree of phenotypic plasticity, makes CSCs hard-to-target tumor cell population. Reprogramming of CSC metabolic pathways plays an essential role in tumor progression and metastatic spread. Many of these pathways confer cell adaptation to the microenvironmental stresses, including a shortage of nutrients and anti-cancer therapies. A better understanding of CSC metabolic dependences as well as metabolic communication between CSCs and the tumor microenvironment are of utmost importance for efficient cancer treatment. In this mini-review, we discuss the general characteristics of CSC metabolism and potential metabolic targeting of CSC populations as a potent strategy to enhance the efficacy of conventional treatment approaches.

Keywords: cancer stem cells, therapy resistance, metabolic targeting, OXPHOS, glycolysis, glutamine metabolism, fatty acid metabolism, tumor microenvironment

INTRODUCTION

According to the world health organization (WHO), cancer is responsible for one in six deaths worldwide, and global cancer rates continue to grow (1, 2). Although the mono-therapy such as surgery, chemotherapy and radiotherapy is a commonly accepted treatment modality for different types of cancers, the combination of two or more types of treatment targeting the key cancer mechanisms in synergistic or additive manners is currently a cornerstone of anticancer therapy especially for advanced and aggressive cancers (3, 4). Recent innovations in treatment technologies as well as in precision of radiation and drug delivery substantially increased efficiency and quality of

treatment. However, treatment-related toxicities and tumor therapy resistance still constitute a fundamental clinical and scientific challenge (5–7).

The difficulty of cancer treatment has its roots in the nature of this disease. Tumors are highly heterogeneous, consisting of different types of cells. Intratumoral heterogeneity is evidenced at the multiple levels, including genetic and epigenetic landscapes, histological and molecular specificities as well as functional differences between tumor cells including their abilities to propagate tumor growth and give rise to other types of cancer cells by the process of differentiation (8).

The process of cell differentiation is initiated from a population of cancer stem cells (CSCs) that possess unique properties such as the unlimited capacity of self-renewal and asymmetric division, which leads to the production of different cell types within tumors. These properties of CSCs make them equipped with tumor-regenerating and tumor-propagating activities and, therefore, responsible for the tumor maintenance and regrowth after treatment. The density of CSCs substantially varies between individual tumors, and its analysis is proven to have prognostic significance for different types of cancers (9, 10). Several CSC-specific markers have been described, among them the expression of CD133, CD44, CD117 (c-kit), Oct4, high aldehyde dehydrogenase (ALDH) activity, etc. as discussed elsewhere (11–13). However, some of these markers can be found in normal stem cells, which make identification and targeting of CSCs more challenging (14). A high plasticity of CSC populations is an additional obstacle on the way of clinical translation as tumor cells possess the ability of shifting their state from the CSC- to non-CSC populations and vice versa that is regulated by multiple genetic, epigenetic and microenvironmental stimuli (15–18). Although tumor stemness is described as a highly dynamic state, eradication of all CSC populations during tumor treatment is of high clinical importance as remaining CSCs might re-initiate local tumor growth and lead to metastatic dissemination.

Many preclinical and clinical studies suggested that some CSC populations can be equipped with intrinsic and extrinsic mechanisms providing them with high radioresistance and chemoresistance compared to the bulk of tumor cells. This relatively high therapy resistance of CSCs is attributed to the efficient DNA repair, low proliferative rate, protective tumor microenvironment, maintenance of cellular redox homeostasis, and immune escape. Altered metabolism of CSCs substantially contributes to their treatment resistance. A deep understanding of the CSC metabolic features and their molecular background will help to develop novel therapeutic strategies that precisely target CSCs and improve the efficiency of cancer control.

METABOLIC CHARACTERISTICS OF CSCS

Reprogramming of cellular metabolism plays a crucial role in tumor initiation, progression, resistance to conventional therapy, and immunosuppression. Unique features of tumor metabolism were noticed almost one hundred years ago. At the beginning of the XX century, Otto Warburg and co-workers described aerobic glycolysis, accompanied by excessive production of lactate, as one of the distinct characteristics of tumor cells and tissue slices (19). Since then, many other alterations of biochemical pathways have been described for cancer cells (11, 20, 21). Studying the metabolism of CSCs is a challenging task due to the small size and high plasticity of these cell populations. Nevertheless, current experimental data shows that the metabolic features of CSCs are highly heterogeneous, and tumor type-dependent (**Table 1**).

Glycolysis is one of the major and best-studied metabolic characteristics of cancer cells. Fast-growing tissues, such as the most malignant tumors, demand more energy. In differentiated cells, energy in the form of adenosine triphosphate (ATP) is produced *via* oxidative phosphorylation (OXPHOS) that occurs in mitochondria. Complete oxidation of glucose molecule leads to the production of about 30 molecules of ATP, whereas about 26 out of these 30 ATP molecules are generated by OXPHOS (42). Fast-proliferating cancer cells switch from OXPHOS to glycolysis that requires the consumption of a high amount of glucose since only two molecules of ATP per one molecule of consumed glucose can be produced *via* this pathway. Lactate, a byproduct of aerobic glycolysis, is shuttled to the extracellular space and was shown to support stemness by upregulation of the expression of genes related to stem cell properties, such as transcription factor SP1, sterol regulatory element-binding protein 1 (SREBP1) which is a transcriptional activator required for regulation of lipid homeostasis, etc., to increase aggressiveness and invasive properties of cancer cells as well as to promote immunosuppression (43–48). Glycolytic CSCs were described for several tumor entities. Song et al. showed that CD133+ liver carcinoma cells had enhanced glycolysis (22). Osteosarcoma-initiating cells also showed a highly glycolytic phenotype (49). Breast CSCs demonstrated the upregulated glycolysis and simultaneously decreased OXPHOS (24). Heterogeneous results were showed for glioblastoma stem cells: Zhou et al. described highly glycolytic glioblastoma cells which were enriched for CSC populations by cell growth conditions (50) while Janiszewska et al. showed the importance of OXPHOS for CD133+ glioblastoma CSCs (28). OXPHOS, as the primary energy production pathway was also shown for leukemic (29), pancreatic (51) and ovarian (32) CSCs.

Many cancer cells demonstrate altered amino acid metabolism. For the majority of cancer cells, glutamine—usually a non-essential amino acid—becomes critically essential as they consume high amounts of it to cover their biosynthetic and energetic needs (52). The rewiring of glutamine metabolism in tumor cells is associated with specific genetic alterations including mitochondrial DNA (mtDNA) mutations (53), oncogenic KRAS (54, 55) and c-Myc overexpression (56). Glutamine enters cells *via* specific transporters (most of them belong to the alanine/serine/cysteine transporter (ASCT) family) and is used in various biochemical pathways. Bi-directional transporters of amino acids export glutamine in exchange for other amino acids (for example,

TABLE 1 | Examples of the metabolic features of CSCs described for the different tumor models.

Metabolic feature of CSCs	Tumor entity	Model	Potential therapeutic targets	References
Glycolysis	Hepatocellular carcinoma	PLC/PRF/5 human hepatocellular cancer cell line; CD133+ subpopulation was obtained by cell sorting	n/a	(22)
	Osteosarcoma	OS13 cell line established by authors; CSC population was obtained by limiting dilution assay *in vitro*	LIN28	(23)
	Breast cancer	Tumor-initiating cells purified from MMTV-*Wnt-1* murine breast tumors	Decreased activity of pyruvate dehydrogenase (Pdh)	(24)
	Breast cancer	$CD44^+/CD24^-$ breast cancer stem cells	Pyruvate dehydrogenase kinase (PDK1)	(25)
Glycolysis and OXPHOS	Lung cancer	CSC-like cells enriched under sphere forming conditions	Glycolysis itself (inhibition with 2-deoxyglucose reduced CSC features)	(26)
	Esophageal cancer	CSC-like cells enriched under sphere forming conditions	HSP27, HK2	(27)
OXPHOS	Glioblastoma	CD133+ CSCs from glioma spheres	IMP2	(28)
	Acute myeloid leukemia	Primary AML patient-derived cells; ROS-low CSC population was isolated by cell sorting	BCL-2	(29)
	Lung cancer	CSCs derived from A549 lung cancer cell line by using single-cell cloning culture	n/a	(30)
	Pancreatic cancer	CD133+ cells derived from patient samples	Mitochondrial complex I (targeted with metformin)	(31)
	Ovarian cancer	CD44+ CD117+ cells from ascitic fluid of ovarian cancer patients	Mitochondrial complex I	(32)
	Breast cancer	MCF7 and MDA-MB-231 cells; CSC-like cells enriched under sphere forming conditions	Mitochondrial respiration	(33)
De novo fatty acid synthesis	Glioma	Patient-derived glioblastoma cell lines; CSC population was enriched by culturing cell lines in serum-free neurobasal medium	FASN (fatty acid synthase)	(34)
	Breast cancer	Epithelial CSCs derived from MCF10A cells; patients' tissue samples; CD24- CD44+ ESA+ CSC-like cells were isolated by magnetic-activated cell sorting	SREBP1 (targeted with resveratrol)	(35)
	Breast cancer	ERBB2-positive breast cancer cells; CSC-like cells were sorted as side population (SP); CSC signature of ERBB2-positive cells was confirmed by high ALDH activity	PPARγ pathway	(36)
	Pancreatic cancer	CSCs derived from Panc1 cell line and enriched under sphere-forming conditions	FASN (targeted with cerulenin); mevalonate pathway (targeted with atorvastatin)	(37)
Glutamine metabolism	Pancreatic cancer	PDAC cells	CD9	(38)
	Non-small cell lung cancer Pancreatic cancer Glioblastoma	Side population of cell lines: A549 AsPC-1 GSC11 GSC23	n/a	(39)
	Neuroblastoma	Cell lines BE(2)-C, SH-SY5Y and SK-N-AS	MycN and c-Myc	(40)
	Hepatocellular carcinoma	Publicly available data from Cancer Genome Atlas; Cell lines HCCLM3 and HC22; Tumor tissue samples from HCC patients	GLS1	(41)

cysteine). In the cytoplasm, glutamine is converted into glutamate and, subsequently, α-ketoglutarate (α-KG). Glutamate is a building block of glutathione—one of the main scavenges of reactive oxygen species (ROS), which protects the cells from oxidative injury and lethal DNA damage (57, 58). In glutamine metabolism, α-KG is an essential intermediate fueling tricarboxylic acid (TCA) cycle in mitochondria. Metabolites of the TCA cycle are, in turn, used for various other pathways, for example, nucleotide and fatty acid biosynthesis. Moreover, α-KG is a co-factor of the ten-eleven translocation (TET) family DNA demethylases and Jumonji-C (JMJ-C) family histone demethylases—enzymes that play a role in epigenetic regulation of gene transcription. Some pieces of evidence suggest that elevated α-KG to succinate ratio is a marker of stemness (59).

Another critical metabolic characteristic of cancer cells is their lipid metabolism. *De novo* lipid biosynthesis, enhanced lipid oxidation, and increased storage of lipids are unique characteristics of many cancers. For some of them, such as prostate cancer, lipid content was proposed as a potential biomarker, since the accumulation of lipids in prostate tissue of mice correlated with tumor stage (60). Increased lipid droplet content was shown for colorectal CSCs (61).

De novo lipid biosynthesis and fatty acid oxidation are among the most targetable features of CSCs (62, 63). CSCs from glioma (34) and pancreatic cancer (37) demonstrated upregulated lipogenesis; interesting that pancreatic CSCs fuelled their lipogenesis *via* enhanced glycolysis. Fatty acid synthase (FASN) is the critical enzyme in *de novo* lipid synthesis. Its expression is

upregulated in many cancers, including lung, colon, breast, and ovarian cancer (64–67). SREBP-2, a transcription factor associated with *de novo* lipid synthesis, was shown to activate transcription of c-Myc in prostate cancer, therefore contributing to the increase of CSC properties (68). Increased fatty acid oxidation is critical for maintaining the stemness of breast cancer (69, 70) and leukemic cells (71).

THE METABOLIC INTERPLAY OF CSCS AND TUMOR MICROENVIRONMENT

Interaction of tumor microenvironment with cancer stem cells can support the survival and phenotype of CSCs. The tumor microenvironment consists of cancer-associated fibroblasts, endothelial cells, immune cells, extracellular matrix. Several factors are critically important for the sustaining of CSC metabolism, and hypoxia is one of them. Hypoxia is one of the major hallmarks of tumor microenvironment playing a critical role in CSC maintenance, quiescence, and therapy resistance (72). Hypoxia can affect CSCs in different ways, including activation of the hypoxia-inducible factor (HIF) mediated signaling that controls the tumorigenicity of CSCs (73). HIF-mediated signaling can interfere with the metabolism of cancer cells by upregulation of many glycolysis-associated genes, including glucose transporters from GLUT family (74). Pharmacological inhibition of GLUT-1 was shown to decrease the self-renewal properties of CSCs *in vitro* (75). Acidic microenvironment associated with hypoxic tumor areas is shown to promote CSC features by activation of the HIF-dependent transcription program (76). Interesting that cervical cancer cells located in hypoxic areas can produce lactate that is scavenged by cancer cells of oxygenated regions, fueling their proliferation (77). Cancer-associated fibroblasts (CAFs) can support the metabolic needs of cancer cells by feeding them via production of alanine (78), lactate, fatty acids or ketone bodies (79). CSCs from certain cancers (e.g., hepatocellular carcinoma and breast cancer) can promote angiogenesis and, therefore, increase nutrient supply, by releasing pro-angiogenic factors (such as VEGF) (80, 81). Tumor-associated immune cells contribute to the cancer progression and survival of CSCs *via* different mechanisms. Thus, cancer-associated macrophages can secrete various cytokines (e.g., TGFβ, IL-6) that induce the conversion of cancer cells to cells with CSC phenotype and contribute to chronic inflammation in tumor region (82, 83). Lactate produced by cancer cells in the hypoxic environment is known to induce conversion of tumor-associated macrophages into their pro-tumorigenic phenotype (84, 85). To survive under nutrient shortage conditions, CSCs may activate autophagy, the process of recycling their own nutrients by degrading organelles and large molecules. Enhanced autophagy as a pro-survival and pro-tumorigenic mechanism was demonstrated for breast (86), liver (87), osteosarcoma (88), and ovarian CSCs (89). Many of the above-described metabolic pathways confer CSC adaptation to the microenvironmental stresses, including a shortage of nutrients and anti-cancer therapies. These pathways are attractive targets for the eradication of CSC populations and better treatment outcomes (**Figure 1**, **Table 2**).

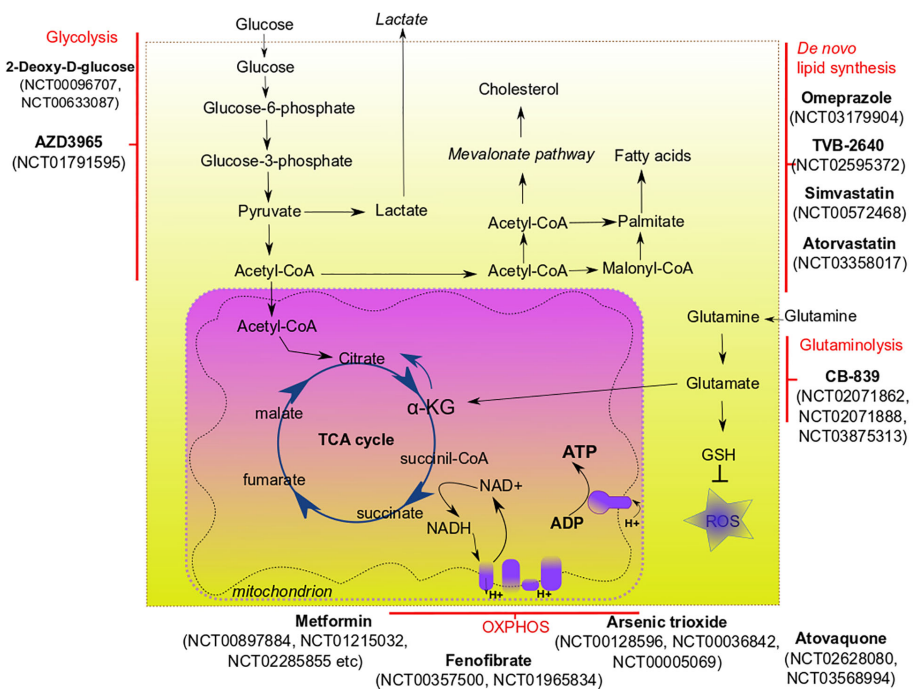

FIGURE 1 | Main metabolic pathways of CSCs and their potential targeting in clinical trials.

TABLE 2 | Compounds for metabolic targeting of cancer stem cells.

Metabolic process	Compound	Cancer type	References
Glycolysis	Metformin	Hepatocellular carcinoma	(90)
		Prostate cancer	(91)
		Colon cancer	(92)
	2-deoxy-D-glucose	Triple-negative breast cancer	(93)
		Colon cancer	(92)
	Epigallocathechine gallate (EGCG)	Pancreatic cancer	(94)
Glutamine metabolism	CB-839	Triple-negative breast cancer	(95)
		Metastatic colorectal cancer	(96)
		Lung cancer	(97)
OXPHOS	Fenofibrate	Prostate cancer Liver cancer Glioma Breast cancer	Reviewed in (98)
	Arsenic trioxide	Acute promyelocytic leukemia	(99)
	Atovaquone	Hepatocellular carcinoma	(100)
		Breast cancer	(101)
	Rosiglitazone	Breast cancer	(102)
		Hepatocellular carcinoma	(103)
De novo lipid synthesis	Cerulenin	Glioblastoma	(34)
		Colon cancer	(104)
	C75	Breast cancer	(105)
	Omeprazole	Breast cancer	(106)
	Fatostatin	Prostate cancer	(107)
		Breast cancer	(108)

TARGETING CSC METABOLISM

Targeting Glycolysis

The most straightforward approach to inhibit glycolysis is to starve tumors for glucose. The effect on patients can be achieved by subjecting them to a ketogenic diet, containing low amounts of carbohydrates and balanced amounts of proteins and fat. Ketogenic diet-mimicking treatment *in vitro* effectively reduced CSC-signature in glioma cells (109). Experimental evidence showing the benefit of a ketogenic diet for cancer patients, especially those with glioblastoma and pancreatic cancer, prompted to investigate the potency of this approach as adjuvant therapy for these types of malignancy. However, current clinical data demonstrates mixed results (110). Although the ketogenic diet is usually well-tolerated, compliance with its strict regimes is generally challenging for patients; therefore, it is not considered as monotherapy, and even its usage as adjuvant therapy is discussable (111).

Compound-mediated targeting of glycolysis demonstrated better results in many preclinical studies. Metformin—an antidiabetic drug—has drawn recent attention in cancer research due to its ability to inhibit various molecular pathways leading to the elimination of cancer cells (112). Metformin attenuates glycolysis in a variety of tumor entities. Interesting that metformin can either downregulate glycolytic flux in hepatocellular carcinoma cells (90) or increase glycolysis in breast cancer cells (113). Moreover, it can also inhibit mitochondrial complex I, therefore impairing OXPHOS (114). Altering cancer cell respiration by metformin treatment led to a significant improvement in radiotherapy response in tumor xenograft models of prostate and colon cancer (91). Epigallocatechin gallate (EGCG) was tested as an inhibitor of glycolysis together with conventional chemotherapeutic drugs, and shown as a potent enhancer of chemotherapy (94). A synthetic analog of glucose, 2-deoxy-D-glucose, was tested *in vitro* and showed the ability to inhibit glycolysis and decrease the CSC phenotype of triple-negative breast cancer cells (93). Experiments on colon cancer cells demonstrated that a combination of 2-deoxyglucose with biguanides (such as 3-bromopyruvate) substantially reduced their proliferation (92). Deoxyglucose is now evaluated in clinical trials as a treatment agent for different cancers, such as lung, breast, and pancreatic cancer (clinicaltrials.gov numbers NCT00096707, NCT00633087).

Targeting OXPHOS

OXPHOS is another promising metabolic target for CSCs. To date, many compounds have been designed to precisely target OXPHOS. Each compound targets a specific protein element of the electron transport chain blocking the transport of electrons and production of ATP. Most compounds that have shown their efficacy *in vitro*, *in vivo*, and in clinical trials, are directed towards mitochondrial complex I (115). The list of these compounds includes, but is not limited to metformin, phenofibrate, pyrvinium, rosiglitazone, pioglitazone, etc. Molecular mechanisms and efficacy of many OXPHOS-targeting compounds are described in reviews by Ashton and co-authors (115) and Sica et al. (116). Such OXPHOS-targeting compounds as atovaquone (clinicaltrials.gov No NCT02628080, NCT03568994), phenformin (NCT03026517) and arsenic trioxide (NCT00128596, NCT00036842, NCT00005069) are now under clinical trials for various solid tumors and leukemias. A combination of OXPHOS inhibition with other treatment modalities (particularly, radiotherapy) shows promising results *in vitro* and *in vivo* (117).

Targeting Glutamine Metabolism

As an essential amino acid for most cancer cells, glutamine represents an attractive anticancer target: depriving cells for glutamine seems to be an effective therapeutic option. However, in reality, targeting glutamine metabolism is a challenging task. Systemic approaches to direct glutamine deprivation may be inefficient as glutamine can be synthesized *de novo* by non-cancerous tissues, such as muscles (118). Other amino acids, such as asparagine and arginine, may also contribute to cancer cell survival under gluatamine deprivation conditions (119, 120). Moreover, some components of tumor microenvironment (e.g. cancer-associated fibroblasts) are able to supplement cancer cells with *de novo* synthesized glutamine, supporting their proliferation (121).

Glutamine metabolism can be precisely targeted *via* blocking critical steps of glutamine utilization. One of the most potent targets is glutaminase 1 (GLS1)—the enzyme that converts glutamine to glutamate. Numerous *in vitro* studies showed that GLS1 was associated with cancer progression, metastasis and CSCs for hepatocellular carcinoma (41), triple-negative breast cancer (122) and pancreatic cancer (123). Inhibition of GLS1 disrupts redox balance in CSCs and can sensitize them to other types of therapy (e.g., radiotherapy) (97, 123). Several inhibitors of GLS1 have been developed, among them BPTES (124) and CB-839. After showing high efficacy *in vitro* (125) and *in vivo*, CB-839 entered clinical trials. Currently, CB-839 is tested in Phase I and II clinical trials alone or in combination with other chemotherapeutic drugs for such malignancies as leukemia, breast cancer, colorectal cancer, and lung cancer (NCT02071862, NCT02071888, NCT03875313).

Targeting Fatty Acid Metabolism

As discussed above, the metabolism of fatty acids is substantially altered in many cancers. Cancer cells can be deprived of exogenous fatty acids or precursors for *de novo* fatty acid synthesis (such as glucose), which may be a promising strategy to slow tumor growth. Indeed, *de novo* fatty acid synthesis, which occurs in CSCs, but not healthy cells, seems to be one of the most promising targetable processes to eliminate the CSC population. Fatty acid synthase (FASN) is a target that received the most attention among all enzymes involved in the lipid metabolism of CSCs. Overexpression of FASN has been shown for a number of cancers, such as lung, prostate, ovarian and colon (66, 67, 126, 127). Inhibitors of FASN have pleiotropic effects on tumor cells, mostly because of the different pathways they can target. Cerulenin, a classical inhibitor of FASN, demonstrated high efficacy in reducing stem cell markers in glioblastoma and colon cells *in vitro* (34, 104). Chemical modifications of cerulenin, such as C75, were developed as the more stable analog of this drug, and C75 showed good results in inhibiting breast cancer cell proliferation (105). Such inhibitors of FASN as omeprazole and TVB-2640 are now evaluated in clinical trials for the treatment of breast cancer (NCT03179904, NCT02595372).

Not only FASN can be inhibited to target *de novo* lipid synthesis in cancer cells. Sterol regulatory element-binding proteins (SREBPs) are essential components of *de novo* lipid synthesis. A few compounds have been synthesized to target their functions. One of the most potent ones is fatostatin (128). It had a remarkable anti-tumor activity for prostate cancer; however, experiments with breast cancer cells showed mixed results, as fatostatin induced accumulation of both pro- and antiapoptotic lipids (108).

CONCLUSIONS AND PERSPECTIVES

Altered tumor metabolism is of utmost clinical importance as it mediates tumor resistance toward conventional anticancer agents, and metabolic co-targeting emerges as a novel, highly promising concept to enhance the efficacy of conventional treatment approaches. Metabolic inhibition of tumor growth by targeting CSCs is of specific interest as these cell populations are responsible for tumor maintenance and regrowth after treatment. Limitations of the current CSC assays and lack of the experimental models representing complex tumor microenvironments are a severe challenge to the development of the metabolic CSC-targeting approaches and their clinical translation. Many pitfalls also arise from the intratumoral heterogeneity of CSC metabolic features as well as the high plasticity of CSC nutritional demand during tumor progression and treatment. Future studies on heterogeneous CSC metabolic states at the level of single-cell resolution and employment advanced computational approaches to merge multi-omics data might yield clues for the development of novel metabolic targeting approaches and their implementation in current treatment regimens.

AUTHOR CONTRIBUTIONS

AM and AD contributed to the conception and design of the figure, tables, and manuscript. AM and AD wrote and edited the manuscript. All authors contributed to the article and approved the submitted version.

FUNDING

Work in AD lab is partially supported by grants from Deutsche Forschungsgemeinschaft (DFG) (273676790, 401326337 SPP 2084: µBONE, and 416001651), from Wilhelm Sander-Stiftung (2017.106.1), BMBF (Grant-No. 03Z1NN11) and DLR Project Management Agency (01DK17047). This work was in part supported by Sächsischen Landesstipendiums for AM (Tyutyunnykova).

REFERENCES

1. Ferlay J, Colombet M, Soerjomataram I, Mathers C, Parkin DM, Piñeros M, et al. Estimating the global cancer incidence and mortality in 2018: GLOBOCAN sources and methods. *Int J Cancer* (2019) 144:1941–53. doi: 10.1002/ijc.31937
2. Lin L, Yan L, Liu Y, Yuan F, Li H, Ni J. Incidence and death in 29 cancer groups in 2017 and trend analysis from 1990 to 2017 from the Global Burden of Disease Study. *J Hematol Oncol* (2019) 12(1):96. doi: 10.1186/s13045-019-0783-9
3. Mokhtari RB, Homayouni TS, Baluch N, Morgatskaya E, Kumar S, Das B, et al. Combination therapy in combating cancer. *Oncotarget* (2017) 8:38022–43. doi: 10.18632/oncotarget.16723
4. Palmer AC, Sorger PK. Combination Cancer Therapy Can Confer Benefit via Patient-to-Patient Variability without Drug Additivity or Synergy. *Cell* (2017) 171(7):1678–91.e13. doi: 10.1016/j.cell.2017.11.009
5. Bristow RG, Alexander B, Baumann M, Bratman SV, Brown JM, Camphausen K, et al. Combining precision radiotherapy with molecular targeting and immunomodulatory agents: a guideline by the American Society for Radiation Oncology. *Lancet Oncol* (2018) 19:e240–51. doi: 10.1016/S1470-2045(18)30096-2

6. Hwang WL, Pike LRG, Royce TJ, Mahal BA, Loeffler JS. Safety of combining radiotherapy with immune-checkpoint inhibition. *Nat Rev Clin Oncol* (2018) 15:477–94. doi: 10.1038/s41571-018-0046-7
7. Cleeland CS, Allen JD, Roberts SA, Brell JM, Giralt SA, Khakoo AY, et al. Reducing the toxicity of cancer therapy: Recognizing needs, taking action. *Nat Rev Clin Oncol* (2012) 9:471–8. doi: 10.1038/nrclinonc.2012.99
8. Gerdes MJ, Sood A, Sevinsky C, Pris AD, Zavodszky MI, Ginty F. Emerging understanding of multiscale tumor heterogeneity. *Front Oncol* (2014) 4:1–12. doi: 10.3389/fonc.2014.00366
9. Krause M, Dubrovska A, Linge A, Baumann M. Cancer stem cells: Radioresistance, prediction of radiotherapy outcome and specific targets for combined treatments. *Adv Drug Delivery Rev* (2017) 109:63–73. doi: 10.1016/j.addr.2016.02.002
10. Bütof R, Dubrovska A, Baumann M. Clinical perspectives of cancer stem cell research in radiation oncology. *Radiother Oncol* (2013) 108:388–96. doi: 10.1016/j.radonc.2013.06.002
11. Bezuidenhout N, Shoshan M. A shifty target: Tumor-initiating cells and their metabolism. *Int J Mol Sci* (2019) 20:1–19. doi: 10.3390/ijms20215370
12. Cojoc M, Peitzsch C, Kurth I, Trautmann F, Kunz-Schughart LA, Telegeev GD, et al. Aldehyde Dehydrogenase Is Regulated by β-Catenin/TCF and Promotes Radioresistance in Prostate Cancer Progenitor Cells. *Cancer Res* (2015) 75(7):1482–94. doi: 10.1158/0008-5472.CAN-14-1924
13. Peitzsch C, Tyutyunnykova A, Pantel K, Dubrovska A. Cancer stem cells: The root of tumor recurrence and metastases. *Semin Cancer Biol* (2017) 44:10–24. doi: 10.1016/j.semcancer.2017.02.011
14. Kim W-T, Ryu CJ. Cancer stem cell surface markers on normal stem cells. *BMB Rep* (2017) 50(6):285–98. doi: 10.5483/BMBRep.2017.50.6.039
15. Linge A, Lock S, Gudziol V, Nowak A, Lohaus F, Von Neubeck C, et al. Low cancer stem cell marker expression and low hypoxia identify good prognosis subgroups in HPV(-) HNSCC after postoperative radiochemotherapy: A multicenter study of the DKTK-ROG. *Clin Cancer Res* (2016) 22(11):2639–49. doi: 10.1158/1078-0432.CCR-15-1990
16. Prasetyanti PR, Medema JP. Intra-tumor heterogeneity from a cancer stem cell perspective. *Mol Cancer* (2017) 16:1–9. doi: 10.1186/s12943-017-0600-4
17. Wang KJ, Wang C, Dai LH, Yang J, Huang H, Ma XJ, et al. Targeting an autocrine regulatory loop in cancer stem-like cells impairs the progression and chemotherapy resistance of bladder cancer. *Clin Cancer Res* (2019) 25 (3):1070–86. doi: 10.1158/1078-0432.CCR-18-0586
18. Kreso A, Dick JE. Evolution of the cancer stem cell model. *Cell Stem Cell* (2014) 14:275–91. doi: 10.1016/j.stem.2014.02.006
19. Warburg O. On the origin of cancer cells. *Sci (80-)* (1956) 123(3191):309–14. doi: 10.1126/science.123.3191.309
20. Intlekofer AM, Finley LWS. Metabolic signatures of cancer cells and stem cells. *Nat Metab* (2019) 1(2):177–88. doi: 10.1038/s42255-019-0032-0
21. DeBerardinis RJ, Chandel NS. Fundamentals of cancer metabolism. *Sci Adv* (2016) 2(5):e1600200. doi: 10.1126/sciadv.1600200
22. Song K, Kwon H, Han C, Zhang J, Dash S, Lim K, et al. Active glycolytic metabolism in CD133(+) hepatocellular cancer stem cells: Regulation by MIR-122. *Oncotarget* (2015) 6(38):40822–35. doi: 10.18632/oncotarget.5812
23. Mizushima E, Tsukahara T, Emori M, Murata K, Akamatsu A, Shibayama Y, et al. Osteosarcoma-initiating cells show high aerobic glycolysis and attenuation of oxidative phosphorylation mediated by LIN28B. *Cancer Sci*.
24. Feng W, Gentles A, Nair RV, Huang M, Lin Y, Lee CY, et al. Targeting unique metabolic properties of breast tumor initiating cells. *Stem Cells* (2014) 32(7):1734–45. doi: 10.1002/stem.1662
25. Peng F, Wang JH, Fan WJ, Meng YT, Li MM, Li TT, et al. Glycolysis gatekeeper PDK1 reprograms breast cancer stem cells under hypoxia. *Oncogene* (2018) 37(8):1062–74. doi: 10.1038/onc.2017.368
26. Hsu HS, Liu CC, Lin JH, Hsu TW, Hsu JW, Li AFY, et al. Involvement of collagen XVII in pluripotency gene expression and metabolic reprogramming of lung cancer stem cells. *J BioMed Sci* (2020) 27(1):115–20. doi: 10.1186/s12929-019-0593-y
27. Liu C, Chou K, Hsu J, Lin J, Hsu T, Yen DH, et al. High metabolic rate and stem cell characteristics of esophageal cancer stem-like cells depend on the Hsp27–AKT–HK2 pathway. *Int J Cancer* (2019) 145(8):2144–56. doi: 10.1002/ijc.32301
28. Janiszewska M, Suvà ML, Riggi N, Houtkooper RH, Auwerx J, Clément-Schatlo V, et al. Imp2 controls oxidative phosphorylation and is crucial for preservin glioblastoma cancer stem cells. *Genes Dev* (2012) 26(17):1926–44. doi: 10.1101/gad.188292.112
29. Lagadinou ED, Sach A, Callahan K, Rossi RM, Neering SJ, Minhajuddin M, et al. BCL-2 inhibition targets oxidative phosphorylation and selectively eradicates quiescent human leukemia stem cells. *Cell Stem Cell* (2013) 12 (3):329–41. doi: 10.1016/j.stem.2012.12.013
30. Ye X-Q, Li Q, Wang G-H, Sun F-F, Huang G-J, Bian X-W, et al. Mitochondrial and energy metabolism-related properties as novel indicators of lung cancer stem cells. *Int J Cancer* (2011) 129(4):820–31. doi: 10.1002/ijc.25944
31. Sancho P, Burgos-Ramos E, Tavera A, Bou Kheir T, Jagust P, Schoenhals M, et al. MYC/PGC-1α balance determines the metabolic phenotype and plasticity of pancreatic cancer stem cells. *Cell Metab* (2015) 22(4):590–605. doi: 10.1016/j.cmet.2015.08.015
32. Pastò A, Bellio C, Pilotto G, Ciminale V, Silic-Benussi M, Guzzo G, et al. Cancer stem cells from epithelial ovarian cancer patients privilege oxidative phosphorylation, and resist glucose deprivation. *Oncotarget* (2014) 5 (12):4305–19. doi: 10.18632/oncotarget.2010
33. De Francesco EM, Ózsvári B, Sotgia F, Lisanti MP. Dodecyl-TPP Targets Mitochondria and Potently Eradicates Cancer Stem Cells (CSCs): Synergy With FDA-Approved Drugs and Natural Compounds (Vitamin C and Berberine). *Front Oncol* (2019) 9::615. doi: 10.3389/fonc.2019.00615/full
34. Yasumoto Y, Miyazaki H, Vaidyan LK, Kagawa Y, Ebrahimi M, Yamamoto Y, et al. Inhibition of fatty acid synthase decreases expression of stemness markers in glioma stem cells. *PloS One* (2016) 11(1):329–41. doi: 10.1371/journal.pone.0147717
35. Pandey PR, Xing F, Sharma S, Watabe M, Pai SK, Iiizumi-Gairani M, et al. Elevated lipogenesis in epithelial stem-like cell confers survival advantage in ductal carcinoma in situ of breast cancer. *Oncogene* (2013) 32(42):5111–22. doi: 10.1038/onc.2012.519
36. Wang X, Sun Y, Wong J, Conklin DS. PPARγ maintains ERBB2-positive breast cancer stem cells. *Oncogene* (2013) 32(49):5512–21. doi: 10.1038/onc.2013.217
37. Brandi J, Dando I, Pozza ED, Biondani G, Jenkins R, Elliott V, et al. Proteomic analysis of pancreatic cancer stem cells: Functional role of fatty acid synthesis and mevalonate pathways. *J Proteomics* (2017) 150:310–22. doi: 10.1016/j.jprot.2016.10.002
38. Wang VMY, Ferreira RMM, Almagro J, Evan T, Legrave N, Zaw Thin M, et al. CD9 identifies pancreatic cancer stem cells and modulates glutamine metabolism to fuel tumour growth. *Nat Cell Biol* (2019) 21(11):1425–35. doi: 10.1038/s41556-019-0407-1
39. Liao J, Liu P-P, Hou G, Shao J, Yang J, Liu K, et al. Regulation of stem-like cancer cells by glutamine through β-catenin pathway mediated by redox signaling. *Mol Cancer* (2017) 16(1):51. doi: 10.1186/s12943-017-0623-x
40. Le Grand M, Mukha A, Püschel J, Valli E, Kamili A, Vittorio O, et al. Interplay between MycN and c-Myc regulates radioresistance and cancer stem cell phenotype in neuroblastoma upon glutamine deprivation. *Theranostics* (2020) 10(14):6411–29. doi: 10.7150/thno.42602
41. Li B, Cao Y, Meng G, Qian L, Xu T, Yan C, et al. Targeting glutaminase 1 attenuates stemness properties in hepatocellular carcinoma by increasing reactive oxygen species and suppressing Wnt/beta-catenin pathway. *EBioMedicine* (2019) 39:239–54. doi: 10.1016/j.ebiom.2018.11.063
42. Koopman WJH, Distelmaier F, Smeitink JA, Willems PH. OXPHOS mutations and neurodegeneration. *EMBO J* (2012) 32(1):9–29. doi: 10.1038/emboj.2012.300
43. Estrella V, Chen T, Lloyd M, Wojtkowiak J, Cornnell HH, Ibrahim-Hashim A, et al. Acidity generated by the tumor microenvironment drives local invasion. *Cancer Res* (2013) 73(5):1524–35. doi: 10.1158/0008-5472.CAN-12-2796
44. Martinez-Outschoorn UE, Prisco M, Ertel A, Tsirigos A, Lin Z, Pavlides S, et al. Ketones and lactate increase cancer cell "stemness", driving recurrence, metastasis and poor clinical outcome in breast cancer: Achieving personalized medicine via metabolo-genomics. *Cell Cycle* (2011) 10 (8):1271–86. doi: 10.4161/cc.10.8.15330
45. Lin S, Sun L, Lyu X, Ai X, Du D, Su N, et al. Lactate-activated macrophages induced aerobic glycolysis and epithelial-mesenchymal transition in breast cancer by regulation of CCL5-CCR5 axis: A positive metabolic feedback loop. *Oncotarget* (2017) 8(66):110426–43. doi: 10.18632/oncotarget.22786

46. Tasdogan A, Faubert B, Ramesh V, Ubellacker JM, Shen B, Solmonson A, et al. Metabolic heterogeneity confers differences in melanoma metastatic potential. *Nature* (2020) 577(7788):115–20. doi: 10.1038/s41586-019-1847-2
47. Brand A, Singer K, Koehl GE, Kolitzus M, Schoenhammer G, Thiel A, et al. LDHA-Associated Lactic Acid Production Blunts Tumor Immunosurveillance by T and NK Cells. *Cell Metab* (2016) 24(5):657–71. doi: 10.1016/j.cmet.2016.08.011
48. Daneshmandi S, Wegiel B, Seth P. Blockade of lactate dehydrogenase-A (LDH-A) improves efficacy of anti-programmed cell death-1 (PD-1) therapy in melanoma. *Cancers (Basel)* (2019) 11(4):2367–78. doi: 10.3390/cancers11040450
49. Mizushima E, Tsukahara T, Emori M, Murata K, Akamatsu A, Shibayama Y, et al. Osteosarcoma-initiating cells show high aerobic glycolysis and attenuation of oxidative phosphorylation mediated by LIN28B. *Cancer Sci* (2020) 111(1):36–46. doi: 10.1111/cas.14229
50. Zhou Y, Zhou Y, Shingu T, Feng L, Chen Z, Ogasawara M, et al. Metabolic alterations in highly tumorigenic glioblastoma cells: Preference for hypoxia and high dependency on glycolysis. *J Biol Chem* (2011) 286(37):32843–53. doi: 10.1074/jbc.M111.260935
51. Sancho P, Burgos-Ramos E, Tavera A, Bou Kheir T, Jagust P, Schoenhals M, et al. MYC/PGC-1α Balance Determines the Metabolic Phenotype and Plasticity of Pancreatic Cancer Stem Cells. *Cell Metab* (2015) 22(4):590–605. doi: 10.1016/j.cmet.2015.08.015
52. Choi Y-K, Park K-G. Targeting Glutamine Metabolism for Cancer Treatment. *Biomol Ther (Seoul)* (2018) 26(1):19–28. doi: 10.4062/biomolther.2017.178
53. Chen Q, Kirk K, Shurubor YI, Zhao D, Arreguin AJ, Shahi I, et al. Rewiring of Glutamine Metabolism Is a Bioenergetic Adaptation of Human Cells with Mitochondrial DNA Mutations. *Cell Metab* (2018) 27(5):1007–25.e5. doi: 10.1016/j.cmet.2018.03.002
54. Mukhopadhyay S, Goswami D, Adiseshaiah PP, Burgan W, Yi M, Guerin TM, et al. Undermining glutaminolysis bolsters chemotherapy while NRF2 promotes chemoresistance in KRAS-driven pancreatic cancers. *Cancer Res* (2020) 41(6):405–9. doi: 10.1158/0008-5472.CAN-19-1363
55. Romero R, Sayin VI, Davidson SM, Bauer MR, Singh SX, Leboeuf SE, et al. Keap1 loss promotes Kras-driven lung cancer and results in dependence on glutaminolysis. *Nat Med* (2017) 23(11):1362–8. doi: 10.1038/nm.4407
56. Wise DR, Deberardinis RJ, Mancuso A, Sayed N, Zhang XY, Pfeiffer HK, et al. Myc regulates a transcriptional program that stimulates mitochondrial glutaminolysis and leads to glutamine addiction. *Proc Natl Acad Sci USA* (2008) 105(48):18782–7. doi: 10.1073/pnas.0810199105
57. Alvarez-Idaboy JR, Galano A. On the Chemical Repair of DNA Radicals by Glutathione: Hydrogen vs Electron Transfer. *J Phys Chem B* (2012) 116 (31):9316–25. doi: 10.1021/jp303116n
58. Evans JW, Taylor YC, Brown JM. The role of glutathione and DNA strand break repair in determining the shoulder of the radiation survival curve. *Br J Cancer Suppl* (1984) 6:49–53. doi: 10.1038/nm.2882
59. Carey BW, Finley LWS, Cross JR, Allis CD, Thompson CB. Intracellular α-ketoglutarate maintains the pluripotency of embryonic stem cells. *Nature* (2015) 518(7539):413–6. doi: 10.1038/nature13981
60. O'Malley J, Kumar R, Kuzmin AN, Pliss A, Yadav N, Balachandar S, et al. Lipid quantification by Raman microspectroscopy as a potential biomarker in prostate cancer. *Cancer Lett* (2017) 397:52–60. doi: 10.1016/j.canlet.2017.03.025
61. Tirinato L, Liberale C, Di Franco S, Candeloro P, Benfante A, La Rocca R, et al. Lipid droplets: A new player in colorectal cancer stem cells unveiled by spectroscopic imaging. *Stem Cells* (2015) 33(1):35–44. doi: 10.1002/stem.1837
62. Yi M, Li J, Chen S, Cai J, Ban Y, Peng Q, et al. Emerging role of lipid metabolism alterations in Cancer stem cells. *J Exp Clin Cancer Res* (2018) 37 (1):118. doi: 10.1186/s13046-018-0784-5
63. Mancini R, Noto A, Pisanu ME, De Vitis C, Maugeri-Saccà M, Ciliberto G. Metabolic features of cancer stem cells: the emerging role of lipid metabolism. *Oncogene* (2018) 37(18):2367–78. doi: 10.1038/s41388-018-0141-3
64. Bartolacci C, Padanad M, Andreani C, Melegari M, Rindhe S, George K, et al. Fatty Acid Synthase Is a Therapeutic Target in Mutant KRAS Lung Cancer. *J Thorac Oncol* (2017) 12(8):S1538. doi: 10.1016/j.jtho.2017.06.030
65. Lupu R, Menendez JA. Targeting Fatty Acid Synthase in Breast and Endometrial Cancer: An Alternative to Selective Estrogen Receptor Modulators? *Endocrinology* (2006) 147(9):4056–66. doi: 10.1210/en.2006-0486
66. Cai Y, Wang J, Zhang L, Wu D, Yu D, Tian X, et al. Expressions of fatty acid synthase and HER2 are correlated with poor prognosis of ovarian cancer. *Med Oncol* (2015) 32(1):1–6. doi: 10.1007/s12032-014-0391-z
67. Cerne D, Prodan Zitnik I, Sok M. Increased Fatty Acid Synthase Activity in Non-small Cell Lung Cancer Tissue Is a Weaker Predictor of Shorter Patient Survival than Increased Lipoprotein Lipase Activity. *Arch Med Res* (2010) 41 (6):405–9. doi: 10.1016/j.arcmed.2010.08.007
68. Li X, Wu JB, Li Q, Shigemura K, Chung LWK, Huang WC. SREBP-2 promotes stem cell-like properties and metastasis by transcriptional activation of c-Myc in prostate cancer. *Oncotarget* (2016) 7(11):12869–84. doi: 10.18632/oncotarget.7331
69. Ann D, Somlo G, Fahrmann JF, Yuan Y, Tripathi SC, Li Y-J, et al. JAK/STAT3-Regulated Fatty Acid β-Oxidation Is Critical for Breast Cancer Stem Cell Self-Renewal and Chemoresistance. *Cell Metab* (2018) 27(6):1357. doi: 10.1016/j.cmet.2017.11.001
70. Wang T, Fahrmann JF, Lee H, Li YJ, Tripathi SC, Yue C, et al. JAK/STAT3-Regulated Fatty Acid β-Oxidation Is Critical for Breast Cancer Stem Cell Self-Renewal and Chemoresistance. *Cell Metab* (2018) 27(1):136–50.e5. doi: 10.1016/j.cmet.2017.11.001
71. Ito K, Carracedo A, Weiss D, Arai F, Ala U, Avigan DE, et al. A PML-PPAR-δ pathway for fatty acid oxidation regulates hematopoietic stem cell maintenance. *Nat Med* (2012) 18(9):1350–8. doi: 10.1038/nm.2882
72. Qiu GZ, Jin MZ, Dai JX, Sun W, Feng JH, Jin WL. Reprogramming of the Tumor in the Hypoxic Niche: The Emerging Concept and Associated Therapeutic Strategies. *Trends Pharmacol Sci* (2017) 38:669–86. doi: 10.1016/j.tips.2017.05.002
73. Li Z, Bao S, Wu Q, Wang H, Eyler C, Sathornsumetee S, et al. Hypoxia-Inducible Factors Regulate Tumorigenic Capacity of Glioma Stem Cells. *Cancer Cell* (2009) 15(6):501–13. doi: 10.1016/j.ccr.2009.03.018
74. Singh D, Arora R, Kaur P, Singh B, Mannan R, Arora S. Overexpression of hypoxia-inducible factor and metabolic pathways: possible targets of cancer. *Cell Biosci* (2017) 7(1):62. doi: 10.1186/s13578-017-0190-2
75. Shibuya K, Okada M, Suzuki S, Seino M, Seino S, Takeda H, et al. Targeting the facilitative glucose transporter GLUT1 inhibits the self-renewal and tumor-initiating capacity of cancer stem cells. *Oncotarget* (2015) 6(2):651–61. doi: 10.18632/oncotarget.2892
76. Filatova A, Seidel S, Böğürcü N, Gräf S, Garvalov BK, Acker T. Acidosis acts through HSP90 in a PHD/ VHL-independent manner to promote HIF function and stem cell maintenance in glioma. *Cancer Res* (2016) 76 (19):5845–56. doi: 10.1158/0008-5472.CAN-15-2630
77. Sonveaux P, Végran F, Schroeder T, Wergin MC, Verrax J, Rabbani ZN, et al. Targeting lactate-fueled respiration selectively kills hypoxic tumor cells in mice. *J Clin Invest* (2008) 118(12):3930–42. doi: 10.1172/JCI36843
78. Sousa CM, Biancur DE, Wang X, Halbrook CJ, Sherman MH, Zhang L, et al. Pancreatic stellate cells support tumour metabolism through autophagic alanine secretion. *Nature* (2016) 536(7617):479–83. doi: 10.1038/nature19084
79. Fu Y, Liu S, Yin S, Niu W, Xiong W, Tan M, et al. The reverse Warburg effect is likely to be an Achilles' heel of cancer that can be exploited for cancer therapy. *Oncotarget* (2017) 8(34):57813–25. doi: 10.18632/oncotarget.18175
80. Yao H, Liu N, Lin MC, Zheng J. Positive feedback loop between cancer stem cells and angiogenesis in hepatocellular carcinoma. *Cancer Lett* (2017) 379:213–9. doi: 10.1016/j.canlet.2016.03.014
81. Sun H, Jia J, Wang X, Ma B, Di L, Song G, et al. CD44+/CD24- breast cancer cells isolated from MCF-7 cultures exhibit enhanced angiogenic properties. *Clin Transl Oncol* (2013) 15(1):46–54. doi: 10.1007/s12094-012-0891-2
82. Chen Y, Tan W, Wang C. Tumor-associated macrophage-derived cytokines enhance cancer stem-like characteristics through epithelial–mesenchymal transition. *OncoTargets Ther* (2018) 11:3817–26. doi: 10.2147/OTT.S168317
83. Yang J, Liao D, Chen C, Liu Y, Chuang TH, Xiang R, et al. Tumor-associated macrophages regulate murine breast cancer stem cells through a novel paracrine egfr/stat3/sox-2 signaling pathway. *Stem Cells* (2013) 31(2):248–58. doi: 10.1002/stem.1281

84. Ohashi T, Aoki M, Tomita H, Akazawa T, Sato K, Kuze B, et al. M2-like macrophage polarization in high lactic acid-producing head and neck cancer. *Cancer Sci* (2017) 108(6):1128–34. doi: 10.1111/cas.13244
85. Mu X, Shi W, Xu Y, Xu C, Zhao T, Geng B, et al. Tumor-derived lactate induces M2 macrophage polarization via the activation of the ERK/STAT3 signaling pathway in breast cancer. *Cell Cycle* (2018) 17(4):428–38. doi: 10.1080/15384101.2018.1444305
86. Gong C, Bauvy C, Tonelli G, Yue W, Deloménie C, Nicolas V, et al. Beclin 1 and autophagy are required for the tumorigenicity of breast cancer stem-like/progenitor cells. *Oncogene* (2013) 32(18):2261–72. doi: 10.1038/onc.2012.252
87. Song YJ, Zhang SS, Guo XL, Sun K, Han ZP, Li R, et al. Autophagy contributes to the survival of CD133+ liver cancer stem cells in the hypoxic and nutrient-deprived tumor microenvironment. *Cancer Lett* (2013) 339(1):70–81. doi: 10.1016/j.canlet.2013.07.021
88. Zhang D, Zhao Q, Sun H, Yin L, Wu J, Xu J, et al. Defective autophagy leads to the suppression of stem-like features of CD271+ osteosarcoma cells. *J BioMed Sci* (2016) 23(1):1–12. doi: 10.1186/s12929-016-0297-5
89. Peng Q, Qin J, Zhang Y, Cheng X, Wang X, Lu W, et al. Autophagy maintains the stemness of ovarian cancer stem cells by FOXA2. *J Exp Clin Cancer Res* (2017) 36(1):171. doi: 10.1186/s13046-017-0644-8
90. Hu L, Zeng Z, Xia Q, Liu Z, Feng X, Chen J, et al. Metformin attenuates hepatoma cell proliferation by decreasing glycolytic flux through the HIF-1α/PFKFB3/PFK1 pathway. *Life Sci* (2019) 239:116966. doi: 10.1016/j.lfs.2019.116966
91. Zannella VE, Pra AD, Muaddi H, McKee TD, Stapleton S, Sykes J, et al. Reprogramming metabolism with metformin improves tumor oxygenation and radiotherapy response. *Clin Cancer Res* (2013) 19(24):6741–50. doi: 10.1158/1078-0432.CCR-13-1787
92. Lea MA, Qureshi MS, Buxhoeveden M, Gengel N, Kleinschmit J, Desbordes C. Regulation of the proliferation of colon cancer cells by compounds that affect glycolysis, including 3-bromopyruvate, 2-deoxyglucose and biguanides. *Anticancer Res* (2013) 33(2):401–7. doi: 10.1158/1538-7445.AM2013-1855
93. O'Neill S, Porter RK, McNamee N, Martinez VG, O'Driscoll L. 2-Deoxy-D-Glucose inhibits aggressive triple-negative breast cancer cells by targeting glycolysis and the cancer stem cell phenotype. *Sci Rep* (2019) 9(1):706–20. doi: 10.1038/s41598-019-39789-9
94. Wei R, Hackman RM, Wang Y, Mackenzie GG. Targeting glycolysis with epigallocatechin-3-gallate enhances the efficacy of chemotherapeutics in pancreatic cancer cells and xenografts. *Cancers (Basel)* (2019) 11(10):685–700. doi: 10.3390/cancers11101496
95. Gross MI, Demo SD, Dennison JB, Chen L, Chernov-Rogan T, Goyal B, et al. Antitumor activity of the glutaminase inhibitor CB-839 in triple-negative breast cancer. *Mol Cancer Ther* (2014) 13(4):890–901. doi: 10.1158/1535-7163.MCT-13-0870
96. Ciombor KK, Whisenant J, Cardin DB, Goff LW, Das S, Schulte M, et al. CB-839, panitumumab, and irinotecan in RAS wildtype (WT) metastatic colorectal cancer (mCRC): Phase I results. *J Clin Oncol* (2019) 37 (4_suppl):574–4. doi: 10.1200/JCO.2019.37.4_suppl.574
97. Boysen G, Jamshidi-Parsian A, Davis MA, Siegel ER, Simecka CM, Kore RA, et al. Glutaminase inhibitor CB-839 increases radiation sensitivity of lung tumor cells and human lung tumor xenografts in mice. *Int J Radiat Biol* (2019) 95(4):436–42. doi: 10.1080/09553002.2018.1558299
98. Lian X, Wang G, Zhou H, Zheng Z, Fu Y, Cai L. Anticancer properties of fenofibrate: A repurposing use. *J Cancer* (2018) 9(9):1527–37. doi: 10.7150/jca.24488
99. Alimoghaddam K. A review of arsenic trioxide and acute promyelocytic Leukemia. *Int J Hematol Stem Cell Res* (2014) 8(3):44–54. doi: 10.1042/BJ20070039
100. Gao X, Liu X, Shan W, Liu Q, Wang C, Zheng J, et al. Anti-malarial atovaquone exhibits anti-tumor effects by inducing DNA damage in hepatocellular carcinoma. *Am J Cancer Res* (2018) 8(9):1697–711. doi: 10.18632/oncotarget.12944
101. Fiorillo M, Lamb R, Tanowitz HB, Mutti L, Krstic-Demonacos M, Cappello AR, et al. Repurposing atovaquone: Targeting mitochondrial complex III and OXPHOS to eradicate cancer stem cells. *Oncotarget* (2016) 7(23):34084–99. doi: 10.18632/oncotarget.9122
102. Mody M, Dharker N, Bloomston M, Wang PS, Chou FS, Glickman TS, et al. Rosiglitazone sensitizes MDA-MB-231 breast cancer cells to anti-tumour effects of tumour necrosis factor-α, CH11 and CYC202. *Endocr Relat Cancer* (2007) 14(2):305–15. doi: 10.1677/ERC-06-0003
103. Liu Y, Hu X, Shan X, Chen K, Tang H. Rosiglitazone metformin adduct inhibits hepatocellular carcinoma proliferation via activation of AMPK/p21 pathway. *Cancer Cell Int* (2019) 19(1):13. doi: 10.1186/s12935-019-0732-2
104. Shiragami R, Murata S, Kosugi C, Tezuka T, Yamazaki M, Hirano A, et al. Enhanced antitumor activity of cerulenin combined with oxaliplatin in human colon cancer cells. *Int J Oncol* (2013) 43(2):431–8. doi: 10.3892/ijo.2013.1978
105. Kridel SJ, Lowther WT, Pemble IV CW. Fatty acid synthase inhibitors: new directions for oncology. *Expert Opin Invest Drugs* (2007) 16(11):1817–29. doi: 10.1517/13543784.16.11.1817
106. Jin UH, Lee SO, Pfent C, Safe S. The aryl hydrocarbon receptor ligand omeprazole inhibits breast cancer cell invasion and metastasis. *BMC Cancer* (2014) 14(1):1–14. doi: 10.1186/1471-2407-14-498
107. Li X, Chen YT, Hu P, Huang WC. Fatostatin displays high antitumor activity in prostate cancer by blocking SREBP-regulated metabolic pathways and androgen receptor signaling. *Mol Cancer Ther* (2014) 13(4):855–66. doi: 10.1158/1535-7163.MCT-13-0797
108. Brovkovych V, Izhar Y, Danes JM, Dubrovskyi O, Sakallioglu IT, Morrow LM, et al. Fatostatin induces pro- and anti-apoptotic lipid accumulation in breast cancer. *Oncogenesis* (2018) 7(8):66. doi: 10.1038/s41389-018-0076-0
109. Ji C, Hu Y, Cheng G, Liang L, Gao B, Ren Y, et al. A ketogenic diet attenuates proliferation and stemness of glioma stem–like cells by altering metabolism resulting in increased ROS production. *Int J Oncol* (2019) 27(1):1–16. doi: 10.3892/ijo.2019.4942
110. Weber DD, Aminzadeh-Gohari S, Tulipan J, Catalano L, Feichtinger RG, Kofler B. Ketogenic diet in the treatment of cancer – Where do we stand? *Mol Metab* (2019) 145(8):2144–56. doi: 10.1016/j.molmet.2019.06.026
111. Erickson N, Boscheri A, Linke B, Huebner J. Systematic review: isocaloric ketogenic dietary regimes for cancer patients. *Med Oncol* (2017) 34:72. doi: 10.1007/s12032-017-0930-5
112. Yu X, Mao W, Zhai Y, Tong C, Liu M, Ma L, et al. Anti-tumor activity of metformin: From metabolic and epigenetic perspectives. *Oncotarget* (2017) 8:5619–28. doi: 10.18632/oncotarget.13639
113. Andrzejewski S, Gravel S-P, Pollak M, St-Pierre J. Metformin directly acts on mitochondria to alter cellular bioenergetics. *Cancer Metab* (2014) 2(1):12. doi: 10.1186/2049-3002-2-12
114. Viollet B, Guigas B, Sanz Garcia N, Leclerc J, Foretz M, Andreelli F. Cellular and molecular mechanisms of metformin: An overview. *Clin Sci* (2012) 122:253–70. doi: 10.1042/CS20110386
115. Ashton TM, Gillies McKenna W, Kunz-Schughart LA, Higgins GS. Oxidative phosphorylation as an emerging target in cancer therapy. *Clin Cancer Res* (2018) 24:2482–90. doi: 10.1158/1078-0432.CCR-17-3070
116. Sica V, Bravo-San Pedro JM, Stoll G, Kroemer G. Oxidative phosphorylation as a potential therapeutic target for cancer therapy. *Int J Cancer* (2020) 146 (1):10–7. doi: 10.1002/ijc.32616
117. Chen D, Barsoumian HB, Fischer G, Yang L, Verma V, Younes AI, et al. Combination treatment with radiotherapy and a novel oxidative phosphorylation inhibitor overcomes PD-1 resistance and enhances antitumor immunity. *J Immunother Cancer* (2020) 8(1):289. doi: 10.1136/jitc-2019-000289
118. Curthoys NP, Watford M. Regulation of glutaminase activity and glutamine metabolism. *Annu Rev Nutr* (1995) 15:133–59. doi: 10.1146/annurev.nu.15.070195.001025
119. Zhang J, Fan J, Venneti S, Cross JR, Takagi T, Bhinder B, et al. Asparagine plays a critical role in regulating cellular adaptation to glutamine depletion. *Mol Cell* (2014) 56(2):205–18. doi: 10.1016/j.molcel.2014.08.018
120. Alkan HF, Walter KE, Luengo A, Madreiter-Sokolowski CT, Stryeck S, Lau AN, et al. Cytosolic Aspartate Availability Determines Cell Survival When Glutamine Is Limiting. *Cell Metab* (2018) 28(5):706–20.e6. doi: 10.1016/j.cmet.2018.07.021
121. Yang L, Achreja A, Yeung T-L, Mangala LS, Jiang D, Han C, et al. Targeting Stromal Glutamine Synthetase in Tumors Disrupts Tumor Microenvironment-Regulated Cancer Cell Growth. *Cell Metab* (2016) 24 (5):685–700. doi: 10.1016/j.cmet.2016.10.011

122. Gross MI, Demo SD, Dennison JB, Chen L, Chernov-Rogan T, Goyal B, et al. Antitumor activity of the glutaminase inhibitor CB-839 in triple-negative breast cancer. *Mol Cancer Ther* (2014) 13(4):890–901. doi: 10.1158/1535-7163.MCT-13-0870
123. Li D, Fu Z, Chen R, Zhao X, Zhou Y, Zeng B, et al. Inhibition of glutamine metabolism counteracts pancreatic cancer stem cell features and sensitizes cells to radiotherapy. *Oncotarget* (2015) 6(31):31151–63. doi: 10.18632/oncotarget.5150
124. Robinson MM, McBryant SJ, Tsukamoto T, Rojas C, Ferraris DV, Hamilton SK, et al. Novel mechanism of inhibition of rat kidney-type glutaminase by BPTES. *Biochem J* (2007) 7(23):34084–99. doi: 10.18632/oncotarget.9122
125. Matre P, Velez J, Jacamo R, Qi Y, Su X, Cai T, et al. Inhibiting glutaminase in acute myeloid leukemia: Metabolic dependency of selected AML subtypes. *Oncotarget* (2016) 7(48):79722–35. doi: 10.18632/oncotarget.12944
126. Migita T, Ruiz S, Fornari A, Fiorentino M, Priolo C, Zadra G, et al. Fatty Acid Synthase: A Metabolic Enzyme and Candidate Oncogene in Prostate Cancer. *JNCI J Natl Cancer Inst* (2009) 101(7):519–32. doi: 10.1093/jnci/djp030
127. Zadra G, Ribeiro CF, Chetta P, Ho Y, Cacciatore S, Gao X, et al. Inhibition of de novo lipogenesis targets androgen receptor signaling in castration-resistant prostate cancer. *Proc Natl Acad Sci USA* (2019) 116(2):631–40. doi: 10.1186/1471-2407-14-498
128. Kamisuki S, Mao Q, Abu-Elheiga L, Gu Z, Kugimiya A, Kwon Y, et al. A Small Molecule That Blocks Fat Synthesis By Inhibiting the Activation of SREBP. *Chem Biol* (2009) 16(8):882–92. doi: 10.1016/j.chembiol.2009.07.007

Conflict of Interest: The authors declare that the research was conducted in the absence of any commercial or financial relationships that could be construed as a potential conflict of interest.

frontiers in Oncology

ORIGINAL RESEARCH
published: 25 February 2021
doi: 10.3389/fonc.2021.612778

Compound C, a Broad Kinase Inhibitor Alters Metabolic Fingerprinting of Extra Cellular Matrix Detached Cancer Cells

Mohammed Razeeth Shait Mohammed[1,2†], *Raed Ahmed Alghamdi*[1†], *Abdulaziz Musa Alzahrani*[1], *Mazin A. Zamzami*[1,2,3], *Hani Choudhry*[1,2,3] *and Mohammad Imran Khan*[1,2,3*]

[1] Biochemistry Department, Faculty of Science, King Abdulaziz University, Jeddah, Saudi Arabia, [2] Cancer Metabolism and Epigenetic Unit, Biochemistry Department, Faculty of Science, King Abdulaziz University, Jeddah, Saudi Arabia, [3] Cancer and Mutagenesis Research Unit, King Fahd Medical Research Centre, King Abdulaziz University, Jeddah, Saudi Arabia

OPEN ACCESS

Edited by:
Federica Sotgia,
University of Salford, United Kingdom

Reviewed by:
Jianrong Lu,
University of Florida, United States
Khalid Omer Alfarouk,
Alfarouk Biomedical Research LLC, United States

***Correspondence:**
Mohammad Imran Khan
mikhan@kau.edu.sa

[†]*These authors have contributed equally to this work*

Specialty section:
This article was submitted to Cancer Metabolism, a section of the journal Frontiers in Oncology

Received: *30 September 2020*
Accepted: *19 January 2021*
Published: *25 February 2021*

Citation:
Shait Mohammed MR, Alghamdi RA, Alzahrani AM, Zamzami MA, Choudhry H and Khan MI (2021) Compound C, a Broad Kinase Inhibitor Alters Metabolic Fingerprinting of Extra Cellular Matrix Detached Cancer Cells. Front. Oncol. 11:612778. doi: 10.3389/fonc.2021.612778

Most of the cancer related deaths are caused mainly by metastasis. Therefore, it is highly important to unfold the major mechanisms governing metastasis process in cancer. Throughout the metastatic cascade, cells need the ability to survive without attachment to neighboring cells and the original Extra Cellular Matrix (ECM). Recent reports showed that loss of ECM attachment shifts cancer cell metabolism towards glycolysis mostly through hypoxia. However, AMPK, a master metabolic regulator was also found to be upregulated under ECM detached conditions. Therefore, in this work we aimed to understand the consequences of targeting AMPK and other metabolic kinases by a broad kinase inhibitor namely Compound C in ECM detached cancer cells. Results showed that Compound C impacts glycolysis as evident by increased levels of pyruvate, but reduces its conversion to lactate thereby negatively regulating the Warburg effect. Simultaneously, Compound C induces block at multiple levels in TCA cycle as evident from accumulation of various TCA metabolites. Interestingly Compound C significantly reduces glutamine and reduced glutathione levels, suggesting loss of antioxidant potential of ECM detached cancer cells. Further, we found increased in metabolites associated with nucleotide synthesis, one carbon metabolism and PPP pathway during Compound C treatment of ECM detached cells. Finally, we also found induction in metabolites associated with DNA damage in ECM detached cancer cells during Compound C treatment, suggesting DNA damage regulatory role of metabolic kinases. Overall, our results showed that Compound C represses pyruvate to lactate conversion, reduces antioxidant potential and invokes DNA damage in ECM detached cancer cells. Our data provides a comprehensive metabolic map of ECM detached cancer cells that can be targeted with a broad kinase inhibitor, is Compound C. The data can be used for designing new combinational therapies to eradicate ECM detached cancer cells.

Keywords: AMP-activated protein kinase, metabolomic analysis, extra cellular matrix detachment, compound C, oxidative phosphorylation

INTRODUCTION

Cancer is the deadliest disease worldwide; it cost nearly 9.6 million lives in 2018. Most cancer deaths associated with the metastasis stage occur during cellular detachment from the primary site of cancer tumour and get attached to secondary metastatic site for growth (1, 2). Cell adhesion to the ECM-extracellular matrix that helps in cell survival and proliferation signal. In the absence of ECM or cell to cell adhesion leads cells to undergo programmed cell death (apoptosis), termed as *anoikis* (3). Metastatic ECM detached cells develop resistance to anoikis for its survival and re-attach to the distal secondary site to develop metastasis tumor. The signaling pathway involved in regulating cells during anoikis resistance is little known. PKB- The serine/threonine-protein kinase Akt regulates several cellular processes in tumors, including proliferation and cell metabolism (4). the AMP-activated protein kinase (AMPK) is regulated under metabolic stress conditions to maintain cell homeostasis by switching energy metabolism. AMPK inhibits anabolic pathway to minimize ATP consumption, sterol and lipid biosynthesis, glycogen synthesis, and cell cycle progression. AMPK promotes a catabolic pathway to restore ATP and increase glucose uptake, autophagy, lipid utilization, and mitochondrial biogenesis (5–7). AMPK is regulated positively by activation of Try172 residue phosphorylation by LKB1 and CaMKKβ kinase. Recent studies showed the AMPK pro-tumorigenic activity under glucose deprivation and hypoxic condition (7–10).

Glucose deprivation reduces NADPH/GSH level and increases H_2O_2 due to impaired PPP. It increases the non-metabolizable 2deoxyglucose(2DG) analogy of glucose, 2DG inhibits glycolysis by mimic glucose starvation and induce cell death (11). AMPK activation protects cancer cells from chemotherapy-induced apoptosis and metabolic stress. Dorsomorphin, also known as Compound C, has the property of inhibiting AMPK that directly effect on blocking metabolic action of AMPK. Dorsomorphin has been effectively anti-apoptotic action of AMPK and causes programmed cell death in many cancer cells type (12, 13).

In this study, we demonstrated the metabolic alteration of dorsomorphin (Compound C) in ECM detached different cancer cells. Interestingly we found dorsomorphin modulates metabolic fingerprinting in cancer cells.

MATERIALS AND METHODS

Cell Culture

The human cancer cell line HCT116 and 22RV1 were kindly gifted from Dr. Hani (Cancer and the epigenetic unit, King Abdulaziz University, Saudi Arabia). Cells were grown at 37˚C with 5% CO_2, in a Dulbecco's Modified Eagle Medium (DMEM) with 10% fetal bovine serum (Sigma).

Matrix Detachment Model

The matrix detachment was done in cell suspension culture. 1×10^6 cells were cultured in ultra-low attachment plate (14) for at 37°C for various time points, which results in formation of spheroids. The spheroids were treated with either vehicle control or with different concentration of compound-C (sigma- P5499) for 5 days. The images were captured by using Nikon (USA) inverted light microscope. Images were analyzed for size measurement using image J software (https://imagej.net/Invasion_assay).

Apoptosis Assay

The apoptosis was detected by using Annexin V-FITC labelled and propidium iodide followed by a flow cytometer. The cells were grown in an ultra-low attachment plate for 6 days with and without treatment with Compound C. After treatment spheroids are harvested and washed with PBS (ice cold) three times. The spheroids were breakdown by multiple pipetting and resuspended in 100 µl 1X binding buffer and 10 µl Annexin V-FITC and 5 µl PI. After incubation for 20 min in RT (dark condition). The cells were analyzed by flow The Guava® easyCyte 5 Flow Cytometer, and the percentage of cells went apoptosis was calculated (15).

Metabolites Extraction

Metabolites were extracted from ECM attached and detached cells and detached cells were treated with dorsomorphin (Compound C, Sigma P5499).ECM detached spheroids were collected and crushed immediately using tissue homogenizer using a combination of ice-cold methanol: acetonitrile: water at a ratio of (2:1:1 v/v) and vortexed for 30s and incubated for 60 min at −20°C, and spin for 15 min at 13,000 rpm at 4°C.

The supernatant was collected, dried in a vacuum concentrator, and reconstituted in 200 µl of acetonitrile in 0.1% formic acid, vortexed for 5 min and centrifuge for 10 min at 13,000 rpm at 4°C. Finally, the samples were taken for LC-MS/MS analysis (15–17).

Mass Spectrometry

Samples were analyzed in LC-MS/MS LTQ XL™ linear ion trap instrument (ThermoFisher Scientific). MSn settings, full scan mode scanning range from 100 to 1000 m/z. Helium was used as buffer gas and Nitrogen was used as sheath gas for run 40 arbitrary units were set as flow rate. The capillary temperature was set at 270°C and voltage 4.0 V; spray voltage was set at −3.0 kV.

Data Analysis

The raw data file was processed using open accesses online XCMS online database. Peaks were searched against human metabolites in the Human Metabolome database. Pathway analysis and statics were Metaboanalyst (15–17).

Real-Time qPCR Analysis for mRNA Expression

Briefly, RNA was extracted from all the cell lines at the end of different experimental conditions by using RNeasy kit (Qiagen), and reverse transcribed a High capacity cDNA Reverse Transcription kit (applied biosystems). cDNA (1–100 ng) was amplified in triplicate using gene specific primers (**Supplementary Table 2**). Threshold cycle (C_T) values

obtained from the instrument's software were used to calculate the fold change of the respective mRNAs. ΔC_T was calculated by subtracting the C_T value of the housekeeping gene from that of the mRNA of interest. $\Delta\Delta C_T$ for each mRNA was then calculated by subtracting the C_T value of the control from the experimental value. Fold change was calculated by the formula $2^{-\Delta\Delta CT}$.

Protein Extraction and Western Blot Analysis

Various cancer cells (HCT116 and 22RV1) were cultured in T_{75} flask (1×10^6/flask). After 24 h cells of cell plating in ultra-low attachment plates cells were treated with Compound C for indicated dose for consecutive 5 days. The fresh treatment was added every 48 h, following completion of treatment, media was aspirated and cells were washed with cold PBS (pH 7.4) and pelleted in 15ml falcon tubes. Ice-cold lysis buffer (RIPA buffer) was added to the pellet, with freshly added protease inhibitor cocktail (Protease Inhibitor Cocktail Set III, Calbiochem, La Jolla, CA). Then cells were passed through needle of the syringe to break up the cell aggregates. The lysate was cleared by centrifugation at 14000 g for 30 min at 4°C and the supernatant was used or immediately stored at −80°C. For western blotting 12% poly acrylamide gels were used to resolve 30µg of protein, transferred on to a nitrocellulose membrane, Equal loading were confirmed with ponceau staining of the membrane. Then probed with appropriate monoclonal primary antibodies and detected by chemiluminescence scanner by LI-COR after incubation with specific secondary antibodies (18). The primary antibodies as follows as follows Phospho-AMPKα (Thr172) (D4D6D), AMPKα (D5A2), LDHA (C4B5)

RESULTS

Compound C Effectively Reduces Proliferation of ECM Detached Cancer Cells

AMPK is a key regulatory during energy deprivation and activated during ECM detached cancer cells. We examined the toxic effect of Compound C on ECM detached cancer cell proliferation. Results showed that low doses of Compound C i.e. 10 µM in HCT116 and 15µM in 22RV1 Compound C significantly reduced cell proliferation (**Figure 1A**). Prolong treatment of Compound C significantly reduces the spheroid formation and size (**Figure 1B**) and simultaneously induces apoptosis in spheroids formed due to ECM detachment (**Figure 1C**)

Metabolic Impact of Compound C in ECM Detached Cancer Cells

To explore the metabolic profile of ECM detached cancer cells treated with broad kinase inhibitor namely Compound C, we performed untargeted metabolomics to comprehend the difference in ECM attached cancer cells with ECM detached cancer cells, and Compound C treated ECM detached cancer cells. Metabolites were acquired using HPLC-MS/MS in DDA-

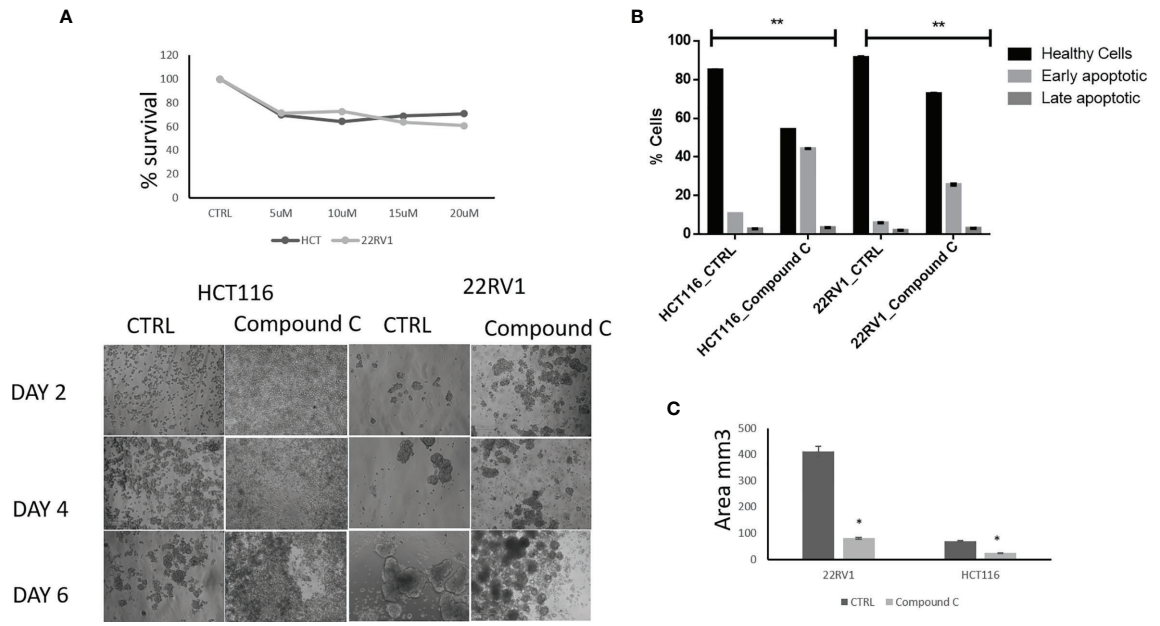

FIGURE 1 | Compound C inhibition reduce cell proliferation and size reduction. **(A)** Cells are grown in ultra-low attachment 96-well plate and treated with different concentration of Compound C and MTT assay were performed. **(B)** Cells are grown in ultra-low attachment plate and treated with Compound C, images were acquired, and size were measured using image J software. **(C)** Cells are grown in ultra-low attachment plat and treated with Compound C; apoptosis assay were performed using Annexin V. * is p-value ≤ 0.05 ** is p-value ≤ 0.01

Data Dependent mode, and spectrum raw files were processed using XCMS online database. The total 649 features were identified using ESI positive mode and 546 metabolites (**Figure 2A**) with (p-value ≤ 0.01) statistically significant. Principal component analysis (PCA) models score plots of all samples showed a significant difference in metabolomics between sample groups (**Figure 2B**). The correlation coefficient of the metabolomics data showed metabolites were self-correlations. However, in the Heatmap for the metabolites showed variation in metabolic expression between ECM attached, ECM detached, and ECM detached cells treated with Compound C (**Figure 2C**). The top highly significant metabolite in terms of PCA analysis with expression index showed the variation in metabolite accumulation in Compound C treated ECM detached cancer cells (**Figure 2D**), Top 275 metabolite with expression value shown in **Table 1**. and their raw table with p-value replicates details given in the **Supplementary Table 1**. The pathway enrichment analysis in ECM detached and Compound C treated ECM detached cancer cells compared with ECM attached cancer cells, pathway enrichment, and pathway linkage analysis were obtained through MetaboAnalyst 4.0. A total of 93 metabolic pathways were shown to be enriched (**Figure 2E**), mainly involved in energy metabolisms like Warburg Effect, Gluconeogenesis, Glycolysis, and TCA Cycle. As well as some other metabolic pathways, such as Methyl histidine Metabolism, Pentose Phosphate Pathway, Mitochondrial Electron Transport Chain, urea cycle, and Lactose Degradation, etc. (**Figure 2F**),

Compound C Reduces Lactate Formation

Lactate production in aerobic glycolysis is a prevalent energy metabolism in cancer cells metabolic pathway. We evaluate mRNA expression and metabolites involved in different steps of glycolysis. Data showed that the mRNA expression of many glycolytic gene namely GLUT1 and 3, Hexokinase 2 (HK2), PFKL (6-phosphofructokinase), PFKFB1 (fructose-2,6-biphosphatase 1), ENO2 (Enolase 2), PGAM1 (Phosphoglycerate Mutase 1), PDK1 (Pyruvate Dehydrogenase Kinase 1), LDHA (Lactate dehydrogenase A), PKM2 (pyruvate kinase M2) and their associated metabolites were high in ECM detached conditions. Compound C reduces both transcripts and associated metabolites of the above-mentioned enzymes in ECM detached cancer cells (**Figures 3A, B**). We further noticed that some enzyme transcript levels i.e. ALDOA (aldolase, fructose-bisphosphate A) GAPDH (glyceraldehyde 3-phosphate dehydrogenase), and PGK1-(Phosphoglycerate Kinase 1) failed to get induced in ECM detached conditions (**Figures 3A, B**).

The reduction of LDHA transcript was well corroborated with lower lactate dehydrogenase activity in Compound C treated cells (**Figure 3C**). These findings suggest that the end product of glycolysis i.e. pyruvate was preferred to enter oxidative phosphorylation rather than lactate formation in ECM detached cancer cells during Compound c treatment. We also observed reduction in phosphorylated-AMPK levels well-known to be targeted by Compound C in treated cells (**Figure 3C**).

Compound C Treatment Results in Malic Acid Accumulation in ECM Detached Cells

ECM detached cancer cells need metabolic reprogramming to survive and within the known metabolic kinases, AMP-activated protein kinase (AMPK) is a primary regulator of metabolism (19). We found that ECM detached cancer cells have accumulation of various TCA intermediates such as malate and fumarate, suggesting their potential role in ECM detached cancer cell metabolism. Compound C treatment induces block at multiple steps of TCA cycle as evident by accumulation of TCA metabolites. We observed a further increase in both malate and fumarate in both cell lines treated with Compound C (**Figure 4**).

Compound C Depletes Glutamine and Alters Cellular Antioxidant Levels

Glutamine have multipurpose roles in cellular metabolism. Glutamine feds TCA cycle along with nucleotide biosynthesis, GSH production and production of nonessential amino acids. We found a significant increase in glutamine and hydroxyglutarate (2HG) in ECM detached cells. 2HG is an oncometabolite. 2HG is known to be produced by mutant IDH ½ enzymes and can also be generated from glutamine derived from αKG (20, 21). Compound C significantly reduces the cellular glutamine levels of ECM detached cancer cells. Since glutamine feeds for reduced glutathione (GSH) production, we measured the GSH levels and

TABLE 1 | Top metabolite with their expression.

	Forward Primer	Reverse
GLUT1	CATCCCATGGTTCATCGTGGCTGAACT	GAAGTAGGTGAAGATGAAGAACAGAAC
GLUT3-	TGCCTTTGGCACTCTCAACCAG	GCCATAGCTCTTCAGACCCAAG
HK2	GCCATCCTGCAACACTTAGGGCTTGAG	GTGAGGATGTAGCTTGTAGAGGGTCCC
PFKL	GGAGAAGCTGCGCGAGGTTTAC	ATTGTGCCAGCATCTTCAGCATGAG
ALDOA	AGGCCATGCTTGCACTCAGAAGT	AGGGCCCAGGGCTTCAGCAGG
GAPDH	TTCCGTGTCCCCACTGCCAACGT	CAAAGGTGGAGGAGTGGGTGTCGC
PGK1	ATGTCGCTTTCTAACAAGCTGA	GCGGAGGTTCTCCAGCA
PGAM1	GGAAACGTGTACTGATTGCAGCCC	TTCCATGGCTTTGCGCACCGTCT
ENO1	GACTTGGCTGGCAACTCTG	GGTCATCGGGAGACTTGAA
ENO2	TCATGGTGAGTCATCGCTCAGGAG	ATGTCCGGCAAAGCGAGCTTCATC
PKM2	GCCCGTGAGGCAGAGGCTGC	TGGTGAGGACGATTATGGCCC
PDK1	CATGTCACGCTGGGTAATGAGG	CTCAACACGAGGTCTTGGTGCA
PFKFBP1	CTACTGAGCCCTTTCCAAGAA	GCAGAGTAGGAGAAGAGCAAA

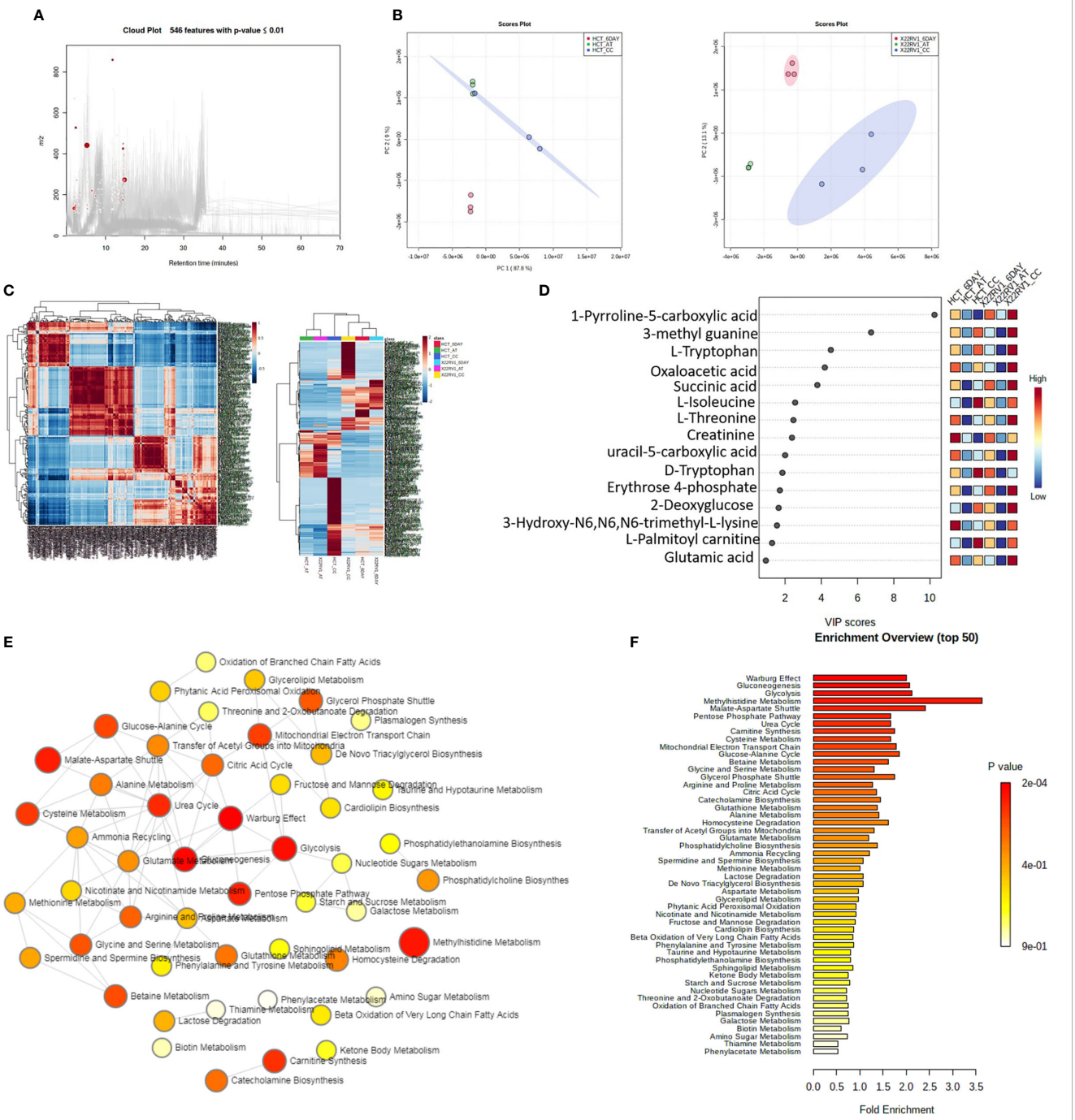

FIGURE 2 | Metabolomic analysis of ECM detached cancer cells and Compound C treated in ECM detached cancer cells, **(A)** Metabolites were extracted and run in LTQ-XL linear ion trap LC-MS and its total ion chromatogram with significate features. **(B)** PCA analysis of total metabolite of HCT 116 and 22RV1 with three different condition. **(C)** Correlation heat map and expression heat map of differential metabolite expressed between ECM attached, ECM detached, and ECM detached cells treated with Compound C. **(D)** VIP score based on PCA analysis of top metabolites. **(E)** Pathway network analysis. **(F)** Top pathway enriched in metabolome analysis between ECM attached, ECM detached, and ECM detached cells treated with Compound C.

as expected ECM detachment showed increased GSH levels which were significantly reduced by Compound C (**Figure 5A**). Next, we measured activity of super oxide dismutase (SOD), reduces ROS, and found that ECM detached cancer cells have high activity and Compound C reduces its activity (**Figure 5B**). Overall, these results showed ECM detached cancer cells possess increase glutamine, GSH and antioxidant capacity and Compound C reduces glutamine, GSH and antioxidant capacity.

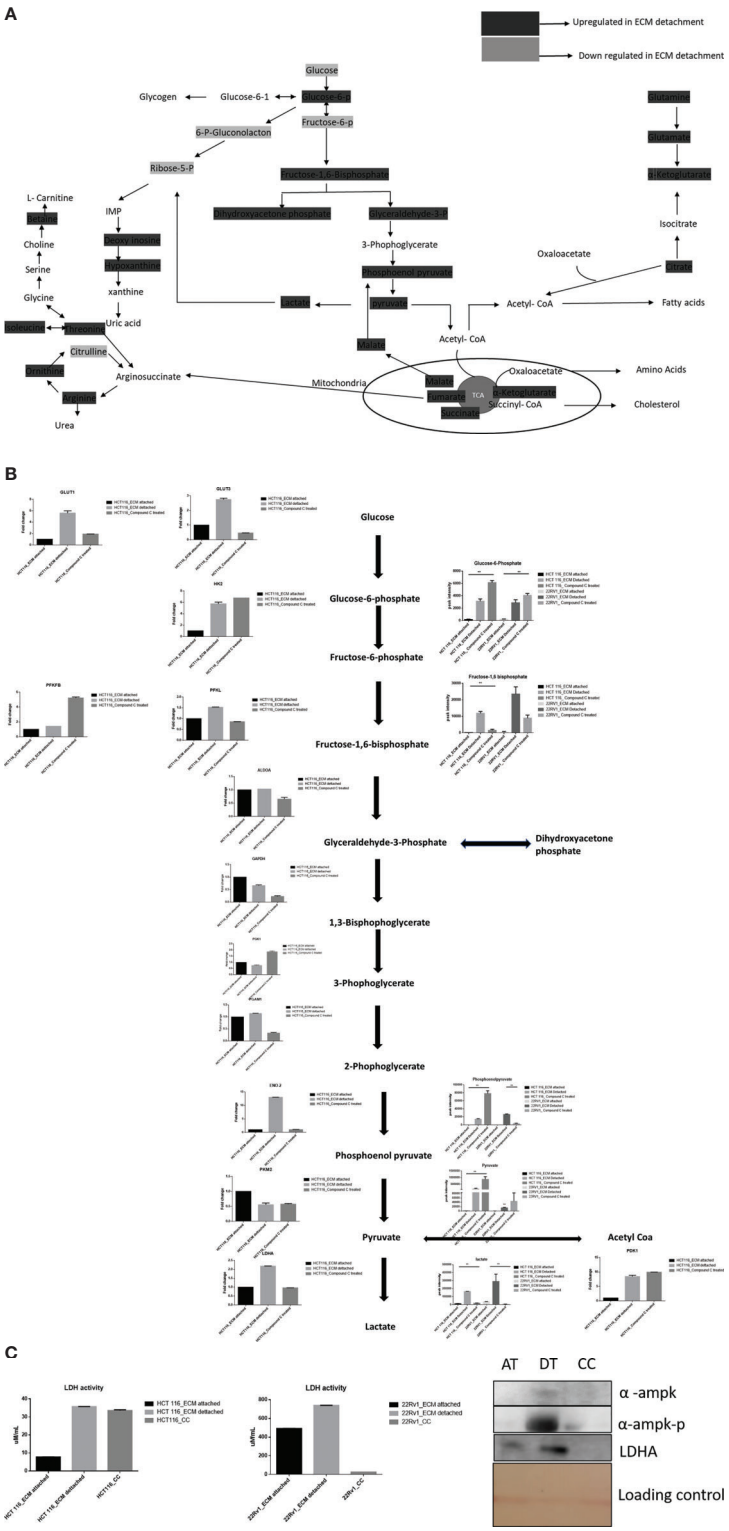

FIGURE 3 | Compound C alter energy enrichment pathway in ECM detachment. **(A)** Overall energy enrichment pathway with metabolite expression index. **(B)** Expression of transcript (HCT116) and metabolite involved in glycolysis during ECM detachment and AMPK inhibited ECM detached cells, P-value $p < 0.01$. **(C)** LDHA assay and Western blot analysis of protein involved in AMPK activation and glycolysis(AT- ECM attached, DT- ECM detached and CC-Compound C treated).

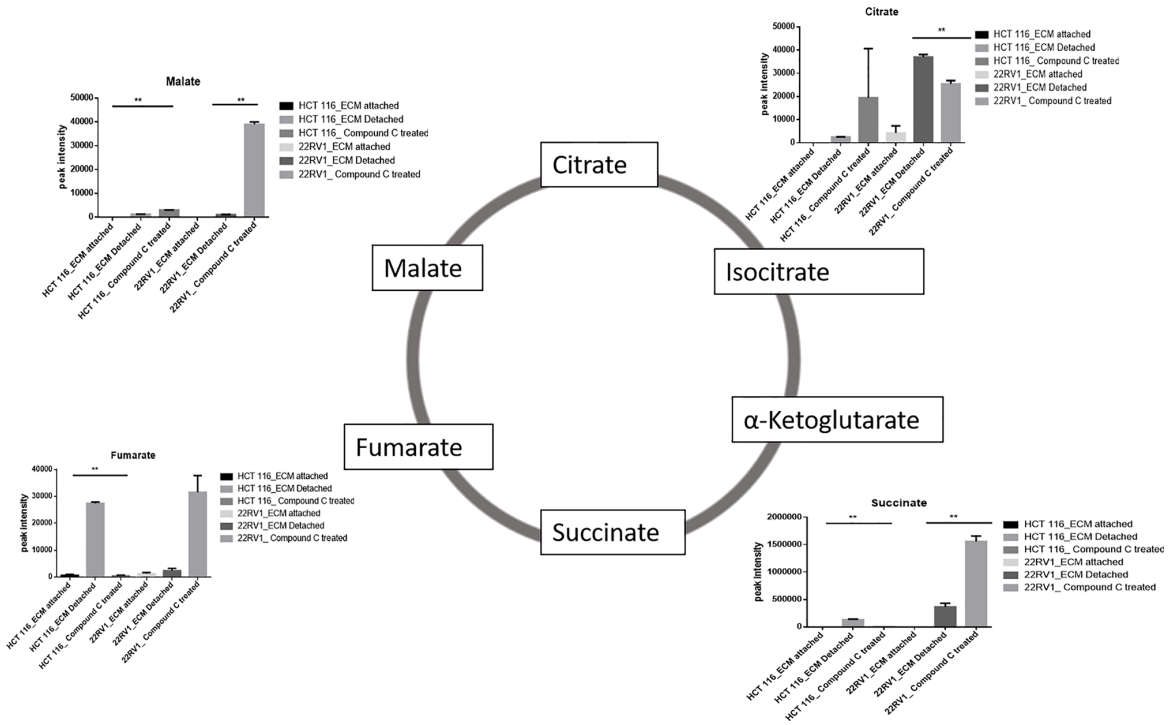

FIGURE 4 | Compound C modulates TCA cycle. ** is p-value ≤ 0.01.

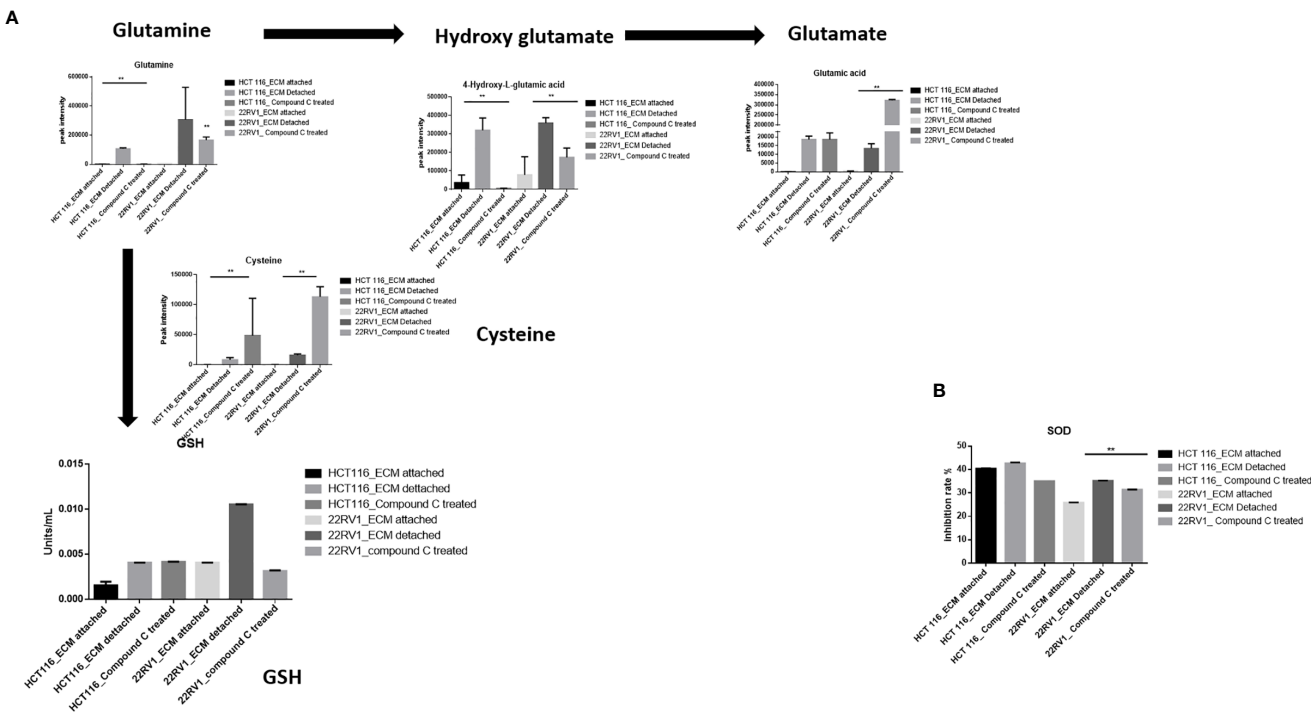

FIGURE 5 | Compound C alters GSH level. **(A)** Overall GSH enrichment pathway with metabolite expression index and GSH assay. **(B)** SOD assay during ECM detachment and AMPK inhibited ECM detached cells, P-value **p < 0.01.

Compound C Favors Ribosugar Synthesis

Hexose monophosphate shunt (HMP), also known as Pentose phosphate pathway (PPP) or phosphogluconate pathway, starts from the branch of glycolysis and the first step of glucose metabolism. HMP activation is demonstrated in different types of cancer and in their role in association with metastasis, invasion, and angiogenesis (22, 23). Our studies showed the ECM detached cells increased intermediate metabolite of HMP shunt in both cell lines. Compound C treatment increases ribose, erythrose and xylose levels. However, there were no significant changes observed in nucleotide levels of adenosine and guanosine (**Figure 6**) (**Table 2**).

Compound C Modulates One Carbon Metabolites

One-carbon (1C) metabolism, which sets a broader set of transformation from folate metabolism. 0ne-carbon metabolism is regulatory in cellular physiology. One-carbon metabolism is mostly derived from glycine and non-essential amino acid serin. One- carbon metabolism generate output metabolites that serve as essential building blocks for a redox reaction, biosynthesis, and methylation (24). We sought to verify the functional effect on one-carbon metabolism by Compound C in detached cells; data showed increased one-carbon metabolite intermediates in ECM detached cells such as SAM, L-cystathionine, methyl-cysteine, homocysteine and cysteine suggesting that ECM detached cancer cells might have more methylation phenotype. Coherent with this observation, Compound C treatment in ECM detached cells showed further increase in S-adenosyl-methionine (SAM), homocysteine, and cysteine in both cell lines, but other intermediate metabolites showed different trends between two cell lines (**Figure 7**) (**Table 3**).

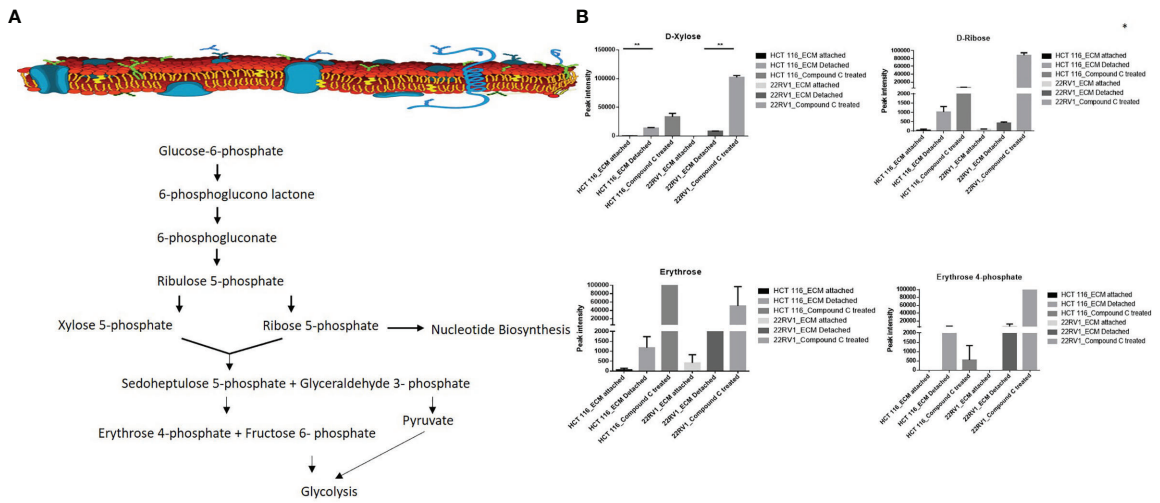

FIGURE 6 | Compound C alter the metabolite involved pentose phosphate pathway. **(A)** Metabolite involved in PPP pathway. **(B)** Expression of metabolite involved in PPP during ECM detachment and AMPK inhibited ECM detached cells, P-value $p < 0.01$. * is p-value ≤ 0.05 ** is p-value ≤ 0.01

TABLE 2 | Fold change of metabolite involved in PPP- fold change was calculated with normalized value of ECM attached and up and down regulation was mention with proposition to ECM detached and Compound C treated.

	22RV1				HCT116				P value
	ECM Attached	ECM detached	Compound C		ECM Attached	ECM detached	Compound C		
Xylulose 5 phosphate	1	221.4749	70.43583	down	1	45.16325	1387.211	up	0.002851
Sorbitol-6-phosphate	1	35.28718	24.27192	down	1	3.658933	11.68237	up	0.00201
Ribose-5-phosphate	1	0.180434	0.056273	down	1	0.558023	0.930893	up	0.00385
Mannitol 1-phosphate	1	11.58318	8.200933	down	1	0.223793	1.231869	up	0.004667
Guanosine	1	19.38104	15.46899	down	1	1.679476	2.855435	up	0.004705
Guanidinosuccinic acid	1	434.0069	82.62108	down	1	101.89	5994.094	up	0.002381
Erythrose 4-phosphate	1	3434.549	527160.1	up	1	1935.108	366.8125	down	0.019394
Erythrose	1	6.659711	276.3982	up	1	25.87366	18793.61	up	0.002141
D-Xylose	1	115.2781	937.4171	up	1	127.792	257.4589	up	0.003406
D-Ribose	1	8.750765	1606.917	up	1	40.64657	167.1691	up	0.002469
adenosine diphosphate	1	253.3069	138.6028	down	1	7.017809	48.89972	up	0.002551
adenosine	1	134.3279	101.9717	down	1	4.509506	9.377341	up	0.002368

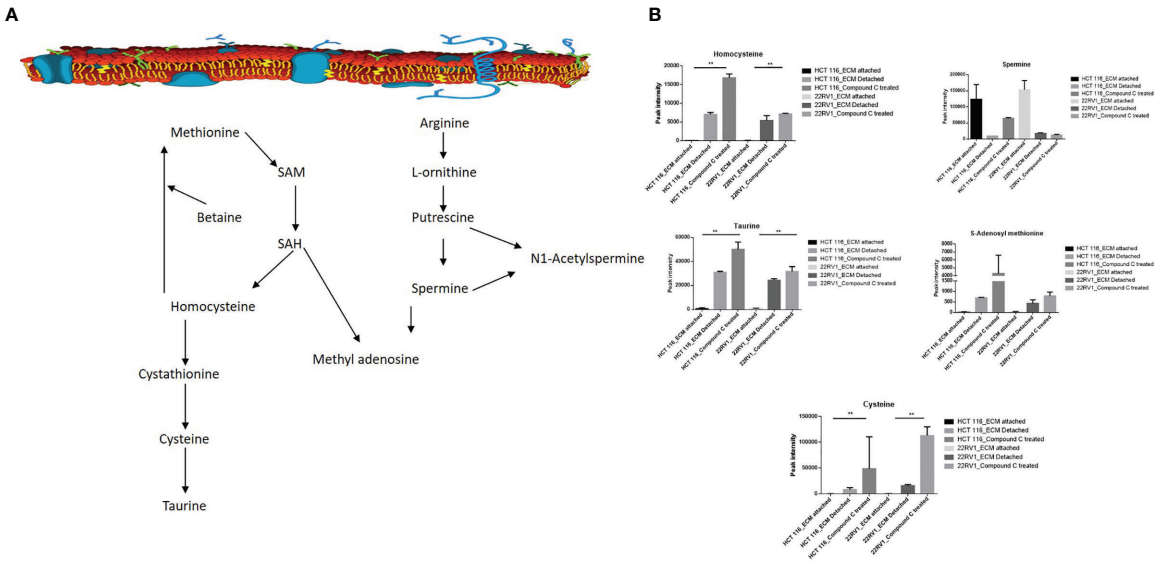

FIGURE 7 | Compound C the modulate metabolite expression of one carbon metabolism **(A)** Metabolite involved in one carbon metabolism pathway. **(B)** Expression of metabolite involved in One carbon metabolite during ECM detachment and AMPK inhibited ECM detached cells, P-value $p < 0.01$. ** is p-value ≤ 0.01.

TABLE 3 | Fold change of metabolite involved in one carbon metabolism- fold change was calculated with normalized value of ECM attached and up and down regulation was mention with proposition to ECM detached and Compound C treated.

	22RV1				HCT116				P value
	ECM Attached	ECM detached	Compound C		ECM Attached	ECM detached	Compound C		
Taurine	1	25.61044	62.29942	up	1	50.94784	95.3329	up	0.001673
Spermine	1	0.119093	0.074492	down	1	0.103608	0.672684	down	0.002103
Selenohomocysteine	1	46.36336	78.14272	up	1	100566.2	2692.212	down	0.002657
S-Adenosyl-l-homocysteine	1	0.398734	0.20135	down	1	0.601573	23.40819	up	0.002926
S-Adenosyl methionine	1	18.2159	20.10414	up	1	43.84777	582.1221	up	0.002815
L-Cystathionine	1	818.562	200.4249	down	1	15.45662	1.346547	down	0.001929
Cytosine	1	106.4612	69.45275	down	1	0.930727	3.676395	up	0.002671
Methylcysteine	1	7.949229	13.74496	up	1	34.12177	99.65528	up	0.003304
Methionine	1	0.999488	0.809505	down	1	11.69524	166.5561	up	0.020447
Homocysteine	1	43.40685	157.0146	up	1	199.278	713.961	up	0.003783
Cysteine	1	110.7534	724.504	up	1	2923.258	112134.5	up	0.003325
Betaine	1	1.888104	0.45807	down	1	2.182797	205.0076	up	0.007133

Compound C Increase Levels of Metabolites Associated With DNA Damage

Genomic DNA damage is instigated by reactive oxygen species (ROS)generated by aerobic metabolism. Both cytotoxic and mutagenic DNA lesions are associated with oxidative DNA damage (25–27). We noticed increased levels of metabolites namely 8-Oxoguanine, 3'-O-Methylguanosine, 6-methyl guanine and 3-Methylcytosine, associated with DNA damage in ECM detached cancer cells. Compound C further increased their levels suggesting a protective role of AMPK and other metabolic kinases in DNA damage conditions [**Figure 8**, (**Table 4**)].

DISCUSSION

Numerous studies have shown that the metabolic reprogramming induced by ECM detachment contributes to cell survival and promotes metastasis. AMPK is a nutrient sensor activated in ECM detachment when ATP : ADP ratio is low (27). In this study, we have shown that metabolic adaption during ECM detachment and during the energy crisis. A metabolic switch happened during Compound C treatment in ECM detached cells. ECM detachment is a signature for metastasis and tumorigenesis (28). Cell depend on glucose metabolism for energy production and biosynthesis need for

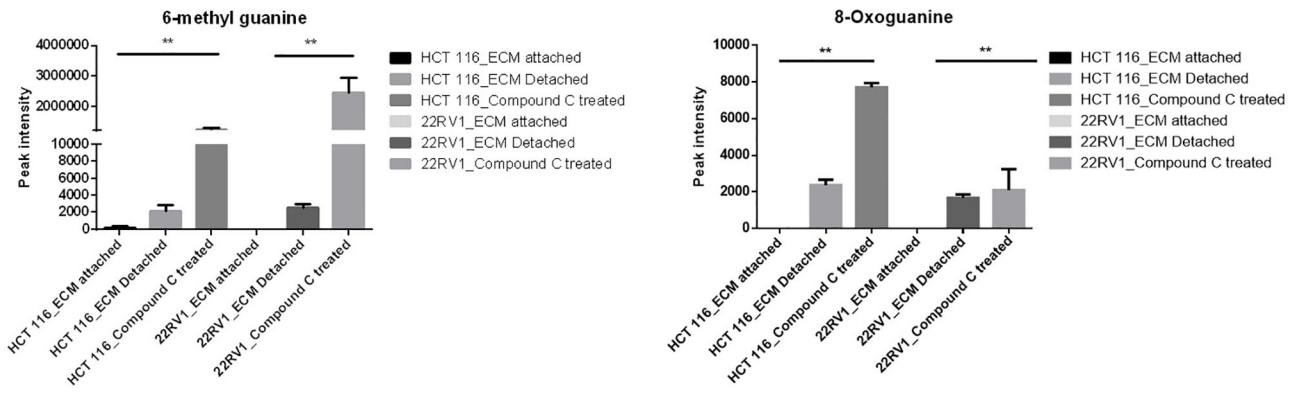

FIGURE 8 | Effect of Compound C on DNA lesion. ** is p-value ≤ 0.01.

TABLE 4 | Fold change of metabolite involved in DNA lesion - fold change was calculated with normalized value of ECM attached and up and down regulation was mention with proposition to ECM detached and Compound C treated.

	22RV1				HCT116				P value
	ECM Attached	ECM detached	Compound C		ECM Attached	ECM detached	Compound C		
Hypoxanthine	1	4718.953	3303.693	down	1	3206.921	49.92634	down	0.00306
Deoxyinosine	1	46.65531	32.8449	down	1	2295.48	137061.3	up	0.001631
Deoxycytidine	1	517.0447	81.81474	down	1	11740.75	84000.85	up	0.002183
8-Oxoguanine	1	1554.729	25277.78	up	1	2146.321	8091.626	up	0.002033
8-Hydroxyguanine	1	0.10706	0.042731	down	1	0.121629	0.731751	up	0.002844
5-Methylcytosine	1	2.945086	6.408358	up	1	9.156975	0.786644	up	0.003468
3'-O-Methylguanosine	1	44.06217	17.30408	down	1	0.900212	1.214881	down	0.006619
3-Methylxanthine	1	0.25198	0.511269	up	1	5.691069	15.18474	up	0.006005
3-Methylthymine	1	0.013313	0.019806	up	1	0.010739	0.052247	up	0.245542
3-Methylcytosine	1	491678.7	149428.8	up	1	652.269	1197.571	up	0.018722
3-methyl guanine	1	608.754	365505.6	up	1	522.408	6618.538	up	0.002785

cell survival and proliferation (29). We showed ECM detachment increase in glycolysis in detached cells. AMPKα1, keeps the high level of reduced glutathione to maintain reduction–oxidation reaction (redox) homeostasis, AMPKα1 regulate the glutathione reductase (GSR) phosphorylation possibly through residue Thr507 which enhances its activity of enzyme (30). Our studies have shown that glutamine levels in ECM detached cells increased and supports metabolic switch reductive carboxylation for energy requirements. Reductive carboxylation is known for mitochondrial disfunction and supports cell proliferation. Our results demonstrated an Compound C was able to reduce glutamine, and other intermediate metabolites. ECM detached activates reductive carboxylation and oxidation glutamine with glycolysis, enabling biomass generation and ATP production; and maintained redox homeostasis, AMPK inhibition reduces glutamine and reduces biomass production and energy deprivation.

ECM detached cancer cells that allow glycolytic intermediate to accumulate and switch to alternate pathway HMP or PPP, which can stimulate macromolecular synthesis and combat oxidative stress (31, 32), our studies showed the ECM detachment activates PPP, intermediate metabolite accumulation was increased on ECM detached cells. The PPP is composed of two functionally interrelated branches: the oxidative and the non-oxidative metabolism. In the oxidative arm of the HMP, three major irreversible reactions involved in the reduction of glucose-6-phosphate to ribose-5-phosphate with reduction of nicotinamide adenine dinucleotide phosphate (NADPH) and ribulose-5-phosphate (Ru5P), In the synthesis of nucleotide (33–35). The non-oxidative branch of the HMP generates nucleotide synthesis from glyceraldehyde-3-phosphate and fructose-6-phosphate. Our studies show the glyceraldehyde-3-phosphate increase in 22RV1 and decrease in HCT116, in both cell lines, AMPK inhibition shows an increase in ribose sugar and erythrose involve in the salvage pathway. In this scenario, we observed that the22RV1 might involve non-oxidative and HCT116 oxidative PPP pathways during AMPK inhibition.

Several pathways are intermediate and generate one-carbon metabolism is include serine and glycine metabolism. Cancer cells show alter DNA, RNA, and histone methylation patterns. Epigenetic modification in DNA, RNA, and histone regulates various gene regulation and function. Post-translational modification (PTM) in protein methylation alter protein-protein interaction (36). Our observation showed, ECM

detachment responsible for the activation of epigenetic modulator metabolite involved in one-carbon metabolism. S-adenosylmethionine (SAM) is a methyl donor; SAM transfer the methyl group to DNA and RNA, it converted to S-adenosylhomocysteine, which is converted to homocysteine and recycled to methionine. Importantly, SAM and homocysteine levels increased in ECM detached cancer cells. This observation is showing that methylation might be high in ECM detached cancer cells. The recent studies revealed that cysteine regulates the mTOR1 activity, cysteine uptake inhibits the mTOR activation and halts protein synthesis, and mTOR is regulated by AMPK. Our studies have shown the cysteine level in ECM detached and AMPK inhibited ECM detached cancer cells are increased, it is showing Compound C induces the cysteine level in ECM detached cells.

DNA lesion and DNA damage is ingested by effect of ROS production by cellular level, 8-oxoguanine is from oxidative DNA damage, effect of oxidative DNA damage results in pathophysiological changes (37). 6-methyl guanine is example for in what way DNA lesion leads to development of DNA damage. DNA damage may responsible apoptotic effect and mutagenesis properties, insertion of mutated 6-methyl guanine pass through cell cycle and causes the secondary DNA lesions and infer in DNA replication. 6-methyl guanine break the double standard DNA and triggered apoptosis (37). The data reported here reveal ECM detachment enhanced the expression of antioxidant enzyme GSH and SOD levels and inhibition of AMPK reduce antioxidant enzyme. Reduction in antioxidant enzyme activity may be increase in ROS levels and causes the DNA damage.

The significant consequence of data presented here represent advance in our understanding of ECM detached cancer cells switch the metabolic pathways., promotes cancer cell survival during metastasis. Compound C reduces pyruvate to lactate conversion, promotes OXPHOS, reduces glutamines and reduced GSH levels, and increases metabolite levels associated with DNA damage suggesting a broad metabolic impact. Beside Compound C, some other AMPK inhibitors are available like Doxorubicin, GSK6906893 and metformin. Our data also provides a detailed metabolic map of ECM detached cells, can be used to extrapolate and design future studies to identify novel targets to eradicate ECM detached cancer cells.

DATA AVAILABILITY STATEMENT

The original contributions presented in the study are included in the article/**Supplementary Material**. Further inquiries can be directed to the corresponding author.

AUTHOR CONTRIBUTIONS

MRSM and RA performed the experiment and wrote the first draft of the manuscript. AA performed a flow cytometry experiment. RA and MZ guidance and proofreading of the manuscript. MRSM and HC supervised and reviewed the manuscript. MK proposed, designed, and supervised the entire study and also wrote and proofread the manuscript. All authors contributed to the article and approved the submitted version.

FUNDING

This project was funded by the Deanship of Scientific Research (DSR) at King Abdulaziz University (KAU), Jeddah, under grant no. (KEP-15-130-41). The authors, therefore, acknowledge with thanks DSR technical and financial support.

ACKNOWLEDGMENTS

The authors thank the Core Metabolomics Facility at the Department of Biochemistry, KAU for providing help for metabolomics study.

SUPPLEMENTARY MATERIAL

The Supplementary Material for this article can be found online at: https://www.frontiersin.org/articles/10.3389/fonc.2021.612778/full#supplementary-material

Supplementary Table 1 | raw metabolite list from XCMS.

Supplementary Table 2 | Primer list.

REFERENCES

1. Mehlen P, Puisieux A. Metastasis: a question of life or death. *Nat Rev Cancer* (2006) 6(6):449–58. doi: 10.1038/nrc1886
2. Giancotti FG, Ruoslahti E. Integrin signaling. *Science* (1999) 285(5430):1028–33. doi: 10.1126/science.285.5430.1028
3. Frisch SM, Francis H. Disruption of epithelial cell-matrix interactions induces apoptosis. *J Cell Biol* (1994) 124(4):619–26. doi: 10.1083/jcb.124.4.619
4. Vivanco I, Sawyers CL. The phosphatidylinositol 3-Kinase AKT pathway in human cancer. *Nat Rev Cancer* (2002) 2(7):489–501. doi: 10.1038/nrc839
5. Miranda-Saavedra D, Gabaldón T, Barton GJ, Langsley G, Doerig C. The kinomes of apicomplexan parasites. *Microbes Infect* (2012) 14(10):796–810. doi: 10.1016/j.micinf.2012.04.007
6. Miranda-Saavedra D, Stark MJ, Packer JC, Vivares CP, Doerig C, Barton GJ. The complement of protein kinases of the microsporidium Encephalitozoon cuniculi in relation to those of Saccharomyces cerevisiae and Schizosaccharomyces pombe. *BMC Genomics* (2007) 8:309. doi: 10.1186/1471-2164-8-309
7. Lin SC, Hardie DG. AMPK: Sensing Glucose as well as Cellular Energy Status. *Cell Metab* (2018) 27(2):299–313. doi: 10.1016/j.cmet.2017.10.009
8. Viollet B, Horman S, Leclerc J, Lantier L, Foretz M, Billaud M, et al. AMPK inhibition in health and disease. *Crit Rev Biochem Mol Biol* (2010) 45(4):276–95. doi: 10.3109/10409238.2010.488215
9. Jeon SM, Hay N. The double-edged sword of AMPK signaling in cancer and its therapeutic implications. *Arch Pharm Res* (2015) 38(3):346–57. doi: 10.1007/s12272-015-0549-z

10. Zadra G, Batista JL, Loda M. Dissecting the Dual Role of AMPK in Cancer: From Experimental to Human Studies. *Mol Cancer Res* (2015) 13(7):1059–72. doi: 10.1158/1541-7786.MCR-15-0068
11. Jeon SM, Chandel NS, Hay N. AMPK regulates NADPH homeostasis to promote tumour cell survival during energy stress. *Nature* (2012) 485 (7400):661–5. doi: 10.1038/nature11066
12. Park HU, Suy S, Danner M, Dailey V, Zhang Y, Li H, et al. AMP-activated protein kinase promotes human prostate cancer cell growth and survival. *Mol Cancer Ther* (2009) 8(4):733–41. doi: 10.1158/1535-7163.MCT-08-0631
13. Xu ZX, Liang J, Haridas V, Gaikwad A, Connolly FP, Mills GB, et al. A plant triterpenoid, avicin D, induces autophagy by activation of AMP-activated protein kinase. *Cell Death Differ* (2007) 14(11):1948–57. doi: 10.1038/sj.cdd.4402207
14. Labuschagne CF, Cheung EC, Blagih J, Domart MC, Vousden KH. Cell Clustering Promotes a Metabolic Switch that Supports Metastatic Colonization. *Cell Metab* (2019) 30(4):720–34.e5. doi: 10.1016/j.cmet.2019.07.014
15. AlGhamdi AA, Mohammed MRS, Zamzami MA, Al-Malki AL, Qari MH, Khan MI, et al. Untargeted Metabolomics Identifies Key Metabolic Pathways Altered by Thymoquinone in Leukemic Cancer Cells. *Nutrients* (2020) 12 (6):1792. doi: 10.3390/nu12061792
16. Hassan MA, Al-Sakkaf K, Shait Mohammed MR, Dallol A, Al-Maghrabi J, Aldahlawi A, et al. Integration of Transcriptome and Metabolome Provides Unique Insights to Pathways Associated With Obese Breast Cancer Patients. *Front Oncol* (2020) 10:804. doi: 10.3389/fonc.2020.00804
17. Gaboon NEA, Banaganapalli B, Nasser K, Razeeth M, Alsaedi MS, Rashidi OM, et al. Exome sequencing and metabolomic analysis of a chronic kidney disease and hearing loss patient family revealed RMND1 mutation induced sphingolipid metabolism defects. *Saudi J Biol Sci* (2020) 27(1):324–34. doi: 10.1016/j.sjbs.2019.10.001
18. Hardie DG. Molecular Pathways: Is AMPK a Friend or a Foe in Cancer? *Clin Cancer Res* (2015) 21(17):3836–40. doi: 10.1158/1078-0432.CCR-14-3300
19. Shait Mohammed MR, Krishnan S, Amrathlal RS, Jayapal JM, Namperumalsamy VP, Prajna L, et al. Local Activation of the Alternative Pathway of Complement System in Mycotic Keratitis Patient Tear. *Front Cell Infect Microbiol* (2020) 10:205. doi: 10.3389/fcimb.2020.00205
20. Intlekofer AM, Dematteo RG, Venneti S, Finley LW, Lu C, Judkins AR, et al. Hypoxia Induces Production of L-2-Hydroxyglutarate. *Cell Metab* (2015) 22 (2):304–11. doi: 10.1016/j.cmet.2015.06.023
21. Jiang L, Shestov A, Swain P, Yang C, Parker SJ, Wang QA, et al. Reductive carboxylation supports redox homeostasis during anchorage-independent growth. *Nature* (2016) 532:255–8. doi: 10.1038/nature17393
22. Riganti C, Gazzano E, Polimeni M, Aldieri E, Ghigo D. The pentose phosphate pathway: an antioxidant defense and a crossroad in tumor cell fate. *Free Radic Biol Med* (2012) 53(3):421–36. doi: 10.1016/j.freeradbiomed.2012.05.006
23. Nathan C, Ding A. SnapShot: Reactive Oxygen Intermediates (ROI). *Cell* (2010) 140(6):951–951.e2. doi: 10.1016/j.cell.2010.03.008
24. Kalhan SC, Hanson RW. Resurgence of serine: an often neglected but indispensable amino Acid. *J Biol Chem* (2012) 287(24):19786–91. doi: 10.1074/jbc.R112.357194
25. Dizdaroglu M. Chemistry of free radical damage to DNA andnucleoproteins. *DNA and Free Radicals*. B Halliwell, OI Arouma, editors. Chichester: Ellis Horwood (1993) p. 19–39.
26. Sies H. Oxidative Stress and Antioxidants. *Exp Physiol*. H Sies, editor. London: Academic (1991) p. 99–116.
27. Grollman AP, Moriya M. Mutagenesis by 8-oxoguanine: an enemy within. *Trends Genet* (1993) 9:246–9. doi: 10.1016/0168-9525(93)90089-z
28. Davison CA, Durbin SM, Thau MR, Zellmer VR, Chapman SE, Diener J, et al. Antioxidant enzymes mediate survival of breast cancer cells deprived of extracellular matrix. *Cancer Res* (2013) 73(12):3704–15. doi: 10.1158/0008-5472.CAN-12-2482
29. Bissell MJ, Radisky D. Putting tumours in context. *Nat Rev Cancer* (2001) 1 (1):46–54. doi: 10.1038/35094059
30. Wang YN, Lu YX, Liu J, Jin Y, Bi HC, Zhao Q, et al. AMPKα1 confers survival advantage of colorectal cancer cells under metabolic stress by promoting redox balance through the regulation of glutathione reductase phosphorylation. *Oncogene* (2020) 39(3):637–50. doi: 10.1038/s41388-019-1004-2
31. Davison CA, Chapman SE, Sasser TA, Wathen C, Diener J, Schafer ZT, et al. Multimodal optical, X-ray CT, and SPECT imaging of a mouse model of breast cancer lung metastasis. *Curr Mol Med* (2013) 13(3):368–76. doi: 10.2174/1566524011313030006
32. Anastasiou D, Poulogiannis G, Asara JM, Boxer MB, Jiang JK, Shen M, et al. Inhibition of pyruvate kinase M2 by reactive oxygen species contributes to cellular antioxidant responses. *Science* (2011) 334(6060):1278–83. doi: 10.1126/science.1211485
33. Stincone A, Prigione A, Cramer T, Wamelink MM, Campbell K, Cheung E, et al. The return of metabolism: biochemistry and physiology of the pentose phosphate pathway. *Biol Rev Camb Philos Soc* (2015) 90(3):927–63. doi: 10.1111/brv.12140
34. Kowalik MA, Columbano A, Perra A. Emerging Role of the Pentose Phosphate Pathway in Hepatocellular Carcinoma. *Front Oncol* (2017) 7:87. doi: 10.3389/fonc.2017.00087
35. Alfarouk KO, Ahmed S, Elliott RL, Benoit A, Alqahtani SS, Ibrahim ME, et al. The Pentose Phosphate Pathway Dynamics in Cancer and Its Dependency on Intracellular pH. *Metabolites* (2020) 10(7):285. doi: 10.3390/metabo10070285
36. Kulis M, Esteller M. DNA methylation and cancer. *Adv Genet* (2010) 70:27–56. doi: 10.1016/B978-0-12-380866-0.60002-2
37. Quiros S, Roos WP, Kaina B. Processing of O6-methylguanine into DNA double-strand breaks requires two rounds of replication whereas apoptosis is also induced in subsequent cell cycles. *Cell Cycle* (2010) 9:168–78. doi: 10.4161/cc.9.1.10363

Conflict of Interest: The authors declare that the research was conducted in the absence of any commercial or financial relationships that could be construed as a potential conflict of interest.

frontiers in Oncology

MINI REVIEW
published: 08 March 2021
doi: 10.3389/fonc.2021.640720

UCP2 as a Potential Biomarker for Adjunctive Metabolic Therapies in Tumor Management

Frederic A. Vallejo[1,2], *Steven Vanni*[1] *and Regina M. Graham*[1,2,3]*

[1] Department of Neurosurgery, University of Miami Miller School of Medicine, Miami, FL, United States, [2] University of Miami Brain Tumor Initiative, Department of Neurosurgery, University of Miami Miller School of Medicine, Miami, FL, United States, [3] Sylvester Comprehensive Cancer Center, University of Miami Miller School of Medicine, Miami, FL, United States

Glioblastoma (GBM) remains one of the most lethal primary brain tumors in both adult and pediatric patients. Targeting tumor metabolism has emerged as a promising-targeted therapeutic strategy for GBM and characteristically resistant GBM stem-like cells (GSCs). Neoplastic cells, especially those with high proliferative potential such as GSCs, have been shown to upregulate UCP2 as a cytoprotective mechanism in response to chronic increased reactive oxygen species (ROS) exposure. This upregulation plays a central role in the induction of the highly glycolytic phenotype associated with many tumors. In addition to shifting metabolism away from oxidative phosphorylation, UCP2 has also been implicated in increased mitochondrial Ca^{2+} sequestration, apoptotic evasion, dampened immune response, and chemotherapeutic resistance. A query of the CGGA RNA-seq and the TCGA GBMLGG database demonstrated that UCP2 expression increases with increased WHO tumor-grade and is associated with much poorer prognosis across a cohort of brain tumors. UCP2 expression could potentially serve as a biomarker to stratify patients for adjunctive anti-tumor metabolic therapies, such as glycolytic inhibition alongside current standard of care, particularly in adult and pediatric gliomas. Additionally, because UCP2 correlates with tumor grade, monitoring serum protein levels in the future may allow clinicians a relatively minimally invasive marker to correlate with disease progression. Further investigation of UCP2's role in metabolic reprogramming is warranted to fully appreciate its clinical translatability and utility.

Keywords: uncoupling protein 2 (UCP2), cancer, glioma, biomarker, metabolism, Warburg effect, Glioblastoma, precision-medicine

OPEN ACCESS

Edited by:
Federica Sotgia,
University of Salford, United Kingdom

Reviewed by:
Khalid Omer Alfarouk,
Alfarouk Biomedical Research LLC, United States
Hsueh-Wei Chang,
Kaohsiung Medical University, Taiwan

***Correspondence:**
Regina M. Graham
RGraham@med.miami.edu

Specialty section:
This article was submitted to Cancer Metabolism, a section of the journal Frontiers in Oncology

Received: *11 December 2020*
Accepted: *01 February 2021*
Published: *08 March 2021*

Citation:
Vallejo FA, Vanni S and Graham RM (2021) UCP2 as a Potential Biomarker for Adjunctive Metabolic Therapies in Tumor Management. Front. Oncol. 11:640720. doi: 10.3389/fonc.2021.640720

INTRODUCTION

In recent years, oncologic treatment plans have continued to emphasize the importance of highly specific, personalized, and targeted therapeutic modalities to combat malignancies in the clinic. Whereas some cancers have seen drastic improvements in prognostic outcomes, certain primary brain tumors have proven to be particularly refractory to most drugs. Very little improvement has been made in the management of patients with gliomas and Glioblastomas, specifically, with 5-year survival in adults and children remaining dismally low (at 7.2% and 17.7%, respectively) (1–3).

With very few efficacious drugs available to these patients, there exists an obvious and desperate need for novel approaches and new potential interventions to improve patients' quality of life. Challenges that have historically hindered glioblastoma drug discovery and utility are impermeability of the blood brain barrier, drastic intra-tumoral heterogeneity, being extremely invasive in nature, and the presence of neurocritical structures commonly surrounding the tumor. Isolating and targeting populations of common progenitor cells, or glioma stem-like cells (GSCs), within the tumor has recently emerged as a potentially effective strategy to eliminate the cells responsible for much of the rapid proliferation commonly observed in these pathologies (4, 5).

Neoplastic cells exhibit a multitude of mitotic, biochemical, and cellular aberrancies. Many solid tumors have been shown to exhibit an increased dependency on glycolytic metabolism and may even forgo oxidative phosphorylation in the presence of oxygen. In fact, it is this often-overlooked increased glycolytic flux on the part of cancer cells that enables clinicians to effectively localize tumors and metastatic outgrowths *via* fluorodeoxyglucose positron emission tomography (PET scan) on a regular basis. This phenomenon, originally described by Otto Warburg nearly a century ago, has been highlighted as one of the central tenants of tumorigenesis and an "emerging hallmark of cancer" (6–8). While this switch in metabolism has been well documented in the literature for some time, the underlying mechanism by which malignant cells undergo this transition is still in question.

Existing hypotheses concerning the Warburg effect posit that forgoing oxidative phosphorylation and generating energy exclusively *via* glycolysis may be a more efficient way to generate metabolic intermediates, nucleotides for further proliferation, and drive angiogenesis to the hypoxic, acidic microenvironment. Another theory is that increased competition for shared metabolic resources in the tumor's vicinity cause the neoplastic cells to seek the path of less resistance and opt for the "evolutionarily less efficient pathway" to generate energy (9). Additionally, this shift in metabolism has been shown to increase cell proliferation as long as the supply of glucose is not limiting. Recent literature suggests that cells may be shutting off mitochondrial cellular respiration by increasing the expression of mitochondrial uncoupling protein 2 (UCP2), in an effort to mitigate the effect of cytotoxic reactive oxygen species (ROS), thereby inducing the Warburg effect *via* UCP2 upregulation (10, 11). In non-cancerous cells, UCP2 upregulation may facilitate, rather than inhibit, continued fatty acid metabolism by mitigating increased ROS generation and actually result in decreased glycolytic flux (12, 13). However, in neurons where basal ROS levels are consistently elevated, as is the case in many cancerous cells, UCP2 upregulation has shown to decrease the cell's ability to sense glucose appropriately and results in disruption of carbohydrate homeostasis (14, 15).

Rapidly dividing stem cells with high proliferative and anabolic capabilities have been shown to overexpress UCP2, whereas induction of neuronal differentiation causes a loss of UCP2 expression (16). Similarly, human pluripotent stem cells have been shown to overexpress UCP2 and metabolize primarily *via* glycolysis until differentiation, wherein they repress UCP2 expression and switch to primarily oxidative phosphorylation (17). These data suggest that UCP2 may be upregulated in situations where proliferative resources are limited, in situations where cells need to generate metabolites quickly to aid in division, and in states of developmental regression into a more anaplastic phenotype as seen in oncogenesis. The central role of UCP2 in driving the metabolic switch in aggressive neoplasms, and its potential therapeutic implications have yet to be thoroughly investigated. Here we sought to investigate the potential role UCP2 could serve as a biomarker to stratify glioma patients for adjunctive metabolic therapies as well as review the implications of prolonged ROS elevation leading to UCP2 overexpression in malignancy.

NORMAL FUNCTION OF UNCOUPLING PROTEIN 2

Three homologous mitochondrial uncoupling protein domains exist at locus 11q13.4. These three isoforms, UCP1, UCP2, and UCP3 all pertain to a family of mitochondrial anion carrier proteins. Although they are differentially expressed in different tissue types, they all function to diminish the proton gradient across the inner mitochondrial membrane in mammalian cells by releasing energy in the form of heat rather than by ATP anabolism. Whereas UCP1 is predominantly expressed in brown adipose tissue and facilitates thermogenesis, UCP2 and UCP3 expression is greatest in skeletal muscle and is thought to be more involved in protecting against the cytotoxic effects of ROS (18, 19). UCP2 is located on the inner mitochondrial membrane (IMM) and acts to uncouple the proton gradient across this membrane, of which the primary function is to drive ATP synthesis *via* ATP synthase. Under normal circumstances, protons accumulate in the inner membrane space and ATP synthase facilitates them to readily flow into the matrix, generating ATP in the process. When UCP2 is upregulated, the opposite occurs, in that the exit of anions and protons from the matrix is facilitated. Although the mechanism by which UCP2 facilitates this proton transport is not fully understood, by allowing protons to leak across the IMM, the driving force behind ATP production *via* the electron transport chain is decreased, resulting in heat-energy release.

As is seen in many cancers, this metabolic shift away from mitochondrial cellular respiration causes cells to increasingly depend on glycolysis to meet their metabolic demands. Additionally, recent studies have suggested that UCP2 may have a role in global homeostatic glucose regulation due to its expression in the arcuate nucleus and pro-opiomelanocortin neurons which project into the hypothalamus (14, 20, 21). Consistent with its potential homeostatic role in metabolic function, UCP2 over-expression has been linked to both α and ß-cell dysfunction and increased mRNA transcripts for UCP2 have been detected in the pancreatic islets of several animal models with type 2 diabetes (22–24). A common UCP2 promoter polymorphism -866G/A has been shown to increase transcriptional activity by allowing for easier

binding of the pancreatic transcription factor PAX6, increasing the risk of glucose dysregulation and type II diabetes in several human populations (25–29).

UNDERSTOOD ROLE OF UNCOUPLING PROTEIN 2 IN GLIOMAS AND OTHER MALIGNANCIES

Several cancers, including gliomas, have been observed to upregulate UCP2 expression when compared with their non-neoplastic cells of origin. Upregulation of this protein has been shown to directly increase AKT pathway signaling and enhance glycolysis by activating phosphofructokinase 2, a key regulatory protein in the glycolytic pathway (30). Recent studies suggest that UCP2 plays a critical role in protecting the cell from metabolically generated reactive oxygen species (ROS), which are known to become increasingly present as cells develop more malignant phenotypes. Neoplastic cells are therefore engaged in a cytotoxic positive feedback loop in which they increase carbohydrate metabolism, dramatically increasing intracellular ROS, leading to the upregulation of UCP2, which further dysregulates glycolytic function allowing cells to continue taking in glucose even in states of "satiety" (31, 32).

This phenomenon in which cells shunt metabolic away from oxidative phosphorylation to protect themselves from free radical damage induced by ROS illustrates one possible reason why cancers exhibit high glycolytic dependence even when oxygen is available. UCP2 has also been shown to facilitate mitochondrial Ca^{2+} sequestration from the endoplasmic reticulum specifically (33). While the link between high intracellular Ca^{2+} and apoptosis has long been understood, recent work posits that multiple potentially apoptogenic Ca^{2+} influx pathways exist, due to entering from the extracellular matrix or release from the endoplasmic reticulum (34–37). Therefore, the dramatic increase in UCP2 expression seen across multiple malignancies may also be, in part, due to aiding in sequestering rising intracellular Ca^{2+} in the mitochondria to protect the cell against apoptosis.

By facilitating apoptotic evasion, overexpression of UCP2 may similarly aide in chemotherapeutic resistance. Overexpression of UCP2 in multiple human cancer cell lines has consistently shown to favor a highly glycolytic phenotype, inhibits ROS accumulation, and prevents apoptosis after exposure to chemotherapeutic agents (38–40). Temozolomide is the chemotherapeutic drug of choice in glioma management and has been shown to trigger dramatic bursts of ROS leading to potential autophagy secondary to ERK activation (41). Previously, our lab has shown that GSCs are resistant to Temozolomide doses well above the peak therapeutic doses reportedly achieved in patient brain tissue and cerebrospinal fluid (42, 43). This resistance may be, in part, due to an increase of UCP2 to protect against ROS accumulation. Taken together, these findings suggest that the upregulation of UCP2 as a cytoprotective mechanism may be largely responsible for inducing this metabolic switch towards aerobic glycolysis, rather than being a consequence of an upstream metabolic alteration (**Figure 1A**).

UNCOUPLING PROTEIN 2 AS A POTENTIAL BIOMARKER IN GLIOMA

Rising levels of cytotoxic ROS have been shown to directly correlate both with increased glioma grade and with UCP2 expression. We sought to analyze if UCP2 expression alone would correlate with tumor grade. Genomic data on GBM patients from TCGA were analyzed using an open-access brain tumor database, GlioVis (gliovis. bioinfo.cnio.es) (44). Consistent with previous findings, UCP2 expression was shown to be significantly greater in GBM tissue than non-tumor tissue in an analysis of the TCGA GBM database containing 10 non-tumor samples and 528 Glioblastoma samples ($p<0.05$, **Figure 1B**). *UCP2 expression was shown to positively correlate with tumor grade* in both the CGGA RNA-seq database containing 625 low-grade glioma samples and 388 high-grade glioma samples and the TCGA GBMLGG database containing 515 low grade and 152 high-grade glioma samples ($p<0.05$, **Figure 1C**).

More notably, in an analysis of Kaplan-Meyer curves based on gene expression the TCGA GBMLGG shows that, across low- and high-grade gliomas, *higher UCP2 expression is associated with significantly shorter median survival when compared to low UCP2 expression* (High=26.4, Low=87.5 months, **Figure 1D**). Additionally, in a combined analysis of samples from oligodendrogliomas, oligoastrocytomas, astrocytomas, anaplastic oligodendrogliomas, anaplastic oligoastrocytomas, anaplastic astrocytomas, and GBMs the CGGA shows a significant and dramatically poorer median prognosis in tumors which have high UCP2 expression (High=19.5, Low=80.1 months, **Figure 1E**). In short, UCP2 expression increases with increased WHO tumor-grade and is associated with much poorer prognosis across a cohort of brain tumors.

Additionally, high UCP2 expression is known to favor a highly glycolytic metabolic profile, therefore suggesting that more aggressive gliomas may have an increased dependency on glycolysis and may be more susceptible to anti-glycolytic treatments. This finding has large implications for metabolic management of high-grade gliomas. Liquid biopsy has recently been proposed as a method of monitoring or diagnosing tumors *via* non-invasive, low-cost methodology by detecting circulating neoplastic cells, DNA, RNA, or proteins secreted by tumor cells (45). The feasibility of measuring UCP2 levels in patient serum has been previously demonstrated (46–48). Theoretically, patients may be able to establish baseline UCP2 measurements after surgical resection and monitor UCP2 trending upward, indicating disease progression, or trending downward, indicating efficacy of treatment due to either cell death or induction of differentiation. Similarly, following UCP2 levels may aide in the surveillance of low-grade gliomas progressing into more aggressive phenotypes. While UCP2 protein levels have been shown to decrease *via* western blot in response to cellular differentiation, the level of mRNA transcripts were shown to remain relatively stable (16). The consistent presence of mRNA is due to an upstream open reading frame in exon 2 of the UCP2 gene coding for ORF1 which has been shown to strongly inhibit the protein's expression (49). By regulating this factor, cells are

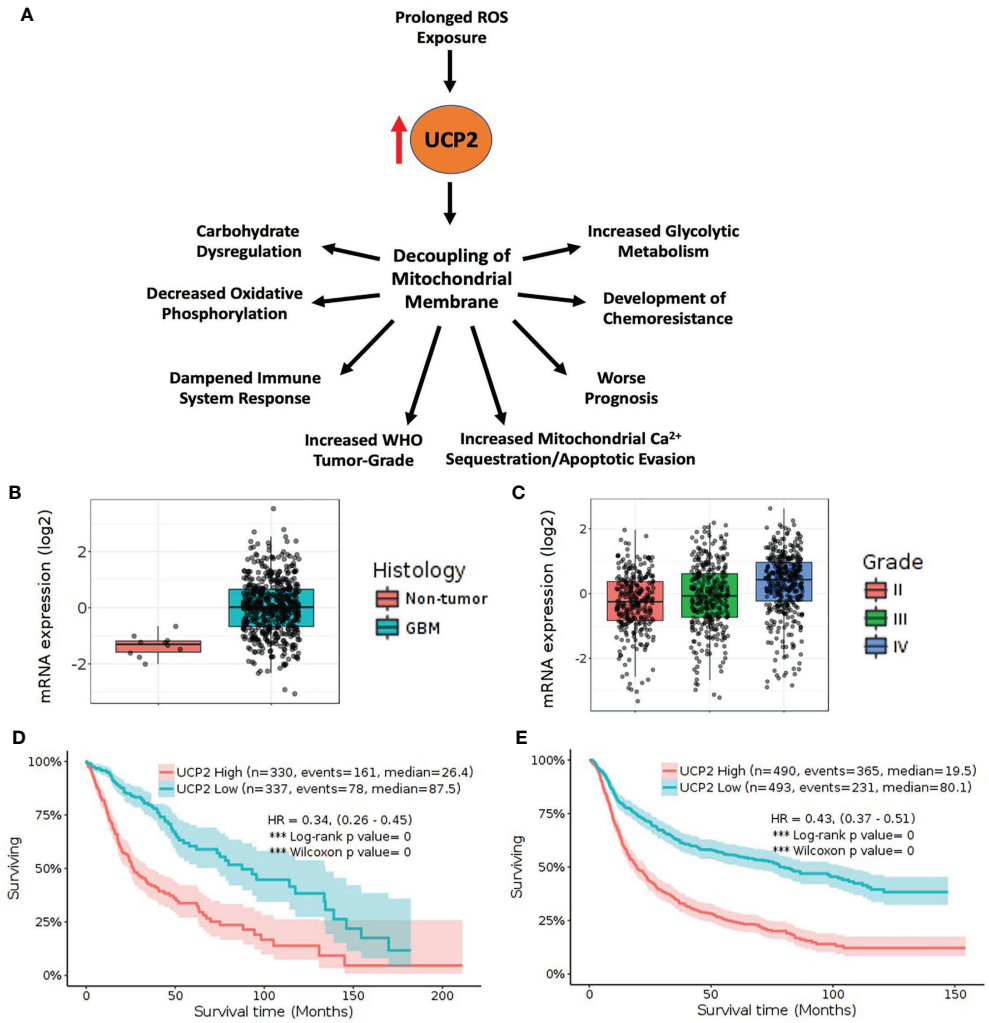

FIGURE 1 | High UCP2 expression is indicative of advanced tumor-grade and is associated with decreased survival. **(A)** UCP2 upregulation has many downstream consequences including worse prognosis. **(B)** TCGA_GBM database platform HG-U133A containing 10 non-tumor and 528 GBM tumor samples shows UCP2 is upregulated in tumor *vs.* non-tumor (p= 1.3E-05). **(C)** UCP2 expression correlates with tumor grade as seen in query of CGGA database including 625 low-grade and 388 high-grade gliomas (Grade II *vs.* Grade III p= 4.2E-02, Grade II *vs.* Grade IV. p= 2.4E-13, Grade III *vs.* Grade IV p= 6.3E-07). **(D)** Elevated UCP2 expression is indicative of worse prognosis in survival data from the TCGA GBMLGG dataset containing 515 low-grade and 152 high-grade tumors. **(E)** Elevated UCP2 expression is indicative of worse prognosis in survival data from the CGGA dataset. (Expression data were analyzed *via* pairwise group comparison using p-value with Bonferroni correction. Kaplan–Meyer data were analyzed *via* computation of Log-rank p-values).

able to quickly increase UCP2 expression in response to metabolic stress without having to generate entirely new transcripts (50, 51). Because of this, UCP2 should be investigated at the protein level should clinicians wish to follow it as a tumor marker in the future. Importantly, determining an individual's intratumoral UCP2 expression level can lead to targeted metabolic therapeutic interventions. Multi-modality treatment plans incorporating metabolic therapies such as glycolytic inhibition or exogenous ketone body supplementation may be more seriously considered in application to more advanced disease with more dramatic glycolytic demands.

THERAPEUTIC IMPLICATIONS OF UNCOUPLING PROTEIN 2 EXPRESSION LEVEL IN GLIOMAS

The role inflammation plays in glioma progression has yet to be fully understood. While the link between glucose and inflammation has been well documented in the scientific literature, the effect on the tumor's microenvironment of the metabolic shift accompanying UCP2 upregulation also warrants further investigation. Several studies have demonstrated that, in UCP2 knockout mice, macrophages mount a higher immune response to pathogens when compared with the UCP2 wild-type

macrophage response, potentially due to the increased peroxide and superoxide generation inside mitochondria (52–54).

This finding suggests that UCP2 upregulation may be due to not only increased need for ROS mitigation, but also as a way to dampen the immune response to the tumor, allowing evasion of immune-system recognition. This potential effect of UCP2 on the microenvironment is consistent with previous studies showing that gliomas and GBMs are "immuno-cold", and are oftentimes not engaged or targeted by patients' immune systems in immunotherapy clinical trials. Conversely, by inducting this metabolic shift which increases glucose availability in the tumor microenvironment, UCP2 may also have a relationship to pro-inflammatory cascades which favor tumorigenesis and progression. Inflammatory tumor associated macrophages (TAMs) in the microenvironment have been associated with more aggressive malignancies with decreased patient survival (55, 56).

Two strategies exist in the metabolic targeting of UCP2 over-expression (**Figure 2**). One strategy is to target tumors with high levels of expression, exhibiting uncoupled oxidative phosphorylation with extremely high levels of glycolytic metabolism, with glycolytic inhibitors or glucose starvation as is suggestive with ketogenic therapy (57). An *in vitro* study on five different GBM cell lines by our lab found that UCP2 was directly upregulated in response to exogenous acetoacetate supplementation, and concurrent glycolytic inhibition produced a dramatic synergistic loss of cell viability (58). Treating UCP2-overexpressing HCT116 cells with 2-deoxy-D-glucose was also shown to halt cell growth, further suggesting the efficacy of glycolytic inhibitor therapy where levels of UCP2 are increased (59). By increasing the glycolytic flux to the tumor, clinicians can aim to lower the supply of glucose available to the tumors while also utilizing anti-glycolytic drugs with minimal toxicity to peripheral tissues.

Another strategy is to inhibit UCP2 directly or preventing its transcription in an effort to slow rampant carbohydrate uptake and restore a more normal metabolic phenotype. In one study, lactate accumulation was diminished after siRNA knockout of UCP2, albeit not to a statistically significantly extent. However, the same study found that a 33% reduction of UCP2 expression resulted in a 22% protection from the proglycolytic-loss of mitochondrial membrane potential, suggesting that UCP2 knockout can restore normal metabolic phenotype *via* enabling oxidative phosphorylation (60). Also, although purine nucleotides are known to inhibit UCP2 expression under normal physiological conditions, the compound genipin successfully inhibited UCP2-mediated proton leak and reversed high-glucose induced ß cell dysfunction in both isolated kidney

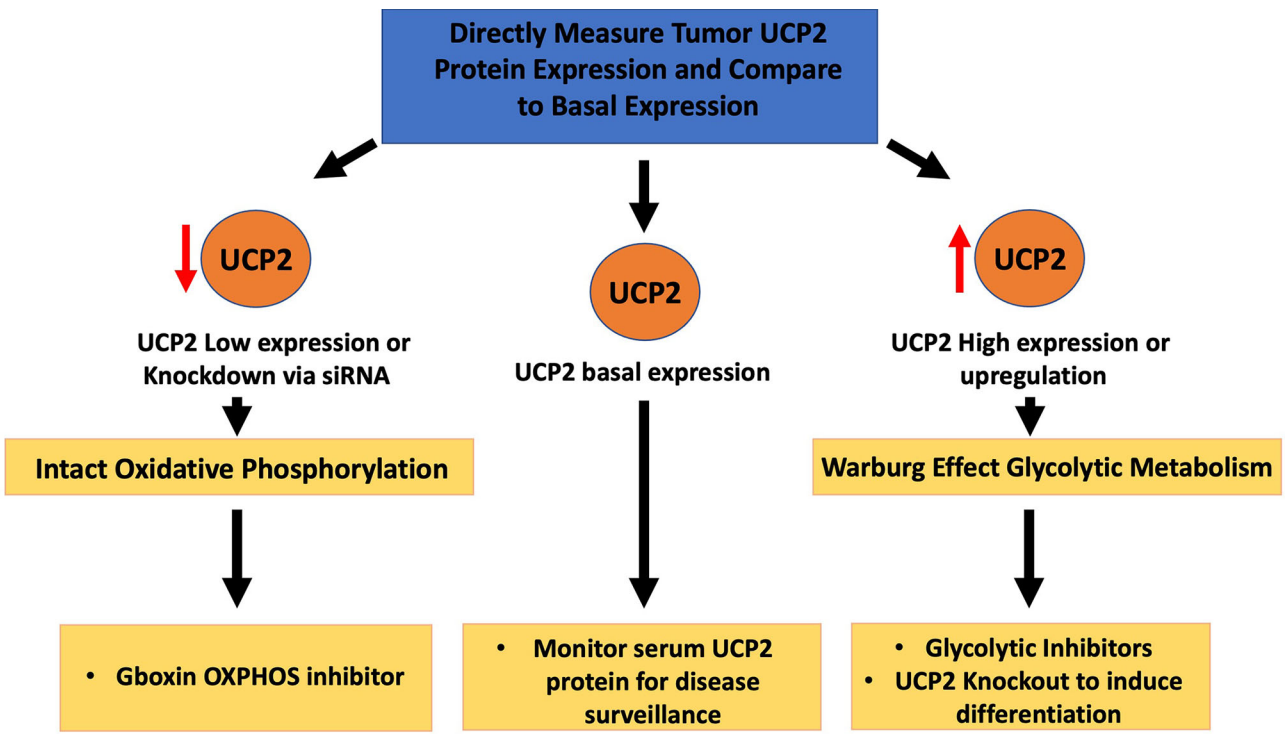

FIGURE 2 | Therapeutic implications of tumor UCP2 expression. UCP2 can be directly measured in tumor tissue and compared to baseline UCP2 expression levels. Tumors with high expression likely to exhibit carbohydrate dysregulation may benefit from adjunctive metabolic treatments such as glycolytic inhibition. Basal levels of UCP2 can be used to monitor tumor progression with potential serum measurements at follow-up. In tumors where UCP2 is inhibited or tumoral expression of UCP2 is very low, mitochondrial metabolism may remain intact suggesting an oxidative phosphorylation inhibitor may be warranted.

mitochondria and pancreatic islets (61, 62). Lending to the idea that UCP2 is expressed in highly proliferative, embryonic, stem-like states, UCP2 knockout was shown to suppress murine skin carcinogenesis of both benign papilloma and malignant squamous cell carcinoma (63). Recently, a series of in-vitro experiments demonstrated that UCP2 knockdown inhibited migration, invasiveness, clonogenicity, proliferation, and promoted *via* ROS-mediated cell apoptosis, in addition to reducing tumorgenicity in nude mice by inhibiting the p38 MAPK pathway (64). As previously described, stem cells with high proliferative potential have increased UCP2 expression which is only downregulated upon differentiation. Therefore, knocking out UCP2 may be a promising strategy to induce differentiation and halt cell-division or conversely facilitate apoptosis *via* ROS accumulation.

In regard to intratumoral heterogeneity, some subpopulations of glioblastoma cells may actually exhibit decreased glycolysis, underscoring the need for multi-modal treatment approaches and regular monitoring of the tumor's metabolic profile to adjust therapy accordingly. One proposed escape mechanism by which cancer cells may evade glycolytic therapy is *via* the p53-mediated induction of SCO2, pushing for oxidative phosphorylation, and TIGAR, which lowers the levels of glycolytic substrate fructose-2,6-bisphosphate (65–67). The mitochondrial permeability transition pore (mPTP) mitigates ROS accumulation *via* transient opening, stabilizing the mitochondrial membrane potential (68). Shi et al. recently demonstrated that glioblastoma and other cancers lack properly functioning mPTP, and that treating these cells with a metabolically stable analogue of Gboxin, an inhibitor of oxidative phosphorylation, inhibits glioblastoma allograft and patient-derived xenografts (69). Therefore, monitoring the expression of UCP2 can help clinicians understand the metabolic profile associated with each unique tumor and give insight as to whether certain metabolic therapies may be effective. Highly glycolytic tumors expressing high levels of UCP2 may benefit from glycolytic inhibition synergizing with glucose deprivation, whereas tumors with low UCP2 expression or with UCP2 knockout metabolizing primarily *via* oxidative phosphorylation may benefit from differentiation and OXPHOS inhibition with Gboxin-like compounds. Patients are in desperate need of novel approaches to combat these malignancies, glioblastoma in particular. UCP2's implications on tumor metabolism warrants more investigation. Just as PET scans are commonplace in oncologic medicine, further understanding of glioma metabolism may allow full clinical exploitation of these aberrant pathways by implementing targeted therapies into future multi-modal treatment plans.

CONCLUSION

Although it has been common scientific knowledge that cancers and gliomas specifically are highly glycolytic, the clinical utility of this tendency has yet to be fully exploited. As ROS increases and gliomas advance in grade, so too does UCP2 expression rise and the tumor become more dependent on glycolytic metabolism. Additionally, high UCP2 expression has shown to correlate with poorer survival outcomes. This finding suggests that more aggressive tumors with high levels of UCP2 expression, which are highly dependent on glycolysis, may benefit from multi-modal treatment approaches which aim to shut down glycolysis. Conversely, UCP2 knockout may aide in restoring normal metabolic phenotype and pushing stem-like cancer cells towards differentiation. UCP2 expression could potentially serve as a biomarker to stratify patients for adjunctive anti-tumor metabolic therapies, particularly in adult and pediatric gliomas.

FUTURE PERSPECTIVE

Clinicians in the future may be able to harness UCP2 expression profiles to better direct targeted treatments against aberrant tumor metabolism. Further investigation of UCP2's role in metabolic reprogramming, the ability to monitor it's expression as a serum tumor marker, and *in vivo* experiments exhibiting a survival benefit with appropriate stratification for additional therapies is warranted to fully appreciate it's clinical translatability and utility.

AUTHOR CONTRIBUTIONS

FV wrote the manuscript, developed the ideas, conducted the review of literature, and made the figures. SV reviewed the manuscript and helped with the editing process, and helped in guiding FV. RG wrote the manuscript, developed the ideas, and guided FV in creating the figures and focusing on the topic idea. All authors contributed to the article and approved the submitted version.

ACKNOWLEDGMENTS

We would like to thank the Mystic Force Foundation for their continued support of our research.

REFERENCES

1. Ostrom QT, Gittleman H, Liao P, Vecchione-Koval T, Wolinsky Y, Kruchko C, et al. CBTRUS Statistical Report: Primary brain and other central nervous system tumors diagnosed in the United States in 2010-2014. *Neuro Oncol* (2017) 19:v1–v88. doi: 10.1093/neuonc/nox158
2. Lukas RV, Wainwright DA, Ladomersky E, Sachdev S, Sonabend AM, Stupp R. Newly Diagnosed Glioblastoma: A Review on Clinical Management. *Oncology* (2019) 33:91–100.
3. Ostrom QT, Patil N, Cioffi G, Waite K, Kruchko C, Barnholtz-Sloan JS. CBTRUS Statistical Report: Primary Brain and Other Central Nervous System Tumors Diagnosed in the United States in 2013-2017. *Neuro Oncol* (2020) 22: iv1–iv96. doi: 10.1093/neuonc/noaa200
4. Garnier D, Renoult O, Alves-Guerra M-C, Paris F, Pecqueur C. Glioblastoma Stem-Like Cells, Metabolic Strategy to Kill a Challenging Target. *Front Oncol* (2019) 9:118. doi: 10.3389/fonc.2019.00118
5. Kalkan R. Glioblastoma Stem Cells as a New Therapeutic Target for Glioblastoma. *Clin Med Insights Oncol* (2015) 9:95–103. doi: 10.4137/CMO.S30271

6. Warburg O, Wind F, Negelein E. The Metabolism Of Tumors In The Body. *J Gen Physiol* (1927) 8:519–30. doi: 10.1085/jgp.8.6.519
7. Hanahan D, Weinberg RA. Hallmarks of cancer: the next generation. *Cell* (2011) 144:646–74. doi: 10.1016/j.cell.2011.02.013
8. Schwartz L, Supuran CT, Alfarouk KO. The Warburg Effect and the Hallmarks of Cancer. *Anticancer Agents Med Chem* (2017) 17:164–70. doi: 10.2174/1871520616666161031143301
9. Epstein T, Gatenby RA, Brown JS. The Warburg effect as an adaptation of cancer cells to rapid fluctuations in energy demand. *PloS One* (2017) 12: e0185085. doi: 10.1371/journal.pone.0185085
10. Baffy G. Uncoupling protein-2 and cancer. *Mitochondrion* (2010) 10:243–52. doi: 10.1016/j.mito.2009.12.143
11. Ji R, Chen W, Wang Y, Gong F, Huang S, Zhong M, et al. The Warburg Effect Promotes Mitochondrial Injury Regulated by Uncoupling Protein-2 in Septic Acute Kidney Injury. *Shock* (2020) 1–24. doi: 10.1097/SHK.0000000000001576
12. Pecqueur C, Bui T, Gelly C, Hauchard J, Barbot C, Bouillaud F, et al. Uncoupling protein-2 controls proliferation by promoting fatty acid oxidation and limiting glycolysis-derived pyruvate utilization. *FASEB J* (2008) 22:9–18. doi: 10.1096/fj.07-8945com
13. Kukat A, Dogan SA, Edgar D, Mourier A, Jacoby C, Maiti P, et al. Loss of UCP2 attenuates mitochondrial dysfunction without altering ROS production and uncoupling activity. *PloS Genet* (2014) 10:e1004385. doi: 10.1371/journal.pgen.1004385
14. Parton LE, Ye CP, Coppari R, Enriori PJ, Choi B, Zhang CY, et al. Glucose sensing by POMC neurons regulates glucose homeostasis and is impaired in obesity. *Nature* (2007) 449:228–32. doi: 10.1038/nature06098
15. Kong D, Vong L, Parton LE, Ye C, Tong Q, Hu X, et al. Glucose stimulation of hypothalamic MCH neurons involves K(ATP) channels, is modulated by UCP2, and regulates peripheral glucose homeostasis. *Cell Metab* (2010) 12:545–52. doi: 10.1016/j.cmet.2010.09.013
16. Rupprecht A, Sittner D, Smorodchenko A, Hilse KE, Goyn J, Moldzio R, et al. Uncoupling protein 2 and 4 expression pattern during stem cell differentiation provides new insight into their putative function. *PloS One* (2014) 9:e88474. doi: 10.1371/journal.pone.0088474
17. Zhang J, Khvorostov I, Hong JS, Oktay Y, Vergnes L, Nuebel E, et al. UCP2 regulates energy metabolism and differentiation potential of human pluripotent stem cells. *EMBO J* (2011) 30:4860–73. doi: 10.1038/emboj.2011.401
18. Echtay KS, Roussel D, St-Pierre J, Jekabsons MB, Cadenas S, Stuart JA, et al. Superoxide activates mitochondrial uncoupling proteins. *Nature* (2002) 415:96–9. doi: 10.1038/415096a
19. Hass DT, Barnstable CJ. Uncoupling proteins in the mitochondrial defense against oxidative stress. *Prog Retin Eye Res* (2021) 1–25. doi: 10.1016/j.preteyeres.2021.100941
20. Coppola A, Liu ZW, Andrews ZB, Paradis E, Roy MC, Friedman JM, et al. A central thermogenic-like mechanism in feeding regulation: an interplay between arcuate nucleus T3 and UCP2. *Cell Metab* (2007) 5:21–33. doi: 10.1016/j.cmet.2006.12.002
21. Haigh JL, New LE, Filippi BM. Mitochondrial Dynamics in the Brain Are Associated With Feeding, Glucose Homeostasis, and Whole-Body Metabolism. *Front Endocrinol (Lausanne)* (2020) 11:580879. doi: 10.3389/fendo.2020.580879
22. Zhang CY, Baffy G, Perret P, Krauss S, Peroni O, Grujic D, et al. Uncoupling protein-2 negatively regulates insulin secretion and is a major link between obesity, beta cell dysfunction, and type 2 diabetes. *Cell* (2001) 105:745–55. doi: 10.1016/S0092-8674(01)00378-6
23. Kassis N, Bernard C, Pusterla A, Casteilla L, Penicaud L, Richard D, et al. Correlation between pancreatic islet uncoupling protein-2 (UCP2) mRNA concentration and insulin status in rats. *Int J Exp Diabetes Res* (2000) 1:185–93. doi: 10.1155/EDR.2000.185
24. Allister EM, Robson-Doucette CA, Prentice KJ, Hardy AB, Sultan S, Gaisano HY, et al. UCP2 regulates the glucagon response to fasting and starvation. *Diabetes* (2013) 62:1623–33. doi: 10.2337/db12-0981
25. Krempler F, Esterbauer H, Weitgasser R, Ebenbichler C, Patsch JR, Miller K, et al. A functional polymorphism in the promoter of UCP2 enhances obesity risk but reduces type 2 diabetes risk in obese middle-aged humans. *Diabetes* (2002) 51:3331–5. doi: 10.2337/diabetes.51.11.3331
26. Sesti G, Cardellini M, Marini MA, Frontoni S, D'Adamo M, Del Guerra S, et al. A common polymorphism in the promoter of UCP2 contributes to the variation in insulin secretion in glucose-tolerant subjects. *Diabetes* (2003) 52:1280–3. doi: 10.2337/diabetes.52.5.1280
27. Sasahara M, Nishi M, Kawashima H, Ueda K, Sakagashira S, Furuta H, et al. Uncoupling protein 2 promoter polymorphism -866G/A affects its expression in beta-cells and modulates clinical profiles of Japanese type 2 diabetic patients. *Diabetes* (2004) 53:482–5. doi: 10.2337/diabetes.53.2.482
28. Andersen G, Dalgaard LT, Justesen JM, Anthonsen S, Nielsen T, Thorner LW, et al. The frequent UCP2 -866G>A polymorphism protects against insulin resistance and is associated with obesity: a study of obesity and related metabolic traits among 17 636 Danes. *Int J Obes (Lond)* (2013) 37:175–81. doi: 10.1038/ijo.2012.22
29. Gomathi P, Samarth AP, Raj N, Sasikumar S, Murugan PS, Nallaperumal S, et al. The -866G/A polymorphism in the promoter of the UCP2 gene is associated with risk for type 2 diabetes and with decreased insulin levels. *Gene* (2019) 701:125–30. doi: 10.1016/j.gene.2019.03.041
30. Sreedhar A, Petruska P, Miriyala S, Panchatcharam M, Zhao Y. UCP2 overexpression enhanced glycolysis via activation of PFKFB2 during skin cell transformation. *Oncotarget* (2017) 8:95504–15. doi: 10.18632/oncotarget.20762
31. Andrews ZB, Liu ZW, Walllingford N, Erion DM, Borok E, Friedman JM, et al. UCP2 mediates ghrelin's action on NPY/AgRP neurons by lowering free radicals. *Nature* (2008) 454:846–51. doi: 10.1038/nature07181
32. Robinson AJ, Hopkins GL, Rastogi N, Hodges M, Doyle M, Davies S, et al. Reactive Oxygen Species Drive Proliferation in Acute Myeloid Leukemia via the Glycolytic Regulator PFKFB3. *Cancer Res* (2020) 80:937–49. doi: 10.1158/0008-5472.CAN-19-1920
33. Waldeck-Weiermair M, Malli R, Naghdi S, Trenker M, Kahn MJ, Graier WF. The contribution of UCP2 and UCP3 to mitochondrial Ca(2+) uptake is differentially determined by the source of supplied Ca(2+). *Cell Calcium* (2010) 47:433–40. doi: 10.1016/j.ceca.2010.03.004
34. Giorgi C, Romagnoli A, Pinton P, Rizzuto R. Ca2+ signaling, mitochondria and cell death. *Curr Mol Med* (2008) 8:119–30. doi: 10.2174/156652408783769571
35. Pinton P, Giorgi C, Siviero R, Zecchini E, Rizzuto R. Calcium and apoptosis: ER-mitochondria Ca2+ transfer in the control of apoptosis. *Oncogene* (2008) 27:6407–18. doi: 10.1038/onc.2008.308
36. Koshenov Z, Oflaz FE, Hirtl M, Bachkoenig OA, Rost R, Osibow K, et al. The contribution of uncoupling protein 2 to mitochondrial Ca(2+) homeostasis in health and disease - A short revisit. *Mitochondrion* (2020) 55:164–73. doi: 10.1016/j.mito.2020.10.003
37. Motloch LJ, Larbig R, Gebing T, Reda S, Schwaiger A, Leitner J, et al. By Regulating Mitochondrial Ca2+-Uptake UCP2 Modulates Intracellular Ca2+. *PloS One* (2016) 11:e0148359. doi: 10.1371/journal.pone.0148359
38. Dalla Pozza E, Fiorini C, Dando I, Menegazzi M, Sgarbossa A, Costanzo C, et al. Role of mitochondrial uncoupling protein 2 in cancer cell resistance to gemcitabine. *Biochim Biophys Acta* (2012) 1823:1856–63. doi: 10.1016/j.bbamcr.2012.06.007
39. Yu G, Liu J, Xu K, Dong J. Uncoupling protein 2 mediates resistance to gemcitabine-induced apoptosis in hepatocellular carcinoma cell lines. *Biosci Rep* (2015) 35:1–7. doi: 10.1042/BSR20150116
40. Yu J, Shi L, Lin W, Lu B, Zhao Y. UCP2 promotes proliferation and chemoresistance through regulating the NF-kappaB/beta-catenin axis and mitochondrial ROS in gallbladder cancer. *Biochem Pharmacol* (2020) 172:113745. doi: 10.1016/j.bcp.2019.113745
41. Lin CJ, Lee CC, Shih YL, Lin TY, Wang SH, Lin YF, et al. Resveratrol enhances the therapeutic effect of temozolomide against malignant glioma in vitro and in vivo by inhibiting autophagy. *Free Radic Biol Med* (2012) 52:377–91. doi: 10.1016/j.freeradbiomed.2011.10.487
42. Gersey ZC, Rodriguez GA, Barbarite E, Sanchez A, Walters WM, Ohaeto KC, et al. Curcumin decreases malignant characteristics of glioblastoma stem cells via induction of reactive oxygen species. *BMC Cancer* (2017) 17:99. doi: 10.1186/s12885-017-3058-2
43. Portnow J, Badie B, Chen M, Liu A, Blanchard S, Synold TW. The neuropharmacokinetics of temozolomide in patients with resectable brain tumors: potential implications for the current approach to chemoradiation. *Clin Cancer Res* (2009) 15:7092–8. doi: 10.1158/1078-0432.CCR-09-1349
44. Bowman RL, Wang Q, Carro A, Verhaak RG, Squatrito M. GlioVis data portal for visualization and analysis of brain tumor expression datasets. *Neuro Oncol* (2017) 19:139–41. doi: 10.1093/neuonc/now247

45. Karachaliou N, Mayo-de-Las-Casas C, Molina-Vila MA, Rosell R. Real-time liquid biopsies become a reality in cancer treatment. *Ann Transl Med* (2015) 3:36. doi: 10.3978/j.issn.2305-5839.2015.01.16
46. Pan HC, Lee CC, Chou KM, Lu SC, Sun CY. Serum levels of uncoupling proteins in patients with differential insulin resistance: A community-based cohort study. *Med (Baltimore)* (2017) 96:e8053. doi: 10.1097/MD.0000000000008053
47. Kakarla M, Puppala VK, Tyagi S, Anger A, Repp K, Wang J, et al. Circulating levels of mitochondrial uncoupling protein 2, but not prohibitin, are lower in humans with type 2 diabetes and correlate with brachial artery flow-mediated dilation. *Cardiovasc Diabetol* (2019) 18:148. doi: 10.1186/s12933-019-0956-4
48. Huang W, Wang X, Zhang H, Wang C, Liu D. The Value of Serum Uncoupling Protein-2 Level for the Patients With Sepsis. *Shock* (2020) 54:301–7. doi: 10.1097/SHK.0000000000001523
49. Pecqueur C, Alves-Guerra MC, Gelly C, Levi-Meyrueis C, Couplan E, Collins S, et al. Uncoupling protein 2, in vivo distribution, induction upon oxidative stress, and evidence for translational regulation. *J Biol Chem* (2001) 276:8705–12. doi: 10.1074/jbc.M006938200
50. Rupprecht A, Moldzio R, Modl B, Pohl EE. Glutamine regulates mitochondrial uncoupling protein 2 to promote glutaminolysis in neuroblastoma cells. *Biochim Biophys Acta Bioenerg* (2019) 1860:391–401. doi: 10.1016/j.bbabio.2019.03.006
51. Yu G, Wang J, Xu K, Dong J. Dynamic regulation of uncoupling protein 2 expression by microRNA-214 in hepatocellular carcinoma. *Biosci Rep* (2016) 36:1–6. doi: 10.1042/BSR20160062
52. Arsenijevic D, Onuma H, Pecqueur C, Raimbault S, Manning BS, Miroux B, et al. Disruption of the uncoupling protein-2 gene in mice reveals a role in immunity and reactive oxygen species production. *Nat Genet* (2000) 26:435–9. doi: 10.1038/82565
53. Carrion J, Abengozar MA, Fernandez-Reyes M, Sanchez-Martin C, Rial E, Dominguez-Bernal G, et al. UCP2 deficiency helps to restrict the pathogenesis of experimental cutaneous and visceral leishmaniosis in mice. *PloS Negl Trop Dis* (2013) 7:e2077. doi: 10.1371/journal.pntd.0002077
54. Bai Y, Onuma H, Bai X, Medvedev AV, Misukonis M, Weinberg JB, et al. Persistent nuclear factor-kappa B activation in Ucp2-/- mice leads to enhanced nitric oxide and inflammatory cytokine production. *J Biol Chem* (2005) 280:19062–9. doi: 10.1074/jbc.M500566200
55. Lin JY, Li XY, Tadashi N, Dong P. Clinical significance of tumor-associated macrophage infiltration in supraglottic laryngeal carcinoma. *Chin J Cancer* (2011) 30:280–6. doi: 10.5732/cjc.010.10336
56. Yagi T, Baba Y, Okadome K, Kiyozumi Y, Hiyoshi Y, Ishimoto T, et al. Tumour-associated macrophages are associated with poor prognosis and programmed death ligand 1 expression in oesophageal cancer. *Eur J Cancer* (2019) 111:38–49. doi: 10.1016/j.ejca.2019.01.018
57. Schwartz L, Seyfried T, Alfarouk KO, Da Veiga Moreira J, Fais S. Out of Warburg effect: An effective cancer treatment targeting the tumor specific metabolism and dysregulated pH. *Semin Cancer Biol* (2017) 43:134–8. doi: 10.1016/j.semcancer.2017.01.005
58. Vallejo FA, Shah SS, de Cordoba N, Walters WM, Prince J, Khatib Z, et al. The contribution of ketone bodies to glycolytic inhibition for the treatment of adult and pediatric glioblastoma. *J Neurooncol* (2020) 147:317–26. doi: 10.1007/s11060-020-03431-w
59. Derdak Z, Mark NM, Beldi G, Robson SC, Wands JR, Baffy G. The mitochondrial uncoupling protein-2 promotes chemoresistance in cancer cells. *Cancer Res* (2008) 68:2813–9. doi: 10.1158/0008-5472.CAN-08-0053
60. Samudio I, Fiegl M, McQueen T, Clise-Dwyer K, Andreeff M. The warburg effect in leukemia-stroma cocultures is mediated by mitochondrial uncoupling associated with uncoupling protein 2 activation. *Cancer Res* (2008) 68:5198–205. doi: 10.1158/0008-5472.CAN-08-0555
61. Zackova M, Skobisova E, Urbankova E, Jezek P. Activating omega-6 polyunsaturated fatty acids and inhibitory purine nucleotides are high affinity ligands for novel mitochondrial uncoupling proteins UCP2 and UCP3. *J Biol Chem* (2003) 278:20761–9. doi: 10.1074/jbc.M212850200
62. Qiu W, Zhou Y, Jiang L, Fang L, Chen L, Su W, et al. Genipin inhibits mitochondrial uncoupling protein 2 expression and ameliorates podocyte injury in diabetic mice. *PloS One* (2012) 7:e41391. doi: 10.1371/journal.pone.0041391
63. Li W, Zhang C, Jackson K, Shen X, Jin R, Li G, et al. UCP2 knockout suppresses mouse skin carcinogenesis. *Cancer Prev Res (Phila)* (2015) 8:487–91. doi: 10.1158/1940-6207.CAPR-14-0297-T
64. Wu S, Luo C, Hameed NUF, Wang Y, Zhuang D. UCP2 silencing in glioblastoma reduces cell proliferation and invasiveness by inhibiting p38 MAPK pathway. *Exp Cell Res* (2020) 394:112110. doi: 10.1016/j.yexcr.2020.112110
65. Matoba S, Kang JG, Patino WD, Wragg A, Boehm M, Gavrilova O, et al. p53 regulates mitochondrial respiration. *Science* (2006) 312:1650–3. doi: 10.1126/science.1126863
66. Bensaad K, Tsuruta A, Selak MA, Vidal MN, Nakano K, Bartrons R, et al. TIGAR, a p53-inducible regulator of glycolysis and apoptosis. *Cell* (2006) 126:107–20. doi: 10.1016/j.cell.2006.05.036
67. Han CY, Patten DA, Richardson RB, Harper ME, Tsang BK. Tumor metabolism regulating chemosensitivity in ovarian cancer. *Genes Cancer* (2018) 9:155–75. doi: 10.18632/genesandcancer.176
68. Zorov DB, Juhaszova M, Sollott SJ. Mitochondrial Reactive Oxygen Species (ROS) and ROS-Induced ROS Release. *Physiol Rev* (2014) 94:909–50. doi: 10.1152/physrev.00026.2013
69. Shi Y, Lim SK, Liang Q, Iyer SV, Wang H-Y, Wang Z, et al. Gboxin is an oxidative phosphorylation inhibitor that targets glioblastoma. *Nature* (2019) 567:341–6. doi: 10.1038/s41586-019-0993-x

Conflict of Interest: The authors declare that the research was conducted in the absence of any commercial or financial relationships that could be construed as a potential conflict of interest.

frontiers in Oncology

ORIGINAL RESEARCH
published: 12 April 2021
doi: 10.3389/fonc.2021.643465

Identification of the Roles of a Stemness Index Based on mRNA Expression in the Prognosis and Metabolic Reprograming of Pancreatic Ductal Adenocarcinoma

Rong Tang[1,2,3,4†], *Xiaomeng Liu*[1,2,3,4†], *Wei Wang*[1,2,3,4†], *Jie Hua*[1,2,3,4], *Jin Xu*[1,2,3,4], *Chen Liang*[1,2,3,4], *Qingcai Meng*[1,2,3,4], *Jiang Liu*[1,2,3,4], *Bo Zhang*[1,2,3,4], *Xianjun Yu*[1,2,3,4*] *and Si Shi*[1,2,3,4*]

[1] Department of Pancreatic Surgery, Fudan University Shanghai Cancer Center, Shanghai, China, [2] Department of Oncology, Shanghai Medical College, Fudan University, Shanghai, China, [3] Shanghai Pancreatic Cancer Institute, Shanghai, China, [4] Pancreatic Cancer Institute, Fudan University, Shanghai, China

OPEN ACCESS

Edited by:
Federica Sotgia,
University of Salford, United Kingdom

Reviewed by:
Olivier Peulen,
University of Liège, Belgium
Erina Vlashi,
University of California, Los Angeles, United States
Y.H. Taguchi,
Chuo University, Japan

***Correspondence:**
Si Shi
shisi@fudanpci.org
Xianjun Yu
yuxianjun@fudanpci.org

†These authors have contributed equally to this work

Specialty section:
This article was submitted to Cancer Metabolism, a section of the journal Frontiers in Oncology

Received: 18 December 2020
Accepted: 16 March 2021
Published: 12 April 2021

Citation:
Tang R, Liu X, Wang W, Hua J, Xu J, Liang C, Meng Q, Liu J, Zhang B, Yu X and Shi S (2021) Identification of the Roles of a Stemness Index Based on mRNA Expression in the Prognosis and Metabolic Reprograming of Pancreatic Ductal Adenocarcinoma. Front. Oncol. 11:643465. doi: 10.3389/fonc.2021.643465

Background: Cancer stem cells (CSCs) are widely thought to contribute to the dismal prognosis of pancreatic ductal adenocarcinoma (PDAC). CSCs share biological features with adult stem cells, such as longevity, self-renewal capacity, differentiation, drug resistance, and the requirement for a niche; these features play a decisive role in cancer progression. A prominent characteristic of PDAC is metabolic reprogramming, which provides sufficient nutrients to support rapid tumor cell growth. However, whether PDAC stemness is correlated with metabolic reprogramming remains unknown.

Method: RNA sequencing data of PDAC, including read counts and fragments per kilobase of transcript per million mapped reads (FPKM), were collected from The Cancer Genome Atlas-Pancreatic Adenocarcinoma (TCGA-PAAD) database. Single-sample gene set enrichment analysis (GSEA) was used to calculate the relative activities of metabolic pathways in each PDAC sample. Quantitative real-time PCR was performed to validate the expression levels of genes of interest.

Results: The overall survival (OS) of patients with high mRNA expression-based stemness index (mRNAsi) values was significantly worse than that of their counterparts with low mRNAsi values (P = 0.003). This survival disadvantage was independent of baseline clinical characteristics. Gene ontology (GO) analysis, Kyoto Encyclopedia of Genes and Genomes (KEGG) analysis and GSEA showed that the differentially expressed genes between patients with high and low mRNAsi values were mainly enriched in oncogenic and metabolic pathways. Weighted gene coexpression network analysis (WGCNA) revealed 8 independent gene modules that were significantly associated with mRNAsi and 12 metabolic pathways. Unsupervised clustering based on the key genes in each module identified two PDAC subgroups characterized by different mRNAsi values and metabolic activities. Univariate Cox regression analysis identified 14 genes beneficial

to OS from 95 key genes selected from the eight independent gene modules from WGCNA. Among them, MAGEH1, MAP3K3, and PODN were downregulated in both pancreatic tissues and cell lines.

Conclusion: The present study showed that PDAC samples with high mRNAsi values exhibited aberrant activation of multiple metabolic pathways, and the patients from whom these samples were obtained had a poor prognosis. Future studies are expected to investigate the underlying mechanism based on the crosstalk between PDAC stemness and metabolic rewiring.

Keywords: pancreatic cancer, stemness, metabolic rewiring, metabolism, transcriptome

INTRODUCTION

Pancreatic ductal adenocarcinoma (PDAC) is one of the most lethal malignancies, with mortality rates almost equal to its incidence (1). In recent decades, the incidence of pancreatic cancer has increased annually, imposing heavy health and economic burdens on many countries (2). Radical surgical resection remains the most efficient treatment method for PDAC (3). Due to the limited understanding of the evolution of its genetic characteristics and the concealed anatomical position of the pancreas, it is difficult to detect PDAC early, which would prevent metastasis and avoid the need for radical treatment (4–6). Many researchers believe that cancer stem cells (CSCs) may contribute to the dismal prognosis of PDAC (7). CSCs share biological features with adult stem cells, such as longevity, capacity for self-renewal, differentiation, drug resistance and the requirement for a niche, features that play a decisive role in cancer progression (8). Malta et al. identified stemness features associated with oncogenic dedifferentiation in a pan-cancer profile using a machine learning algorithm (9). They introduced stem cell indices to evaluate the stemness of each tumor sample in The Cancer Genome Atlas (TCGA) database and found that such indices could accurately predict metastatic events and interpret intratumoral heterogeneity. In particular, the mRNA expression-based stemness index (mRNAsi) reflects cancer stemness by analyzing transcriptomic data of cancer samples; signatures for cancer stemness are derived from the pre-analysis of normal stem cells and their progeny using one-class logistic regression.

A prominent characteristic of PDAC is metabolic rewiring, which provides sufficient nutrients to support rapid tumor cell growth (10, 11). Driven by oncogene-mediated cell-autonomous pathways and the unique physiology of the tumor microenvironment, PDAC cell metabolism is extensively reprogrammed, including increased glycolysis and glutamine metabolism. Our previous work revealed that different SMAD4 mutation statuses dictate various metabolic preferences in PDAC (12). Hence, targeting tumor metabolism may be an efficient weapon to curb tumor progression (13).

CSCs possess unique metabolic plasticity, allowing them to rapidly respond and adapt to environmental disturbances (14). The metabolism of CSCs is thought to be tumor type-specific: some tumors (such as nasopharyngeal and liver cancers) rely on a glycolytic program, whereas others (such as lung, glioma or colon cancer) use oxidative phosphorylation, suggesting that metabolic plasticity confers on CSCs the ability to adapt to challenges from the environment and support self-renewal (15). Nonetheless, the correlation between stemness and metabolic landscapes in PDAC has yet to be systematically analyzed.

Here, we performed a bioinformatics analysis to systematically investigate whether the stemness of PDAC affects patient prognosis and intratumoral metabolic rewiring.

METHODS

Data Source and Selection

RNA sequencing (RNA-seq) data, including read counts and fragments per kilobase of transcript per million mapped reads (FPKM), were collected from The Cancer Genome Atlas-Pancreatic Adenocarcinoma (TCGA-PAAD). According to the annotation of TCGA-PAAD, we excluded nonductal-derived tumors and normal adjacent samples. Only PDAC samples remained for subsequent bioinformatics analysis. Clinical data, such as overall survival (OS), were also downloaded from the abovementioned data sets. Two GEO data sets, GSE11838 and GSE32676, were included to validate the expression of key genes between tumor and adjacent tissues. The stem cell indices based on the transcriptome of each PDAC sample were acquired from a previously reported study (9) and referred to as the mRNA expression-based stemness index (mRNAsi) in the following sections. Gene sets involved in arginine and proline metabolism; glycine, serine, and threonine metabolism; branched chain amino acid catabolism; glycolysis; glutamate and glutamine metabolism; glutathione synthesis and recycling; phospholipid metabolism; gluconeogenesis; oxidative phosphorylation; pentose phosphate pathway; lipolysis in adipose tissue; and triglyceride biosynthesis were downloaded from the Molecular Signatures Database (MSigDB) (https://www.gsea-msigdb.org/gsea/msigdb/index.jsp). The genes involved in each pathway are presented in **Supplementary Table 1**.

Mutation Analysis

Whole-exome sequencing data were downloaded from TCGA-PAAD-VarScan. The gene mutation distribution and abundance were visualized using the "maftools" R package.

Gene Ontology (GO) and KOBAS-Kyoto Encyclopedia of Genes and Genomes (KEGG) Pathway Analyses

Differentially expressed genes (DEGs) between the mRNAsi_high and mRNAsi_low groups were detected using the Wilcoxon test with the "limma" R package (version 3.4). The cutoff values to define the DEGs were log [fold change (FC)] > 2 and false discovery rate (FDR) < 0.05. GO functional enrichment analysis and KEGG pathway enrichment analysis of DEGs were performed by the "clusterProfiler," "org.Hs.eg.db," "plot," and "ggplot2" R packages. Gene set enrichment analysis (GSEA) was also performed to explore the functions of the DEGs using the "clusterProfiler," "org.Hs.eg.db," "enrichplot," and "limma" R packages.

Single-Sample GSEA (ssGSEA)

Based on the transcriptomes of PDAC samples and metabolism-related gene sets, we performed ssGSEA to calculate the activity of each metabolic pathway in every PDAC sample. The R packages "GSEABase" and "GSVA" were used to conduct ssGSEA.

Weighted Gene Coexpression Network Analysis (WGCNA)

WGCNA was performed using the WGCNA R package (16). According to the WGCNA manual, the coexpression of genes in the pan-gene landscape was analyzed instead of only DEGs. Initially, RNA-seq data were filtered to exclude outliers. The coexpression similarity matrix consisted of the absolute values of the correlations between transcript expression levels. A Pearson correlation matrix was constructed for paired genes. Then, we constructed a weighted adjacency matrix using the power function amn = |cmn|β, where cmn = the Pearson correlation between gene m and gene n and amn = the adjacency between gene m and gene n. The β value emphasizes strong correlations between genes and penalizes weak correlations. Next, an appropriate β value was taken to increase the similarity matrix and achieve a scale-free coexpression network. The adjacency matrix was then converted into a topological overlap matrix (TOM), which reflects the network connectivity of genes defined as the sum of adjacent genes generated by other networks. Average linkage hierarchical clustering was further conducted based on TOM-based dissimilarity measurements, and the minimum size (genome) of the gene dendrogram was 30. Through further analysis of modules, we calculated their dissimilarity and constructed module dendrograms.

To evaluate the significance of each module, gene significance (GS) was calculated to reflect the correlations between genes and sample traits. Module eigengenes (MEs) were considered the major components in the principal component analysis of each gene module, and the expression patterns of all genes were summarized as a single feature expression profile within a given module. Next, GS was determined by the log10 conversion of the *P* value in the linear regression of gene expression and clinical data (GS = $\log_{10}P$). Module significance (MS) was the average GS within the module and was calculated to measure the correlation between the module and sample traits. Statistical significance was determined using the relevant *P* values. To increase the capacity of the modules, we selected a cutoff (<0.25) to merge some modules with similar heights. The resulting gene models contained genes that were highly correlated and might exert identical biological functions or have associations with the same phenotypes.

To identify key genes in each module, we calculated GS and module membership (MM, correlation between the module's own genes and gene expression profiles) for each key gene and set their thresholds. The thresholds for screening key genes in the module were defined as cor. gene MM > 0.8 and cor. gene GS > 0.5.

Survival Analysis

PDAC patients were assigned to two groups based on the median of each stem cell index. A Kaplan-Meier curve was depicted to present the variation in the OS rate along with an increased follow-up period. A log-rank test was conducted to evaluate the difference between two groups in terms of survival expectancy.

Univariate Cox regression analysis was conducted to assess whether the selected key genes were correlated with patient survival. $P < 0.05$ was considered statistically significant.

Cell Culture and qRT-PCR

The human pancreatic cancer cell lines Capan-1, Panc-1, Mia-paca2, CF-PAC1, and BxPC-3 were obtained from the American Type Culture Collection. The human pancreatic ductal cell line HPDE was also obtained from the American Type Culture Collection. Capan-1 and CF-PAC1 cells were cultured in Iscove's modified Dulbecco's medium (IMDM) with 10% fetal bovine serum. Panc-1, BxPC-3, Mia-paca2, and HPDE cells were cultured in Dulbecco's modified Eagle's medium (DMEM) with 10% fetal bovine serum. CAFs were first separated and purified from human pancreatic cancer tissues in our laboratory based on the study by Walter et al. and then subjected to immortalization treatment (17). Fresh pancreatic cancer tissue was minced into 1–3 mm^3 fragments and digested with 0.25% trypsin at 37°C for 30 min. The resulting fragments were centrifuged at 600*g* for 5 min and washed once with Dulbecco's modified Eagle's medium (DMEM) containing 10% fetal bovine serum (FBS). The tissue fragments were then plated and allowed to adhere. After incubation at 37°C for several days, fibroblast outgrowth from the tissue fragments occurred. Fibroblasts were sub-cultured by trypsinization for two to three passages until free of epithelial cell contamination and maintained in DMEM supplemented with 10% FBS, 2% penicillin and streptomycin (Invitrogen). Cells were grown at 37°C in a humidified atmosphere containing 5% CO_2. CAFs were cultured in DMEM with 10% fetal bovine serum. Quantitative real-time PCR was performed as described previously (12). All reactions were run in triplicate, and the primer sequences are listed in **Supplementary Table 2**. RNA was extracted from 43 pairs of resected pancreatic cancer tissues and adjacent normal tissues preserved in RNAlater using the SteadyPure Universal RNA Extraction Kit (AG21017). The paired t test was performed to assess the statistical significance

of the differential expression between tumor and adjacent normal tissues.

RESULTS

Lower mRNAsi Predicts Prolonged OS in Patients With Pancreatic Cancer

A total of 145 PDAC samples with complete follow-up data were divided into two groups based on the median mRNAsi (**Figure 1A**). Then, we compared the baseline clinical data between the two groups; the distribution of sex, age, race, liver metastasis, history of chronic pancreatitis, residual tumor, number of lymph nodes, location, T stage, N stage, and American Joint Committee on Cancer (AJCC) grade were comparable between the two groups (**Table 1**). Next, we depicted the survival curve for each group and compared differences in OS using the log-rank test. The OS of patients with high mRNAsi values was significantly worse than that of their counterparts with low mRNAsi values (P = 0.003) (**Figure 1B**).

GO and KEGG Analyses of DEGs Between Patients With High and Low mRNAsi Values

A total of 2116 DEGs were identified with the criteria logFC>2 and adjusted P value<0.05 (**Figure 1C**). GO analysis suggested that these DEGs were highly enriched for functions associated with cancer initiation and progression, such as focal adhesion, collagen-containing extracellular matrix and substantially activated RNA transcription and protein translation (**Supplementary Figure 1**).

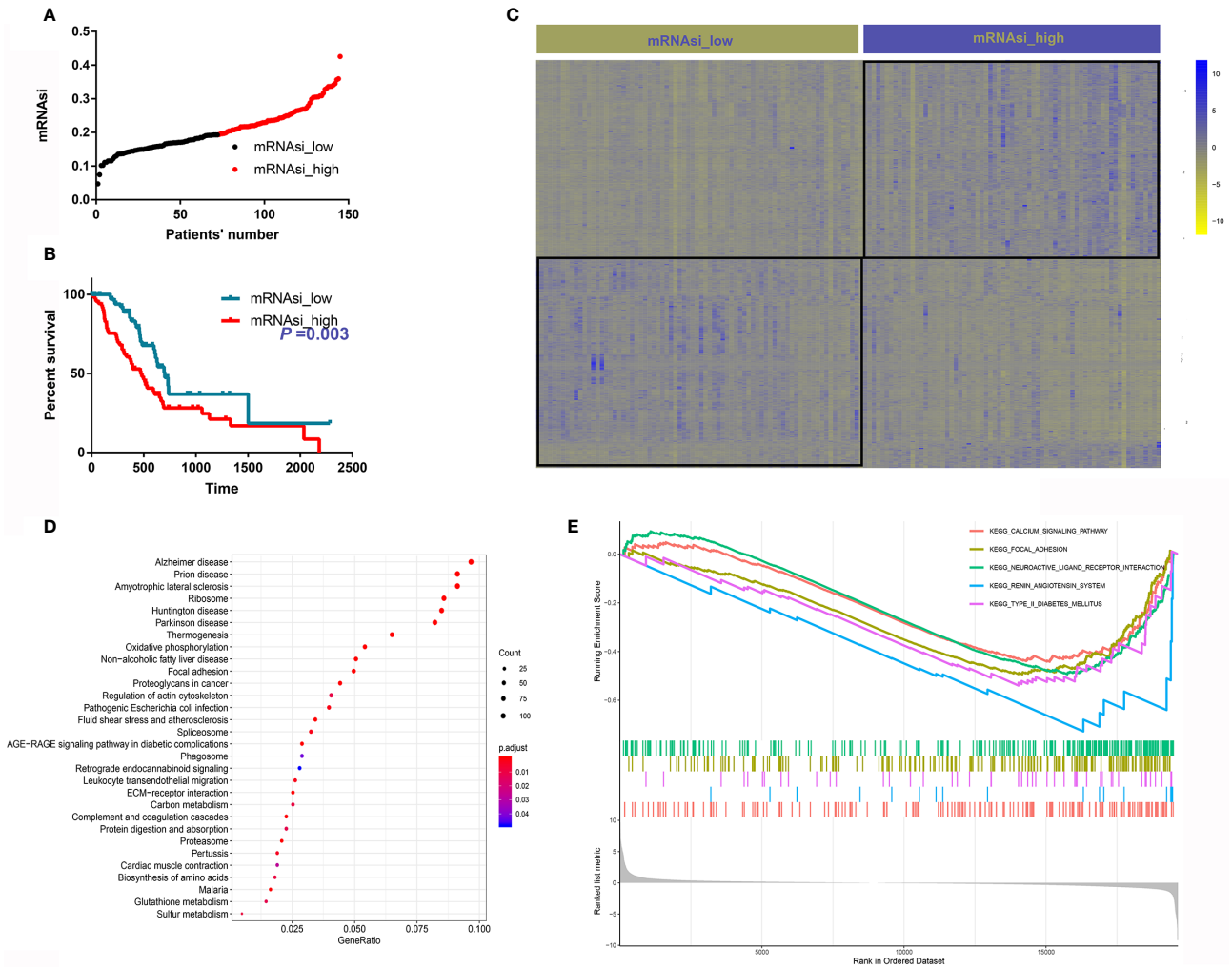

FIGURE 1 | mRNAsi is associated with PDAC patient survival and oncogenic and metabolic pathways. **(A)** Patients were divided into two groups based on the median mRNAsi. **(B)** High mRNAsi values predicted poor OS of patients with PDAC. **(C)** DEGs between samples with high and low mRNAsi values. **(D)** KEGG analysis of the DEGs. **(E)** The top five pathways upregulated in samples with high mRNAsi values.

TABLE 1 | Basic characteristics of patients with different mRNAsi values.

	mRNAsi_low (n = 72)	mRNAsi_high (n = 73)	Significance
Sex (male)	52.80%	56.20%	$P = 0.682$
Age (year)	63.64	66.45	$P = 0.121$
Race (white)	88.90%	86.30%	$P = 0.637$
Liver metastasis (yes)	25.00%	17.81%	$P = 0.291$
History of chronic pancreatitis (yes)	8.33%	9.59%	$P = 0.791$
Residual tumor (R0)	56.90%	54.80%	$P = 0.794$
Number of lymph nodes (median)	2	2	$P = 0.780$
Location(head)	81.94%	78.08%	$P = 0.561$
T stage (T3/4)	81.94%	87.67%	$P = 0.337$
N stage (N1)	79.17%	68.49%	$P = 0.144$
AJCC (>2b)	80.56%	68.49%	$P = 0.096$
Grade	45.83%	47.95%	$P = 0.799$

KEGG analysis showed that these DEGs were enriched in some oncogenic mechanisms, such as focal adhesion and were also enriched in many metabolic pathways, such as oxidative phosphorylation, carbon metabolism, glutathione metabolism and biosynthesis of amino acids (**Figure 1D**). GSEA was also performed, and calcium signaling and focal adhesion were the two most enriched signaling pathways (**Figure 1E**).

PDAC Samples With High and Low mRNAsi Values Have Different Mutational Landscapes and Match Different Previously Reported Molecular Subtypes

We further compared the differences in mutation profiles between patients with high and low mRNAsi values. The top 30 most frequently mutated genes in the two groups are shown in **Figures 2A, B**. Notably, these genes were mutated in 91.04% of PDAC samples with high mRNAsi values but only 68.25% of samples with low mRNAsi values, suggesting that the frequencies of these mutations increased with mRNAsi elevation. In addition, as expected, KRAS was the most frequently mutated gene in samples with high mRNAsi values; however, the most mutated gene in the low- mRNAsi group was TP53. Another important finding was that the cooccurrence of gene mutations was more common in samples with high mRNAsi values than in samples with low mRNAsi values (**Figures 2C, D**). The mutation landscape profiles of the two groups are shown in **Supplementary Figure 2**.

Next, we analyzed the proportions of patients with the three previously reported molecular subtypes with high and low mRNAsi values (**Table 2**). We found a significant inconsistency between different subtypes of the Collisson and Bailey clusters in PDAC samples with high and low mRNAsi values ($P = 0.0145$ and $P = 0.0001$, respectively). Specifically, the proportion of the classic subtype in the Collisson cluster was larger among high-mRNAsi samples than among low-mRNAsi samples; similarly, the percentage of the progenitor subtype in the Bailey cluster was also larger in high-mRNAsi samples (**Figures 2E–G**).

We also compared differences in the immune microenvironment between the high and low mRNAsi groups. Differences in the infiltration of a many types of immune were observed between the high and low mRNAsi groups. Notably, low-mRNAsi samples were enriched in fibroblasts and M2-polarized macrophages, whereas high-mRNAsi samples were enriched in activated CD4+ T cells (**Supplementary Figure 3**).

Identification of Eight Independent Gene Modules Associated With mRNAsi and Metabolic Reprogramming in Pancreatic Cancer by WGCNA

The RNA-seq data were first filtered to exclude outliers (**Supplementary Figure 4A**). Then, we visualized the associations between mRNAsi and metabolic activities in the PDAC samples (**Supplementary Figure 4B**). Next, an appropriate β value (0.9) was identified to increase the similarity matrix and obtain a scale-free coexpression network (**Figures 3A, B**). Average linkage hierarchical clustering was further conducted based on topological overlap matrix (TOM)-based dissimilarity measurements, and the minimum size (genome) of the gene dendrogram was 30 (**Supplementary Figures 4C, D**). To reduce the number of gene modules, dynamic tree cuts with high similarities were merged based on a cutoff height of (0.25) (**Supplementary Figure 4E**), and the distribution of genes in every module was visualized as shown in **Figure 3C**. Finally, eight independent gene modules were identified.

We presented the module-trait relationships by showing the correlations among eight clustered gene modules, mRNAsi and the activity of each metabolic pathway (**Figure 4A**). The eight gene modules were further divided into two gene clusters: gene cluster 1 was inversely associated with mRNAsi and most metabolic pathways except for lipolysis activity, while gene cluster 2 was positively correlated with mRNAsi and lipolysis activity.

Then, we investigated the key genes that were highly associated with mRNAsi in each module by setting the threshold parameters as MM > 0.8 and GS > 0.5. A total of 95 genes in six modules met these criteria (**Figure 4B**). Among them, ten genes belonged to the modules in gene cluster 2, while the others belonged to the modules in gene cluster 1 (**Figure 4C**).

Unsupervised Clustering Based on the Key Genes Identified in Each Module

Based on the expression levels of the 95 selected key genes, the PDAC samples were clustered into two groups (referred to as cluster 1 and cluster 2) (**Figure 5A**). Samples in cluster 2 were characterized by significantly higher mRNAsi values (**Figure 5B**). We further investigated the activity of each metabolic pathway between high and low mRNAsi samples. The activities of arginine and proline metabolism, branched chain amino acid catabolism, glutamate and glutamine metabolism, glycolysis, oxidative phosphorylation, pentose phosphate pathway, and triglyceride biosynthesis were significantly upregulated in PDAC samples with high mRNAsi values compared with

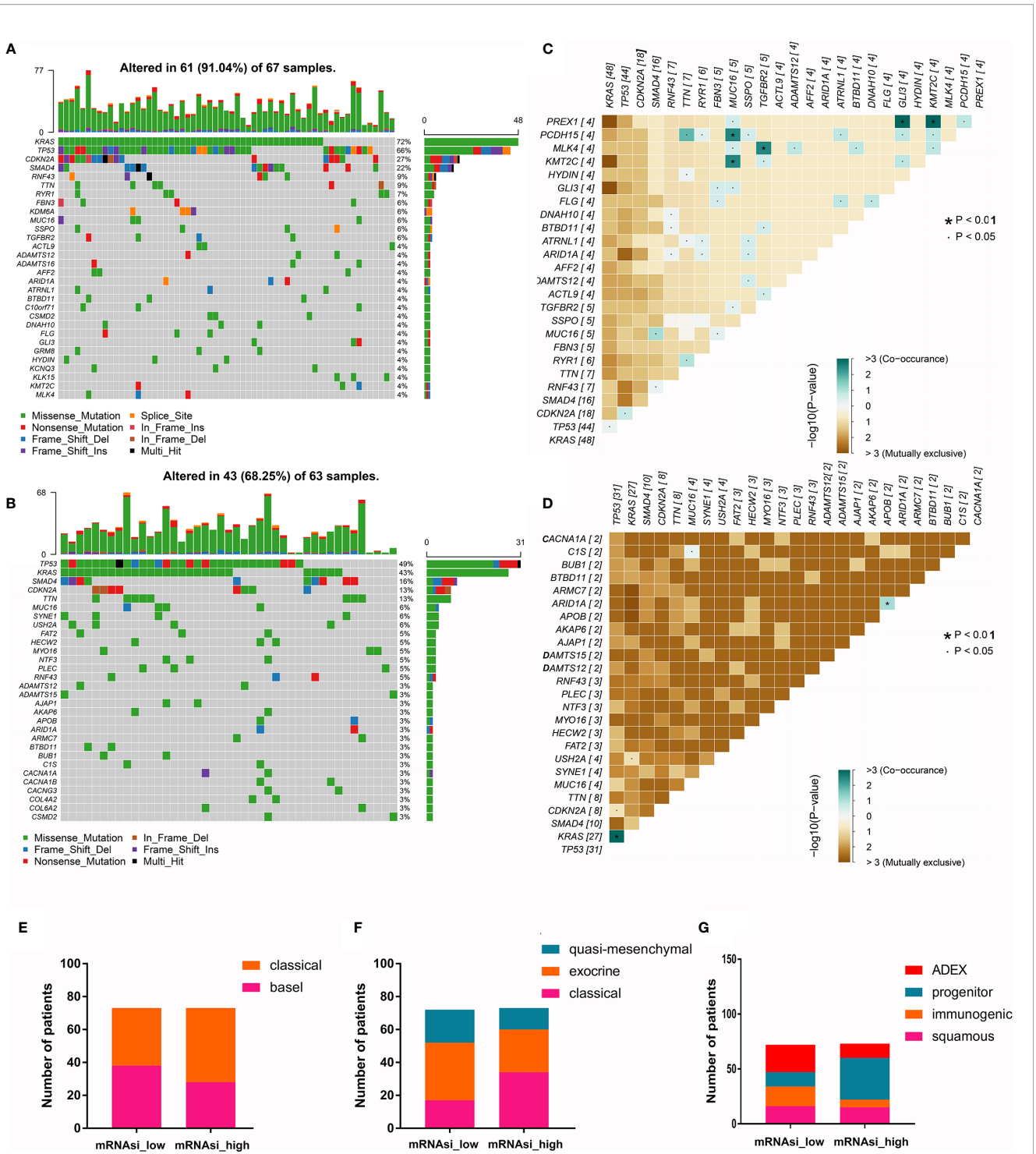

FIGURE 2 | The mutational landscape and molecular subtypes of samples with high and low mRNAsi values. **(A, B)** The top 30 most mutated genes in PDAC samples with high and low mRNAsi values. **(C, D)** Cooccurrence and mutual exclusion of mutated genes in PDAC samples with high and low mRNAsi values. **(E–G)** Proportions of PDAC samples of different molecular subtypes (Moffitt cluster, Collison cluster and Bailey cluster) with high and low mRNAsi values.

samples with low mRNAsi values, whereas lipolysis activity decreased with increasing mRNAsi value (**Figure 5C**). In addition, the activities of branched chain amino acid catabolism; glutathione synthesis and recycling; glycine, serine and threonine metabolism; and phospholipid metabolism were increased in cluster 2 (**Figure 5D**). Hence, the activity of branched chain amino acid catabolism was increased in both cluster 2 and in samples with high mRNAsi values, suggesting

TABLE 2 | The distribution of patients with previously reported molecular subtypes between the different mRNAsi groups.

	mRNAsi_low(n=72)	mRNAsi_high(n=73)	
Moffitt clusters			
Basel	38	28	
Classical	35	45	$P = 0.096$
Collisson clusters			
Classical	17	34	
Exocrine	35	26	
Quasi-mesenchymal	20	13	$P = 0.0145$
Bailey Clusters			
Squamous	16	15	
Immunogenic	18	7	
Progenitor	13	38	
ADEX	25	13	$P = 0.0001$

that the key genes used to define cluster 2 could partially explain the concurrently increased mRNAsi values and branched chain amino acid catabolism.

In Vitro Validation of Differentially Expressed Prognosis-Related Genes USsing qRT-PCR in Pancreatic Cancer Cell Lines, CAFs and HPDE Cells

Due to the heterogeneity of tumor tissue, differential gene expression may occur only in some cell types and not throughout the entire tumor. We used qRT-PCR to validate the expression of the genes of interest (**Figure 6A**) in pancreatic cancer cell lines and normal pancreatic ductal cells (HPDE). A total of 14 of 95 key genes were found to be associated with the OS of patients with PDAC. Interestingly, all 14 genes were predicted to favor survival (**Figure 6B**) and were expected to be downregulated in tumor tissues and cells. Therefore, if a specific gene was downregulated in tumor tissues (GSE11838 or GSE32676), we further validated the expression of this gene using qRT-PCR in vitro. MAGEH1 and PODN were downregulated in PDAC tissues in GSE32676, and MAGEH1 was downregulated in PDAC tissues in GSE11838. These in silico

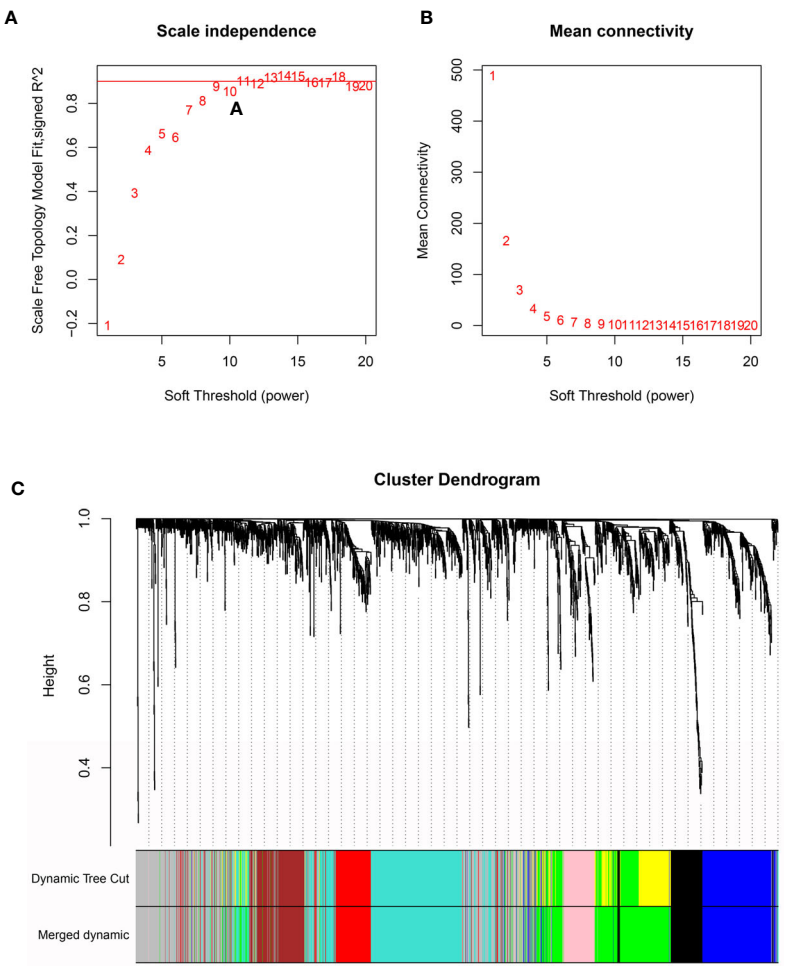

FIGURE 3 | WGCNA-based identification of 8 independent gene modules based on PDAC transcriptome data. **(A, B)** An appropriate β value was selected to increase the similarity matrix and obtain a scale-free coexpression network. **(C)** Eight gene modules remained after adjacent gene modules with high similarity were merged.

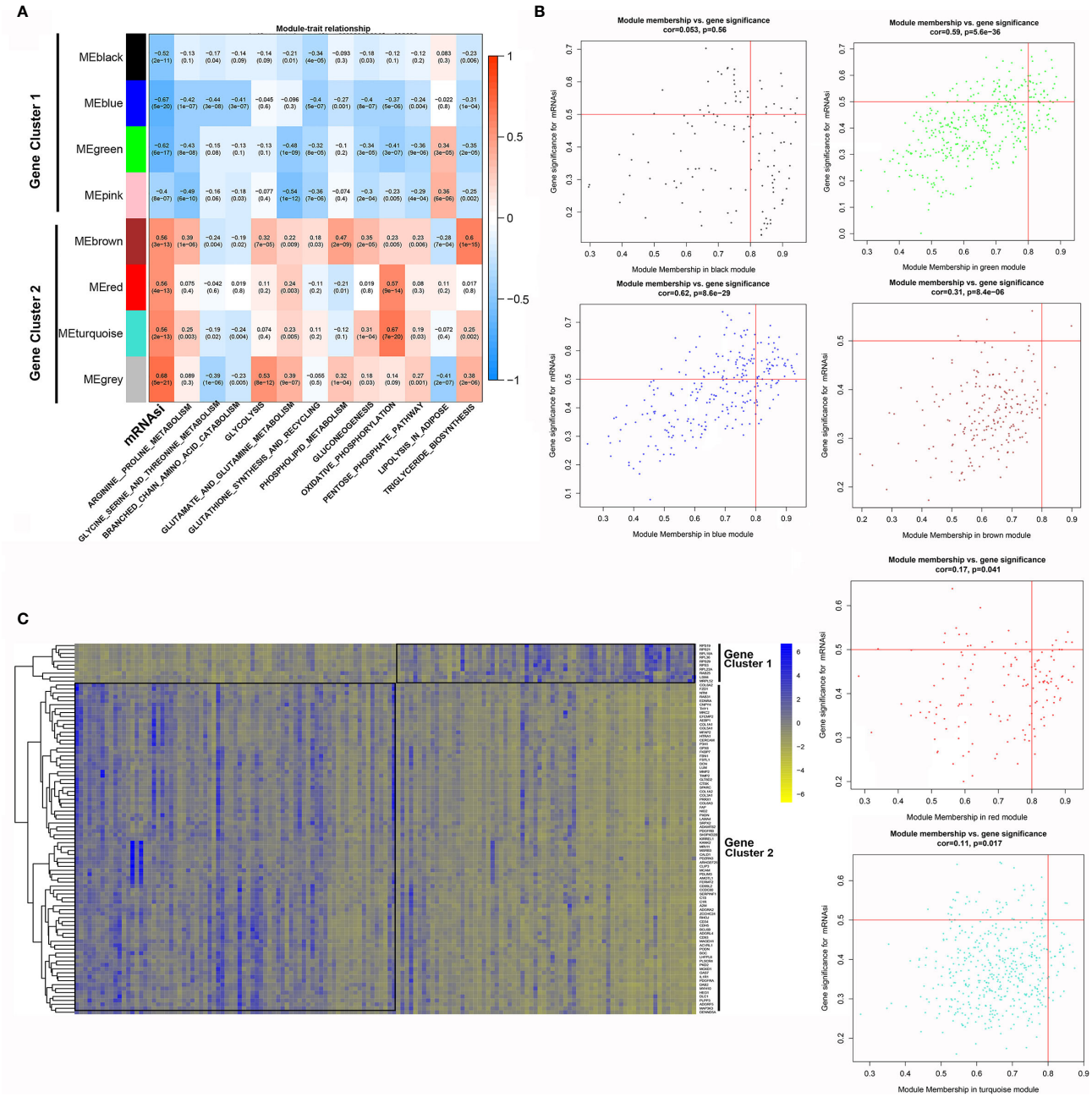

FIGURE 4 | WGCNA-based identification of gene modules and key genes associated with PDAC stemness. **(A)** Module-trait relationships revealed the correlations among gene modules, mRNAsi and metabolic pathways. **(B)** Identification of key genes significantly associated with both mRNAsi and modules in each gene module. **(C)** The differential expression of the selected key genes between the mRNAsi_high and mRNAsi_low groups.

results were validated using 43 pairs of resected pancreatic cancer samples, which also showed that the expression levels of MAGEH1, MAP3K3 and PODN were downregulated in tumor tissues. The relative mRNA expression levels of these genes were also decreased in most pancreatic cancer cell lines compared with HPDE cells (**Figure 6C**). In addition, the expression levels of these genes were comparable between CAFs and HPDEs (**Supplementary Figure 5**).

DISCUSSION

Tumor heterogeneity is an ongoing challenge for cancer therapy (18). Many studies have demonstrated that tumors harbor subclones that differ with respect to karyotype and chemotherapy sensitivity (19, 20), and CSCs are thought to be one of the determining factors of intratumor heterogeneity. Recently, Wang et al. identified tetraspanin CD9 as a marker

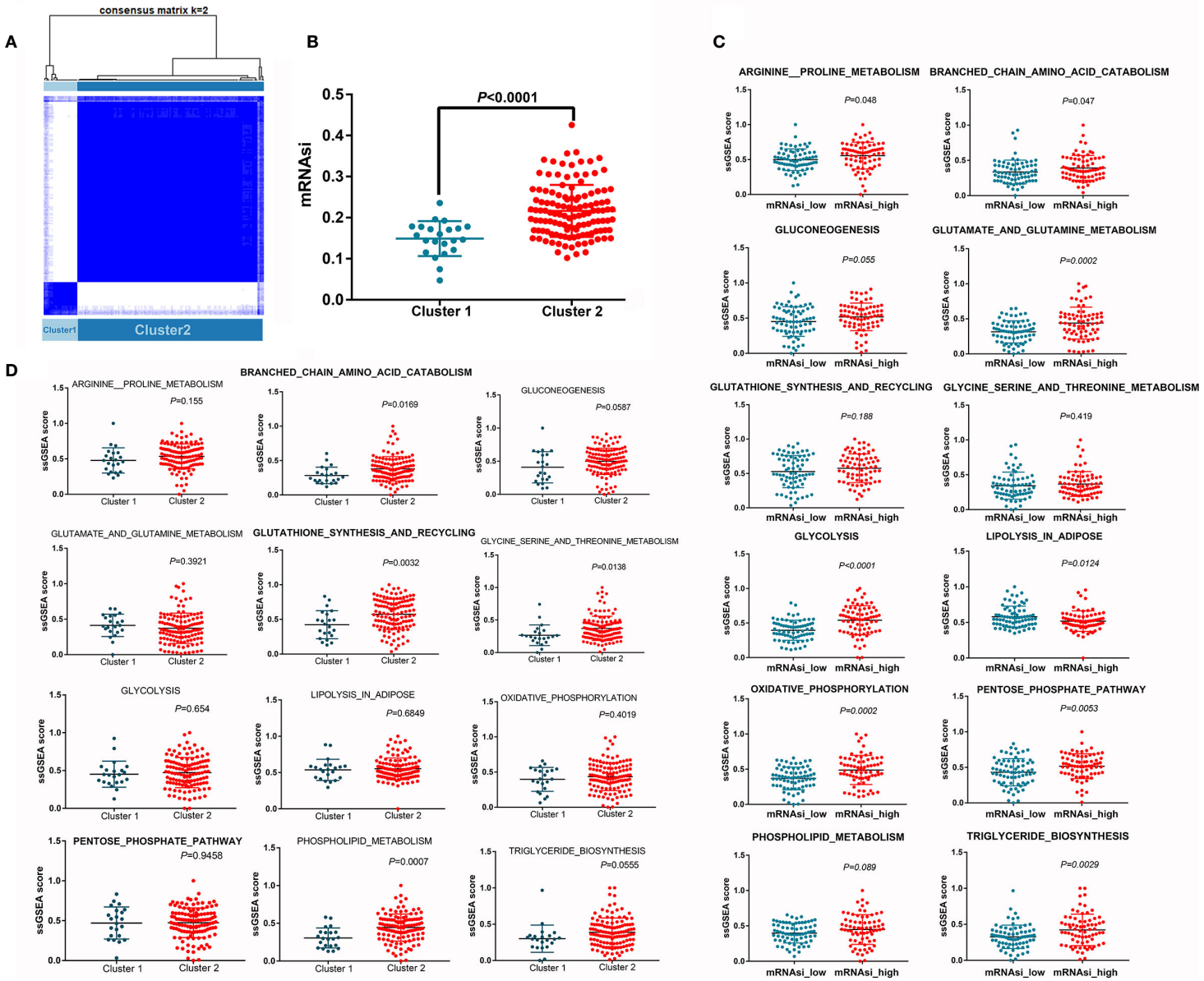

FIGURE 5 | Differences in metabolic pathway activity between different clusters. **(A)** Unsupervised clustering distinguished two clusters based on the selected key genes. **(B)** mRNAsi is increased in cluster 2. **(C)** Differences in metabolic pathway activity between the mRNAsi_high and mRNAsi_low groups. **(D)** Differences in metabolic pathway activity between clusters 1 and 2.

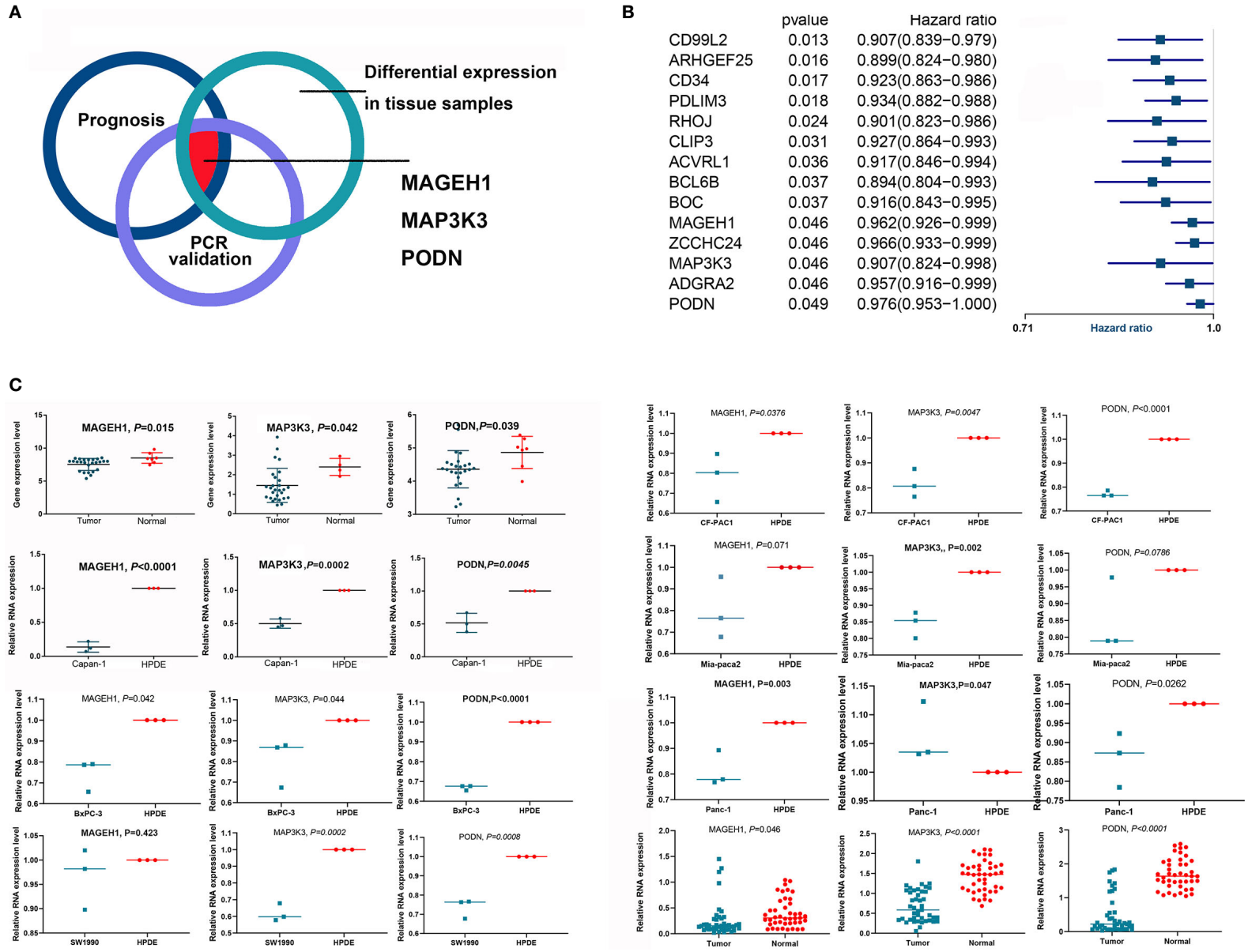

FIGURE 6 | Validation of the differential expression of key OS-related genes. **(A)** The diagram shows that MAGEH1, MAP3K3 and PODN were validated in silico and by qRT-PCR. **(B)** Fourteen key genes were associated with the OS of patients with PDAC. **(C)** MAGEH1, MAP3K3 and PODN were downregulated in tumor tissues and cell lines.

of PDAC tumor-initiating cells (21). Cells with high CD9 expression have increased organoid formation capability and generate tumor grafts more easily in vivo. Tumors originating from cells with high CD9 expression recapitulate the cellular heterogeneity of primary PDAC, whereas cells with low CD9 expression produce only duct-like epithelial progeny. Interestingly, this study also illustrated that CD9 promotes plasma membrane localization of the glutamine transporter ASCT2 and further increases uptake of glutamine, an essential metabolite for cancer progression, in PDAC cells.

In fact, metabolic rewiring is a widely acknowledged phenomenon in cancer development, and several metabolic pathways are aberrantly activated intratumorally, such as glycolysis and glutamine metabolism (13, 22). A recent study uncovered the robust dependence of PDAC on cysteine metabolism. Through upregulated uptake of cysteine from the tumor microenvironment, PDAC cells can instantly clear lipid peroxides and evade ferroptosis, a potent nonapoptotic cell death mechanism (23). Similarly, another study reported that genetic ablation of the cystine transporter in PDAC cells inhibits mTORC1, proliferation and tumor formation via nutrient and oxidative stresses (24).

In this context, systematically investigating the association and crosstalk between PDAC stemness and metabolic reprogramming is significant but experimentally challenging using traditional methods. Advances in next-generation sequencing and RNA-seq have provided useful tools to investigate the correlations between different gene signatures (25, 26). The activity of a specific signaling pathway can be estimated by related gene expression using the algorithm "GSVA" (27). PDAC stemness can be estimated using transcriptome data through one-class logistic regression as innovated by Malta et al. (9). In the present study, we first revealed that a higher mRNAsi predicts worse OS in PDAC patients, suggesting that increased stemness is associated with a dismal prognosis of PDAC. Then, we identified 8 independent gene modules based on PDAC transcriptome data by WGCNA and analyzed their associations with mRNAsi and various metabolic pathways. Ninety-five key genes tightly associated with both gene modules and stemness were selected, and their prognostic implications in PDAC were also established. Finally, MAGEH1, PODN, and MAP3K3 were identified as three mRNAsi-related tumor suppressor genes that were downregulated in tumor tissues and whose overexpression was associated with prolonged OS. Several previous studies have reported roles of these genes in other types of cancer. For example, Wang et al. suggested that MAGEH1 expression is downregulated in HCC tumor tissues (28). MAGEH1 reduces HCC cell proliferation, migration and invasion abilities. Low MAGEH1 expression is significantly correlated with poor prognosis in HCC patients (28). Few studies have reported the role of PODN in cancer. Bai et al. recently reported that PODN is hypermethylated and could be used to predict patient survival in gastric cancer (29). MAP3K3 seems to play a dual role in cancer. Some studies have shown that it acts as a tumor suppressor that inhibits Hedgehog pathway-dependent medulloblastoma, and its overexpression in tumor cells and tumor-infiltrating lymphocytes is correlated with favorable lung cancer patient survival (30, 31). Some other studies have implied that MAP3K3 is a protumor molecule (32, 33).

This study has notable strengths. First, few previous studies have systematically investigated the associations among stemness, prognosis and metabolic rewiring in PDAC. Second, most of the clinical characteristics were comparable between the two groups with high and low mRNAsi values, and the sample size of our study was relatively large, which ensured the reliability of our results. However, this study also has some limitations. External validation based on transcriptome, proteome and metabolome analyses using fresh PDAC samples is needed to further confirm our conclusions. Such studies are hindered by the difficulty of collecting PDAC samples and the high cost of sequencing. In addition, we revealed only the association between stemness and metabolic rewiring in PDAC, and the causality between them was not elucidated. Furthermore, a common weakness of GO and KEGG analyses is that they do not reveal which differentially expressed pathways are enriched in which group. Hence, we provide the differentially expressed genes between the high- and low-mRNAsi groups as **Supplementary Table 3**. More basic studies are warranted to determine whether CSCs can induce intratumoral metabolic rewiring or metabolite alteration in the tumor microenvironment to promote PDAC stemness.

In conclusion, the present study showed that high mRNAsi values were associated with a poor prognosis of PDAC patients and the aberrant activation of multiple metabolic pathways in PDAC samples. Future studies are expected to investigate the underlying mechanism based on the crosstalk between PDAC stemness and metabolic rewiring.

DATA AVAILABILITY STATEMENT

The datasets presented in this study can be found in online repositories. The names of the repository/repositories and accession number(s) can be found in the article/**Supplementary Material**.

AUTHOR CONTRIBUTIONS

RT and XL performed the bioinformatics analysis. WW and JH were responsible for the statistical analysis. JX, CL, and JL revised the tables and figures. BZ, XY, and SS designed the study. All authors contributed to the article and approved the submitted version.

FUNDING

This work was supported in part by the National Natural Science Foundation of China (81802352), the National Science Foundation for Distinguished Young Scholars of China (81625016), the Scientific Innovation Project of Shanghai Education Committee (2019-01-07-00-07-E00057), and the Clinical and Scientific Innovation Project of Shanghai Hospital Development Center (SHDC12018109).

ACKNOWLEDGMENTS

We appreciate the joint effort of all researchers who have contributed to TCGA.

SUPPLEMENTARY MATERIAL

The Supplementary Material for this article can be found online at: https://www.frontiersin.org/articles/10.3389/fonc.2021.643465/full#supplementary-material

Supplementary Figure 1 | GO analysis of DEGs between PDAC samples with high and low mRNAsi values.

Supplementary Figure 2 | Summary of mutation information from patients with high and low mRNAsi values.

Supplementary Figure 3 | Differences in immune microenvironment between samples with high and low mRNAsi values.

Supplementary Figure 4 | The process of WGCNA. **(A)** RNA-seq data were filtered to exclude outliers. **(B)** The corresponding associations among PDAC samples, their mRNAsi and metabolic activities were determined. **(C, D)** Average linkage hierarchical clustering was further conducted based on TOM-based dissimilarity measurements. **(E)** To reduce the number of gene modules, dynamic tree cuts with high similarities were merged based on a cutoff height of 0.25.

Supplementary Figure 5 | The expression of target genes in fibroblasts derived from pancreatic cancer.

REFERENCES

1. Moore A, Donahue T. Pancreatic Cancer. *Jama* (2019) 322:1426. doi: 10.1001/jama.2019.14699
2. Gordon-Dseagu VL, Devesa SS, Goggins M, Stolzenberg-Solomon R. Pancreatic cancer incidence trends: evidence from the Surveillance, Epidemiology and End Results (SEER) population-based data. *Int J Epidemiol* (2018) 47:427–39. doi: 10.1093/ije/dyx232
3. Tummers WS, Groen JV. Impact of resection margin status on recurrence and survival in pancreatic cancer surgery. *Br J Surg* (2019) 106:1055–65. doi: 10.1002/bjs.11115
4. Hezel AF, Kimmelman AC, Stanger BZ, Bardeesy N, Depinho RA. Genetics and biology of pancreatic ductal adenocarcinoma. *Genes Dev* (2006) 20:1218–49. doi: 10.1101/gad.1415606
5. Mueller S, Engleitner T, Maresch R, Zukowska M, Lange S, Kaltenbacher T, et al. Evolutionary routes and KRAS dosage define pancreatic cancer phenotypes. *Nature* (2018) 554:62–8. doi: 10.1038/nature25459
6. Pelosi E, Castelli G, Testa U. Pancreatic Cancer: Molecular Characterization, Clonal Evolution and Cancer Stem Cells. *Biomedicines* (2017) 5(4):65. doi: 10.3390/biomedicines5040065
7. Lytle NK, Ferguson LP, Rajbhandari N, Gilroy K, Fox RG, Deshpande A, et al. A Multiscale Map of the Stem Cell State in Pancreatic Adenocarcinoma. *Cell* (2019) 177:572–86.e22. doi: 10.1016/j.cell.2019.03.010
8. Heiler S, Wang Z, Zöller M. Pancreatic cancer stem cell markers and exosomes - the incentive push. *World J Gastroenterol* (2016) 22:5971–6007. doi: 10.3748/wjg.v22.i26.5971
9. Malta TM, Sokolov A, Gentles AJ, Burzykowski T, Poisson L, Weinstein JN, et al. Machine Learning Identifies Stemness Features Associated with Oncogenic Dedifferentiation. *Cell* (2018) 173:338–54.e15. doi: 10.1016/j.cell.2018.03.034
10. Hosein AN, Beg MS. Pancreatic Cancer Metabolism: Molecular Mechanisms and Clinical Applications. *Curr Oncol Rep* (2018) 20:56. doi: 10.1007/s11912-018-0699-5
11. Son J, Lyssiotis CA, Ying H, Wang X, Hua S, Ligorio M, et al. Glutamine supports pancreatic cancer growth through a KRAS-regulated metabolic pathway. *Nature* (2013) 496:101–5. doi: 10.1038/nature12040
12. Liang C, Shi S, Qin Y, Meng Q, Hua J, Hu Q, et al. Localisation of PGK1 determines metabolic phenotype to balance metastasis and proliferation in patients with SMAD4-negative pancreatic cancer. *Gut* (2020) 69:888–900. doi: 10.1136/gutjnl-2018-317163
13. Halbrook CJ, Lyssiotis CA. Employing Metabolism to Improve the Diagnosis and Treatment of Pancreatic Cancer. *Cancer Cell* (2017) 31:5–19. doi: 10.1016/j.ccell.2016.12.006
14. Peiris-Pagès M, Martinez-Outschoorn UE, Pestell RG, Sotgia F, Lisanti MP. Cancer stem cell metabolism. *Breast Cancer Res BCR* (2016) 18:55. doi: 10.1186/s13058-016-0712-6
15. Perusina Lanfranca M, Thompson JK, Bednar F, Halbrook C, Lyssiotis C, Levi B, et al. Metabolism and epigenetics of pancreatic cancer stem cells. *Semin Cancer Biol* (2019) 57:19–26. doi: 10.1016/j.semcancer.2018.09.008
16. Langfelder P, Horvath S. WGCNA: an R package for weighted correlation network analysis. *BMC Bioinf* (2008) 9:559. doi: 10.1186/1471-2105-9-559
17. Walter K, Omura N, Hong SM, Griffith M, Goggins M. Pancreatic cancer associated fibroblasts display normal allelotypes. *Cancer Biol Ther* (2008) 7:882–8. doi: 10.4161/cbt.7.6.5869
18. Dagogo-Jack I, Shaw AT. Tumour heterogeneity and resistance to cancer therapies. *Nat Rev Clin Oncol* (2018) 15:81–94. doi: 10.1038/nrclinonc.2017.166
19. McGranahan N, Swanton C. Clonal Heterogeneity and Tumor Evolution: Past, Present, and the Future. *Cell* (2017) 168:613–28. doi: 10.1016/j.cell.2017.01.018
20. Meacham CE, Morrison SJ. Tumour heterogeneity and cancer cell plasticity. *Nature* (2013) 501:328–37. doi: 10.1038/nature12624
21. Wang VM, Ferreira RMM, Almagro J. CD9 identifies pancreatic cancer stem cells and modulates glutamine metabolism to fuel tumour growth. *Nat Cell Biol* (2019) 21:1425–35. doi: 10.1038/s41556-019-0407-1
22. Biancur DE, Kimmelman AC. The plasticity of pancreatic cancer metabolism in tumor progression and therapeutic resistance. *Biochim Biophys Acta Rev Cancer* (2018) 1870:67–75. doi: 10.1016/j.bbcan.2018.04.011
23. Badgley MA, Kremer DM. Cysteine depletion induces pancreatic tumor ferroptosis in mice. *Sci (New York NY)* (2020) 368:85–9. doi: 10.1126/science.aaw9872
24. Daher B, Parks SK, Durivault J. Genetic Ablation of the Cystine Transporter xCT in PDAC Cells Inhibits mTORC1, Growth, Survival, and Tumor Formation via Nutrient and Oxidative Stresses. *Cancer Res* (2019) 79:3877–90. doi: 10.1158/0008-5472.CAN-18-3855
25. Morganti S, Tarantino P, Ferraro E, D'Amico P, Duso BA, Curigliano G. Next Generation Sequencing (NGS): A Revolutionary Technology in Pharmacogenomics and Personalized Medicine in Cancer. *Adv Exp Med Biol* (2019) 1168:9–30. doi: 10.1007/978-3-030-24100-1_2
26. Pareek CS, Smoczynski R, Tretyn A. Sequencing technologies and genome sequencing. *J Appl Genet* (2011) 52:413–35. doi: 10.1007/s13353-011-0057-x
27. Hänzelmann S, Castelo R, Guinney J. GSVA: gene set variation analysis for microarray and RNA-seq data. *BMC Bioinf* (2013) 14:7. doi: 10.1186/1471-2105-14-7
28. Wang PC, Hu ZQ, Zhou SL, Zhan H, Zhou ZJ, Luo CB, et al. Downregulation of MAGE family member H1 enhances hepatocellular carcinoma progression and serves as a biomarker for patient prognosis. *Future Oncol (London England)* (2018) 14:1177–86. doi: 10.2217/fon-2017-0672
29. Bai Y, Wei C, Zhong Y, Zhang Y, Long J, Huang S, et al. Development and Validation of a Prognostic Nomogram for Gastric Cancer Based on DNA Methylation-Driven Differentially Expressed Genes. *Int J Biol Sci* (2020) 16:1153–65. doi: 10.7150/ijbs.41587
30. He Y, Wang L, Liu W, Zhong J, Bai S, Wang Z, et al. MAP3K3 expression in tumor cells and tumor-infiltrating lymphocytes is correlated with favorable patient survival in lung cancer. *Sci Rep* (2015) 5:11471. doi: 10.1038/srep11471
31. Lu J, Liu L, Zheng M, Li X, Wu A, Wu Q, et al. MEKK2 and MEKK3 suppress Hedgehog pathway-dependent medulloblastoma by inhibiting GLI1 function. *Oncogene* (2018) 37:3864–78. doi: 10.1038/s41388-018-0249-5
32. Fan Y, Ge N, Wang X, Sun W, Mao R, Bu W, et al. Amplification and over-expression of MAP3K3 gene in human breast cancer promotes formation and survival of breast cancer cells. *J Pathol* (2014) 232:75–86. doi: 10.1002/path.4283

33. Yin W, Shi L, Mao Y. MiR-194 regulates nasopharyngeal carcinoma progression by modulating MAP3K3 expression. *FEBS Open Bio* (2019) 9:43–52. doi: 10.1002/2211-5463.12545

Conflict of Interest: The authors declare that the research was conducted in the absence of any commercial or financial relationships that could be construed as a potential conflict of interest.

frontiers in Oncology

ORIGINAL RESEARCH
published: 30 July 2021
doi: 10.3389/fonc.2021.678343

MitoTracker Deep Red (MTDR) Is a Metabolic Inhibitor for Targeting Mitochondria and Eradicating Cancer Stem Cells (CSCs), With Anti-Tumor and Anti-Metastatic Activity *In Vivo*

Camillo Sargiacomo, Sophie Stonehouse, Zahra Moftakhar, Federica Sotgia and Michael P. Lisanti**

Translational Medicine, School of Science, Engineering and Environment (SEE), University of Salford, Greater Manchester, United Kingdom

OPEN ACCESS

Edited by:
Chris Albanese, Georgetown University, United States

Reviewed by:
Olivier Peulen, University of Liège, Belgium
Barbara Marengo, University of Genoa, Italy

***Correspondence:**
Federica Sotgia
fsotgia@gmail.com
Michael P. Lisanti
michaelp.lisanti@gmail.com

Specialty section:
This article was submitted to Cancer Metabolism, a section of the journal Frontiers in Oncology

Received: *09 March 2021*
Accepted: *17 June 2021*
Published: *30 July 2021*

Citation:
Sargiacomo C, Stonehouse S, Moftakhar Z, Sotgia F and Lisanti MP (2021) MitoTracker Deep Red (MTDR) Is a Metabolic Inhibitor for Targeting Mitochondria and Eradicating Cancer Stem Cells (CSCs), With Anti-Tumor and Anti-Metastatic Activity In Vivo. Front. Oncol. 11:678343. doi: 10.3389/fonc.2021.678343

MitoTracker Deep Red (MTDR) is a relatively non-toxic, carbocyanine-based, far-red, fluorescent probe that is routinely used to chemically mark and visualize mitochondria in living cells. Previously, we used MTDR at low nano-molar concentrations to stain and metabolically fractionate breast cancer cells into Mito-high and Mito-low cell sub-populations, by flow-cytometry. Functionally, the Mito-high cell population was specifically enriched in cancer stem cell (CSC) activity, i) showing increased levels of ESA cell surface expression and ALDH activity, ii) elevated 3D anchorage-independent growth, iii) larger overall cell size (>12-μm) and iv) Paclitaxel-resistance. The Mito-high cell population also showed enhanced tumor-initiating activity, in an *in vivo* preclinical animal model. Here, we explored the hypothesis that higher nano-molar concentrations of MTDR could also be used to therapeutically target and eradicate CSCs. For this purpose, we employed an ER(+) cell line (MCF7) and two triple negative cell lines (MDA-MB-231 and MDA-MB-468), as model systems. Remarkably, MTDR inhibited 3D mammosphere formation in MCF7 and MDA-MB-468 cells, with an IC-50 between 50 to 100 nM; similar results were obtained in MDA-MB-231 cells. In addition, we now show that MTDR exhibited near complete inhibition of mitochondrial oxygen consumption rates (OCR) and ATP production, in all three breast cancer cell lines tested, at a level of 500 nM. However, basal glycolytic rates in MCF7 and MDA-MB-468 cells remained unaffected at levels of MTDR of up to 1 μM. We conclude that MTDR can be used to specifically target and eradicate CSCs, by selectively interfering with mitochondrial metabolism, by employing nano-molar concentrations of this chemical entity. In further support of this notion, MTDR significantly inhibited tumor growth and prevented metastasis *in vivo*, in a xenograft model employing MDA-MB-231 cells, with little or no toxicity observed. In contrast, Abemaciclib, an FDA-approved CDK4/6 inhibitor, failed to inhibit metastasis. Therefore, in the future, MTDR could be modified and optimized *via* medicinal chemistry, to further increase its

potency and efficacy, for its ultimate clinical use in the metabolic targeting of CSCs for their eradication.

Keywords: MitoTracker Deep Red (MTDR), near-infrared dyes (NIR), cancer stem-like cells (CSCs), mitochondria, cancer therapy, anti-tumor activity, anti-metastatic activity

INTRODUCTION

Cancer stem-like cells (CSCs) are a relatively small sub-population of tumor cells that share characteristic features with normal adult stem cells and embryonic stem cells (1–4). As such, CSCs are thought to be a 'primary biological cause' for i) tumor regeneration and ii) systemic organismal spread, resulting in the clinical features of tumor recurrence and distant metastasis, ultimately driving treatment failure and premature death in cancer patients undergoing chemo- and radio-therapy (1, 2, 4, 5).

Evidence indicates that CSCs also function in tumor initiation, as isolated CSCs experimentally behave as tumor-initiating cells (TICs) in pre-clinical animal models (1, 2). As approximately 90% of all cancer patients die pre-maturely from metastatic disease world-wide (4), there is a great urgency and unmet clinical need, to develop novel therapies for effectively targeting and eradicating CSCs. Most conventional therapies do not target CSCs and often increase the frequency of CSCs, in the primary tumor and at distant sites.

One new approach to the elimination of CSCs has been through the exploitation of cellular metabolism (4). As CSCs are amongst the most energetic cancer cells, new metabolic inhibitors could be employed to induce ATP depletion to "starve" CSCs to death (4–7). So far, we have identified numerous FDA-approved drugs with off-target mitochondrial side effects that have anti-CSC properties and induce ATP depletion, including the antibiotic Doxycycline, which functions as an inhibitor of mitochondrial protein translation (5). Doxycycline, a long-acting Tetracycline analogue, is currently used for treating diverse forms of infections, such as acne, acne rosacea, and malaria prevention, amongst others. In a recent Phase II clinical study, pre-operative oral Doxycycline (200 mg/day for 14 days) reduced the CSC burden in early breast cancer patients between 17.65% and 66.67%, with a near 90% positive response rate (8).

Therefore, it is imperative that we identify other complementary approaches with higher potency, to metabolically starve CSCs by targeting mitochondria and driving ATP depletion. Previous studies have shown that, in general, cyanine dyes accumulate in cells derived from solid tumors, e.g., prostate (9), gastric (10), kidney (11), hepatocytes (12, 13), lung (14) and glioblastoma (15), but not in healthy cells *in vitro* (16–20). More specifically, they observed that cyanine dyes preferentially target mitochondria in cancer cells, by generating a selective chemically-induced cytotoxicity, through redox-based mechanisms (21). In addition, *in vivo* experiments have shown that NIR cyanine derivatives (e.g. IR-780) in general are safe to use, with short-term accumulation and a serum half-life of minutes to hours (22), whereas, in tumors its fluorescent signal persists for days in animals. In addition, they observed that the thiol reactive chloromethyl moiety (*meso*-chlorine-group) increased IR-780 tumor localization *in vivo*. Therefore, these compounds have been used mainly for theranostic approaches, as well as for photodynamic and photothermal therapy (17, 23–25).

Here, we propose to repurpose the heptamethine cyanine dye MitoTracker Deep Red (MTDR) as a potential therapeutic for targeting mitochondrial metabolism in CSCs. MTDR is currently used as a non-toxic fluorescent chemical probe with a thiol reactive chloromethyl-moiety for visualizing, in the long term, the distribution of mitochondria in living cells and, in the short term, to quantitate mitochondrial potential by FACS or fluorescent microscopy analysis. Recent evidence also indicates that MTDR can also be used as a marker to purify drug-resistant CSC activity by flow-cytometry (26, 27), which was validated by other functional assays, including pre-clinical animal models that documented higher tumor-initiating activity *in vivo* (26).

In the current work, we investigated the anti-cancer properties of MTDR and other NIR dyes, namely HITC, DDI, and IR-780. Interestingly, we found that MTDR, HITC and DDI were all effective inhibitors of anchorage-independent CSC propagation. However, IR-780 had no significant effect in the nanomolar range. In addition, we tested seven Cyanine 5 (Cy5) heptamethine analogs, with different reactive groups, for their ability to inhibit CSC growth. Overall, we observed that Cy5-Azide and Cy5-Alkyne are both effective inhibitors of CSCs, in the nanomolar range.

MATERIALS AND METHODS

Compounds

MitoTracker™ Deep Red FM

MTDR (1-{4-[(chloromethyl)phenyl]methyl}-3,3-dimethyl-2-[5-(1,3,3-trimethyl-1,3-dihydro-2H indol-2-ylidene)penta-1,3-dien-1-yl]-3H-indolium chloride 2-[5-(1-{[4-(chloromethyl) phenyl]methyl}-3,3-dimethyl-1,3-dihydro-2H-indol-2 ylidene) penta-1,3 dien-1-yl]-1,3,3-trimethyl-3H-indolium chloride) was purchased from ThermoFisher (# M22426).

Near-Infrared Compounds

HITC iodine (B-1,1',3,3,3',3'-Hexamethylindotri-carbocyanine) (# 252034, Merk), DDI iodine (1,1'Diethyl-2-2'-dicarbo-cyanine) (# 392197, Merk) and IR780 iodine (2-[2-[2-Chloro-3-[(1,3-dihydro-3,3-dimethyl-1-propyl-2H-indol 2ylidene)ethylidene]-1-cyclohexen-1-l] ethenyl] -3,3-dimethyl-1 propylindolium iodide) (# 425311, Merk). To prepare a 10 mM stock solution all NIR compounds were first dissolved in PBS, DMEM with 10% FBS, DMEM/F-12. DDI and HITC were dissolved best in water, whereas IR780 in DMEM media (10% FBS). All compounds were

left to dissolve for a few hours rolling at room temperature and filtered using a 0.02 μm filter, prior to treating cells. Stock solutions were kept at -20°C.

Cy5 Analogs

Cy5 analogs were purchased from Lumiprobe (Cyanine5 NHS ester (#13020), Cyanine5 Maleimide (#13080), Cyanine5 Azide (#A3030), Cyanine5 Alkyne (#A30B0), Cyanine5 Hydrazide (#13070), Cyanine5 Amine (#130C0), Cyanine5 Carboxylic Acid (#13090). All Cy5 compounds were dissolved at 10 mM in DMSO and stored at -20°C.

Cell Lines

Human breast cancer cell lines (MCF7, MDA-MB-231 and MDA-MB-468) were all obtained from the American Type Culture Collection (ATCC).

3D-Mammosphere Formation

A single cell suspension was prepared using enzymatic (1x Trypsin-EDTA, Sigma Aldrich, cat. #T3924), and manual disaggregation (25-gauge needle). Five thousand cells were plated with in mammosphere medium (DMEM-F12/B27/20ng/ml EGF/PenStrep), under non-adherent conditions, in six wells plates coated with 2-hydroxyethylmethacrylate (poly-HEMA, Sigma, cat. #P3932). Cells were grown for 5 days and maintained in a humidified incubator at 37°C at an atmospheric pressure in 5% (v/v) carbon dioxide/air. After 5 days, 3D mammospheres with a diameter greater than 50-μm were counted using a microscope, fitted with a graticule eye-piece, and the percentage of cells which formed spheroids was calculated and normalized to one (1 = 100% MFE; mammosphere forming efficiency). Mammosphere assays were performed in triplicate and repeated three times independently.

Metabolic Flux Analysis on the Total Cell Population

Extracellular acidification rates (ECAR) and oxygen consumption rates (OCR) were analyzed using the Seahorse XFe96 analyzer (Agilent/Seahorse Bioscience, USA). Cells were maintained in DMEM supplemented with 10% FBS (fetal bovine serum), 2 mM GlutaMAX, and 1% Pen- Strep. Twenty-thousand breast cancer cells were seeded per well, into XFe96-well cell culture plates, and incubated at 37°C in a 5% CO_2 humidified atmosphere. After 24-48 hours, MCF7 cells were washed in pre-warmed XF assay media, as previously described. ECAR and OCR measurements were normalized for cell protein content, by the SRB colorimetric assay. Data sets were analyzed using XFe96 software and Excel software.

Measuring the Metabolic Effects of MTDR in a CSC-Enriched MCF7 Cell Population

To quantitatively measure the mitochondrial-specific effects of MTDR on a CSC-enriched cell population, we used the Seahorse XFe96 Analyzer to perform the XF Cell Mito Stress Test. Briefly, MCF7 cells were seeded for 3D-mammosphere formation and were grown for 5-days using the standard protocol, but in the absence or presence of MTDR at a low concentration (100 nM), to avoid cell death. Then, the resulting 3D-mammospheres were collected, dissociated into single cells by incubation with trypsin (for 10 minutes at 37°C) and passage through a syringe. The single cell suspension was then passed through a 40-μm strainer, to remove potentially aggregated material and then washed with OCR media. Single cells were counted using Trypan blue to assess their vitality, prior to metabolic analysis. Then, thirty-thousand single cells were dispensed into each well of the 96-well XF microplate pre-coated with Corning™ Cell-Tak Cell and Tissue Adhesive (Catalog No. CB-40240), to ensure rapid adhesion of the cells. Finally, the single cells were briefly centrifuged (200 x g for 1 minute) to further ensure their attachment to the bottom of the wells. Finally, OCR was measured using the Seahorse Metabolic Flux Analyser (XFe96), under standard conditions at 37°C.

Cell Viability Assays

The effects of MTDR on cell viability were measured by staining cell monolayers with the nuclear fluorescent dye Hoechst 33342, which labels DNA in living cells. Quantitation was performed using a Varioskan LUX multimode microplate reader. The treatment was conducted for 72 hours prior to microplate analysis.

Fluorescent Microscopy Analysis

Microscopy analysis was performed by analyzing samples in live cell imaging with EVOS imaging platform (ThermoFisher) using the Cy5 channel and bright field.

Tumor Growth, Metastasis and Embryo Toxicity Assays

Xenograft studies were performed, essentially as previously described (28). According to the French legislation, no ethical approval is needed for scientific experimentation using oviparous embryos (decree n° 2013–118, February 1, 2013; art. R-214–88). Animal studies were performed under animal experimentation permit N° 381029 and B3851610001 to Jean Viallet (INOVOTION). Briefly, fertilized White Leghorn eggs were incubated at 37.5°C with 50% relative humidity for 9 days. At that moment (E9), the chorioallantoic membrane (CAM) was dropped down by drilling a small hole through the eggshell into the air sac, and a 1 cm^2 window was cut in the eggshell above the CAM. For amplification and grafting of the tumor cells, the MDA-MB-231 tumor cell line was cultivated in DMEM supplemented with 10% FBS and 1% penicillin/streptomycin. On day E9, MDA-MB-231 cells were trypsinized, washed with complete medium and suspended in graft medium. More specifically, we applied Corning® Matrigel® Matrix (Catalogue number: 354230) for tumor cell xenografting. This was performed because it has been demonstrated that the increased viscosity of the cell suspension can prevent the diffusion of cells at the injection site. Briefly, tumor cells are suspended in Matrigel diluted with complete media at 1:1 ratio and then grafted in 50 μl/egg. For the MDA-MB-231 tumor model, an inoculum of 1 x 10^6 cells in 50μL (i.e., 25 μl Matrigel + 25μl complete culture media) was added onto the CAM of each egg at E9. On day E10, tumors were detectable, and they were then treated daily for 8 days with vehicle alone (1% DMSO in PBS) or with different dosages of MTDR. The therapeutic solution was added dropwise onto the tumor. At day 18 (E18), the upper portion of the CAM was removed from each egg, washed in PBS and then

directly transferred to paraformaldehyde (fixation for 48 h) and weighed. For tumor growth assays, at least 10 tumor samples were collected and analyzed per group ($n \geq 10$). On day E18, a 1 cm^2 portion of the lower CAM was collected to evaluate the number of metastatic cells in 7 to 8 samples per group ($n \geq 7$). Genomic DNA was extracted from the CAM (commercial kit) and analyzed by qPCR with specific primers for Human Alu sequences. Calculation of Cq for each sample, mean Cq and relative amounts of metastases for each group were directly managed by the Bio-Rad® CFX Maestro software. A one-way ANOVA analysis with post-tests was performed on all the data. To measure embryo tolerability, before each administration, the treatment toxicity was evaluated by scoring the number of dead embryos.

Statistical Significance

The statistical tests used were the unpaired Student's t-test and one-way ANOVA. Bar graphs are shown as the average ± SEM (standard error of the mean). A p-value of less than 0.05 was considered statistically significant and is indicated by asterisks: *$p < 0.05$, **$p < 0.01$, ***$p < 0.001$ and ****$p < 0.0001$. ns, not significant.

Software

All statistical analysis was performed using GraphPad version 8. All compounds chemical structures were drawn by using ChemDraw 18.

RESULTS

Here, we directly assessed the suitability of using MitoTracker Deep Red (MTDR), a well-known mitochondrial fluorescent probe, for targeting mitochondria and effectively inhibiting the propagation of breast CSCs. For this purpose, we employed three model cell lines of breast cancer: MCF7, MDA-MB-231, MDA-MB-468, as well as an hTERT-BJ1 skin fibroblasts cell line.

MCF7 is an ER (+) breast cancer cell line, while MDA-MB-231 and MDA-MB-468 are both triple negative [ER (-), PR (-), HER2 (-)] cell lines. In this context, we assessed the targeted effects of MTDR on 3D CSC propagation and overall metabolic rates in 2D monolayer cultures.

The structure of MTDR is shown in **Figure 1A**.

MTDR Inhibits the 3D Anchorage-Independent Propagation of CSCs

In order to assess the effects of MTDR on CSC propagation, we used the mammosphere assay as a functional readout of "stemness" and 3D anchorage-independent growth. As CSCs are highly-resistant to many types of cell stress, they can undergo anchorage-independent propagation, under low-attachment conditions. Ultimately, this results in the generation of >50 μm sized 3D spheroid-like structures. These "mammospheres" are highly enriched in CSCs and progenitor-like cells, and

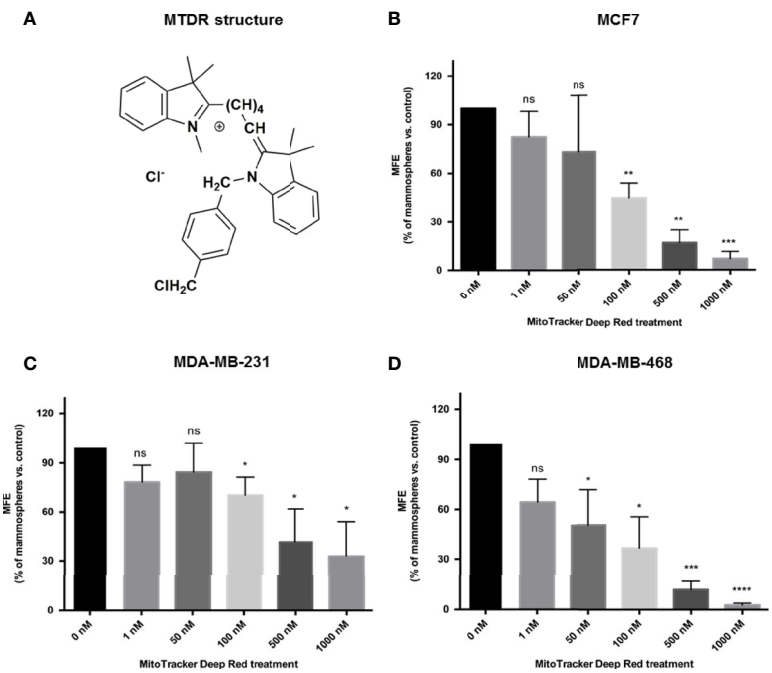

FIGURE 1 | MTDR inhibits mammosphere formation in MCF7, MDA-MB-231 and MDA-MB-468 cells. **(A)** *Structure of MitoTracker Deep Red FM (MTDR).* MTDR is a far-red fluorescent dye that stains active mitochondria. Note that MTDR is a lipophilic cation, which is a chemical characteristic that results its high-efficiency targeting to mitochondria. **(B)** *Effects of MTDR on 3D mammosphere formation in MCF7 cells.* Note that MTDR inhibits 3D anchorage-independent growth in MCF7 cells, with an IC-50 of <100 nM. **(C)** *Effects of MTDR on 3D mammosphere formation in MDA-MB-231 cells.* Note that MTDR inhibits 3D anchorage-independent growth in MDA-MB-231 cells, with an IC-50 between 100 and 500 nM. **(D)** *Effects of MTDR on 3D mammosphere formation in MDA-MB-468 cells.* Note that MTDR inhibits 3D anchorage-independent growth in MDA-MB-468 cells, with an IC-50 between 50 and 100 nM. The statistical test used was a one-tail unpaired t-test.

morphologically resemble the morula stage of embryonic development, a solid "ball" of cells without a hollow lumen. Under these culture conditions of non-attachment, the majority of epithelioid cancer cells die, *via* an unusual form of apoptosis, known as "anoikis" (29).

Remarkably, each single 3D mammosphere is constructed from the anchorage-independent clonal propagation of an individual CSC, and does not involve the process of self-aggregation, under these limiting dilution conditions. As a consequence, the growth of 3D spheroids provides functional culture conditions to select for a population of epithelioid CSCs, with EMT properties. As such this provides an ideal assay for identifying small molecules that can target the anchorage-independent growth of CSCs.

Figure 1B shows that MTDR potently inhibits 3D spheroid formation in MCF7 cells, with an IC-50 of less than 100 nM. Similarly, MTDR also inhibited the anchorage-independent growth of MDA-MB-231 cells, in the range of 100 to 500 nM (**Figure 1C**). Finally, MTDR inhibited 3D sphere formation in MDA-MB-468 cells, with an IC-50 of approximately 50 nM (**Figure 1D**). Therefore, MTDR is clearly effective in targeting CSCs, in both ER (+) and triple-negative breast cancer-derived cell lines, in the nano-molar range.

MTDR Specifically Inhibits Mitochondrial Metabolism

To validate the idea that MTDR was specifically targeting mitochondrial metabolism, we next subjected monolayer cultures to metabolic flux analysis, using the Seahorse XFe96 analyzer.

Figures 2, 3 and **Supplemental Figure S1** show the effects of MTDR on the mitochondrial oxygen consumption rate (OCR) in MCF7, MDA-MB-231 and MDA-MB-468 monolayer cells, respectively. In all three cell lines, MTDR treatment induced near complete inhibition of mitochondrial basal and maximal respiration and ATP production, starting at a concentration of 500 nM.

The extracellular acidification rate (ECAR), a measure of glycolytic function, remained largely unchanged in MCF7 and MDA-MB-468 cell monolayers, at levels of MTDR of up to 1 μM. Similarly, in MDA-MB-231 cells, the levels of glycolysis remained unchanged from 1 nM to 100 nM MTDR, but glycolysis was decreased at levels of 500 to 1,000 nM, especially for glycolytic reserve (**Figures 4, 5** and **Supplemental Figure S2**). Therefore, high nano-molar concentrations of MTDR, of 500 nM or greater, preferentially affected mitochondrial metabolism in all three breast cancer cell lines tested.

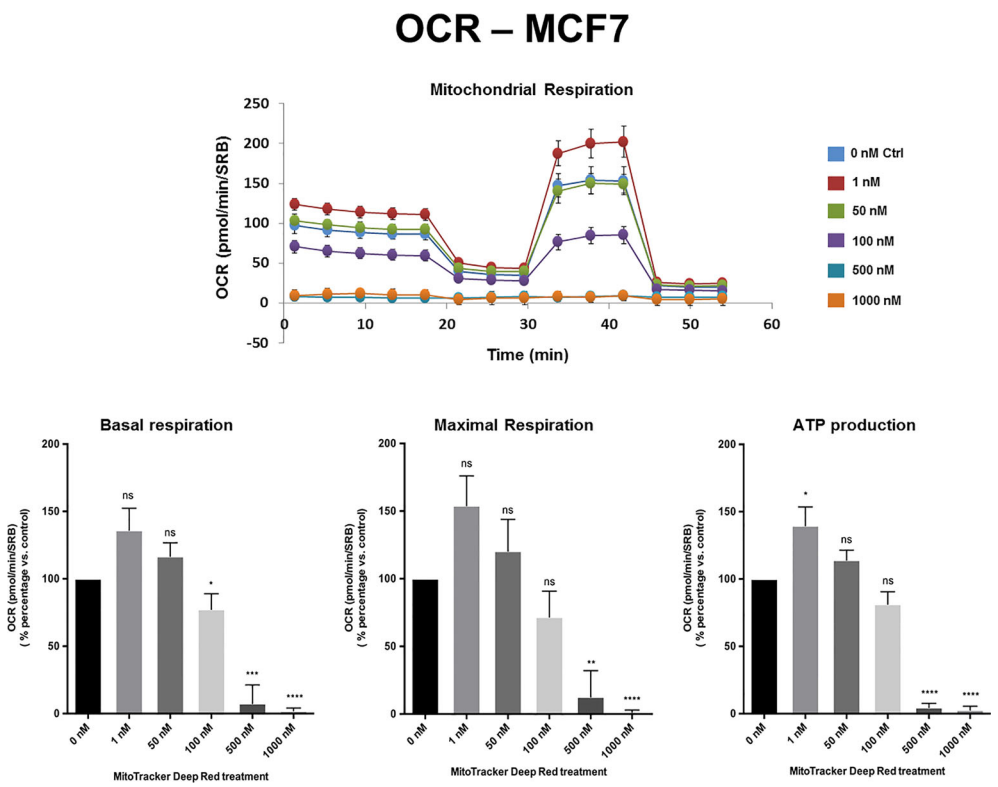

FIGURE 2 | MTDR potently inhibits the mitochondrial oxygen consumption rate (OCR) in MCF7 cells. A representative Seahorse tracing is shown, with bar graphs highlighting the quantitative, dose-dependent effects of MTDR on basal respiration, maximal respiration and ATP production. Note that MTDR treatment exhibits near complete inhibition of OCR in MCF7 cells at 500 nM. The statistical test used was a one-tail unpaired t-test.

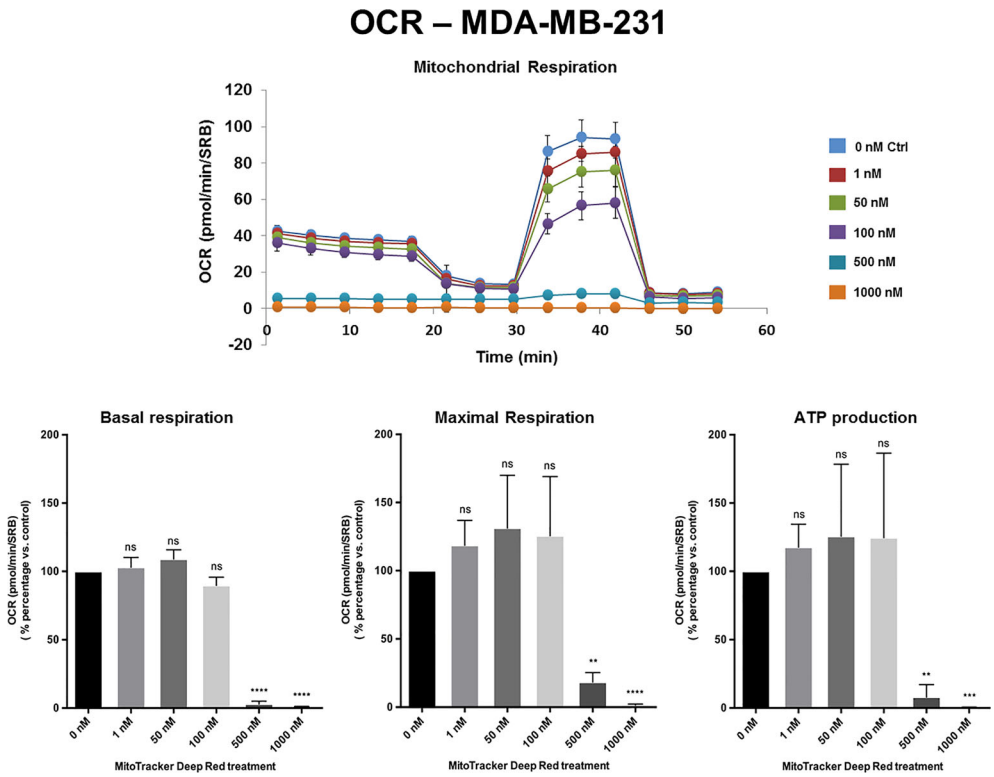

FIGURE 3 | MTDR potently inhibits the mitochondrial OCR in MDA-MB-231 cells. A representative Seahorse tracing is shown, with bar graphs highlighting the quantitative, dose-dependent effects of MTDR on basal respiration, maximal respiration and ATP production. Note that MTDR treatment exhibits near complete inhibition of OCR in MDA-MB-231 cells at 500 nM. The statistical test used was a one-tail unpaired t-test.

Validating the Metabolic Effects of MTDR in a CSC-Enriched MCF7 Cell Population

To further evaluate the metabolic effects of MTDR, we measured the mitochondrial-specific effects of MTDR on a CSC-enriched MCF7 cell population, using the Seahorse XFe96 Analyzer to perform the XF Cell Mito Stress Test.

Briefly, MCF7 cells were seeded for 3D-mammosphere formation and were grown for 5-days using the standard protocol, but in the absence or presence of MTDR at a lower concentration (100 nM), to avoid cell death. Then, the resulting 3D-mammospheres were collected, dissociated into single cells and subjected to OCR analysis.

Figure 6 shows that at a concentration as low as 100 nM, MDTR significantly inhibited OCR in this CSC-enriched MCF7 cell population. Under these conditions, mitochondrial ATP production was reduced by nearly 50%.

MTDR Preferentially and Selectively Targets Cancer Cells

To examine the selectivity of MTDR for the preferential targeting of cancer cells, we used a Hoechst-based viability assay. Briefly, MCF7, MDA-MB-231 and MDA-MB-468 cell monolayers were all treated with MTDR, at concentrations ranging from 1 nM to 1 μM, for a period of 72 hours and their viability was assessed using Hoechst 33342, a nuclear dye that stains DNA in live cells. The viability of normal human fibroblasts (hTERT-BJ1) treated with MTDR was also assessed in parallel. Quantitation was performed with a plate-reader.

Figure 7 shows that MTDR more effectively killed MCF7, MDA-MB-231 and MDA-MB-468, but was less effective on hTERT-BJ1 (a non-transformed fibroblast cell line). Therefore, MTDR was more potent and selective for the targeting of breast cancer cells, with little or no effect on normal fibroblast viability.

MCF7 Treatment With Other Near-Infrared (NIR) Compounds

To evaluate the anti-cancer properties other carbocyanine dyes with similar spectral emission as MTDR, we next selected three compounds with a spectral emission in the NIR range (**Figures 8** and **9**) and performed the MCF7 3D-mammosphere assay to assess their effect on CSC propagation. Namely, HITC, DDI and IR-780 were all tested, using the same nanomolar concentration range used for MTDR.

Figure 9 illustrates that both HITC and DDI significantly inhibited CSC propagation, between 100 and 1,000 nM. In contrast, IR-780, was not effective. In support of these findings, **Figure 8** shows that only HITC and DDI were efficiently incorporated into 3D-mammospheres, while IR780 was not taken up by MCF7 CSCs, at concentrations in the nanomolar range.

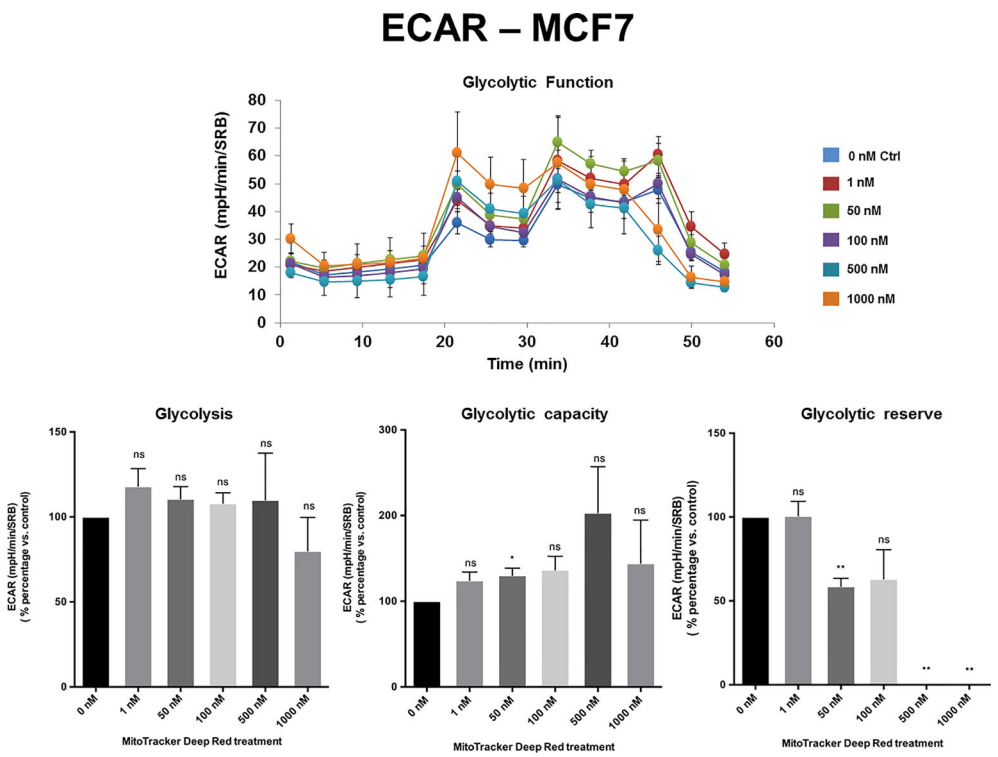

FIGURE 4 | MTDR has no effect on glycolysis in MCF7 cells. A representative Seahorse tracing is shown, with bar graphs highlighting the quantitative, dose-dependent effects of MTDR on glycolysis, glycolytic capacity and glycolytic reserve. Note that MTDR has no significant effect on glycolysis, at concentrations up to 1 μM. The statistical test used was a one-tail unpaired t-test.

To examine the effects of HITC and DDI on mitochondrial respiration and aerobic glycolysis, we treated adherent MCF7 and then measured their OCR and ECAR. **Supplemental Figure S3** shows that basal and maximal OCR, as well as ATP production levels, were both significantly inhibited, as compared to vehicle-alone control cells. In contrast, ECAR levels were increased significantly, at 500 and 1,000 nM (**Supplemental Figure S4**). Surprisingly, DDI did not affect OCR and ECAR in MCF7 cells (**Supplemental Figures S5**, **S6**).

In summary, our results indicate that HITC specifically targets mitochondrial metabolism and inhibits 3D-mammosphere formation. In contrast, DDI also inhibits 3D-mammosphere formation, but by a mitochondrial-independent mechanism. Finally, IR780 did not inhibit CSC propagation in the nanomolar range.

MCF7 Treatment With Cyanine 5 (Cy5) Analogs

To assess the possible anti-cancer properties of Cy5 lipophilic fluorophores, we next tested the potential inhibitory activity of seven commercially available Cy5 analogs (**Figure 10**).

We found that Cy5-Azide and Cy5-Alkyne analogs were the only two compounds out of seven, to significantly inhibit MCF7 3D-mammosphere formation, between 500 nM to 1,000 nM (**Figure 11**). However, all the Cy5 analogs were internalized by mammospheres, at low nanomolar concentrations (50 nM), independently from their anti-CSC effects, and suggesting that Cy5 retention lasts for days in CSCs (**Supplemental Figure S7**).

Furthermore, we found that both carbocyanine compounds (Cy5-Azide and Cy5-Alkyne) are mitochondrial OXPHOS inhibitors that act, in the range of 500 nM and 1000 nM, and they induce glycolysis to compensate for mitochondrial ATP depletion (data not shown).

MTDR Potently Inhibits Cancer Cell Tumor Growth and Metastasis *In Vivo*

To determine the potential therapeutic effects of MTDR *in vivo*, we next used a human breast cancer cell line, namely MDA-MB-231 cells, and the well-known chorio-allantoic membrane (CAM) assay in chicken eggs, to evaluate the effects of MTDR on tumor growth and metastasis (28, 30).

More specifically, an inoculum of 1 x 10^6 MDA-MB-231 cells was added on top of the Upper CAM of each egg (day E9). On day E10, tumors were detectable and they were then treated daily for 8 days with vehicle alone (1% DMSO in PBS) or MTDR. After 8 days of MTDR administration, on day E18 all tumors were weighed, and the Lower CAM was collected to evaluate the number of metastatic cells, as analyzed by qPCR with specific primers for Human Alu sequences.

Figure 12 shows the effects of MTDR on MDA-MB-231 tumor growth. Note that MTDR showed a significant effect on tumor growth, with inhibition of up to nearly 30%, as a result of the

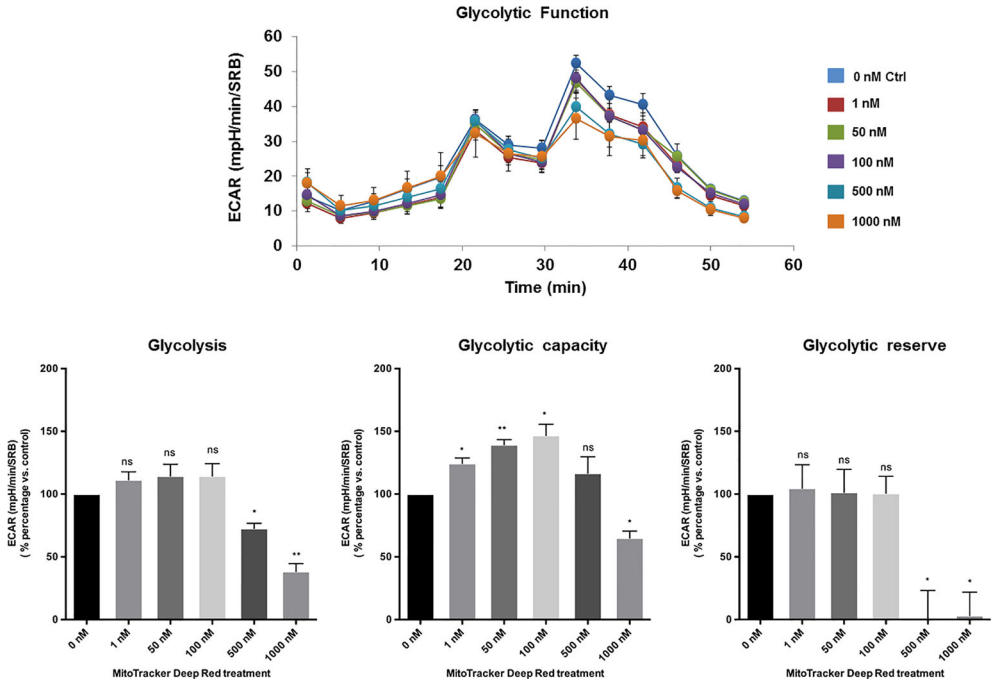

FIGURE 5 | MTDR has minor effects on glycolysis in MDA-MB-231 cells. A representative Seahorse tracing is shown, with bar graphs highlighting the quantitative, dose-dependent effects of MTDR on glycolysis, glycolytic capacity and glycolytic reserve. Note that MTDR has no significant effect on glycolysis, at concentrations up to 100 nM. Mild to moderate inhibition of glycolysis was only observed, starting at 500 nM. The statistical test used was a one-tail unpaired t-test.

8-day period of drug administration. In addition, MTDR showed significant effects on MDA-MB-231 cancer cell metastasis. **Figure 13** illustrates that MTDR inhibited metastasis (by >60%) at the same concentrations tested. Interestingly, the effects of MTDR on metastasis were significantly more pronounced.

Surprisingly, little or no embryo toxicity was observed for MTDR (**Figure 14**). Therefore, we conclude that MTDR can be further developed as an anti-cancer agent, for inhibiting both tumor growth and metastasis, without showing significant toxicity.

Abemaciclib, a CDK4/6 Inhibitor, Does Not Prevent Metastasis *In Vivo*

For comparison purposes, in parallel, we also assessed the functional activity of an FDA-approved CDK4/6 inhibitor, namely Abemaciclib, which was developed by Eli Lilly. Abemaciclib was first approved in 2017, with breakthrough status, for the treatment of breast cancer patients with advanced or metastatic disease. Results from the MONARCH 3 clinical trial indicated that there was significant clinical benefit for progression-free survival (28.18 versus 14.76 months; hazard ratio [95% confidence interval], 0.540 [0.418–0.698]; p = .000002). As a consequence, Abemaciclib is considered standard-of-care for patients with advanced or metastatic breast cancer (31).

Therefore, here we evaluated the efficacy of Abemaciclib, using the CAM assay, to measure its effects on MDA-MB-231 tumor growth, metastasis and embryo toxicity.

Interestingly, treatment with Abemaciclib (in a similar concentration range as with MTDR) resulted in the significant inhibition of tumor growth by up to 47%, at a 90 µM (**Figure 15A**). Importantly, little or no embryo toxicity was observed in this concentration range (**Figure 15B**). However, Abemaciclib was completely ineffective for the prevention of metastasis (**Figure 15C**).

Thus, as compared with the standard-of-care for advanced breast cancer (Abemaciclib), MTDR was clearly more effective for the prevention of metastatic dissemination, using MDA-MB-231 cells (**Figure 13**).

DISCUSSION

MTDR is a carbocyanine-based fluorescent probe that chemically behaves as a lipophilic cation. MTDR is functionally localized to mitochondria and is normally used to measure mitochondrial mass in living cells, by fluorescence microscopy and/or FACS analysis. Here, we assessed whether MTDR could be used to target mitochondria in CSCs, to prevent their anchorage-independent propagation. For this purpose, we used three independent breast cancer cell lines, namely MCF7, MDA-MB-231 and MDA-MB-468 cells, representing both ER(+) and triple-negative breast cancer sub-types. Remarkably, we observed that MTDR potently inhibited the

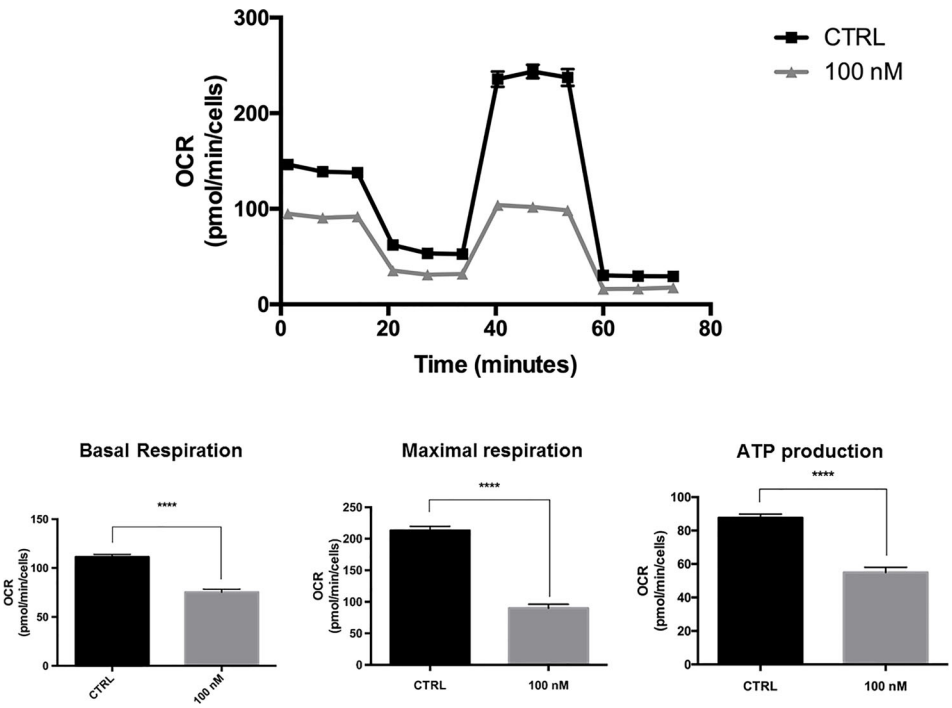

FIGURE 6 | MTDR potently inhibits the mitochondrial OCR in a CSC-enriched MCF7 cell population. A representative Seahorse tracing is shown, with bar graphs highlighting the quantitative effects of MTDR on basal respiration, maximal respiration and ATP production. Note that MTDR treatment exhibits inhibition of OCR at 100 nM. Briefly, MCF7 cells were seeded for 3D-mammosphere formation and were grown for 5-days using the standard protocol, but in the absence or presence of MTDR at a lower concentration (100 nM), to avoid cell death. Then, the resulting 3D-mammospheres were collected, dissociated into single cells and subjected to OCR analysis. Under these conditions, mitochondrial ATP production was reduced by nearly 50%. The statistical test used was a one-tail unpaired t-test.

3D propagation CSCs from all three cancer cell lines, using nanomolar concentrations of the near-infrared fluorescent probe. Furthermore, we directly validated that MTDR specifically targeted mitochondrial metabolism and induced ATP depletion, by using the Seahorse XFe96 metabolic flux analyzer. However, we did not see a significant induction of glycolysis by MTDR, in all three cell lines.

Originally, it was thought that MTDR could be used as a probe to measure mitochondrial mass, independently of mitochondrial activity or membrane potential. However, recent experiments directly show that MTDR staining is prevented and/or reduced by treatment with FCCP (carbonyl cyanide 4-(trifluoromethoxy) phenylhydrazone), a potent mitochondrial uncoupling agent (32). Therefore, MTDR may preferentially accumulate in highly-active mitochondria, potentially making it a better therapeutic drug for targeting and inhibiting mitochondrial function.

In addition, we found that other NIR compounds such as HITC and DDI, but not IR780, accumulate in MCF7 cells and inhibit CSC anchorage-independent growth. Our results demonstrated that HITC effectively blocks CSCs growth in a mitochondrial-dependent manner, and induces glycolysis starting at 500 nM. In contrast, we showed that DDI, did not produce any noticeable metabolic effects, but was able to inhibit CSC growth in the nanomolar range in MCF7 cells. Furthermore, we showed that IR-780 was not effective against CSCs growth and was not internalized by tumor cells, at nanomolar concentrations. Thereafter, we compared seven Cy5 carbocyanine analogs with different reactive groups for their ability to inhibit MCF7 CSC growth. Our results showed that all compounds tested were internalized after five days of treatment (**Supplemental Figure S7**). However, only Cy5-Alkyne and Cy5-Azide blocked 3D mammosphere growth and also targeted energized mitochondria in cancer cells (data not shown) within the nanomolar range, which is line with previous studies (33).

We have previously shown that other lipophilic cations, such as derivatives of triphenyl-phosphonium (TPP) (34), can be effectively used to target mitochondria in CSCs, significantly preventing 3D mammosphere formation. However, these TPP derivatives were much less potent, inhibiting 3D spheroid formation in MCF7 cells, with an IC-50 between 500 nM to 5 μM. Therefore, MTDR is clearly more potent than these TPP-derivatives, such as 2,4-dichlorobenzyl-TPP, 1-naphthylmethyl-TPP, 3-methylbenzyl-TPP, 2-chlorobenzyl-TPP, and 2-butene-1,4-bis-TPP. As such, MTDR, HITC, Cy5-Alkyne and Cy5-Azide are clearly more efficacious.

Interestingly, in our work, we identified four carbocyanines that target mitochondria (MTDR, HITC, Cy5-Alkyne and Cy5-Azid) and we found that DDI did not target mitochondria, but it showed the same potency in inhibiting CSC growth. In contrast, IR-780 at nanomolar concentrations, was not internalized and this is in line with previous *in vitro* studies (23). The fact that IR-780 at

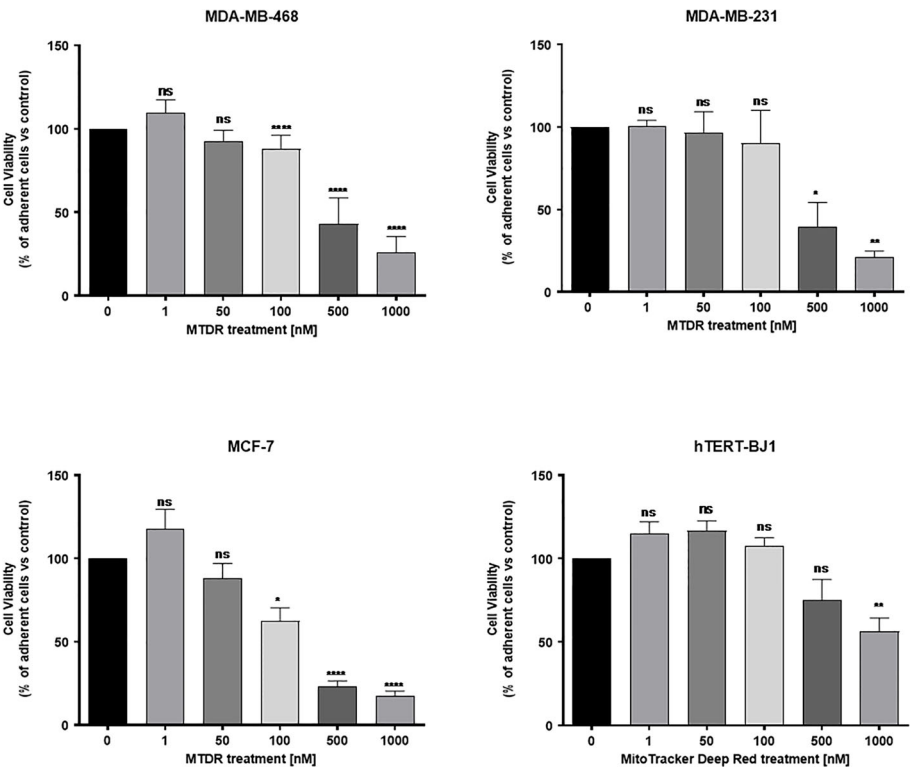

FIGURE 7 | MTDR preferentially and selectively targets cancer cells. MCF7, MDA-MB-231 and MDA-MB-468 cell monolayers were all treated with MTDR for a period of 72 hours and viability was assessed using Hoechst 33342, a nuclear dye that stains DNA in live cells. Effects of MTDR on the viability in normal human fibroblasts (hTERT-BJ1) were assessed in parallel. Note that MTDR effectively killed MCF7, MDA-MB-231 and MDA-MB-468 cells, but had little or no effect on normal cell viability (hTERT-BJ1), in the same concentration range. Therefore, MTDR was more potent and selective for the targeting of breast cancer cells, relative to normal fibroblasts. The statistical test used was a one-tail unpaired t-test.

nanomolar concentrations does not have anti-tumor activity (23, 35), highlights that MTDR, HITC, Cy5-Alkyne and Cy5-Azide are all more effective in eradicating CSCs than IR-780.

In principal, "energized" cancer cell mitochondria present a higher membrane potential (about ~60 mV more negative than in normal cells) (36). Therefore, mitochondria in cancer cells produce more ATP and play a key role for CSC metastatic growth. Indeed, our results are in line with the general theory that CSC strictly depend on mitochondria. We report that in our experiments that glycolysis alone was not sufficient to allow for 3D mammosphere formation, when OCR was targeted by carbocyanines in breast cancer cells. We speculate, as previously demonstrated elsewhere (21), that the lipophilic carbocyanine mechanism of action is through chemical alkylation between electrophilic carbocyanines and nucleophilic atoms within cysteine residues found in mitochondrial proteins (chemical intoxication). In addition, the low pH of the mitochondrial matrix increases chemical alkylation reactions that generate electrophile-protein adducts that are toxic to tumor cells. Therefore, one can speculate that this "non-selective", chemical intoxication by carbocyanines would presumably allow the avoidance of possible resistance to such broad, but yet organelle-specific, intoxication of cancer cell mitochondria.

Indeed, after observing the Cy5-Alkyne mitochondrial-dependent inhibition of breast CSCs, the same analog was found to show anti-tumor effect, both in *in vitro* and *in vivo*, in the nanomolar range (33), further confirming our findings. Interestingly, Cy5-NHS was found to successfully deliver nanoparticles and other compounds such as doxorubicin to mitochondria, and to retain their mitochondrial targeting of tumor cells. Furthermore, in other *in vivo* studies, they found that carbocyanines have a strong safety profile, with low toxicity and fast clearance as theranostic agents, and are considered non-toxic agents for cell live imaging applications *in vitro* (17). Furthermore, acute toxicity studies conducted on mice using 100 nM concentrations of IR-780 demonstrated no acute toxicity, and low organ accumulation was observed (25).

Lipophilic carbocyanine uptake has been found to depend on the Organic Anionic Transporter Protein (OATP) family of transporters (37). OATP transporters function as non-selective sodium-independent co-transporter proteins that regulate the flux of ions and small molecules across the plasma membrane of the cell (e.g., bile salts, bilirubin, steroids and thyroid hormones) (38). OATP transporters influx of small molecules is coupled to the passive efflux of intracellular bicarbonate, glutathione and glutathione adducts. Interestingly, the OATP1B3 isoform was previously described to selectively transport Cy5.5, IR-780 as well

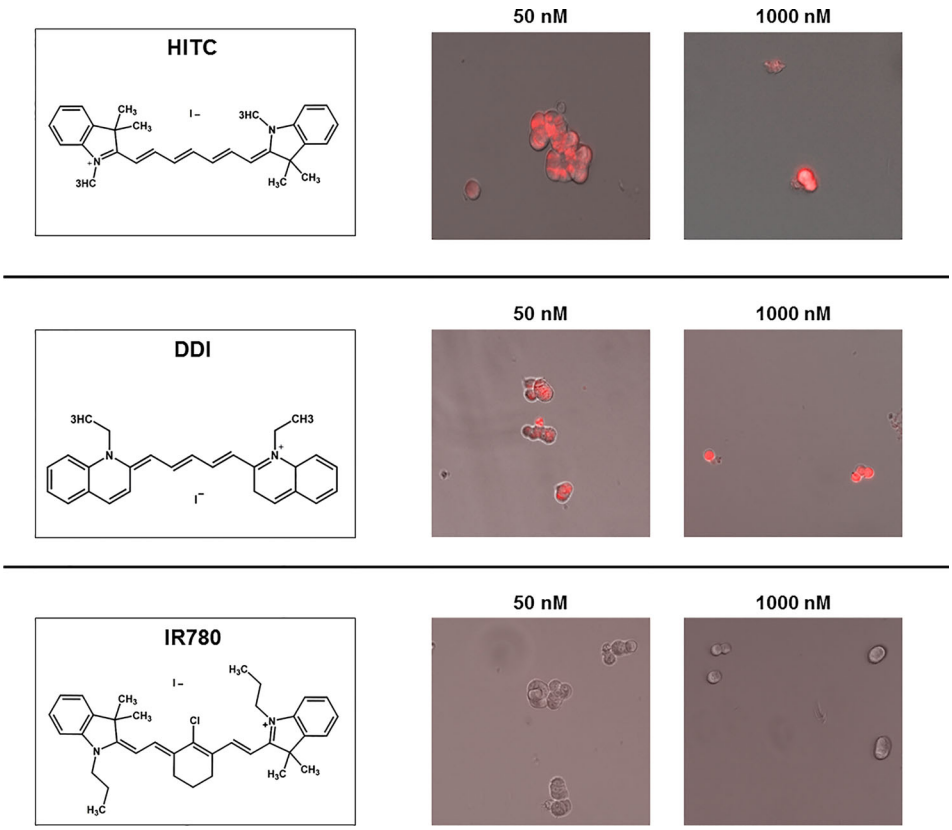

FIGURE 8 | Structure and uptake of NIR compounds in MCF7 cells. (Left). Near-infrared (NIR) compounds. Chemical structures of HITC (B-1,1',3,3,3',3'-Hexamethylindotricarbocyanine iodide), DDI (1,1'Diethyl-2-2'-dicarboccyanine iodide) and IR780 (2-[2-[2-Chloro-3-[(1,3-dihydro-3,3-dimethyl-1-propyl-2H-indol-2-ylidene)ethylidene]-1-cyclohexen-1-l]ethenyl]-3,3-dimethyl-1-propylindolium iodide). NIR compounds present a characteristic peak fluorescent emission in the NIR light spectrum. (Middle and Right). MCF7 mammosphere cellular uptake. Treatment of mammospheres using 50 nM and 1000 nM concentrations of HITC, DDI and IR780 for five days. Note that HITC and DDI is localized within the cell and was observed with the Cy5 channel (near infrared signal), whereas IR780 cellular uptake was not detectable, even at higher concentrations.

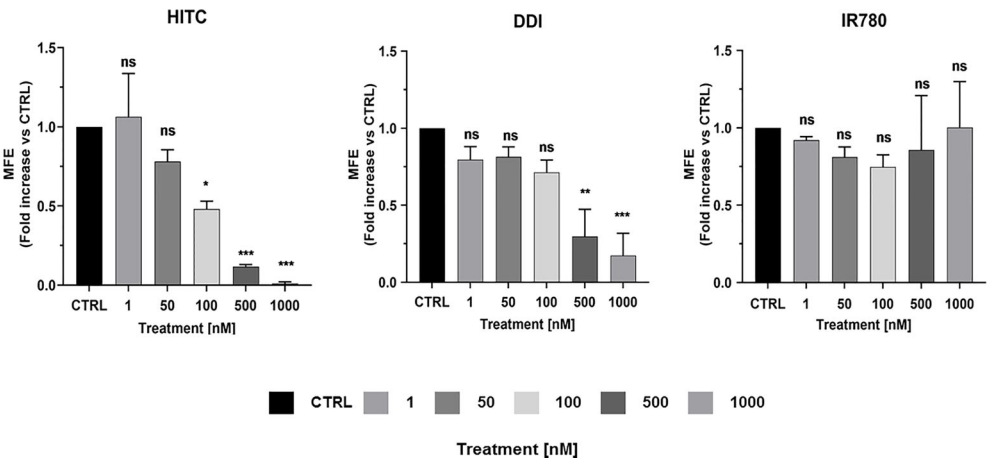

FIGURE 9 | HITC and DDI behave as cancer stem cell inhibitors. Non-adherent MCF7 cells were treated using different drug concentrations of HITC, DDI and IR780 (1, 50, 100, 500, 1,000 nM) for five days and then mammospheres were counted. Data are expressed as fold increase Vs control. Statistical analysis was conducted using one-way ANOVA.

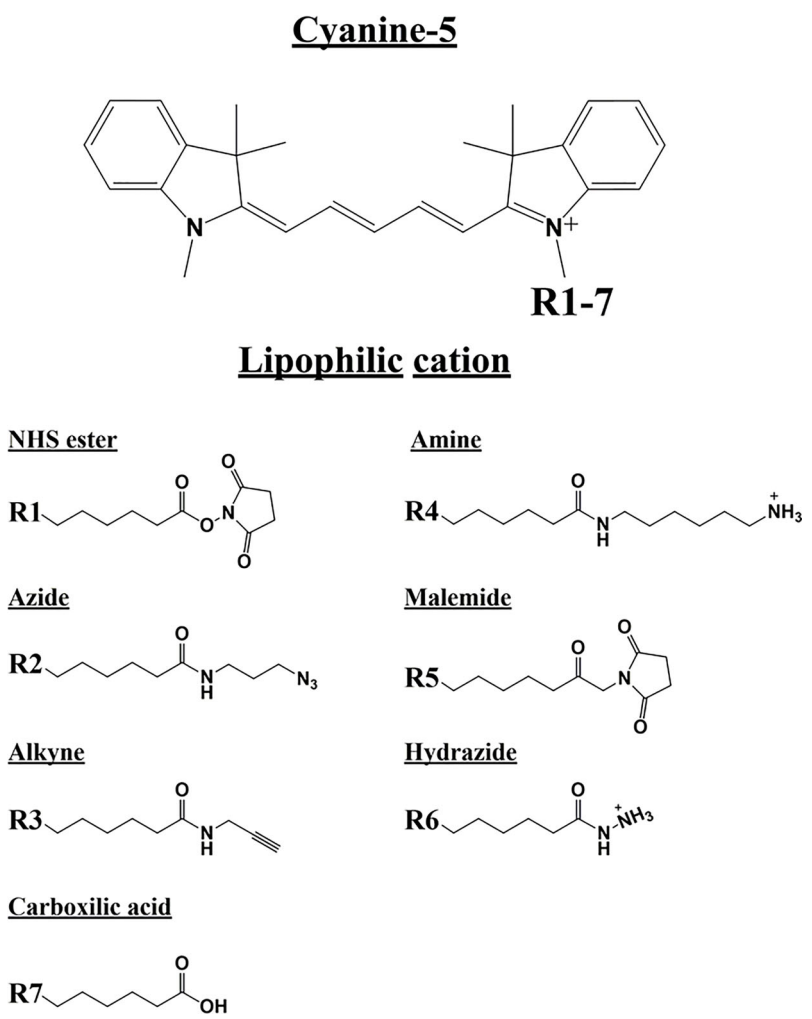

FIGURE 10 | Cyanine 5 structure and analogue structures. Upper: The chemical structure of cyanine 5 compounds is characterized by a polymethine bridge in between the two nitrogen atoms. The positive charge (+) is delocalized within the scaffold on one of the two amine groups (N+). The amine group can be used to attach several different side chains (R1-7). Lower: Below are different Cyanine 5 analogue with their side chain structure highlighted.

as Cy5-Alkyne heptamethine carbocyanines both *in vitro* and *in vivo* (37, 39–42). Furthermore, OATPs expression in cells was found to be induced by hypoxia, i.e., lowering oxygen conditions or inducing pseudo-hypoxia *via* DMOG (dimethyloalyglycine) treatment. OATP expression is positively regulated by the transcription factor of hypoxia induction factor 1 (HIF1α). Therefore, cellular hypoxia increases carbocyanine uptake in tumor cells *via* OATP (33, 42), suggesting that hypoxic cancer cells would be more susceptible to carbocyanines, as compared to normoxic cells, and can be preferentially eliminated by using mitochondrially-targeted carbocyanine dyes.

The *de novo* expression of OATP1B3 and 1B1, in general, is considered specific for the liver, but it was found to increase in several tumors. In breast cancer tissue, as well as other cells lines, OATP1B3 transporters are upregulated (38). However, in normal breast tissue, it is absent. Hence, we believe that carbocyanine absorption could depend on OATP functional expression also for breast CSCs. Therefore, in addition to carbocyanine's chemical electrophilic properties previously discussed, we must consider the key role of OATP in carbocyanines uptake by CSCs. As far as we are aware, OATP expression has not been examined in CSCs and should be further investigated.

Thiol reactive groups are present in both MTDR and IR-780 carbocyanine structures and are thought to react with cysteine residues through *meso*-chlorine motility inside their chemical structure. Nevertheless, we observed that MTDR, compared to IR-780, was more potent in mitochondrial inhibition. A possible explanation is that IR-780 is a Cy7, whereas MTDR is Cy5 member, indicating specific chemical differences between carbocyanine families regarding their potential anti-tumor properties. Nevertheless, Cy7 compounds, such as HITC, goes against such a hypothesis as it blocked mitochondrial respiration in the nanomolar range, and it is a heptamethine without *meso*-

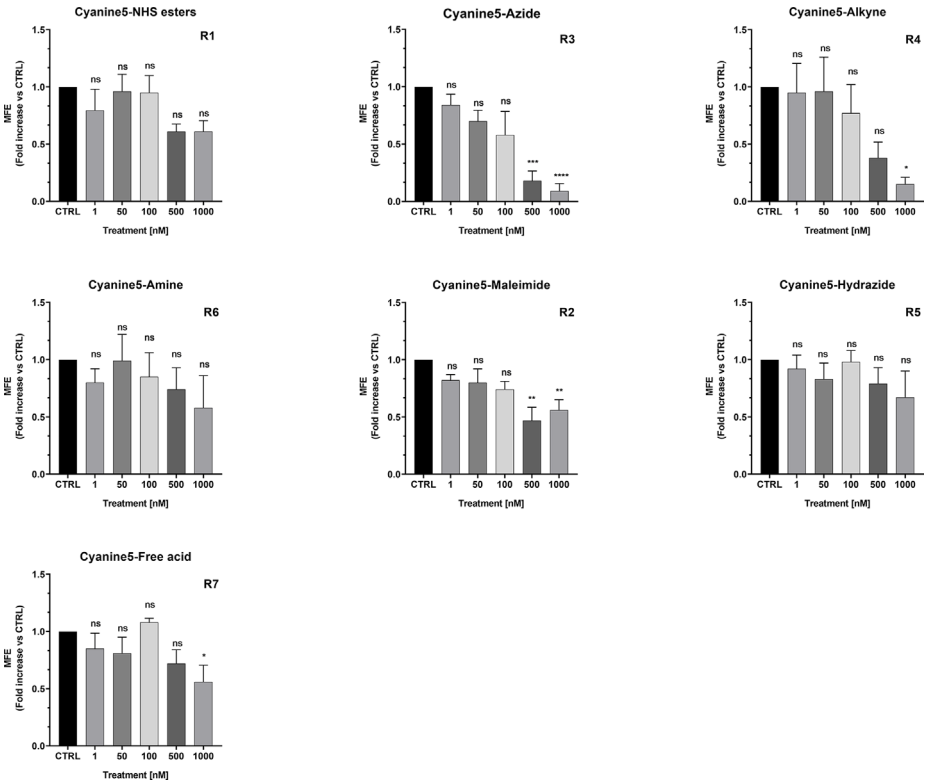

FIGURE 11 | Effects of Cyanine 5 on 3D mammosphere formation in MCF7 cells. MCF7 mammospheres cells were treated with different concentrations of each compound (1, 50, 100, 500 and 1,000 nM) for five days. Mammospheres >50-µm were counted manually using a bright field microscope (n = 4). Data is expressed as fold increase Vs control. Statistical analysis was conducted using one-way ANOVA.

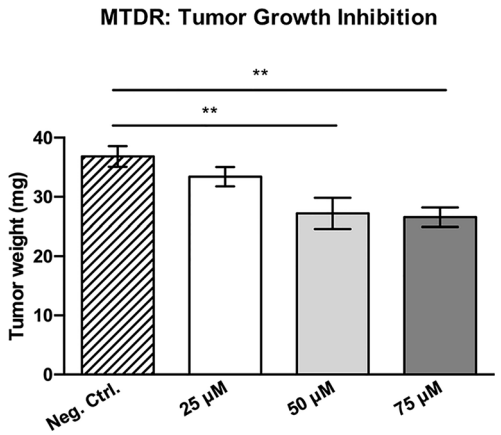

FIGURE 12 | MTDR significantly inhibits tumor growth. MDA-MB-231 cells and the well-established chorio-allantoic membrane (CAM) assay in chicken eggs were used to quantitatively measure tumor growth. See Materials & Methods for specific details. After 8 days of MTDR administration, on day E18 all tumors were weighed. Note that MTDR significantly inhibited tumor growth, by up to nearly 30%, at a concentration of 75 µM (n ≥ 15). Averages are shown ± SEM. **p < 0.01; *p < 0.05. Statistical analysis was conducted using ANOVA.

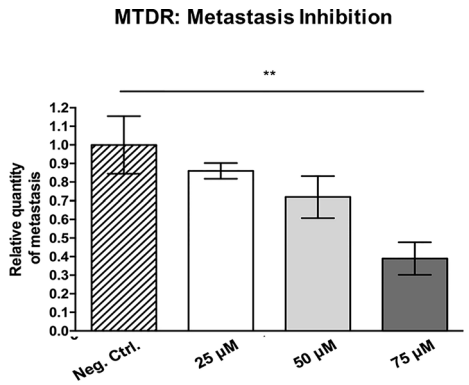

FIGURE 13 | MTDR preferentially targets and prevent cancer cell metastasis. MDA-MB-231 cells and the well-established chorio-allantoic membrane (CAM) assay in chicken eggs were used to quantitatively measure spontaneous tumor cell metastasis. See Materials & Methods for specific details. After 8 days of drug administration, the Lower CAM was collected to evaluate the number of metastatic cells, as analyzed by qPCR with specific primers for Human Alu sequences. Note that MTDR showed significant effects on MDA-MB-231 metastasis, with an inhibition of >60%, at a concentration of 75 µM (n ≥ 7). Averages are shown ± SEM. **p < 0.01. Statistical analysis was conducted using ANOVA.

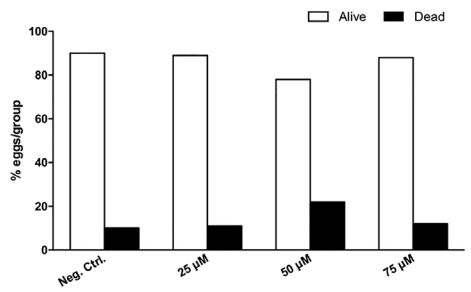

FIGURE 14 | Chick embryo toxicity of MTDR. Note that MTDR was non-toxic, as compared to the vehicle alone control (n ≥ 17), over a dose range of 25, 50, and 75 µM.

chlorin motility. As such, the differences observed between IR-780 and MTDR anti-CSC efficacy may account for other chemical properties. In addition, an FDA-approved carbocyanine Indocyanines green (ICG), which is very similar to IR-780, and is used as an optical marker routinely in the clinic, is not taken up by tumor cells. One possible explanation that was advanced is that ICG is missing a thiol reactive group, which is responsible for IR-780 adduct formation in tumors (22).

In a recent study, human serum albumin (HSA) was found to bind to IR-780 carbocyanines, *via* reactive thiol group to albumin cysteine residues (22), which explains its rapid decrease in the blood (approximately 30 minutes in the serum for IR-780-like dies). They found that IR-780 generated a higher fluorescent signal in the serum compared to ICG (that does not bind to albumin), and they speculate that IR-780-albumin adducts increase the half-life and the tumor uptake capacity of carbocyanines. Interestingly, Usama et al. also reported that IR-780 albumin-adduct uptake by glioblastoma cells was not inhibited by BSP, or increased by DMOG (hypoxia inducer). However, it was abolished only by applying low temperatures (4°C), which strongly suggests an OATP-independent mechanism of uptake for IR-780-albumin adducts.

Overall, in this work, we have shown how the energetic state of malignant cancer cells can be targeted *via* "tumor-seeking" drugs, by taking advantage of the chemical properties of carbocyanine dyes. Hence, we believe that based on our findings, both *in vitro* and *in vivo*, that carbocyanine-induced mitochondrial cytotoxicity should be generally applicable for preventing CSC-driven metastatic growth, and could be used as a preventive treatment against breast cancer relapse, either shortly after or concurrently with chemo- or radiation therapy.

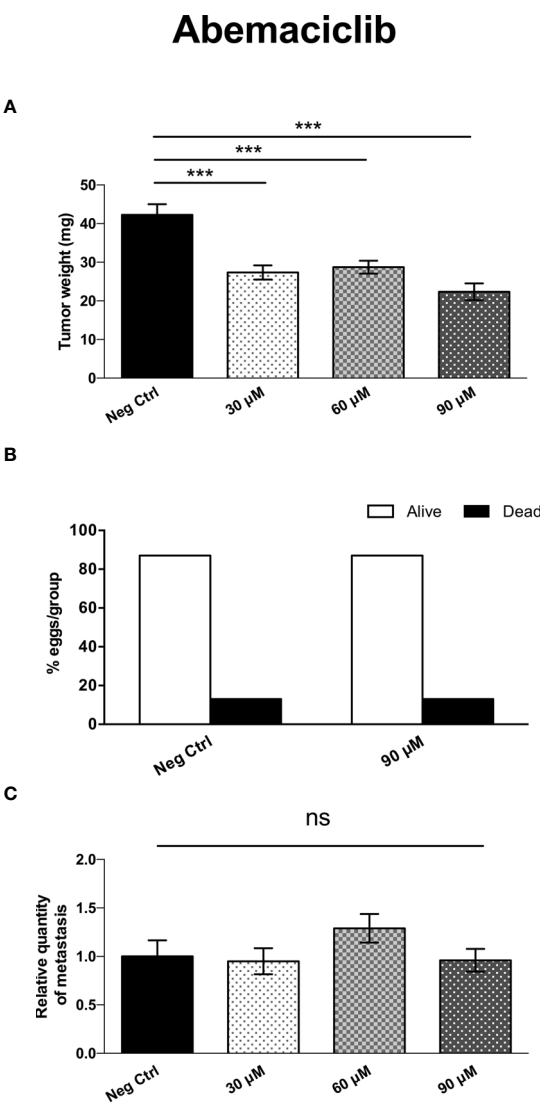

FIGURE 15 | Abemaciclib significantly inhibits tumor growth, without preventing cancer cell metastasis. **(A)** MDA-MB-231 cells and the well-established chorio-allantoic membrane (CAM) assay in chicken eggs were used to quantitatively measure tumor growth. See Materials & Methods for specific details. After 8 days of Abemaciclib administration, on day E18 all tumors were weighed. Note that Abemaciclib significantly inhibited tumor growth, by nearly 50%, at a concentration of 90 µM (n > 11). Averages are shown ± SEM. ***p < 0.001. Statistical analysis was conducted using ANOVA. **(B)** Note that Abemaciclib was non-toxic, as compared to the vehicle alone control (n > 15), up to 90 µM. **(C)** MDA-MB-231 cells and the well-established chorio-allantoic membrane (CAM) assay in chicken eggs were used to quantitatively measure spontaneous tumor cell metastasis. See Materials & Methods for specific details. After 8 days of drug administration, the Lower CAM was collected to evaluate the number of metastatic cells, as analyzed by qPCR with specific primers for Human Alu sequences. Note that Abemaciclib did not show any significant effects on MDA-MB-231 metastasis, at concentrations up to 90 µM (n = 8). Averages are shown + SEM. ns, not significant. Statistical analysis was conducted using ANOVA.

CONCLUSIONS

In conclusion, here we show that MTDR can be used effectively as a metabolic inhibitor to target mitochondrial function and halt CSC propagation, in the nano-molar range. The metabolic effects of MTDR on mitochondrial OCR and ATP production were directly validated, using the Searhorse XFe96 flux analyzer. Therefore, we propose that MTDR, and other related compounds, could be

repurposed, as potent and selective anti-cancer agents, to target the CSC population, in a variety of cancer types.

DATA AVAILABILITY STATEMENT

The original contributions presented in the study are included in the article/**Supplementary Material**. Further inquiries can be directed to the corresponding authors.

AUTHOR CONTRIBUTIONS

ML, FS, and CS conceived and initiated this project. Experiments described in this paper were performed by CS, a post-doctoral fellow in the Lisanti/Sotgia laboratory, and SS, a placement student, as well as ZM, a PhD student. ML and FS wrote the first draft of the manuscript, which was then further edited by CS. All authors contributed to the article and approved the submitted version.

FUNDING

This work was supported by research grant funding, provided by Lunella Biotech, Inc. The funder, Lunella Biotech, Inc., only provided the necessary monetary resources to carry out the current study.

ACKNOWLEDGMENTS

We are grateful to Rumana Rafiq, for her kind and dedicated assistance, in keeping the Translational Medicine Laboratory at Salford running very smoothly. We would like to thank the Foxpoint Foundation and the Healthy Life Foundation for their philanthropic donations, towards new equipment and infrastructure, in the Translational Medicine Laboratory at the University of Salford. We are thankful to Inovotion, Inc. (Grenoble, France), for independently performing the tumor growth and metastasis studies, using the CAM assay, as well as evaluating chicken embryo toxicity, through a research contract with Lunella Biotech, Inc. (Ottawa, Canada). We also thank Luma Godoy Magalhães for determining the solubility of Abemaciclib.

SUPPLEMENTARY MATERIAL

The Supplementary Material for this article can be found online at: https://www.frontiersin.org/articles/10.3389/fonc.2021.678343/full#supplementary-material

Supplementary Figure 1 | MTDR potently inhibits the mitochondrial oxygen consumption rate in MDA-MB-468 cells. A representative Seahorse tracing is shown, with bar graphs highlighting the quantitative, dose-dependent effects of MTDR on basal respiration, maximal respiration and ATP production. Note that MTDR treatment exhibits near complete inhibition of OCR in MDA-MB-468 cells at 500 nM. The statistical test used was an unpaired one-tail t-test.

Supplementary Figure 2 | MTDR has no effect on glycolysis in MDA-MB-468 cells. A representative Seahorse tracing is shown, with bar graphs highlighting the quantitative, dose-dependent effects of MTDR on glycolysis, glycolytic capacity and glycolytic reserve. Note that MTDR has no significant effect on glycolysis, at concentrations up to 1 μM. The statistical test used was an unpaired one-tail t-test.

Supplementary Figure 3 | HITC inhibits mitochondria aerobic respiration. Adherent MCF7 cells were treated with HITC using five different concentrations for 16 hours. After treatment, the mitochondrial oxygen consumption rate (OCR) was measured using the Seahorse XFe96 analyzer. Data is expressed as percentage of OCR vs control. All data was normalized for cell number. Statistical analysis was conducted using one-way ANOVA.

Supplementary Figure 4 | HITC induces glycolysis. Adherent MCF7 cells were treated with HITC using five different concentrations for 16 hours. After treatment, the extracellular acidification rate (ECAR) was measured using the Seahorse XFe96 analyzer. Data is expressed as percentage of ECAR vs control. All data was normalized for cell number. Statistical analysis was conducted using one-way ANOVA.

Supplementary Figure 5 | DDI does not inhibit mitochondria aerobic respiration. Adherent MCF7 cells were treated with DDI using five different concentrations for 16 hours and the mitochondrial OCR was measured using the Seahorse XFe96 analyzer. Data is expressed as percentage of OCR vs control. Statistical analysis was conducted using one-way ANOVA.

Supplementary Figure 6 | DDI does not induce glycolysis. Adherent MCF7 cells were treated with DDI using five different treatment concentrations, the ECAR was measured using the Seahorse XFe96 analyzed. Data is expressed as percentage of ECAR vs control. Statistical analysis was conducted using one-way ANOVA.

Supplementary Figure 7 | Cyanine 5 analog uptake by MCF7 mammospheres. Microscopy analysis of MCF7 dye internalization at a concentration 50 nM for each analog was detected in the Cy5 fluorescent channel (red) and is visualized with nuclear staining detected in the DAPI channel (blue). Images were acquired with an EVOS fluorescent microscope, using Cy5 channel and a 20x objective.

REFERENCES

1. Luo M, Wicha MS. Targeting Cancer Stem Cell Redox Metabolism to Enhance Therapy Responses. *Semin Radiat Oncol* (2019) 29(1):42–54. doi: 10.1016/j.semradonc.2018.10.003
2. Sehl M, Wicha MS. Modelling of Interaction Between Cancer Stem Cells and Their Microenviroment: Prediciting Clinical Response. *Methods Mol Biol* (2018) 1711:333–49. doi: 10.1007/978-1-4939-7493-1_16
3. De Francesco E, Sotgia F, Lisanti MP. Cancer Stem Cells (CSCs): Metabolic Strategies for Their Identification and Eradication. *Biochem J* (2018) 475 (9):1611–34. doi: 10.1042/BCJ20170164
4. Martinez-Outschoorn U, Peiris-Pagés M, Pestell RG, Sotgia F, Lisanti MP. Cancer Metabolism: A Therapeutic Perspective. *Nat Rev Clin Oncol* (2017) 14 (1):11–31. doi: 10.1038/nrclinonc.2017.1
5. Sotgia F, Ozsvari B, Fiorillo M, De Francesco EM, Bonuccelli G, Lisanti MP. A Mitochondrial Based Oncology Platform for Targeting Cancer Stem Cells (CSCs). *Cell Cycle* (2018) 17(17):2091–100. doi: 10.1080/15384101.2018.1515551
6. Fiorillo M, Sotgia F, Lisanti MP. "Energetic" Cancer Stem Cells (E-CSCs): A New Hyper-Metabolic and Proliferative Tumor Cell Phenotype, Driven by Mitochondrial Energy. *Front Oncol* (2018) 8:677. doi: 10.3389/fonc.2018.00677
7. Sotgia F, Fiorillo M, Lisanti MP. Hallmarks of the Cancer Cell of Origin: Comparisons With "Energetic" Cancer Stem Cells (E-CSCs). *Aging (Albany NY)* (2019) 11(3):1065–8. doi: 10.18632/aging.101822
8. Scatena C, Roncella M, Di Paolo A, Aretini P, Menicagli M, Fanelli G, et al. Doxycycline, An Inhibitor of Mitochondrial Biogenesis, Effectively Reduces Cancer Stem Cells (CSCs) in Early Breast Cancer Patients: A Clinical Pilot Study. *Front Oncol* (2018) 8:452. doi: 10.3389/fonc.2018.00452
9. Yuan J, Yi X, Yan F, Wang F, Qin W, Wu G, et al. Near-Infrared Fluorescence Imaging of Prostate Cancer Using Heptamethine Carbocyanine Dyes. *Mol Med Rep* (2015) 11:821–8. doi: 10.3892/mmr.2014.2815

10. Zhao N, Zhang C, Zhao Y, Bai B, An J, Zhang H, et al. Optical Imaging of Gastric Cancer With Near-Infrared Heptamethine Carbocyanine Fluorescence Dyes. *Oncotarget* (2016) 7(35):57277–89. doi: 10.18632/oncotarget.10031
11. Yang X, Shao C, Wang R, Chu CY, Hu P, Master V, et al. Optical Imaging of Kidney Cancer With Novel Near Infrared Heptamethine Carbocyanine Fluorescent Dyes. *J Urol* (2013) 189:702–10. doi: 10.1016/j.juro.2012.09.056
12. An J, Zhao N, Zhang C, Zhao Y, Tan D, Zhao Y, et al. Heptamethine Carbocyanine DZ-1 Dye for Near-Infrared Fluorescence Imaging of Hepatocellular Carcinoma. *Oncotarget* (2017) 8:56880–92. doi: 10.18632/oncotarget.18131
13. Zhang C, Zhao Y, Zhang H, Chen X, Zhao N, Tan D, et al. The Application of Heptamethine Cyanine Dye DZ-1 and Indocyanine Green for Imaging and Targeting in Xenograft Models of Hepatocellular Carcinoma. *Int J Mol Sci* (2017) 18(6):1332. doi: 10.3390/ijms18061332
14. Luo S, Tan X, Qi Q, Guo Q, Ran X, Zhang L, et al. A Multifunctional Heptamethine Near-Infrared Dye for Cancer Theranosis. *Biomaterials* (2013) 34(9):2244–51. doi: 10.1016/j.biomaterials.2012.11.057
15. Wu JB, Shi C, Chu GC, Xu Q, Zhang Y, Li Q, et al. Near-Infrared Fluorescence Heptamethine Carbocyanine Dyes Mediate Imaging and Targeted Drug Delivery for Human Brain Tumor. *Biomaterials* (2015) 67:1–10. doi: 10.1016/j.biomaterials.2015.07.028
16. Yang X, Shi C, Tong R, Qian W, Zhau HE, Wang R, et al. Near IR Heptamethine Cyanine Dye-Mediated Cancer Imaging. *Clin Cancer Res* (2010) 16:2833–44. doi: 10.1158/1078-0432.CCR-10-0059
17. Zhang C, Liu T, Su YP, Luo SL, Zhu Y, Tan X, et al. A Near-Infrared Fluorescent Heptamethine Indocyanine Dye With Preferential Tumor Accumulation for *In Vivo* Imaging. *Biomaterials* (2010) 31(25):6612–7. doi: 10.1016/j.biomaterials.2010.05.007
18. Luo S, Yang X, Shi ,C. Newly Emerging Theranostic Agents for Simultaneous Cancer Targeted Imaging and Therapy. *Curr Med Chem* (2016) 23:483–97. doi: 10.2174/0929867323666151223095718
19. Gao M, Yu F, Lv C, Choo J, Chen L. Fluorescent Chemical Probes for Accurate Tumor Diagnosis and Targeting Therapy. *Chem Soc Rev* (2017) 46:2237–71. doi: 10.1039/c6cs00908e
20. Tan X, Luo S, Wang D, Su Y, Cheng T, Shi C. A NIR Heptamethine Dye With Intrinsic Cancer Targeting, Imaging and Photosensitizing Properties. *Biomaterials* (2012) 33(7):2230–9. doi: 10.1016/j.biomaterials.2011.11.081
21. Vayalil P, Oh J-Y, Zhou F, Diers AR, Smith MR, Golzarian H, et al. A Novel Class of Mitochondria-Targeted Soft Electrophiles Modifies Mitochondrial Proteins and Inhibits Mitochondrial Metabolism in Breast Cancer Cells Through Redox Mechanisims. *PloS One* (2015) 3(10):e0120460. doi: 10.1371/journal.pone.0120460
22. Usama S, Lin CM, Burgess K. On the Mechanisim of Uptake of Tumor-Seeking Cyanine Dyes. *Bioconj Chem* (2018) 29:3886–95. doi: 10.1021/acs.bioconjchem.8b00708
23. Pais-Silva C, de Melo-Diogo D, Correia IJ. IR780-Loaded TPGS-TOS Micelles for Breast Cancer Photodynamic Therapy. *Eur J Pharm Biopharm* (2017) 113:108–17. doi: 10.1016/j.ejpb.2017.01.002
24. Alves CG, Lima-Sousa R, de Melo-Diogo D, Louro RO, Correia IJ. IR780 Based Nanomaterials for Cancer Imaging and Photothermal, Photodynamic and Combinatorial Therapies. *Int J Pharm* (2018) 542(1-2):164–75. doi: 10.1016/j.ijpharm.2018.03.020
25. Zhang CWS, Xiao J, Tan X, Zhu Y, Su Y, Cheng T, et al. Sentinel Lymph Node Mapping by a Near-Infrared Fluorescent Heptamethine Dye. *Biomaterials* (2010a) 7(31):1911–7. doi: 10.1016/j.biomaterials.2009.11.061
26. Farnie G, Sotgia F, Lisanti MP. High Mitochondrial Mass Identifies a Sub-Population of Stem-Like Cancer Cells That Are Chemo-Resistant. *Oncotarget* (2015) 6(31):30472–86. doi: 10.18632/oncotarget.5401
27. Lamb R, Harrison H, Hulit J, Smith DL, Lisanti MP, Sotgia F. Mitochondria as New Therapeutic Targets for Eradicating Cancer Stem Cells: Quantitative Proteomics and Functional Validation *Via* MCT1/2 Inhibition. *Oncotarget* (2014) 5(22):11029–37. doi: 10.18632/oncotarget.2789
28. Nascimento BFO, Laranjo M, Pereira NAM, Dias-Ferreira J, Pineiro M, Botelho MF, et al. Ring-Fused Diphenylchlorins as Potent Photosensitizers for Photodynamic Therapy Applications: *In Vitro* Tumor Cell Biology and *In Vivo* Chick Embryo Chorioallantoic Membrane Studies. *ACS Omega* (2019) 4(17):17244–50. doi: 10.1021/acsomega.9b01865
29. De Luca A, Fiorillo M, Peiris-Pagès M, Ozsvari B, Smith DL, Sanchez-Alvarez R, et al. Mitochondrial Biogenesis Is Required for the Anchorage-Independent Survival and Propagation of Stem-Like Cancer Cells. *Oncotarget* (2015) 17 (6):14777–95. doi: 10.18632/oncotarget.4401
30. Alsamri H, El Hasasna H, Al Dhaheri Y, Eid AH, Attoub S, Iratni R. Carnosol, a Natural Polyphenol, Inhibits Migration, Metastasis, and Tumor Growth of Breast Cancer *via* a ROS-Dependent Proteasome Degradation of STAT3. *Front Oncol* (2019) 9:743. doi: 10.3389/fonc.2019.00743
31. Johnston S, Martin M, Di Leo A, Im SA, Awada A, Forrester T, et al. MONARCH 3 Final PFS: A Randomized Study of Abemaciclib as Initial Therapy for Advanced Breast Cancer. *NPJ Breast Cancer* (2019) 5:5. doi: 10.1038/s41523-018-0097-z
32. Mot AI, Liddell JR, White AR, Crouch PJ. Circumventing the Crabtree Effect: A Method to Induce Lactate Consumption and Increase Oxidative Phosphorylation in Cell Culture. *Int J Biochem Cell Biol* (2016) 79:128–38. doi: 10.1016/j.biocel.2016.08.029
33. Zhao LWY, Luo Y, Li H, Meng X, Liu C, Xiang J, et al. Mitochondria-Localized Self-Reporting Small-Molecule-Decorated Theranostic Agents for Cancer-Organelle Transporting and Imaging. *ACS Appl Bio Mater* (2019) 2:5164–73. doi: 10.1021/acsabm.9b00811
34. Ozsvari B, Sotgia F, Lisanti MP. Exploiting Mitochondrial Targeting Signal(s), TPP and Bis-TPP, for Eradicating Cancer Stem Cells (CSCs). *Aging (Albany NY)* (2018) 10(2):229–40. doi: 10.18632/aging.101384
35. Wang Y, Liu T, Zhang E, Luo S, Tan X, Shi C. Preferential Accumulation of the Near Infrared Heptamethine Dye IR-780 in the Mitochondria of Drug-Resistant Lung Cancer Cells. *Biomaterials* (2014) 35(13):4116–24. doi: 10.1016/j.biomaterials.2014.01.061
36. C. L B. Mitochondrial Membrane Potential in Living Cells. *Annu Rev Cell Biol* (1988) 4:155–81. doi: 10.1146/annurev.cb.04.110188.001103
37. Karlgren M, Vildhede A, Norinder U, Wisniewski JR, Kimoto E, Lai Y, et al. Classification of Inhibitors of Hepatic Organic Anion Transporting Polypeptides (OATPs): Influence of Protein Expression on Drug-Drug Interactions. *J Med Chem* (2012) 55(10):4740–63. doi: 10.1021/jm300212s
38. Obiadat A, Roth M, Hagencuch B. The Expression and Function of Organic Anion Transporting Polypeptides in Normal and in Cancer. *Annu Rev Pharmacol Toxicol* (2012) 52:135–51. doi: 10.1146/annurev-pharmtox-010510-100556
39. Yu CY, Xu H, Ji S, Kwok RT, Lam JW, Li X, et al. Mitochondrion-Anchoring Photosensitizer With Aggregation-Induced Emission Characteristics Synergistically Boosts the Radiosensitivity of Cancer Cells to Ionizing Radiation. *Adv Mater* (2017) 29(15):1606167. doi: 10.1002/adma.201606167
40. Zhou L, Wu Y, Meng X, Li S, Zhang J, Gong P, et al. Dye-Anchored MnO Nanoparticles Targeting Tumor and Inducing Enhanced Phototherapy Effect *Via* Mitochondria-Mediated Pathway. *Small* (2018) 14(36):e1801008. doi: 10.1002/smll.201801008
41. Jiang T, Zhou L, Liu H, Zhang P, Liu G, Gong P, et al. Monitorable Mitochondria-Targeting DNAtrain for Image-Guided Synergistic Cancer Therapy. *Anal Chem* (2019) 91(11):6996–7000. doi: 10.1021/acs.analchem.9b01777
42. Wu JB, Shao C, Li XY, Shi CH, Li QL, Hu PZ, et al. Near-Infrared Fluorescence Imaging of Cancer Mediated by Tumor Hypoxia and HIFI Alpha/OATPs Signaling Axis. *Biomaterials* (2014) 35(28):8175–85. doi: 10.1016/j.biomaterials.2014.05.073

Conflict of Interest: ML and FS hold a minority interest in Lunella Biotech, Inc.

The remaining authors declare that the research was conducted in the absence of any commercial or financial relationships that could be construed as a potential conflict of interest.

Publisher's Note: All claims expressed in this article are solely those of the authors and do not necessarily represent those of their affiliated organizations, or those of the publisher, the editors and the reviewers. Any product that may be evaluated in this article, or claim that may be made by its manufacturer, is not guaranteed or endorsed by the publisher.

frontiers in Oncology

REVIEW
published: 07 October 2021
doi: 10.3389/fonc.2021.745924

Mitochondrial Effects on Seeds of Cancer Survival in Leukemia

Hend E. El-Shaqanqery[1], *Rania Hassan Mohamed*[2*] *and Ahmed A. Sayed*[1,2*]

[1] Genomics Program, Children's Cancer Hospital Egypt, Cairo, Egypt, [2] Department of Biochemistry, Faculty of Science, Ain Shams University, Cairo, Egypt

The cancer metabolic alteration is considered a hallmark and fast becoming a road for therapeutic intervention. Mitochondria have been regarded as essential cell elements that fuel the metabolic needs of most cancer cell types. Leukemia stem cells (LSCs) are a heterogeneous, highly self-renewing, and pluripotent cell population within leukemic cells. The most important source of ATP and metabolites to fulfill the bioenergetics and biosynthetic needs of most cancer stem cells is the mitochondria. In addition, mitochondria have a core role in autophagy and cell death and are the main source of reactive oxygen species (ROS) generation. Overall, growing evidence now shows that mitochondrial activities and pathways have changed to adapt with different types of leukemia, thus mitochondrial metabolism could be targeted for blood malignancy therapy. This review focuses on the function of mitochondria in LSC of the different leukemia types.

Keywords: leukemia, leukemia stem cell, metabolism, mitochondria, mitophagy

OPEN ACCESS

Edited by:
Michael P. Lisanti,
University of Salford Manchester,
United Kingdom

Reviewed by:
Pritam Sadhukhan,
Johns Hopkins University,
United States
Cinzia Domenicotti,
Università di Genova,
Italy

***Correspondence:**
Rania Hassan Mohamed
rania.hassan@sci.asu.edu.eg
Ahmed A. Sayed
ahmad.sayed@57357.org

Specialty section:
This article was submitted to Cancer Metabolism, a section of the journal Frontiers in Oncology

Received: *22 July 2021*
Accepted: *13 September 2021*
Published: *07 October 2021*

Citation:
El-Shaqanqery HE, Mohamed RH and Sayed AA (2021) Mitochondrial Effects on Seeds of Cancer Survival in Leukemia. Front. Oncol. 11:745924. doi: 10.3389/fonc.2021.745924

INTRODUCTION

Leukemia is described as an excessive division of blood-forming cells, resulting from failure of hematopoietic stem cell (HSC) death and abrogation of its differentiation (1, 2). Although these events occur in white blood cells, different blood cells are implicated in leukemia. Commonly, this kind of cancer is divided into two subtypes such as acute (speedy developing) or chronic (slow developing) leukemia (3). Hematologic disorders are still the most common cancer worldwide (4). Leukemia is one of the important causes of mortality in both developed and developing countries; as a result, it burdens high expenses to health scope (5). It has been predicted that deaths of about 50% younger patients and 90% older patients are because of acute myeloid leukemia (AML) or acute lymphoid leukemia (ALL), respectively (6, 7).

Leukemic stem cells (LSCs) are a biologically and functionally defined entity. They are not always named because they arise from an ordinary stem cell but because they fulfill the standards used to define ordinary stem cells. LSCs are multipotent, incredibly proliferative, and self-renewing (8). Cancer stem cell (CSC) is called LSC when it exists in leukemia. It shares many characteristics with normal HSCs, including being $CD38^{+}$ $CD34^{-}$ stem cells (9). However, LSCs often upregulate the expression of other membrane markers such as CD123, TIM3, CD25, CD32, and CD96 that are absent from HSCs and vary among patients. Moreover, like HSCs and unlike leukemia myeloblasts, LSCs divide slowly (10). During normal progression from stem cell to progenitor cell to mature cell, mutations may probably arise at any stage, giving upward thrust to malignancy. Self-renewing HSCs that carry out genetic and epigenetic modifications can downregulate cell death and boost their self-renewal capability. A mutation in a normal stem cell can lead to the formation of a unit that could be

considered an LSC. However, there may be experimental evidence suggesting that mutations in progenitor cells that do not have the complete characters of a stem cell can also lead to initiation and maintenance of the leukemic disease (11). A mutation of some genes (SRSF2, DNMT3A) in normal stem cells can lead to the formation of pre-leukemic stem cell (pre-LSC), while such pre-LSCs are capable of giving rise to healthy blood and immune cells. Additional mutations in CCAAT-enhancer-binding protein alpha (CEBPA) and nucleophosmin (NPM1) can cause a complete block in differentiation and thereby result in malignant expansion of aberrant progenitor cells that could be considered LSCs (**Figure 1**) (12). However, there may be experimental evidence suggesting that mutations in progenitor cells that do not have the complete characteristics of a stem cell can also lead to initiation and maintenance of the leukemic disease. The mutations of genes encoding mitochondrial enzymes, FMS-like tyrosine kinase-3 internal tandem duplication (FLT3-ITD) and isocitrate dehydrogenase (IDH), play a vital role in leukemia cell survival and chemoresistance. Recently, the IDH mutations offer the evidence for the relation between metabolism and leukemogenesis. These mutations play a pivotal role in the reprogramming of energetic metabolism in leukemic cells and in deregulation of ROS production. IDH mutations also enhance generation of 2-hydroxyglutarate (2-HG) instead of α-ketoglutarate (α-KG) (13). LSCs are often resistant to conventional chemotherapy, and their maintenance after therapy is a common reason for relapse. Therefore, it is vital to recognize the biological mechanisms that contribute to leukemia (14, 15). LSCs are characterized by a low rate of metabolism with a decreased basal reactive oxygen species (ROS) manufacturing as compared to bulk leukemic cells (16). These ROS-low LSCs are also unable to upregulate glycolysis after inhibiting oxidative phosphorylation (OXPHOS), which is in line with other reports showing that LSCs have unprecedented mitochondrial characteristics and an expanded sensitivity to strategies that block oxidative phosphorylation (17). Mitochondria play an essential role in metabolism, hypoxia, iron–sulfur clusters, cell differentiation, innate immunity, metabolism of amino acids, calcium, and heme biosynthesis (18). Furthermore, the redox balance of cells and the proapoptotic factor expression are managed by mitochondria to regulate cell death. Thus, there are critical functions of mitochondria inside the neoplastic phenotype, which include resistance to apoptosis, out of control proliferation, and metabolic reprogramming (15, 19).

CSCs ought to adapt their metabolism, especially by elevating nutrient uptake, to keep their uninhibited proliferation (20). Actually, CSC metabolism is not only an indirect by-product of

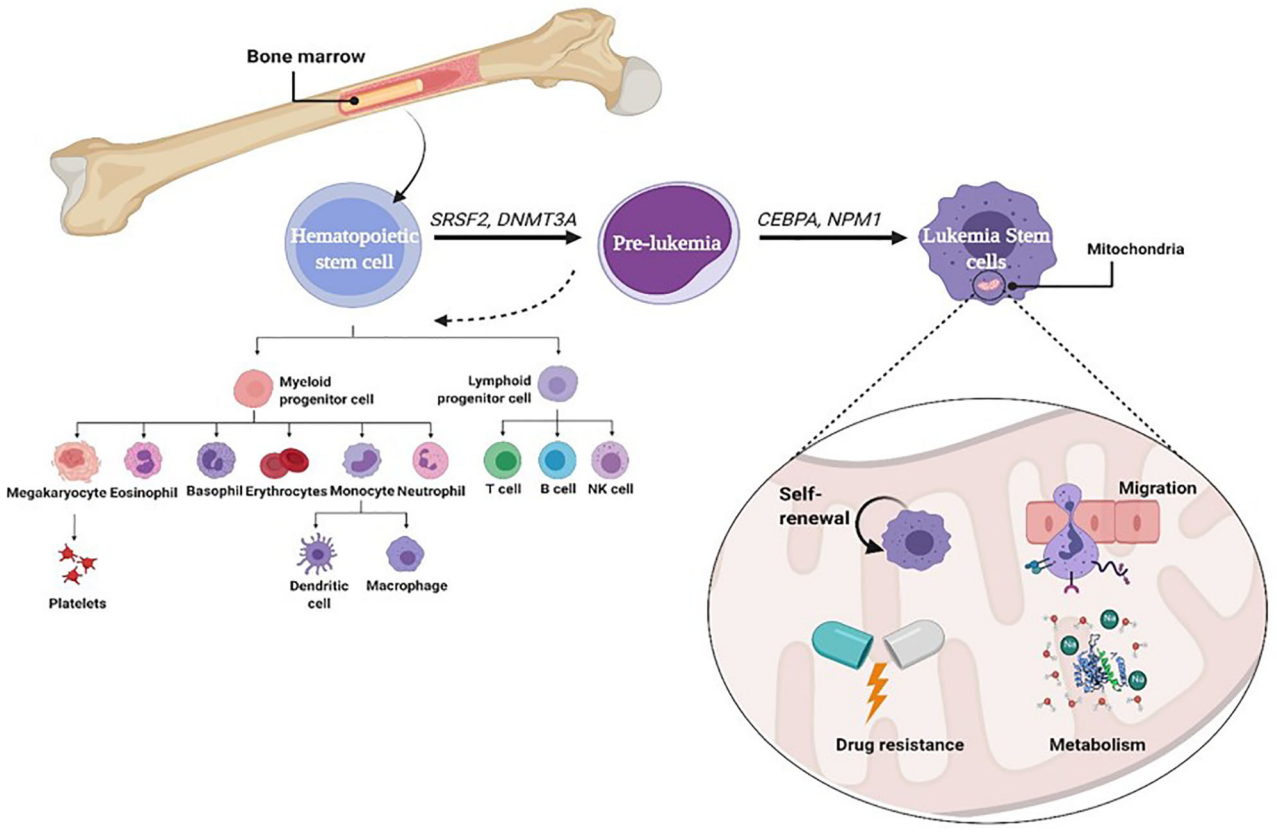

FIGURE 1 | Role of mitophagy in leukemia stem cell.

proliferation but also an immediate reprogramming orchestrated through the use of oncogenic signals (21, 22). Studying the metabolic phenotype of LSCs would potentially clarify their mechanism of survival, persistence, and progression through the development of the disease. Understanding how they differ metabolically from HSCs can help better characterize any type of leukemia stem cell.

METABOLIC FLEXIBILITY OF LEUKEMIC STEM CELLS

There are multiple levels of tumorigenesis process and mitochondrial biology interactions: tumorigenesis may start by direct signals from mitochondria (may be by mutations in mitochondrial DNA) or the alteration of mitochondrial functions of metabolism and bioenergetics by oncogenic signaling pathways. So, understanding the mechanisms of cancer-initiating cell metabolism will effectively aid to develop novel anticancer drugs targeting these aspects. **Table 1** summarizes the metabolic steps potentially implicated in the survival and therapy resistance of LSCs.

BIOENERGETICS OF LEUKEMIC STEM CELLS

LSCs are flexible and able to take advantage of more than one metabolic pathway to continue and survive. LSCs can use fatty acids and amino acids in addition to glucose to provide precursors to the tricarboxylic acid (TCA) cycle and to maintain mitochondrial metabolism (22). Most CSCs are dependent on and upregulate OXPHOS; hence, CSCs can be a target to mitochondrial inhibition. A study carried out in primary lymphocytes and $CD34^+$ progenitors of patients with ALL suggests that, being an inhibitor of mitochondrial translation, tigecycline is capable of sensitizing them to multiplied apoptosis and would improve the levels of oxidative metabolism (29). Moreover, cytarabine-resistant AML cells are shown to be enriched in dormant LSCs and have higher functional mitochondrial mass, which is translated as increasing in OXPHOS levels with subsequent peak in ROS. Interestingly, although cytarabine was not effective, residual cells showed an increase in OXPHOS gene expression. In the study by Kuntz et al. (30), enriched and differentiated $CD34^-$ cells were derived from patients with CML for metabolic analyses on each $CD34^+CD38^-$ stem cell, it has been proven that most primitive LSCs have higher mitochondrial efficacy than differentiated LSCs and normal CD34+CD38- cells. These studies show that primitive CML cells are reliant on oxidative metabolism for their survival (30). We will explain here the central carbon metabolism in LSC to fulfill their energy desires.

GLUCOSE METABOLISM IN LEUKEMIC STEM CELLS

The glycolytic pathway is the primary process in the metabolism of HSCs. Ordinarily, HSCs are energetically dormant with active glycolysis. In glycolysis, glucose is converted to pyruvate. In presence of oxygen, pyruvate can be metabolized to acetyl-CoA that is oxidized in the TCA cycle to drive OXPHOS and generation of ATP. LSCs often lack the ability to enhance glycolysis and therefore switch from anaerobic glycolysis to mitochondria-mediated OXPHOS as their major pathway to generate energy. LSCs rely upon OXPHOS for ATP generation instead of glycolysis and lactic acid fermentation, which gives a chance for ROS production, which can force cells out of quiescence and trigger programmed cell death pathways. Most ROS are generated in mitochondria *via* electron transport. As a result, LSCs respond to this action by upregulating autophagy, which is critical for the maintenance of stemness and the eradication of damaged mitochondria and production of ROS. This also upregulates the expression of the hypoxic response transcription factor [hypoxia-inducible factor 1-alpha (HIF-1-α], even in normoxia (23).

On the other hand, Song et al. (24) showed that bone marrow (BM) cells separated from AML patients without remission produce higher levels of HIF-1α and glucose transporter 1 (GLUT1), as well as hexokinase 2 (HK2) and lactate dehydrogenase (LDH), which are considered the main controlling stages of glycolytic flux, than those from patients with full or partial remission and healthy donors (31). By using metabolomics analysis in the study conducted by Bhanot et al. (31), UDP-P-glucose, a glycogen precursor to glucose, has been reported to be upregulated in AML independently of low glycogen levels. Additionally, adjustments in glucose metabolism have been

TABLE 1 | Summary of the metabolic steps implicated in the survival and therapy resistance of LSCs.

Condition	Role	Ref.
Glucose metabolism	ATP production ROS production Cell stemness	(23)
Glutamine Metabolism	ATP production Regulate leukemia stem cell programing	(19, 24)
Fatty acid metabolism	ATP production Responsible for leukemia stem cell resistance to chemotherapy	(25)
Hypoxia	Maintaining leukemia stem cell stemness and drug resistance	(26, 27)
Mitophagy	Leukemia stem cell maintenance	(28)

LSC, leukemic stem cell; ROS, reactive oxygen species.

linked to end-stage medical outcomes and drug resistance. Kreitz et al. (32) showed that there is excessive glycolytic level in blast AML reluctant to treatment. Also, it was suggested that myeloblast glycolytic rate may be an effective and effortless approach to decide the pretreatment prognosis of AML (25). Unfortunately, current studies are not sufficient to outline the LSC glycolytic phenotype, and extra studies are needed.

GLUTAMINE METABOLISM IN LEUKEMIC STEM CELLS

Metabolism of glutamine (glutaminolysis) is an alternative source of energy. Glutamine is the most considerable amino acid in circulation and can be supplied with the aid of adipose tissue as one of its fundamental sources to the LSCs (33). The mechanism by which tumor cells adjust the balance between glycolysis and oxidative metabolism to meet their energy needs is not fully understood.

It is known that the Warburg shift is an exquisite mark of the extra-proliferating cancer cells, which have an intact TCA cycle and gradually more dependent on glutamine metabolism compared to normal cells for ATP synthesis. Knoechel and Aster confirmed that a signal from the phosphoinositide 3-kinase (PI3K)–AKT pathway shifts NOTCH-dependent T-ALL cells from glutamine metabolism to aerobic glycolysis. Using murine models and the primary human T-ALL xenograft transplantation model, they showed that T-ALL cells with activating NOTCH1 mutations use glutamine as the main substrate for anaplerotic reactions that fuel the TCA cycle (34). In another study, MYC transcription factor and its "super enhancer" sequence have a critical function in hematopoietic malignancies by regulating the LSC programming (33). MYC promotes the uptake of essential amino acids (i.e., glutamine) through SLC7A5/SLC43A1 in lymphoma cells, which in turn stimulate the MYC translation and tumorigenesis (35, 36). Likewise, mutated IDH in AML-LSCs gains increased enzymatic feature to generate R-2-hydroxyglutarate (R2HG) from α-KG, rather than unmutated IDH, which catalyzes the conversion of isocitrate to α-KG. The subsequent accumulation of the oncometabolite R2HG inhibits the α-KG-dependent ten-eleven translocation (TET) protein family, which leads to DNA demethylation and consequently to tumorigenesis (36). The results of previous studies strongly recommend the glutamine metabolism key steps as a target for therapeutic strategies against LSCs.

FATTY ACID METABOLISM IN LEUKEMIC STEM CELLS

The adipocytes have a central role in offering fatty acids to fulfill the high energy needs of the LSCs. Adipocytes can preserve energy as triglycerides, which at some point of lipolysis, it can be catabolized into glycerol and free fatty acids (FFAs). Therefore, adipocytes can also deliver FFA to cancer cells to meet their needs for lipid synthesis and energy.

Woolthuis et al. (37) showed that adipocytes offer FFAs as a source of energy to leukemia cells by a mouse model of blast-crisis CML. Surprisingly, they found a niche of LSCs in gonadal adipose tissue (GAT), and by using limiting-dilution transplantation techniques, it was found that GAT resident LSCs elevated in leukemia are similar to that derived from bone marrow. Likewise, the GAT-associated LSCs have elevated expression of the fatty acid transporter CD36. Gene expression analysis suggested that LSCs have a pro-inflammatory phenotype that will increase lipolysis to provide energy to LSCs with high levels of fatty acid oxidation (FAO) compared to highly differentiated progeny or normal HSCs. These characteristics control LSC quiescence and resistance to chemotherapy. A preceding study on primary human samples of AML recorded a subpopulation expressing CD36 in the $CD34^+$ LSCs. This $CD36^+$ phenotype was used as a poor prognosis indicator (38). In these cases, the $CD36^+$ LSCs also showed an increase in FFAs and their subsequent oxidation, assuming that CD36 can adapt the LSC metabolism in at least one subgroup of human myeloid leukemia. Moreover, cytarabine-resistant AML cells located in quiescent LSCs have elevated levels of mitochondrial mass, which is translated into elevation of OXPHOS levels with high level in ROS. Surprisingly, although treatment with cytarabine was ineffective, residual cells exhibited high expression of OXPHOS genes collectively with increased FAO and upregulation of CD36 that can predict response to treatment in patients with AML (39). Tucci et al. (40) clarified that ALL cells accelerate adipocyte lipolysis and use the produced FFA to complement lipogenesis and *de novo* proliferation. In another study, Chronic Lymphocytic Leukemia (CLL) cells, in comparison with normal B lymphocytes, are able to catabolize lipids that allows usage of FFAs for oxidative respiration (41). FFAs also can interact with the nuclear receptor peroxisome proliferator-activated receptor α (PPARα). The interaction between FFAs and PPARα leads to generation of a complex that, much like a transcription factor, turns on the transcription of enzymes necessary for OXPHOS (42). Adipose tissue can also be protective for LSCs throughout stressful conditions, which includes drug treatment. Orgel et al. (43) showed that glutamine secreted by adipocytes protects leukemia cells from treatment with L-asparaginase. This is especially true, considering that L-asparaginase is used in the treatment of ALL, because leukemic lymphoblasts are quite sensitive to exogenous asparagine and glutamine depletion (41, 43).

This can show how LSCs can make the use of the surrounding microenvironment differential through several routes of metabolisms in different leukemia types. Furthermore, this suggests that targeting combined aspects of metabolism can be a complementary and powerful therapeutic strategy.

HYPOXIA AND HYPOXIA-INDUCIBLE FACTORS IN LEUKEMIC STEM CELLS

Cells have a balanced antioxidant system to neutralize the extra ROS consisting of enzymatic antioxidants such as superoxide

dismutase (SOD), glutathione peroxidases (GPxs), thioredoxin (Trx), and catalase (CAT) and non-enzymatic antioxidants to reduce the oxidative stress state (44). Human SOD can be classified into cytosolic CuZn-SOD, mitochondrial Mn-SOD, and extracellular SOD. The SOD seems to be the first line of defense against oxygen-derived free radicals as it can be rapidly induced in some conditions when exposed to oxidative stress as it catalyzes superoxide into oxygen and hydrogen peroxide (26). CAT can neutralize hydrogen peroxide through decomposing it into molecular oxygen and water. It is now well established that the mitochondria are the major producers of ROS and also the main targets of ROS. Immense accumulation of ROS and free radicals in mitochondria leads to elevated expression of Mn-SOD to inhibit oxidative damage in mitochondria. The accumulation of ROS will lead to mitochondrial permeability transition and disrupt the mitochondrial membrane stability (27). Disruption of mitochondrial outer membrane leads to cytochrome c release and other proapoptotic factors, such as serine protease OMI/HtrA2, Smac/Diablo, endonuclease G, and apoptosis-inducing factor (AIF), and consequently caspase activation and cell death (45). GPx family has antioxidative function at different cellular components: GPx1 is present ubiquitously in the cytosol and mitochondria, GPx2 is in the cytosol and nucleus, GPx3 is in the plasma, and GPx4 is membrane-associated and appears to protect membranes from oxidative challenge (46).

The Trx antioxidant system, composed of nicotinamide adenine dinucleotide phosphate (NADPH), thioredoxin reductase (TrxR), and Trx, is very important against oxidative stress as an endogenous antioxidant system. Trx antioxidants have a function in DNA and protein repair by reducing ribonucleotide reductase and methionine sulfoxide reductases. In addition, Trx systems have a significant role in the immune response (47). Homodimeric TrxR is a member of the pyridine nucleotide-disulfide oxidoreductase family, which includes TrxR, glutathione reductase (GR), TryR, alkyl hydroperoxide reductase, lipoamide dehydrogenase, and mercuric reductase. Trx and TrxR are the dimeric FAD-containing enzyme that catalyzes the NADPH-dependent reduction of the active-site disulfide in oxidized Trx (Trx-S2) to give a dithiol in reduced Trx [Trx-(SH)2] (48). Trx-(SH)2 is a hydrogen donor for ribonucleotide reductase and a disulfide reductase regulating thiol redox. Trx systems in cells can use the thiol and selenol groups to maintain redox level. Trx and its binding proteins [Apoptosis signal-regulating kinase 1 (ASK1) and TATA-box-binding protein 2 (TBP2)] appear to control apoptosis or metabolic states such as carbohydrate and lipid metabolism (49). Both GSH system and Trx system can defend against oxidative stress *via* the efficient removal of various ROS. Cytosolic Trx1 and mitochondrial Trx2 are the major disulfide reductases that affect cell proliferation and viability. The reduced/dithiol form of Trxs binds to ASK1 and inhibits its activity to induce apoptosis. When Trx is oxidized, it dissociates from ASK1 and apoptosis is induced (50). Non-enzymatic antioxidants like vitamin A or retinol, vitamin E, and vitamin C (51).

The role of hypoxia within the generation of LSCs remains debatable perhaps because of addressing hypoxia as a stemness factor in conflicting studies and the difference in duration and degree of hypoxia (52, 53). In any case, further investigations are required so as to clarify its impact on LSC maintenance and survival. Hypoxia by means of HIFs may drive powerful support and advancement through different pathways, for example, energy metabolism, cell cycle, and immune response. These physiological procedures can be upregulated or downregulated in malignancy. In AML, the presence of different oxygen levels in the BM permits upkeep of essential AML cells (28). The downregulation of HIF-2α or HIF-1α to a lesser degree was recorded by Rouault-Pierre et al. (54). Hypoxia promotes apoptosis and inhibits leukemic engraftment in human AML transplantation cells into mice. There are ongoing studies proving that keeping on the redox stability is fundamental for maintaining the stemness and drug resistance characteristics in most cancer cells (55, 56). The function of the PI3K/Akt/mammalian target of rapamycin (mTOR) signaling pathway in developing CSC traits of low apoptotic potential is reported to be partially through enhancement of the ROS elimination *via* CAT production downstream of nuclear localization of FoxOs and stimulation of the HIF-1α (57). In addition, Osellame et al. (58) validated that loss of mitochondrial outer membrane permeability is an indication for intrinsic apoptosis. These observations propose that HIF-2α or HIF-1α is important for development of LSCs and may possibly work as therapeutic targets for AML. Furthermore, the research by Velasco-Hernandez et al. (59) showed that the HIF-1α deletion does not influence the maintenance of AML in mice, which presents the inconsistencies in the role of HIF in AML. In any case, these variations may depend on the specific hereditary change that initiates the malignancy, again revealing the enormous heterogeneity of this disease. In addition, Vukovic et al. (60) developed a genetic model to investigate the effects of the deficiency in HIF-1α and HIF-2α during leukemogenesis. The model indicated that while HIF-2α had no effect on AML cell expansion in a murine model, it is significant in obstructing the development of LSC in malignancy. HIF-2α deletion enhances LSC differentiation, yet does not influence LSC maintenance of AML (60). In CML, Zhang et al. (61) recorded that deletion of HIF-1α prevents CML progression by inhibiting cell cycle and inducing LSC apoptosis. breakpoint cluster region-Abelson fusion gene (BCR-ABL) oncogene in CML-LSCs regulates HIF-1α to induce cell expansion. Regardless of whether HIF-1α has a function in the LSC survival in CLL is as yet obscure. In CLL, HIF-1α is regulated even under normoxia *via* downregulation of von Hippel–Lindau (VHL) protein, whose articulation is controlled by microRNAs (62). This system enables the formation of a complex (HIF-1α/p300/p-STAT3), which is responsible for the expression of the vascular endothelial growth factor (VEGF) (62). It was shown that upregulation of VEGF by HIF-1α assumes a significant role in the microenvironment controlling leukemic cell progression. In T-ALL, HIF-1α control promotes Wnt pathway through enhancing translation of β-catenin (63). Loss of HIF-1α diminishes the LSC recurrence without influencing the development and viability of leukemic cell mass.

MITOPHAGY IN LEUKEMIC STEM CELLS

Autophagy is defined as a self-digestion of the cell, wherein cytoplasmic materials, proteins (macroautophagy), damaged organelles like mitochondria (mitophagy), and lipids are segregated into vesicles, termed autophagosomes, for degradation and reusing. The quality and integrity of the mitochondria are basic to the typical elements of the mitochondria. Damaged mitochondria can be eliminated by mitophagy, which acts as a basic factor in the maintenance of stem cells. Various studies showed that stem cell self-renewal depends on mitophagy (64), illustrated in **Figure 1**. Decreasing Fis1 (mitochondrial division 1) in human LSCs weakens mitophagy, prompts cell cycle arrest, and disables self-renewal. It has been indicated that adenosine monophosphate-activated protein kinase (AMPK) enhances Fis1-dependent mitophagy, and AMPK inactivation mimics the mitophagy defect as a result of lack of Fis1 (14, 15). Mitochondrial dynamics likewise has a significant role in controlling mitophagy (65). LSCs indicated a constitutive activation of AMPK, a key player of controlling energy and mitochondrial homeostasis that arranges the initiation of autophagy and mitophagy through ULK1 activation (66). AMPK is a heterotrimeric serine/threonine kinase that phosphorylates plenty of cell substrates involved in various metabolic pathways through quick versatile reactions to various metabolites (66). AMPK mediates the crosstalk between various key cell signaling pathways regulating energy status, cell expansion, and autophagy through its negative control of the PI3K/AKT/mTOR pathway and its stimulatory impact on phosphorylation of ULK1 (67, 68). In addition, AMPK is a fundamental controller and sensor of cell energy status in mammalian cells. This kinase coordinates changes in the AMP/ATP and ADP/ATP ratios, adjusting the balance between ATP utilization and synthesis (69, 70)and acts to raise the catabolic processes and to diminish the anabolic processes to support intracellular energy homeostasis (71). It is stimulated by many conditions, such as nutrient deprivation (72), cell stresses (73), fasting or caloric limitation (74, 75), and nucleoside analogs like 5-aminoimidazole-4-carboxamide-1-β-D-ribofuranoside (AICAR) (76). In clinical trials, AMPK has been assessed for metabolic illness treatment and malignancies, including both hematopoietic cancers and solid tumors (77, 78), which showed that AMPK has a significant role in tumor regression. Notwithstanding, AMPK has a central role in controlling energy homeostasis and broadly associated with autophagy initiation (64, 79), life span, and tumor suppression (80, 81).

MITOCHONDRIA AND LEUKEMIC STEM CELL MICROENVIRONMENT

The connection between tumor cells and the tumor microenvironment (TME) impacts the phenotype of tumor cells (82). The TME involved different cell types including fibroblasts; immune, endothelial, and perivascular cells; and extracellular matrix (ECM) compartments, such as cytokines, growth factors, and extracellular vesicles. CSCs are thought to be inside or surrounded by the tumor environment maintaining the CSC "niche" and controlling its properties (83). CSC niche is thought to promote the formation of CSCs, keep the CSCs in stem-like state, shield them to resist the immune system, and induce the epithelial-to-mesenchymal transition (EMT), which improves tumor metastasis. Although the CSC niche has a major role in cancer growth, survival, and recurrence, it is still an obscure point needing more studies to solve its unique role in cancer dilemma.

BONE MARROW MICROENVIRONMENT CROSSTALK WITH LEUKEMIC STEM CELLS

In light of the mentioned behavior of the LSC, the BM metabolic microenvironment supports the development of the leukemia cell stemness and pre-metastatic niche. Interestingly, Marlein et al. (15) showed that NADPH oxidase 2 (NOX2) generates superoxide, which causes BM stromal cells to move mitochondria through AML-derived tunnel nanotubes to AML blasts. Indeed, the quiescent CLL cells cultured in the presence of three distinctive stromal cell lines exhibit higher OXPHOS when compared to CLL cells cultured alone. A group of 28 CLL patient-derived cells cocultured with BM could stimulate natural killer (NK) cells, M2-10B4 fibroblasts, or HS-5 stromal cells to feature the significance of considering cell–cell communications (84). Cai et al. (85) revealed that culturing the T-ALL cells with mesenchymal stem cells (MSCs) decreases their mitochondrial ROS levels and initiate a Warburg-like shift that is portrayed by an expansion in glucose uptake and generation of lactate with decrease in ATP synthesis and mitochondrial membrane potential. Moreover, T-ALL cells cocultured with MSCs have adjusted mitochondrial morphology because of the extracellular signals involved in the phosphorylation of the factor, the protein related to dynamin 1 (Drp1) at residue S616. Consistently, phosphorylated Drp1 expression in S616 retained mitochondrial ROS levels, mitochondrial dynamics, metabolic exchange, and chemoresistance in T-ALL cells cocultured with MSCs (85). In addition, the BM mesenchymal stromal cells increase the metabolism and proliferation of their CML cell neighbors by secreting placental growth factor (86, 87). Moreover, the BM stroma uses multiple metabolic regulatory strategies to enhance the stemness traits of the leukemic cells, such as the induction of resistance of ALL cells to asparaginase treatment by secreting high concentrations of asparagine from MSCs (88). Conversion of cystine to cysteine by the BM stroma also protects CLL cells from the oxidative damage (89). The activated p53 pathway and secretion of inflammatory mediators from BM stromal cells activate the initiation of leukemia *via* activation of TLR4, which induces the mitochondria hyperpolarization, ROS production, and DNA double-strand breaks in hematopoietic stem and progenitor cells (HSPCs) (90). On the other hand, the BM stromal cells protect the LSCs from chemotherapy by upregulation of mitochondrial proteins

[i.e., B-cell lymphoma 2 (BCL2) and Uncoupling Protein 2 (UCP2)] to uncouple the leukemic mitochondria and support the glycolytic pathways (91, 92). Another regulator for the metabolic niche of the LSC is the microRNA; LIN28B has been proven to enhance the stemness of the LSC by repression of Let-7, which regulates the insulin-like growth factor 2 mRNA-binding protein 1 (IGF2BP1) (93). Leukemia cells need metabolic adaptation not only for its survival and growth but also to educate the BM milieu to support the LSC reprogramming. Leukemic cells induce a state of insulin resistance in the surrounding cells by increasing the IGFBP1 production from the adipose tissue to save sufficient glucose level for LSC usage (94). After depletion of glucose in the BM microenvironment, the AML cells are encouraged to consume fructose as a source of energy by upregulation of GLUT5 on leukemic cells (95). Moreover, leukemic cells in contact with adipocytes enhance lipolysis by increasing the Fatty Acid-Binding Protein 4 (FABP4) to provide the fatty acids, which are essential for LSC survival (96).

IMMUNOMETABOLIC REGULATION IN LEUKEMIC STEM CELLS

CSCs exhibit metabolic flexibility not only to promote the biosynthetic and bioenergetic needs of tumor malignancy but also to evade the antitumor immunity. The increased consumption of nutrients for the high metabolic competitive CSC deteriorates the metabolic resources of the immune cells in the TME (97, 98). The tumor infiltrated immune cells can act as protumor or antitumor, but both mechanisms are influenced by the metabolic activities of leukemic cells of AML (99). In support of that, the high consumption of glucose and amino acids in cancer cells downregulates the cytotoxic T and NK cell energy metabolism and subsequently their activation and effector functions (100). Also, lactate production suppresses monocyte activation (101) while increasing the tumor-promoting cytokine expression [i.e., interleukin (IL) -23] (102). Also, oxidative stress metabolic products can alter the functions of regulatory T cells (T regs) and myeloid dendritic cells (103, 104). In line with the mentioned immune-metabolic adaptation and to feed the gluttonous needs of the CSCs, leukemia cells secrete several inflammatory mediators such as IL-6, IL-1β, tumor necrosis factor (TNF)α, and granulocyte colony-stimulating factor (G-CSF), along with the endothelial granulocyte-macrophage colony-stimulating factor (GM-CSF), to enhance vasculogenesis for supplying the AML LSC with the essential metabolites for its growth and proliferation (85). Also, the AML blasts suppress T-cell proliferation and enhance the polarization into the M2 suppressive monocyte by secreting high levels of arginase II (88).

Although ROS is a direct effector for killing pathogens *via* innate immune cells, ROS has a crucial role as an immunosuppressive agent helping CSCs/LSCs to evade the immune system and to enhance cancer stemness and anti-leukemic lymphocyte resistance (105, 106). One suggested mechanism for its role in immune evasion, ROS released from these malignant cells is able to induce apoptosis and to reduce the cytokine production of the anti-leukemic lymphocytes. The CSCs maintain their redox balance to keep their stemness traits, survival, and immune evasion. Hence, AML cells with low ROS level represent more CSC and quiescent characteristics (56, 57). Therefore, antioxidants are considered double-edged weapons. They can act as tumor suppressors by decreasing the ROS apoptotic effect on NK and T cells against leukemic cells. On the other hand, antioxidants act as cancer stemness inducers through targeting of ROS-mediated signaling. For example, the GSH precursor N-acetylcysteine can reduce the effect of ROS in Acute myeloid leukemia stem cells (AMLSCs), which resists the niclosamide antineoplastic and apoptotic effect through inhibition of TNFα-induced nuclear factor (NF)-κB activation and increase of the intracellular ROS levels (107).

Signal transducer and activator of transcription (STAT3) can modulate the immune TME to maintain CSC characteristics and renewal. This can be by promoting the functions of MDSC *via* increased ROS and NOX2 expression. Some anticancer candidates such as fluorinated β-amino-ketone and AZD9159, antisense oligonucleotides, are used to inhibit the T regs, MDSC, and tumor growth *via* suppression of STAT3 expression and cascade. One other way is by increasing the expression of HIF-1α, as STAT3 is an upstream transcription factor for HIF-1α, in cancer cells and myeloid cells in the TME, which is critical for immunosuppression and tumor immune evasion (107). HIF-1α, STAT3, and CBP/p300 are known as transcriptional complex components that regulate the response to hypoxia in cancer. HIF-1α/p300/p-STAT3 axis enhances the immune evasion mechanisms of CSC by inhibition of T-cell proliferation, activation, and induction of T regs *via* VEGF upregulation (108). In line with this, HIF-1α/p300/p-STAT3 axis is considered a therapeutic target to eradicate cancer progression. Triptolidenol-1 (LB-1) was used to inhibit the HIF-1α activity, increase its degradation, and suppress the connection between HIF-1α, p-STAT3, and p300. Also, TEL03 is used as a phosphorylation inhibitor for STAT3, which suppresses HIF-1α expression (109). On the other hand, HIF-1α regulates the expression of natural killer group 2 member D (NKG2D) ligands to enhance tumor immunosurveillance by NK and γδ T cells. HIF-1α downregulation increases the shedding of soluble NKG2D ligands (sNKG2D) such as soluble Major Histocompatibility class I polypeptide–related sequence A (sMICA) to enhance the tumor immune evasion (110). Furthermore, it was reported that STAT3 can work as a tumor suppressor by inhibiting aerobic glycolysis of tumor cells, which decreases glucose consumption, lactate production, and expression of HIF-1α target genes in the tumor cells. In such a way, STAT3 and HIF-1α can mediate tumor immunity and immune evasion (111). So, finding the balance between the pros and cons of targeting HIF-1α and STAT3 can be a direction to solve the problems associated with tumor therapy through modulating the immune response.

The hematopoietic stem cell transplantation (HSCT) therapy of leukemia has been greatly improved due to the accurate typing and selection of the donors. However, there is a high level of

relapse and low rates of survival. This challenge is supported by BM microenvironment, which can be reprogrammed by LSC to enhance the stemness characteristics of both HSCs and LSCs and promote leukemia initiation (112). Although the metabolic immunoregulation of LSCs is not completely and directly addressed so far, Du et al. (113) have investigated the metabolic axis of the hematopoietic progenitor microenvironment to suppress the anti-leukemic immunity. They connected inflammation, metabolism, and cancer immunity through cyclooxygenase (COX)2/prostaglandin (PG)/The nuclear orphan receptor 4A (NR4A)/Wingless/int1 (WNT) immunometabolism-regulatory axis. The role of pro-inflammatory (COX2) upregulation and its products, PGs, has been reported in hematological malignancies (114). The elevated COX2 and PGs in AML-MSCs in the BM niche increased the expression of NR4A transcription factors and the WNT signaling pathways, which has been known to be associated with many CSC traits (115). Inhibition of this axis could ameliorate anti-leukemic reactive T effector cells (113). All the previous links suggest the possibility of immunotherapeutic targeting through metabolic routes.

CONCLUSION AND FUTURE PROSPECTIVE

LSC is a mutated stem cell with normal stemness characteristics and also can differentiate to give rise to a cancerous hematopoietic lineage that accumulates the immature blast cells. Mitochondria not only is a main player in the LSC survival and malignancy development but also change the TME to keep the LSC alive. It regulates the redox status, bioenergetics, nutritional dependence, and metabolic products according to the available substrates, as well as modifies the surrounding immune milieu of the tumor. In this review, we highlighted the role of mitochondria in the adaptation of the demanding LSCs to the microenvironment and the development of their stemness traits. LSCs are resilient to use a range of sources such as glucose, amino acids, and fatty acids as precursors for TCA cycle. These leukemia seeds might easily switch between OXPHOS and glycolysis to provide their needs of energy, biogenesis, and drug resistance. Regulation of essential amino acid transporter expression and glutamine metabolism is not only a source of ATP but also considered an immune evasion strategy of LSCs. The crosstalk between adipocytes and LSCs by delivering fatty acids resulting from lipolysis is an unescapable factor for LSC survival. Also, keeping the ROS and oxygen gradient allows the maintenance of the LSCs. Here, we shed light on LSC flexibility to gain their needs of energy, which offers a new therapeutic strategy to target the metabolic reprogramming of LSCs, maybe specifically, in the different types of leukemia. We also focused on mitophagy and AMPK as an initiator of autophagy and mitophagy. AMPK is considered a potential therapeutic target to control the progression of LSCs in different types of leukemia. Moreover, the disruption of the interaction between the BM stroma and LSC may be of great importance to eliminate LSCs and improve HSCT outcomes in different types of leukemia.

AUTHOR CONTRIBUTIONS

HE-S and RM performed the literature search and drafted the manuscript. HE-S drew the figure. AS edited and revised the manuscript. All authors contributed to the article and approved the submitted version.

FUNDING

This study was supported by the Department of Basic Research, Children's Cancer Hospital Egypt 57357 (CCHE 57357).

REFERENCES

1. Yamashita M, Dellorusso PV, Olson OC, Passegué E. Dysregulated Haematopoietic Stem Cell Behaviour in Myeloid Leukaemogenesis. *Nat Rev Cancer* (2020) 20(7):365–82. doi: 10.1038/s41568-020-0260-3
2. Pal K. Cell Growth Inhibition and Apoptosis by Extract of BASELLA ALBA Plant on U937 Cells. *World J Pharm Pharm Sci* (2016) 5(02):1251–61.
3. Takam Kamga P. Signaling Pathways in Leukemia: Any Role for Medicinal Plants in Leukemia Therapy. *J Dis Med Plants* (2015) 1:76. doi: 10.11648/j.jdmp.20150105.12
4. MKeykhaei M, Masinaei M, Mohammadi E, Azadnajafabad S, Rezaei N, Moghaddam SS, et al. A Global, Regional, and National Survey on Burden and Quality of Care Index (QCI) of Hematologic Malignancies; Global Burden of Disease Systematic Analysis 1990–2017. *Exp Hematol Oncol* (2021) 10:11. doi: 10.1186/s40164-021-00198-2
5. Siegel RL, Miller KD, Jemal A. Cancer Statistics, 2015. *CA. Cancer J Clin* (2015) 65:5–29. doi: 10.3322/caac.21254
6. Döhner H, Estey E, Grimwade D, Amadori S, Appelbaum FR, Büchner T, et al. Diagnosis and Management of AML in Adults: 2017 ELN Recommendations From an International Expert Panel. *Blood* (2017) 129:424–47. doi: 10.1182/blood-2016-08-733196
7. Harrison CJ, Johansson B. *Acute Lymphoblastic Leukemia. In Cancer Cytogenetics: Fourth Edition 198–251*. New Jersey: Wiley Blackwell (2015). doi: 10.1002/9781118795569.ch10
8. Riether C, Schürch CM, Ochsenbein AF. Regulation of Hematopoietic and Leukemic Stem Cells by the Immune System. *Cell Death Differ* (2015) 22 (2):187–98. doi: 10.1038/cdd.2014.89
9. Villatoro A, Konieczny J, Cuminetti V, Arranz L. Leukemia Stem Cell Release From the Stem Cell Niche to Treat Acute Myeloid Leukemia. *Front Cell Dev Biol* (2020) 8:607. doi: 10.3389/fcell.2020.00607
10. Ding Y, Gao H, Zhang Q. The Biomarkers of Leukemia Stem Cells in Acute Myeloid Leukemia. *Stem Cell Investig* (2017) 4:19. doi: 10.21037/sci.2017.02.10
11. Thomas D, Majeti R. Biology and Relevance of Human Acute Myeloid Leukemia Stem Cells. *Blood* (2017) 129(12):1577–85. doi: 10.1182/blood-2016-10-696054
12. Velten L, Story BA, Hernández-Malmierca P, Raffel S, Leonce DR, Milbank J, et al. Identification of Leukemic and Pre-Leukemic Stem Cells by Clonal Tracking From Single-Cell Transcriptomics. *Nat Commun* (2021) 12:1366. doi: 10.1038/s41467-021-21650-1
13. Presti CL, Fauvelle F, Jacob MC, Mondet J, Mossuz P. The Metabolic Reprogramming in Acute Myeloid Leukemia Patients Depends on Their

Genotype and Is a Prognostic Marker. *Blood Adv* (2021) 5(1):156–66. doi: 10.1182/bloodadvances.2020002981
14. Pei S, Minhajuddin M, Adane B, Khan N, Stevens BM, Mack SC, et al. AMPK/FIS1-Mediated Mitophagy Is Required for Self-Renewal of Human AML Stem Cells. *Cell Stem Cell* (2018) 23:86–100.e6. doi: 10.1016/j.stem.2018.05.021
15. Marlein CR, Zaitseva L, Piddock RE, Robinson SD, Edwards DR, Shafat MS, et al. NADPH Oxidase-2 Derived Superoxide Drives Mitochondrial Transfer From Bone Marrow Stromal Cells to Leukemic Blasts. *Blood* (2017) 130:1649–60. doi: 10.1182/blood-2017-03-772939
16. Lagadinou ED, Sach A, Jordan CT, Rossi RM, Neering SJ, Minhajuddin M, et al. BCL-2 Inhibition Targets Oxidative Phosphorylation and Selectively Eradicates Quiescent Human Leukemia Stem Cells. *Cell Stem Cell* (2013) 12:329–41. doi: 10.1016/j.stem.2012.12.013
17. Cole A, Wang Z, Coyaud E, Voisin V, Gronda M, Jitkova Y, et al. Inhibition of the Mitochondrial Protease ClpP as a Therapeutic Strategy for Human Acute Myeloid Leukemia. *Cancer Cell* (2015) 27:864–76. doi: 10.1016/j.ccell.2015.05.004
18. Subir Roy Chowdhury SR, Banerji V. Targeting Mitochondrial Bioenergetics as a Therapeutic Strategy for Chronic Lymphocytic Leukemia. *Oxid Med Cell Longevity* (2018) 2018:10. doi: 10.1155/2018/2426712. Article ID 2426712.
19. Peiris-Pagès M, Martinez-Outschoorn UE, Pestell RG, Lisanti FSMP. Cancer Stem Cell Metabolism. *Breast Cancer Res* (2016) 18:55. doi: 10.1186/s13058-016-0712-6
20. Ward PS, Thompson CB. Metabolic Reprogramming: A Cancer Hallmark Even Warburg Did Not Anticipate. *Cancer Cell* (2012) 21:297–308. doi: 10.1016/j.ccr.2012.02.014
21. Pavlova NN, Thompson CB. The Emerging Hallmarks of Cancer Metabolism. *Cell Metab* (2016) 23:27–47. doi: 10.1016/j.cmet.2015.12.006
22. Ianniciello A, Rattigan KM, Helgason GV. The Ins and Outs of Autophagy and Metabolism in Hematopoietic and Leukemic Stem Cells: Food for Thought. *Front Cell Dev Biol* (2018) 6:120. doi: 10.3389/fcell.2018.00120
23. Panina SB, Pei J, . Kirienko NV. Mitochondrial Metabolism as a Target for Acute Myeloid Leukemia Treatment. *Cancer Metab* (2021) 9:17. doi: 10.1186/s40170-021-00253-w
24. Song K, Li M, Xu X, Xuan LI, Huang G, Liu Q. Resistance to Chemotherapy Is Associated With Altered Glucose Metabolism in Acute Myeloid Leukemia. *Oncol Lett* (2016) 12:334–42. doi: 10.3892/ol.2016.4600
25. Chen WL, Wang JH, Zhao AH, Xu X, Wang YH, Chen TL, et al. A Distinct Glucose Metabolism Signature of Acute Myeloid Leukemia With Prognostic Value. *Blood* (2014) 124:1645–54. doi: 10.1182/blood-2014-02-554204
26. Hea L, Hea T, Farrarb S, Jia L, Liua T, Maa X. Antioxidants Maintain Cellular Redox Homeostasis by Elimination of Reactive Oxygen Species. *Cell Physiol Biochem* (2017) 44:532–53. doi: 10.1159/000485089
27. He L, Eslamfam S, Ma X, Li D. Autophagy and the Nutritional Signaling Pathway. *Front Agr Sci Eng* (2016) 3:222–30. doi: 10.15302/J-FASE-2016106
28. Griessinger E, Afonso FA, Pizzitola I, Pierre KR, Vargaftig J, Taussig D, et al. A Niche-Like Culture System Allowing the Maintenance of Primary Human Acute Myeloid Leukemia-Initiating Cells: A New Tool to Decipher Their Chemoresistance and Self-Renewal Mechanisms. *Stem Cells Transl Med* (2014) 3:520–9. doi: 10.5966/sctm.2013-0166
29. Fu X, Liu W, Huang Q, Wang Y, Li H, Xiong Y. Targeting Mitochondrial Respiration Selectively Sensitizes Pediatric Acute Lymphoblastic Leukemia Cell Lines and Patient Samples to Standard Chemotherapy. *Am J Cancer Res* (2017) 7:2395–405.
30. Kuntz EM, Baquero P, Michie AM, Dunn K, Tardito S, Holyoake TL, et al. Targeting Mitochondrial Oxidative Phosphorylation Eradicates Therapy-Resistant Chronic Myeloid Leukemia Stem Cells. *Nat Med* (2017) 23:1234–40. doi: 10.1038/nm.4399
31. Bhanot H, Reddy MM, Nonami A, Weisberg EL, Bonal D, Kirschmeier PT, et al. Pathological Glycogenesis Through Glycogen Synthase 1 and Suppression of Excessive AMP Kinase Activity in Myeloid Leukemia Cells. *Leukemia* (2015) 29:1555–63. doi: 10.1038/leu.2015.46
32. Kreitz J, Schönfeld C, Seibert M, Stolp V, Alshamleh I, Oellerich T, et al. Metabolic Plasticity of Acute Myeloid Leukemia. *Cells* (2019) 8(8):805. doi: 10.3390/cells8080805
33. Bahr C, Paleske l V, Uslu VV, Remeseiro S, Takayama N, Ng SW, et al. A Myc Enhancer Cluster Regulates Normal and Leukaemic Haematopoietic Stem Cell Hierarchies. *Nature* (2018) 553:515–20. doi: 10.1038/nature25193
34. Knoechel B, Aster JC. Metabolic Mechanisms of Drug Resistance in Leukemia. *Cell Metabolism* (2015) 759:760. doi: 10.1016/j.cmet.2015.10.005
35. Yue M, Jiang J, Gao P, Liu H, Qing G. Oncogenic MYC Activates a Feedforward Regulatory Loop Promoting Essential Amino Acid Metabolism and Tumorigenesis. *Cell Rep* (2017) 21:3819–32. doi: 10.1016/j.celrep.2017.12.002
36. Yoo HC, Yu YC, Sung Y, Han JM. Glutamine Reliance in Cell Metabolism. *Exp Mol Med* (2020) 52:1496–516. doi: 10.1038/s12276-020-00504-8
37. Woolthuis CM, Adane B, Khan N, Sullivan T, Minhajuddin M, Gasparetto M, et al. Leukemic Stem Cells Evade Chemotherapy by Metabolic Adaptation to an Adipose Tissue Niche. *Cell Stem Cell* (2016) 19:23–37. doi: 10.1016/j.stem.2016.06.001
38. Zhang T, Yang J, Vaikari VP, Beckford JS, Wu S, Akhtari M, et al. Apolipoprotein C2 - CD36 Promotes Leukemia Growth and Presents a Targetable Axis in Acute Myeloid Leukemia. *Blood Cancer Discov* (2020) 1 (2):198–213. doi: 10.1158/2643-3230.BCD-19-0077
39. Farge T, Saland E, De Toni F, Aroua N, Hosseini M, Perry R, et al. Chemotherapy-Resistant Human Acute Myeloid Leukemia Cells Are Not Enriched for Leukemic Stem Cells But Require Oxidative Metabolism. *Cancer Discov* (2017) 7:716–35. doi: 10.1158/2159-8290.CD-16-0441
40. Tucci J, Sheng X, Mittelman SD. Acute Lymphoblastic Leukemia Cells Stimulate Adipocyte Lipolysis and Utilize Adipocyte-Derived Free-Fatty Acids for Proliferation. In: *Molecular and Cellular Biology*. Philadelphia, Pennsylvania: American Association for Cancer Research (2014). p. 4339–9. doi: 10.1158/1538-7445.AM2014-4339
41. Jiang J, Batra S, Zhang J. Asparagine: A Metabolite to Be Targeted in Cancers. *Metabolites* (2021) 11:402. doi: 10.3390/metabo11060402
42. Rozovski U, Grgurevic S, Ramos CB, Harris DM, Li P, Liu Z, et al. Aberrant LPL Expression, Driven by STAT3, Mediates Free Fatty Acid Metabolism in Cll Cells. *Mol Cancer Res* (2015) 13:944–53. doi: 10.1158/1541-7786.MCR-14-0412
43. Orgel E, Sea JL, Mittelman SD. Mechanisms by Which Obesity Impacts Survival From Acute Lymphoblastic Leukemia. *JNCI Monogr* (2019) 2019 (54):152–6. doi: 10.1093/jncimonographs/lgz020
44. Radadiya A, Zhu W, Coricello A, Alcaro S, Richards NGJ. Improving the Treatment of Acute Lymphoblastic Leukemia. *Biochemistry* (2020) 59:3193–200. doi: 10.1021/acs.biochem.0c00354
45. Zhang M, Shi J, Jiang L. Modulation of Mitochondrial Membrane Integrity and ROS Formation by High Temperature in Saccharomyces Cerevisiae. *Electron J Biotechnol* (2015) 18:202–9. doi: 10.1016/j.ejbt.2015.03.008
46. Suen DF, Norris KL, Youle RJ. Mitochondrial Dynamics and Apoptosis. *Genes Dev* (2008) 22:1577–90. doi: 10.1101/gad.1658508
47. Liu H, Zhang J, Zhang S, Yang F, Thacker PA, Zhang G, et al. Oral Administration of Lactobacillus Fermentum I5007 Favors Intestinal Development and Alters the Intestinal Microbiota in Formula-Fed Piglets. *J Agric Food Chem* (2014) 62:860–6. doi: 10.1021/jf403288r
48. Lu J, Holmgren A. The Thioredoxin Antioxidant System. *Free Radic Biol Med* (2014) 66:75–87. doi: 10.1016/j.freeradbiomed.2013.07.036
49. Holmgren A. Thioredoxin and Glutaredoxin Systems. *J Biol Chem* (1989) 264:13963–1396. doi: 10.1016/S0021-9258(18)71625-6
50. Lillig CH, Holmgren A. Thioredoxin and Related Molecules–From Biology to Health and Disease. *Antioxid Redox Signal* (2007) 9:25–47. doi: 10.1089/ars.2007.9.25
51. Lu J, Holmgren A. Thioredoxin System in Cell Death Progression. *Antioxid Redox Signal* (2012) 17:1738–47. doi: 10.1089/ars.2012.4650
52. Deynoux M, Sunter N, Hérault O, Mazurier F. Hypoxia and Hypoxia-Inducible Factors in Leukemias. *Front Oncol* (2016) 6(41). doi: 10.3389/fonc.2016.00041
53. Huang X, Trinh T, Aljoufi A, Broxmeyer HE. Hypoxia Signaling Pathway in Stem Cell Regulation: Good and Evil. *Curr Stem Cell Rep* (2018) 4:149–57. doi: 10.1007/s40778-018-0127-7
54. Rouault-Pierre K, Lopez-Onieva L, Foster K, Anjos-Afonso F, Lamrissi-Garcia I, Serrano-Sanchez M, et al. HIF-2α Protects Human Hematopoietic Stem/Progenitors and Acute Myeloid Leukemic Cells From Apoptosis Induced by Endoplasmic Reticulum Stress. *Cell Stem Cell* (2013) 13:549–63. doi: 10.1016/j.stem.2013.08.011
55. Liao J, Liu PP, Hou G, Shao J, Yang J, Liu K, et al. Regulation of Stem-Like Cancer Cells by Glutamine Through β-Catenin Pathway Mediated by Redox Signaling. *Mol Cancer* (2017) 16:51. doi: 10.1186/s12943-017-0623-x

56. Mohamed RH, Abu-Shahba N, Mahmoud M, Abdelfattah AMH, Zakaria W, ElHefnawi M. Co-Regulatory Network of Oncosuppressor miRNAs and Transcription Factors for Pathology of Human Hepatic Cancer Stem Cells (HCSC). *Sci Rep* (2019) 9:5564. doi: 10.1038/s41598-019-41978-5
57. Ding S, Li C, Cheng N, Cui X, Xu X, Zhou G. Redox Regulation in Cancer Stem Cells. *Oxid Med Cell Longevity* (2015) 2015:750798. doi: 10.1155/2015/750798. Article ID 750798.
58. Osellame LD, Blacker TS, Duchen MR. Cellular and Molecular Mechanisms of Mitochondrial Function. *Best Pract Research: Clin Endocrinol Metab* (2012) 26:711–23. doi: 10.1016/j.beem.2012.05.003
59. Velasco-Hernandez T, Hyrenius-Wittsten A, Rehn M, Bryder D, Cammenga J. HIF-1α can Act as a Tumor Suppressor Gene in Murine Acute Myeloid Leukemia. *Blood* (2014) 124:3597–607. doi: 10.1182/blood-2014-04-567065
60. Vukovic M, Guitart AV, Sepulveda C, Villacreces A, O'Duibhir E, Panagopoulou TI, et al. Hif-1α and Hif-2α Synergize to Suppress AML Development But Are Dispensable for Disease Maintenance. *J Exp Med* (2015) 212:2223–34. doi: 10.1084/jem.20150452
61. Zhang H, Li H, Xi HS, Li S. Hif1α is Required for Survival Maintenance of Chronic Myeloid Leukemia Stem Cells. *Blood* (2012) 119:2595–607. doi: 10.1182/blood-2011-10-387381
62. Seiffert M. HIF-1α: A Potential Treatment Target in Chronic Lymphocytic Leukemia. *Haematologica* (2020) 105(4):856–8. doi: 10.3324/haematol.2019.246330
63. Giambra V, Jenkins CE, Lam SH, Hoofd C, Belmonte M, Wang X, et al. Leukemia Stem Cells in T-ALL Require Active Hif1α and Wnt Signaling. *Blood* (2015) 125:3917–27. doi: 10.1182/blood-2014-10-609370
64. Ho TT, Warr MR, Adelman ER, Lansinger OM, Flach J, Verovskaya EV. Autophagy Maintains the Metabolism and Function of Young and Old Stem Cells. *Nature* (2017) 543:205–10. doi: 10.1038/nature21388
65. Wang Y, Liu HH, Cao YT, Zhang LL, Huang F, Yi C. The Role of Mitochondrial Dynamics and Mitophagy in Carcinogenesis, Metastasis and Therapy. *Front Cell Dev Biol* (2020) 8:413. doi: 10.3389/fcell.2020.00413
66. Herzig S, Shaw RJ. AMPK: Guardian of Metabolism and Mitochondrial Homeostasis. *Nat Rev Mol Cell Biol* (2018) 19(2):121–35. doi: 10.1038/nrm.2017.95
67. Tamargo-Gómez I, Mariño G. AMPK: Regulation of Metabolic Dynamics in the Context of Autophagy. *Int J Mol Sci* (2018) 19(12):3812. doi: 10.3390/ijms19123812
68. Laker RC, Drake JC, Wilson RJ, Lira VA, Lewellen BM, Ryall KA, et al. Ampk Phosphorylation of Ulk1 Is Required for Targeting of Mitochondria to Lysosomes in Exercise-Induced Mitophagy. *Nat Commun* (2017) 8:548. doi: 10.1038/s41467-017-00520-9
69. Lin SC, Hardie DG. AMPK: Sensing Glucose as Well as Cellular Energy Status. *Cell Metab* (2018) 27:299–313. doi: 10.1016/j.cmet.2017.10.009
70. Hardie DG. AMPK: Positive and Negative Regulation, and Its Role in Whole-Body Energy Homeostasis. *Curr Opin Cell Biol* (2015) 33:1–7. doi: 10.1016/j.ceb.2014.09.004
71. Hardie DG, Schaffer BE, Brunet A. AMPK: An Energy-Sensing Pathway With Multiple Inputs and Outputs. *Trends Cell Biol* (2016) 26:190–201. doi: 10.1016/j.tcb.2015.10.013
72. Yi D, Yu H, Lu K, Ruan C, Ding C, Tong L, et al. Chen D.AMPK Signaling in Energy Control, Cartilage Biology, and Osteoarthritis. *Front Cell Dev Biol* (2021) 9:696602. doi: 10.3389/fcell.2021.696602
73. Zhang S, Sheng H, Zhang X, Qi Q, Chan CB, Li L, et al. Cellular Energy Stress Induces AMPK-Mediated Regulation of Glioblastoma Cell Proliferation by PIKE-A Phosphorylation. *Cell Death Dis* (2019) 10:222. doi: 10.1038/s41419-019-1452-1. 1:13.
74. López-Lluch G, Navas P. Calorie Restriction as an Intervention in Ageing. *J Physiol* (2016) 594:2043–60. doi: 10.1113/JP270543
75. Pietrocola F, Castoldi F, Markaki M, Lachkar S, Chen G, Enot DP, et al. Aspirin Recapitulates Features of Caloric Restriction. *Cell Rep* (2018) 22:2395–407. doi: 10.1016/j.celrep.2018.02.024
76. Višnji´ c.D., Lali´ c.H., Dembitz V, Tomi´ c B., Smoljo T. AICAr. A Widely Used AMPK Activator With Important AMPK-Independent Effects: A Systematic Review. *Cells* (2021) 10:1095. doi: 10.3390/cells10051095
77. Yuan J, Dong X, Yap J, Hu I. The MAPK and AMPK Signalings: Interplay and Implication in Targeted Cancer Therapy. *J Hematol Oncol* (2020) 13:113. doi: 10.1186/s13045-020-00949-4
78. Li W, Saud SM, Young MR, Chen G, Hua B. Targeting AMPK for Cancer Prevention and Treatment. *Oncotarget* (2015) 6: (10):7365–78. doi: 10.18632/oncotarget.3629
79. Yuan J, Zhao X, Hu Y, Sun H, Gong G, Huang X, et al. Autophagy Regulates the Generation of the Auditory Cortex Through the AMPK-mTOR-ULK1 Signaling Pathway. *Int J Mol Med* (2018) 41(4):2086–98. doi: 10.3892/ijmm.2018.3393
80. Vara-Ciruelos D, Dandapani M, Grahame DH. AMP-Activated Protein Kinase: Friend or Foe in Cancer? *Annu Rev Cancer Biol* (2020) 4:1–16. doi: 10.1146/annurev-cancerbio-030419-033619
81. Templeman NM, Murphy CT. Regulation of Reproduction and Longevity by Nutrient-Sensing Pathways. *J Cell Biol* (2018) 217:93–106. doi: 10.1083/jcb.201707168
82. Peitzsch C, Tyutyunnykova A, Pantel K, Dubrovska A. Cancer Stem Cells: The Root of Tumor Recurrence and Metastases. *Semin Cancer Biol* (2017) 44:10–24. doi: 10.1016/j.semcancer.2017.02.011
83. Plaks V, Kong N, Werb Z. The Cancer Stem Cell Niche: How Essential Is the Niche in Regulating Stemness of Tumor Cells? *Cell Stem Cell* (2015) 16:225–38. doi: 10.1016/j.stem.2015.02.015
84. Vangapandu HV, Ayres ML, Bristow CA, Wierda WG, Keating MJ, Balakrishnan K, et al. The Stromal Microenvironment Modulates Mitochondrial Oxidative Phosphorylation in Chronic Lymphocytic Leukemia Cells. *Neoplasia (United States)* (2017) 19:762–71. doi: 10.1016/j.neo.2017.07.004
85. Cai J, Wang J, Huang Y, Wu H, Xia T, Xiao J, et al. ERK/Drp1-Dependent Mitochondrial Fission Is Involved in the MSC-Induced Drug Resistance of T-Cell Acute Lymphoblastic Leukemia Cells. *Cell Death Dis* (2016) 7(11): e2459. doi: 10.1038/cddis.2016.370
86. Houshmand M, Blanco TM, Circosta P, Yazdi N, Kazemi A, Saglio G, et al. Bone Marrow Microenvironment: The Guardian of Leukemia Stem Cells. *World J Stem Cells* (2019) 11(8):476–90. doi: 10.4252/wjsc.v11.i8.476
87. Ni Y, Zhou X, Yang J, Shi H, Li H, Zhao X, et al. The Role of Tumor-Stroma Interactions in Drug Resistance Within Tumor Microenvironment. *Front Cell Dev Biol* (2021) 9:637675. doi: 10.3389/fcell.2021.637675
88. Chen Y, Liang Y, Luo X, Hu Q. Oxidative Resistance of Leukemic Stem Cells and Oxidative Damage to Hematopoietic Stem Cells Under Pro-Oxidative Therapy. *Cell Death Dis* (2020) 11:291. doi: 10.1038/s41419-020-2488-y
89. Zambetti NA, Ping Z, Chen S, Kenswil KJG, Mylona MA, Sanders MA, et al. Mesenchymal Inflammation Drives Genotoxic Stress in Hematopoietic Stem Cells and Predicts Disease Evolution in Human Pre-Leukemia. *Cell Stem Cell* (2016) 19:613–27. doi: 10.1016/j.stem.2016.08.021
90. Singh AK, Cancelas JA. Gap Junctions in the Bone Marrow Lympho-Hematopoietic Stem Cell Niche, Leukemia Progression, and Chemoresistance. *Int J Mol Sci* (2020) 21(3):796. doi: 10.3390/ijms21030796
91. Mohammadalipour A, Dumbali SP, Wenzel PL. Mitochondrial Transfer and Regulators of Mesenchymal Stromal Cell Function and Therapeutic Efficacy. *Front Cell Dev Biol* (2020) 8:603292. doi: 10.3389/fcell.2020.603292
92. Zhou J, Bi C, Ching YQ, Chooi JY, Lu X, Quah JY, et al. Inhibition of LIN28B Impairs Leukemia Cell Growth and Metabolism in Acute Myeloid Leukemia. *J Hematol Oncol* (2017) 10:138. doi: 10.1186/s13045-017-0507-y
93. Forte D, Krause DS, Andreeff M, Bonnet D, Méndez-Ferrer S. Updates on the Hematologic Tumor Microenvironment and Its Therapeutic Targeting. *Haematologica* (2019) 104:1928–34. doi: 10.3324/haematol.2018.195396
94. Chen WL, Wang YY, Zhao A, Xia L, Xie G, Su M, et al. Enhanced Fructose Utilization Mediated by SLC2A5 Is a Unique Metabolic Feature of Acute Myeloid Leukemia With Therapeutic Potential. *Cancer Cell* (2016) 30:779–91. doi: 10.1016/j.ccell.2016.09.006
95. Shafat MS, Oellerich T, Mohr S, Robinson SD, Edwards DR, Marlein CR, et al. Leukemic Blasts Program Bone Marrow Adipocytes to Generate a Protumoral Microenvironment. *Blood* (2017) 129:1320–32. doi: 10.1182/blood-2016-08-734798
96. Renner K, Singer K, Koehl GE, Geissler EK, Peter K, Siska PJ, et al. Metabolic Hallmarks of Tumor and Immune Cells in the Tumor Microenvironment. *Front Immunol* (2017) 8:248. doi: 10.3389/fimmu.2017.00248
97. Konopleva MY, Jordan CT. Leukemia Stem Cells and Microenvironment: Biology and Therapeutic Targeting. *J Clin Oncol* (2011) 29:591–9. doi: 10.1200/JCO.2010.31.0904

98. Mougiakakos D. The Induction of a Permissive Environment to Promote T Cell Immune Evasion in Acute Myeloid Leukemia : The Metabolic Perspective. *Front Oncol* (2019) 9:1–9. doi: 10.3389/fonc.2019.01166
99. Knaus HA, Berglund S, Hackl H, Blackford AL, Zeidner JF, Montiel-Esparza R, et al. Signatures of CD8+ T Cell Dysfunction in AML Patients and Their Reversibility With Response to Chemoterapy. *JCI Insight* (2018) 3 (21):e120974. doi: 10.1172/jci.insight.120974
100. Dietl K, Renner K, Dettmer K, Timischl B, Eberhart K, Dorn C, et al. Lactic Acid and Acidification Inhibit TNF Secretion and Glycolysis of Human Monocytes. *J Immunol* (2010) 184:1200–9. doi: 10.4049/jimmunol.0902584
101. Shime H, Yabu M, Akazawa T, Kodama K, Matsumoto M, Seya T, et al. Tumor-Secreted Lactic Acid Promotes IL-23/IL-17 Proinflammatory Pathway. *J Immunol* (2008) 180:7175–83. doi: 10.4049/jimmunol.180.11.7175
102. Cubillos-Ruiz JR, Silberman PC, Rutkowski MR, Chopra S, Perales-Puchalt A, Song M, et al. ER Stress Sensor XBP1 Controls Anti-Tumor Immunity by Disrupting Dendritic Cell Homeostasis. *Cell* (2015) 161:1527–38. doi: 10.1016/j.cell.2015.05.025
103. Maj T, Wang W, Crespo J, Zhang H, Wang W, Wei S, et al. Oxidative Stress Controls Regulatory T Cell Apoptosis and Suppressor Activity and PD-L1-Blockade Resistance in Tumor. *Nat Immunol* (2017) 18:1332–41. doi: 10.1038/ni.3868
104. Mussai F, De Santo C, Abu-Dayyeh I, Booth S, Quek L, McEwen-Smith RM, et al. Acute Myeloid Leukemia Creates an Arginase-Dependent Immunosuppressive Microenvironment. *Blood* (2013) 122:749–58. doi: 10.1182/blood-2013-01-480129
105. Kumari S, Badana AK, Murali Mohan G, Shailender G, Malla R. Reactive Oxygen Species: A Key Constituent in Cancer Survival. *Biomark Insights* (2018) 13:1177271918755391. doi: 10.1177/1177271918755391
106. Zhou F, Shen Q, Claret FX. Novel Roles of Reactive Oxygen Species in the Pathogenesis of Acute Myeloid Leukemia. *J Leukocyte Biol* (2013) 94(3):423–9. doi: 10.1189/jlb.0113006
107. Garg M, Shanmugam MK, Bhardwaj V, Goel A, Gupta R, Sharma A, et al. The Pleiotropic Role of Transcription Factor STAT3 in Oncogenesis and Its Targeting Through Natural Products for Cancer Prevention and Therapy. *Medicinal Res Rev* (2021) 41(3):1291–336. doi: 10.1002/med.21761
108. Jin X, Dai L, Ma Y, Wang J, Liu Z. Implications of HIF-1α in the Tumorigenesis and Progression of Pancreatic Cancer. *Cancer Cell Int* (2020) 20(1):1–11. doi: 10.1186/s12935-020-01370-0
109. Niu G, Briggs J, Deng J, Ma Y, Lee H, Kortylewski M, et al. Signal Transducer and Activator of Transcription 3 Is Required for Hypoxia-Inducible Factor-1alpha RNA Expression in Both Tumor Cells and Tumor-Associated Myeloid Cells. *Mol Cancer Res* (2008) 6(7):1099–105. doi: 10.1158/1541-7786.MCR-07-2177
110. Zhang Q, Han Z, Zhu Y, Chen J, Li W. Role of Hypoxia Inducible Factor-1 in Cancer Stem Cells. *Mol Med Rep* (2021) 23(1):1–1. doi: 10.3892/mmr.2020.11655
111. Zhang H-F, Lai R. STAT3 in Cancer—Friend or Foe? *Cancers* (2014) 6 (3):1408–40. doi: 10.3390/cancers6031408
112. Van den Brink MRM, Burakoff SJ. Cytolytic Pathways in Haematopoietic Stem-Cell Transplantation. *Nat Rev Immunol* (2002) 2:273–81. doi: 10.1038/nri775
113. Wu L, Amarachintha S, Xu J, Oley F, Du W. Mesenchymal COX2-PG Secretome Engages NR4A-WNT Signalling Axis in Haematopoietic Progenitors to Suppress Anti-Leukaemia Immunity. *Br J Haematol* (2018) 183:445–56. doi: 10.1111/bjh.15548
114. Bernard M, Bancos S, Sime P, Phipps R. Targeting Cyclooxygenase-2 in Hematological Malignancies: Rationale and Promise. *Curr Pharm Des* (2008) 14:2051–60. doi: 10.2174/138161208785294654
115. de Sousa e Melo F, Vermeulen L. Wnt Signaling in Cancer Stem Cell Biology. *Cancers* (2016) 8(7):60. doi: 10.3390/cancers8070060

Conflict of Interest: The authors declare that the research was conducted in the absence of any commercial or financial relationships that could be construed as a potential conflict of interest.

Publisher's Note: All claims expressed in this article are solely those of the authors and do not necessarily represent those of their affiliated organizations, or those of the publisher, the editors and the reviewers. Any product that may be evaluated in this article, or claim that may be made by its manufacturer, is not guaranteed or endorsed by the publisher.

frontiers in Oncology

REVIEW
published: 15 October 2021
doi: 10.3389/fonc.2021.740720

High ATP Production Fuels Cancer Drug Resistance and Metastasis: Implications for Mitochondrial ATP Depletion Therapy

Marco Fiorillo[1,2], *Béla Ózsvári*[1], *Federica Sotgia*[1*] and *Michael P. Lisanti*[1*]

[1] Translational Medicine, School of Science, Engineering and Environment (SEE), University of Salford, Greater Manchester, United Kingdom, [2] The Department of Pharmacy, Health and Nutritional Sciences, The University of Calabria, Cosenza, Italy

OPEN ACCESS

Edited by:
Chris Albanese,
Georgetown University, United States

Reviewed by:
Pau B. Esparza-Moltó,
Salk Institute for Biological Studies, United States
Sujit Kumar Bhutia,
National Institute of Technology Rourkela, India
Stefano Falone,
University of L'Aquila, Italy

***Correspondence:**
Federica Sotgia
fsotgia@gmail.com
Michael P. Lisanti
michaelp.lisanti@gmail.com

Specialty section:
This article was submitted to Cancer Metabolism, a section of the journal Frontiers in Oncology

Received: 13 July 2021
Accepted: 07 September 2021
Published: 15 October 2021

Citation:
Fiorillo M, Ózsvári B, Sotgia F and Lisanti MP (2021) High ATP Production Fuels Cancer Drug Resistance and Metastasis: Implications for Mitochondrial ATP Depletion Therapy. Front. Oncol. 11:740720. doi: 10.3389/fonc.2021.740720

Recently, we presented evidence that high mitochondrial ATP production is a new therapeutic target for cancer treatment. Using ATP as a biomarker, we isolated the "metabolically fittest" cancer cells from the total cell population. Importantly, ATP-high cancer cells were phenotypically the most aggressive, with enhanced stem-like properties, showing multi-drug resistance and an increased capacity for cell migration, invasion and spontaneous metastasis. In support of these observations, ATP-high cells demonstrated the up-regulation of both mitochondrial proteins and other protein biomarkers, specifically associated with stemness and metastasis. Therefore, we propose that the "energetically fittest" cancer cells would be better able to resist the selection pressure provided by i) a hostile micro-environment and/or ii) conventional chemotherapy, allowing them to be *naturally-selected* for survival, based on their high ATP content, ultimately driving tumor recurrence and distant metastasis. In accordance with this energetic hypothesis, ATP-high MDA-MB-231 breast cancer cells showed a dramatic increase in their ability to metastasize in a pre-clinical model *in vivo*. Conversely, metastasis was largely prevented by treatment with an FDA-approved drug (Bedaquiline), which binds to and inhibits the mitochondrial ATP-synthase, leading to ATP depletion. Clinically, these new therapeutic approaches could have important implications for preventing treatment failure and avoiding cancer cell dormancy, by employing ATP-depletion therapy, to target even the fittest cancer cells.

Keywords: anti-oxidant capacity, ATP, bedaquiline, cancer stem cells (CSCs), dormancy, mitochondria, metastasis, multi-drug resistance

ATP, THE ENERGETIC CURRENCY OF LIFE: HISTORY, CHEMISTRY AND BIOLOGY

ATP is the vital energetic "currency" of all living things, including micro-organisms (1–11). Viruses also energetically require sufficient ATP levels, for replication in host cells.

Historically, ATP was initially discovered in 1929, by Karl Lohmann, a German chemist (**Figure 1**). Then, in 1937, Herman Kalckar, from Denmark, showed that ATP synthesis is driven by cell

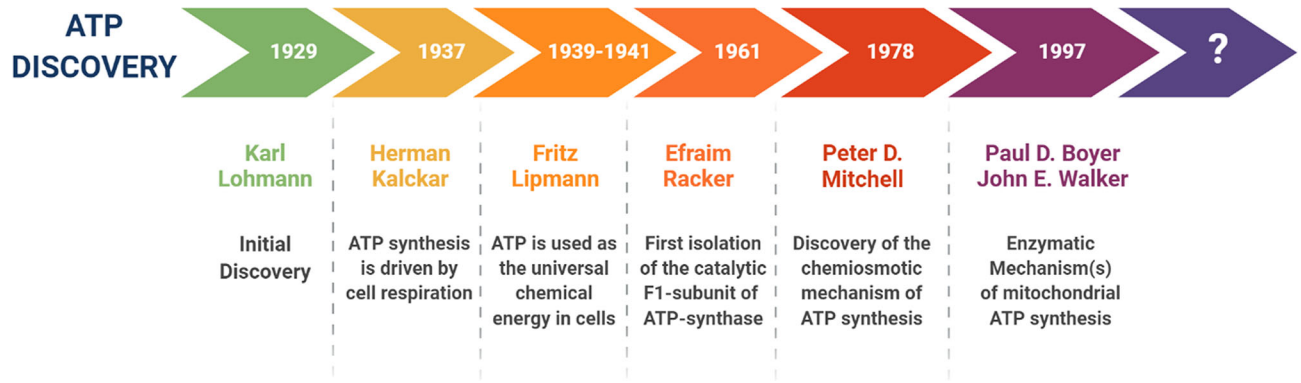

FIGURE 1 | A brief history of the discovery of ATP and its energetic function. This timeline highlights the key scientists and the events that contributed to our deeper understanding the structure, function and molecular machinery responsible for the synthesis of ATP, especially within mitochondrial organelles.

respiration. From 1939 to 1941, Fritz Lipmann, a German-born scientist, was the first to demonstrate that ATP is used as the universal chemical energy in cells. However, it wasn't until 1961, that an American biochemist, namely Efraim Racker, first isolated the catalytic F1-subunit of the mitochondrial ATP-synthase. Then, in 1978, Peter D. Mitchell proposed that the asymmetric distribution of protons across a topologically enclosed membrane, plays an important role in mitochondrial ATP generation. In 1997, the Nobel Prize in Chemistry was jointly awarded to Paul D. Boyer and John E. Walker, for discovering the enzymatic mechanism(s), underpinning mitochondrial ATP synthesis (4–7, 12–16). The mitochondrial ATP-synthase (Complex V) is an excellent example of a rotary molecular motor, with an architecture of nanoscale dimensions (4–7).

Chemically, at the molecular level, ATP is a nucleoside triphosphate, which contains adenine, a ribose sugar, and three phosphate groups (i.e., adenosine-5'-triphosphate) (1–3). Enzymatic cleavage of ATP at its terminal phosphate group, produces two main reaction products, ADP and inorganic phosphate (Pi), thereby releasing high levels of stored chemical energy (-30.5 kJ/mole) (1–3). Importantly, free energy released by the hydrolysis of ATP is also due to the higher stability of the reaction products, because the reaction is kept away from equilibrium in living cells. As a consequence, the free energy released by the hydrolysis of ATP into ADP and Pi, is actually higher than under standard biochemical conditions.

Biologically, ATP is a required co-factor for a plethora of biochemical reactions, involved in cellular catabolism, as well as in anabolic metabolism (8–11). During passive diffusion, small molecules randomly move *via* Brownian motion, down the concentration gradient. Therefore, in living cells, in order to maintain normal physiology and organismal homeostasis, active transport is necessary to move molecules directionally and vectorially, against the concentration gradient, from an area of low concentration to an area of high concentration. This process of active transport also involves energy expenditures, in the form of ATP.

Kinases employ ATP for auto- and trans-phosphorylation reactions, to rapidly transmit information *via* cellular signaling cascades, from the plasma membrane to the cytoplasm, intracellular organelles and, ultimately, to the nucleus. The enzyme adenylate cyclase (a family of ten human genes; ADCY1-10) uses ATP as a precursor, for the generation of the second messenger, cyclic AMP (3',5'-cyclic adenosine monophosphate).

ATP is involved in various aspects of protein synthesis. For example, tRNA-ligases employ ATP hydrolysis for coupling the 20 amino acids to their appropriate tRNAs, for their use by cellular and mitochondrial ribosomes, during protein synthesis. During protein translation, molecular chaperones (e.g., HSP70 and HSP90 family members) facilitate proper protein folding, by acting as enzymatically active ATPases, consuming large amounts of ATP.

In summary, ATP energetically "fuels" most cellular processes, including metabolism, active transport, intracellular signaling, as well as DNA, RNA and protein synthesis. Therefore, it is perhaps surprising that nutrient fasting and/or caloric restriction (17, 18) are believed to be one of the best strategies for extending both healthspan and lifespan, as evidenced by studies using model organisms (*C. elegans, Drosophila* and mice), as well as preventing cancer (19, 20). For example, Resveratrol, a natural anti-aging phytochemical and caloric restriction mimetic, is a known inhibitor of the mitochondrial ATP-synthase (21). Moreover, Resveratrol is also thought to exert its powerful anti-aging effects, *via* its sirtuin-dependent mechanisms of action.

More specifically, calorie restriction activates pro-longevity signaling pathways in model organisms, such as AMPK and the mitochondrial unfolded protein response (UPRmt), and inhibits mTOR and insulin/IGF1 signaling (22, 23). These effects may mechanistically reduce or restrict different processes that contribute to aging, such as inflammation, loss of proteostasis and senescence.

Energy for the mitochondrial synthesis of ATP is derived from the oxidation of NADH and $FADH_2$ by Complexes I-IV of the mitochondrial electron transport chain (ETC). NADH and $FADH_2$ are generated mainly from the TCA cycle, but some NADH is also donated by glycolysis and from the conversion of pyruvate into acetyl-CoA. However, cytosolic NADH (obtained

through glycolysis) does not directly feed into the mitochondrial electron transport chain, but it gives electron equivalents *via* the malate-aspartate and/or glycerol shuttles. In contrast, NADPH, generated by the pentose-phosphate pathway (PPP), is used to maintain glutathione in a reduced state, providing anti-oxidant buffering capacity against ROS and oxidative stress.

Because of the central importance of ATP as a "barometer" of cell metabolism, many luminescent and fluorescent probes have been developed, to measure and track ATP levels, in response to various cellular stimuli (24–28). For example, BioTracker ATP-Red 1 is a vital dye that is only fluorescent when bound to ATP, but does not recognize ADP or other nutrients (29). Morphologically, BioTracker ATP-Red 1 specifically localizes to mitochondria, as seen by fluorescence microscopy, and co-localizes with the mitochondrial probe MitoTracker-Green (29). Therefore, BioTracker ATP-Red 1 allows for the dynamic detection and visualization of mitochondrial ATP in living cells and tissues.

As mitochondrial activity is specifically increased in human tumor cells and metastatic cancer cells *in vivo*, as measured by specific functional activity assays, high ATP production may be a key driving force in promoting tumor progression, therapy-resistance and, ultimately, in metastatic dissemination (30, 31). However, more mechanistic studies are needed to experimentally support this hypothesis.

USING ATP AS A BIOMARKER TO METABOLICALLY FRACTIONATE THE CANCER CELL POPULATION: IMPLICATIONS FOR ATP-DEPLETION THERAPY

In our recent studies, we took advantage of a vital fluorescent dye that allows one to measure ATP levels in living cells, namely BioTracker ATP-Red 1 (32, 33). More specifically, we coupled BioTracker ATP-Red 1 staining with a bioenergetic fractionation scheme, in which the total cell population was subjected to flow cytometry, to isolate the ATP-high and ATP-low sub-populations of MCF7 cells, an ER(+) human breast cancer cell line. This metabolic fractionation approach allowed us to isolate the most "energetic" cancer cells within the total cell population. One possibility is that increased mitochondrial metabolism and/or ROS production may contribute to this phenotype, *via* mitochondrial retrograde signalling (34, 35). Therefore, we proposed that the ATP-high cancer cell population should be targeted for eradication *via* ATP-depletion therapy (36–40). ATP-depletion therapy would be expected to result in rapid energy-depletion, especially in highly aggressive cancer cells, thereby halting their propagation, by inducing autophagy, apoptosis and/or necrosis.

In a parallel line of research, we have previously identified >20 mitochondrially-targeted therapeutics that could be used to effectively achieve ATP-depletion therapy (**Figure 2**). These potential therapeutics include: FDA-approved drugs (Doxycycline, Tigecycline, Azithromycin, Pyrvinium pamoate, Atovaquone, Bedaquiline, Niclosamide, Irinotecan); natural products/nutraceuticals (Actinonin, CAPE, Berberine, Brutieridin, Melitidin); and experimental compounds [Oligomycin, AR-C155858, Mitoriboscins, Mitoketoscins, Mitoflavoscins, TPP derivatives (including Dodecyl-TPP and 2-Butene-1,4-bis-TPP)] (41–47). A triple-combination of two antibiotics together with Vitamin C (Doxycycline, Azithromycin and Ascorbic acid) was found to be particularly potent for targeting mitochondria, inducing ATP-depletion and inhibiting CSC propagation (48), at sub-antimicrobial levels.

As many of these are repurposed FDA-approved antibiotics, with excellent safety profiles, Phase II clinical trials are warranted. For example, a Phase II clinical pilot study of Doxycycline (49) has already shown that this >50-year-old antibiotic is indeed effective in metabolically targeting the CSC population in early breast cancer patients, as demonstrated using CD44 and ALDH1 as specific CSC markers (49). Mitochondrial ATP-depletion therapy is expected to functionally mimic fasting and/or caloric restriction, thereby more effectively starving CSCs to death. This has important implications for cancer prevention (50–52) and for potentially extending human lifespan during aging (53).

Recently, we also demonstrated that treatment with a panel of mitochondrially-targeted therapeutics, which potently inhibit mitochondrial protein translation or OXPHOS, could block tumor cell metastasis, using an *in vivo* pre-clinical model (54–56). These results indicated that ATP levels are functionally critical for the processes fueling aggressive tumor cell behaviors and spontaneous metastasis.

In further support of our hypothesis, other mitochondrial inhibitors are known to have promising anti-cancer effects, including IACS-010759, Gboxin, β1-blockers, Nebivolol, and Benzethonium (57–60).

SURVIVAL OF THE "FITTEST": ATP-HIGH CANCER CELLS SHOW A MULTI-DRUG RESISTANT PHENOTYPE, WITH ENHANCED ANTI-OXIDANT CAPACITY

Previous studies have shown that high anti-oxidant capacity, due to increased levels of reduced glutathione, elevated NADPH, and activated NRF2 signaling, significantly contributes to the onset of multi-drug resistance (61–67). Consistent with this hypothesis, recently we directly showed that ATP-high MCF7 cells have an increased anti-oxidant capacity, with elevated levels of reduced glutathione, and are intrinsically resistant to four different classes of drugs (Tamoxifen, Palbociclib, Doxycycline and DPI) (33). Therefore, the existence of the ATP-high CSC phenotype may help to mechanistically explain the pathogenesis of multi-drug resistance, during cancer therapy (**Figure 3**). In this context, current cancer therapy may allow only the metabolically "fittest" cancer cells to survive.

More specifically, as we have shown that the ATP-high phenotype is indeed transient, consistent with a "stemness" phenotype, external selection pressure created by a hostile environment, such as chemo-therapy, may further stabilize this

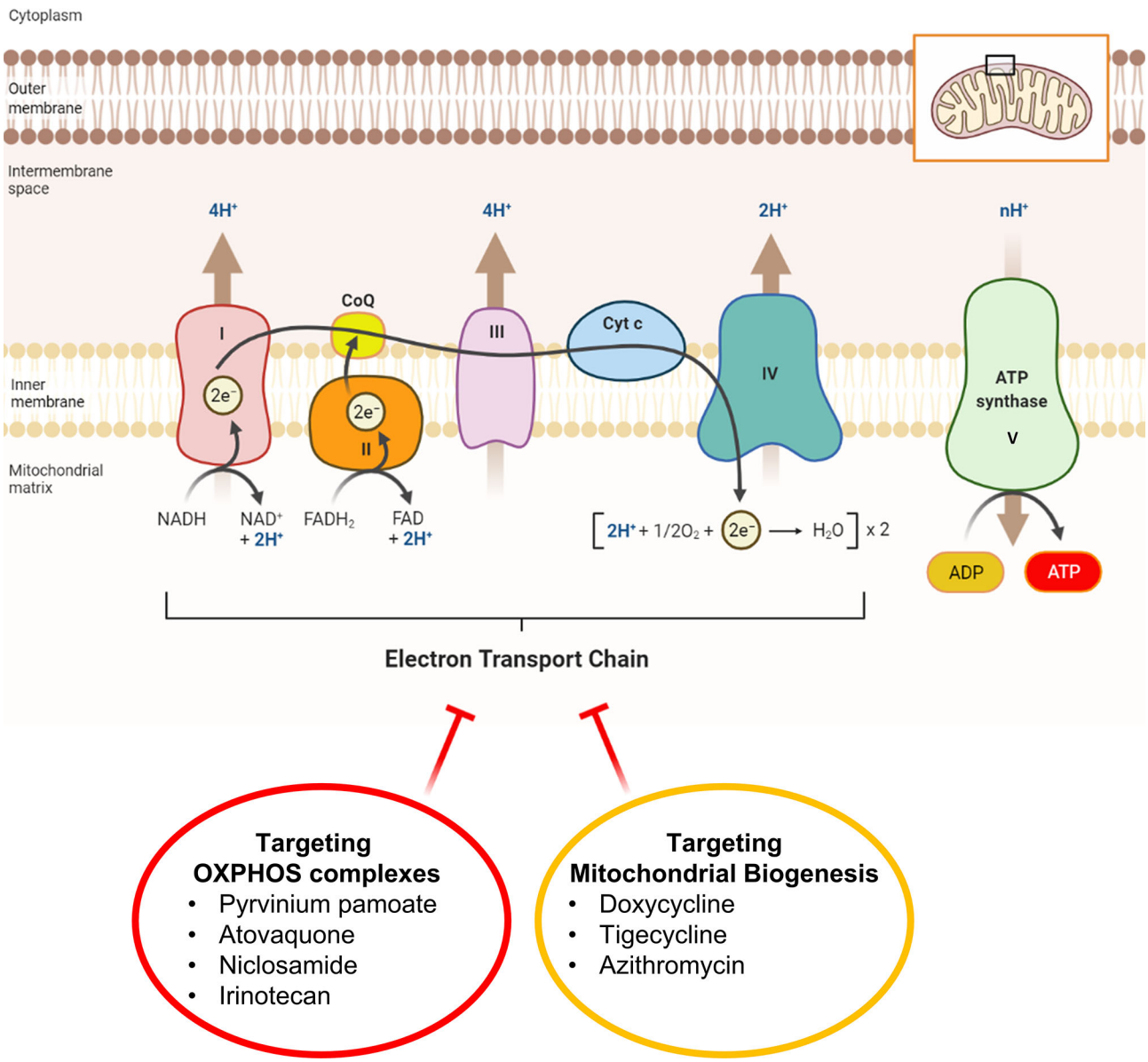

FIGURE 2 | Mitochondrial complexes I to IV can be safely targeted with FDA-approved drugs. This diagram illustrates that ATP-depletion can be induced in cancer cells by employing FDA-approved mitochondrial inhibitors that either i) block OXPHOS directly or ii) block OXPHOS indirectly, by halting mitochondrial protein translation. Inhibition of mitochondrial ATP production is a manageable side-effect that can re-purposed as a therapeutic effect to target and halt the propagation of CSCs. Inhibitors of mitochondrial protein translation (Doxycycline, Tigecycline and Azithromycin) prevent the production of the 13 proteins encoded by mitochondrial DNA (mt-DNA), including key subunits of complex I, III, and IV, as well as complex V (MT-ATP6, MT-ATP8) and Humanin (MT-RNR2).

metabolic state. As such, this high energy phenotype may be required for the survival of only the "fittest" cancer cells, allowing their propagation, under these harsh conditions.

Our recent findings with ATP-high MCF7 cells are also consistent with several other studies that establish a direct causal relationship between mitochondrial "power" and Tamoxifen-resistance. For example, MCF7-TAMR cells that were generated *via* chronic exposure to increasing concentrations of Tamoxifen, resulting in Tamoxifen-resistance, showed elevated levels of mitochondrial OXPHOS and ATP production (66). In MCF7-TAMR cells, acquired Tamoxifen-resistance was due to the over-expression of two key anti-oxidant proteins (NQO1 and GCLC) and their positive metabolic effects on mitochondrial metabolism, as revealed by unbiased proteomics analysis (66). In addition, recombinant over-expression of either NQO1 or GCLC in MCF7 cells autonomously conferred an ~2-fold increase in mitochondrial ATP-production and Tamoxifen-resistance (66). Moreover, recombinant over-expression of a somatic mutation

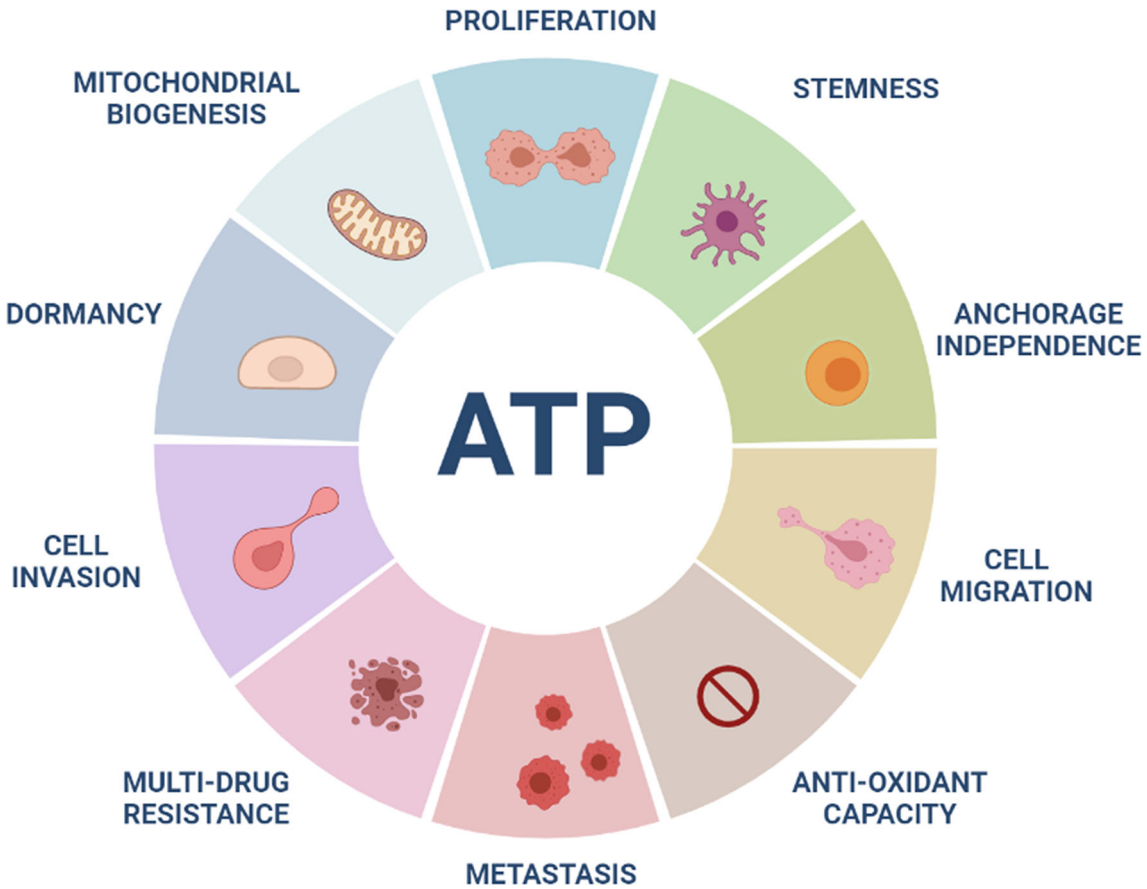

FIGURE 3 | High ATP levels are a major driver of aggressive cancer cell phenotypes. ATP-high cancer cells show increases in many aggressive properties or behaviors, including cell proliferation, stemness, anchorage-independence, migration, invasion, metastasis, anti-oxidant capacity and drug-resistance. In contrast, more "dormant" CSCs show low ATP levels. High mitochondrial ATP production may be related to increases in mitochondrial mass in ATP-high cancer cells.

(Y537S) in the estrogen receptor (ER-alpha; ESR1), clinically associated with acquired Tamoxifen-resistance in breast cancer patients, genetically conferred elevated mitochondrial biogenesis, OXPHOS and high ATP production (68). The proteomic profiles of MCF7-TAMR cells and MCF7-ESR1(Y537S) cells also showed considerable overlap in the biological processes that were functionally activated (68). Finally, 60 gene products functionally-associated with mitochondrial ATP production, were predictive of Tamoxifen-resistance in ER(+)/Luminal A breast cancer patients (69). These predictive biomarkers included 18 different mitochondrial ribosomal proteins (MRPs) and >20 distinct components of the mitochondrial OXPHOS complexes. Therefore, our recent results showing that "naïve" ATP-high MCF7 cells are intrinsically Tamoxifen-resistant, without any prior exposure to the drug, have important clinical implications for optimizing the effectiveness of hormonal breast cancer therapy.

Interestingly, it has been previously reported that treatment with conventional chemotherapeutic regimens, actually increases the number of CSCs, while selectively killing "bulk" cancer cells (70), but no metabolic hypotheses have been proposed to explain this phenomenon. In accordance with our "ATP-based hypothesis", Chan and colleagues (from Genentech, Inc.) examined the effects of gemcitabine and etoposide on the total cancer cell population (71). Remarkably, they observed that after treatment with gemcitabine and etoposide, the population of surviving cells showed an increase in ATP content, elevated mitochondrial mass, with more mitochondrial respiration (71). However, they did not propose a mechanistic explanation for these observations, nor did they consider the CSC population. Instead, they simply concluded that measuring ATP is not a good read-out to assess the effectiveness of chemo-therapeutic agents. Given our current findings with ATP-high cells, an alternate interpretation of their results is that gemcitabine and etoposide selectively killed the ATP-low sub-population of cancer cells, thereby enriching for the "energetic" ATP-high sub-population, which are more stem-like and drug-resistant. Therefore, new drug discovery should be initiated to help eradicate the ATP-high sub-population of cancer cells.

Higher intracellular ATP levels have also been suggested to account for acquired drug-resistance to oxaliplatin and cisplatin, in a variety of chronically-treated colon and ovarian cancer cell

lines (HT29, HCT116, A2780), although a diverse number of mechanisms have been proposed, including increased glycolysis and/or mitochondrial metabolism (72, 73). However, in these previous studies, ATP levels were measured only after chronically selecting for the drug resistant cell population. Therefore, a direct cause-effect relationship between ATP production and drug resistance could not be established.

Taken together, these findings are internally consistent with the idea that the high selection pressure afforded by these conventional chemotherapeutic agents ultimately drives the natural-selection and survival of only the "energetically fittest" cancer cells, namely the ATP-high sub-population. Therefore, in the future, new drug therapies must be implemented, to target and eradicate the ATP-high population of cancer cells, to prevent the accumulation of an aggressive, metastatic sub-population of tumor cells.

TUMOR DORMANCY AND MULTI-DRUG RESISTANCE: ARE THEY INTER-RELATED?

According to the conventional view of tumor dormancy, dormant cancer cells undergo slower rates of cell proliferation and/or cell cycle arrest (quiescence), to avoid therapy-induced cell death, leading to multi-drug resistance (67, 74). Surprisingly, recently we observed just the opposite phenomenon. ATP-low MCF7 cells were less proliferative, with >87% of the cells in the G0/G1 phase of the cell cycle, but were actually more sensitive to 4 different classes of drugs, using the 3D-mammosphere assay as a readout (33). Conversely, ATP-high MCF7 cells were significantly more proliferative, with >38% of the cells in either S-phase or G2/M, showing a clear multi-drug resistance phenotype. Therefore, high levels of mitochondrial ATP appear to be a key driver of both elevated cell proliferation and drug-resistance, as they represent the energetically "fittest" population of cancer cells (**Figure 3**).

DEFINING A METASTASIS GENE SIGNATURE, USING BIOINFORMATICS: VALIDATING THE IMPORTANCE OF ATP5F1C, USING SEVERAL INDEPENDENT DATA SETS AND MDA-MB-231 CELLS

To interrogate the possible role of mitochondrial ATP production in the process of metastasis, we also used a bioinformatics approach (33). Briefly, we intersected a series of publicly-available GEO breast cancer DataSets and defined a metastasis-associated gene-signature consisting of five ATP-related genes, namely ATP5F1C, UQCRB, COX20, NDUFA2, and ABCA2 (**Figure 4**). Notably, two members of the signature, ATP5F1C and UQCRB, are both known markers of maximal oxygen uptake ($V0_{2max}$) in mitochondrial-rich human skeletal muscle fibers (75).

Interestingly, ATP5F1C appeared to be the most relevant member of this metastasis signature, as it is directly connected to ATP-synthesis (76). ATP5F1C is the gamma subunit of the mitochondrial ATP synthase (Complex V) and is directly involved in converting physical energy (torque) into chemical energy (ATP) (33, 76).

To further validate and confirm the relevance of ATP5F1C, we next used a third completely independent database, namely the "The Metastatic Breast Cancer Project", which includes mRNA expression profiling data (RNA Seq V2 RSEM) from the RNA-sequencing of metastatic breast cancer samples, derived from N=146 patients (**Figure 4**). In this context, the mRNA expression of ATP5F1C was positively correlated with the co-expression of numerous breast CSC markers, circulating tumor cell (CTC) markers, metastasis markers, cell cycle regulatory proteins, and other mitochondrial-related genes, as well as three other members of the metastasis gene signature (UQCRB, COX20, NDUFA2). Independently, using Kaplan-Meier (K-M) analysis, high levels of ATP5F1C mRNA transcripts specifically predicted poor clinical outcomes in breast, ovarian and lung cancer patients (33).

To provide functional validation, we next used MDA-MB-231 cells as a metastatic model for triple-negative breast cancer. Interestingly, ATP-high MDA-MB-231 cells over-expressed ATP5F1C, as well as other members of mitochondrial complexes I-V and CTC markers (Ep-CAM1 and VCAM1), all relative to ATP-low MDA-MB-231 cells. ATP-high MDA-MB-231 cells also showed notable increases in ATP-production, proliferation, anchorage-independent growth, cell migration, invasion and spontaneous metastasis (**Figure 3**). Conversely, inducible knock-down of ATP5F1C in MDA-MB-231 cells was indeed sufficient to inhibit ATP-production, anchorage-independent growth and cell migration.

Moreover, ATP-high sub-populations of MDA-MB-231 and MCF7 cells both showed features of multi-drug resistance, consistent with a more aggressive cancer cell phenotype.

Therefore, ATP5F1C may be an attractive target for new drug development and metastasis prevention.

REPURPOSING BEDAQUILINE TO PREVENT ATP PRODUCTION, CANCER CELL MOTILITY, AND SPONTANEOUS METASTASIS *IN VIVO*: TARGETED DOWN-REGULATION OF ATP5F1C

Are there any existing FDA-approved inhibitors of the mitochondrial ATP-synthase that could be repurposed to target and prevent cancer metastasis? This would certainly accelerate future clinical trials, as FDA-approved drugs can re-enter Phase II trials, for another clinical indication, completely skipping Phase I, which is specifically focused on safety and toxicity.

Bedaquiline is a clinically-approved drug, that is usually used for anti-tuberculosis therapy, especially in the context of drug-resistant TB strains. More specifically, Bedaquiline was originally designed to target and block the activity of the ATP-synthase in mycobacteria. Perhaps surprisingly, recent studies have also demonstrated that

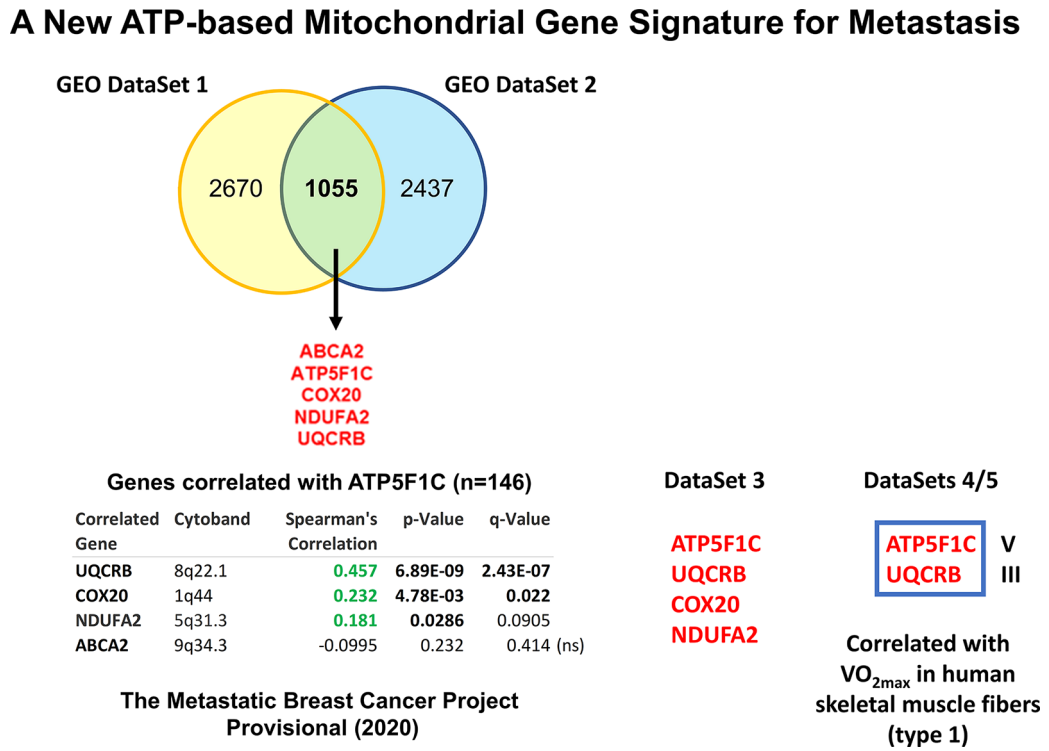

FIGURE 4 | Using several independent data sets to identify ATP5F1C as a key biomarker and therapeutic target for metastasis prevention. In order to define an ATP-related metastasis gene signature we first intersected two GEO DataSets focused on breast cancer metastasis (namely, GSE2034 and GSE59000), resulting in 5 common genes. The positive co-expression of ATP5F1C, with 3 other members of this gene signature (UQCRB, COX20, NDUFA2), was indeed confirmed by analyzing data from The Metastatic Breast Cancer Project (Provisional, February 2020; DataSet 3; https://mbcproject.org). Finally, 2 of these 4 gene transcripts (ATP5F1C and UQCRB) were independently found to be specifically-associated with i) maximal oxygen uptake (VO_{2max}) and ii) a higher percentage of mitochondrial-rich (type 1) fibers, in human skeletal muscle (DataSets 4/5), especially during exercise training. Therefore, ATP5F1C and UQCRB are likely to be key biomarkers of high OXPHOS and high mitochondrial ATP production in cancer cells. *Modified from Reference 33 and reproduced with permission, under a Creative Commons License*.

Bedaquiline significantly inhibits the human and the yeast mitochondrial ATP-synthase, as an off-target side effect (77). In addition, using cryo-EM as a tool for structural studies, investigators have localized the binding site of Bedaquiline to the integral membrane subunit (F_0), using the yeast mitochondrial ATP-synthase. Since the soluble F_1 subunit is physically tethered to the membrane-bound F_0 subunit *via* the gamma-subunit (ATP5F1C) (76), we hypothesized that ATP5F1C might be mis-folded and degraded in the presence of Bedaquiline. This would effectively disrupt ATP synthesis, as ATP5F1C functions as the rotating central stalk that helps convert torque into chemical energy, in the form of ATP (**Figure 5**).

Interestingly, we observed that ATP5F1C was effectively down-regulated after Bedaquiline treatment in MDA-MB-231 cells, resulting in significant reductions in ATP production, stemness, anchorage-independent growth and cell migration (33).

Bedaquiline-induced cell death in MDA-MB-231 cells was related to the onset of autophagy and necrosis, but apoptosis was not observed. Remarkably, the expression of ATP5F1C and ATP-production, as well as cell growth, remained unaffected after Bedaquiline treatment in MCF-10A cells, a non-tumor-producing human breast epithelial cell line. Therefore, the effects of Bedaquiline appeared to be restricted to cancer cells. Similarly, Bedaquiline inhibited ATP-production in MCF7 breast cancer cells, but not in hTERT-BJ1 cells, a normal human fibroblast cell line (44).

As a result of these findings, we tested the efficacy of Bedaquiline in a pre-clinical xenograft model, namely the CAM assay, which uses chicken eggs as the host for measuring tumor growth, spontaneous metastasis and drug toxicity (33). Our results demonstrated that Bedaquiline had no effect on MDA-MB-231 tumor growth, but effectively prevented spontaneous metastasis, by nearly 85%, at a concentration that did not show any significant chicken embryo toxicity (**Figure 5**).

As a consequence, we suggest that Bedaquiline could be re-purposed to prevent spontaneous metastasis, by driving ATP-depletion *via* its targeting of the ATP5F1C subunit, within the mitochondrial ATP-synthase multi-subunit complex. As such, clinical trials may be warranted.

We speculate that Bedaquiline, by mechanistically targeting the gamma-subunit of the ATP synthase, may promote dissociation of the F1-domain of the enzyme and thereby promote the opening of the transition pore (78–80). Recent

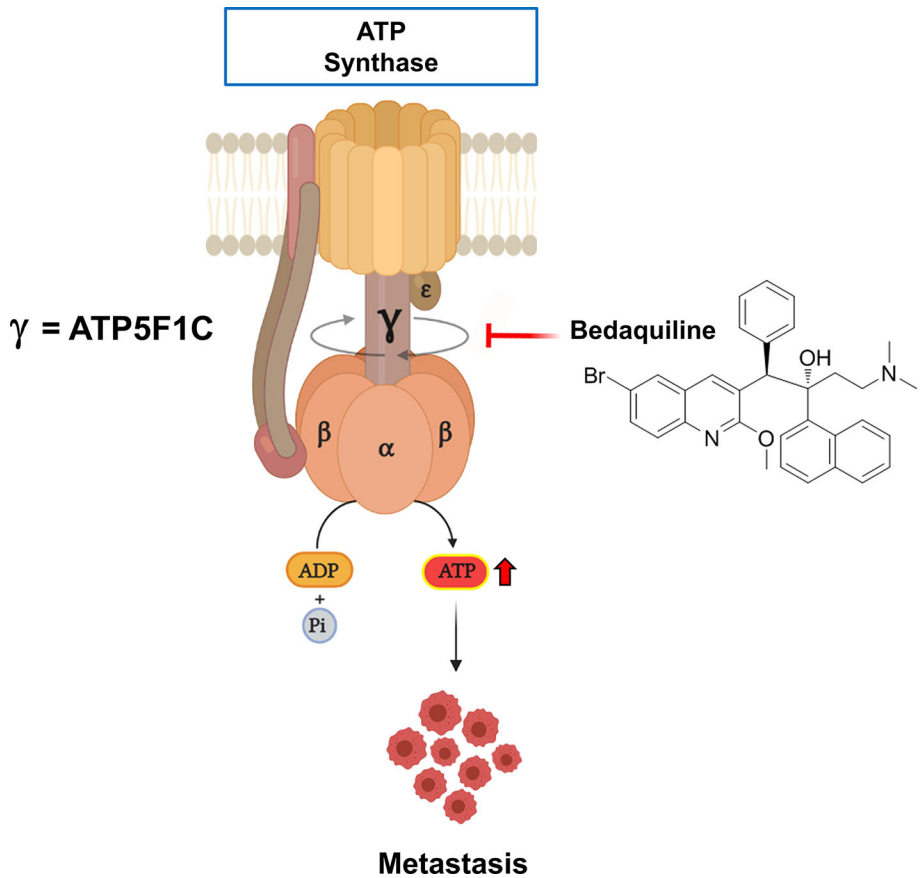

FIGURE 5 | Targeting the human mitochondrial ATP synthase with Bedaquiline, an FDA-approved drug, prevents spontaneous metastasis. Mitochondrial ATP-synthase is a nano-scale rotary molecular motor that uses the transport of hydrogen ions to generate physical energy in the form of torque that is then converted into chemical energy in the form of ATP. Rotation of the gamma-subunit (ATP5F1C) helps to convert physical energy into chemical energy. Note that Bedaquiline treatment induces the degradation or down-regulation of the gamma-subunit (ATP5F1C), resulting in ATP-depletion and the prevention of metastasis.

findings strongly support the idea that the ATP synthase forms the permeability transition pore (PTP) (78, 79). Prolonged opening of the PTP permeabilizes the inner mitochondrial membrane to small solutes and constitutes the point of no return in the execution of cell death.

Finally, the mitochondrial ATP-synthase is indeed subjected to numerous post-translational modifications (such as phosphorylation, as well as acetylation and succinylation on key lysine residues). Of course, this can potentially affect its level of enzymatic activity, and could perhaps explain the phenotypic differences between ATP-high and ATP-low cancer cells. Regarding Bedaquiline, this FDA-approved drug is known to bind directly to the ATP-synthase, but it is not known if Bedaquiline affects the status of these post-translational modifications.

CONCLUSIONS

In conclusion, we recently employed bioenergetic cell "stratification" using an ATP-based biomarker to isolate the metabolically "fittest" cancer cells. Using this novel approach, we obtained the first evidence that high levels of mitochondrial ATP are a primary determinant of aggressive cancer cell behavior(s), including spontaneous metastasis. These findings have important therapeutic implications for preventing treatment failure in cancer patients, which remains an urgent unmet clinical need.

For example, energetic cell profiling, using ATP as a biomarker, can provide a reliable source of ATP-high CSCs i) for establishing "living" tumor bio-banks and ii) for conducting small-molecule library screening, targeting drug resistance. This new conceptual framework will allow novel strategies to be developed to therapeutically target and eradicate even the energetically "fittest" CSCs, to ultimately abrogate drug resistance and metastasis.

In direct support of these observations, Kalluri and colleagues (81) observed that shRNA-mediated down-regulation of the key mitochondrial transcription factor, namely PGC-1α, significantly inhibited lung metastasis, in several independent cell lines (MDA-MB-231, 4T1 and B16F10 melanoma cells), but had little or no effect on tumor growth. These observations are consistent with the idea that targeted down-regulation of

PGC-1α inhibited the propagation of the "fittest" CSC sub-population (31, 32, 82), although the authors did not directly address the issue of the CSC phenotype.

Similarly, high expression levels of the ATP synthase inhibitory factor 1 (IF1), which inhibits the activity of the mitochondrial ATP synthase, predicts a better outcome for breast cancer patients, especially in the case of triple-negative breast cancer (83, 84). Moreover, IF1 over-expression reduces the production of ATP in mitochondria and decreases the proliferation and invasiveness of triple-negative breast cancer cells (84).

Finally, mitochondrial DNA-encoded (mt-DNA) cytochrome c oxidase II (MT-CO2) is an essential component of mitochondrial complex IV of the respiratory chain; without MT-CO2, electron transport and mitochondrial ATP production cannot proceed. Recently, Lebok and colleagues (85) showed that high levels of MT-CO2 protein expression in a cohort of approximately 2,000 breast cancer patients, from Germany and Switzerland, were clinically associated with advanced tumor stage, higher tumor grade, lymph nodal metastasis and shorter overall survival ($P < 0.0001$ each). Moreover, at the molecular level, high MT-CO2 protein expression was associated with elevated Ki67 (a marker of cell proliferation), the genetic amplification of several oncogenes (HER2, MYC, CCND1 and MDM2), the deletion of PTEN (a known tumor suppressor) and the down-regulation of estrogen receptor (ER-alpha) expression (85). As MT-CO2 is a well-established surrogate marker of mitochondrial DNA content and mitochondrial protein translation, these results clinically establish that high mitochondrial content (85) is a functional biomarker of aggressive tumor progression and metastasis, as well as poor prognosis and reduced overall survival. In further support of these clinical observations, MT-CO2 is over-expressed by >20-fold in an hTERT-enriched sub-population of breast cancer stem cells (86). Pharmacologically, MT-CO2 is effectively targeted by the FDA-approved antibiotic Doxycycline (87), which behaves as an inhibitor of mitochondrial protein translation and prevents ATP production (87), ultimately blocking metastasis in preclinical models (54). Therefore, Doxycycline may also provide a therapeutic solution for inhibiting MT-CO2 in breast cancer patients, to help prevent disease progression.

Taken together, these multiple lines of experimental evidence are all consistent with the idea that mitochondrial ATP-depletion therapy should be pursued as a viable means to provide metastasis prophylaxis in cancer patients.

AUTHOR CONTRIBUTIONS

ML wrote the first draft of this review article, which was then further edited by MF, BÓ, and FS. MF prepared the figures, which were edited by BÓ, ML, and FS. All authors contributed to the article and approved the submitted version.

FUNDING

This work was supported by research grant funding, provided by Lunella Biotech, Inc. (to FS and ML). The funder was not involved in the study design, collection, analysis, interpretation of data, the writing of this article or the decision to submit it for publication.

ACKNOWLEDGMENTS

We would like to thank the Foxpoint Foundation and the Healthy Life Foundation for their philanthropic donations toward new equipment and infrastructure, in the Translational Medicine Laboratory, at the University of Salford. We are grateful to Rumana Rafiq, for her kind and dedicated assistance, in keeping the Translational Medicine Laboratory at Salford running very smoothly.

REFERENCES

1. Langen P, Hucho F. Karl Lohmann and the Discovery of ATP. *Angew Chem Int Ed Engl* (2008) 47(10):1824–7. doi: 10.1002/anie.200702929
2. Khakh BS, Burnstock G. The Double Life of ATP. *Sci Am* (2009) 301(6):84–90, 92. doi: 10.1038/scientificamerican1209-84
3. Bonora M, Patergnani S, Rimessi A, De Marchi E, Suski JM, Bononi A, et al. ATP Synthesis and Storage. *Purinergic Signal* (2012) 8(3):343–57. doi: 10.1007/s11302-012-9305-8
4. Noji H, Yasuda R, Yoshida M, Kinosita KJr. Direct Observation of the Rotation of F1-ATPase. *Nature* (1997) 386(6622):299–302. doi: 10.1038/386299a0
5. Shampo MA, Kyle RA, Steensma DP, Paul D. Boyer-Nobel Prize for Work on ATP Synthase. *Mayo Clin Proc* (2011) 86(11):e51. doi: 10.4065/mcp.2011.0615
6. Senior AE, Weber J. Happy Motoring With ATP Synthase. *Nat Struct Mol Biol* (2004) 11(2):110–2. doi: 10.1038/nsmb0204-110
7. Ahmad Z, Cox JL. ATP Synthase: The Right Size Base Model for Nanomotors in Nanomedicine. *Sci World J* (2014) 2014:567398. doi: 10.1155/2014/567398
8. Hargreaves M, Spriet LL. Exercise Metabolism: Fuels for the Fire. *Cold Spring Harb Perspect Med* (2018) 8(8):a029744. doi: 10.1101/cshperspect.a029744
9. Neufer PD. The Bioenergetics of Exercise. *Cold Spring Harb Perspect Med* (2018) 8(5):a029678. doi: 10.1101/cshperspect.a029678
10. Wilson DF. Oxidative Phosphorylation: Regulation and Role in Cellular and Tissue Metabolism. *J Physiol* (2017) 595(23):7023–38. doi: 10.1113/JP273839
11. Morelli AM, Ravera S, Calzia D, Panfoli I. An Update of the Chemiosmotic Theory as Suggested by Possible Proton Currents Inside the Coupling Membrane. *Open Biol* (2019) 9(4):180221. doi: 10.1098/rsob.180221
12. Stock D, Leslie AG, Walker JE. Molecular Architecture of the Rotary Motor in ATP Synthase. *Science* (1999) 286(5445):1700–5. doi: 10.1126/science.286.5445.1700
13. Spikes TE, Montgomery MG, Walker JE. Structure of the Dimeric ATP Synthase From Bovine Mitochondria. *Proc Natl Acad Sci USA* (2020) 117 (38):23519–26. doi: 10.1073/pnas.2013998117
14. He J, Ford HC, Carroll J, Douglas C, Gonzales E, Ding S, et al. Assembly of the Membrane Domain of ATP Synthase in Human Mitochondria. *Proc Natl Acad Sci USA* (2018) 115(12):2988–93. doi: 10.1073/pnas.1722086115
15. Hayashi S, Ueno H, Shaikh AR, Umemura M, Kamiya M, Ito Y, et al. Molecular Mechanism of ATP Hydrolysis in F1-ATPase Revealed by Molecular Simulations and Single-Molecule Observations. *J Am Chem Soc* (2012) 134(20):8447–54. doi: 10.1021/ja211027m
16. Abrahams JP, Leslie AG, Lutter R, Walker JE. Structure at 2.8 A Resolution of F1-ATPase From Bovine Heart Mitochondria. *Nature* (1994) 370(6491):621–8. doi: 10.1038/370621a0
17. McCay CM, Crowell MF, Maynard LA. The Effect of Retarded Growth Upon the Length of Life Span and Upon the Ultimate Body Size: One Figure. *J Nutr* (1935) 10(1):63–79. doi: 10.1093/jn/10.1.63
18. Muller I, Zimmermann M, Becker D, Flomer M. Calendar Life Span Versus Budding Life Span of Saccharomyces Cerevisiae. *Mech Ageing Dev* (1980) 12 (1):47–52. doi: 10.1016/0047-6374(80)90028-7

19. Palliyaguru DL, Moats JM, Di Germanio C, Bernier M, de Cabo R. Frailty Index as a Biomarker of Lifespan and Healthspan: Focus on Pharmacological Interventions. *Mech Ageing Dev* (2019) 180:42–8. doi: 10.1016/j.mad.2019.03.005
20. Madeo F, Carmona-Gutierrez D, Hofer SJ, Kroemer G. Caloric Restriction Mimetics Against Age-Associated Disease: Targets, Mechanisms, and Therapeutic Potential. *Cell Metab* (2019) 29(3):592–610. doi: 10.1016/j.cmet.2019.01.018
21. Zheng J, Ramirez VD. Inhibition of Mitochondrial Proton F0F1-ATPase/ATP Synthase by Polyphenolic Phytochemicals. *Br J Pharmacol* (2000) 130 (5):1115–23. doi: 10.1038/sj.bjp.0703397
22. Lopez-Otin C, Blasco MA, Partridge L, Serrano M, Kroemer G. The Hallmarks of Aging. *Cell* (2013) 153(6):1194–217. doi: 10.1016/j.cell.2013.05.039
23. Esparza-Molto PB, Nuevo-Tapioles C, Cuezva JM. Regulation of the H (+)-ATP Synthase by IF1: A Role in Mitohormesis. *Cell Mol Life Sci* (2017) 74(12):2151–66. doi: 10.1007/s00018-017-2462-8
24. Rajendran M, Dane E, Conley J, Tantama M. Imaging Adenosine Triphosphate (ATP). *Biol Bull* (2016) 231(1):73–84. doi: 10.1086/689592
25. Iannetti EF, Prigione A, Smeitink JAM, Koopman WJH, Beyrath J, Renkema H. Live-Imaging Readouts and Cell Models for Phenotypic Profiling of Mitochondrial Function. *Front Genet* (2019) 10:131. doi: 10.3389/fgene.2019.00131
26. Depaoli MR, Hay JC, Graier WF, Malli R. The Enigmatic ATP Supply of the Endoplasmic Reticulum. *Biol Rev Camb Philos Soc* (2019) 94(2):610–28. doi: 10.1111/brv.12469
27. Arai HC, Yukawa A, Iwatate RJ, Kamiya M, Watanabe R, Urano Y, et al. Torque Generation Mechanism of F1-ATPase Upon NTP Binding. *Biophys J* (2014) 107(1):156–64. doi: 10.1016/j.bpj.2014.05.016
28. Farnie G, Sotgia F, Lisanti MP. High Mitochondrial Mass Identifies a Sub-Population of Stem-Like Cancer Cells That Are Chemo-Resistant. *Oncotarget* (2015) 6(31):30472–86. doi: 10.18632/oncotarget.5401
29. Wang L, Yuan L, Zeng X, Peng J, Ni Y, Er JC, et al. A Multisite-Binding Switchable Fluorescent Probe for Monitoring Mitochondrial ATP Level Fluctuation in Live Cells. *Angew Chem Int Ed Engl* (2016) 55(5):1773–6. doi: 10.1002/anie.201510003
30. Whitaker-Menezes D, Martinez-Outschoorn UE, Flomenberg N, Birbe RC, Witkiewicz AK, Howell A, et al. Hyperactivation of Oxidative Mitochondrial Metabolism in Epithelial Cancer Cells in Situ: Visualizing the Therapeutic Effects of Metformin in Tumor Tissue. *Cell Cycle* (2011) 10(23):4047–64. doi: 10.4161/cc.10.23.18151
31. Sotgia F, Whitaker-Menezes D, Martinez-Outschoorn UE, Flomenberg N, Birbe RC, Witkiewicz AK, et al. Mitochondrial Metabolism in Cancer Metastasis: Visualizing Tumor Cell Mitochondria and the "Reverse Warburg Effect" in Positive Lymph Node Tissue. *Cell Cycle* (2012) 11 (7):1445–54. doi: 10.4161/cc.19841
32. Fiorillo M, Sotgia F, Lisanti MP. "Energetic" Cancer Stem Cells (E-CSCs): A New Hyper-Metabolic and Proliferative Tumor Cell Phenotype, Driven by Mitochondrial Energy. *Front Oncol* (2018) 8:677. doi: 10.3389/fonc.2018.00677
33. Fiorillo M, Scatena C, Naccarato AG, Sotgia F, Lisanti MP. Bedaquiline, an FDA-Approved Drug, Inhibits Mitochondrial ATP Production and Metastasis In Vivo, by Targeting the Gamma Subunit (ATP5F1C) of the ATP Synthase. *Cell Death Differ* (2021) 28(9):2797–817. doi: 10.1038/s41418-021-00788-x
34. Weinberg F, Hamanaka R, Wheaton WW, Weinberg S, Joseph J, Lopez M, et al. Mitochondrial Metabolism and ROS Generation Are Essential for Kras-Mediated Tumorigenicity. *Proc Natl Acad Sci USA* (2010) 107(19):8788–93. doi: 10.1073/pnas.1003428107
35. Formentini L, Sanchez-Arago M, Sanchez-Cenizo L, Cuezva JM. The Mitochondrial ATPase Inhibitory Factor 1 Triggers a ROS-Mediated Retrograde Prosurvival and Proliferative Response. *Mol Cell* (2012) 45 (6):731–42. doi: 10.1016/j.molcel.2012.01.008
36. Martinez-Outschoorn UE, Peiris-Pages M, Pestell RG, Sotgia F, Lisanti MP. Cancer Metabolism: A Therapeutic Perspective. *Nat Rev Clin Oncol* (2017) 14 (1):11–31. doi: 10.1038/nrclinonc.2016.60
37. Martinez-Outschoorn UE, Sotgia F, Lisanti MP. Power Surge: Supporting Cells "Fuel" Cancer Cell Mitochondria. *Cell Metab* (2012) 15(1):4–5. doi: 10.1016/j.cmet.2011.12.011
38. Sotgia F, Ozsvari B, Fiorillo M, De Francesco EM, Bonuccelli G, Lisanti MP. A Mitochondrial Based Oncology Platform for Targeting Cancer Stem Cells (CSCs): MITO-ONC-RX. *Cell Cycle* (2018) 17(17):2091–100. doi: 10.1080/15384101.2018.1515551
39. De Francesco EM, Sotgia F, Lisanti MP. Cancer Stem Cells (CSCs): Metabolic Strategies for Their Identification and Eradication. *Biochem J* (2018) 475 (9):1611–34. doi: 10.1042/BCJ20170164
40. Peiris-Pages M, Martinez-Outschoorn UE, Pestell RG, Sotgia F, Lisanti MP. Cancer Stem Cell Metabolism. *Breast Cancer Res* (2016) 18(1):55. doi: 10.1186/s13058-016-0712-6
41. Lamb R, Ozsvari B, Lisanti CL, Tanowitz HB, Howell A, Martinez-Outschoorn UE, et al. Antibiotics That Target Mitochondria Effectively Eradicate Cancer Stem Cells, Across Multiple Tumor Types: Treating Cancer Like an Infectious Disease. *Oncotarget* (2015) 6(7):4569–84. doi: 10.18632/oncotarget.3174
42. Fiorillo M, Peiris-Pages M, Sanchez-Alvarez R, Bartella L, Di Donna L, Dolce V, et al. Bergamot Natural Products Eradicate Cancer Stem Cells (CSCs) by Targeting Mevalonate, Rho-GDI-Signalling and Mitochondrial Metabolism. *Biochim Biophys Acta Bioenerg* (2018) 1859(9):984–96. doi: 10.1016/j.bbabio.2018.03.018
43. Ozsvari B, Sotgia F, Lisanti MP. Exploiting Mitochondrial Targeting Signal(s), TPP and Bis-TPP, for Eradicating Cancer Stem Cells (CSCs). *Aging (Albany NY)* (2018) 10(2):229–40. doi: 10.18632/aging.101384
44. Fiorillo M, Lamb R, Tanowitz HB, Cappello AR, Martinez-Outschoorn UE, Sotgia F, et al. Bedaquiline, an FDA-Approved Antibiotic, Inhibits Mitochondrial Function and Potently Blocks the Proliferative Expansion of Stem-Like Cancer Cells (CSCs). *Aging (Albany NY)* (2016) 8(8):1593–607. doi: 10.18632/aging.100983
45. Fiorillo M, Lamb R, Tanowitz HB, Mutti L, Krstic-Demonacos M, Cappello AR, et al. Repurposing Atovaquone: Targeting Mitochondrial Complex III and OXPHOS to Eradicate Cancer Stem Cells. *Oncotarget* (2016) 7 (23):34084–99. doi: 10.18632/oncotarget.9122
46. Ozsvari B, Bonuccelli G, Sanchez-Alvarez R, Foster R, Sotgia F, Lisanti MP. Targeting Flavin-Containing Enzymes Eliminates Cancer Stem Cells (CSCs), by Inhibiting Mitochondrial Respiration: Vitamin B2 (Riboflavin) in Cancer Therapy. *Aging (Albany NY)* (2017) 9(12):2610–28. doi: 10.18632/aging.101351
47. Ozsvari B, Sotgia F, Simmons K, Trowbridge R, Foster R, Lisanti MP. Mitoketoscins: Novel Mitochondrial Inhibitors for Targeting Ketone Metabolism in Cancer Stem Cells (CSCs). *Oncotarget* (2017) 8(45):78340–50. doi: 10.18632/oncotarget.21259
48. Fiorillo M, Toth F, Sotgia F, Lisanti MP. Doxycycline, Azithromycin and Vitamin C (DAV): A Potent Combination Therapy for Targeting Mitochondria and Eradicating Cancer Stem Cells (CSCs). *Aging (Albany NY)* (2019) 11(8):2202–16. doi: 10.18632/aging.101905
49. Scatena C, Roncella M, Di Paolo A, Aretini P, Menicagli M, Fanelli G, et al. Doxycycline, an Inhibitor of Mitochondrial Biogenesis, Effectively Reduces Cancer Stem Cells (CSCs) in Early Breast Cancer Patients: A Clinical Pilot Study. *Front Oncol* (2018) 8:452. doi: 10.3389/fonc.2018.00452
50. Lamb R, Harrison H, Smith DL, Townsend PA, Jackson T, Ozsvari B, et al. Targeting Tumor-Initiating Cells: Eliminating Anabolic Cancer Stem Cells With Inhibitors of Protein Synthesis or by Mimicking Caloric Restriction. *Oncotarget* (2015) 6(7):4585–601. doi: 10.18632/oncotarget.3278
51. Saleh AD, Simone BA, Palazzo J, Savage JE, Sano Y, Dan T, et al. Caloric Restriction Augments Radiation Efficacy in Breast Cancer. *Cell Cycle* (2013) 12(12):1955–63. doi: 10.4161/cc.25016
52. Champ CE, Baserga R, Mishra MV, Jin L, Sotgia F, Lisanti MP, et al. Nutrient Restriction and Radiation Therapy for Cancer Treatment: When Less is More. *Oncologist* (2013) 18(1):97–103. doi: 10.1634/theoncologist.2012-0164
53. Vermeij WP, Dolle ME, Reiling E, Jaarsma D, Payan-Gomez C, Bombardieri CR, et al. Restricted Diet Delays Accelerated Ageing and Genomic Stress in DNA-Repair-Deficient Mice. *Nature* (2016) 537(7620):427–31. doi: 10.1038/nature19329
54. Ozsvari B, Magalhaes LG, Latimer J, Kangasmetsa J, Sotgia F, Lisanti MP. A Myristoyl Amide Derivative of Doxycycline Potently Targets Cancer Stem Cells (CSCs) and Prevents Spontaneous Metastasis, Without Retaining Antibiotic Activity. *Front Oncol* (2020) 10:1528. doi: 10.3389/fonc.2020.01528
55. Ozsvari B, Sotgia F, Lisanti MP. First-In-Class Candidate Therapeutics That Target Mitochondria and Effectively Prevent Cancer Cell Metastasis: Mitoriboscins and TPP Compounds. *Aging (Albany NY)* (2020) 12 (11):10162–79. doi: 10.18632/aging.103336
56. Sargiacomo C, Stonehouse S, Moftakhar Z, Sotgia F, Lisanti MP. MitoTracker Deep Red (MTDR) Is a Metabolic Inhibitor for Targeting Mitochondria and Eradicating Cancer Stem Cells (CSCs), With Anti-Tumor and Anti-Metastatic Activity *In Vivo*. *Front Oncol* (2021) 11:678343. doi: 10.3389/fonc.2021.678343

57. Molina JR, Sun Y, Protopopova M, Gera S, Bandi M, Bristow C, et al. An Inhibitor of Oxidative Phosphorylation Exploits Cancer Vulnerability. *Nat Med* (2018) 24(7):1036–46. doi: 10.1038/s41591-018-0052-4
58. Shi Y, Lim SK, Liang Q, Iyer SV, Wang HY, Wang Z, et al. Gboxin is an Oxidative Phosphorylation Inhibitor That Targets Glioblastoma. *Nature* (2019) 567(7748):341–6. doi: 10.1038/s41586-019-0993-x
59. Nuevo-Tapioles C, Santacatterina F, Stamatakis K, Nunez de Arenas C, Gomez de Cedron M, Formentini L, et al. Coordinate Beta-Adrenergic Inhibition of Mitochondrial Activity and Angiogenesis Arrest Tumor Growth. *Nat Commun* (2020) 11(1):3606. doi: 10.1038/s41467-020-17384-1
60. De Mario A, Tosatto A, Hill JM, Kriston-Vizi J, Ketteler R, Vecellio Reane D, et al. Identification and Functional Validation of FDA-Approved Positive and Negative Modulators of the Mitochondrial Calcium Uniporter. *Cell Rep* (2021) 35(12):109275. doi: 10.1016/j.celrep.2021.109275
61. Cort A, Ozben T, Saso L, De Luca C, Korkina L. Redox Control of Multidrug Resistance and Its Possible Modulation by Antioxidants. *Oxid Med Cell Longev* (2016) 2016:4251912. doi: 10.1155/2016/4251912
62. Greenwood HE, McCormick PN, Gendron T, Glaser M, Pereira R, Maddocks ODK, et al. Measurement of Tumor Antioxidant Capacity and Prediction of Chemotherapy Resistance in Preclinical Models of Ovarian Cancer by Positron Emission Tomography. *Clin Cancer Res* (2019) 25(8):2471–82. doi: 10.1158/1078-0432.CCR-18-3423
63. Hatem E, El Banna N, Huang ME. Multifaceted Roles of Glutathione and Glutathione-Based Systems in Carcinogenesis and Anticancer Drug Resistance. *Antioxid Redox Signal* (2017) 27(15):1217–34. doi: 10.1089/ars.2017.7134
64. Peiris-Pages M, Martinez-Outschoorn UE, Sotgia F, Lisanti MP. Metastasis and Oxidative Stress: Are Antioxidants a Metabolic Driver of Progression? *Cell Metab* (2015) 22(6):956–8. doi: 10.1016/j.cmet.2015.11.008
65. Kahroba H, Shirmohamadi M, Hejazi MS, Samadi N. The Role of Nrf2 Signaling in Cancer Stem Cells: From Stemness and Self-Renewal to Tumorigenesis and Chemoresistance. *Life Sci* (2019) 239:116986. doi: 10.1016/j.lfs.2019.116986
66. Fiorillo M, Sotgia F, Sisci D, Cappello AR, Lisanti MP. Mitochondrial "Power" Drives Tamoxifen Resistance: NQO1 and GCLC Are New Therapeutic Targets in Breast Cancer. *Oncotarget* (2017) 8(12):20309–27. doi: 10.18632/oncotarget.15852
67. Liu S, Cong Y, Wang D, Sun Y, Deng L, Liu Y, et al. Breast Cancer Stem Cells Transition Between Epithelial and Mesenchymal States Reflective of Their Normal Counterparts. *Stem Cell Rep* (2014) 2(1):78–91. doi: 10.1016/j.stemcr.2013.11.009
68. Fiorillo M, Sanchez-Alvarez R, Sotgia F, Lisanti MP. The ER-Alpha Mutation Y537S Confers Tamoxifen-Resistance via Enhanced Mitochondrial Metabolism, Glycolysis and Rho-GDI/PTEN Signaling: Implicating TIGAR in Somatic Resistance to Endocrine Therapy. *Aging (Albany NY)* (2018) 10 (12):4000–23. doi: 10.18632/aging.101690
69. Sotgia F, Fiorillo M, Lisanti MP. Mitochondrial Markers Predict Recurrence, Metastasis and Tamoxifen-Resistance in Breast Cancer Patients: Early Detection of Treatment Failure With Companion Diagnostics. *Oncotarget* (2017) 8(40):68730–45. doi: 10.18632/oncotarget.19612
70. Chiodi I, Belgiovine C, Dona F, Scovassi AI, Mondello C. Drug Treatment of Cancer Cell Lines: A Way to Select for Cancer Stem Cells? *Cancers (Basel)* (2011) 3(1):1111–28. doi: 10.3390/cancers3011111
71. Chan GK, Kleinheinz TL, Peterson D, Moffat JG. A Simple High-Content Cell Cycle Assay Reveals Frequent Discrepancies Between Cell Number and ATP and MTS Proliferation Assays. *PLoS One* (2013) 8(5):e63583. doi: 10.1371/journal.pone.0063583
72. Zhou Y, Tozzi F, Chen J, Fan F, Xia L, Wang J, et al. Intracellular ATP Levels Are a Pivotal Determinant of Chemoresistance in Colon Cancer Cells. *Cancer Res* (2012) 72(1):304–14. doi: 10.1158/0008-5472.CAN-11-1674
73. Schneider V, Krieger ML, Bendas G, Jaehde U, Kalayda GV. Contribution of Intracellular ATP to Cisplatin Resistance of Tumor Cells. *J Biol Inorg Chem* (2013) 18(2):165–74. doi: 10.1007/s00775-012-0960-6
74. Recasens A, Munoz L. Targeting Cancer Cell Dormancy. *Trends Pharmacol Sci* (2019) 40(2):128–41. doi: 10.1016/j.tips.2018.12.004
75. Parikh H, Nilsson E, Ling C, Poulsen P, Almgren P, Nittby H, et al. Molecular Correlates for Maximal Oxygen Uptake and Type 1 Fibers. *Am J Physiol Endocrinol Metab* (2008) 294(6):E1152–9. doi: 10.1152/ajpendo.90255.2008
76. Walker JE. The ATP Synthase: The Understood, the Uncertain and the Unknown. *Biochem Soc Trans* (2013) 41(1):1–16. doi: 10.1042/BST20110773
77. Luo M, Zhou W, Patel H, Srivastava AP, Symersky J, Bonar MM, et al. Bedaquiline Inhibits the Yeast and Human Mitochondrial ATP Synthases. *Commun Biol* (2020) 3(1):452. doi: 10.1038/s42003-020-01173-z
78. Urbani A, Giorgio V, Carrer A, Franchin C, Arrigoni G, Jiko C, et al. Purified F-ATP Synthase Forms a Ca(2+)-Dependent High-Conductance Channel Matching the Mitochondrial Permeability Transition Pore. *Nat Commun* (2019) 10(1):4341. doi: 10.1038/s41467-019-12331-1
79. Mnatsakanyan N, Llaguno MC, Yang Y, Yan Y, Weber J, Sigworth FJ, et al. A Mitochondrial Megachannel Resides in Monomeric F1FO ATP Synthase. *Nat Commun* (2019) 10(1):5823. doi: 10.1038/s41467-019-13766-2
80. Mnatsakanyan N, Jonas EA. ATP Synthase C-Subunit Ring as the Channel of Mitochondrial Permeability Transition: Regulator of Metabolism in Development and Degeneration. *J Mol Cell Cardiol* (2020) 144:109–18. doi: 10.1016/j.yjmcc.2020.05.013
81. LeBleu VS, O'Connell JT, Gonzalez Herrera KN, Wikman H, Pantel K, Haigis MC, et al. PGC-1alpha Mediates Mitochondrial Biogenesis and Oxidative Phosphorylation in Cancer Cells to Promote Metastasis. *Nat Cell Biol* (2014) 16(10):992–1003, 1-15. doi: 10.1038/ncb3039
82. De Luca A, Fiorillo M, Peiris-Pages M, Ozsvari B, Smith DL, Sanchez-Alvarez R, et al. Mitochondrial Biogenesis is Required for the Anchorage-Independent Survival and Propagation of Stem-Like Cancer Cells. *Oncotarget* (2015) 6 (17):14777–95. doi: 10.18632/oncotarget.4401
83. Sanchez-Arago M, Formentini L, Martinez-Reyes I, Garcia-Bermudez J, Santacatterina F, Sanchez-Cenizo L, et al. Expression, Regulation and Clinical Relevance of the ATPase Inhibitory Factor 1 in Human Cancers. *Oncogenesis* (2013) 2:e46. doi: 10.1038/oncsis.2013.9
84. Garcia-Ledo L, Nuevo-Tapioles C, Cuevas-Martin C, Martinez-Reyes I, Soldevilla B, Gonzalez-Llorente L, et al. Overexpression of the ATPase Inhibitory Factor 1 Favors a Non-Metastatic Phenotype in Breast Cancer. *Front Oncol* (2017) 7:69. doi: 10.3389/fonc.2017.00069
85. Lebok P, Schütt K, Kluth M, Witzel I, Wölber L, Paluchowski P, et al. High Mitochondrial Content Is Associated With Breast Cancer Aggressiveness. *Mol Clin Oncol* (2021) 15(4):203. doi: 10.3892/mco.2021.2365
86. Lamb R, Ozsvari B, Bonuccelli G, Smith DL, Pestell RG, Martinez-Outschoorn UE, et al. Dissecting Tumor Metabolic Heterogeneity: Telomerase and Large Cell Size Metabolically Define a Sub-Population of Stem-Like, Mitochondrial-Rich, Cancer Cells. *Oncotarget* (2015) 6(26):21892–905. doi: 10.18632/oncotarget.5260
87. De Francesco EM, Bonuccelli G, Maggiolini M, Sotgia F, Lisanti MP. Vitamin C and Doxycycline: A Synthetic Lethal Combination Therapy Targeting Metabolic Flexibility in Cancer Stem Cells (CSCs). *Oncotarget* (2017) 8 (40):67269–86. doi: 10.18632/oncotarget.18428

Conflict of Interest: ML and FS hold a minority interest in Lunella Biotech, Inc.

The remaining authors declare that the research was conducted in the absence of any commercial or financial relationships that could be construed as a potential conflict of interest.

The reviewer, SF, declared a past co-authorship with one of the authors, ML, to the handling editor.

Publisher's Note: All claims expressed in this article are solely those of the authors and do not necessarily represent those of their affiliated organizations, or those of the publisher, the editors and the reviewers. Any product that may be evaluated in this article, or claim that may be made by its manufacturer, is not guaranteed or endorsed by the publisher.

frontiers in Oncology

MINI REVIEW
published: 05 November 2021
doi: 10.3389/fonc.2021.756888

Cancer Stem Cells: Metabolic Characterization for Targeted Cancer Therapy

Jasmeet Kaur and Shalmoli Bhattacharyya *

Department of Biophysics, Postgraduate Institute of Medical Education and Research (PGIMER), Chandigarh, India

The subpopulation of cancer stem cells (CSCs) within tumor bulk are known for tumor recurrence and metastasis. CSCs show intrinsic resistance to conventional therapies and phenotypic plasticity within the tumor, which make these a difficult target for conventional therapies. CSCs have different metabolic phenotypes based on their needs as compared to the bulk cancer cells. CSCs show metabolic plasticity and constantly alter their metabolic state between glycolysis and oxidative metabolism (OXPHOS) to adapt to scarcity of nutrients and therapeutic stress. The metabolic characteristics of CSCs are distinct compared to non-CSCs and thus provide an opportunity to devise more effective strategies to target CSCs. Mechanism for metabolic switch in CSCs is still unravelled, however existing evidence suggests that tumor microenvironment affects the metabolic phenotype of cancer cells. Understanding CSCs metabolism may help in discovering new and effective clinical targets to prevent cancer relapse and metastasis. This review summarises the current knowledge of CSCs metabolism and highlights the potential targeted treatment strategies.

Keywords: metabolism, cancer stem cell, glucose, glutamine, OxPhos

OPEN ACCESS

Edited by:
Michael P. Lisanti,
University of Salford Manchester,
United Kingdom

Reviewed by:
Pritam Sadhukhan,
Johns Hopkins University,
United States
Herbert Levine,
Rice University, United States

***Correspondence:**
Shalmoli Bhattacharyya
shalmoli2007@yahoo.co.in;
shalmolib@gmail.com

Specialty section:
This article was submitted to Cancer Metabolism, a section of the journal Frontiers in Oncology

Received: *11 August 2021*
Accepted: *18 October 2021*
Published: *05 November 2021*

Citation:
Kaur J and Bhattacharyya S (2021) Cancer Stem Cells: Metabolic Characterization for Targeted Cancer Therapy. Front. Oncol. 11:756888. doi: 10.3389/fonc.2021.756888

INTRODUCTION

Cancer causes significant deaths worldwide, despite major innovations in treatment therapy strategies, radiation- and chemo-therapy and drug delivery technologies. A major contributor to the cancer treatment-associated toxicities and resistance (1–3), is their inability to eradicate subset of cancer stem cells (CSCs) which drive tumour growth and heterogeneity. CSCs presence makes tumors resistant to conventional therapies (4). Density of CSCs is a proven prognostic marker in various cancers (5, 6), thus targeting CSCs is an effective way for treating cancer.

CSCs self-renewal and asymmetric division capacity help tumors to regenerate and propagate post-treatment. CSCs populations provide high radio- and chemo-resistance due to efficient DNA repair and cellular redox homeostasis, protective tumor microenvironment, escape from immune response and unique metabolic phenotype (7–10). CSCs use metabolic reprogramming to escape immune system (11) and grant them plasticity (12). Metabolic reprogramming induce M2 phenotype in tumor-associated macrophages (TAMs) (13, 14) and glycolysis induce IL-6 secretion in M2 macrophages (15). Secreted IL-6 promotes CSC phenotype in cancer cells (16) *via* activation of STAT3/NFκB signaling pathways (17). CSCs in turn induce M2 phenotype in TAMs to confer drug

resistance and tumorigenicity in CSCs by blocking the anti-tumor $CD8^+$ response during chemotherapy (18).

Till date the origin of CSCs remains elusive. Two models are postulated to explain the genetic and functional heterogeneity of cancer in a single patient: the clonal evolution model and the cancer stem cell (CSC) hypothesis (19). The clonal evolution model suggests that multiple stepwise oncogenic mutations in somatic cells leads to tumor formation and natural selection favors the tumor cells with aggressive phenotype (20, 21). The CSC hypothesis suggests that metabolic events occurring in cancer epithelial cells may generate CSCs (**Figure 1**). Altered metabolic events in cancer cells may affect chromatin organization and activate epigenetic program (22) which may further fuel metabolic-reprogramming of CSCs. Two proposed models explain how metabolic alterations could affect epigenetics (22). In the first model, metabolism reprogramming facilitates differentiation of one cell type to another by altering chromatin modifications without affecting the epigenomic landscape. The second model proposes that altered metabolism induces new potential cell types *via* creation of novel stable epigenetic states, thus reshaping the entire epigenomic landscape. In this model, altered metabolism remodels chromatin by either inducing gene expression or affecting availability of substrates and cofactors for chromatin-modifying enzymes. In either case, the end-result is a novel cell state that is irreversible as epigenomic landscape has changed.

Metabolic characterization of CSCs has been a challenging task, as CSCs lack a common metabolic phenotype across cancer types. CSCs metabolic pattern differ from adult stem cells (SCs) and use either glycolysis or OXPHOS (**Figure 1**) triggering cellular plasticity in CSCs (23). Thus, an understanding of CSCs metabolic features will help target CSCs specifically and prevent cancer progression. Current review summarizes the various metabolic features of CSCs along with therapeutic interventions that can be adopted to target key energy processes in CSCs. Targeting the metabolic flexibility in CSCs can emerge as an effective strategy for preventing or minimizing disease progression and recurrence.

METABOLIC FEATURES OF CSCs

Growth factors, nutrients and oxygen in the tumor microenvironment provide necessary energy sources and growth signals for CSCs generation and proliferation. Recently, metabolism has been identified as a major component in CSCs biology, as oncogenic alterations has been observed to cause metabolite-driven dissemination of CSCs (19). Multipotent SCs use glycolysis (24, 25), have fewer mitochondria and produce less reactive oxygen species (ROS) (26, 27). Higher ROS levels cause SCs dysfunction (28–30) and shift to OXPHOS with increased ROS production leads to differentiated SCs progeny.

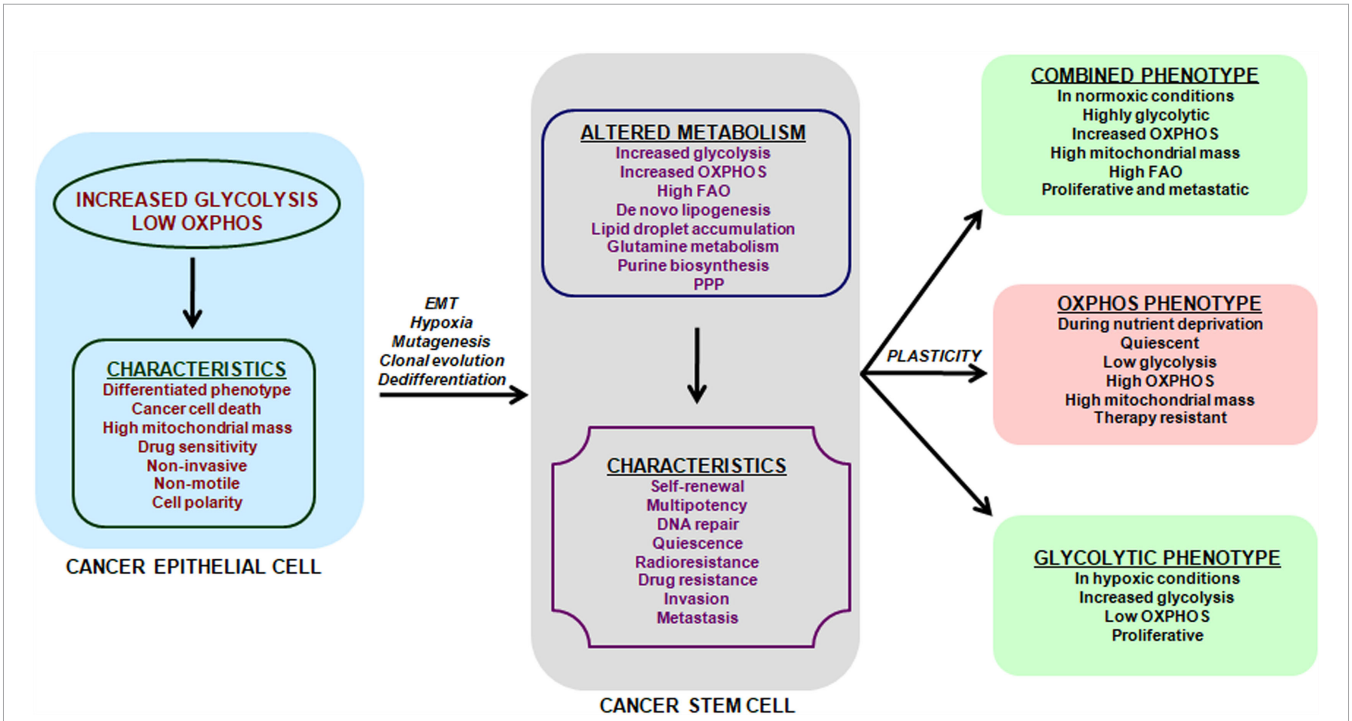

FIGURE 1 | Metabolic features and plasticity of CSCs. Cancer is a heterogeneous disease with multiple sub-populations of cells and CSCs form the self-renewing and tumorigenic core in a tumor. Cancer cells have a predominant glycolytic phenotype and use aerobic glycolysis for tumor growth. This altered metabolism in cancer cells may trigger EMT, hypoxia, cell de-differentiation, mutagenesis and clonal evolution for acquisition of CSCs phenotype. The metabolic alterations in CSCs promote cell-renewal, immune system escape and invasive and metastatic potential. CSCs unlike cancer cells can use glycolysis, OXPHOS or both, depending on their oncogenic background and bio-energetic needs. This freedom of metabolic choice makes CSCs metabolically plastic and they easily shuffle between metabolic phenotypes, based on their state i.e. proliferative or quiescent. EMT, epithelial to mesenchymal transition; FAO, fatty acid oxidation; PPP, Pentose phosphate pathway.

Glycolysis

CSCs were hypothesized to be glycolytic (31), as SCs rely primarily on glycolysis to generate energy (32). However, CSCs are more glycolytic than SCs in various cancers (33–35). Upregulation of glycolytic genes precede pluripotency markers expression, thus switching from OXPHOS to glycolysis promotes stemness in CSCs and is not an outcome of attaining pluripotency (36). CSCs' glucose uptake and hence lactate and ATP production is higher (37) and glycolysis inhibition or glucose starvation cause CSCs' death (19, 38). Glycolytic CSCs are shown in $CD133^+$ liver carcinoma cells (39), osteosarcoma-initiating cells (40), breast cells (41) and glioblastoma cells (35).

Glycolysis is preferred in breast $CD44^+CD24^{low}EPCAM^+$ CSCs, sphere-forming radio-resistant nasopharyngeal carcinoma cells (42) and $CD133^+CD49f^+$ tumor initiating cells (TICs) in hepatocellular carcinoma (43). Elevated expression of oncogenic MYC drove stemness in these cancer types (44) and MYC-driven glycolytic program determined tumorigenic potential (45), thus making MYC a likely candidate linking glycolysis and stemness.

Lactate supports stemness by upregulation of transcription factor SP1 and increases aggressiveness, invasiveness and immune-suppression through sterol regulatory element-binding protein 1 (SREBP1) (46–51). Hypoxia-inducible factor-1 (HIF-1) promotes glycolysis in CSCs and declines OXPHOS and TCA cycle (52). HIF-1 reduces ROS production and upregulates glucose transporters (GLUT) and hexokinase (HK2) expression, pyruvate kinase (PK) activity and LDHA levels and downregulates pyruvate dehydrogenase (PDH) levels (52). HIF-1 promotes self-renewal and pluripotency in various cancers making them treatment resistant (19, 53, 54).

NANOG-expressing hepatocellular CSCs have higher glycolysis and fatty acid oxidation (FAO) rates, and lower OXPHOS and ROS generation (43). CSCs secretome have enriched levels of glycolytic and antioxidant pathways proteins and secreted high levels of ALDH than differentiated cells from colorectal tumors (24). ALDH detoxifies anticancer drugs such as maphosphamide and CSCs secreting ALDH promoted self-preservation and protected nearby differentiated mature cancer cells, leading to therapy resistance (24). Ovarian CSCs with glycolysis enrichment, *de novo* fatty acid synthesis, and decreased mitochondrial respiration and anaplerotic flux, led to aggressive tumors with therapy resistance to cisplatin in comparison to mature cancer cells (34).

Mitochondrial Respiration

As an energy source, OXPHOS is more efficient than glycolysis, but has a slower rate to produce energy. Quiescent or slow-cycling tumor-initiating CSCs prefer OXPHOS metabolism over glycolysis (**Figure 1**), consume less glucose, have lower lactate and higher ATP levels (55–57). OXPHOS-dependent CSCs with low glycolytic reserves are shown in acute myeloid leukemia, $CD133^+$ glioblastoma, melanoma, pancreatic and ovarian cancer (58–63). In breast CSCs, elevated OXPHOS levels trigger chemotherapeutic resistance through synergistic action of MYC and MCL1 (64).

CSCs using OXPHOS have higher mitochondrial mass with increase in membrane potential and rates of oxygen consumption (62, 65, 66). Mitochondrial mass is a vital metabolic biomarker of CSCs (65, 67). Tumor cells without mitochondrial DNA (mtDNA) grew slowly and acquisition of mtDNA from host cells led to tumor-initiation and drug resistance in these tumor cells (68), suggesting mitochondrial function as a target for CSCs treatment. Master mitochondrial biogenesis regulator, peroxisome proliferator-activator 1 alpha (PGC1α) maintained stemness characteristics (69) in breast cancer (70) and pancreatic $CD133^+$ CSCs (66) and increased chemoresistance in CSCs (64, 71–73). NANOG is a pluripotency gene that supports tumorigenesis through OXPHOS and fatty acid metabolism (43). Some breast CSCs show elevated glucose consumption and ATP production, higher mitochondrial activity but lower lactate levels, suggesting that OXPHOS and glycolysis may not be mutually exclusive to CSCs (62).

Glutamine Metabolism

Glycolysis and OXPHOS may not completely support CSCs metabolism, thus glutamine compensates for glucose shortage (74, 75). Although a non-essential amino acid, glutamine becomes essential for cancer cells (76) and CSCs from lung, pancreatic and ovarian cancer have shown glutamine dependence (77, 78). CSCs rely on glutamine for carbon and amino-nitrogen for protein, nucleotide and lipids biosynthesis (79). Glutamine metabolism is rewired by mutations in mitochondrial DNA (mtDNA) (80) and oncogenic alterations in KRAS (81, 82) and c-Myc (83) in tumor cells. Glutamine metabolism in c-Myc-over-expressing cells suggests a pluripotency gene profile dependence on glutamine (84). In pancreatic CSCs, glutamine unavailability reduced stemness characteristics and increased radiation therapy sensitivity (77). L-DON (a glutamine analog) inhibited glucose metabolism and prevented systemic metastasis to liver, lung and kidney in mice (85).

Lipid Metabolism

Cells use an anabolic process of fatty acid synthesis (FAS) to derive energy from fatty acid metabolism for cell growth and proliferation, and a catabolic process of fatty acid oxidation (FAO) for NADH and ATP production (86). CSCs are extremely reliant on *de novo* lipid biosynthesis, lipid oxidation and lipid metabolizing enzymes (87, 88).

Lipid accumulation correlates with tumor stage in mice with prostate cancer (89). *De novo* lipid synthesis associated transcription factor, SREBP-2 activated c-Myc transcription in prostate cancer, enhancing CSCs properties (90). Increased lipid droplet content in colorectal CSCs (91), upregulated lipogenesis in glioma (92) and pancreatic cancer CSCs (93), and increased fatty acid oxidation (FAO) in breast cancer (94) and leukemic cells (95) maintained stemness. High levels of unsaturated lipids in ovarian CSCs promotes cancer stemness and tumor initiation capacity (96).

CSCs use mitochondrial FAO for ATP and NADPH generation to survive loss of matrix attachment (97, 98).

Pluripotency factor NANOG-induced FAO genes expression promoted chemoresistance in TICs in hepatocellular carcinoma (43). Hematopoietic stem cells (HSCs) and leukemia-initiating cells depend on FAO for self-renewal (95, 99) and thus FAO inhibition is a potential pharmacological opportunity to target CSCs (98). Lipid metabolism enzymes, ACSVL3 (acyl-CoA synthetase very-long-chain 3) and ALOX5 (arachidonic acid 5-lipoxygenase) promoted glioblastoma CSCs self-renewal and tumorigenicity (100, 101).

Other Metabolic Features

Mutations in isocitrate dehydrogenase (IDH1 and 2) promote stem-ness in leukemia by aberrant conversion of α-ketoglutarate (αKG) to an analogue named 2-hydroxyglutarate (2-HG). Intracellular accumulation of 2-HG promoted a pro-leukemic phenotype by inhibiting tet methylcytosine dioxygenase 2 (TET2) function, increased self-renewal and impaired differentiation of hematopoietic SCs (102–104).

Elevated purine synthesis promoted stemness in brain tumor initiating cells (BTICs) and correlated with significantly poorer overall survival in glioblastoma patients (105). MYC regulates purine synthesis enzymes and its liaison with *de novo* purine synthesis mediated selective dependence of BTICs on glucose-sustained anabolic metabolism. Inhibition of purine synthesis prevented BTICs growth by inhibiting their self-renewal capacity, but differentiated glioma cells remained unaffected (105). Thus frailty of purine synthesis in CSCs makes it a potential therapeutic target,

Lysine catabolism promoted self-renewal of $CD110^+$ colorectal cancer tumor-initiating cells (TICs) by generating acetyl-CoA. Acetyl-CoA triggered LDL receptor-related protein 6 (LRP6) acetylation and phosphorylation, and finally activation of WNT signaling (106). Lysine catabolism promoted drug-resistance and metastasis to liver in $CD110^+$ TICs by glutamate and glutathione synthesis, which modulated the redox status (106). Collectively, CSCs use an array of metabolism alterations to fuel their self-renewal, thus making these metabolic dependencies open to targeted therapies.

CLINICAL IMPLICATIONS

CSCs have both distinct and flexible metabolic phenotypes between glycolysis and OXPHOS-dependent. Despite limited clinical evidence, targeting CSCs through selective metabolic modulation is an effective and promising avenue for cancer treatment. In our view, synergistic treatments using a standard cytotoxic agent and a metabolic-based therapy will improve eradication of CSCs. **Table 1** lists the available metabolic targeting agents undergoing clinical trials in various cancers.

Targeting Glycolysis

Glycolytic CSCs can be targeted for glycolytic enzymes (hexokinase (HK), phosphoglycerate kinase, pyruvate kinase) and glucose transporters (GLUT1-4). Direct inhibition of GLUTs results in a total disruption of glucose uptake and hence energy metabolism, and GLUT inhibitors such as phloretin, fasentin and WZB117 have shown anticancer effects in preclinical models (107–110). However, ubiquitous expression of GLUTs even in normal cells challenges the explicit inhibition of CSCs glucose uptake and leads to side-effects.

HK enzymes catalyze the first step of glycolysis and their inhibition *via* 2-deoxy-D-glucose (2-DG), benserazide, lonidamine (LN) and genistein-27 (GEN-27) are being used for cancer treatment (111–114). 2-DG is a synthetic analog of glucose that competitively inhibits glucose transport (115) and can be used in combination with cisplatin/docetaxel as an anti-cancer agent (116, 117). 2-DG inhibited glycolysis and CSCs phenotype in triple-negative breast cancer cells (118) and 2-DG with biguanides (such as 3-bromopyruvate, 3-BP) prevented colon cancer cell proliferation (119).

Pyruvate is converted into mitochondrial acetyl-CoA in the cytosol and is negatively regulated by pyruvate dehydrogenase kinase (PDK) enzyme. This shifts cellular metabolism from OXPHOS to glycolysis and thus targeting PDK can inhibit cellular proliferation of CSCs. Dichloroacetate (DCA) activates mitochondrial pyruvate dehydrogenase (PDH) by inhibiting PDK (120), is fairly well-tolerated with fewer side effects and is being tested in several anticancer clinical trials (121, 122).

CSCs can oscillate between metabolic phenotypes during oxygen deprivation and glucose starvation, and thus targeting mechanisms underlying these metabolic adaptations can effectively eliminate CSCs. Hypoxia-inducible factors (HIFs) promote tumor progression in response to localized hypoxia by switching to glycolysis from OXPHOS, activating Notch pathway and expression of Oct4 transcription factor (123, 124). This suggests HIF-1α's role in self-renewal and multipotency and targeting HIFs can be a prospective treatment for CSCs. Metformin, although an antidiabetic drug, attenuated glycolysis flux in hepatocellular carcinoma cells (125) and improved radiotherapy response in prostate and colon cancer tumor xenograft models (126). Epigallocatechin gallate (EGCG) is an inhibitor of glycolysis and its co-treatment with gemcitabine enhanced pancreatic cancer cell death both *in vitro* and in xenografts (127).

Targeting Mitochondrial Respiration

Several OXPHOS-targeting pharmacological agents are being explored in clinical trials for cancer treatment (**Table 1**) and have potential to target CSCs. OXPHOS inhibition overcame drug resistance in slow-cycling melanoma cells and mitochondria-targeted antibiotics prevented sphere formation and tumorigenesis in CSCs (61, 128). Metformin inhibited mitochondrial electron transport chain complex I and diminished OXPHOS (129). Metformin caused energy emergency and hence apoptosis in OXPHOS-dependent pancreatic cancer stem cells (CSCs), but spared their glycolytic differentiated progenies (66). Diabetic patients receiving metformin have a lower mortality rate from cancer and hence a better prognosis (130, 131). Phenformin, a biguanide formerly used in diabetes and a mitochondrial inhibitor induced non-small cell lung cancer (NSCLC) cells apoptosis (132).

CSCs mitochondrial mass and metabolism can be targeted using approved antibiotics like tetracyclines, salinomycin and erythromycins. Antibiotic salinomycin inhibits OXPHOS (133)

TABLE 1 | Clinical trial status of drugs targeting metabolic pathways.

METABOLIC PATHWAYS	TARGET MOLECULE	DRUG	CANCER TYPE	CLINICAL TRIAL PHASE	RECRUITMENT STATUS	CLINICAL TRIAL NUMBER
Amino acid metabolism	Glutaminase	**Phenylacetate**	Brain tumor	Phase-II	Completed	NCT00003241
		CB-839	Renal Cell Carcinoma	Phase-II	Active	NCT03428217
			Hematological tumor	Phase-I	Completed	NCT02071888
			Leukemia	Phase-I	Completed	NCT02071927
	Asparagine	**Asparaginase**	Acute myloid leukemia	Phase-III	Active	NCT00369317
				Phase-III	Recruiting	NCT02521493
		Pegylated L-Asparaginase	Epithelial Ovarian Cancer, Fallopian Tube Cancer, and/or Primary Peritoneal Cancer	Phase II	Completed	NCT01313078
	Arginine	**Arginine deiminase**	Soft Tissue Sarcoma, Osteosarcoma, Ewing's Sarcoma, and Small Cell Lung Cancer	Phase-II	Active	NCT03449901
Fatty acid synthesis	FASN	**TVB-2640**	Colon Cancer	Phase-I	Recruiting	NCT02980029
			Solid Malignant Tumor	Phase-I	Completed	NCT02223247
			Breast Cancer	Phase-II	Recruiting	NCT03179904
			Non-Small Cell Lung Carcinomas	Phase-II	Recruiting	NCT03808558
			Astrocytoma	Phase-II	Active, not recruiting	NCT03032484
Cholesterol synthesis	HMGCR	**Statins**	Breast Cancer	Phase-III	Recruiting	NCT03971019
			Prostate Cancer	NA	Completed	NCT01428869
			Gastric Cancer	NA	Completed	NCT01813994
			Breast Cancer	Phase-II	Completed	NCT00816244
Lipid-Mediated Signaling	Prostaglandin-endoperoxide synthase 2	**Celecoxib**	Breast Cancer	Phase-III	Completed	NCT02429427
			Pancreatic Cancer	Phase-II	Completed	NCT00068432
			Lung Cancer	Phase-II	Completed	NCT00030407
	EP4 receptor (prostaglandin receptor)	**PGE1**	Prostate Cancer	Phase-II	Completed	NCT00080808
			Penile Cancer	NA	Completed	NCT00955929
		Omega-3 polyunsaturated fatty acids (ω-3 PUFAs)	Skin Cancer	NA	Completed	NCT01032343
			Bladder Cancer	NA	Recruiting	NCT04664816
			Breast Cancer	NA	Active, not recruiting	NCT02295059
Tricarboxylic acid cycle (TCA) Cycle	Pyruvate dehydrogenase kinase (PDK1)	**Dichloroacetate (DCA)**	Head and neck cancer	Phase-I	Completed	NCT01163487
			Glioblastoma and Other Recurrent Brain Tumors	Phase-I	Completed	NCT01111097
			Brain cancer	Phase-II	Completed	NCT00540176
			Metastatic solid tumor	Phase-I	Completed	NCT00566410
Glycolysis	GLUT4	**Ritonavir**	HER2-expressing Advanced Solid Malignant Tumors	Phase-I	Active	NCT03383692
	Hexokinase	**2-deoxy-D-glucose (2-DG)**	Lung cancer	Phase-III	Active	NCT01394679
			Prostate cancer	NA	Active	NCT00002981
	Pyruvate kinase (PK)	**TLN-232**	Renal Cell Carcinoma	Phase-II	Completed	NCT00422786
OXPHOS	Cytochrome b	**Atovaquone**	Acute myloid leukemia	Phase-I	Active	NCT03568994
			Lung cancer	Phase-I	Recruiting	NCT04648033
	Respiratory complex I, mitochondrial glycerol-3-phosphate dehydrogenase (mGPDH)	**Metformin**	Breast cancer	Phase-II	Active	NCT02028221
			Prostate cancer	Phase-II	Active	NCT02945813
			Endometrial cancer	Phase-II	Active	NCT02755844
			Lung cancer	Phase-II	Active	NCT03048500
Pentose phosphate pathway (PPP)	Glucose-6-phosphate dehydrogenase (G6PDH)	**Resveratrol**	Colon cancer	Phase-I	Completed	NCT00256334
			Gastrointestinal Tumors	NA	Completed	NCT01476592
			Colorectal Cancer	Phase-I	Completed	NCT00433576
			Colorectal Cancer	Phase-I	Completed	NCT00920803
	G6PDH and ribose-5-phosphate (R-5P)	**Dehydroepiandrosterone (DHEA)**	Vaginal Atrophy In Breast Cancer Survivors	Phase-IV	Recruiting	NCT04705883
			Multiple myeloma	Phase-II	Completed	NCT00006219
	G6PDH, 6PGDH and Transaldolase TA	**Arginine and ascorbic acid combination**	Head and Neck Cancer	NA	Completed	NCT03531190
Nucleotide biosynthesis	DNA & RNA synthesis	**5-Fluorouracil (5-FU)**	Pancreatic cancer	Phase-II	Active	NCT02352337
			Colon cancer	Phase-I	Active	NCT02724202
			Biliary tract cancer	Phase-II	Active	NCT03524508

(Continued)

TABLE 1 | Continued

METABOLIC PATHWAYS	TARGET MOLECULE	DRUG	CANCER TYPE	CLINICAL TRIAL PHASE	RECRUITMENT STATUS	CLINICAL TRIAL NUMBER
			Bladder cancer	Phase-II	Active	NCT00777491
		Cytarabine	Multiple myeloma	Phase-II	Active	NCT02416206
		Methotrexate	Head and Neck Cancers	Phase-II	Active	NCT03193931
			Breast Cancer	NA	Completed	NCT00615901
			Head and Neck Cancer	Phase-III	Active	NCT01884623
			Brain Tumors	Phase-I	Completed	NCT02458339
	DNA synthesis	**Folate**	Colorectal Cancer	Phase-I	Completed	NCT00096330
			Non-Small Cell Lung Cancer	Phase-II	Completed	NCT00609518
			Head and Neck Squamous Cell Cancer	Phase-II	Completed	NCT01183065
	Methyltransferases	**Genistein**	Breast cancer	Phase-II	Completed	NCT00244933
			Prostate cancer	Phase-II	Completed	NCT00584532
			Colorectal cancer	Phase-I	Completed	NCT01985763
			Pancreatic cancer	Phase-II	Completed	NCT00376948
		Epigallocatechin Gallate (EGCG)	Colorectal Cancer	Phase-I	Recruiting	NCT02891538
			Lung Cancer	Phase-II	Enrolling by invitation	NCT02577393
	Histone deacetylases (HDAC)	**Butyrate**	Rectal cancer	Phase-II	Completed	NCT04795180
		Sulforaphane	Prostate cancer	Phase-II	Completed	NCT01228084
		3,3 Diindolylmethane	Prostate Cancer	Phase-II	Completed	NCT00888654
	Histone acetyltransferase	**Curcumin**	Colon cancer	Phase-I	Active	NCT02724202
			Breast cancer	Phase-II	Completed	NCT01042938
			Prostate cancer	Phase-II	Active	NCT02724618
			Colon cancer	Phase-I	Active	NCT02724202
			Gastric cancer	Phase-II	Active	NCT02782949
	Acetylation of non-histone proteins	**Butyrate**	Epstein Barr virus-induced malignancies	Phase-I	Completed	NCT00006340
Combination treatments	mTOR (mammalian target of rapamycin)	**Everolimus**	Pancreatic cancer	Phase-II	Active, not recruiting	NCT02294006
	Respiratory complex I, mGPDH	**Metformin**				
	Cyclooxygenase (COX)	**Aspirin**	Colorectal Cancer	Phase-II	Unknown	NCT03047837
	Respiratory complex I, mGPDH	**Metformin**				
	HMG-CoA reductase	**Atorvastatin**	Triple Negative Breast Cancer	Phase-II	Recruiting	NCT03358017
	Farnesyl pyrophosphate (FPP) synthase	**Zoledronate**				
	Arginase	**INCB001158**	Advanced/Metastatic Solid Tumors	Phase-I Phase-II	Active, not recruiting	NCT02903914
	Programmed cell death protein 1 (PD-1)	**Pembrolizumab**				
	Glutaminase	**CB-839**	Solid Tumors	Phase-I Phase-II	Terminated (Slow Enrollment)	NCT03875313
	Poly ADP ribose polymerase (PARP)	**Talazoparib**				
	Respiratory complex I, mGPDH	**Metformin**	Prostate Cancer	Phase-II	Completed	NCT01796028
	Microtubules	**Taxotere**				
	Respiratory complex I, mGPDH	**Metformin**	Cancer	Phase-III	Not yet recruiting	NCT02201381
	HMG-CoA reductase	**Atorvastatin**				
	30S ribosomal subunit	**Doxycycline**				
	Tubulin	**Mebendazole**				
	Coenzyme A	**Coenzyme A**	Castration-resistant Prostate Cancer	Phase-I Phase-II	Recruiting	NCT04839055
	CYP17A1 (17 alpha-hydroxylase/ C17,20 lyase)	**Abiraterone**				
	Respiratory complex I, mGPDH	**Metformin**	Endometrial Cancer	Phase-II Phase-I	Active, not recruiting	NCT02755844
	PARP	**Olaparib**				
	Phosphoramide mustard	**Metronomic cyclophosphamide**				
	Respiratory complex I, mGPDH	**Metformin**	Colorectal Cancer	Phase-II	Completed	NCT01941953
	DNA & RNA synthesis	**Fluorouracil**	Pancreatic Cancer	Phase-II	Completed	NCT01666730
	Respiratory complex I, mGPDH	**Metformin**	Breast Cancer	Phase-II	Completed	NCT01310231
	Athracyclines, platinum, taxanes or capecitabine; first or second line	**Standard chemotherapy**				
	Respiratory complex I, mGPDH	**Metformin Hydrochloride**	Endometrial Cancer	Phase-II		NCT02065687

(Continued)

TABLE 1 | Continued

METABOLIC PATHWAYS	TARGET MOLECULE	DRUG	CANCER TYPE	CLINICAL TRIAL PHASE	RECRUITMENT STATUS	CLINICAL TRIAL NUMBER
	DNA	**Carboplatin**			Active, not recruiting	
	Respiratory complex I, mGPDH	**Metformin**	Liver Cancer	Phase-III	Unknown	NCT03184493
	Prostaglandin-endoperoxide synthase 2	**Celecoxib**	Prostate Cancer	Phase-II & III	Recruiting	NCT00268476

and salinomycin treatment reduced breast CSCs gene expression. Antibiotic tigecycline inhibited mitochondrial translation in mitochondrial associated ribosomes in OXPHOS-dependent leukemia cells (134).

CSCs using OXPHOS have a higher mitochondrial membrane potential ($\Delta\psi m$) and thus $\Delta\psi m$ can be explored for selective accumulation of cytotoxic drugs. Triphenylphosphonium (TPP) accumulates in the mitochondrial matrix (135) and conjugation of TPP to doxorubicin prevented drug efflux by enhancing drug selectivity in cancer cells (136). Dual inhibition of glycolysis and OXPHOS in sarcoma cells, using 2-DG and oligomycin/metformin co-treatment (137), suggests that simultaneous inhibition of glycolytic and mitochondrial respiration is more effective to eradicate CSCs (138, 139).

Targeting Glutamine Metabolism

Although a non-essential amino acid, glutamine becomes essential as a favored respiratory fuel for cancer cells and thus depriving glutamine is a potential anti-cancer strategy. Glutamine metabolism can be blocked by inhibiting glutaminase 1 (GLS1), an enzyme that converts glutamine to glutamate. GLS1 inhibition disrupted redox balance in CSCs and sensitized lung and pancreatic cancers to radiotherapy (77, 140). GLS1 inhibitors, BPTES (141) and CB-839 reduce intracellular glutamate and 2-hydroxyglutarate (an oncometabolite) levels. Lower glutamate levels inhibited cell growth, induced apoptosis and differentiation in Acute Myeloid Leukemia (AML) cells (142). CB-839 is under clinical trials for various cancers including renal cell carcinoma, hematologic cancer and leukemia (**Table 1**).

Targeting Lipid Metabolism

Cancer cells predominately use glycolysis for ATP production instead of oxidizing energy-rich substrates. However, unlike non-cancerous cells dependence on dietary lipids, cancer cells use *de novo* lipogenesis. Thus targeting fatty acid synthase (FASN), a central enzyme to lipogenesis, is a promising strategy to eliminate CSCs. FASN inhibitor cerulenin reduced *de novo* lipogenesis and in turn proliferation, migration and stemness of glioma stem cells (GSCs), induced apoptosis in colon cancer cell lines (92, 143) and blocked proliferation of pancreatic spheres (93). C75 decreased HER2+ breast cancer cells self-renewal capacity at non-cytotoxic concentrations (144). However, due to toxicity issues in *in-vivo* studies owing to high selectivity of FASN inhibitors, only one FASN inhibitor (TVB-2640) is under clinical trials to date (**Table 1**).

Studies show that increased fatty acid production in cancer cells raises their dependence on desaturases (enzymes that add double bonds into acyl-CoA chains). Thus targeting desaturase enzyme activity may provide a novel approach to selectively interfere lipid metabolism in CSCs. Several stearoyl-CoA desaturase-1 (SCD-1) inhibitors have effectively targeted stemness in pre-clinical models of cancer. Inhibitors like CAY10556 and SC-26196 reduced stem-ness markers and inhibited *in-vitro* sphere formation and *in-vivo* tumorigenicity, by down-regulating Hedgehog and Notch expression in aldehyde dehydrogenase (ALDH)- and CD133-enriched ovarian cells and had no effect on differentiated cells (96). Similarly, SCD-1 inhibitors (SSI-4 or A939572) promoted differentiation in chemo-resistant hepatospheres with little toxicity *in vivo* (145). MF-438 reduced expression of self-renewal and pluripotency markers in lung $ALDH1^+$ cells (146).

Along with *de novo* lipogenesis, cancer cells also take lipids from the extracellular milieu (147) using LDL receptor (LDLR) (148), CD36 fatty acid translocase, fatty acid transport proteins (FATPs) (149) or fatty acid-binding proteins (FABPs) (150). Inhibition of CD36 transporter with 2-methylthio-1,4-naphtoquinone reduced self-renewal and promoted apoptosis in $CD133^+$ glioblastoma (151) and sulfosuccinimidyl oleate reduced chemo-resistant leukemic stem cells (152). CD36-neutralizing antibodies inhibited progression and metastasis of oral squamous cell carcinoma and had no reported toxicity *in-vivo* (153).

Highly proliferating cells also have a higher demand for components of cell membrane like cholesterol. Cholesterol is either taken up from exogenous sources or synthesized using FASN or mevalonate pathway (154). Statins inhibit cholesterol synthesis through the mevalonate pathway and their target enzyme is 3-hydroxy-3-methyl-glutharyl-coenzyme A reductase (HMGCR). Statins treatment decreased CSCs self-renewal capacity and number in breast (155), nasopharyngeal (156) carcinomas and $CD133^+$ brain TICs (157). MYC controls over-expression of mevalonate pathway genes and thus anti-CSCs effects of statins could be due to MYC inhibition (157).

Synthesized or accumulated fatty acids are also converted to signaling lipids and energy *via* FAO, in addition to membrane incorporation or being stored. FAO is an essential energy source in non-glycolytic tumors (158, 159), as CSCs show higher FAO in nutrient-deprived conditions (63, 86, 160, 161). FAO promotes pluripotency and chemoresistance (94) by reducing ROS production (162, 163) and promoted metastatic capacity in sphere-derived cells (164). Etomoxir, an inhibitor of FAO,

inhibited mammosphere formation in hypoxic breast CSCs (165) and eradicated half of quiescent leukemia SCs (99), suggesting that FAO inhibitors hinder CSCs survival. In hepatocellular carcinoma, etomoxir sensitized CSCs to sorafenib treatment (43). Soraphen A, cerulenin and resveratrol inhibited FAO and lowered stemness markers and spheroid formation in CSCs (92, 166, 167).

Lipids also support CSCs functionality by being second messengers in signal transduction pathways. Sphingolipids, eicosanoids (prostaglandin E2) and glycerophospholipids (lysophosphatidic acid (LPA)) boost CSCs number by activation of Notch, AKT and NF-kB pathways in breast, bladder, colorectal (CRC) and ovarian cancer (168–171). Lipid-mediated signaling in CSCs thus can be targeted using inhibitors and dietary supplements. Inhibition of autotoxin (ATX) (a lysophosphatidic acid (LPA)-producing enzyme) with S32826 or PF8380 reduced tumorigenicity and chemoresistance *in-vivo* (171). Inhibition of LPA production in cancer cells modulated the immune system by inducing monocytes differentiation to macrophages and launching cancer-associated fibroblasts (CAFs) phenotype (172, 173). Prostaglandins are major lipid mediator in CSCs and celecoxib treatment of Apc^{Min}/þ mice reduced number of $CD133^+CD44^+$ cells and tumor burden (170). Celecoxib reduced patient-derived CSCs content and liver metastatic tumors number in NOD scid gamma (NSG) mice and weakened chemoresistance in bladder carcinomas, indicating its potential as an adjuvant therapy (169). In contrast, reduction of $CD34^+$ cells in chronic myelogenous leukemia (CML) xenograft model by EP4 receptor (prostaglandin receptor) agonist misoprostol or PGE1 (FDA-approved), suggests a context-dependent role of prostaglandins in stem-ness (174). Further, dietary omega-3 polyunsaturated fatty acids (ω-3 PUFA) decreased CRC risk and reduced $CD133^+$ content in CRC cell lines (175, 176). Eicosapentaenoic acid (EPA) and docosahexaenoic acid (DHA) supplementation decreased breast tumorspheres proliferation (177) and EPA with chemotherapy suppressed tumor growth in mice (178), suggesting an anti-CSCs properties of ω-3 PUFAs.

Combination Treatments

CSCs can also attain a combined metabolic phenotype where both glycolysis and OXPHOS are utilized (**Figure 1**). This phenotype can be attained by direct association of AMP-activated protein kinase (AMPK, master regulator of OXPHOS) and HIF-1 (master regulator of glycolysis) activities (179). High AMPK/HIF-1 activities leads to higher glycolysis and OXPHOS, and provide enhanced proliferation and clonogenicity compared to only glycolytic or OXPHOS phenotype (179). In addition, CSCs metabolize glutamine along with glucose for carbon and amino-nitrogen to synthesize amino acids, nucleotides and lipids (79). Additionally, CSCs also use *de novo* lipogenesis to increase their bioenergetic requirements and are linked in tumor metastasis (88). Also preclinical and clinical setting has shown that targeting a single metabolic pathway like glycolysis has low success rates and enhanced side effects as GLUT transporters are ubiquitous. Also, inhibition of hexokinase II with ionidamine showed no significant improvement in overall survival but led to elevated toxicity (114, 180–182). Thus combination treatments targeting two or more metabolic pathways will majorly erase CSCs, prevent tumor relapse and prevent side-effects of a single treatment.

Further, combining a standard cytotoxic therapy with a metabolic inhibitor will probably enhance CSCs eradication. Combinations of metformin and JQ-1 (bromodomain and extraterminal motif (BET) inhibitor) in pancreatic cancer (66) or PI3K inhibitor in ovarian cancer (183) blocked both OXPHOS and glycolysis. Apart from direct metabolic inhibition, targeting oncogenes regulating cellular metabolism will also eradicate CSCs effectively. KRAS mutation occurs in about 90% of pancreatic cancer cases (184) and KRAS drives glycolysis and nucleic acids synthesis (185, 186). c-MYC is essential for glycolysis in cancer (187, 188) and MYC suppression prevents mitochondrial inhibitors resistance (66, 75). Thus combination approaches can be extended to target CSCs as an anti-cancer strategy. **Table 1** lists the clinical trials using combination treatments for various cancers.

FUTURE CHALLENGES

Figure 1 summarizes the known CSCs' metabolic phenotypes and how these phenotypes switch with metabolic stressors like nutrient deprivation and hypoxia. However, melanoma cells attain a drug-tolerant "idling state" after enduring MAPK inhibition (MAPKi) and this state has a metabolically Low/Low (L/L) phenotype, where both AMPK/HIF-1 activity and OXPHOS/glycolysis are minimal (189). L/L phenotype does not favor tumorigenicity but supports cell division. These idle L/L drug-tolerant cells accumulate mutations to promote relapse post MAPKi melanoma treatment (189).

Further adding to the complexity of CSCs metabolism, Luo et al. (190) showed that breast cancer stem cells (BCSCs) have two states: quiescent mesenchymal-like (M) and proliferative epithelial-like (E). Proliferative E-BCSCs showed higher mitochondrial OXPHOS, whereas M-BCSCs have enrichment of glycolysis and gluconeogenesis pathways and hypoxia promotes M to E transition in BCSCs (190). Thus CSCs' multiple metabolic phenotypes (glycolytic, OXPHOS, combined and L/L) explain the futility of current efforts to eradicate CSCs and a deeper understanding of CSCs metabolic plasticity would translate to better therapeutic strategies.

CONCLUDING REMARKS

CSCs provide treatment resistance and promote metastasis during tumor growth and targeting metabolism holds potential in overcoming cancer recurrence and metastasis by CSCs. Deciphering metabolic reprogramming in cancer showed differences between metabolic phenotypes of CSCs and their differentiated counterparts. CSCs metabolism shuffles between glycolysis and OXPHOS primarily, however the mechanisms of CSCs metabolic heterogeneity are still unknown. Current knowledge suggests that carefully designed metabolic therapies have potential to be more effective against CSCs. Further,

co-targeting CSCs using metabolic drugs and traditional anticancer treatments could be more efficient. The ongoing clinical trials targeting CSCs show a promising future for cancer therapy and are worth exploring further. More preclinical and clinical studies are thus required to uncover novel metabolic targets in CSCs.

AUTHOR CONTRIBUTIONS

SB conceptualized the article and reviewed the literature, JK did literature search and drafted the manuscript. Both SB and JK contributed to the final version.

REFERENCES

1. Bristow RG, Alexander B, Baumann M, Bratman SV, Brown JM, Camphausen K, et al. Combining Precision Radiotherapy With Molecular Targeting and Immunomodulatory Agents: A Guideline by the American Society for Radiation Oncology. *Lancet Oncol* (2018) 19:e240–51. doi: 10.1016/S1470-2045(18)30096-2
2. Hwang WL, Pike LRG, Royce TJ, Mahal BA, Loeffler JS. Safety of Combining Radiotherapy With Immune-Checkpoint Inhibition. *Nat Rev Clin Oncol* (2018) 15:477–94. doi: 10.1038/s41571-018-0046-7
3. Cleeland CS, Allen JD, Roberts SA, Brell JM, Giralt SA, Khakoo AY, et al. Reducing the Toxicity of Cancer Therapy: Recognizing Needs, Taking Action. *Nat Rev Clin Oncol* (2012) 9:471–8. doi: 10.1038/nrclinonc.2012.99
4. Lytle NK, Barber AG, Reya T. Stem Cell Fate in Cancer Growth, Progression and Therapy Resistance. *Nat Rev Cancer* (2018) 18:669–80. doi: 10.1038/s41568-018-0056-x
5. Krause M, Dubrovska A, Linge A, Baumann M. Cancer Stem Cells: Radioresistance, Prediction of Radiotherapy Outcome and Specific Targets for Combined Treatments. *Adv Drug Delivery Rev* (2017) 109:63–73. doi: 10.1016/j.addr.2016.02.002
6. Bütof R, Dubrovska A, Baumann M. Clinical Perspectives of Cancer Stem Cell Research in Radiation Oncology. *Radiother Oncol* (2013) 108:388–96. doi: 10.1016/j.radonc.2013.06.002
7. Linge A, Löck S, Gudziol V, Nowak A, Lohaus F, von Neubeck C, et al. Low Cancer Stem Cell Marker Expression and Low Hypoxia Identify Good Prognosis Subgroups in HPV(-) HNSCC After Postoperative Radiochemotherapy: A Multicenter Study of the DKTK-ROG. *Clin Cancer Res* (2016) 22:2639–49. doi: 10.1158/1078-0432.CCR-15-1990
8. Prasetyanti PR, Medema JP. Intra-Tumor Heterogeneity From a Cancer Stem Cell Perspective. *Mol Cancer* (2017) 16:41. doi: 10.1186/s12943-017-0600-4
9. Wang K-J, Wang C, Dai L-H, Yang J, Huang H, Ma X-J, et al. Targeting an Autocrine Regulatory Loop in Cancer Stem-Like Cells Impairs the Progression and Chemotherapy Resistance of Bladder Cancer. *Clin Cancer Res* (2019) 25:1070–86. doi: 10.1158/1078-0432.CCR-18-0586
10. Kreso A, Dick JE. Evolution of the Cancer Stem Cell Model. *Cell Stem Cell* (2014) 14:275–91. doi: 10.1016/j.stem.2014.02.006
11. Ahmed N, Escalona R, Leung D, Chan E, Kannourakis G. Tumour Microenvironment and Metabolic Plasticity in Cancer and Cancer Stem Cells: Perspectives on Metabolic and Immune Regulatory Signatures in Chemoresistant Ovarian Cancer Stem Cells. *Semin Cancer Biol* (2018) 53:265–81. doi: 10.1016/j.semcancer.2018.10.002
12. Mukha A, Dubrovska A. Metabolic Targeting of Cancer Stem Cells. *Front Oncol* (2020) 10:537930. doi: 10.3389/fonc.2020.537930
13. Tan Z, Xie N, Cui H, Moellering DR, Abraham E, Thannickal VJ, et al. Pyruvate Dehydrogenase Kinase 1 Participates in Macrophage Polarization *via* Regulating Glucose Metabolism. *J Immunol* (2015) 194:6082–9. doi: 10.4049/jimmunol.1402469
14. Palsson-McDermott EM, Curtis AM, Goel G, Lauterbach MAR, Sheedy FJ, Gleeson LE, et al. Pyruvate Kinase M2 Regulates Hif-1α Activity and IL-1β Induction and Is a Critical Determinant of the Warburg Effect in LPS-Activated Macrophages. *Cell Metab* (2015) 21:65–80. doi: 10.1016/j.cmet.2014.12.005
15. Freemerman AJ, Johnson AR, Sacks GN, Milner JJ, Kirk EL, Troester MA, et al. Metabolic Reprogramming of Macrophages: Glucose Transporter 1 (GLUT1)-Mediated Glucose Metabolism Drives a Proinflammatory Phenotype. *J Biol Chem* (2014) 289:7884–96. doi: 10.1074/jbc.M113.522037
16. Chen Y, Tan W, Wang C. Tumor-Associated Macrophage-Derived Cytokines Enhance Cancer Stem-Like Characteristics Through Epithelial-Mesenchymal Transition. *Onco Targets Ther* (2018) 11:3817–26. doi: 10.2147/OTT.S168317
17. Korkaya H, Liu S, Wicha MS. Regulation of Cancer Stem Cells by Cytokine Networks: Attacking Cancer's Inflammatory Roots. *Clin Cancer Res* (2011) 17:6125–9. doi: 10.1158/1078-0432.CCR-10-2743
18. Mitchem JB, Brennan DJ, Knolhoff BL, Belt BA, Zhu Y, Sanford DE, et al. Targeting Tumor-Infiltrating Macrophages Decreases Tumor-Initiating Cells, Relieves Immunosuppression, and Improves Chemotherapeutic Responses. *Cancer Res* (2013) 73:1128–41. doi: 10.1158/0008-5472.CAN-12-2731
19. De Francesco EM, Sotgia F, Lisanti MP. Cancer Stem Cells (CSCs): Metabolic Strategies for Their Identification and Eradication. *Biochem J* (2018) 475:1611–34. doi: 10.1042/BCJ20170164
20. Meacham CE, Morrison SJ. Tumour Heterogeneity and Cancer Cell Plasticity. *Nature* (2013) 501:328–37. doi: 10.1038/nature12624
21. Nowell PC. The Clonal Evolution of Tumor Cell Populations. *Science* (1976) 194:23–8. doi: 10.1126/science.959840
22. Reid MA, Dai Z, Locasale JW. The Impact of Cellular Metabolism on Chromatin Dynamics and Epigenetics. *Nat Cell Biol* (2017) 19:1298–306. doi: 10.1038/ncb3629
23. Sancho P, Barneda D, Heeschen C. Hallmarks of Cancer Stem Cell Metabolism. *Br J Cancer* (2016) 114:1305–12. doi: 10.1038/bjc.2016.152
24. Emmink BL, Verheem A, Van Houdt WJ, Steller EJA, Govaert KM, Pham TV, et al. The Secretome of Colon Cancer Stem Cells Contains Drug-Metabolizing Enzymes. *J Proteomics* (2013) 91:84–96. doi: 10.1016/j.jprot.2013.06.027
25. Hammoudi N, Ahmed KBR, Garcia-Prieto C, Huang P. Metabolic Alterations in Cancer Cells and Therapeutic Implications. *Chin J Cancer* (2011) 30:508–25. doi: 10.5732/cjc.011.10267
26. Jang Y-Y, Sharkis SJ. A Low Level of Reactive Oxygen Species Selects for Primitive Hematopoietic Stem Cells That may Reside in the Low-Oxygenic Niche. *Blood* (2007) 110:3056–63. doi: 10.1182/blood-2007-05-087759
27. Prigione A, Fauler B, Lurz R, Lehrach H, Adjaye J. The Senescence-Related Mitochondrial/Oxidative Stress Pathway Is Repressed in Human Induced Pluripotent Stem Cells. *Stem Cells* (2010) 28:721–33. doi: 10.1002/stem.404
28. Simsek T, Kocabas F, Zheng J, Deberardinis RJ, Mahmoud AI, Olson EN, et al. The Distinct Metabolic Profile of Hematopoietic Stem Cells Reflects Their Location in a Hypoxic Niche. *Cell Stem Cell* (2010) 7:380–90. doi: 10.1016/j.stem.2010.07.011
29. Suda T, Takubo K, Semenza GL. Metabolic Regulation of Hematopoietic Stem Cells in the Hypoxic Niche. *Cell Stem Cell* (2011) 9:298–310. doi: 10.1016/j.stem.2011.09.010
30. Maryanovich M, Zaltsman Y, Ruggiero A, Goldman A, Shachnai L, Zaidman SL, et al. An MTCH2 Pathway Repressing Mitochondria Metabolism Regulates Haematopoietic Stem Cell Fate. *Nat Commun* (2015) 6:7901. doi: 10.1038/ncomms8901
31. Folmes CDL, Dzeja PP, Nelson TJ, Terzic A. Metabolic Plasticity in Stem Cell Homeostasis and Differentiation. *Cell Stem Cell* (2012) 11:596–606. doi: 10.1016/j.stem.2012.10.002
32. Jang H, Yang J, Lee E, Cheong J-H. Metabolism in Embryonic and Cancer Stemness. *Arch Pharm Res* (2015) 38:381–8. doi: 10.1007/s12272-015-0558-y
33. Ciavardelli D, Rossi C, Barcaroli D, Volpe S, Consalvo A, Zucchelli M, et al. Breast Cancer Stem Cells Rely on Fermentative Glycolysis and Are Sensitive to 2-Deoxyglucose Treatment. *Cell Death Dis* (2014) 5:e1336. doi: 10.1038/cddis.2014.285
34. Liao J, Qian F, Tchabo N, Mhawech-Fauceglia P, Beck A, Qian Z, et al. Ovarian Cancer Spheroid Cells With Stem Cell-Like Properties Contribute to Tumor Generation, Metastasis and Chemotherapy Resistance Through Hypoxia-Resistant Metabolism. *PloS One* (2014) 9:e84941. doi: 10.1371/journal.pone.0084941

35. Zhou Y, Zhou Y, Shingu T, Feng L, Chen Z, Ogasawara M, et al. Metabolic Alterations in Highly Tumorigenic Glioblastoma Cells: Preference for Hypoxia and High Dependency on Glycolysis. *J Biol Chem* (2011) 286:32843–53. doi: 10.1074/jbc.M111.260935
36. Folmes CDL, Nelson TJ, Martinez-Fernandez A, Arrell DK, Lindor JZ, Dzeja PP, et al. Somatic Oxidative Bioenergetics Transitions Into Pluripotency-Dependent Glycolysis to Facilitate Nuclear Reprogramming. *Cell Metab* (2011) 14:264–71. doi: 10.1016/j.cmet.2011.06.011
37. Liu P-P, Liao J, Tang Z-J, Wu W-J, Yang J, Zeng Z-L, et al. Metabolic Regulation of Cancer Cell Side Population by Glucose Through Activation of the Akt Pathway. *Cell Death Differ* (2014) 21:124–35. doi: 10.1038/cdd.2013.131
38. Palorini R, Votta G, Balestrieri C, Monestiroli A, Olivieri S, Vento R, et al. Energy Metabolism Characterization of a Novel Cancer Stem Cell-Like Line 3AB-OS. *J Cell Biochem* (2014) 115:368–79. doi: 10.1002/jcb.24671
39. Song K, Kwon H, Han C, Zhang J, Dash S, Lim K, et al. Active Glycolytic Metabolism in CD133(+) Hepatocellular Cancer Stem Cells: Regulation by MIR-122. *Oncotarget* (2015) 6:40822–35. doi: 10.18632/oncotarget.5812
40. Mizushima E, Tsukahara T, Emori M, Murata K, Akamatsu A, Shibayama Y, et al. Osteosarcoma-Initiating Cells Show High Aerobic Glycolysis and Attenuation of Oxidative Phosphorylation Mediated by LIN28B. *Cancer Sci* (2020) 111:36–46. doi: 10.1111/cas.14229
41. Feng W, Gentles A, Nair RV, Huang M, Lin Y, Lee CY, et al. Targeting Unique Metabolic Properties of Breast Tumor Initiating Cells. *Stem Cells* (2014) 32:1734–45. doi: 10.1002/stem.1662
42. Shen Y-A, Wang C-Y, Hsieh Y-T, Chen Y-J, Wei Y-H. Metabolic Reprogramming Orchestrates Cancer Stem Cell Properties in Nasopharyngeal Carcinoma. *Cell Cycle* (2015) 14:86–98. doi: 10.4161/15384101.2014.974419
43. Chen C-L, Uthaya Kumar DB, Punj V, Xu J, Sher L, Tahara SM, et al. NANOG Metabolically Reprograms Tumor-Initiating Stem-Like Cells Through Tumorigenic Changes in Oxidative Phosphorylation and Fatty Acid Metabolism. *Cell Metab* (2016) 23:206–19. doi: 10.1016/j.cmet.2015.12.004
44. Gabay M, Li Y, Felsher DW. MYC Activation Is a Hallmark of Cancer Initiation and Maintenance. *Cold Spring Harb Perspect Med* (2014) 4:a014241. doi: 10.1101/cshperspect.a014241
45. Folmes CDL, Martinez-Fernandez A, Faustino RS, Yamada S, Perez-Terzic C, Nelson TJ, et al. Nuclear Reprogramming With C-Myc Potentiates Glycolytic Capacity of Derived Induced Pluripotent Stem Cells. *J Cardiovasc Transl Res* (2013) 6:10–21. doi: 10.1007/s12265-012-9431-2
46. Estrella V, Chen T, Lloyd M, Wojtkowiak J, Cornnell HH, Ibrahim-Hashim A, et al. Acidity Generated by the Tumor Microenvironment Drives Local Invasion. *Cancer Res* (2013) 73:1524–35. doi: 10.1158/0008-5472.CAN-12-2796
47. Martinez-Outschoorn UE, Prisco M, Ertel A, Tsirigos A, Lin Z, Pavlides S, et al. Ketones and Lactate Increase Cancer Cell "Stemness," Driving Recurrence, Metastasis and Poor Clinical Outcome in Breast Cancer: Achieving Personalized Medicine *via* Metabolo-Genomics. *Cell Cycle* (2011) 10:1271–86. doi: 10.4161/cc.10.8.15330
48. Lin S, Sun L, Lyu X, Ai X, Du D, Su N, et al. Lactate-Activated Macrophages Induced Aerobic Glycolysis and Epithelial-Mesenchymal Transition in Breast Cancer by Regulation of CCL5-CCR5 Axis: A Positive Metabolic Feedback Loop. *Oncotarget* (2017) 8:110426–43. doi: 10.18632/oncotarget.22786
49. Tasdogan A, Faubert B, Ramesh V, Ubellacker JM, Shen B, Solmonson A, et al. Metabolic Heterogeneity Confers Differences in Melanoma Metastatic Potential. *Nature* (2020) 577:115–20. doi: 10.1038/s41586-019-1847-2
50. Brand A, Singer K, Koehl GE, Kolitzus M, Schoenhammer G, Thiel A, et al. LDHA-Associated Lactic Acid Production Blunts Tumor Immunosurveillance by T and NK Cells. *Cell Metab* (2016) 24:657–71. doi: 10.1016/j.cmet.2016.08.011
51. Daneshmandi S, Wegiel B, Seth P. Blockade of Lactate Dehydrogenase-A (LDH-A) Improves Efficacy of Anti-Programmed Cell Death-1 (PD-1) Therapy in Melanoma. *Cancers (Basel)* (2019) 11:450. doi: 10.3390/cancers11040450
52. Yuen CA, Asuthkar S, Guda MR, Tsung AJ, Velpula KK. Cancer Stem Cell Molecular Reprogramming of the Warburg Effect in Glioblastomas: A New Target Gleaned From an Old Concept. *CNS Oncol* (2016) 5:101–8. doi: 10.2217/cns-2015-0006
53. Schito L, Semenza GL. Hypoxia-Inducible Factors: Master Regulators of Cancer Progression. *Trends Cancer* (2016) 2:758–70. doi: 10.1016/j.trecan.2016.10.016
54. Tong W-W, Tong G-H, Liu Y. Cancer Stem Cells and Hypoxia-Inducible Factors (Review). *Int J Oncol* (2018) 53:469–76. doi: 10.3892/ijo.2018.4417
55. Cuyàs E, Corominas-Faja B, Menendez JA. The Nutritional Phenome of EMT-Induced Cancer Stem-Like Cells. *Oncotarget* (2014) 5:3970–82. doi: 10.18632/oncotarget.2147
56. LaBarge MA. The Difficulty of Targeting Cancer Stem Cell Niches. *Clin Cancer Res* (2010) 16:3121–9. doi: 10.1158/1078-0432.CCR-09-2933
57. Moore KA, Lemischka IR. Stem Cells and Their Niches. *Science* (2006) 311:1880–5. doi: 10.1126/science.1110542
58. Adams JM, Strasser A. Is Tumor Growth Sustained by Rare Cancer Stem Cells or Dominant Clones? *Cancer Res* (2008) 68:4018–21. doi: 10.1158/0008-5472.CAN-07-6334
59. Janiszewska M, Suvà ML, Riggi N, Houtkooper RH, Auwerx J, Clément-Schatlo V, et al. Imp2 Controls Oxidative Phosphorylation and Is Crucial for Preserving Glioblastoma Cancer Stem Cells. *Genes Dev* (2012) 26:1926–44. doi: 10.1101/gad.188292.112
60. Lagadinou ED, Sach A, Callahan K, Rossi RM, Neering SJ, Minhajuddin M, et al. BCL-2 Inhibition Targets Oxidative Phosphorylation and Selectively Eradicates Quiescent Human Leukemia Stem Cells. *Cell Stem Cell* (2013) 12:329–41. doi: 10.1016/j.stem.2012.12.013
61. Roesch A, Vultur A, Bogeski I, Wang H, Zimmermann KM, Speicher D, et al. Overcoming Intrinsic Multidrug Resistance in Melanoma by Blocking the Mitochondrial Respiratory Chain of Slow-Cycling JARID1B(high) Cells. *Cancer Cell* (2013) 23:811–25. doi: 10.1016/j.ccr.2013.05.003
62. Vlashi E, Lagadec C, Vergnes L, Matsutani T, Masui K, Poulou M, et al. Metabolic State of Glioma Stem Cells and Nontumorigenic Cells. *Proc Natl Acad Sci USA* (2011) 108:16062–7. doi: 10.1073/pnas.1106704108
63. Pastò A, Bellio C, Pilotto G, Ciminale V, Silic-Benussi M, Guzzo G, et al. Cancer Stem Cells From Epithelial Ovarian Cancer Patients Privilege Oxidative Phosphorylation, and Resist Glucose Deprivation. *Oncotarget* (2014) 5:4305–19. doi: 10.18632/oncotarget.2010
64. Lee K-M, Giltnane JM, Balko JM, Schwarz LJ, Guerrero-Zotano AL, Hutchinson KE, et al. MYC and MCL1 Cooperatively Promote Chemotherapy-Resistant Breast Cancer Stem Cells *via* Regulation of Mitochondrial Oxidative Phosphorylation. *Cell Metab* (2017) 26:633–647.e7. doi: 10.1016/j.cmet.2017.09.009
65. Lamb R, Bonuccelli G, Ozsvári B, Peiris-Pagès M, Fiorillo M, Smith DL, et al. Mitochondrial Mass, a New Metabolic Biomarker for Stem-Like Cancer Cells: Understanding WNT/FGF-Driven Anabolic Signaling. *Oncotarget* (2015) 6:30453–71. doi: 10.18632/oncotarget.5852
66. Sancho P, Burgos-Ramos E, Tavera A, Bou Kheir T, Jagust P, Schoenhals M, et al. MYC/PGC-1α Balance Determines the Metabolic Phenotype and Plasticity of Pancreatic Cancer Stem Cells. *Cell Metab* (2015) 22:590–605. doi: 10.1016/j.cmet.2015.08.015
67. Farnie G, Sotgia F, Lisanti MP. High Mitochondrial Mass Identifies a Sub-Population of Stem-Like Cancer Cells That Are Chemo-Resistant. *Oncotarget* (2015) 6:30472–86. doi: 10.18632/oncotarget.5401
68. Tan J, Ong CK, Lim WK, Ng CCY, Thike AA, Ng LM, et al. Genomic Landscapes of Breast Fibroepithelial Tumors. *Nat Genet* (2015) 47:1341–5. doi: 10.1038/ng.3409
69. Lamb R, Ozsvari B, Bonuccelli G, Smith DL, Pestell RG, Martinez-Outschoorn UE, et al. Dissecting Tumor Metabolic Heterogeneity: Telomerase and Large Cell Size Metabolically Define a Sub-Population of Stem-Like, Mitochondrial-Rich, Cancer Cells. *Oncotarget* (2015) 6:21892–905. doi: 10.18632/oncotarget.5260
70. De Luca A, Fiorillo M, Peiris-Pagès M, Ozsvari B, Smith DL, Sanchez-Alvarez R, et al. Mitochondrial Biogenesis is Required for the Anchorage-Independent Survival and Propagation of Stem-Like Cancer Cells. *Oncotarget* (2015) 6:14777–95. doi: 10.18632/oncotarget.4401
71. Vazquez F, Lim J-H, Chim H, Bhalla K, Girnun G, Pierce K, et al. Pgc1α Expression Defines a Subset of Human Melanoma Tumors With Increased Mitochondrial Capacity and Resistance to Oxidative Stress. *Cancer Cell* (2013) 23:287–301. doi: 10.1016/j.ccr.2012.11.020

72. Yajima T, Ochiai H, Uchiyama T, Takano N, Shibahara T, Azuma T. Resistance to Cytotoxic Chemotherapy-Induced Apoptosis in Side Population Cells of Human Oral Squamous Cell Carcinoma Cell Line Ho-1-N-1. *Int J Oncol* (2009) 35:273–80.
73. Zhang G, Frederick DT, Wu L, Wei Z, Krepler C, Srinivasan S, et al. Targeting Mitochondrial Biogenesis to Overcome Drug Resistance to MAPK Inhibitors. *J Clin Invest* (2016) 126:1834–56. doi: 10.1172/JCI82661
74. Oburoglu L, Tardito S, Fritz V, de Barros SC, Merida P, Craveiro M, et al. Glucose and Glutamine Metabolism Regulate Human Hematopoietic Stem Cell Lineage Specification. *Cell Stem Cell* (2014) 15:169–84. doi: 10.1016/j.stem.2014.06.002
75. Kim JH, Lee KJ, Seo Y, Kwon J-H, Yoon JP, Kang JY, et al. Effects of Metformin on Colorectal Cancer Stem Cells Depend on Alterations in Glutamine Metabolism. *Sci Rep* (2018) 8:409. doi: 10.1038/s41598-017-18762-4
76. Choi Y-K, Park K-G. Targeting Glutamine Metabolism for Cancer Treatment. *Biomol Ther (Seoul)* (2018) 26:19–28. doi: 10.4062/biomolther.2017.178
77. Li D, Fu Z, Chen R, Zhao X, Zhou Y, Zeng B, et al. Inhibition of Glutamine Metabolism Counteracts Pancreatic Cancer Stem Cell Features and Sensitizes Cells to Radiotherapy. *Oncotarget* (2015) 6:31151–63. doi: 10.18632/oncotarget.5150
78. Sato M, Kawana K, Adachi K, Fujimoto A, Yoshida M, Nakamura H, et al. Spheroid Cancer Stem Cells Display Reprogrammed Metabolism and Obtain Energy by Actively Running the Tricarboxylic Acid (TCA) Cycle. *Oncotarget* (2016) 7:33297–305. doi: 10.18632/oncotarget.8947
79. Cluntun AA, Lukey MJ, Cerione RA, Locasale JW. Glutamine Metabolism in Cancer: Understanding the Heterogeneity. *Trends Cancer* (2017) 3:169–80. doi: 10.1016/j.trecan.2017.01.005
80. Chen Q, Kirk K, Shurubor YI, Zhao D, Arreguin AJ, Shahi I, et al. Rewiring of Glutamine Metabolism Is a Bioenergetic Adaptation of Human Cells With Mitochondrial DNA Mutations. *Cell Metab* (2018) 27:1007–1025.e5. doi: 10.1016/j.cmet.2018.03.002
81. Mukhopadhyay S, Goswami D, Adiseshaiah PP, Burgan W, Yi M, Guerin TM, et al. Undermining Glutaminolysis Bolsters Chemotherapy While NRF2 Promotes Chemoresistance in KRAS-Driven Pancreatic Cancers. *Cancer Res* (2020) 80:1630–43. doi: 10.1158/0008-5472.CAN-19-1363
82. Romero R, Sayin VI, Davidson SM, Bauer MR, Singh SX, LeBoeuf SE, et al. Keap1 Loss Promotes Kras-Driven Lung Cancer and Results in Dependence on Glutaminolysis. *Nat Med* (2017) 23:1362–8. doi: 10.1038/nm.4407
83. Wise DR, DeBerardinis RJ, Mancuso A, Sayed N, Zhang X-Y, Pfeiffer HK, et al. Myc Regulates a Transcriptional Program That Stimulates Mitochondrial Glutaminolysis and Leads to Glutamine Addiction. *Proc Natl Acad Sci USA* (2008) 105:18782–7. doi: 10.1073/pnas.0810199105
84. Lu W, Pelicano H, Huang P. Cancer Metabolism: Is Glutamine Sweeter Than Glucose? *Cancer Cell* (2010) 18:199–200. doi: 10.1016/j.ccr.2010.08.017
85. Shelton LM, Huysentruyt LC, Seyfried TN. Glutamine Targeting Inhibits Systemic Metastasis in the VM-M3 Murine Tumor Model. *Int J Cancer* (2010) 127:2478–85. doi: 10.1002/ijc.25431
86. Carracedo A, Cantley LC, Pandolfi PP. Cancer Metabolism: Fatty Acid Oxidation in the Limelight. *Nat Rev Cancer* (2013) 13:227–32. doi: 10.1038/nrc3483
87. Yi M, Li J, Chen S, Cai J, Ban Y, Peng Q, et al. Emerging Role of Lipid Metabolism Alterations in Cancer Stem Cells. *J Exp Clin Cancer Res* (2018) 37:118. doi: 10.1186/s13046-018-0784-5
88. Mancini R, Noto A, Pisanu ME, De Vitis C, Maugeri-Saccà M, Ciliberto G. Metabolic Features of Cancer Stem Cells: The Emerging Role of Lipid Metabolism. *Oncogene* (2018) 37:2367–78. doi: 10.1038/s41388-018-0141-3
89. O'Malley J, Kumar R, Kuzmin AN, Pliss A, Yadav N, Balachandar S, et al. Lipid Quantification by Raman Microspectroscopy as a Potential Biomarker in Prostate Cancer. *Cancer Lett* (2017) 397:52–60. doi: 10.1016/j.canlet.2017.03.025
90. Li X, Wu JB, Li Q, Shigemura K, Chung LWK, Huang W-C. SREBP-2 Promotes Stem Cell-Like Properties and Metastasis by Transcriptional Activation of C-Myc in Prostate Cancer. *Oncotarget* (2016) 7:12869–84. doi: 10.18632/oncotarget.7331
91. Tirinato L, Liberale C, Di Franco S, Candeloro P, Benfante A, La Rocca R, et al. Lipid Droplets: A New Player in Colorectal Cancer Stem Cells Unveiled by Spectroscopic Imaging. *Stem Cells* (2015) 33:35–44. doi: 10.1002/stem.1837
92. Yasumoto Y, Miyazaki H, Vaidyan LK, Kagawa Y, Ebrahimi M, Yamamoto Y, et al. Inhibition of Fatty Acid Synthase Decreases Expression of Stemness Markers in Glioma Stem Cells. *PloS One* (2016) 11:e0147717. doi: 10.1371/journal.pone.0147717
93. Brandi J, Dando I, Pozza ED, Biondani G, Jenkins R, Elliott V, et al. Proteomic Analysis of Pancreatic Cancer Stem Cells: Functional Role of Fatty Acid Synthesis and Mevalonate Pathways. *J Proteomics* (2017) 150:310–22. doi: 10.1016/j.jprot.2016.10.002
94. Wang T, Fahrmann JF, Lee H, Li Y-J, Tripathi SC, Yue C, et al. JAK/STAT3-Regulated Fatty Acid β-Oxidation Is Critical for Breast Cancer Stem Cell Self-Renewal and Chemoresistance. *Cell Metab* (2018) 27:1357. doi: 10.1016/j.cmet.2018.04.018
95. Ito K, Carracedo A, Weiss D, Arai F, Ala U, Avigan DE, et al. A PML–PPAR-δ Pathway for Fatty Acid Oxidation Regulates Hematopoietic Stem Cell Maintenance. *Nat Med* (2012) 18:1350–8. doi: 10.1038/nm.2882
96. Li J, Condello S, Thomes-Pepin J, Ma X, Xia Y, Hurley TD, et al. Lipid Desaturation Is a Metabolic Marker and Therapeutic Target of Ovarian Cancer Stem Cells. *Cell Stem Cell* (2017) 20:303–314.e5. doi: 10.1016/j.stem.2016.11.004
97. Schafer ZT, Grassian AR, Song L, Jiang Z, Gerhart-Hines Z, Irie HY, et al. Antioxidant and Oncogene Rescue of Metabolic Defects Caused by Loss of Matrix Attachment. *Nature* (2009) 461:109–13. doi: 10.1038/nature08268
98. Carracedo A, Weiss D, Leliaert AK, Bhasin M, de Boer VCJ, Laurent G, et al. A Metabolic Prosurvival Role for PML in Breast Cancer. *J Clin Invest* (2012) 122:3088–100. doi: 10.1172/JCI62129
99. Samudio I, Harmancey R, Fiegl M, Kantarjian H, Konopleva M, Korchin B, et al. Pharmacologic Inhibition of Fatty Acid Oxidation Sensitizes Human Leukemia Cells to Apoptosis Induction. *J Clin Invest* (2010) 120:142–56. doi: 10.1172/JCI38942
100. Wang B, Yu S, Jiang J, Porter GW, Zhao L, Wang Z, et al. An Inhibitor of Arachidonate 5-Lipoxygenase, Nordy, Induces Differentiation and Inhibits Self-Renewal of Glioma Stem-Like Cells. *Stem Cell Rev Rep* (2011) 7:458–70. doi: 10.1007/s12015-010-9175-9
101. Sun P, Xia S, Lal B, Shi X, Yang KS, Watkins PA, et al. Lipid Metabolism Enzyme ACSVL3 Supports Glioblastoma Stem Cell Maintenance and Tumorigenicity. *BMC Cancer* (2014) 14:401. doi: 10.1186/1471-2407-14-401
102. Figueroa ME, Abdel-Wahab O, Lu C, Ward PS, Patel J, Shih A, et al. Leukemic IDH1 and IDH2 Mutations Result in a Hypermethylation Phenotype, Disrupt TET2 Function, and Impair Hematopoietic Differentiation. *Cancer Cell* (2010) 18:553–67. doi: 10.1016/j.ccr.2010.11.015
103. Cimmino L, Abdel-Wahab O, Levine RL, Aifantis I. TET Family Proteins and Their Role in Stem Cell Differentiation and Transformation. *Cell Stem Cell* (2011) 9:193–204. doi: 10.1016/j.stem.2011.08.007
104. Kats LM, Reschke M, Taulli R, Pozdnyakova O, Burgess K, Bhargava P, et al. Proto-Oncogenic Role of Mutant IDH2 in Leukemia Initiation and Maintenance. *Cell Stem Cell* (2014) 14:329–41. doi: 10.1016/j.stem.2013.12.016
105. Wang X, Yang K, Xie Q, Wu Q, Mack SC, Shi Y, et al. Purine Synthesis Promotes Maintenance of Brain Tumor Initiating Cells in Glioma. *Nat Neurosci* (2017) 20:661–73. doi: 10.1038/nn.4537
106. Wu Z, Wei D, Gao W, Xu Y, Hu Z, Ma Z, et al. TPO-Induced Metabolic Reprogramming Drives Liver Metastasis of Colorectal Cancer CD110+ Tumor-Initiating Cells. *Cell Stem Cell* (2015) 17:47–59. doi: 10.1016/j.stem.2015.05.016
107. Lin S-T, Tu S-H, Yang P-S, Hsu S-P, Lee W-H, Ho C-T, et al. Apple Polyphenol Phloretin Inhibits Colorectal Cancer Cell Growth *via* Inhibition of the Type 2 Glucose Transporter and Activation of P53-Mediated Signaling. *J Agric Food Chem* (2016) 64:6826–37. doi: 10.1021/acs.jafc.6b02861
108. Wu K-H, Ho C-T, Chen Z-F, Chen L-C, Whang-Peng J, Lin T-N, et al. The Apple Polyphenol Phloretin Inhibits Breast Cancer Cell Migration and Proliferation *via* Inhibition of Signals by Type 2 Glucose Transporter. *J Food Drug Anal* (2018) 26:221–31. doi: 10.1016/j.jfda.2017.03.009
109. Wood TE, Dalili S, Simpson CD, Hurren R, Mao X, Saiz FS, et al. A Novel Inhibitor of Glucose Uptake Sensitizes Cells to FAS-Induced Cell Death. *Mol Cancer Ther* (2008) 7:3546–55. doi: 10.1158/1535-7163.MCT-08-0569

110. Liu Y, Cao Y, Zhang W, Bergmeier S, Qian Y, Akbar H, et al. A Small-Molecule Inhibitor of Glucose Transporter 1 Downregulates Glycolysis, Induces Cell-Cycle Arrest, and Inhibits Cancer Cell Growth *In Vitro* and *In Vivo*. *Mol Cancer Ther* (2012) 11:1672–82. doi: 10.1158/1535-7163.MCT-12-0131
111. Tao L, Wei L, Liu Y, Ding Y, Liu X, Zhang X, et al. Gen-27, a Newly Synthesized Flavonoid, Inhibits Glycolysis and Induces Cell Apoptosis *via* Suppression of Hexokinase II in Human Breast Cancer Cells. *Biochem Pharmacol* (2017) 125:12–25. doi: 10.1016/j.bcp.2016.11.001
112. Li W, Zheng M, Wu S, Gao S, Yang M, Li Z, et al. Benserazide, a Dopadecarboxylase Inhibitor, Suppresses Tumor Growth by Targeting Hexokinase 2. *J Exp Clin Cancer Res* (2017) 36:58. doi: 10.1186/s13046-017-0530-4
113. Coleman MC, Asbury CR, Daniels D, Du J, Aykin-Burns N, Smith BJ, et al. 2-Deoxy-D-Glucose Causes Cytotoxicity, Oxidative Stress, and Radiosensitization in Pancreatic Cancer. *Free Radic Biol Med* (2008) 44:322–31. doi: 10.1016/j.freeradbiomed.2007.08.032
114. Berruti A, Bitossi R, Gorzegno G, Bottini A, Alquati P, De Matteis A, et al. Time to Progression in Metastatic Breast Cancer Patients Treated With Epirubicin Is Not Improved by the Addition of Either Cisplatin or Lonidamine: Final Results of a Phase III Study With a Factorial Design. *J Clin Oncol* (2002) 20:4150–9. doi: 10.1200/JCO.2002.08.012
115. Dwarakanath B, Jain V. Targeting Glucose Metabolism With 2-Deoxy-D-Glucose for Improving Cancer Therapy. *Future Oncol* (2009) 5:581–5. doi: 10.2217/fon.09.44
116. Raez LE, Papadopoulos K, Ricart AD, Chiorean EG, Dipaola RS, Stein MN, et al. A Phase I Dose-Escalation Trial of 2-Deoxy-D-Glucose Alone or Combined With Docetaxel in Patients With Advanced Solid Tumors. *Cancer Chemother Pharmacol* (2013) 71:523–30. doi: 10.1007/s00280-012-2045-1
117. Simons AL, Ahmad IM, Mattson DM, Dornfeld KJ, Spitz DR. 2-Deoxy-D-Glucose Combined With Cisplatin Enhances Cytotoxicity *via* Metabolic Oxidative Stress in Human Head and Neck Cancer Cells. *Cancer Res* (2007) 67:3364–70. doi: 10.1158/0008-5472.CAN-06-3717
118. O'Neill S, Porter RK, McNamee N, Martinez VG, O'Driscoll L. 2-Deoxy-D-Glucose Inhibits Aggressive Triple-Negative Breast Cancer Cells by Targeting Glycolysis and the Cancer Stem Cell Phenotype. *Sci Rep* (2019) 9:3788. doi: 10.1038/s41598-019-39789-9
119. Lea MA, Qureshi MS, Buxhoeveden M, Gengel N, Kleinschmit J, Desbordes C. Regulation of the Proliferation of Colon Cancer Cells by Compounds That Affect Glycolysis, Including 3-Bromopyruvate, 2-Deoxyglucose and Biguanides. *Anticancer Res* (2013) 33:401–7.
120. Michelakis ED, Sutendra G, Dromparis P, Webster L, Haromy A, Niven E, et al. Metabolic Modulation of Glioblastoma With Dichloroacetate. *Sci Transl Med* (2010) 2:31ra34. doi: 10.1126/scitranslmed.3000677
121. Dunbar EM, Coats BS, Shroads AL, Langaee T, Lew A, Forder JR, et al. Phase 1 Trial of Dichloroacetate (DCA) in Adults With Recurrent Malignant Brain Tumors. *Invest New Drugs* (2014) 32:452–64. doi: 10.1007/s10637-013-0047-4
122. Chu QS-C, Sangha R, Spratlin J, Vos LJ, Mackey JR, McEwan AJB, et al. A Phase I Open-Labeled, Single-Arm, Dose-Escalation, Study of Dichloroacetate (DCA) in Patients With Advanced Solid Tumors. *Invest New Drugs* (2015) 33:603–10. doi: 10.1007/s10637-015-0221-y
123. Peng F, Wang J-H, Fan W-J, Meng Y-T, Li M-M, Li T-T, et al. Glycolysis Gatekeeper PDK1 Reprograms Breast Cancer Stem Cells Under Hypoxia. *Oncogene* (2018) 37:1119. doi: 10.1038/onc.2017.407
124. Keith B, Simon MC. Hypoxia-Inducible Factors, Stem Cells, and Cancer. *Cell* (2007) 129:465–72. doi: 10.1016/j.cell.2007.04.019
125. Hu L, Zeng Z, Xia Q, Liu Z, Feng X, Chen J, et al. Metformin Attenuates Hepatoma Cell Proliferation by Decreasing Glycolytic Flux Through the HIF-1α/PFKFB3/PFK1 Pathway. *Life Sci* (2019) 239:116966. doi: 10.1016/j.lfs.2019.116966
126. Zannella VE, Dal Pra A, Muaddi H, McKee TD, Stapleton S, Sykes J, et al. Reprogramming Metabolism With Metformin Improves Tumor Oxygenation and Radiotherapy Response. *Clin Cancer Res* (2013) 19:6741–50. doi: 10.1158/1078-0432.CCR-13-1787
127. Wei R, Hackman RM, Wang Y, Mackenzie GG. Targeting Glycolysis With Epigallocatechin-3-Gallate Enhances the Efficacy of Chemotherapeutics in Pancreatic Cancer Cells and Xenografts. *Cancers (Basel)* (2019) 11:1496. doi: 10.3390/cancers11101496
128. Lamb R, Ozsvari B, Lisanti CL, Tanowitz HB, Howell A, Martinez-Outschoorn UE, et al. Antibiotics That Target Mitochondria Effectively Eradicate Cancer Stem Cells, Across Multiple Tumor Types: Treating Cancer Like an Infectious Disease. *Oncotarget* (2015) 6:4569–84. doi: 10.18632/oncotarget.3174
129. Wheaton WW, Weinberg SE, Hamanaka RB, Soberanes S, Sullivan LB, Anso E, et al. Metformin Inhibits Mitochondrial Complex I of Cancer Cells to Reduce Tumorigenesis. *Elife* (2014) 3:e02242. doi: 10.7554/eLife.02242
130. Bowker SL, Yasui Y, Veugelers P, Johnson JA. Glucose-Lowering Agents and Cancer Mortality Rates in Type 2 Diabetes: Assessing Effects of Time-Varying Exposure. *Diabetologia* (2010) 53:1631–7. doi: 10.1007/s00125-010-1750-8
131. Kheirandish M, Mahboobi H, Yazdanparast M, Kamal W, Kamal MA. Anti-Cancer Effects of Metformin: Recent Evidences for Its Role in Prevention and Treatment of Cancer. *Curr Drug Metab* (2018) 19:793–7. doi: 10.2174/1389200219666180416161846
132. Shackelford DB, Abt E, Gerken L, Vasquez DS, Seki A, Leblanc M, et al. LKB1 Inactivation Dictates Therapeutic Response of non-Small Cell Lung Cancer to the Metabolism Drug Phenformin. *Cancer Cell* (2013) 23:143–58. doi: 10.1016/j.ccr.2012.12.008
133. Gupta PB, Onder TT, Jiang G, Tao K, Kuperwasser C, Weinberg RA, et al. Identification of Selective Inhibitors of Cancer Stem Cells by High-Throughput Screening. *Cell* (2009) 138:645–59. doi: 10.1016/j.cell.2009.06.034
134. Skrtić M, Sriskanthadevan S, Jhas B, Gebbia M, Wang X, Wang Z, et al. Inhibition of Mitochondrial Translation as a Therapeutic Strategy for Human Acute Myeloid Leukemia. *Cancer Cell* (2011) 20:674–88. doi: 10.1016/j.ccr.2011.10.015
135. Murphy MP. Targeting Lipophilic Cations to Mitochondria. *Biochim Biophys Acta* (2008) 1777:1028–31. doi: 10.1016/j.bbabio.2008.03.029
136. Chamberlain GR, Tulumello DV, Kelley SO. Targeted Delivery of Doxorubicin to Mitochondria. *ACS Chem Biol* (2013) 8:1389–95. doi: 10.1021/cb400095v
137. Issaq SH, Teicher BA, Monks A. Bioenergetic Properties of Human Sarcoma Cells Help Define Sensitivity to Metabolic Inhibitors. *Cell Cycle* (2014) 13:1152–61. doi: 10.4161/cc.28010
138. Cheong J-H, Park ES, Liang J, Dennison JB, Tsavachidou D, Nguyen-Charles C, et al. Dual Inhibition of Tumor Energy Pathway by 2-Deoxyglucose and Metformin Is Effective Against a Broad Spectrum of Preclinical Cancer Models. *Mol Cancer Ther* (2011) 10:2350–62. doi: 10.1158/1535-7163.MCT-11-0497
139. Peiris-Pagès M, Martinez-Outschoorn UE, Pestell RG, Sotgia F, Lisanti MP. Cancer Stem Cell Metabolism. *Breast Cancer Res* (2016) 18:55. doi: 10.1186/s13058-016-0712-6
140. Boysen G, Jamshidi-Parsian A, Davis MA, Siegel ER, Simecka CM, Kore RA, et al. Glutaminase Inhibitor CB-839 Increases Radiation Sensitivity of Lung Tumor Cells and Human Lung Tumor Xenografts in Mice. *Int J Radiat Biol* (2019) 95:436–42. doi: 10.1080/09553002.2018.1558299
141. Robinson MM, McBryant SJ, Tsukamoto T, Rojas C, Ferraris DV, Hamilton SK, et al. Novel Mechanism of Inhibition of Rat Kidney-Type Glutaminase by Bis-2-(5-Phenylacetamido-1,2,4-Thiadiazol-2-Yl)Ethyl Sulfide (BPTES). *Biochem J* (2007) 406:407–14. doi: 10.1042/BJ20070039
142. Matre P, Velez J, Jacamo R, Qi Y, Su X, Cai T, et al. Inhibiting Glutaminase in Acute Myeloid Leukemia: Metabolic Dependency of Selected AML Subtypes. *Oncotarget* (2016) 7:79722–35. doi: 10.18632/oncotarget.12944
143. Shiragami R, Murata S, Kosugi C, Tezuka T, Yamazaki M, Hirano A, et al. Enhanced Antitumor Activity of Cerulenin Combined With Oxaliplatin in Human Colon Cancer Cells. *Int J Oncol* (2013) 43:431–8. doi: 10.3892/ijo.2013.1978
144. Corominas-Faja B, Vellon L, Cuyàs E, Buxó M, Martin-Castillo B, Serra D, et al. Clinical and Therapeutic Relevance of the Metabolic Oncogene Fatty Acid Synthase in HER2+ Breast Cancer. *Histol Histopathol* (2017) 32:687–98. doi: 10.14670/HH-11-830
145. Ma MKF, Lau EYT, Leung DHW, Lo J, Ho NPY, Cheng LKW, et al. Stearoyl-CoA Desaturase Regulates Sorafenib Resistance *via* Modulation of ER Stress-Induced Differentiation. *J Hepatol* (2017) 67:979–90. doi: 10.1016/j.jhep.2017.06.015

146. Pisanu ME, Noto A, De Vitis C, Morrone S, Scognamiglio G, Botti G, et al. Blockade of Stearoyl-CoA-Desaturase 1 Activity Reverts Resistance to Cisplatin in Lung Cancer Stem Cells. *Cancer Lett* (2017) 406:93–104. doi: 10.1016/j.canlet.2017.07.027
147. Medes G, Thomas A, Weinhouse S. Metabolism of Neoplastic Tissue. IV. A Study of Lipid Synthesis in Neoplastic Tissue Slices *In Vitro*. *Cancer Res* (1953) 13:27–9.
148. Brown MS, Goldstein JL. A Receptor-Mediated Pathway for Cholesterol Homeostasis. *Science* (1986) 232:34–47. doi: 10.1126/science.3513311
149. Kazantzis M, Stahl A. Fatty Acid Transport Proteins, Implications in Physiology and Disease. *Biochim Biophys Acta (BBA) - Mol Cell Biol Lipids* (2012) 1821:852–7. doi: 10.1016/j.bbalip.2011.09.010
150. Furuhashi M, Hotamisligil GS. Fatty Acid-Binding Proteins: Role in Metabolic Diseases and Potential as Drug Targets. *Nat Rev Drug Discovery* (2008) 7:489–503. doi: 10.1038/nrd2589
151. Hale JS, Otvos B, Sinyuk M, Alvarado AG, Hitomi M, Stoltz K, et al. Cancer Stem Cell-Specific Scavenger Receptor CD36 Drives Glioblastoma Progression. *Stem Cells* (2014) 32:1746–58. doi: 10.1002/stem.1716
152. Ye H, Adane B, Khan N, Sullivan T, Minhajuddin M, Gasparetto M, et al. Leukemic Stem Cells Evade Chemotherapy by Metabolic Adaptation to an Adipose Tissue Niche. *Cell Stem Cell* (2016) 19:23–37. doi: 10.1016/j.stem.2016.06.001
153. Pascual G, Avgustinova A, Mejetta S, Martín M, Castellanos A, Attolini CS-O, et al. Targeting Metastasis-Initiating Cells Through the Fatty Acid Receptor CD36. *Nature* (2017) 541:41–5. doi: 10.1038/nature20791
154. Beloribi-Djefaflia S, Vasseur S, Guillaumond F. Lipid Metabolic Reprogramming in Cancer Cells. *Oncogenesis* (2016) 5:e189. doi: 10.1038/oncsis.2015.49
155. Ginestier C, Monville F, Wicinski J, Cabaud O, Cervera N, Josselin E, et al. Mevalonate Metabolism Regulates Basal Breast Cancer Stem Cells and Is a Potential Therapeutic Target. *Stem Cells* (2012) 30:1327–37. doi: 10.1002/stem.1122
156. Peng Y, He G, Tang D, Xiong L, Wen Y, Miao X, et al. Lovastatin Inhibits Cancer Stem Cells and Sensitizes to Chemo- and Photodynamic Therapy in Nasopharyngeal Carcinoma. *J Cancer* (2017) 8:1655–64. doi: 10.7150/jca.19100
157. Wang X, Huang Z, Wu Q, Prager BC, Mack SC, Yang K, et al. MYC-Regulated Mevalonate Metabolism Maintains Brain Tumor-Initiating Cells. *Cancer Res* (2017) 77:4947–60. doi: 10.1158/0008-5472.CAN-17-0114
158. Liu Y, Zuckier LS, Ghesani NV. Dominant Uptake of Fatty Acid Over Glucose by Prostate Cells: A Potential New Diagnostic and Therapeutic Approach. *Anticancer Res* (2010) 30:369–74.
159. Caro P, Kishan AU, Norberg E, Stanley IA, Chapuy B, Ficarro SB, et al. Metabolic Signatures Uncover Distinct Targets in Molecular Subsets of Diffuse Large B Cell Lymphoma. *Cancer Cell* (2012) 22:547–60. doi: 10.1016/j.ccr.2012.08.014
160. Kamphorst JJ, Cross JR, Fan J, de Stanchina E, Mathew R, White EP, et al. Hypoxic and Ras-Transformed Cells Support Growth by Scavenging Unsaturated Fatty Acids From Lysophospholipids. *Proc Natl Acad Sci USA* (2013) 110:8882–7. doi: 10.1073/pnas.1307237110
161. Daniëls VW, Smans K, Royaux I, Chypre M, Swinnen JV, Zaidi N. Cancer Cells Differentially Activate and Thrive on *De Novo* Lipid Synthesis Pathways in a Low-Lipid Environment. *PloS One* (2014) 9:e106913. doi: 10.1371/journal.pone.0106913
162. Lee EA, Angka L, Rota S-G, Hanlon T, Mitchell A, Hurren R, et al. Targeting Mitochondria With Avocatin B Induces Selective Leukemia Cell Death. *Cancer Res* (2015) 75:2478–88. doi: 10.1158/0008-5472.CAN-14-2676
163. Chen X, Song M, Zhang B, Zhang Y. Reactive Oxygen Species Regulate T Cell Immune Response in the Tumor Microenvironment. *Oxid Med Cell Longev* (2016) 2016:1580967. doi: 10.1155/2016/1580967
164. Aguilar E, Marin de Mas I, Zodda E, Marin S, Morrish F, Selivanov V, et al. Metabolic Reprogramming and Dependencies Associated With Epithelial Cancer Stem Cells Independent of the Epithelial-Mesenchymal Transition Program. *Stem Cells* (2016) 34:1163–76. doi: 10.1002/stem.2286
165. De Francesco EM, Maggiolini M, Tanowitz HB, Sotgia F, Lisanti MP. Targeting Hypoxic Cancer Stem Cells (CSCs) With Doxycycline: Implications for Optimizing Anti-Angiogenic Therapy. *Oncotarget* (2017) 8:56126–42. doi: 10.18632/oncotarget.18445
166. Corominas-Faja B, Cuyàs E, Gumuzio J, Bosch-Barrera J, Leis O, Martin ÁG, et al. Chemical Inhibition of Acetyl-CoA Carboxylase Suppresses Self-Renewal Growth of Cancer Stem Cells. *Oncotarget* (2014) 5:8306–16. doi: 10.18632/oncotarget.2059
167. Pandey PR, Okuda H, Watabe M, Pai SK, Liu W, Kobayashi A, et al. Resveratrol Suppresses Growth of Cancer Stem-Like Cells by Inhibiting Fatty Acid Synthase. *Breast Cancer Res Treat* (2011) 130:387–98. doi: 10.1007/s10549-010-1300-6
168. Hirata N, Yamada S, Shoda T, Kurihara M, Sekino Y, Kanda Y. Sphingosine-1-Phosphate Promotes Expansion of Cancer Stem Cells *via* S1PR3 by a Ligand-Independent Notch Activation. *Nat Commun* (2014) 5:4806. doi: 10.1038/ncomms5806
169. Kurtova AV, Xiao J, Mo Q, Pazhanisamy S, Krasnow R, Lerner SP, et al. Blocking PGE2-Induced Tumour Repopulation Abrogates Bladder Cancer Chemoresistance. *Nature* (2015) 517:209–13. doi: 10.1038/nature14034
170. Wang D, Fu L, Sun H, Guo L, DuBois RN. Prostaglandin E2 Promotes Colorectal Cancer Stem Cell Expansion and Metastasis in Mice. *Gastroenterology* (2015) 149:1884–1895.e4. doi: 10.1053/j.gastro.2015.07.064
171. Seo EJ, Kwon YW, Jang IH, Kim DK, Lee SI, Choi EJ, et al. Autotaxin Regulates Maintenance of Ovarian Cancer Stem Cells Through Lysophosphatidic Acid-Mediated Autocrine Mechanism. *Stem Cells* (2016) 34:551–64. doi: 10.1002/stem.2279
172. Ray R, Rai V. Lysophosphatidic Acid Converts Monocytes Into Macrophages in Both Mice and Humans. *Blood* (2017) 129:1177–83. doi: 10.1182/blood-2016-10-743757
173. Radhakrishnan R, Ha JH, Jayaraman M, Liu J, Moxley KM, Isidoro C, et al. Ovarian Cancer Cell-Derived Lysophosphatidic Acid Induces Glycolytic Shift and Cancer-Associated Fibroblast-Phenotype in Normal and Peritumoral Fibroblasts. *Cancer Lett* (2019) 442:464–74. doi: 10.1016/j.canlet.2018.11.023
174. Li F, He B, Ma X, Yu S, Bhave RR, Lentz SR, et al. Prostaglandin E1 and Its Analog Misoprostol Inhibit Human CML Stem Cell Self-Renewal *via* EP4 Receptor Activation and Repression of AP-1. *Cell Stem Cell* (2017) 21:359–373.e5. doi: 10.1016/j.stem.2017.08.001
175. De Carlo F, Witte TR, Hardman WE, Claudio PP. Omega-3 Eicosapentaenoic Acid Decreases CD133 Colon Cancer Stem-Like Cell Marker Expression While Increasing Sensitivity to Chemotherapy. *PloS One* (2013) 8:e69760. doi: 10.1371/journal.pone.0069760
176. Yang T, Fang S, Zhang H-X, Xu L-X, Zhang Z-Q, Yuan K-T, et al. N-3 PUFAs Have Antiproliferative and Apoptotic Effects on Human Colorectal Cancer Stem-Like Cells *In Vitro*. *J Nutr Biochem* (2013) 24:744–53. doi: 10.1016/j.jnutbio.2012.03.023
177. Erickson KL, Hubbard NE. Fatty Acids and Breast Cancer: The Role of Stem Cells. *Prostaglandins Leukot Essent Fatty Acids* (2010) 82:237–41. doi: 10.1016/j.plefa.2010.02.019
178. Vasudevan A, Yu Y, Banerjee S, Woods J, Farhana L, Rajendra SG, et al. Omega-3 Fatty Acid Is a Potential Preventive Agent for Recurrent Colon Cancer. *Cancer Prev Res (Phila)* (2014) 7:1138–48. doi: 10.1158/1940-6207.CAPR-14-0177
179. Jia D, Lu M, Jung KH, Park JH, Yu L, Onuchic JN, et al. Elucidating Cancer Metabolic Plasticity by Coupling Gene Regulation With Metabolic Pathways. *Proc Natl Acad Sci USA* (2019) 116:3909–18. doi: 10.1073/pnas.1816391116
180. Gadducci A, Brunetti I, Muttini MP, Fanucchi A, Dargenio F, Giannessi PG, et al. Epidoxorubicin and Lonidamine in Refractory or Recurrent Epithelial Ovarian Cancer. *Eur J Cancer* (1994) 30A:1432–5. doi: 10.1016/0959-8049(94)00231-s
181. De Lena M, Lorusso V, Bottalico C, Brandi M, De Mitrio A, Catino A, et al. Revertant and Potentiating Activity of Lonidamine in Patients With Ovarian Cancer Previously Treated With Platinum. *J Clin Oncol* (1997) 15:3208–13. doi: 10.1200/JCO.1997.15.10.3208
182. De Marinis F, Rinaldi M, Ardizzoni A, Bruzzi P, Pennucci MC, Portalone L, et al. The Role of Vindesine and Lonidamine in the Treatment of Elderly Patients With Advanced non-Small Cell Lung Cancer: A Phase III Randomized FONICAP Trial. Italian Lung Cancer Task Force. *Tumori* (1999) 85:177–82. doi: 10.1177/030089169908500306
183. Li C, Liu VWS, Chan DW, Yao KM, Ngan HYS. LY294002 and Metformin Cooperatively Enhance the Inhibition of Growth and the Induction of Apoptosis of Ovarian Cancer Cells. *Int J Gynecol Cancer* (2012) 22:15–22. doi: 10.1097/IGC.0b013e3182322834

184. Bailey P, Chang DK, Nones K, Johns AL, Patch A-M, Gingras M-C, et al. Genomic Analyses Identify Molecular Subtypes of Pancreatic Cancer. *Nature* (2016) 531:47–52. doi: 10.1038/nature16965
185. Blum R, Kloog Y. Metabolism Addiction in Pancreatic Cancer. *Cell Death Dis* (2014) 5:e1065. doi: 10.1038/cddis.2014.38
186. Ying H, Kimmelman AC, Lyssiotis CA, Hua S, Chu GC, Fletcher-Sananikone E, et al. Oncogenic Kras Maintains Pancreatic Tumors Through Regulation of Anabolic Glucose Metabolism. *Cell* (2012) 149:656–70. doi: 10.1016/j.cell.2012.01.058
187. Lin W, Rajbhandari N, Liu C, Sakamoto K, Zhang Q, Triplett AA, et al. Dormant Cancer Cells Contribute to Residual Disease in a Model of Reversible Pancreatic Cancer. *Cancer Res* (2013) 73:1821–30. doi: 10.1158/0008-5472.CAN-12-2067
188. He T-L, Zhang Y-J, Jiang H, Li X-H, Zhu H, Zheng K-L. The C-Myc-LDHA Axis Positively Regulates Aerobic Glycolysis and Promotes Tumor Progression in Pancreatic Cancer. *Med Oncol* (2015) 32:187. doi: 10.1007/s12032-015-0633-8
189. Jia D, Paudel BB, Hayford CE, Hardeman KN, Levine H, Onuchic JN, et al. Drug-Tolerant Idling Melanoma Cells Exhibit Theory-Predicted Metabolic Low-Low Phenotype. *Front Oncol* (2020) 10:1426. doi: 10.3389/fonc.2020.01426
190. Luo M, Shang L, Brooks MD, Jiagge E, Zhu Y, Buschhaus JM, et al. Targeting Breast Cancer Stem Cell State Equilibrium Through Modulation of Redox Signaling. *Cell Metab* (2018) 28:69–86.e6. doi: 10.1016/j.cmet.2018.06.006

Conflict of Interest: The authors declare that the research was conducted in the absence of any commercial or financial relationships that could be construed as a potential conflict of interest.

Advantages of publishing in Frontiers

OPEN ACCESS
Articles are free to read for greatest visibility and readership

FAST PUBLICATION
Around 90 days from submission to decision

HIGH QUALITY PEER-REVIEW
Rigorous, collaborative, and constructive peer-review

TRANSPARENT PEER-REVIEW
Editors and reviewers acknowledged by name on published articles

Frontiers
Avenue du Tribunal-Fédéral 34
1005 Lausanne | Switzerland

Visit us: www.frontiersin.org
Contact us: frontiersin.org/about/contact

REPRODUCIBILITY OF RESEARCH
Support open data and methods to enhance research reproducibility

DIGITAL PUBLISHING
Articles designed for optimal readership across devices

FOLLOW US
@frontiersin

IMPACT METRICS
Advanced article metrics track visibility across digital media

EXTENSIVE PROMOTION
Marketing and promotion of impactful research

LOOP RESEARCH NETWORK
Our network increases your article's readership